CC CHM 411: ADVANCED ANALYTICAL CHEMISTRY



Cynthia Strong
Cornell College

LibreTexts™

Coe College (CHM 411) and Cornell College (CHE 333)

Advanced Analytical Chemistry

Martin St. Clair and Cynthia Strong

This text is disseminated via the Open Education Resource (OER) LibreTexts Project (https://LibreTexts.org) and like the thousands of other texts available within this powerful platform, it is freely available for reading, printing, and "consuming."

The LibreTexts mission is to bring together students, faculty, and scholars in a collaborative effort to provide an accessible, and comprehensive platform that empowers our community to develop, curate, adapt, and adopt openly licensed resources and technologies; through these efforts we can reduce the financial burden born from traditional educational resource costs, ensuring education is more accessible for students and communities worldwide.

Most, but not all, pages in the library have licenses that may allow individuals to make changes, save, and print this book. Carefully consult the applicable license(s) before pursuing such effects. Instructors can adopt existing LibreTexts texts or Remix them to quickly build course-specific resources to meet the needs of their students. Unlike traditional textbooks, LibreTexts' web based origins allow powerful integration of advanced features and new technologies to support learning.



LibreTexts is the adaptable, user-friendly non-profit open education resource platform that educators trust for creating, customizing, and sharing accessible, interactive textbooks, adaptive homework, and ancillary materials. We collaborate with individuals and organizations to champion open education initiatives, support institutional publishing programs, drive curriculum development projects, and more.

The LibreTexts libraries are Powered by NICE CXone Expert and was supported by the Department of Education Open Textbook Pilot Project, the California Education Learning Lab, the UC Davis Office of the Provost, the UC Davis Library, the California State University Affordable Learning Solutions Program, and Merlot. This material is based upon work supported by the National Science Foundation under Grant No. 1246120, 1525057, and 1413739.

Any opinions, findings, and conclusions or recommendations expressed in this material are those of the author(s) and do not necessarily reflect the views of the National Science Foundation nor the US Department of Education.

Have questions or comments? For information about adoptions or adaptions contact info@LibreTexts.org or visit our main website at https://LibreTexts.org.

This text was compiled on 01/11/2026

TABLE OF CONTENTS

Licensing

1: Spectroscopic Methods

- 1.1: Overview of Spectroscopy
- 1.2: Spectroscopy Based on Absorption
- 1.3: UV/Vis and IR Spectroscopy
- 1.4: Fourier-Transform Infrared Spectroscopy -- Additional Readings
- 1.5: Raman Spectroscopy
  - 1.5.1: Raman- Application
  - 1.5.2: Raman- Theory
  - 1.5.3: Resonant vs. Nonresonant Raman Spectroscopy
- 1.6: Current Applications of IR and Raman Spectroscopy
- 1.7: Atomic Absorption Spectroscopy
- 1.8: Emission Spectroscopy
- 1.9: Photoluminescent Spectroscopy
- 1.10: Atomic Emission Spectroscopy
- 1.11: Nuclear Magnetic Resonance Spectrometry
  - 1.11.1: Additional Readings on NMR
  - 1.11.2: Applications of NMR
- 1.12: Spectroscopy Based on Scattering
- 1.13: Neutron Activation Analysis
- 1.14: Problems
- 1.15: Additional Resources
- 1.16: Chapter Summary and Key Terms

2: Chromatographic and Electrophoretic Methods

- 2.1: Overview of Analytical Separations
- 2.2: General Theory of Column Chromatography
- 2.3: Optimizing Chromatographic Separations
- 2.4: Gas Chromatography
- 2.5: High-Performance Liquid Chromatography
  - 2.5.1: HPLC Simulator
  - 2.5.2: HPLC Method Development
- 2.6: Other Forms of Chromatography
- 2.7: Electrophoresis
- 2.8: Problems
- 2.9: Additional Resources
- 2.10: Chapter Summary and Key Terms

3: Mass Spectrometry

- 3.1: Accelerator Mass Spectroscopy
- 3.2: Fragmentation Patterns in Mass Spectra
- 3.3: GC/MS Combination- Shockwave

- 3.4: How the Mass Spectrometer Works
- 3.5: Introductory Mass Spectrometry
  - 3.5.1: Fragmentation
  - 3.5.2: High Resolution vs Low Resolution
  - 3.5.3: Introduction to Mass Spectrometry
  - 3.5.4: Isotopes- 13C
  - 3.5.5: Isotopes- Br and Cl
  - 3.5.6: Molecular Ions
  - 3.5.7: Molecular Ion and Nitrogen
  - 3.5.8: The Mass Spectrometry Experiment
- 3.6: MALDI-TOF
- 3.7: Mass Spectra
  - 3.7.1: Interpreting a Mass Spectrum
  - 3.7.2: Mass Spectrometry - Fragmentation Patterns
  - 3.7.3: Mass Spectroscopy- Quizzes
- 3.8: Mass Spectra Interpretation- ALDEHYDES
- 3.9: Mass Spectrometers (Instrumentation)
  - 3.9.1: Electrospray Ionization Mass Spectrometry
  - 3.9.2: Injection Stage
  - 3.9.3: Mass Analyzers (Mass Spectrometry)
- 3.10: Mass Spectrometry- Isotope Effects
- 3.11: Organic Compounds Containing Halogen Atoms
- 3.12: Selected Ion Monitoring- Shockwave
- 3.13: The Mass Spectra of Elements
- 3.14: The Molecular Ion (M^+) Peak
- 3.15: The M+1 Peak
- 3.16: Current Applications of Mass Spectrometry

4: Electrochemical Methods

- 4.1: Overview of Electrochemistry
- 4.2: Potentiometric Methods
- 4.3: Coulometric Methods
- 4.4: Voltammetric and Amperometric Methods
  - 4.4.1: Cyclic Voltammetry
  - 4.4.2: Anodic Stripping Voltammetry
- 4.5: Problems
- 4.6: Additional Resources
- 4.7: Chapter Summary and Key Terms

5: Surface Techniques

- 5.1: Applications of Surface Techniques

6: Elemental Analysis

- 6.1: Neutron Activation Analysis

Index

Glossary

Detailed Licensing

Licensing

*A detailed breakdown of this resource's licensing can be found in **Back Matter/Detailed Licensing**.*

CHAPTER OVERVIEW

1: Spectroscopic Methods

An early example of a colorimetric analysis is Nessler's method for ammonia, which was introduced in 1856. Nessler found that adding an alkaline solution of HgI_2 and KI to a dilute solution of ammonia produced a yellow-to-reddish brown colloid, in which the colloid's color depended on the concentration of ammonia. By visually comparing the color of a sample to the colors of a series of standards, Nessler was able to determine the concentration of ammonia. Colorimetry, in which a sample absorbs visible light, is one example of a spectroscopic method of analysis. At the end of the nineteenth century, spectroscopy was limited to the absorption, emission, and scattering of visible, ultraviolet, and infrared electromagnetic radiation. Since then, spectroscopy has expanded to include other forms of electromagnetic radiation—such as X-rays, microwaves, and radio waves—and other energetic particles—such as electrons and ions.

1.1: Overview of Spectroscopy
1.2: Spectroscopy Based on Absorption
1.3: UV/Vis and IR Spectroscopy
1.4: Fourier-Transform Infrared Spectroscopy -- Additional Readings
1.5: Raman Spectroscopy
1.5.1: Raman- Application
1.5.2: Raman- Theory
1.5.3: Resonant vs. Nonresonant Raman Spectroscopy
1.6: Current Applications of IR and Raman Spectroscopy
1.7: Atomic Absorption Spectroscopy
1.8: Emission Spectroscopy
1.9: Photoluminescent Spectroscopy
1.10: Atomic Emission Spectroscopy
1.11: Nuclear Magnetic Resonance Spectrometry
1.11.1: Additional Readings on NMR
1.11.2: Applications of NMR
1.12: Spectroscopy Based on Scattering
1.13: Neutron Activation Analysis
1.14: Problems
1.15: Additional Resources
1.16: Chapter Summary and Key Terms

This page titled 1: Spectroscopic Methods is shared under a CC BY-NC-SA 4.0 license and was authored, remixed, and/or curated by David Harvey.

1.1: Overview of Spectroscopy

The focus of this chapter is on the interaction of ultraviolet, visible, and infrared radiation with matter. Because these techniques use optical materials to disperse and focus the radiation, they often are identified as optical spectroscopies. For convenience we will use the simpler term spectroscopy in place of optical ***spectroscopy***; however, you should understand we will consider only a limited piece of what is a much broader area of analytical techniques.

Despite the difference in instrumentation, all spectroscopic techniques share several common features. Before we consider individual examples in greater detail, let's take a moment to consider some of these similarities. As you work through the chapter, this overview will help you focus on the similarities between different spectroscopic methods of analysis. You will find it easier to understand a new analytical method when you can see its relationship to other similar methods.

What is Electromagnetic Radiation?

Electromagnetic radiation—light—is a form of energy whose behavior is described by the properties of both waves and particles. Some properties of electromagnetic radiation, such as its refraction when it passes from one medium to another (Figure 10.1.1), are explained best when we describe light as a wave. Other properties, such as absorption and emission, are better described by treating light as a particle. The exact nature of electromagnetic radiation remains unclear, as it has since the development of quantum mechanics in the first quarter of the 20th century [Home, D.; Gribbin, J. *New Scientist* 1991, 2 Nov. 30–33]. Nevertheless, this dual model of wave and particle behavior provide a useful description for electromagnetic radiation.



Figure 10.1.1 . The Golden Gate bridge as seen through rain drops. Refraction of light by the rain drops produces the distorted images. Source: Brocken Inaglory (commons. Wikipedia.org).

Wave Properties of Electromagnetic Radiation

Electromagnetic radiation consists of oscillating electric and magnetic fields that propagate through space along a linear path and with a constant velocity. In a vacuum, electromagnetic radiation travels at the speed of light, c, which is $\mathbf{2.99792 \times 10^8}$ m/s. When electromagnetic radiation moves through a medium other than a vacuum, its velocity, v, is less than the speed of light in a vacuum. The difference between v and c is sufficiently small (<0.1%) that the speed of light to three significant figures, $\mathbf{3.00 \times 10^8}$ m/s, is accurate enough for most purposes.

The oscillations in the electric field and the magnetic field are perpendicular to each other and to the direction of the wave's propagation. Figure 10.1.2 shows an example of plane-polarized electromagnetic radiation, which consists of a single oscillating electric field and a single oscillating magnetic field.

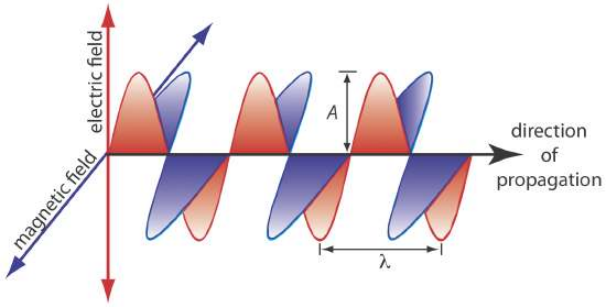


Figure 10.1.2 . Plane-polarized electromagnetic radiation showing the oscillating electric field in blue and the oscillating magnetic field in red. The radiation's amplitude, A, and its wavelength, λ, are shown. Normally, electromagnetic radiation is unpolarized, with oscillating electric and magnetic fields present in all possible planes perpendicular to the direction of propagation.

An electromagnetic wave is characterized by several fundamental properties, including its velocity, amplitude, frequency, phase angle, polarization, and direction of propagation [Ball, D. W. *Spectroscopy* **1994**, *9(5)*, 24–25]. For example, the amplitude of the oscillating electric field at any point along the propagating wave is

$$A_t = A_e \sin(2\pi\nu t + \Phi)$$

where A_t is the magnitude of the electric field at time t, A_e is the electric field's maximum ***amplitude***, ν is the wave's ***frequency***—the number of oscillations in the electric field per unit time—and Φ is a ***phase angle*** that accounts for the fact that A_t need not have a value of zero at $t = 0$. The identical equation for the magnetic field is

$$A_t = A_m \sin(2\pi\nu t + \Phi)$$

where A_m is the magnetic field's maximum amplitude.

Other properties also are useful for characterizing the wave behavior of electromagnetic radiation. The ***wavelength***, λ, is defined as the distance between successive maxima (see Figure 10.1.2). For ultraviolet and visible electromagnetic radiation the wavelength usually is expressed in nanometers (1 nm = 10^{-9} m), and for infrared radiation it is expressed in microns (1 mm = 10^{-6} m). The relationship between wavelength and frequency is

$$\lambda = \frac{c}{\nu}$$

Another unit useful unit is the ***wavenumber***, $\bar{\nu}$, which is the reciprocal of wavelength

$$\bar{\nu} = \frac{1}{\lambda}$$

Wavenumbers frequently are used to characterize infrared radiation, with the units given in cm^{-1}.

When electromagnetic radiation moves between different media—for example, when it moves from air into water—its frequency, ν, remains constant. Because its velocity depends upon the medium in which it is traveling, the electromagnetic radiation's wavelength, λ, changes. If we replace the speed of light in a vacuum, c, with its speed in the medium, v, then the wavelength is

$$\lambda = \frac{v}{\nu}$$

This change in wavelength as light passes between two media explains the refraction of electromagnetic radiation shown in Figure 10.1.1 .

Example 10.1.1

In 1817, Josef Fraunhofer studied the spectrum of solar radiation, observing a continuous spectrum with numerous dark lines. Fraunhofer labeled the most prominent of the dark lines with letters. In 1859, Gustav Kirchhoff showed that the D line in the

sun's spectrum was due to the absorption of solar radiation by sodium atoms. The wavelength of the sodium D line is 589 nm. What are the frequency and the wavenumber for this line?

Solution

The frequency and wavenumber of the sodium D line are

$$\nu = \frac{c}{\lambda} = \frac{3.00 \times 10^{8}\ \text{m/s}}{589 \times 10^{-9}\ \text{m}} = 5.09 \times 10^{14}\ \text{s}^{-1}$$

$$\overline{\nu} = \frac{1}{\lambda} = \frac{1}{589 \times 10^{-9}\ \text{m}} \times \frac{1\ \text{m}}{100\ \text{cm}} = 1.70 \times 10^{4}\ \text{cm}^{-1}$$

Exercise 10.1.1

Another historically important series of spectral lines is the Balmer series of emission lines from hydrogen. One of its lines has a wavelength of 656.3 nm. What are the frequency and the wavenumber for this line?

Answer

The frequency and wavenumber for the line are

$$\nu = \frac{c}{\lambda} = \frac{3.00 \times 10^{8}\ \text{m/s}}{656.3 \times 10^{-9}\ \text{m}} = 4.57 \times 10^{14}\ \text{s}^{-1}$$

$$\overline{\nu} = \frac{1}{\lambda} = \frac{1}{656.3 \times 10^{-9}\ \text{m}} \times \frac{1\ \text{m}}{100\ \text{cm}} = 1.524 \times 10^{4}\ \text{cm}^{-1}$$

Particle Properties of Electromagnetic Radiation

When matter absorbs electromagnetic radiation it undergoes a change in energy. The interaction between matter and electromagnetic radiation is easiest to understand if we assume that radiation consists of a beam of energetic particles called photons. When a ***photon*** is absorbed by a sample it is "destroyed" and its energy acquired by the sample [Ball, D. W. *Spectroscopy* **1994**, *9(6)* 20–21]. The energy of a photon, in joules, is related to its frequency, wavelength, and wavenumber by the following equalities

$$E = h\nu = \frac{hc}{\lambda} = hc\overline{\nu}$$

where *h* is Planck's constant, which has a value of 6.626×10^{-34} Js.

Example 10.1.2

What is the energy of a photon from the sodium D line at 589 nm?

Solution

The photon's energy is

$$E = \frac{hc}{\lambda} = \frac{\left(6.626 \times 10^{-34}\ \text{Js}\right)\left(3.00 \times 10^{8}\ \text{m/s}\right)}{589 \times 10^{-7}\ \text{m}} = 3.37 \times 10^{-19}\ \text{J}$$

Exercise 10.1.2

What is the energy of a photon for the Balmer line at a wavelength of 656.3 nm?

Answer

The photon's energy is

$$E = \frac{hc}{\lambda} = \frac{(6.626 \times 10^{-34}\ \text{Js})\,(3.00 \times 10^{8}\ \text{m/s})}{656.3 \times 10^{-9}\ \text{m}} = 3.03 \times 10^{-19}\ \text{J}$$

The Electromagnetic Spectrum

The frequency and the wavelength of electromagnetic radiation vary over many orders of magnitude. For convenience, we divide electromagnetic radiation into different regions—the ***electromagnetic spectrum***—based on the type of atomic or molecular transitions that gives rise to the absorption or emission of photons (Figure 10.1.3). The boundaries between the regions of the electromagnetic spectrum are not rigid and overlap between spectral regions is possible.

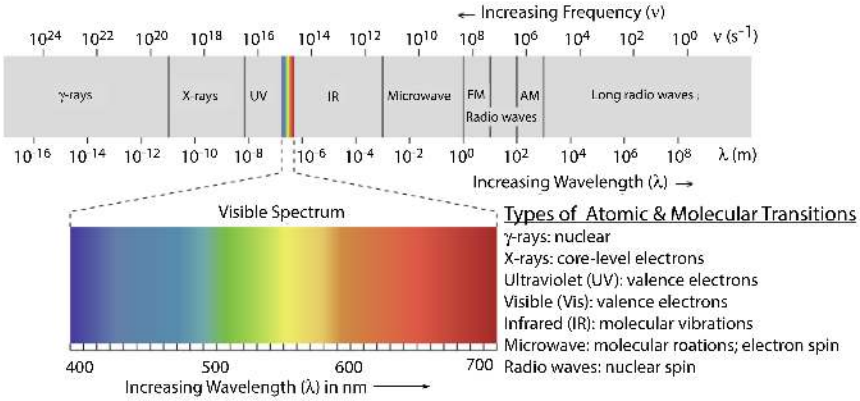


Figure 10.1.3 . The electromagnetic spectrum showing the boundaries between different regions and the type of atomic or molecular transitions responsible for the change in energy. The colored inset shows the visible spectrum. Source: modified from Zedh (www.commons.Wikipedia.org).

Photons as a Signal Source

In the previous section we defined several characteristic properties of electromagnetic radiation, including its energy, velocity, amplitude, frequency, phase angle, polarization, and direction of propagation. A spectroscopic measurement is possible only if the photon's interaction with the sample leads to a change in one or more of these characteristic properties.

We will divide spectroscopy into two broad classes of techniques. In one class of techniques there is a transfer of energy between the photon and the sample. Table 10.1.1 provides a list of several representative examples.

Table 10.1.1 . Examples of Spectroscopic Techniques That Involve an Exchange of Energy Between a Photon and the Sample

type of energy transfer	region of electromagnetic spectrum	spectroscopic technique
absorption	γ-ray	Mossbauer spectroscopy
	X-ray	X-ray absorption spectroscopy
	UV/Vis	*UV/Vis spectroscopy*
	IR	*infrared spectroscopy*
	microwave	raman spectroscopy
	radio wave	electron spin resonance nuclear magnetic resonance
emission (thermal excitation)	UV/Vis	*atomic emission spectroscopy*
photoluminescence	X-ray	X-ray fluorescence
	UV/Vis	*fluorescence spectroscopy* *phosphorescence spectroscopy* atomic fluorescence spectroscopy
chemiluminescence	UV/Vis	chemiluminescence spectroscopy
techniques discussed in this chapter are shown in *italics*		

In absorption spectroscopy a photon is absorbed by an atom or molecule, which undergoes a transition from a lower-energy state to a higher-energy, or excited state (Figure 10.1.4). The type of transition depends on the photon's energy. The electromagnetic spectrum in Figure 10.1.3 , for example, shows that absorbing a photon of visible light promotes one of the atom's or molecule's valence electrons to a higher-energy level. When an molecule absorbs infrared radiation, on the other hand, one of its chemical bonds experiences a change in vibrational energy.

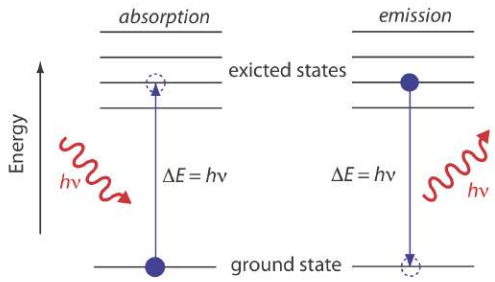


Figure 10.1.4 . A simplified energy diagram that shows the absorption and emission of a photon by an atom or a molecule. When a photon of energy $h\nu$ strikes the atom or molecule, absorption may occur if the difference in energy, ΔE, between the ground state and the excited state is equal to the photon's energy. An atom or molecule in an excited state may emit a photon and return to the ground state. The photon's energy, $h\nu$, equals the difference in energy, ΔE, between the two states.

When it absorbs electromagnetic radiation the number of photons passing through a sample decreases. The measurement of this decrease in photons, which we call ***absorbance***, is a useful analytical signal. Note that each energy level in Figure 10.1.4 has a well-defined value because each is quantized. Absorption occurs only when the photon's energy, $h\nu$, matches the difference in energy, ΔE, between two energy levels. A plot of absorbance as a function of the photon's energy is called an ***absorbance spectrum***. Figure 10.1.5 , for example, shows the absorbance spectrum of cranberry juice.

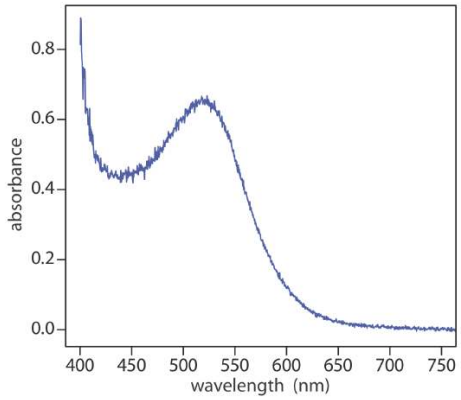


Figure 10.1.5 . Visible absorbance spectrum for cranberry juice. The anthocyanin dyes in cranberry juice absorb visible light with blue, green, and yellow wavelengths (see Figure 10.1.3). As a result, the juice appears red.

When an atom or molecule in an excited state returns to a lower energy state, the excess energy often is released as a photon, a process we call ***emission*** (Figure 10.1.4). There are several ways in which an atom or a molecule may end up in an excited state, including thermal energy, absorption of a photon, or as the result of a chemical reaction. Emission following the absorption of a photon is also called ***photoluminescence***, and that following a chemical reaction is called ***chemiluminescence***. A typical emission spectrum is shown in Figure 10.1.6 .

> Molecules also can release energy in the form of heat. We will return to this point later in the chapter.

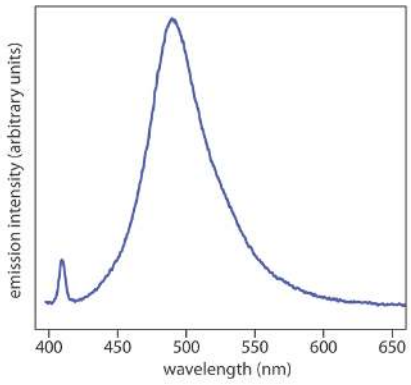


Figure 10.1.6 . Photoluminescence spectrum of the dye coumarin 343, which is incorporated in a reverse micelle suspended in cyclohexanol. The dye's absorbance spectrum (not shown) has a broad peak around 400 nm. The sharp peak at 409 nm is from the laser source used to excite coumarin 343. The broad band centered at approximately 500 nm is the dye's emission band. Because the dye absorbs blue light, a solution of coumarin 343 appears yellow in the absence of photoluminescence. Its photoluminescent emission is blue-green. Source: data from Bridget Gourley, Department of Chemistry & Biochemistry, DePauw University.

In the second broad class of spectroscopic techniques, the electromagnetic radiation undergoes a change in amplitude, phase angle, polarization, or direction of propagation as a result of its refraction, reflection, scattering, diffraction, or dispersion by the sample. Several representative spectroscopic techniques are listed in Table 10.1.2 .

Table 10.1.2 . Examples of Spectroscopic Techniques That Do Not Involve an Exchange of Energy Between a Photon and the Sample

region of electromagnetic spectrum	type of interaction	spectroscopic technique
X-ray	diffraction	X-ray diffraction
UV/Vis	refraction	refractrometry
	scattering	*nephelometry* *turbidimetry*
	dispersion	optical rotary dispersion
techniques discussed in this chapter are shown in *italics*		

Basic Components of Spectroscopic Instruments

The spectroscopic techniques in Table 10.1.1 and Table 10.1.2 use instruments that share several common basic components, including a source of energy, a means for isolating a narrow range of wavelengths, a detector for measuring the signal, and a signal processor that displays the signal in a form convenient for the analyst. In this section we introduce these basic components. Specific instrument designs are considered in later sections.

> You will find a more detailed treatment of these components in the additional resources for this chapter.

Sources of Energy

All forms of spectroscopy require a source of energy. In absorption and scattering spectroscopy this energy is supplied by photons. Emission and photoluminescence spectroscopy use thermal, radiant (photon), or chemical energy to promote the analyte to a suitable excited state.

Sources of Electromagnetic Radiation. A source of electromagnetic radiation must provide an output that is both intense and stable. Sources of electromagnetic radiation are classified as either continuum or line sources. A ***continuum source*** emits radiation over a broad range of wavelengths, with a relatively smooth variation in intensity (Figure 10.1.7). A ***line source***, on the other hand, emits radiation at selected wavelengths (Figure 10.1.8). Table 10.1.3 provides a list of the most common sources of electromagnetic radiation.

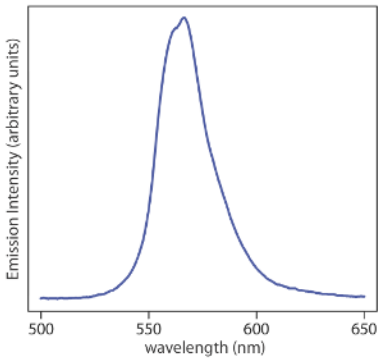


Figure 10.1.7 . Spectrum showing the emission from a green LED, which provides continuous emission over a wavelength range of approximately 530–640 nm.

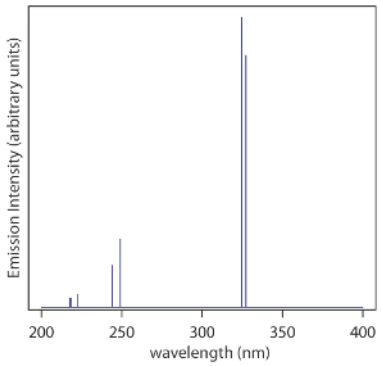


Figure 10.1.8 . Emission spectrum from a Cu hollow cathode lamp. This spectrum consists of seven distinct emission lines (the first two differ by only 0.4 nm and are not resolved at the scale shown in this spectrum). Each emission line has a width of approximately 0.01 nm at 1⁄2 of its maximum intensity.

Table 10.1.3 . Common Source of Electromagnetic Radiation

source	wavelength region	useful for...
H_2 and D_2 lamp	continuum source from 160–380 nm	molecular absorption
tungsten lamp	continuum source from 320–2400 nm	molecular absorption
Xe arc lamp	continuum source from 200–1000 nm	molecular fluorescence
nernst glower	continuum source from 0.4–20 μm	molecular absorption
globar	continuum source from 1–40 μm	molecular absorption
nichrome wire	continuum source from 0.75–20 μm	molecular absorption
hollow cathode lamp	line source in UV/Vis	atomic absorption
Hg vapor lamp	line source in UV/Vis	molecular fluorescence
laser	line source in UV/Vis/Ir	atomic and molecular absorption, fluorescence, and scattering

Sources of Thermal Radiation. The most common sources of thermal energy are flames and plasmas. A flame source uses a combustion of a fuel and an oxidant to achieve temperatures of 2000–3400 K. Plasmas, which are hot, ionized gases, provide temperatures of 6000–10000 K.

Chemical Sources of Energy. Exothermic reactions also may serve as a source of energy. In chemiluminescence the analyte is raised to a higher-energy state by means of a chemical reaction, emitting characteristic radiation when it returns to a lower-energy state. When the chemical reaction results from a biological or enzymatic reaction, the emission of radiation is called bioluminescence. Commercially available “light sticks” and the flash of light from a firefly are examples of chemiluminescence and bioluminescence.

Wavelength Selection

In Nessler’s original colorimetric method for ammonia, which was described at the beginning of the chapter, the sample and several standard solutions of ammonia are placed in separate tall, flat-bottomed tubes. As shown in Figure 10.1.9 , after adding the reagents and allowing the color to develop, the analyst evaluates the color by passing ambient light through the bottom of the tubes and looking down through the solutions. By matching the sample’s color to that of a standard, the analyst is able to determine the concentration of ammonia in the sample.

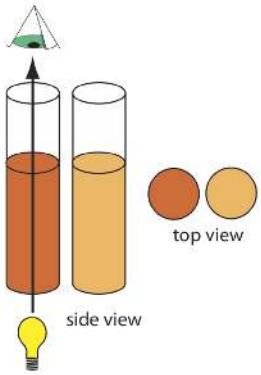


Figure 10.1.9 . Nessler's original method for comparing the color of two solutions. Natural light passes upwards through the samples and standards and the analyst views the solutions by looking down toward the light source. The top view, shown on the right, is what the analyst sees. To determine the analyte's concentration, the analyst exchanges standards until the two colors match.

In Figure 10.1.9 every wavelength of light from the source passes through the sample. This is not a problem if there is only one absorbing species in the sample. If the sample contains two components, then a quantitative analysis using Nessler's original method is impossible unless the standards contains the second component at the same concentration it has in the sample.

To overcome this problem, we want to select a wavelength that only the analyte absorbs. Unfortunately, we can not isolate a single wavelength of radiation from a continuum source, although we can narrow the range of wavelengths that reach the sample. As seen in Figure 10.1.10 , a wavelength selector always passes a narrow band of radiation characterized by a ***nominal wavelength***, an ***effective bandwidth***, and a maximum throughput of radiation. The effective bandwidth is defined as the width of the radiation at half of its maximum throughput.

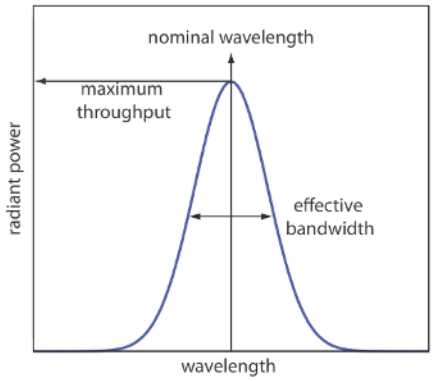


Figure 10.1.10 . Radiation exiting a wavelength selector showing the band's nominal wavelength and its effective bandwidth.

The ideal wavelength selector has a high throughput of radiation and a narrow effective bandwidth. A high throughput is desirable because the more photons that pass through the wavelength selector, the stronger the signal and the smaller the background noise. A narrow effective bandwidth provides a higher ***resolution***, with spectral features separated by more than twice the effective bandwidth being resolved. As shown in Figure 10.1.11 , these two features of a wavelength selector often are in opposition. A larger effective bandwidth favors a higher throughput of radiation, but provide less resolution. Decreasing the effective bandwidth improves resolution, but at the cost of a noisier signal [Jiang, S.; Parker, G. A. *Am. Lab.* **1981**, October, 38–43]. For a qualitative analysis, resolution usually is more important than noise and a smaller effective bandwidth is desirable; however, in a quantitative analysis less noise usually is desirable.

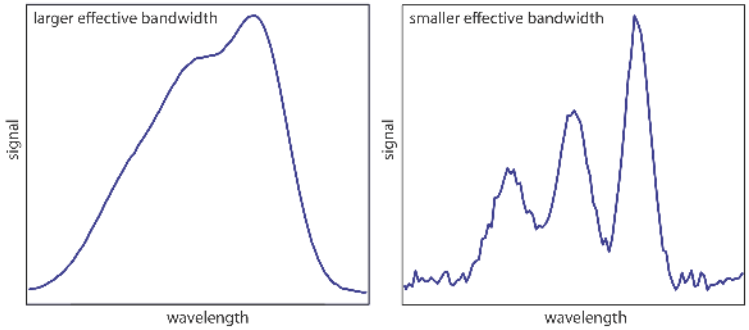


Figure 10.1.11 . Example showing the effect of the wavelength selector's effective bandwidth on resolution and noise. The spectrum with the smaller effective bandwidth (on the right) has a better resolution, allowing us to see the presence of three peaks, but at the expense of a noisier signal. The spectrum with the larger effective bandwidth (on the left) has less noise, but at the expense of less resolution between the three peaks.

Wavelength Selection Using Filters. The simplest method for isolating a narrow band of radiation is to use an absorption or interference ***filter***. Absorption filters work by selectively absorbing radiation from a narrow region of the electromagnetic spectrum. Interference filters use constructive and destructive interference to isolate a narrow range of wavelengths. A simple example of an absorption filter is a piece of colored glass. A purple filter, for example, removes the complementary color green from 500–560 nm.

Commercially available absorption filters provide effective bandwidths of 30–250 nm, although the throughput at the low end of this range often is only 10% of the source's emission intensity. Interference filters are more expensive than absorption filters, but have narrower effective bandwidths, typically 10–20 nm, with maximum throughputs of at least 40%.

Wavelength Selection Using Monochromators. A filter has one significant limitation—because a filter has a fixed nominal wavelength, if we need to make measurements at two different wavelengths, then we must use two different filters. A ***monochromator*** is an alternative method for selecting a narrow band of radiation that also allows us to continuously adjust the band's nominal wavelength.

The construction of a typical monochromator is shown in Figure 10.1.12 . Radiation from the source enters the monochromator through an entrance slit. The radiation is collected by a collimating mirror, which reflects a parallel beam of radiation to a diffraction grating. The diffraction grating is an optically reflecting surface with a large number of parallel grooves (see insert to Figure 10.1.12). The diffraction grating disperses the radiation and a second mirror focuses the radiation onto a planar surface that contains an exit slit. In some monochromators a prism is used in place of the diffraction grating.

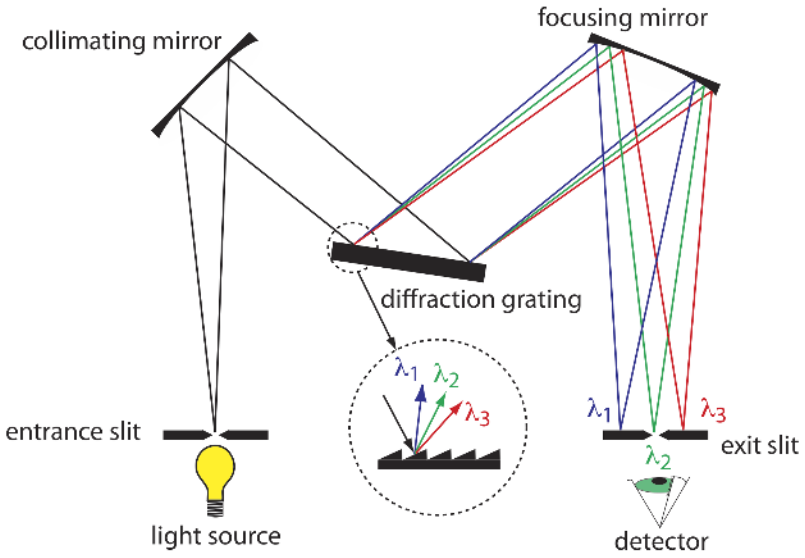


Figure 10.1.12 . Schematic diagram of a monochromator that uses a diffraction grating to disperse the radiation.

Radiation exits the monochromator and passes to the detector. As shown in Figure 10.1.12 , a monochromator converts a ***polychromatic*** source of radiation at the entrance slit to a ***monochromatic*** source of finite effective bandwidth at the exit slit. The

choice of which wavelength exits the monochromator is determined by rotating the diffraction grating. A narrower exit slit provides a smaller effective bandwidth and better resolution than does a wider exit slit, but at the cost of a smaller throughput of radiation.

> Polychromatic means many colored. Polychromatic radiation contains many different wavelengths of light. Monochromatic means one color, or one wavelength. Although the light exiting a monochromator is not strictly of a single wavelength, its narrow effective bandwidth allows us to think of it as monochromatic.

Monochromators are classified as either fixed-wavelength or scanning. In a fixed-wavelength monochromator we manually select the wavelength by rotating the grating. Normally a fixed-wavelength monochromator is used for a quantitative analysis where measurements are made at one or two wavelengths. A scanning monochromator includes a drive mechanism that continuously rotates the grating, which allows successive wavelengths of light to exit from the monochromator. A scanning monochromator is used to acquire spectra, and, when operated in a fixed-wavelength mode, for a quantitative analysis.

Interferometers. An ***interferometer*** provides an alternative approach for wavelength selection. Instead of filtering or dispersing the electromagnetic radiation, an interferometer allows source radiation of all wavelengths to reach the detector simultaneously (Figure 10.1.13). Radiation from the source is focused on a beam splitter that reflects half of the radiation to a fixed mirror and transmits the other half to a moving mirror. The radiation recombines at the beam splitter, where constructive and destructive interference determines, for each wavelength, the intensity of light that reaches the detector. As the moving mirror changes position, the wavelength of light that experiences maximum constructive interference and maximum destructive interference also changes. The signal at the detector shows intensity as a function of the moving mirror's position, expressed in units of distance or time. The result is called an ***interferogram*** or a time domain spectrum. The time domain spectrum is converted mathematically, by a process called a Fourier transform, to a spectrum (a frequency domain spectrum) that shows intensity as a function of the radiation's energy.

> The mathematical details of the Fourier transform are beyond the level of this textbook. You can consult the chapter's additional resources for additional information.

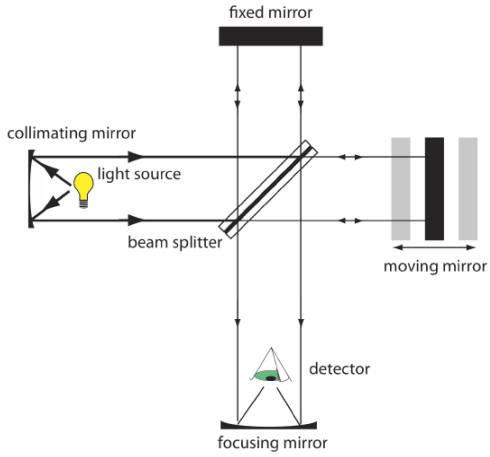


Figure 10.1.13 . Schematic diagram of an interferometers.

In comparison to a monochromator, an interferometer has two significant advantages. The first advantage, which is termed ***Jacquinot's advantage***, is the greater throughput of source radiation. Because an interferometer does not use slits and has fewer optical components from which radiation is scattered and lost, the throughput of radiation reaching the detector is $80 - 200\times$ greater than that for a monochromator. The result is less noise. The second advantage, which is called ***Fellgett's advantage***, is a savings in the time needed to obtain a spectrum. Because the detector monitors all frequencies simultaneously, a spectrum takes approximately one second to record, as compared to 10–15 minutes when using a scanning monochromator.

Detectors

In Nessler's original method for determining ammonia (Figure 10.1.9) the analyst's eye serves as the detector, matching the sample's color to that of a standard. The human eye, of course, has a poor range—it responds only to visible light—and it is not particularly sensitive or accurate. Modern detectors use a sensitive ***transducer*** to convert a signal consisting of photons into an easily measured electrical signal. Ideally the detector's signal, *S*, is a linear function of the electromagnetic radiation's power, *P*,

$$S = kP + D$$

where *k* is the detector's sensitivity, and *D* is the detector's ***dark current***, or the background current when we prevent the source's radiation from reaching the detector.

There are two broad classes of spectroscopic transducers: thermal transducers and photon transducers. Table 10.1.4 provides several representative examples of each class of transducers.

> Transducer is a general term that refers to any device that converts a chemical or a physical property into an easily measured electrical signal. The retina in your eye, for example, is a transducer that converts photons into an electrical nerve impulse; your eardrum is a transducer that converts sound waves into a different electrical nerve impulse.

Table 10.1.4 . Examples of Transducers for Spectroscopy

transducer	class	wavelength range	output signal
phototube	photon	200–1000 nm	current
photomultiplier	photon	110–1000 nm	current
Si photodiode	photon	250–1100 nm	current
photoconductor	photon	750–6000 nm	change in resistance
photovoltaic cell	photon	400–5000 nm	current or voltage
thermocouple	thermal	0.8–40 μm	voltage
thermistor	thermal	0.8–40 μm	change in resistance
pneumatic	thermal	0.8–1000 μm	membrane displacement
pyroelectric	thermal	0.3–1000 μm	current

Photon Transducers. Phototubes and photomultipliers use a photosensitive surface that absorbs radiation in the ultraviolet, visible, or near IR to produce an electrical current that is proportional to the number of photons reaching the transducer (Figure 10.1.14). Other photon detectors use a semiconductor as the photosensitive surface. When the semiconductor absorbs photons, valence electrons move to the semiconductor's conduction band, producing a measurable current. One advantage of the Si photodiode is that it is easy to miniaturize. Groups of photodiodes are gathered together in a linear array that contains 64–4096 individual photodiodes. With a width of 25 μm per diode, a linear array of 2048 photodiodes requires only 51.2 mm of linear space. By placing a ***photodiode array*** along the monochromator's focal plane, it is possible to monitor simultaneously an entire range of wavelengths.

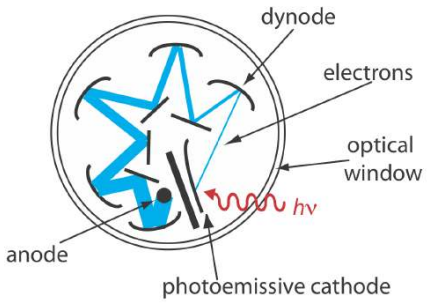


Figure 10.1.14 . Schematic of a photomultiplier. A photon strikes the photoemissive cathode producing electrons, which accelerate toward a positively charged dynode. Collision of these electrons with the dynode generates additional electrons, which accelerate toward the next dynode. A total of 10^6–10^7 electrons per photon eventually reach the anode, generating an electrical current.

Thermal Transducers. Infrared photons do not have enough energy to produce a measurable current with a photon transducer. A thermal transducer, therefore, is used for infrared spectroscopy. The absorption of infrared photons increases a thermal transducer's temperature, changing one or more of its characteristic properties. A pneumatic transducer, for example, is a small tube of xenon gas with an IR transparent window at one end and a flexible membrane at the other end. Photons enter the tube and are absorbed by a blackened surface, increasing the temperature of the gas. As the temperature inside the tube fluctuates, the gas expands and contracts and the flexible membrane moves in and out. Monitoring the membrane's displacement produces an electrical signal.

Signal Processors

A transducer's electrical signal is sent to a ***signal processor*** where it is displayed in a form that is more convenient for the analyst. Examples of signal processors include analog or digital meters, recorders, and computers equipped with digital acquisition boards. A signal processor also is used to calibrate the detector's response, to amplify the transducer's signal, to remove noise by filtering, or to mathematically transform the signal.

> If the retina in your eye and the eardrum in your ear are transducers, then your brain is the signal processor.

This page titled 1.1: Overview of Spectroscopy is shared under a CC BY-NC-SA 4.0 license and was authored, remixed, and/or curated by David Harvey.

- **10.1: Overview of Spectroscopy** by David Harvey is licensed CC BY-NC-SA 4.0.

1.2: Spectroscopy Based on Absorption

In absorption spectroscopy a beam of electromagnetic radiation passes through a sample. Much of the radiation passes through the sample without a loss in intensity. At selected wavelengths, however, the radiation's intensity is attenuated. This process of attenuation is called absorption.

Absorption Spectra

There are two general requirements for an analyte's absorption of electromagnetic radiation. First, there must be a mechanism by which the radiation's electric field or magnetic field interacts with the analyte. For ultraviolet and visible radiation, absorption of a photon changes the energy of the analyte's valence electrons. A bond's vibrational energy is altered by the absorption of infrared radiation.

> Figure 10.1.3 provides a list of the types of atomic and molecular transitions associated with different types of electromagnetic radiation.

The second requirement is that the photon's energy, $h\nu$, must exactly equal the difference in energy, ΔE, between two of the analyte's quantized energy states. Figure 10.1.4 shows a simplified view of a photon's absorption, which is useful because it emphasizes that the photon's energy must match the difference in energy between a lower-energy state and a higher-energy state. What is missing, however, is information about what types of energy states are involved, which transitions between energy states are likely to occur, and the appearance of the resulting spectrum.

We can use the energy level diagram in Figure 10.2.1 to explain an absorbance spectrum. The lines labeled E_0 and E_1 represent the analyte's ground (lowest) electronic state and its first electronic excited state. Superimposed on each electronic energy level is a series of lines representing vibrational energy levels.

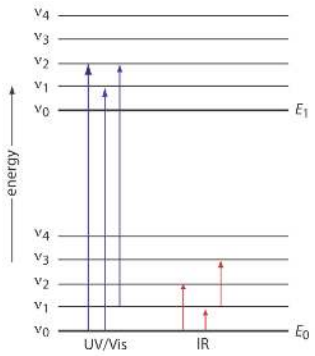


Figure 10.2.1 . Diagram showing two electronic energy levels (E_0 and E_1), each with five vibrational energy levels ν_{0-4}. Absorption of ultraviolet and visible radiation (shown by the blue arrows) leads to a change in the analyte's electronic energy levels and, possibly, a change in vibrational energy as well. A change in vibrational energy without a change in electronic energy levels occurs with the absorption of infrared radiation (shown by the red arrows).

Infrared Spectra for Molecules and Polyatomic Ions

The energy of infrared radiation produces a change in a molecule's or a polyatomic ion's vibrational energy, but is not sufficient to effect a change in its electronic energy. As shown in Figure 10.2.1 , vibrational energy levels are quantized; that is, a molecule or polyatomic ion has only certain, discrete vibrational energies. The energy for an allowed vibrational mode, E_ν, is

$$E_\nu = \nu + \frac{1}{2}h\nu_0$$

where ν is the vibrational quantum number, which has values of 0, 1, 2, ..., and ν_0 is the bond's fundamental vibrational frequency. The value of ν_0, which is determined by the bond's strength and by the mass at each end of the bond, is a characteristic property of a bond. For example, a carbon-carbon single bond (C–C) absorbs infrared radiation at a lower energy than a carbon-carbon double bond (C=C) because a single bond is weaker than a double bond.

At room temperature most molecules are in their ground vibrational state ($\nu = 0$) . A transition from the ground vibrational state to the first vibrational excited state ($\nu = 1$) requires absorption of a photon with an energy of $h\nu_0$. Transitions in which $\Delta\nu = \pm 1$ give rise to the fundamental absorption lines. Weaker absorption lines, called overtones, result from transitions in which $\Delta\nu$ is ±2 or ±3. The number of possible normal vibrational modes for a linear molecule is $3N - 5$, and for a non-linear molecule is $3N - 6$, where N is the number of atoms in the molecule. Not surprisingly, infrared spectra often show a considerable number of absorption bands. Even a relatively simple molecule, such as ethanol (C_2H_6O), for example, has $3 \times 9 - 6$, or 21 possible normal modes of vibration, although not all of these vibrational modes give rise to an absorption. The IR spectrum for ethanol is shown in Figure 10.2.2 .

Why does a non-linear molecule have $3N - 6$ vibrational modes? Consider a molecule of methane, CH_4. Each of methane's five atoms can move in one of three directions (x, y, and z) for a total of $5 \times 3 = 15$ different ways in which the molecule's atoms can move. A molecule can move in three ways: it can move from one place to another, which we call translational motion; it can rotate around an axis, which we call rotational motion; and its bonds can stretch and bend, which we call vibrational motion. Because the entire molecule can move in the x, y, and z directions, three of methane's 15 different motions are translational. In addition, the molecule can rotate about its x, y, and z axes, accounting for three additional forms of motion. This leaves $15 - 3 - 3 = 9$ vibrational modes. A linear molecule, such as CO_2, has $3N - 5$ vibrational modes because it can rotate around only two axes.

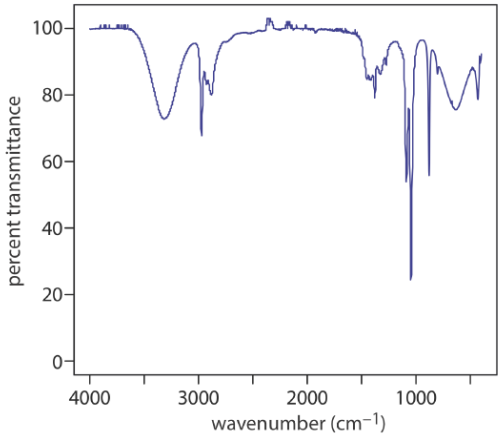


Figure 10.2.2 . Infrared spectrum of ethanol.

UV/Vis Spectra for Molecules and Ions

The valence electrons in organic molecules and polyatomic ions, such as CO_3^{2-}, occupy quantized sigma bonding (σ), pi bonding (π), and non-bonding (n) molecular orbitals (MOs). Unoccupied sigma antibonding (σ^*) and pi antibonding (π^*) molecular orbitals are slightly higher in energy. Because the difference in energy between the highest-energy occupied MOs and the lowest-energy unoccupied MOs corresponds to ultraviolet and visible radiation, absorption of a photon is possible.

Four types of transitions between quantized energy levels account for most molecular UV/Vis spectra. Table 10.2.1 lists the approximate wavelength ranges for these transitions, as well as a partial list of bonds, functional groups, or molecules responsible for these transitions. Of these transitions, the most important are $n \rightarrow \pi^*$ and $\pi \rightarrow \pi^*$ because they involve important functional groups that are characteristic of many analytes and because the wavelengths are easily accessible. The bonds and functional groups that give rise to the absorption of ultraviolet and visible radiation are called ***chromophores***.

Table 10.2.1 . Electronic Transitions Involving n, σ, and π Molecular Orbitals

transition	wavelength range	examples
$\sigma \rightarrow \sigma^*$	<200 nm	C—C, C—H
$n \rightarrow \sigma^*$	160–260 nm	H_2O, CH_3OH, CH_3Cl
$\pi \rightarrow \pi^*$	200–500 nm	C=C, C=O, C=N, C≡C
$n \rightarrow \pi^*$	250–600 nm	C=O, C=N, N=N, N=O

Many transition metal ions, such as Cu^{2+} and Co^{2+}, form colorful solutions because the metal ion absorbs visible light. The transitions that give rise to this absorption are valence electrons in the metal ion's *d*-orbitals. For a free metal ion, the five *d*-orbitals are of equal energy. In the presence of a complexing ligand or solvent molecule, however, the *d*-orbitals split into two or more groups that differ in energy. For example, in an octahedral complex of $\mathbf{Cu(H_2O)_6^{2+}}$ the six water molecules perturb the *d*-orbitals into the two groups shown in Figure 10.2.3 . The resulting $d \rightarrow d$ transitions for transition metal ions are relatively weak.

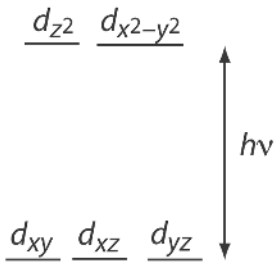


Figure 10.2.3 . Splitting of the *d*-orbitals in an octahedral field.

A more important source of UV/Vis absorption for inorganic metal–ligand complexes is charge transfer, in which absorption of a photon produces an excited state in which there is transfer of an electron from the metal, *M*, to the ligand, *L*.

$$M - L + h\nu \rightarrow (M^+ - L^-)^*$$

Charge-transfer absorption is important because it produces very large absorbances. One important example of a charge-transfer complex is that of *o*-phenanthroline with Fe^{2+}, the UV/Vis spectrum for which is shown in Figure 10.2.4 . Charge-transfer absorption in which an electron moves from the ligand to the metal also is possible.

> Why is a larger absorbance desirable? An analytical method is more sensitive if a smaller concentration of analyte gives a larger signal.

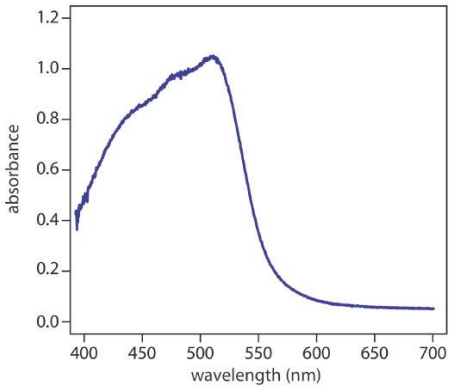


Figure 10.2.4 . UV/Vis spectrum for the metal–ligand complex $\mathbf{Fe(phen)_3^{2+}}$, where phen is the ligand *o*-phenanthroline.

Comparing the IR spectrum in Figure 10.2.2 to the UV/Vis spectrum in Figure 10.2.4 shows us that UV/Vis absorption bands are often significantly broader than those for IR absorption. We can use Figure 10.2.1 to explain why this is true. When a species

absorbs UV/Vis radiation, the transition between electronic energy levels may also include a transition between vibrational energy levels. The result is a number of closely spaced absorption bands that merge together to form a single broad absorption band.

UV/Vis Spectra for Atoms

The energy of ultraviolet and visible electromagnetic radiation is sufficient to cause a change in an atom's valence electron configuration. Sodium, for example, has a single valence electron in its 3*s* atomic orbital. As shown in Figure 10.2.5 , unoccupied, higher energy atomic orbitals also exist.

> The valence shell energy level diagram in Figure 10.2.5 might strike you as odd because it shows that the 3*p* orbitals are split into two groups of slightly different energy. The reasons for this splitting are unimportant in the context of our treatment of atomic absorption. For further information about the reasons for this splitting, consult the chapter's additional resources.

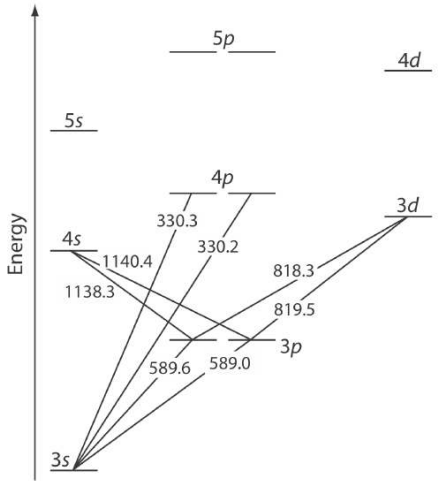


Figure 10.2.5 . Valence shell energy level diagram for sodium. The wavelengths (in wavenumbers) corresponding to several transitions are shown.

Absorption of a photon is accompanied by the excitation of an electron from a lower-energy atomic orbital to an atomic orbital of higher energy. Not all possible transitions between atomic orbitals are allowed. For sodium the only allowed transitions are those in which there is a change of ±1 in the orbital quantum number (l); thus transitions from $s \rightarrow p$ orbitals are allowed, but transitions from $s \rightarrow s$ and from $s \rightarrow d$ orbitals are forbidden.

The atomic absorption spectrum for Na is shown in Figure 10.2.6 , and is typical of that found for most atoms. The most obvious feature of this spectrum is that it consists of a small number of discrete absorption lines that correspond to transitions between the ground state (the 3*s* atomic orbital) and the 3*p* and the 4*p* atomic orbitals. Absorption from excited states, such as the $3p \rightarrow 4s$ and the $3p \rightarrow 3d$ transitions included in Figure 10.2.5 , are too weak to detect. Because an excited state's lifetime is short—an excited state atom typically returns to a lower energy state in 10^{-7} to 10^{-8} seconds—an atom in the exited state is likely to return to the ground state before it has an opportunity to absorb a photon.

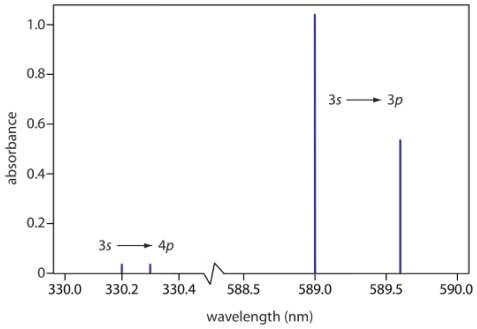


Figure 10.2.6 . Atomic absorption spectrum for sodium. Note that the scale on the *x*-axis includes a break.

Another feature of the atomic absorption spectrum in Figure 10.2.6 is the narrow width of the absorption lines, which is a consequence of the fixed difference in energy between the ground state and the excited state, and the lack of vibrational and rotational energy levels. Natural line widths for atomic absorption, which are governed by the uncertainty principle, are approximately 10^{-5} nm. Other contributions to broadening increase this line width to approximately 10^{-3} nm.

Transmittance and Absorbance

As light passes through a sample, its power decreases as some of it is absorbed. This attenuation of radiation is described quantitatively by two separate, but related terms: transmittance and absorbance. As shown in Figure 10.2.7 a, transmittance is the ratio of the source radiation's power as it exits the sample, P_T, to that incident on the sample, P_0.

$$T = \frac{P_T}{P_0} \tag{1.2.1}$$

Multiplying the transmittance by 100 gives the percent transmittance, $\%T$, which varies between 100% (no absorption) and 0% (complete absorption). All methods of detecting photons—including the human eye and modern photoelectric transducers—measure the transmittance of electromagnetic radiation.

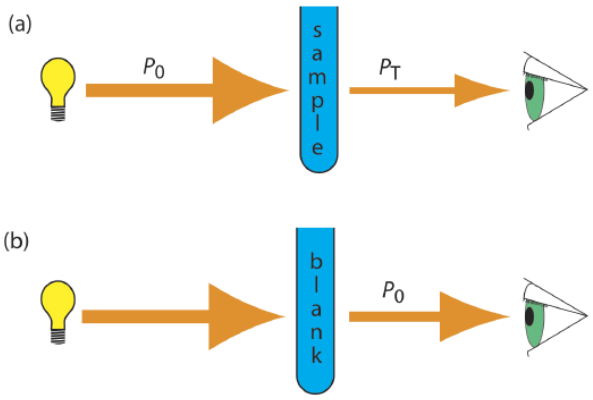


Figure 10.2.7 . (a) Schematic diagram showing the attenuation of radiation passing through a sample; P_0 is the source's radiant power and P_T is the radiant power transmitted by the sample. (b) Schematic diagram showing how we redefine P_0 as the radiant power transmitted by the blank. Redefining P_0 in this way corrects the transmittance in (a) for the loss of radiation due to scattering, reflection, absorption by the sample's container, and absorption by the sample's matrix.

Equation 1.2.1 does not distinguish between different mechanisms that prevent a photon emitted by the source from reaching the detector. In addition to absorption by the analyte, several additional phenomena contribute to the attenuation of radiation, including reflection and absorption by the sample's container, absorption by other components in the sample's matrix, and the scattering of radiation. To compensate for this loss of the radiation's power, we use a method blank. As shown in Figure 10.2.7 b, we redefine P_0 as the power exiting the method blank.

An alternative method for expressing the attenuation of electromagnetic radiation is absorbance, A, which we define as

$$A = -\log T = -\log \frac{P_T}{P_0} \tag{1.2.2}$$

Absorbance is the more common unit for expressing the attenuation of radiation because it is a linear function of the analyte's concentration.

> We will show that this is true in the next section when we introduce Beer's law.

Example 10.2.1

A sample has a percent transmittance of 50%. What is its absorbance?

Solution

A percent transmittance of 50.0% is the same as a transmittance of 0.500. Substituting into Equation 1.2.2 gives

$$A = -\log T = -\log(0.500) = 0.301$$

Exercise 10.2.1

What is the %T for a sample if its absorbance is 1.27?

Answer

To find the transmittance, T, we begin by noting that

$$A = 1.27 = -\log T$$

Solving for T

$$-1.27 = \log T$$
$$10^{-1.27} = T$$

gives a transmittance of 0.054, or a %T of 5.4%.

Equation 1.2.1 has an important consequence for atomic absorption. As we learned from Figure 10.2.6 , atomic absorption lines are very narrow. Even with a high quality monochromator, the effective bandwidth for a continuum source is $100 - 1000\times$ greater than the width of an atomic absorption line. As a result, little radiation from a continuum source is absorbed when it passes through a sample of atoms; because $P_0 \approx P_T$ the measured absorbance effectively is zero. For this reason, atomic absorption requires that we use a line source instead of a continuum source.

Absorbance and Concentration: Beer's Law

When monochromatic electromagnetic radiation passes through an infinitesimally thin layer of sample of thickness dx, it experiences a decrease in its power of dP (Figure 10.2.8).

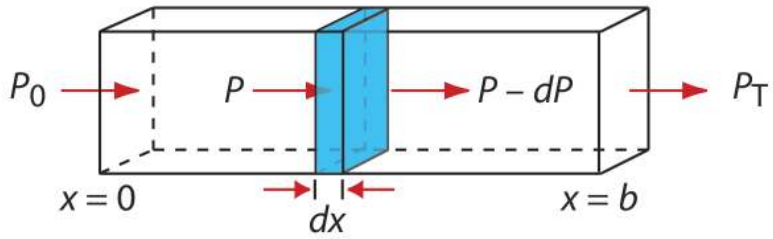


Figure 10.2.8 . Factors used to derive the Beer's law.

This fractional decrease in power is proportional to the sample's thickness and to the analyte's concentration, C; thus

$$-\frac{dP}{P} = \alpha C dx \tag{1.2.3}$$

where P is the power incident on the thin layer of sample and α is a proportionality constant. Integrating the left side of Equation 1.2.3 over the sample's full thickness

$$-\int_{P=P_0}^{P=P_t} \frac{dP}{P} = \alpha C \int_{x=0}^{x=b} dx$$

$$\ln \frac{P_0}{P_T} = \alpha b C$$

converting from ln to log, and substituting into Equation 1.2.2, gives

$$A = abC \tag{1.2.4}$$

where a is the analyte's ***absorptivity*** with units of cm^{-1} $conc^{-1}$. If we express the concentration using molarity, then we replace a with the ***molar absorptivity***, ε, which has units of cm^{-1} M^{-1}.

$$A = \varepsilon b C \tag{1.2.5}$$

The absorptivity and the molar absorptivity are proportional to the probability that the analyte absorbs a photon of a given energy. As a result, values for both a and ε depend on the wavelength of the absorbed photon.

Example 10.2.2

A 5.00×10^{-4} M solution of analyte is placed in a sample cell that has a pathlength of 1.00 cm. At a wavelength of 490 nm, the solution's absorbance is 0.338. What is the analyte's molar absorptivity at this wavelength?

Solution

Solving Equation 1.2.5 for ϵ and making appropriate substitutions gives

$$\varepsilon = \frac{A}{bC} = \frac{0.338}{(1.00 \text{ cm})\left(5.00 \times 10^{-4} \text{ M}\right)} = 676 \text{ cm}^{-1} \text{ M}^{-1}$$

Exercise 10.2.2

A solution of the analyte from Example 10.2.2 has an absorbance of 0.228 in a 1.00-cm sample cell. What is the analyte's concentration?

Answer

Making appropriate substitutions into Beer's law

$$A = 0.228 = \varepsilon b C = \left(676 \text{ M}^{-1} \text{ cm}^{-1}\right)(1 \text{ cm}) C$$

and solving for C gives a concentration of 3.37×10^{-4} M.

Equation 1.2.4 and Equation 1.2.5, which establish the linear relationship between absorbance and concentration, are known as Beer's law. Calibration curves based on Beer's law are common in quantitative analyses.

As is often the case, the formulation of a law is more complicated than its name suggests. This is the case, for example, with Beer's law, which also is known as the Beer-Lambert law or the Beer-Lambert-Bouguer law. Pierre Bouguer, in 1729, and Johann Lambert, in 1760, noted that the transmittance of light decreases exponentially with an increase in the sample's thickness.

$$T \propto e^{-b}$$

Later, in 1852, August Beer noted that the transmittance of light decreases exponentially as the concentration of the absorbing species increases.

$$T \propto e^{-C}$$

Together, and when written in terms of absorbance instead of transmittance, these two relationships make up what we know as Beer's law.

Beer's Law and Multicomponent Samples

We can extend Beer's law to a sample that contains several absorbing components. If there are no interactions between the components, then the individual absorbances, A_i, are additive. For a two-component mixture of analyte's X and Y, the total absorbance, A_{tot}, is

$$A_{tot} = A_X + A_Y = \varepsilon_X b C_X + \varepsilon_Y b C_Y$$

Generalizing, the absorbance for a mixture of n components, A_{mix}, is

$$A_{mix} = \sum_{i=1}^{n} A_i = \sum_{i=1}^{n} \varepsilon_i b C_i \tag{1.2.6}$$

Limitations to Beer's Law

Beer's law suggests that a plot of absorbance vs. concentration—we will call this a Beer's law plot—is a straight line with a *y*-intercept of zero and a slope of *ab* or εb. In some cases a Beer's law plot deviates from this ideal behavior (see Figure 10.2.9), and such deviations from linearity are divided into three categories: fundamental, chemical, and instrumental.

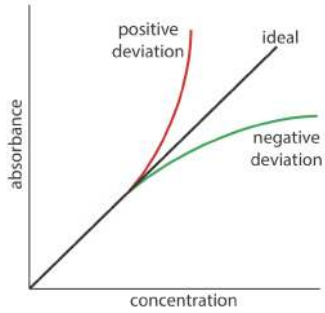


Figure 10.2.9 . Plots of absorbance vs. concentration showing positive and negative deviations from the ideal Beer's law relationship, which is a straight line.

Fundamental Limitations to Beer's Law

Beer's law is a limiting law that is valid only for low concentrations of analyte. There are two contributions to this fundamental limitation to Beer's law. At higher concentrations the individual particles of analyte no longer are independent of each other. The resulting interaction between particles of analyte may change the analyte's absorptivity. A second contribution is that an analyte's absorptivity depends on the solution's refractive index. Because a solution's refractive index varies with the analyte's concentration, values of *a* and ε may change. For sufficiently low concentrations of analyte, the refractive index essentially is constant and a Beer's law plot is linear.

Chemical Limitations to Beer's Law

A chemical deviation from Beer's law may occur if the analyte is involved in an equilibrium reaction. Consider, for example, the weak acid, HA. To construct a Beer's law plot we prepare a series of standard solutions—each of which contains a known total concentration of HA—and then measure each solution's absorbance at the same wavelength. Because HA is a weak acid, it is in equilibrium with its conjugate weak base, A^-.

> In the equations that follow, the conjugate weak base A^- is written as A as it is easy to mistake the symbol for anionic charge as a minus sign.

$$HA(aq) + H_2O(l) \rightleftharpoons H_3O^+(aq) + A^-(aq)$$

If both HA and A^- absorb at the selected wavelength, then Beer's law is

$$A = \varepsilon_{HA} b C_{HA} + \varepsilon_A b C_A \tag{1.2.7}$$

Because the weak acid's total concentration, C_{total}, is

$$C_{total} = C_{HA} + C_A$$

we can write the concentrations of HA and A^- as

$$C_{HA} = \alpha_{HA} C_{total} \tag{1.2.8}$$

$$C_A = (1 - \alpha_{HA}) C_{total} \tag{1.2.9}$$

where α_{HA} is the fraction of weak acid present as HA. Substituting Equation 1.2.8 and Equation 1.2.9 into Equation 1.2.7 and rearranging, gives

$$A = (\varepsilon_{HA}\alpha_{HA} + \varepsilon_{A} - \varepsilon_{A}\alpha_{A})\, bC_{total} \tag{1.2.10}$$

To obtain a linear Beer's law plot, we must satisfy one of two conditions. If ε_{HA} and ε_{A} have the same value at the selected wavelength, then Equation 1.2.10 simplifies to

$$A = \varepsilon_{A} bC_{total} = \varepsilon_{HA} bC_{total}$$

Alternatively, if α_{HA} has the same value for all standard solutions, then each term within the parentheses of Equation 1.2.10 is constant—which we replace with *k*—and a linear calibration curve is obtained at any wavelength.

$$A = kbC_{total}$$

Because HA is a weak acid, the value of α_{HA} varies with pH. To hold α_{HA} constant we buffer each standard solution to the same pH. Depending on the relative values of α_{HA} and α_{A}, the calibration curve has a positive or a negative deviation from Beer's law if we do not buffer the standards to the same pH.

Instrumental Limitations to Beer's Law

There are two principal instrumental limitations to Beer's law. The first limitation is that Beer's law assumes that radiation reaching the sample is of a single wavelength—that is, it assumes a purely monochromatic source of radiation. As shown in Figure 10.1.10, even the best wavelength selector passes radiation with a small, but finite effective bandwidth. Polychromatic radiation always gives a negative deviation from Beer's law, but the effect is smaller if the value of ε essentially is constant over the wavelength range passed by the wavelength selector. For this reason, as shown in Figure 10.2.10 , it is better to make absorbance measurements at the top of a broad absorption peak. In addition, the deviation from Beer's law is less serious if the source's effective bandwidth is less than one-tenth of the absorbing species' natural bandwidth [(a) Strong, F. C., III *Anal. Chem.* **1984**, *56*, 16A–34A; Gilbert, D. D. *J. Chem. Educ.* **1991**, *68*, A278–A281]. When measurements must be made on a slope, linearity is improved by using a narrower effective bandwidth.

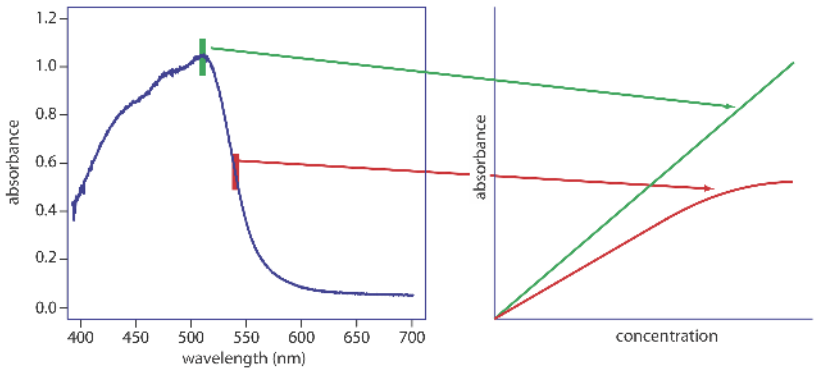


Figure 10.2.10 . Effect of wavelength selection on the linearity of a Beer's law plot. Another reason for measuring absorbance at the top of an absorbance peak is that it provides for a more sensitive analysis. Note that the green Beer's law plot has a steeper slope—and, therefore, a greater sensitivity—than the red Beer's law plot. A Beer's law plot, of course, is equivalent to a calibration curve.

Stray radiation is the second contribution to instrumental deviations from Beer's law. Stray radiation arises from imperfections in the wavelength selector that allow light to enter the instrument and to reach the detector without passing through the sample. Stray radiation adds an additional contribution, P_{stray}, to the radiant power that reaches the detector; thus

$$A = -\log \frac{P_T + P_{stray}}{P_0 + P_{stray}}$$

For a small concentration of analyte, P_{stray} is significantly smaller than P_0 and P_T, and the absorbance is unaffected by the stray radiation. For higher concentrations of analyte, less light passes through the sample and P_T and P_{stray} become similar in magnitude. This results is an absorbance that is smaller than expected, and a negative deviation from Beer's law.

This page titled 1.2: Spectroscopy Based on Absorption is shared under a CC BY-NC-SA 4.0 license and was authored, remixed, and/or curated by David Harvey.

- **10.2: Spectroscopy Based on Absorption** by David Harvey is licensed CC BY-NC-SA 4.0.

https://chem.libretexts.org/@go/page/379416

1.3: UV/Vis and IR Spectroscopy

In Figure 10.1.9 we examined Nessler's original method for matching the color of a sample to the color of a standard. Matching colors is a labor intensive process for the analyst and, not surprisingly, spectroscopic methods of analysis were slow to find favor. The 1930s and 1940s saw the introduction of photoelectric transducers for ultraviolet and visible radiation, and thermocouples for infrared radiation. As a result, modern instrumentation for absorption spectroscopy routinely became available in the 1940s—further progress has been rapid ever since.

Instrumentation

Frequently an analyst must select from among several instruments of different design, the one instrument best suited for a particular analysis. In this section we examine several different instruments for molecular absorption spectroscopy, with an emphasis on their advantages and limitations. Methods of sample introduction also are covered in this section.

Instrument Designs for Molecular UV/Vis Absorption

Filter Photometer. The simplest instrument for molecular UV/Vis absorption is a ***filter photometer*** (Figure 10.3.1), which uses an absorption or interference filter to isolate a band of radiation. The filter is placed between the source and the sample to prevent the sample from decomposing when exposed to higher energy radiation. A filter photometer has a single optical path between the source and detector, and is called a ***single-beam*** instrument. The instrument is calibrated to 0% T while using a shutter to block the source radiation from the detector. After opening the shutter, the instrument is calibrated to 100% T using an appropriate blank. The blank is then replaced with the sample and its transmittance measured. Because the source's incident power and the sensitivity of the detector vary with wavelength, the photometer is recalibrated whenever the filter is changed. Photometers have the advantage of being relatively inexpensive, rugged, and easy to maintain. Another advantage of a photometer is its portability, making it easy to take into the field. Disadvantages of a photometer include the inability to record an absorption spectrum and the source's relatively large effective bandwidth, which limits the calibration curve's linearity.

> The percent transmittance varies between 0% and 100%. As we learned from Figure 10.2.7, we use a blank to determine P_0, which corresponds to 100%T. Even in the absence of light the detector records a signal. Closing the shutter allows us to assign 0%T to this signal. Together, setting 0% T and 100%T calibrates the instrument. The amount of light that passes through a sample produces a signal that is greater than or equal to 0%T and smaller than or equal to 100%T.

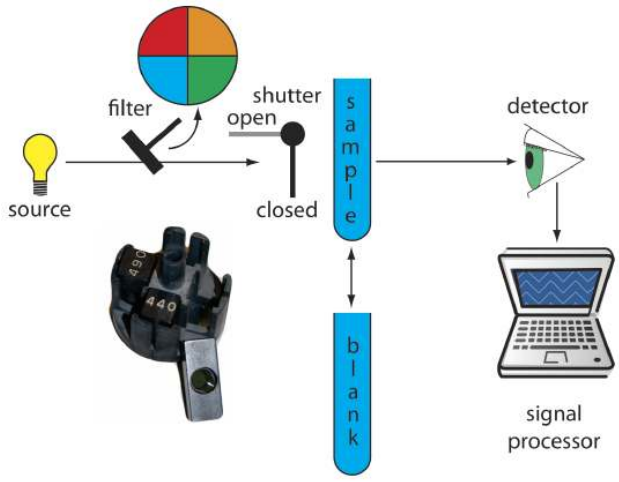


Figure 10.3.1 . Schematic diagram of a filter photometer. The analyst either inserts a removable filter or the filters are placed in a carousel, an example of which is shown in the photographic inset. The analyst selects a filter by rotating it into place.

Single-Beam Spectrophotometer. An instrument that uses a monochromator for wavelength selection is called a ***spectrophotometer***. The simplest spectrophotometer is a single-beam instrument equipped with a fixed-wavelength monochromator (Figure 10.3.2). Single-beam spectrophotometers are calibrated and used in the same manner as a photometer. One example of a single-beam spectrophotometer is Thermo Scientific's Spectronic 20D+, which is shown in the photographic insert to Figure 10.3.2 . The Spectronic 20D+ has a wavelength range of 340–625 nm (950 nm when using a red-sensitive detector), and a fixed effective bandwidth of 20 nm. Battery-operated, hand-held single-beam spectrophotometers are available, which are easy to transport into the field. Other single-beam spectrophotometers also are available with effective bandwidths of 2–8 nm. Fixed wavelength single-beam spectrophotometers are not practical for recording spectra because manually adjusting the wavelength and recalibrating the spectrophotometer is awkward and time-consuming. The accuracy of a single-beam spectrophotometer is limited by the stability of its source and detector over time.

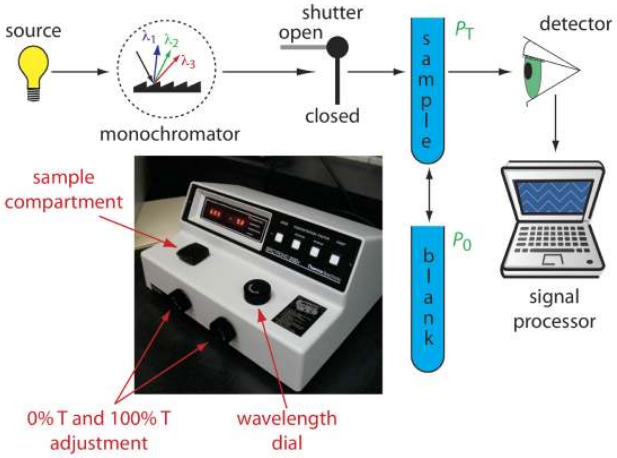


Figure 10.3.2 . Schematic diagram of a fixed-wavelength, single-beam spectrophotometer. The photographic inset shows a typical instrument. The shutter remains closed until the sample or blank is placed in the sample compartment. The analyst manually selects the wavelength by adjusting the wavelength dial. Inset photo modified from: Adi (www.commons.Wikipedia.org).

Double-Beam Spectrophotometer. The limitations of a fixed-wavelength, single-beam spectrophotometer is minimized by using a ***double-beam*** spectrophotometer (Figure 10.3.3). A chopper controls the radiation's path, alternating it between the sample, the blank, and a shutter. The signal processor uses the chopper's speed of rotation to resolve the signal that reaches the detector into the transmission of the blank, P_0, and the sample, P_T. By including an opaque surface as a shutter, it also is possible to continuously adjust 0%T. The effective bandwidth of a double-beam spectrophotometer is controlled by adjusting the monochromator's entrance and exit slits. Effective bandwidths of 0.2–3.0 nm are common. A scanning monochromator allows for the automated recording of spectra. Double-beam instruments are more versatile than single-beam instruments, being useful for both quantitative and qualitative analyses, but also are more expensive and not particularly portable.

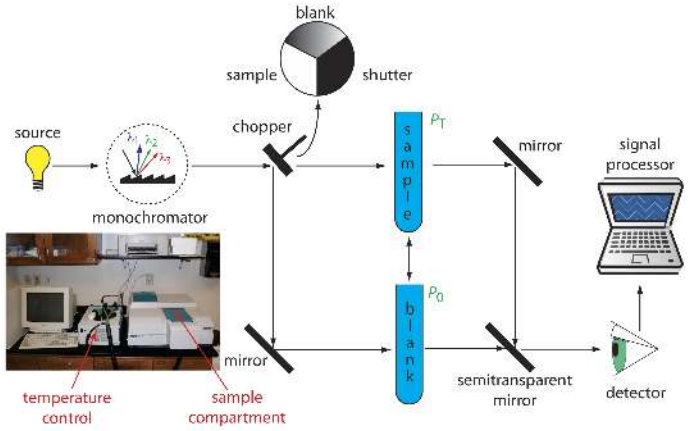


Figure 10.3.3 . Schematic diagram of a scanning, double-beam spectrophotometer. A chopper directs the source's radiation, using a transparent window to pass radiation to the sample and a mirror to reflect radiation to the blank. The chopper's opaque surface serves as a shutter, which allows for a constant adjustment of the spectrophotometer's 0%T. The photographic insert shows a typical instrument. The module in the middle of the photo is a temperature control unit that makes it possible to heat or cool the sample to a constant temperature.

Diode Array Spectrometer. An instrument with a single detector can monitor only one wavelength at a time. If we replace a single photomultiplier with an array of photodiodes, we can use the resulting detector to record a full spectrum in as little as 0.1 s. In a diode array spectrometer the source radiation passes through the sample and is dispersed by a grating (Figure 10.3.4). The photodiode array detector is situated at the grating's focal plane, with each diode recording the radiant power over a narrow range of wavelengths. Because we replace a full monochromator with just a grating, a diode array spectrometer is small and compact.

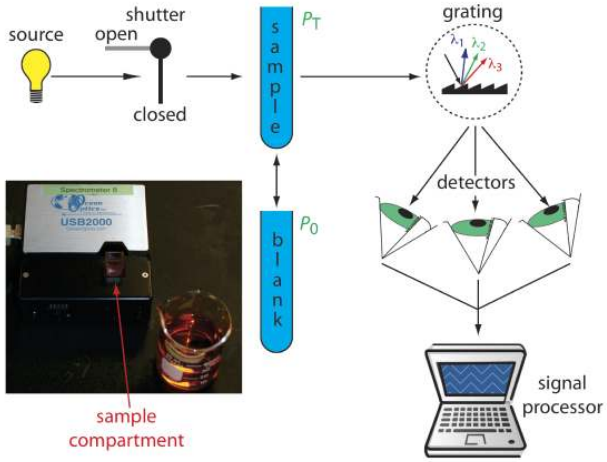


Figure 10.3.4 . Schematic diagram of a diode array spectrophotometer. The photographic insert shows a typical instrument. Note that the 50-mL beaker provides a sense of scale. Because the spectrometer is small and compact, it is easy to transport into the field.

One advantage of a diode array spectrometer is the speed of data acquisition, which allows us to collect multiple spectra for a single sample. Individual spectra are added and averaged to obtain the final spectrum. This ***signal averaging*** improves a spectrum's signal-to-noise ratio. If we add together n spectra, the sum of the signal at any point, x, increases as nS_x, where S_x is the signal. The noise at any point, N_x, is a random event, which increases as $\sqrt{n}N_x$ when we add together n spectra. The ***signal-to-noise ratio*** after n scans, $(S/N)_n$ is

$$\left(\frac{S}{N}\right)_n = \frac{nS_x}{\sqrt{n}N_x} = \sqrt{n}\frac{S_x}{N_x}$$

where S_x/N_x is the signal-to-noise ratio for a single scan. The impact of signal averaging is shown in Figure 10.3.5 . The first spectrum shows the signal after one scan, which consists of a single, noisy peak. Signal averaging using 4 scans and 16 scans decreases the noise and improves the signal-to-noise ratio. One disadvantage of a photodiode array is that the effective bandwidth per diode is roughly an order of magnitude larger than that for a high quality monochromator.

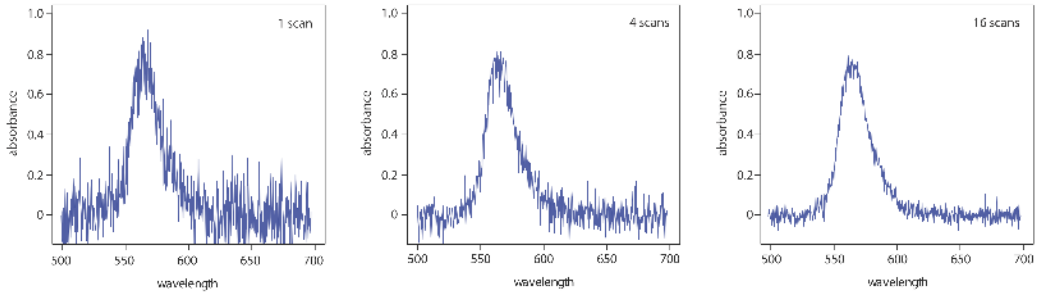


Figure 10.3.5 . Effect of signal averaging on a spectrum's signal-to-noise ratio. From top to bottom: spectrum for a single scan; average spectrum after four scans; and average spectrum after adding 16 scans.

For more details on signals and noise, see Introduction to Signals and Noise by Steven Petrovic, an on-line resource that is part of the Analytical Sciences Digital Library.

Sample Cells. The sample compartment provides a light-tight environment that limits stray radiation. Samples normally are in a liquid or solution state, and are placed in cells constructed with UV/Vis transparent materials, such as quartz, glass, and plastic (Figure 10.3.6). A quartz or fused-silica cell is required when working at a wavelength <300 nm where other materials show a significant absorption. The most common pathlength is 1 cm (10 mm), although cells with shorter (as little as 0.1 cm) and longer pathlengths (up to 10 cm) are available. Longer pathlength cells are useful when analyzing a very dilute solution or for gas samples. The highest quality cells allow the radiation to strike a flat surface at a 90^{o} angle, minimizing the loss of radiation to reflection. A test tube often is used as a sample cell with simple, single-beam instruments, although differences in the cell's pathlength and optical properties add an additional source of error to the analysis.

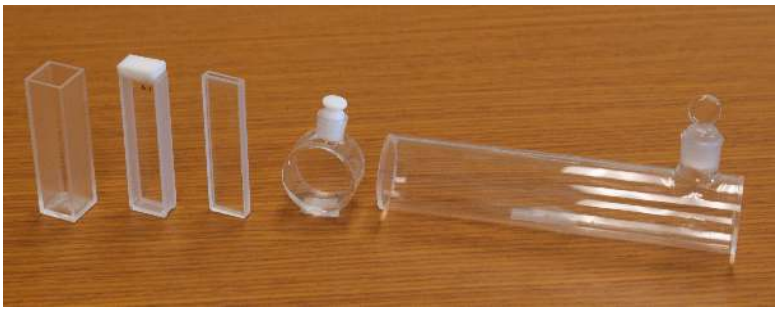


Figure 10.3.6 . Examples of sample cells for UV/Vis spectroscopy. From left to right (with path lengths in parentheses): rectangular plastic cuvette (10.0 mm), rectangular quartz cuvette (5.000 mm), rectangular quartz cuvette (1.000 mm), cylindrical quartz cuvette (10.00 mm), cylindrical glass cuvette with quartz windows (100.0 mm). Cells often are available as a matched pair, which is important when using a double-beam instrument.

If we need to monitor an analyte's concentration over time, it may not be possible to remove samples for analysis. This often is the case, for example, when monitoring an industrial production line or waste line, when monitoring a patient's blood, or when monitoring an environmental system, such as stream. With a ***fiber-optic probe*** we can analyze samples *in situ*. An example of a remote sensing fiber-optic probe is shown in Figure 10.3.7 . The probe consists of two bundles of fiber-optic cable. One bundle transmits radiation from the source to the probe's tip, which is designed to allow the sample to flow through the sample cell. Radiation from the source passes through the solution and is reflected back by a mirror. The second bundle of fiber-optic cable transmits the nonabsorbed radiation to the wavelength selector. Another design replaces the flow cell shown in Figure 10.3.7 with a membrane that contains a reagent that reacts with the analyte. When the analyte diffuses into the membrane it reacts with the reagent, producing a product that absorbs UV or visible radiation. The nonabsorbed radiation from the source is reflected or scattered back to the detector. Fiber optic probes that show chemical selectivity are called optrodes [(a) Seitz, W. R. *Anal. Chem.* **1984**, *56*, 16A–34A; (b) Angel, S. M. *Spectroscopy* **1987**, *2(2)*, 38–48].

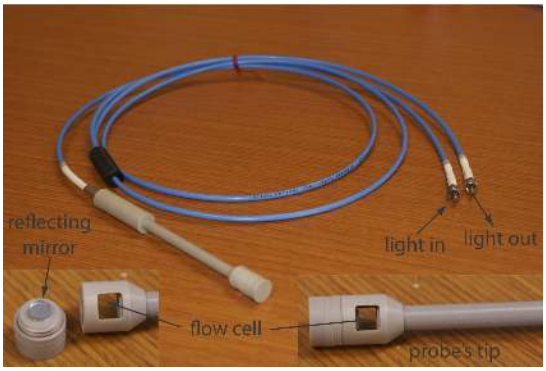


Figure 10.3.7 . Example of a fiber-optic probe. The inset photographs at the bottom of the figure provide close-up views of the probe's flow cell and the reflecting mirror.

Instrument Designs for Infrared Adsorption

Filter Photometer. The simplest instrument for IR absorption spectroscopy is a filter photometer similar to that shown in Figure 10.3.1 for UV/Vis absorption. These instruments have the advantage of portability and typically are used as dedicated analyzers for gases such as HCN and CO.

Double-beam spectrophotometer. Infrared instruments using a monochromator for wavelength selection use double-beam optics similar to that shown in Figure 10.3.3 . Double-beam optics are preferred over single-beam optics because the sources and detectors for infrared radiation are less stable than those for UV/Vis radiation. In addition, it is easier to correct for the absorption of infrared radiation by atmospheric CO_2 and H_2O vapor when using double-beam optics. Resolutions of 1–3 cm^{-1} are typical for most instruments.

Fourier transform spectrometer. In a Fourier transform infrared spectrometer, or FT–IR, the monochromator is replaced with an interferometer (Figure 10.1.13). Because an FT-IR includes only a single optical path, it is necessary to collect a separate spectrum to compensate for the absorbance of atmospheric CO_2 and H_2O vapor. This is done by collecting a background spectrum without the sample and storing the result in the instrument's computer memory. The background spectrum is removed from the sample's spectrum by taking the ratio the two signals. In comparison to other instrument designs, an FT–IR provides for rapid data acquisition, which allows for an enhancement in signal-to-noise ratio through signal-averaging.

Sample Cells. Infrared spectroscopy routinely is used to analyze gas, liquid, and solid samples. Sample cells are made from materials, such as NaCl and KBr, that are transparent to infrared radiation. Gases are analyzed using a cell with a pathlength of approximately 10 cm. Longer pathlengths are obtained by using mirrors to pass the beam of radiation through the sample several times.

A liquid sample may be analyzed using a variety of different sample cells (Figure 10.3.8). For non-volatile liquids a suitable sample is prepared by placing a drop of the liquid between two NaCl plates, forming a thin film that typically is less than 0.01 mm thick. Volatile liquids are placed in a sealed cell to prevent their evaporation.

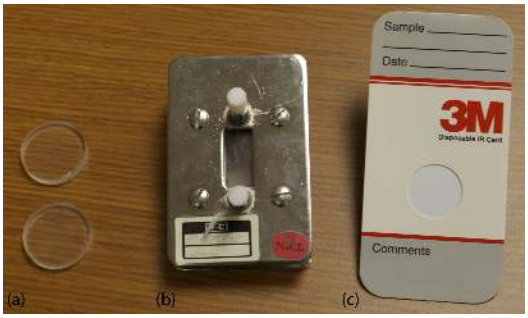


Figure 10.3.8 . Three examples of IR sample cells: (a) NaCl salts plates; (b) fixed pathlength (0.5 mm) sample cell with NaCl windows; (c) disposable card with a polyethylene window that is IR transparent with the exception of strong absorption bands at 2918 cm^{-1} and 2849 cm^{-1}.

The analysis of solution samples is limited by the solvent's IR absorbing properties, with CCl_4, CS_2, and $CHCl_3$ being the most common solvents. Solutions are placed in cells that contain two NaCl windows separated by a Teflon spacer. By changing the

Teflon spacer, pathlengths from 0.015–1.0 mm are obtained.

Transparent solid samples are analyzed by placing them directly in the IR beam. Most solid samples, however, are opaque, and are first dispersed in a more transparent medium before recording the IR spectrum. If a suitable solvent is available, then the solid is analyzed by preparing a solution and analyzing as described above. When a suitable solvent is not available, solid samples are analyzed by preparing a mull of the finely powdered sample with a suitable oil. Alternatively, the powdered sample is mixed with KBr and pressed into an optically transparent pellet.

The analysis of an aqueous sample is complicated by the solubility of the NaCl cell window in water. One approach to obtaining an infrared spectrum of an aqueous solution is to use ***attenuated total reflectance*** instead of transmission. Figure 10.3.9 shows a diagram of a typical attenuated total reflectance (ATR) FT–IR instrument. The ATR cell consists of a high refractive index material, such as ZnSe or diamond, sandwiched between a low refractive index substrate and a lower refractive index sample. Radiation from the source enters the ATR crystal where it undergoes a series of internal reflections before exiting the crystal. During each reflection the radiation penetrates into the sample to a depth of a few microns, which results in a selective attenuation of the radiation at those wavelengths where the sample absorbs. ATR spectra are similar, but not identical, to those obtained by measuring the transmission of radiation.

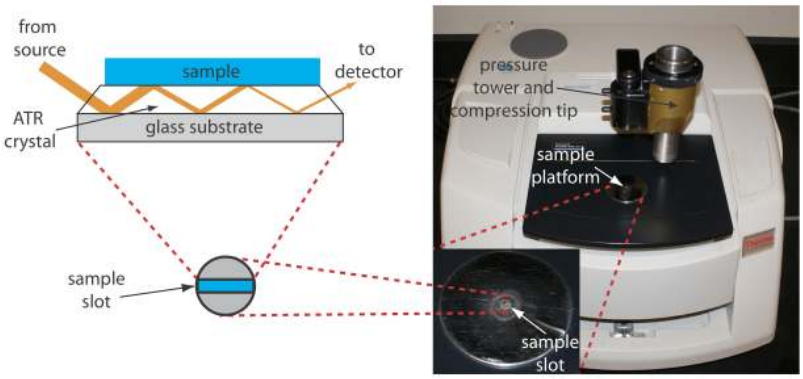


Figure 10.3.9 . FT-IR spectrometer equipped with a diamond ATR sample cell. The inserts show a close-up photo of the sample platform, a sketch of the ATR's sample slot, and a schematic showing how the source's radiation interacts with the sample. The pressure tower is used to ensure proper contact of a solid sample with the ATR crystal.

Solid samples also can be analyzed using an ATR sample cell. After placing the solid in the sample slot, a compression tip ensures that it is in contact with the ATR crystal. Examples of solids analyzed by ATR include polymers, fibers, fabrics, powders, and biological tissue samples. Another reflectance method is diffuse reflectance, in which radiation is reflected from a rough surface, such as a powder. Powdered samples are mixed with a non-absorbing material, such as powdered KBr, and the reflected light is collected and analyzed. As with ATR, the resulting spectrum is similar to that obtained by conventional transmission methods. Further details about these, and other methods for preparing solids for infrared analysis can be found in this chapter's additional resources.

Quantitative Applications

The determination of an analyte's concentration based on its absorption of ultraviolet or visible radiation is one of the most frequently encountered quantitative analytical methods. One reason for its popularity is that many organic and inorganic compounds have strong absorption bands in the UV/Vis region of the electromagnetic spectrum. In addition, if an analyte does not absorb UV/Vis radiation—or if its absorbance is too weak—we often can react it with another species that is strongly absorbing. For example, a dilute solution of Fe^{2+} does not absorb visible light. Reacting Fe^{2+} with *o*-phenanthroline, however, forms an orange–red complex of $\mathbf{Fe(phen)_3^{2+}}$ that has a strong, broad absorbance band near 500 nm. An additional advantage to UV/Vis absorption is that in most cases it is relatively easy to adjust experimental and instrumental conditions so that Beer's law is obeyed.

A quantitative analysis based on the absorption of infrared radiation, although important, is encountered less frequently than with UV/Vis absorption. One reason is the greater tendency for instrumental deviations from Beer's law when using infrared radiation. Because an infrared absorption band is relatively narrow, any deviation due to the lack of monochromatic radiation is more pronounced. In addition, infrared sources are less intense than UV/Vis sources, which makes stray radiation more of a problem.

Differences between the pathlengths for samples and for standards when using thin liquid films or KBr pellets are a problem, although an internal standard can correct for any difference in pathlength. Finally, establishing a 100%T (A = 0) baseline often is difficult because the optical properties of NaCl sample cells may change significantly with wavelength due to contamination and degradation. We can minimize this problem by measuring absorbance relative to a baseline established for the absorption band. Figure 10.3.10 shows how this is accomplished.

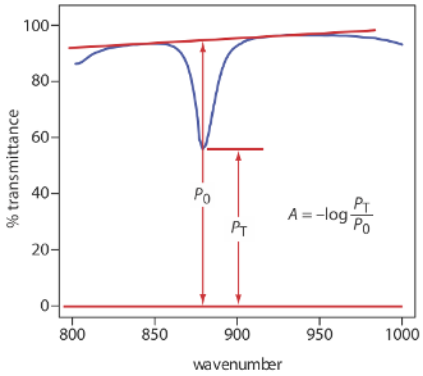


Figure 10.3.10 . Method for determining absorbance from an IR spectrum.

> Another approach is to use a cell with a fixed pathlength, such as that shown in Figure 10.3.8 b.

Environmental Applications

The analysis of waters and wastewaters often relies on the absorption of ultraviolet and visible radiation. Many of these methods are outlined in Table 10.3.1 . Several of these methods are described here in more detail.

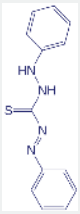
Table 10.3.1 . Examples of Molecular UV/Vis Analysis of Waters and Wastewaters

analyte	method	γ (nm)
trace metals		
aluminum	react with Eriochrome cyanide R dye at pH 6; forms red to pink complex	535
arsenic	reduce to AsH_3 using Zn and react with silver diethyldithiocarbamate; forms red complex	535
cadmium	extract into $CHCl_3$ containing dithizone from a sample made basic with NaOH; forms pink to red complex	518
chromium	oxidize to Cr(VI) and react with diphenylcarbazide; forms 540 red-violet product	540
copper	react with neocuprine in neutral to slightly acid solution and extract into $CHCl_3/CH_3OH$; forms yellow complex	457
iron	reduce to Fe^{2+} and react with *o*-phenanthroline; forms orange-red complex	510
lead	extract into $CHCl_3$ containing dithizone from sample made basic with NH_3/ NH_4^+ buffer; forms cherry red complex	510
manganese	oxidize to MnO_4^- with persulfate; forms purple solution	525
mercury	extract into $CHCl_3$ containing dithizone from acidic sample; forms orange complex	492
zinc	react with zincon at pH 9; forms blue complex	620
inorganic nonmetals		
ammonia	reaction with hypochlorite and phenol using a manganous 630 salt catalyst; forms blue indophenol as product	630
cyanide	react with chloroamine-T to form CNCl and then with a pyridine-barbituric acid; forms a red-blue dye	578
fluoride	react with red Zr-SPADNS lake; formation of ZrF_6^{2-} decreases color of the red lake	570
chlorine (residual)	react with leuco crystal violet; forms blue product	592
nitrate	react with Cd to form NO_2^- and then react with sulfanilamide and *N*-(1-napthyl)-ethylenediamine; forms red azo 543 dye	543
phosphate	react with ammonium molybdate and then	690

analyte	method	λ (nm)
	reduce with $SnCl_2$; forms molybdenum blue	
organics		
phenol	react with 4-aminoantipyrine and $K_3Fe(CN)_6$; forms yellow antipyrine dye	460
anionic surfactants	react with cationic methylene blue dye and extract into $CHCl_3$; forms blue ion pair	652

Although the quantitative analysis of metals in waters and wastewaters is accomplished primarily by atomic absorption or atomic emission spectroscopy, many metals also can be analyzed following the formation of a colored metal–ligand complex. One advantage to these spectroscopic methods is that they easily are adapted to the analysis of samples in the field using a filter photometer. One ligand used for the analysis of several metals is diphenylthiocarbazone, also known as dithizone. Dithizone is not soluble in water, but when a solution of dithizone in $CHCl_3$ is shaken with an aqueous solution that contains an appropriate metal ion, a colored metal–dithizonate complex forms that is soluble in $CHCl_3$. The selectivity of dithizone is controlled by adjusting the sample's pH. For example, Cd^{2+} is extracted from solutions made strongly basic with NaOH, Pb^{2+} from solutions made basic with an NH_3/ NH_4^+ buffer, and Hg^{2+} from solutions that are slightly acidic.

The structure of dithizone is shown below. See Chapter 7 for a discussion of extracting metal ions using dithizone.

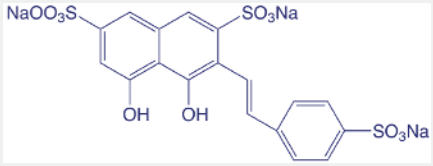


When chlorine is added to water the portion available for disinfection is called the chlorine residual. There are two forms of chlorine residual. The free chlorine residual includes Cl_2, HOCl, and OCl^-. The combined chlorine residual, which forms from the reaction of NH_3 with HOCl, consists of monochloramine, NH_2Cl, dichloramine, $NHCl_2$, and trichloramine, NCl_3. Because the free chlorine residual is more efficient as a disinfectant, there is an interest in methods that can distinguish between the total chlorine residual's different forms. One such method is the leuco crystal violet method. The free residual chlorine is determined by adding leuco crystal violet to the sample, which instantaneously oxidizes to give a blue-colored compound that is monitored at 592 nm. Completing the analysis in less than five minutes prevents a possible interference from the combined chlorine residual. The total chlorine residual (free + combined) is determined by reacting a separate sample with iodide, which reacts with both chlorine residuals to form HOI. When the reaction is complete, leuco crystal violet is added and oxidized by HOI, giving the same blue-colored product. The combined chlorine residual is determined by difference.

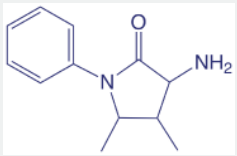
In Chapter 9 we explored how the total chlorine residual can be determined by a redox titration; see Representative Method 9.4.1 for further details. The method described here allows us to divide the total chlorine residual into its component parts.

The concentration of fluoride in drinking water is determined indirectly by its ability to form a complex with zirconium. In the presence of the dye SPADNS, a solution of zirconium forms a red colored compound, called a lake, that absorbs at 570 nm. When fluoride is added, the formation of the stable ZrF_6^{2-} complex causes a portion of the lake to dissociate, decreasing the absorbance. A plot of absorbance versus the concentration of fluoride, therefore, has a negative slope.

SPADNS, the structure of which is shown below, is an abbreviation for the sodium salt of 2-(4-sulfophenylazo)-1,8-dihydroxy-3,6-napthalenedisulfonic acid, which is a mouthful to say.



Spectroscopic methods also are used to determine organic constituents in water. For example, the combined concentrations of phenol and ortho- and meta-substituted phenols are determined by using steam distillation to separate the phenols from nonvolatile impurities. The distillate reacts with 4-aminoantipyrine at pH 7.9 ± 0.1 in the presence of $K_3Fe(CN)_6$ to a yellow colored antipyrine dye. After extracting the dye into $CHCl_3$, its absorbance is monitored at 460 nm. A calibration curve is prepared using only the unsubstituted phenol, C_6H_5OH. Because the molar absorptivity of substituted phenols generally are less than that for phenol, the reported concentration represents the minimum concentration of phenolic compounds.



4-aminoantipyrene

Molecular absorption also is used for the analysis of environmentally significant airborne pollutants. In many cases the analysis is carried out by collecting the sample in water, converting the analyte to an aqueous form that can be analyzed by methods such as those described in Table 10.3.1 . For example, the concentration of NO_2 is determined by oxidizing NO_2 to $\mathbf{NO_3^-}$. The concentration of $\mathbf{NO_3^-}$ is then determined by first reducing it to $\mathbf{NO_2^-}$ with Cd, and then reacting $\mathbf{NO_2^-}$ with sulfanilamide and *N*-(1-naphthyl)-ethylenediamine to form a red azo dye. Another important application is the analysis for SO_2, which is determined by collecting the sample in an aqueous solution of $\mathbf{HgCl_4^{2-}}$ where it reacts to form $\mathbf{Hg(SO_3)_2^{2-}}$. Addition of *p*-rosaniline and formaldehyde produces a purple complex that is monitored at 569 nm. Infrared absorption is useful for the analysis of organic vapors, including HCN, SO_2, nitrobenzene, methyl mercaptan, and vinyl chloride. Frequently, these analyses are accomplished using portable, dedicated infrared photometers.

Clinical Applications

The analysis of clinical samples often is complicated by the complexity of the sample's matrix, which may contribute a significant background absorption at the desired wavelength. The determination of serum barbiturates provides one example of how this problem is overcome. The barbiturates are first extracted from a sample of serum with $CHCl_3$ and then extracted from the $CHCl_3$ into 0.45 M NaOH (pH ≈ 13). The absorbance of the aqueous extract is measured at 260 nm, and includes contributions from the barbiturates as well as other components extracted from the serum sample. The pH of the sample is then lowered to approximately 10 by adding NH_4Cl and the absorbance remeasured. Because the barbiturates do not absorb at this pH, we can use the absorbance at pH 10, $A_{\text{pH 10}}$, to correct the absor-ance at pH 13, $A_{\text{pH 13}}$

$$A_{\text{barb}} = A_{\text{pH 13}} - \frac{V_{\text{samp}} + V_{\text{NH}_4\text{Cl}}}{V_{\text{samp}}} \times A_{\text{pH 10}}$$

where A_{barb} is the absorbance due to the serum barbiturates and V_{samp} and $V_{\text{NH}_4\text{Cl}}$ are the volumes of sample and NH_4Cl, respectively. Table 10.3.2 provides a summary of several other methods for analyzing clinical samples.

Table 10.3.2 . Examples of the Molecular UV/Vis Analysis of Clinical Samples

analyte	method	λ (nm)
total serum protein	react with NaOH and Cu^{2+}; forms blue-violet complex	540
serum cholesterol	react with Fe^{3+} in presence of isopropanol, acetic acid, and H_2SO_4; forms blue-violet complex	540
uric acid	react with phosphotungstic acid; forms tungsten blue	710
serum barbituates	extract into $CHCl_3$ to isolate from interferents and then extract into 0.45 M NaOH	260
glucose	react with *o*-toludine at 100°C; forms blue-green complex	630
protein-bound iodine	decompose protein to release iodide, which catalyzes redox reaction between Ce^{3+} and As^{3+}; forms yellow colored Ce^{4+}	420

Industrial Applications

UV/Vis molecular absorption is used for the analysis of a diverse array of industrial samples including pharmaceuticals, food, paint, glass, and metals. In many cases the methods are similar to those described in Table 10.3.1 and in Table 10.3.2 . For example, the amount of iron in food is determined by bringing the iron into solution and analyzing using the *o*-phenanthroline method listed in Table 10.3.1 .

Many pharmaceutical compounds contain chromophores that make them suitable for analysis by UV/Vis absorption. Products analyzed in this fashion include antibiotics, hormones, vitamins, and analgesics. One example of the use of UV absorption is in determining the purity of aspirin tablets, for which the active ingredient is acetylsalicylic acid. Salicylic acid, which is produced by the hydrolysis of acetylsalicylic acid, is an undesirable impurity in aspirin tablets, and should not be present at more than 0.01% w/w. Samples are screened for unacceptable levels of salicylic acid by monitoring the absorbance at a wavelength of 312 nm. Acetylsalicylic acid absorbs at 280 nm, but absorbs poorly at 312 nm. Conditions for preparing the sample are chosen such that an absorbance of greater than 0.02 signifies an unacceptable level of salicylic acid.

Forensic Applications

UV/Vis molecular absorption routinely is used for the analysis of narcotics and for drug testing. One interesting forensic application is the determination of blood alcohol using the Breathalyzer test. In this test a 52.5-mL breath sample is bubbled through an acidified solution of $K_2Cr_2O_7$, which oxidizes ethanol to acetic acid. The concentration of ethanol in the breath sample is determined by a decrease in the absorbance at 440 nm where the dichromate ion absorbs. A blood alcohol content of 0.10%, which is above the legal limit, corresponds to 0.025 mg of ethanol in the breath sample.

Developing a Quantitative Method for a Single Component

To develop a quantitative analytical method, the conditions under which Beer's law is obeyed must be established. First, the most appropriate wavelength for the analysis is determined from an absorption spectrum. In most cases the best wavelength corresponds to an absorption maximum because it provides greater sensitivity and is less susceptible to instrumental limitations. Second, if the instrument has adjustable slits, then an appropriate slit width is chosen. The absorption spectrum also aids in selecting a slit width by choosing a width that is narrow enough to avoid instrumental limita- tions to Beer's law, but wide enough to increase the throughput of source radiation. Finally, a calibration curve is constructed to determine the range of concentrations for which Beer's law is valid. Additional considerations that are important in any quantitative method are the effect of potential interferents and establishing an appropriate blank.

Representative Method 10.3.1: Determination of Iron in Water and Wastewater

The best way to appreciate the theoretical and the practical details discussed in this section is to carefully examine a typical analytical method. Although each method is unique, the following description of the determination of iron in water and wastewater provides an instructive example of a typical procedure. The description here is based on Method 3500-Fe B as published in *Standard Methods for the Examination of Water and Wastewater*, 20th Ed., American Public Health Association: Washington, D. C., 1998.

Description of Method

Iron in the +2 oxidation state reacts with *o*-phenanthroline to form the orange-red $\mathbf{Fe(phen)_3^{2+}}$ complex. The intensity of the complex's color is independent of the solution's acidity between a pH of 3 and 9. Because the complex forms more rapidly at lower pH levels, the reaction usually is carried out within a pH range of 3.0–3.5. Any iron present in the +3 oxidation state is reduced with hydroxylamine before adding *o*-phenanthroline. The most important interferents are strong oxidizing agents, polyphosphates, and metal ions such as Cu^{2+}, Zn^{2+}, Ni^{2+}, and Cd^{2+}. An interference from oxidizing agents is minimized by adding an excess of hydroxylamine, and an interference from polyphosphate is minimized by boiling the sample in the presence of acid. The absorbance of samples and standards are measured at a wavelength of 510 nm using a 1-cm cell (longer pathlength cells also may be used). Beer's law is obeyed for concentrations of within the range of 0.2–4.0 mg Fe/L.

Procedure

For a sample that contains less than 2 mg Fe/L, directly transfer a 50-mL portion to a 125-mL Erlenmeyer flask. Samples that contain more than 2 mg Fe/L are diluted before acquiring the 50-mL portion. Add 2 mL of concentrated HCl and 1 mL of hydroxylamine to the sample. Bring the solution to a boil and continue boiling until the solution's volume is reduced to between 15 and 20 mL. After cooling to room temperature, transfer the solution to a 50-mL volumetric flask, add 10 mL of an ammonium acetate buffer, 2 mL of a 1000 ppm solution of *o*-phenanthroline, and dilute to volume. Allow 10–15 minutes for color development before measuring the absorbance, using distilled water to set 100% T. Calibration standards, including a blank, are prepared by the same procedure using a stock solution that contains a known concentration of Fe^{2+}.

Questions

1. Explain why strong oxidizing agents are interferents and why an excess of hydroxylamine prevents the interference.

   A strong oxidizing agent will oxidize some Fe^{2+} to Fe^{3+}. Because $\mathbf{Fe(phen)_3^{3+}}$ does not absorb as strongly as $\mathbf{Fe(phen)_3^{2+}}$, the absorbance is smaller than expected, which produces a negative determinate error. The excess hydroxylamine reacts with the oxidizing agents, removing them from the solution.

2. The color of the complex is stable between pH levels of 3 and 9. What are some possible complications at more acidic or at more basic pH's?

   Because *o*-phenanthroline is a weak base, its conditional formation constant for $\mathbf{Fe(phen)_3^{2+}}$ becomes smaller at more acidic pH levels, where *o*-phenanthroline is present in its protonated form. The result is a decrease in absorbance and a less sensitive analytical method. When the pH is greater than 9, competition between OH^- and *o*-phenanthroline for Fe^{2+} also decreases the absorbance. In addition, if the pH is sufficiently basic there is a risk that the iron will precipitate as $Fe(OH)_2$.

3. Cadmium is an interferent because it forms a precipitate with *o*-phenanthroline. What effect does the formation of precipitate have on the determination of iron?

   Because *o*-phenanthroline is present in large excess (2000 µg of *o*-phenanthroline for 100 µg of $Fe2^+$), it is not likely that the interference is due to an insufficient amount of *o*-phenanthroline being available to react with the Fe^{2+}. The presence of a precipitate in the sample cell results in the scattering of radiation, which causes an apparent increase in absorbance. Because the measured absorbance increases, the reported concentration is too high. Although scattering is a problem here, it can serve as the basis of a useful analytical method. See Chapter 10.8 for further details.

4. Even high quality ammonium acetate contains a significant amount of iron. Why is this source of iron not a problem?

   Because all samples and standards are prepared using the same volume of ammonium acetate buffer, the contribution of this source of iron is accounted for by the calibration curve's reagent blank.

Quantitative Analysis for a Single Sample

To determine the concentration of an analyte we measure its absorbance and apply Beer's law using any of the standardization methods described in Chapter 5. The most common methods are a normal calibration curve using external standards and the method of standard additions. A single point standardization also is possible, although we must first verify that Beer's law holds for the concentration of analyte in the samples and the standard.

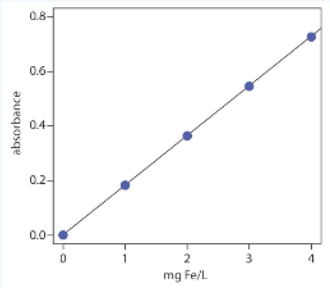
Example 10.3.1

The determination of iron in an industrial waste stream is carried out by the *o*-phenanthroline described in Representative Method 10.3.1. Using the data in the following table, determine the mg Fe/L in the waste stream.

mg Fe/L	absorbance
0.00	0.000
1.00	0.183
2.00	0.364
3.00	0.546
4.00	0.727
sample	0.269

Solution

Linear regression of absorbance versus the concentration of Fe in the standards gives the calibration curve and calibration equation shown here



$$A = 0.0006 + (0.1817\ \text{mg}^{-1}\text{L}) \times (\text{mgFe/L})$$

Substituting the sample's absorbance into the calibration equation gives the concentration of Fe in the waste stream as 1.48 mg Fe/L

Exercise 10.3.1

The concentration of Cu^{2+} in a sample is determined by reacting it with the ligand cuprizone and measuring its absorbance at 606 nm in a 1.00-cm cell. When a 5.00-mL sample is treated with cuprizone and diluted to 10.00 mL, the resulting solution has an absorbance of 0.118. A second 5.00-mL sample is mixed with 1.00 mL of a 20.00 mg/L standard of Cu^{2+}, treated with cuprizone and diluted to 10.00 mL, giving an absorbance of 0.162. Report the mg Cu^{2+}/L in the sample.

Answer

For this standard addition we write equations that relate absorbance to the concentration of Cu^{2+} in the sample before the standard addition

$$0.118 = \varepsilon b \left[C_{Cu} \times \frac{5.00\ mL}{10.00\ mL} \right]$$

and after the standard addition

$$0.162 = \varepsilon b \left(C_{Cu} \times \frac{5.00\ mL}{10.00\ mL} + \frac{20.00\ mg\ Cu}{L} \times \frac{1.00\ mL}{10.00\ mL} \right)$$

in each case accounting for the dilution of the original sample and for the standard. The value of εb is the same in both equation. Solving each equation for εb and equating

$$\frac{0.162}{C_{Cu} \times \frac{5.00\ mL}{10.00\ mL} + \frac{20.00\ mg\ Cu}{L} \times \frac{1.00\ mL}{10.00\ mL}} = \frac{0.118}{C_{Cu} \times \frac{5.00\ mL}{10.00\ mL}}$$

leaves us with an equation in which C_{Cu} is the only variable. Solving for C_{Cu} gives its value as

$$\frac{0.162}{0.500 \times C_{Cu} + 2.00\ mg\ Cu/L} = \frac{0.118}{0.500 \times C_{Cu}}$$

$$0.0810 \times C_{Cu} = 0.0590 \times C_{Ca} + 0.236\ mg\ Cu/L$$

$$0.0220 \times C_{Cu} = 0.236\ mg\ Cu/L$$

$$C_{Cu} = 10.7\ mg\ Cu/L$$

Quantitative Analysis of Mixtures

Suppose we need to determine the concentration of two analytes, *X* and *Y*, in a sample. If each analyte has a wavelength where the other analyte does not absorb, then we can proceed using the approach in Example 10.3.5 . Unfortunately, UV/Vis absorption bands are so broad that frequently it is not possible to find suitable wavelengths. Because Beer's law is additive the mixture's absorbance, A_{mix}, is

$$(A_{mix})_{\lambda_1} = (\varepsilon_x)_{\lambda_1} bC_X + (\varepsilon_Y)_{\lambda_1} bC_Y \tag{1.3.1}$$

where λ_1 is the wavelength at which we measure the absorbance. Because Equation 1.3.1 includes terms for the concentration of both *X* and *Y*, the absorbance at one wavelength does not provide enough information to determine either C_X or C_Y. If we measure the absorbance at a second wavelength

$$(A_{mix})_{\lambda_2} = (\varepsilon_x)_{\lambda_2} bC_X + (\varepsilon_Y)_{\lambda_2} bC_Y \tag{1.3.2}$$

then we can determine C_X and C_Y by solving simultaneously Equation 1.3.1 and Equation 1.3.2. Of course, we also must determine the value for ε_X and ε_Y at each wavelength. For a mixture of *n* components, we must measure the absorbance at *n* different wavelengths.

Example 10.3.2

The concentrations of Fe^{3+} and Cu^{2+} in a mixture are determined following their reaction with hexacyanoruthenate (II), $Ru(CN)_6^{4-}$, which forms a purple-blue complex with Fe^{3+} (λ_{max} = 550 nm) and a pale-green complex with Cu^{2+} (λ_{max} = 396 nm) [DiTusa, M. R.; Schlit, A. A. *J. Chem. Educ.* **1985**, *62*, 541–542]. The molar absorptivities (M^{-1} cm^{-1}) for the metal complexes at the two wavelengths are summarized in the following table.

analyte	ε_{550}	ε_{396}
Fe^{3+}	9970	84
Cu^{2+}	34	856

When a sample that contains Fe^{3+} and Cu^{2+} is analyzed in a cell with a pathlength of 1.00 cm, the absorbance at 550 nm is 0.183 and the absorbance at 396 nm is 0.109. What are the molar concentrations of Fe^{3+} and Cu^{2+} in the sample?

Solution

Substituting known values into Equation 1.3.1 and Equation 1.3.2 gives

$$A_{550} = 0.183 = 9970C_{Fe} + 34C_{Cu}$$
$$A_{396} = 0.109 = 84C_{Fe} + 856C_{Cu}$$

To determine C_{Fe} and C_{Cu} we solve the first equation for C_{Cu}

$$C_{Cu} = \frac{0.183 - 9970C_{Fe}}{34}$$

and substitute the result into the second equation.

$$0.109 = 84C_{Fe} + 856 \times \frac{0.183 - 9970C_{Fe}}{34}$$
$$= 4.607 - \left(2.51 \times 10^5\right) C_{Fe}$$

Solving for C_{Fe} gives the concentration of Fe^{3+} as 1.8×10^{-5} M. Substituting this concentration back into the equation for the mixture's absorbance at 396 nm gives the concentration of Cu^{2+} as 1.3×10^{-4} M.

Another approach to solving Example 10.3.2 is to multiply the first equation by 856/34 giving

$$4.607 = 251009C_{Fe} + 856C_{Cu}$$

Subtracting the second equation from this equation

$$4.607 = 251009C_{Fe} + 856C_{Cu}$$
$$-0.109 = 84C_{Fe} + 856C_{Cu}$$

gives

$$4.498 = 250925C_{Fe}$$

and we find that C_{Fe} is 1.8×10^{-5}. Having determined C_{Fe} we can substitute back into one of the other equations to solve for C_{Cu}, which is 1.3×10^{-5}.

? Exercise 10.3.2

The absorbance spectra for Cr^{3+} and Co^{2+} overlap significantly. To determine the concentration of these analytes in a mixture, its absorbance is measured at 400 nm and at 505 nm, yielding values of 0.336 and 0.187, respectively. The individual molar absorptivities (M^{-1} cm^{-1}) for $Cr3^{+}$ are 15.2 at 400 nm and 0.533 at 505 nm; the values for Co^{2+} are 5.60 at 400 nm and 5.07 at 505 nm.

Answer

Substituting into Equation 1.3.1 and Equation 1.3.2 gives

$$A_{400} = 0.336 = 15.2C_{Cr} + 5.60C_{Co}$$

$$A_{400} = 0187 = 0.533C_{Cr} + 5.07C_{Co}$$

To determine C_{Cr} and C_{Co} we solve the first equation for C_{Co}

$$C_{Co} = \frac{0.336 - 15.2C_{Co}}{5.60}$$

and substitute the result into the second equation.

$$0.187 = 0.533C_{Cr} + 5.07 \times \frac{0.336 - 15.2C_{Co}}{5.60}$$

$$0.187 = 0.3042 - 13.23C_{Cr}$$

Solving for C_{Cr} gives the concentration of Cr^{3+} as 8.86×10^{-3} M. Substituting this concentration back into the equation for the mixture's absorbance at 400 nm gives the concentration of Co^{2+} as 3.60×10^{-2} M.

To obtain results with good accuracy and precision the two wavelengths should be selected so that $\varepsilon_X > \varepsilon_Y$ at one wavelength and $\varepsilon_X < \varepsilon_Y$ at the other wavelength. It is easy to appreciate why this is true. Because the absorbance at each wavelength is dominated by one analyte, any uncertainty in the concentration of the other analyte has less of an impact. Figure 10.3.11 shows that the choice of wavelengths for Practice Exercise 10.3.2 are reasonable. When the choice of wavelengths is not obvious, one method for locating the optimum wavelengths is to plot $\varepsilon_X/\varepsilon_y$ as function of wavelength, and determine the wavelengths where $\varepsilon_X/\varepsilon_y$ reaches maximum and minimum values [Mehra, M. C.; Rioux, J. *J. Chem. Educ.* **1982**, *59*, 688–689].

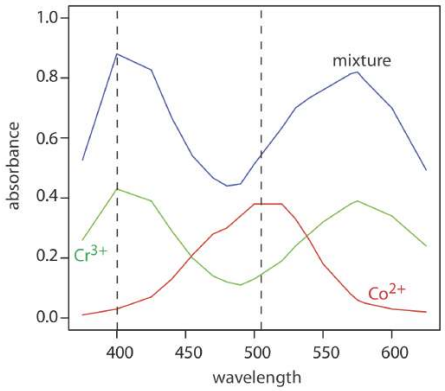


Figure 10.3.11 . Visible absorption spectra for 0.0250 M Cr^{3+}, 0.0750 M Co^{2+}, and for a mixture of Cr^{3+} and Co^{2+}. The two wavelengths used to analyze the mixture of Cr^{3+} and Co^{2+} are shown by the dashed lines. The data for the two standards are from Brewer, S. *Solving Problems in Analytical Chemistry*, John Wiley & Sons: New York, 1980.

When the analyte's spectra overlap severely, such that $\varepsilon_X \approx \varepsilon_Y$ at all wavelengths, other computational methods may provide better accuracy and precision. In a multiwavelength linear regression analysis, for example, a mixture's absorbance is compared to that for a set of standard solutions at several wavelengths [Blanco, M.; Iturriaga, H.; Maspoch, S.; Tarin, P. *J. Chem. Educ.* **1989**, *66*, 178–180]. If A_{SX} and A_{SY} are the absorbance values for standard solutions of components *X* and *Y* at any wavelength, then

$$A_{SX} = \varepsilon_X b C_{SX} \tag{1.3.3}$$

$$A_{SY} = \varepsilon_Y b C_{SY} \tag{1.3.4}$$

where C_{SX} and C_{SY} are the known concentrations of *X* and *Y* in the standard solutions. Solving Equation 1.3.3 and Equation 1.3.4 for ε_X and for ε_Y, substituting into Equation 1.3.1, and rearranging, gives

$$\frac{A_{mix}}{A_{SX}} = \frac{C_X}{C_{SX}} + \frac{C_Y}{C_{SY}} \times \frac{A_{SY}}{A_{SX}}$$

To determine C_X and C_Y the mixture's absorbance and the absorbances of the standard solutions are measured at several wavelengths. Graphing A_{mix}/A_{SX} versus A_{SY}/A_{SX} gives a straight line with a slope of C_Y/C_{SY} and a *y*-intercept of C_X/C_{SX}. This approach is particularly helpful when it is not possible to find wavelengths where $\varepsilon_X > \varepsilon_Y$ and $\varepsilon_X < \varepsilon_Y$.

The approach outlined here for a multiwavelength linear regression uses a single standard solution for each analyte. A more rigorous approach uses multiple standards for each analyte. The math behind the analysis of such data—which we call a multiple linear regression—is beyond the level of this text. For more details about multiple linear regression see Brereton, R. G. *Chemometrics: Data Analysis for the Laboratory and Chemical Plant*, Wiley: Chichester, England, 2003.

Example 10.3.3

Figure ***PageIndex*10.11** shows visible absorbance spectra for a standard solution of 0.0250 M Cr^{3+}, a standard solution of 0.0750 M Co^{2+}, and a mixture that contains unknown concentrations of each ion. The data for these spectra are shown here.

λ (nm)	A_{Cr}	A_{Cu}	A_{mix}	λ (nm)	A_{Cr}	A_{Cu}	A_{mix}
375	0.26	0.01	0.53	520	0.19	0.38	0.63
400	0.43	0.03	0.88	530	0.24	0.33	0.70
425	0.39	0.07	0.83	540	0.28	0.26	0.73
440	0.29	0.13	0.67	550	0.32	0.18	0.76
455	0.20	0.21	0.54	570	0.38	0.08	0.81
470	0.14	0.28	0.47	575	0.39	0.06	0.82
480	0.12	0.30	0.44	580	0.38	0.05	0.79
490	0.11	0.34	0.45	600	0.34	0.03	0.70
500	0.13	0.38	0.51	625	0.24	0.02	0.49

Use a multiwavelength regression analysis to determine the composition of the unknown.

Solution

First we need to calculate values for A_{mix}/A_{SX} and for A_{SY}/A_{SX}. Let's define X as Co^{2+} and Y as Cr^{3+}. For example, at a wavelength of 375 nm A_{mix}/A_{SX} is 0.53/0.01, or 53 and A_{SY}/A_{SX} is 0.26/0.01, or 26. Completing the calculation for all wavelengths and graphing A_{mix}/A_{SX} versus A_{SY}/A_{SX} gives the calibration curve shown in Figure 10.3.12 . Fitting a straight-line to the data gives a regression model of

$$\frac{A_{mix}}{A_{SX}} = 0.636 + 2.01 \times \frac{A_{SY}}{A_{SX}}$$

Using the *y*-intercept, the concentration of Co^{2+} is

$$\frac{C_X}{C_{SX}} = \frac{[Co^{2+}]}{0.0750 M} = 0.636$$

or $[Co^{2+}]$ = 0.048 M; using the slope the concentration of Cr^{3+} is

$$\frac{C_Y}{C_{SY}} = \frac{[Cr^{3+}]}{0.0250 M} = 2.01$$

or $[Cr^{3+}]$ = 0.050 M.

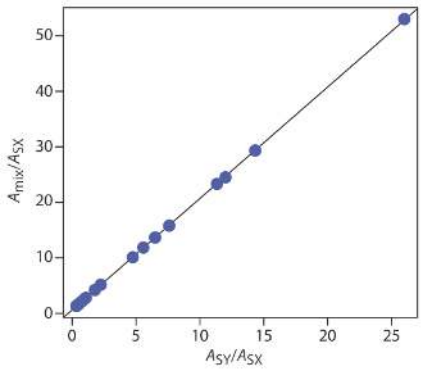


Figure 10.3.12 . Multiwavelength linear regression analysis for the data in Example 10.3.3 .

? Exercise 10.3.3

A mixture of MnO_4^- and $Cr_2O_7^{2-}$, and standards of 0.10 mM $KMnO_4$ and of 0.10 mM $K_2Cr_2O_7$ give the results shown in the following table. Determine the composition of the mixture. The data for this problem is from Blanco, M. C.; Iturriaga, H.; Maspoch, S.; Tarin, P. *J. Chem. Educ.* **1989**, *66*, 178–180.

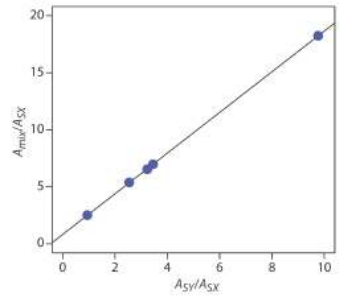
λ (nm)	A_{Mn}	A_{Cr}	A_{mix}
266	0.042	0.410	0.766
288	0.082	0.283	0.571
320	0.168	0.158	0.422
350	0.125	0.318	0.672
360	0.036	0.181	0.366

Answer

Letting *X* represent MnO_4^- and letting *Y* represent $Cr_2O_7^{2-}$, we plot the equation

$$\frac{A_{mix}}{A_{SX}} = \frac{C_X}{C_{SX}} + \frac{C_Y}{C_{SY}} \times \frac{A_{SY}}{A_{SX}}$$

placing A_{mix}/A_{SX} on the *y*-axis and A_{SY}/A_{SX} on the *x*-axis. For example, at a wavelength of 266 nm the value A_{mix}/A_{SX} of is 0.766/0.042, or 18.2, and the value of A_{SY}/A_{SX} is 0.410/0.042, or 9.76. Completing the calculations for all wavelengths and plotting the data gives the result shown here



Fitting a straight-line to the data gives a regression model of

$$\frac{A_{mix}}{A_{SX}} = 0.8147 + 1.7839 \times \frac{A_{SY}}{A_{SX}}$$

Using the *y*-intercept, the concentration of MnO_4^- is

$$\frac{C_X}{C_{SX}} = 0.8147 = \frac{[MnO_4^-]}{1.0 \times 10^{-4}\ \text{M}\ MnO_4^-}$$

or 8.15×10^{-5} M MnO_4^-, and using the slope, the concentration of $Cr_2O_7^{2-}$ is

$$\frac{C_Y}{C_{SY}} = 1.7839 = \frac{[Cr_2O_7^{2-}]}{1.00 \times 10^{-4}\ \text{M}\ Cr_2O_7^{2-}}$$

or 1.78×10^{-4} M $Cr_2O_7^{2-}$.

Qualitative Applications

As discussed in Chapter 10.2, ultraviolet, visible, and infrared absorption bands result from the absorption of electromagnetic radiation by specific valence electrons or bonds. The energy at which the absorption occurs, and the intensity of that absorption, is determined by the chemical environment of the absorbing moiety. For example, benzene has several ultraviolet absorption bands due to $\pi \rightarrow \pi^*$ transitions. The position and intensity of two of these bands, 203.5 nm (ε = 7400 M^{-1} cm^{-1}) and 254 nm (ε = 204 M^{-}

^{1} cm^{-1}), are sensitive to substitution. For benzoic acid, in which a carboxylic acid group replaces one of the aromatic hydrogens, the two bands shift to 230 nm (ε = 11600 M^{-1} cm^{-1}) and 273 nm (ε = 970 M^{-1} cm^{-1}). A variety of rules have been developed to aid in correlating UV/Vis absorption bands to chemical structure. Similar correlations are available for infrared absorption bands. For example a carbonyl's C=O stretch is sensitive to adjacent functional groups, appearing at 1650 cm^{-1} for acids, 1700 cm^{-1} for ketones, and 1800 cm^{-1} for acid chlorides. The interpretation of UV/ Vis and IR spectra receives adequate coverage elsewhere in the chemistry curriculum, notably in organic chemistry, and is not considered further in this text.

With the availability of computerized data acquisition and storage it is possible to build digital libraries of standard reference spectra. The identity of an a unknown compound often can be determined by comparing its spectrum against a library of reference spectra, a process known as ***spectral searching***. Comparisons are made using an algorithm that calculates the cumulative difference between the sample's spectrum and a reference spectrum. For example, one simple algorithm uses the following equation

$$D = \sum_{i=1}^{n} |(A_{sample})_i - (A_{reference})_i|$$

where D is the cumulative difference, A_{sample} is the sample's absorbance at wavelength or wavenumber i, $A_{reference}$ is the absorbance of the reference compound at the same wavelength or wavenumber, and n is the number of digitized points in the spectra. The cumulative difference is calculated for each reference spectrum. The reference compound with the smallest value of D is the closest match to the unknown compound. The accuracy of spectral searching is limited by the number and type of compounds included in the library, and by the effect of the sample's matrix on the spectrum.

Another advantage of computerized data acquisition is the ability to subtract one spectrum from another. When coupled with spectral searching it is possible to determine the identity of several components in a sample without the need of a prior separation step by repeatedly searching and sub- tracting reference spectra. An example is shown in Figure 10.3.13 in which the composition of a two-component mixture is determined by successive searching and subtraction. Figure 10.3.13 a shows the spectrum of the mixture. A search of the spectral library selects cocaine•HCl (Figure 10.3.13 b) as a likely component of the mixture. Subtracting the reference spectrum for cocaine•HCl from the mixture's spectrum leaves a result (Figure 10.3.13 c) that closely matches mannitol's reference spectrum (Figure 10.3.13 d). Subtracting the reference spectrum for mannitol leaves a small residual signal (Figure 10.3.13 e).

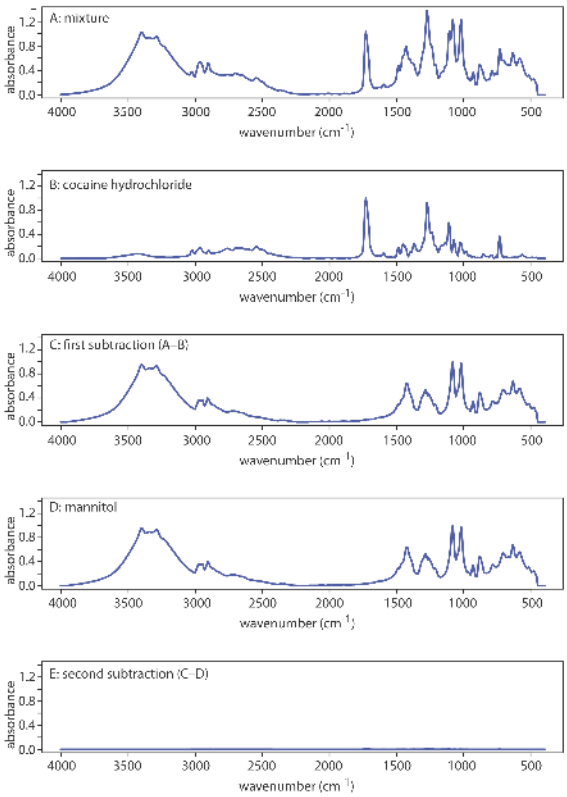


Figure 10.3.13 . Identifying the components of a mixture by spectral searching and subtracting. (a) IR spectrum of the mixture; (b) Reference IR spectrum of cocaine•HCl; (c) Result of subtracting the spectrum of cocaine•HCl from the mixture's spectrum; (d) Reference IR spectrum of mannitol; and (e) The residual spectrum after removing mannitol's contribution to the mixture's spectrum. IR spectra traditionally are displayed using percent transmittance, %T, along the *y*-axis (for example, see Figure 10.2.2). Because absorbance—not percent transmittance—is a linear function of concentration, spectral searching and spectral subtraction, is easier to do when displaying absorbance on the *y*-axis.

Characterization Applications

Molecular absorption, particularly in the UV/Vis range, has been used for a variety of different characterization studies, including determining the stoichiometry of metal–ligand complexes and determining equilibrium constants. Both of these examples are examined in this section.

Stoichiometry of a Metal-Ligand Complex

We can determine the stoichiometry of the metal–ligand complexation reaction

$$\mathrm{M} + y\mathrm{L} \rightleftharpoons \mathrm{ML}_y$$

using one of three methods: the method of continuous variations, the mole-ratio method, and the slope-ratio method. Of these approaches, the ***method of continuous variations***, also called Job's method, is the most popular. In this method a series of solutions is prepared such that the total moles of metal and of ligand, n_{total}, in each solution is the same. If $(n_{\mathrm{M}})_i$ and $(n_{\mathrm{L}})_i$ are, respectively, the moles of metal and ligand in solution *i*, then

$$n_{\text{total}} = (n_{\mathrm{M}})_i + (n_{\mathrm{L}})_i$$

The relative amount of ligand and metal in each solution is expressed as the mole fraction of ligand, $(X_{\mathrm{L}})i$, and the mole fraction of metal, $(X_{\mathrm{M}})_i$,

$$(X_{\mathrm{L}})_i = \frac{(n_{\mathrm{L}})_i}{n_{\text{total}}}$$

$$(X_M)_i = 1 - \frac{(n_{\mathrm{L}})_i}{n_{\text{total}}} = \frac{(n_{\mathrm{M}})_i}{n_{\text{total}}}$$

The concentration of the metal–ligand complex in any solution is determined by the limiting reagent, with the greatest concentration occurring when the metal and the ligand are mixed stoichiometrically. If we monitor the complexation reaction at a wavelength where only the metal–ligand complex absorbs, a graph of absorbance versus the mole fraction of ligand has two linear branches—one when the ligand is the limiting reagent and a second when the metal is the limiting reagent. The intersection of the two branches represents a stoichiometric mixing of the metal and the ligand. We use the mole fraction of ligand at the intersection to determine the value of y for the metal–ligand complex ML_y.

$$y = \frac{n_L}{n_M} = \frac{X_L}{X_M} = \frac{X_L}{1 - X_L}$$

You also can plot the data as absorbance versus the mole fraction of metal. In this case, y is equal to $(1 - X_M)/X_M$.

Example 10.3.4

To determine the formula for the complex between Fe^{2+} and *o*-phenanthroline, a series of solutions is prepared in which the total concentration of metal and ligand is held constant at 3.15×10^{-4} M. The absorbance of each solution is measured at a wavelength of 510 nm. Using the following data, determine the formula for the complex.

X_L	absorbance	X_L	absorbance
0.000	0.000	0.600	0.693
0.100	0.116	0.700	0.809
0.200	0.231	0.800	0.693
0.300	0.347	0.900	0.347
0.400	0.462	1.000	0.000
0.500	0.578		

Solution

A plot of absorbance versus the mole fraction of ligand is shown in Figure 10.3.14 . To find the maximum absorbance, we extrapolate the two linear portions of the plot. The two lines intersect at a mole fraction of ligand of 0.75. Solving for y gives

$$y = \frac{X_L}{1 - X_L} = \frac{0.75}{1 - 0.75} = 3$$

The formula for the metal–ligand complex is $\mathbf{Fe(phen)_3^{2+}}$.

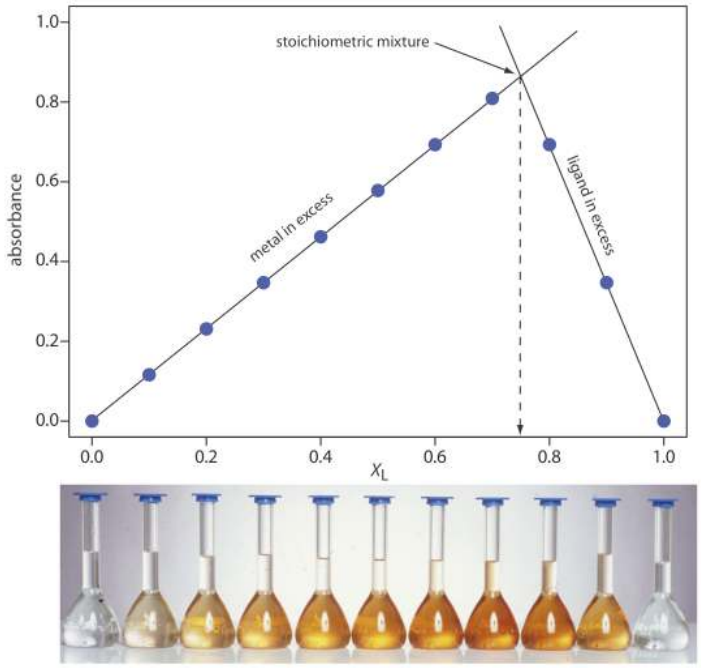


Figure 10.3.14 . Continuous variations plot for Example 10.3.4 . The photo shows the solutions used to gather the data. Each solution is displayed directly below its coresponding point on the continuous variations plot. To prepare these solutions I first prepared a solution of $\mathbf{3.15 \times 10^{-4}}$ M Fe^{2+} and a solution of $\mathbf{3.15 \times 10^{-4}}$ M *o*-phenanthroline. Because the two stock solutions have the same concentration, diluting a portion of one solution with the other solution gives a mixture in which the combined concentration of *o*-phenanthroline and Fe^{2+} is $\mathbf{3.15 \times 10^{-4}}$ M. Because each solution has the same volume, each solution also contains the same total moles of metal and ligand.

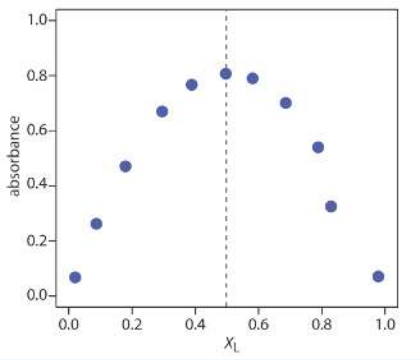
? Exercise 10.3.4

Use the continuous variations data in the following table to determine the formula for the complex between Fe^{2+} and SCN^-. The data for this problem is adapted from Meloun, M.; Havel, J.; Högfeldt, E. *Computation of Solution Equilibria*, Ellis Horwood: Chichester, England, 1988, p. 236.

X_L	absorbance	X_L	absorbance	X_L	absorbance	X_L	absorbance
0.0200	0.068	0.2951	0.670	0.5811	0.790	0.8923	0.324
0.0870	0.262	0.3887	0.767	0.6860	0.701	0.9787	0.071
0.1792	0.471	0.4964	0.807	0.7885	0.540		

Answer

The figure below shows a continuous variations plot for the data in this exercise. Although the individual data points show substantial curvature—enough curvature that there is little point in trying to draw linear branches for excess metal and excess ligand—the maximum absorbance clearly occurs at $X_L \approx 0.5$. The complex's stoichiometry, therefore, is $Fe(SCN)^{2+}$.



Several precautions are necessary when using the method of continuous variations. First, the metal and the ligand must form only one metal–ligand complex. To determine if this condition is true, plots of absorbance versus X_L are constructed at several different wavelengths and for several different values of n_{total}. If the maximum absorbance does not occur at the same value of X_L for each set of conditions, then more than one metal–ligand complex is present. A second precaution is that the metal–ligand complex's absorbance must obey Beer's law. Third, if the metal–ligand complex's formation constant is relatively small, a plot of absorbance versus X_L may show significant curvature. In this case it often is difficult to determine the stoichiometry by extrapolation. Finally, because the stability of a metal–ligand complex may be influenced by solution conditions, it is necessary to control carefully the composition of the solutions. When the ligand is a weak base, for example, each solutions must be buffered to the same pH.

In the ***mole-ratio method*** the moles of one reactant, usually the metal, is held constant, while the moles of the other reactant is varied. The absorbance is monitored at a wavelength where the metal–ligand complex absorbs. A plot of absorbance as a function of the ligand-to-metal mole ratio, n_L/n_M, has two linear branches that intersect at a mole–ratio corresponding to the complex's formula. Figure 10.3.15 a shows a mole-ratio plot for the formation of a 1:1 complex in which the absorbance is monitored at a wavelength where only the complex absorbs. Figure 10.3.15 b shows a mole-ratio plot for a 1:2 complex in which all three species —the metal, the ligand, and the complex—absorb at the selected wavelength. Unlike the method of continuous variations, the mole-ratio method can be used for complexation reactions that occur in a stepwise fashion if there is a difference in the molar absorptivities of the metal–ligand complexes, and if the formation constants are sufficiently different. A typical mole-ratio plot for the step-wise formation of ML and ML_2 is shown in Figure 10.3.15 c.

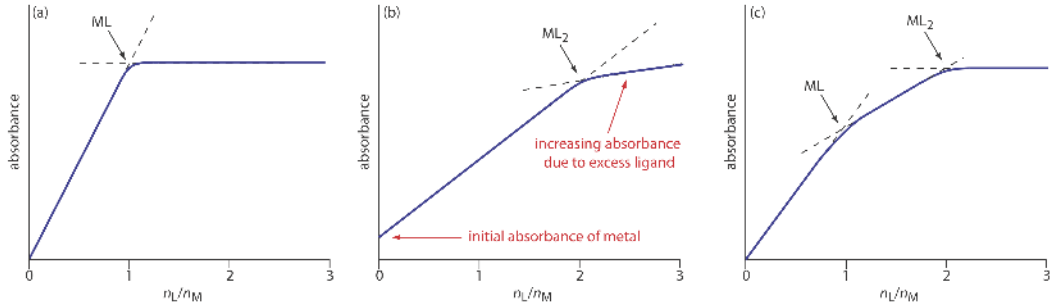


Figure 10.3.15 . Mole-ratio plots for: (a) a 1:1 metal–ligand complex in which only the complex absorbs; (b) a 1:2 metal–ligand complex in which the metal, the ligand, and the complex absorb; and (c) the stepwise formation of a 1:1 and a 1:2 metal–ligand complex.

For both the method of continuous variations and the mole-ratio method, we determine the complex's stoichiometry by extrapolating absorbance data from conditions in which there is a linear relationship between absorbance and the relative amounts of metal and ligand. If a metal–ligand complex is very weak, a plot of absorbance versus X_L or n_L/n_M becomes so curved that it is impossible to determine the stoichiometry by extrapolation. In this case the slope-ratio is used.

In the ***slope-ratio method*** two sets of solutions are prepared. The first set of solutions contains a constant amount of metal and a variable amount of ligand, chosen such that the total concentration of metal, C_M, is much larger than the total concentration of ligand, C_L. Under these conditions we may assume that essentially all the ligand reacts to form the metal–ligand complex. The concentration of the complex, which has the general form M_xL_y, is

$$[\mathrm{M}_x\mathrm{L}_y] = \frac{C_\mathrm{L}}{y}$$

If we monitor the absorbance at a wavelength where only $\mathrm{M}_x\mathrm{L}_y$ absorbs, then

$$A = \varepsilon b\,[\mathrm{M}_x\mathrm{L}_y] = \frac{\varepsilon b C_\mathrm{L}}{y}$$

and a plot of absorbance versus C_L is linear with a slope, s_L, of

$$s_\mathrm{L} = \frac{\varepsilon b}{y}$$

A second set of solutions is prepared with a fixed concentration of ligand that is much greater than a variable concentration of metal; thus

$$[\mathrm{M}_x\mathrm{L}_y] = \frac{C_\mathrm{M}}{x}$$

$$A = \varepsilon b\,[\mathrm{M}_x\mathrm{L}_y] = \frac{\varepsilon b C_\mathrm{M}}{x}$$

$$s_M = \frac{\varepsilon b}{x}$$

A ratio of the slopes provides the relative values of x and y.

$$\frac{s_\mathrm{M}}{s_\mathrm{L}} = \frac{\varepsilon b/x}{\varepsilon b/y} = \frac{y}{x}$$

An important assumption in the slope-ratio method is that the complexation reaction continues to completion in the presence of a sufficiently large excess of metal or ligand. The slope-ratio method also is limited to systems in which only a single complex forms and for which Beer's law is obeyed.

Determination of Equilibrium Constants

Another important application of molecular absorption spectroscopy is the determination of equilibrium constants. Let's consider, as a simple example, an acid–base reaction of the general form

$$\mathrm{HIn}(aq) + \mathrm{H_2O}(l) \rightleftharpoons \mathrm{H_3O^+}(aq) + \mathrm{In^-}(aq)$$

where HIn and $\mathrm{In^-}$ are the conjugate weak acid and weak base forms of an acid–base indicator. The equilibrium constant for this reaction is

$$K_\mathrm{a} = \frac{[\mathrm{H_3O^+}]\,[\mathrm{A^-}]}{[\mathrm{HA}]}$$

To determine the equilibrium constant's value, we prepare a solution in which the reaction is in a state of equilibrium and determine the equilibrium concentration for $\mathrm{H_3O^+}$, HIn, and $\mathrm{In^-}$. The concentration of $\mathrm{H_3O^+}$ is easy to determine by measuring the solution's pH. To determine the concentration of HIn and $\mathrm{In^-}$ we can measure the solution's absorbance.

If both HIn and $\mathrm{In^-}$ absorb at the selected wavelength, then, from Beer's law, we know that

$$A = \varepsilon_\mathrm{HIn} b[\mathrm{HIn}] + \varepsilon_\mathrm{In} b[\mathrm{In^-}] \tag{1.3.5}$$

where ε_HIn and ε_In are the molar absorptivities for HIn and $\mathrm{In^-}$. The indicator's total concentration, C, is given by a mass balance equation

$$C = [\mathrm{HIn}] + [\mathrm{In^-}] \tag{1.3.6}$$

Solving Equation 1.3.6 for [HIn] and substituting into Equation 1.3.5 gives

$$A = \varepsilon_\mathrm{HIn} b\,(C - [\mathrm{In^-}]) + \varepsilon_\mathrm{In} b\,[\mathrm{In^-}]$$

which we simplify to

$$A = \varepsilon_{\text{HIn}} bC - \varepsilon_{\text{HIn}} b\,[\text{In}^-] + \varepsilon_{\text{In}} b\,[\text{In}^-]$$

$$A = A_{\text{HIn}} + b\,[\text{In}^-]\,(\varepsilon_{\text{In}} - \varepsilon_{\text{HIn}}) \tag{1.3.7}$$

where A_{HIn}, which is equal to $\varepsilon_{\text{HIn}} bC$, is the absorbance when the pH is acidic enough that essentially all the indicator is present as HIn. Solving Equation 1.3.7 for the concentration of In^- gives

$$[\text{In}^-] = \frac{A - A_{\text{HIn}}}{b\,(\varepsilon_{\text{In}} - \varepsilon_{\text{HIn}})} \tag{1.3.8}$$

Proceeding in the same fashion, we derive a similar equation for the concentration of HIn

$$[\text{HIn}] = \frac{A_{\text{In}} - A}{b\,(\varepsilon_{\text{In}} - \varepsilon_{\text{HIn}})} \tag{1.3.9}$$

where A_{In}, which is equal to $\varepsilon_{\text{In}} bC$, is the absorbance when the pH is basic enough that only In^- contributes to the absorbance. Substituting Equation 1.3.8 and Equation 1.3.9 into the equilibrium constant expression for HIn gives

$$K_a = \frac{[\text{H}_3\text{O}^+][\text{In}^-]}{[\text{HIn}]} = [\text{H}_3\text{O}^+] \times \frac{A - A_{\text{HIn}}}{A_{\text{In}} - A} \tag{1.3.10}$$

We can use Equation 1.3.10 to determine K_a in one of two ways. The simplest approach is to prepare three solutions, each of which contains the same amount, C, of indicator. The pH of one solution is made sufficiently acidic such that [HIn] >> [In^-]. The absorbance of this solution gives A_{HIn}. The value of A_{In} is determined by adjusting the pH of the second solution such that [In^-] >> [HIn]. Finally, the pH of the third solution is adjusted to an intermediate value, and the pH and absorbance, A, recorded. The value of K_a is calculated using Equation 1.3.10.

Example 10.3.5

The acidity constant for an acid–base indicator is determined by preparing three solutions, each of which has a total concentration of indicator equal to 5.00×10^{-5} M. The first solution is made strongly acidic with HCl and has an absorbance of 0.250. The second solution is made strongly basic and has an absorbance of 1.40. The pH of the third solution is 2.91 and has an absorbance of 0.662. What is the value of K_a for the indicator?

Solution

The value of K_a is determined by making appropriate substitutions into 10.20 where [H_3O^+] is 1.23×10^{-3}; thus

$$K_a = (1.23 \times 10^{-3}) \times \frac{0.662 - 0.250}{1.40 - 0.662} = 6.87 \times 10^{-4}$$

Exercise 10.3.5

To determine the K_a of a merocyanine dye, the absorbance of a solution of 3.5×10^{-4} M dye was measured at a pH of 2.00, a pH of 6.00, and a pH of 12.00, yielding absorbances of 0.000, 0.225, and 0.680, respectively. What is the value of K_a for this dye? The data for this problem is adapted from Lu, H.; Rutan, S. C. *Anal. Chem.*, **1996**, *68*, 1381–1386.

Answer

The value of K_a is

$$K_a = (1.00 \times 10^{-6}) \times \frac{0.225 - 0.000}{0.680 - 0.225} = 4.95 \times 10^{-7}$$

A second approach for determining K_a is to prepare a series of solutions, each of which contains the same amount of indicator. Two solutions are used to determine values for A_{HIn} and A_{In}. Taking the log of both sides of Equation 1.3.10 and rearranging leave us with the following equation.

$$\log \frac{A - A_{\text{Hin}}}{A_{\text{In}^-} - A} = \text{pH} - \text{p}K_a \tag{1.3.11}$$

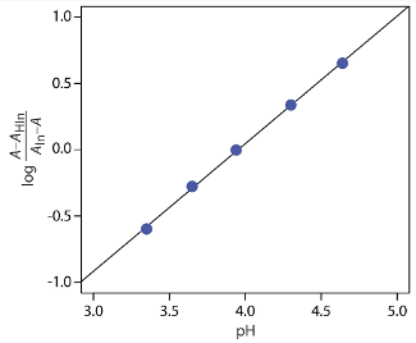
A plot of $\log[(A - A_{HIn})/(A_{In} - A)]$ versus pH is a straight-line with a slope of +1 and a *y*-intercept of $-pK_a$.

Exercise 10.3.6

To determine the K_a for the indicator bromothymol blue, the absorbance of each a series of solutions that contain the same concentration of bromothymol blue is measured at pH levels of 3.35, 3.65, 3.94, 4.30, and 4.64, yielding absorbance values of 0.170, 0.287, 0.411, 0.562, and 0.670, respectively. Acidifying the first solution to a pH of 2 changes its absorbance to 0.006, and adjusting the pH of the last solution to 12 changes its absorbance to 0.818. What is the value of K_a for bromothymol blue? The data for this problem is from Patterson, G. S. *J. Chem. Educ.*, **1999**, *76*, 395–398.

Answer

To determine K_a we use Equation 1.3.11, plotting $\log[(A - A_{HIn})/(A_{In} - A)]$ versus pH, as shown below.



Fitting a straight-line to the data gives a regression model of

$$\log \frac{A - A_{HIn}}{A_{In} - A} = -3.80 + 0.962\text{pH}$$

The *y*-intercept is $-pK_a$; thus, the pK_a is 3.80 and the K_a is 1.58×10^{-4}.

In developing these approaches for determining K_a we considered a relatively simple system in which the absorbance of HIn and In^- are easy to measure and for which it is easy to determine the concentration of H_3O^+. In addition to acid–base reactions, we can adapt these approaches to any reaction of the general form

$$X(aq) + Y(aq) \rightleftharpoons Z(aq)$$

including metal–ligand complexation reactions and redox reactions, provided we can determine spectrophotometrically the concentration of the product, *Z*, and one of the reactants, either *X* or *Y*, and that we can determine the concentration of the other reactant by some other method. With appropriate modifications, a more complicated system in which we cannot determine the concentration of one or more of the reactants or products also is possible [Ramette, R. W. *Chemical Equilibrium and Analysis*, Addison-Wesley: Reading, MA, 1981, Chapter 13].

Evaluation of UV/Vis and IR Spectroscopy

Scale of Operations

Molecular UV/Vis absorption routinely is used for the analysis of trace analytes in macro and meso samples. Major and minor analytes are determined by diluting the sample before analysis, and concentrating a sample may allow for the analysis of ultratrace analytes. The scale of operations for infrared absorption is generally poorer than that for UV/Vis absorption.

Accuracy

Under normal conditions a relative error of 1–5% is easy to obtained with UV/Vis absorption. Accuracy usually is limited by the quality of the blank. Examples of the type of problems that are encountered include the pres- ence of particulates in the sample that scatter radiation, and the presence of interferents that react with analytical reagents. In the latter case the interferent may react to form an absorbing species, which leads to a positive determinate error. Interferents also may prevent the analyte from reacting,

which leads to a negative determinate error. With care, it is possible to improve the accuracy of an analysis by as much as an order of magnitude.

Precision

In absorption spectroscopy, precision is limited by indeterminate errors—primarily instrumental noise—which are introduced when we measure absorbance. Precision generally is worse for low absorbances where $P_0 \approx P_T$, and for high absorbances where P_T approaches 0. We might expect, therefore, that precision will vary with transmittance.

We can derive an expression between precision and transmittance by applying the propagation of uncertainty as described in Chapter 4. To do so we rewrite Beer's law as

$$C = -\frac{1}{\varepsilon b}\log T \tag{1.3.12}$$

Table 4.3.1 in Chapter 4 helps us complete the propagation of uncertainty for Equation 1.3.12; thus, the absolute uncertainty in the concentration, s_C, is

$$s_c = -\frac{0.4343}{\varepsilon b} \times \frac{s_T}{T} \tag{1.3.13}$$

where s_T is the absolute uncertainty in the transmittance. Dividing Equation 1.3.13 by Equation 1.3.12 gives the relative uncertainty in concentration, s_C/C, as

$$\frac{s_c}{C} = \frac{0.4343 s_T}{T \log T}$$

If we know the transmittance's absolute uncertainty, then we can determine the relative uncertainty in concentration for any measured transmittance.

Determining the relative uncertainty in concentration is complicated because s_T is a function of the transmittance. As shown in Table 10.3.3 , three categories of indeterminate instrumental error are observed [Rothman, L. D.; Crouch, S. R.; Ingle, J. D. Jr. *Anal. Chem.* **1975**, *47*, 1226–1233]. A constant s_T is observed for the uncertainty associated with reading %T on a meter's analog or digital scale. Typical values are ±0.2–0.3% (a k_1 of ±0.002–0.003) for an analog scale and ±0.001% a (k_1 of ±0.00001) for a digital scale.

Table 10.3.3 . Effect of Indeterminate Errors on Relative Uncertainty in Concentration

category	sources of indeterminate error	relative uncertainty in concentration
$s_T = k_1$	%T readout resolution noise in thermal detectors	$\frac{s_C}{C} = \frac{0.4343 k_1}{T \log T}$
$s_T = k_2\sqrt{T^2 + T}$	noise in photon detectors	$\frac{s_C}{C} = \frac{0.4343 k_2}{\log T}\sqrt{1 + \frac{1}{T}}$
$s_T = k_3 T$	positioning of sample cell fluctuations in source intensity	$\frac{s_C}{C} = \frac{0.4343 k_3}{\log T}$

A constant s_T also is observed for the thermal transducers used in infrared spectrophotometers. The effect of a constant s_T on the relative uncertainty in concentration is shown by curve A in Figure 10.3.16 . Note that the relative uncertainty is very large for both high absorbances and low absorbances, reaching a minimum when the absorbance is 0.4343. This source of indeterminate error is important for infrared spectrophotometers and for inexpensive UV/Vis spectrophotometers. To obtain a relative uncertainty in concentration of ±1–2%, the absorbance is kept within the range 0.1–1.

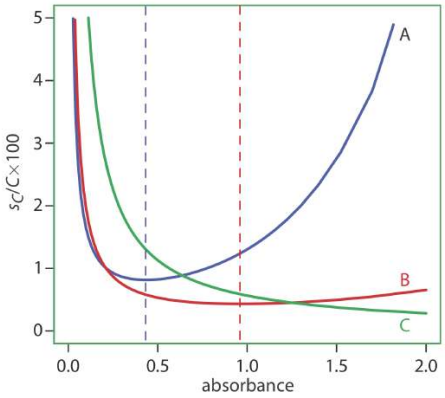


Figure 10.3.16 . Percent relative uncertainty in concentration as a function of absorbance for the categories of indeterminate errors in Table **1.3.10.3**. A: k_1 = ±0.0030; B: k_2 = ±0.0030; and C: k_3= ±0.0130. The dashed lines correspond to the minimum uncertainty for curve A (absorbance of 0.4343) and for curve B (absorbance of 0.963).

Values of s_T are a complex function of transmittance when indeterminate errors are dominated by the noise associated with photon detectors. Curve B in Figure 10.3.16 shows that the relative uncertainty in concentration is very large for low absorbances, but is smaller at higher absorbances. Although the relative uncertainty reaches a minimum when the absorbance is 0.963, there is little change in the relative uncertainty for absorbances between 0.5 and 2. This source of indeterminate error generally limits the precision of high quality UV/Vis spectrophotometers for mid-to-high absorbances.

Finally, the value of s_T is directly proportional to transmittance for indeterminate errors that result from fluctuations in the source's intensity and from uncertainty in positioning the sample within the spectrometer. The latter is particularly important because the optical properties of a sample cell are not uniform. As a result, repositioning the sample cell may lead to a change in the intensity of transmitted radiation. As shown by curve C in Figure 10.3.16 , the effect is important only at low absorbances. This source of indeterminate errors usually is the limiting factor for high quality UV/Vis spectrophotometers when the absorbance is relatively small.

When the relative uncertainty in concentration is limited by the %*T* readout resolution, it is possible to improve the precision of the analysis by redefining 100% T and 0% T. Normally 100% T is established using a blank and 0% T is established while preventing the source's radiation from reaching the detector. If the absorbance is too high, precision is improved by resetting 100% T using a standard solution of analyte whose concentration is less than that of the sample (Figure 10.3.17 a). For a sample whose absorbance is too low, precision is improved by redefining 0% T using a standard solution of the analyte whose concentration is greater than that of the analyte (Figure 10.3.17 b). In this case a calibration curve is required because a linear relationship between absorbance and concentration no longer exists. Precision is further increased by combining these two methods (Figure 10.3.17 c). Again, a calibration curve is necessary since the relation- ship between absorbance and concentration is no longer linear.

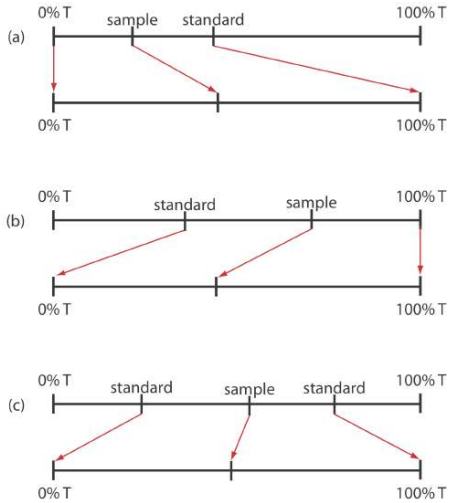


Figure 10.3.17 . Methods for improving the precision of absorption methods: (a) high-absorbance method; (b) low-absorbance method; (c) maximum precision method.

https://chem.libretexts.org/@go/page/379417

Sensitivity

The sensitivity of a molecular absorption method, which is the slope of a Beer's law calibration curve, is the product of the analyte's absorptivity and the pathlength of the sample cell (εb). You can improve a method's sensitivity by selecting a wavelength where absorbance is at a maximum or by increasing pathlength.

> See Figure 10.2.10 for an example of how the choice of wavelength affects a calibration curve's sensitivity.

Selectivity

Selectivity rarely is a problem in molecular absorption spectrophotometry. In many cases it is possible to find a wavelength where only the analyte absorbs. When two or more species do contribute to the measured absorbance, a multicomponent analysis is still possible, as shown in Example 10.3.2 and Example 10.3.3 .

Time, Cost, and Equipment

The analysis of a sample by molecular absorption spectroscopy is relatively rapid, although additional time is required if we need to convert a nonabsorbing analyte into an absorbing form. The cost of UV/Vis instrumentation ranges from several hundred dollars for a simple filter photometer, to more than $50,000 for a computer-controlled, high-resolution double-beam instrument equipped with variable slit widths, and operating over an extended range of wavelengths. Fourier transform infrared spectrometers can be obtained for as little as $15,000–$20,000, although more expensive models are available.

This page titled 1.3: UV/Vis and IR Spectroscopy is shared under a CC BY-NC-SA 4.0 license and was authored, remixed, and/or curated by David Harvey.

- **10.3: UV/Vis and IR Spectroscopy** by David Harvey is licensed CC BY-NC-SA 4.0.

1.4: Fourier-Transform Infrared Spectroscopy -- Additional Readings

1.4: Fourier-Transform Infrared Spectroscopy -- Additional Readings is shared under a not declared license and was authored, remixed, and/or curated by LibreTexts.

SECTION OVERVIEW

1.5: Raman Spectroscopy

Raman spectroscopy is a chemical instrumentation technique that exploits molecular vibrations.

1.5.1: Raman- Application

1.5.2: Raman- Theory

1.5.3: Resonant vs. Nonresonant Raman Spectroscopy

Template:HideTOC

1.5: Raman Spectroscopy is shared under a CC BY 4.0 license and was authored, remixed, and/or curated by LibreTexts.

1.5.1: Raman- Application

If one can extract all of the vibrational information corresponds a molecule, its molecular structure can then be determined. In the field of spectroscopy, two main techniques are applied in order to detect molecular vibrational motions: Infrared spectroscopy (IR) and Raman spectroscopy. Raman Spectroscopy has its unique properties which have been used very commonly and widely in Inorganic, Organic, Biological systems [1] and Material Science [2], [3], etc.

Introduction

Generally speaking, vibrational and rotational motions are unique for every molecule. The uniqueness to molecules are in analogous to fingerprint identification of people hence the term molecular fingerprint. Study the nature of molecular vibration and rotation is particularly important in structure identification and molecular dynamics. Two of the most important techniques in studying vibration/rotation information are IR spectroscopy and Raman spectroscopy. IR is an absorption spectroscopy which measures the transmitted light. Coupling with other techniques, such as Fourier Transform, IR has been highly successful in both organic and inorganic chemistry.

Unlike IR, Raman spectroscopy measures the scattered light (Figure 2). There are three types of scattered lights: Rayleigh scattering, Stokes scattering, and anti-stokes scattering. Rayleigh scattering is elastic scattering where there is no energy exchange between the incident light and the molecule. Stokes scattering happens when there is an energy absorption from the incident light, while anti-stokes scattering happens when the molecule emites energy to the incident light. Thus, Stokes scattering results in a red shift, while anti-stokes scattering results in a blue shift. (Figure 1) Stokes and Anti-Stokes scattering are called Raman scattering which can provide the vibration/rotation information

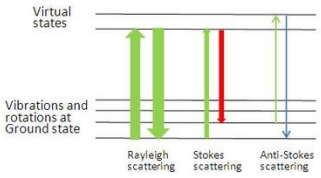


Figure 1: Scattered lights (The line thickness represents the intensity of the signal)

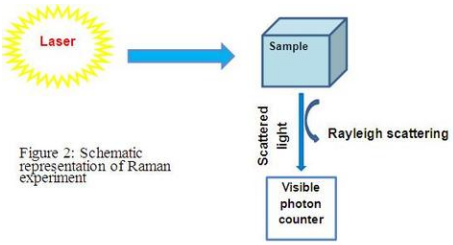


Figure 2: Schematic representation of Raman experiment

The intensity of Rayleigh scattering is around 10^7 times that of Stokes scattering. [4]According to the Boltzmann distribution, anti-Stokes is weaker than Stokes scattering. Thus, the main difficulty of Raman spectroscopy is to detect the Raman scattering by filtering out the strong Rayleigh scattering. In order to reduce the intensity of the Rayleigh scattering, multiple monochromators are applied to selectively transmit the needed wave range. An alternative way is to use Rayleigh filters. There are many types of Rayleigh filters. One common way to filter the Rayleigh light is by interference.

Because of the weakness of Raman scattering, the resolving power of a Raman spectrometer is much higher than an IR specctrometer. A resolution of 10^5 is needed in Raman while 10^3 is sufficient in IR. [5] In order to achieve high resolving power, prisms, grating spectrometers or interferometers are applied in Raman instruments.

Despite the limitations above, Raman spectroscopy has some advantages over IR spectroscopy as follows:

1. Raman Spectroscopy can be used in aqueous solutions (while water can absorb the infrared light strongly and affect the IR spectrum).
2. Because of the different selection rules, vibrations inactive in IR spectroscopy may be seen in Raman spectroscopy. This helps to complement IR spectroscopy.
3. There is no destruction to the sample in Raman Spectroscopy. In IR spectroscopy, samples need to disperse in transparent matrix. For example grind the sample in solid KBr. In RS, no such destructions are needed.
4. Glass vials can be used in RS *(this should only work in the visible region. If in UV region, glass is not applicable because it can strongly absorb light too.)*
5. Raman Spectroscopy needs relative short time. So we can do Raman Spectroscopy detection very quickly.

After analysis of the advantages and disadvantages of Raman Spectroscopy technique, we can begin to consider the application of Raman Spectroscopy in inorganic, organic, biological systems and Material Science, etc.

Applications

Raman Spectroscopy application in inorganic systems

X-ray diffraction (XRD) has been developed into a standard method of determining structure of solids in inorganic systems. Compared to XRD, it is usually necessary to obtain other information (NMR, electron diffraction, or UV-Visible) besides vibrational information from IR/Raman in order to elucidate the structure. Nevertheless, vibrational spectroscopy still plays an important role in inorganic systems. For example, some small reactive molecules only exist in gas phase and XRD can only be applied for solid state. Also, XRD cannot distinguish between the following bonds: –CN vs. –NC, –OCN vs. –NCO,–CNO vs. –ONC, -SCN vs. –NCS. [7] Furthermore, IR and Raman are fast and simple analytical method, and are commonly used for the first approximation analysis of an unknown compound.

Raman spectroscopy has considerable advantages over IR in inorganic systems due to two reasons. First, since the laser beam used in RS and the Raman-scattered light are both in the visible region, glass (Pyrex) tubes can be used in RS. On the other hand, glass absorbs infrared radiation and cannot be used in IR. However, some glass tubes, which contain rare earth salts, will gives rises to fluorescence or spikes. Thus, using of glass tubes in RS still need to be careful. Secondly, since water is a very weak Raman scatter but has a very broad signal in IR, aqueous solution can be directly analyzed using RS.

Raman Spectroscopy and IR have different selection rules. RS detects the polarizability change of a molecule, while IR detects the dipole momentum change of a molecule. Principle about the RS and IR can be found at Chemwiki Infrared Theory and Raman Theory. Thus, some vibration modes that are active in Raman may not be active IR, vice versa. As a result, both of Raman and IR spectrum are provided in the stucture study. As an example, in the study of Xenon Tetrafluoride. There are 3 strong bands in IR and solid Raman shows 2 strong bands and 2 weaker bands. These information indicates that Xenon Tetrafluoride is a planar molecule and has a symmetry of D4h. [8] Another example is the application of Raman Spectroscopy in homonuclear diatomic molecules. Homonuclear diatomic molecules are all IR inactive, fortunately, the vibration modes for all the homonuclear diatomic molecules are always Raman Spectroscopy active.

Raman Spectroscopy Application in Organic Systems

Unlike inorganic compounds, organic compounds have less elements mainly carbons, hydrogens and oxygens. And only a certain function groups are expected in organic specturm. Thus, Raman and IR spectroscopy are widely used in organic systems. Characteristic vibrations of many organic compounds both in Raman and IR are widely studied and summarized in many literature. [5] Qualitative analysis of organic compounds can be done base on the characteristic vibrations table.

Table 1: Characteristic frequencies of some organic function group in Raman and IR

Vibration	Region(cm^{-1})	Raman intensity	IR intensity
v(O-H)	3650~3000	weak	strong
v(N-H)	3500~3300	medium	medium
v(C=O)	1820~1680	strong~weak	very strong
v(C=C)	1900~1500	very strong~medium	0~weak

“RS is similar to IR in that they have regions that are useful for functional group detection and fingerprint regions that permit the identification of specific compounds.”[1] While from the different selection rules of Raman Spectroscopy and IR, we can get the Mutual Exclusion rule [5], which says that for a molecule with a center of symmetry, no mode can be both IR and Raman Spectroscopy active. So, if we find a strong bond which is both IR and Raman Spectroscopy active, the molecule doesn't have a center of symmetry.

Non-classical Raman Spectroscopy

Although classical Raman Spectroscopy has been successfully applied in chemistry, this technique has some major limitations as follows[5]:

1. The probability for photon to undergo Raman Scattering is much lower than that of Rayleigh scattering, which causes low sensitivity of Raman Spectroscopy technique. Thus, for low concentration samples, we have to choose other kinds of techniques.
2. For some samples which are very easily to generate fluorescence, the fluorescence signal may totally obscure the Raman signal. We should consider the competition between the Raman Scattering and fluorescence.
3. In some point groups, such as C_6 , D_6 , D_{6h} , C_{4h} , D_{2h}, there are some vibrational modes that is neither Raman or IR active.
4. The resolution of the classical Raman Spectroscopy is limited by the resolution of the monochromator.

In order to overcome the limitations, special techniques are used to modify the classical Raman Spectroscopy. These non-classical Raman Spectroscopy includes: Resonance Raman Spectroscopy, surface enhanced Raman Spectroscopy, and nonlinear coherent Raman techniques, such as hyper Raman spectroscopy

Resonance Raman Scattering (RRS)

The resonance effect is observed when the photon energy of the exciting laser beam is equal to the energy of the allowed electronic transition. Since only the allowed transition is affected, (in terms of group theory, these are the totally symmetric vibrational ones.), only a few Raman bands are enhanced (by a factor of 10^6). As a result, RRS can increase the resolution of the classical Raman Spectroscopy, which makes the detection of dilution solution possible (concentrations as low as 10^{-3} M). RRS is extensively used for biological molecules because of its ability to selectively study the local environment. As an example, the Resonance Raman labels are used to study the biologically active sites on the bond ligand. RRS can also be used to study the electronic excited state. For example, the excitation profile which is the Raman intensity as a function of incident laser intensity can tell the interaction between the electronic states and the vibrational modes. Also, it can be used to measure the atomic displacement between the ground state and the excited state.

Surface Enhanced Raman Scattering (SERS)

At 1974, Fleischmann discovered that pyridine adsorbed onto silver electrodes showed enhanced Raman signals. This phenomenon is now called surface enhanced Raman Scattering (SERS). Although the mechanism of SERS is not yet fully understood, it is believed to result from an enhancement either of transition polarizability, α,or the electric field, E, by the interaction with the rough metallic support.

Unlike RRS, SERS enhances every band in the Raman spectrum and has a high sensitivity. Due to the high enhancement (by a factor of $10^{10\sim11}$), the SERS results in a rich spectrum and is an ideal tool for trace analysis and in situ study of interfacial process. Also, it is a better tool to study highly diluted solutions. A concentration of $4x10^{-12}$ M was reported by Kneipp using SERS. [5]

Nonlinear Raman Spectroscopy

In a nonlinear process, the output is not linearly proportional to its input. This happens when the perturbation become large enough that the response to the perturbation doesn’t follows the perturbation’s magnitude. Nonlinear Raman Spectroscopy includes: Hyper Raman spectroscopy, coherent anti-Stokes Raman Spectroscopy, coherent Stokes Raman spectroscopy, stimulated Raman gain and inverse Ramen spectroscopy. Nonlinear Raman spectroscopy is more sensitive than classical Raman spectroscopy and can effectively reduce/remove the influence of fluorescence. The following paragraph will focus on the most useful nonlinear Raman spectroscopy---coherent anti-Stokes Raman Spectroscopy (CARS):

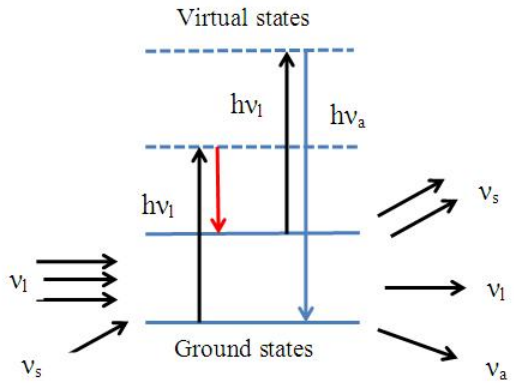


Figure 3: Schematic representation of coherent anti-Stoke Raman. ν is the frequency of the light. The subscript1 represents laser light; s represents Stoke scattering light; a represents anti-Stoke scattering light.

Figure 3) The two laser sources generate a coherent beam at frequency ν_3. There is a signal enhancement when ν_3 equal the anti-Stokes scattering (ν_a), and the vibrational transition equals to the energy difference between two light sources. Since CARS signal is at anti-Stoke region (a higher energy region than fluorescence), the influence of fluorescence is eliminated. Thus, CARS is very useful for molecules with high fluorescence effect, for example, some biological molecules. Another important advantage of CARS is that the resolution is no longer limited by the monochromator as in classical Raman because only the anti-Stokes frequency is studied in CARS. High-resolution CARS has been developed as a tool for small-time scale process, such as photochemical analysis and chemical kinetics studies. [6]

References

1. Principles of Instrumental Analysis, fifth edition. Skoog, Holler and Nieman.
2. Infrared and Raman Spectra of Inorganic and Coordination Compounds, fifth edition. Kazuo Nakamoto.
3. Symmetry and Spectroscopy an introduction to vibrational and electronic spectroscopy. Daniel C. Harris, etc.
4. P. Bisson, G. Parodi, D. Rigos, J.E. Whitten, The Chemical Educator, 2006, Vol. 11, No. 2
5. B. Schrader, Infrared and Raman Spectroscopy, VCH, 1995, ISBN:3-527-26446-9
6. S.A. Borman, Analytical Chemistry, 1982, Vol. 54, No. 9, 1021A-1026A
7. K. Nakamoto, Infrared Spectra of Inorganic and Coordination Compounds, 3rd edition. Wiley Intrsc John Wiley & Sons, New York London Sydney Toronto, 1978
8. H.H. Claassen, C.L. Chernick, J.G. Malm, 1963 J. Am. Chem. Soc., 85, 1927

Problems

1. What are the advantages and disadvantages for Raman spectroscopy, comparing with IR spectroscopy?
2. Please briefly explain the mutual exclusive principle in Raman and IR spectroscopy.

1.5.1: Raman- Application is shared under a CC BY 4.0 license and was authored, remixed, and/or curated by Xu Yuntao & Qiuting Hong.

- **Raman: Application** by Qiuting Hong, Xu Yuntao is licensed CC BY 4.0.

1.5.2: Raman- Theory

The phenomenon of Raman scattering of light was first postulated by Smekai in 1923 and first observed experimentally in 1928 by Raman and Krishnan. Raman scattering is most easily seen as the change in frequency for a small percentage of the intensity in a monochromatic beam as the result of coupling between the incident radiation and vibrational energy levels of molecules. A vibrational mode will be Raman active only when it changes the polariazbility of the molecule.

Introduction

When monochromatic radiation with a wavenumber $\tilde{\nu}_0$ is incident on systems, most of it is transmitted without change, but, in addition, some scattering of the radiation occurs. If the frequency content of the scattered radiation is analyzed, there will be observed to be present not only the wavenumber $\tilde{\nu}_0$ associated with the incident radiation but also, in general, pairs of new wavenumbers of the type $\tilde{\nu}' = \tilde{\nu}_0 + \tilde{\nu}_M$. In molecular systems, the wavenumbers $\tilde{\nu}_M$ are found to lie principally in the ranges associated with transitions between rotational, vibrational, and electronic levels.

Such scattering of radiation with change of wavenumber is called Raman Scattering, after the Indian scientist C. V. Raman who, with K. S. Krishnan, first observed this phenomenon in liquids in 1928. The effect had been predicted on theoretical grounds in 1923 by A. Smekal. Due to its very low scattering efficiency, Raman spectroscopy did not become popular until powerful laser systems were available after the 1960s. Now, Raman spectroscopy has become one of the most popular approaches to study the vibrational structures of molecules together with infrared spectrum.

The origin of the modified frequencies found in Raman scattering is explained in terms of energy transfer between the scattering system and the incident radiation. When a system interacts with radiation of wavenumber $\tilde{\nu}_0$, it makes an upward transition from a lower energy level E_1 to an upper energy level E_2. It must then acquire the necessary energy, $\Delta E = E_2 - E_1$, from the incident radiation. The energy ΔE is expressed in terms of a wavenumber $\tilde{\nu}_M$ associated with the two levels involved, where

$$\Delta E = hc\tilde{\nu}_M \tag{1.5.2.1}$$

This energy requirement is regarded as being provided by the absorption of one photon of the incident radiation of energy $hc\tilde{\nu}_0$ and the simultaneous emission of a photon of smaller energy $hc(\tilde{\nu}_0 - \tilde{\nu}_M)$, so that scattering of radiation of lower wavenumber, $\tilde{\nu}_0 - \tilde{\nu}_M$, occurs. Alternatively, the interaction of the radiation with the system may cause a downward transition from a higher energy level E_2 to a lower energy level E_1, in which case it makes available energy

$$E_2 - E_1 = hc\tilde{\nu}_M \tag{1.5.2.2}$$

Again a photon of the incident radiation of energy $hc\tilde{\nu}_0$ and the simultaneous emission of a photon of higher energy $hc(\tilde{\nu}_0 + \tilde{\nu}_M)$, so that scattering of radiation of higher wavenumber, $\tilde{\nu}_0 + \tilde{\nu}_M$, occurs.

In the case of Rayleigh scattering, although there is no resultant change in the energy state of the system, the system still participates directly in the scattering act, causing one photon of incident radiation $hc\tilde{\nu}_0$ to be absorbed and a photon of the same energy to be emitted simultaneously, so that scattering of radiation of unchanged wavenumber, $\tilde{\nu}_0$, occurs.

It is clear that, as far as wavenumber is concerned, a Raman band is to be characterized not by its absolute wavenumber, $\tilde{\nu}' = \tilde{\nu}_0 \pm \tilde{\nu}_M$, but by the magnitude of its wavenumber shift $\tilde{\nu}_M$ from the incident wavenumber. Such wavenumber shifts are often referred to as Raman wavenumbers. Where it is necessary to distinguish Stokes and anti-Stokes Raman scattering we shall define $\Delta\tilde{\nu}$ to be positive for Stokes scattering and negative for anti-Stokes scattering, that is $\Delta\tilde{\nu} = \tilde{\nu}_0 + \tilde{\nu}'$ (see Fig. 1).

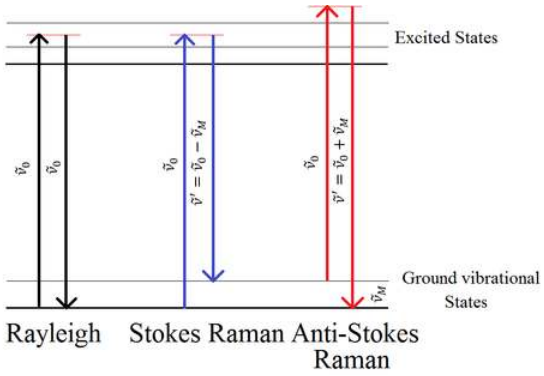


Figure 1. Diagrammatic representation of an energy transfer model of Rayleigh scattering, Stokes Raman and anti-Stokes Raman scattering.

The intensity of anti-Stokes relative to Stokes Raman scattering decreases rapidly with increase in the wavenumber shift. This is because anti-Stokes Raman scattering involves transitions to a lower energy state from a populated higher energy states.

Classical theory

According to the classical theory of electromagnetic radiation, electric and magnetic fields oscillating at a given frequency are able to give out electromagnetic radiation of the same frequency. One could use electromagnetic radiation theory to explain light scattering phenomena.

For a majority of systems, only an induced electric dipole moment $\boldsymbol{\mu}$ is taken into consideration. This dipole moment which is induced by the electric field $\boldsymbol{E}$ could be expressed by the power series

$$\mu = \mu^{(1)} + \mu^{(2)} + \mu^{(3)} + \cdots \tag{1.5.2.3}$$

where

$$\mu^{(1)} = \alpha \cdot \mathbf{E} \tag{1.5.2.4}$$

$$\mu^{(2)} = \tfrac{1}{2}\beta \cdot \mathbf{EE}$$

$$\mu^{(3)} = \tfrac{1}{6}\gamma \cdot \mathbf{EEE}$$

$\boldsymbol{\alpha}$ is termed the polarizability tensor. It is a second-rank tensor with all the components in the unit of $CV^{-1}m^2$. Typically, orders of magnitude for components in $\boldsymbol{\alpha}$, $\boldsymbol{\beta}$, and $\boldsymbol{\gamma}$ are as follows, $\boldsymbol{\alpha}$, 10^{-40} $CV^{-1}m^2$; $\boldsymbol{\beta}$, 10^{-50} $CV^{-2}m^3$; and $\boldsymbol{\gamma}$, 10^{-61} $CV^{-3}m^4$. According to the values, the contributions of $\boldsymbol{\mu}^{(2)}$and $\boldsymbol{\mu}^{(3)}$ are quite small unless electric field is very high. Since Rayleigh and Raman scattering are observed quite readily with very much lower electric field intensities, one may expect to explain Rayleigh and Raman scattering in terms of $\boldsymbol{\mu}^{(1)}$ only.

We shall now consider the interaction of a molecular system with the harmonically oscillating electric field in the frequency ω_0. To make the explanation easily, we shall ignore the rotation but just consider the vibration part. It is to be expected that the polarizability will be a function of the nuclear coordinates. The variation of components in polarizability tensor with vibrational coordinates is expressed in a Taylor series

$$\alpha_{ij} = (\alpha_{ij})_0 + \sum_k \left(\frac{\partial \alpha_{ij}}{\partial Q_k}\right)_0 Q_k + \frac{1}{2}\sum_{k,l}\left(\frac{\partial^2 \alpha_{ij}}{\partial Q_k \partial Q_l}\right)_0 Q_k Q_l + \cdots$$

where $(\alpha_{ij})_0$ is the α_{ij} value at the equilibrium configuration, Q_k, Q_l are normal coordinates of vibration at frequencies ω_k, ω_l. We shall make a harmonic approximation to neglect the terms which involve powers of Q higher than first. After initially fixing our attention on one normal mode, Q_k, we could get

$$\alpha_{ij} = (\alpha_{ij})_0 + \left(\frac{\partial \alpha_{ij}}{\partial Q_k}\right)_0 Q_k$$

As for a harmonic vibration,

$$Q_k = Q_{k0}\cos(\omega_k t + \delta_k) \tag{1.5.2.5}$$

Then we could get the expression of $\boldsymbol{\alpha}$ tensor resulting from k-th vibration,

$$\alpha_k = \alpha_0 + \left(\frac{\partial \alpha_k}{\partial Q_k}\right)_0 Q_{k0} \cos\left(\omega_k t + \delta_k\right)$$

Now, under the influence of electromagnetic radiation at frequency ω_0, the induced electric dipole moment $\boldsymbol{\mu}^{(1)}$ is expressed,

$$\mu^{(1)} = \alpha_k \cdot \mathbf{E}_0 \cos\omega_0 t = \alpha_0 \cdot \mathbf{E}_0 \cos\omega_0 t + \left(\frac{\partial \alpha_k}{\partial Q_k}\right)_0 \cdot \mathbf{E}_0 Q_{k0} \cos\omega_0 t \cos\left(\omega_k t + \delta_k\right) t = \tag{1.5.2.6}$$

$$\alpha_0 \cdot \mathbf{E}_0 \cos\omega_0 t + \frac{1}{2}\left(\frac{\partial \alpha_k}{\partial Q_k}\right)_0 \cdot \mathbf{E}_0 Q_{k0} \cos\left(\omega_0 t + \omega_k t + \delta_k\right) \tag{1.5.2.7}$$

$$+ \frac{1}{2}\left(\frac{\partial \alpha_k}{\partial Q_k}\right)_0 \cdot \mathbf{E}_0 Q_{k0} \cos\left(\omega_0 t - \omega_k t - \delta_k\right)$$

We see that the linear induced dipole moment $\boldsymbol{\mu}^{(1)}$ has three components with different frequencies,

$\boldsymbol{\alpha_0} \cdot \mathbf{E_0} \cos\omega_0 t$ which gives rise to radiation at ω_0 and accounts for the Rayleigh scattering;

$$\tfrac{1}{2}\left(\tfrac{\partial \alpha_k}{\partial Q_k}\right)_0 \cdot \mathbf{E}_0 Q_{k0} \cos\left(\omega_0 t + \omega_k t + \delta_k\right)$$

which gives rise to radiation at ω_0+ω_k and accounts for the anti-Stokes Raman scattering; and

$$\frac{1}{2}\left(\frac{\partial \alpha_k}{\partial Q_k}\right)_0 \cdot \mathbf{E}_0 Q_{k0} \cos\left(\omega_0 t \omega_k t \delta_k\right) \tag{1.5.2.8}$$

which gives rise to radiation at ω_0-ω_k and accounts for the Stokes Raman scattering.

From these mathematical manipulations, there emerges a useful qualitative picture of the mechanisms of Rayleigh and Raman scattering in terms of classical radiation theory. Rayleigh scattering comes from the dipole oscillating at ω_0 induced in the molecule by the electric field of the incident radiation at frequency ω_0. Raman scattering arises from the dipole moment oscillating at $\omega_0 \pm \omega_k$ produced by the modulation of dipole oscillating at ω_0 with molecular vibration at frequency ω_k. In other words, the frequencies we observe in Raman scattering are beat frequencies of the radiation frequency ω_0 and the molecular vibrational frequency ω_k.

Quantum mechanical treatment

According to the quantum theory, radiation is emitted or absorbed as a result of a system making a downward or upward transition between two discrete energy levels. A quantum theory of spectroscopic processes should, therefore, treat the radiation and molecule together as a complete system, and explore how energy is transferred between the radiation and the molecule as a result of their interaction.

A transition between energy levels of the molecular systems takes place with the emission or absorption of radiation, provided a transition moment associated with the initial and final molecular states is non-zero. The transition moment could be defined as

$$\mathbf{M}_{fi} = \langle \Psi_f \mid \mu \mid \Psi_i \rangle$$

in the Dirac bracket notation, where Ψ_i and Ψ_f are the wave function of initial and final states, respectively, and $\boldsymbol{\mu}$ is the dipole moment operator.

As we have discussed in the classical part, the linear induced dipole moment could be expressed by

$$\mu^{(1)} = \alpha \cdot \mathbf{E} \tag{1.5.2.9}$$

Therefore, in quantum mechanical treatment, if a transition from an initial state to a final state is induced by incident radiation at frequency ω_0, the transition moment is given by

$$\mu_{fi}^{(1)} = \langle \Psi_f \mid \alpha \mid \Psi_i \rangle \cdot \mathbf{E} \tag{1.5.2.10}$$

Now we will examine in more detail the nature of a typical matrix element of the polarizability tensor, like $[\alpha_{xy}]_{fi}$, for Raman scattering. Just like in the classical theory, we will ignore the rotational wave function and consider the vibrational part only.

$$[\alpha_{xy}]_{fi} = \langle \Phi_f \mid \alpha_{xy} \mid \Phi_i \rangle \tag{1.5.2.11}$$

where Φ is the vibrational wave function.

In classical theory,

$$\alpha_{xy} = (\alpha_{xy})_0 + \sum_k \left(\frac{\partial \alpha_{xy}}{\partial Q_k}\right)_0 Q_k + \frac{1}{2}\sum_{k,l}\left(\frac{\partial^2 \alpha_{ij}}{\partial Q_k \partial Q_l}\right)_0 Q_k Q_l + \cdots \quad (1.5.2.12)$$

Introducing the quantum part, we obtain (just consider the first order term)

$$[\alpha_{xy}]_{fi} = (\alpha_{xy})_0 \langle \Phi_f \mid \Phi_i \rangle + \sum_k \left(\frac{\partial \alpha_{xy}}{\partial Q_k}\right)_0 \langle \Phi_f \mid Q_k \mid \Phi_i \rangle$$

In the harmonic oscillator model, the total vibrational wave function is product of the harmonic oscillator wave functions for each of the normal modes of vibration. Thus, for Φ,

$$\Phi_i = \prod_k \Phi_{v_k^i}(Q_k) \quad (1.5.2.13)$$

where $\Phi_{v_k^i}(Q_k)$ is the harmonic oscillator wave function associated with the normal coordinate Q_k, which has a vibrational quantum number v_k^i in a certain state. For harmonic oscillator functions, we have

$$\left\langle \Phi_{v_k^f}(Q_k) \mid \Phi_{v_k^i}(Q_k) \right\rangle = \begin{cases} 0 & \text{for } v_k^f \neq v_k^i \\ 1 & \text{for } v_k^f = v_k^i \end{cases} \quad (1.5.2.14)$$

and

$$\left\langle \Phi_{v_k^f}(Q_k) \mid Q_k \mid \Phi_{v_k^i}(Q_k) \right\rangle = \begin{cases} 0 & for\ v_k^f = v_k^i \\ (v_k^i+1)^{\frac{1}{2}} b_{v_k} & for\ v_k^f = v_k^i + 1 \\ (v_k^i)^{\frac{1}{2}} b_{v_k} & for\ v_k^f = v_k^i - 1 \end{cases} \quad (1.5.2.15)$$

where

$$b_{v_k} = \sqrt{\frac{h}{8\pi^2 v_k}} \quad (1.5.2.16)$$

Selection rules

We are now able to find out the conditions which have to be satisfied if the transition moment is non-zero. We will consider the zero order term which accounts for the Rayleigh scattering part first. This term is none-zero only if $v_k^f = v_k^i$ which means none of the vibrational quantum numbers change during this transition from initial state *i* to final state *f*. Thus, for Rayleigh scattering, the quantum mechanical treatment and the classical theory give the same results.

Then we could go to the first order term $\sum_k \left(\frac{\partial \alpha_{xy}}{\partial Q_k}\right)_0 \langle \Phi_f \mid Q_k \mid \Phi_i \rangle$ which accounts for the Raman scattering part. For the *k*-th summand, it is zero unless every term in the product is non-zero, and to achieve this the following conditions must be satisfied, for all modes except the *k*-th: the vibrational quantum numbers must be the same during the transition, i.e. $v_j^f = v_j^i$ where j≠k; and, for the *k*-th mode, and the vibrational quantum number must change by one unit, i.e. $v_k^f = v_k^i \pm 1$. The transition moment is associated with Stokes Raman scattering for Δv_k=1, and with anti-Stokes Raman scattering for Δv_k=-1. These conditions are a result of the properties of harmonic oscillator wave functions.

It follows from these arguments that, in the harmonic approximation, only vibrational fundamentals, i.e., transitions with only one vibrational quantum number changes by one unit, can be observed in the Raman scattering. However, this Δv_k=±1 restriction is only a necessary but not a sufficient condition for the occurrence of Raman scattering at the *k*-th vibrational mode. The vibrational mode should be Raman active, i.e., at least one of the elements of the derived polarizability tensor should be non-zero.

It can be rigorously established by group theory that the elements of the derived polarizability will be non-zero only if they have the same symmetry with the second order terms, i.e., x^2, y^2, z^2, xy, yz, xz. In other words, the irreducible representation of a certain vibrational mode should have a basis in x^2, y^2, z^2, xy, yz or xz.

Finally, we could establish a much better basis for determining selection rules for vibrational transitions in the Raman effect, if we consider the properties of the vibrational transition polarizability components, rather than the derived prolarizability tensor components. For fundamental vibrational transitions, where in the initial state all vibrational quantum numbers are zero and in the final state only the *k*-th vibrational quantum number has changed to unity,

$$[\alpha_{xy}]_{fi} = \langle \Phi_1 \mid \alpha_{xy} \mid \Phi_0 \rangle$$

According to the group theory, this integral will be non-zero, only if α_{xy} and $\Phi_1(Q_k)$ belong to the same symmetry species, which implies that, under each symmetry operation of the molecule in question, α_{xy} and $\Phi_1(Q_k)$ transform in the same way. This constitutes a general selection rule for the Raman activity of a fundamental transition.

In its most general way, covering all types of transitions, the selection rule is as follows: a transition between two states, $\Psi_i$and Ψ_f, is Raman forbidden unless at least one of the triple products of the type $\Psi_i\alpha_{xy}\Psi_f$ belongs to a representation whose structure contains the totally symmetric species.

References

1. Long, D.A., *Raman Spectoscopy*, McGraw-Hill, Inc., New York, 1977.
2. Szymanski, H. A., *Raman Spectroscopy: Theory and Practice*, Plenum Press, New York, 1967.
3. McCreery, R. L., *Raman Spectroscopy for Chemical Analysis*, John Wiley & Sons, Inc., New York, 2000.
4. Stencel, J. M., *Raman Spectroscopy for Catalysis*, Van Nostrand Reinhold, New York, 1990.
5. Grasselli, J. G.; Bulkin, B. J., *Analytical Raman Spectroscopy*, John Wiley & Sons, Inc., New York, 1991.
6. Harris, D. C.; Bertolucci, M. D.; *Symmetry and Spectroscopy: an introduction to vibrational and electronic spectroscopy*, Dover Publications, Inc., New York, 1989.

1.5.2: Raman- Theory is shared under a CC BY 4.0 license and was authored, remixed, and/or curated by Yang Liu & Hong Gao.

- **Raman: Theory** by Hong Gao, Yang Liu is licensed CC BY 4.0.

1.5.3: Resonant vs. Nonresonant Raman Spectroscopy

Raman spectroscopy is a chemical instrumentation technique that exploits molecular vibrations. It does not require large sample sizes and is non-destructive to samples. It is capable of qualitative analysis of samples and the intensity of spectral bands produced assist in quantitative analysis as well. Raman spectroscopy is even being used in areas outside of physical science (i.e. archeology and art preservation) due to the characteristics mentioned above.

Introduction

Raman spectroscopy is based on scattering of radiation (Raman scattering), which is a phenomenon discovered in 1928 by physicist Sir C. V. Raman. The field of Raman spectroscopy was greatly enhanced by the advent of laser technology during the 1960s.[1] Resonance Raman also helped to advance the field. This technique is more selective compared to non-resonance Raman spectroscopy. It works by exciting the analyte with incident radiation corresponding to the electronic absorption bands.[2] This causes an augmentation of the emission up to a factor of 10^6 in comparison to non-resonance Raman.[2,3]

In this section readers will be introduced to the theory behind resonance and non-resonance Raman spectroscopy. Each technique has its share of advantages and challenges. Each of these aspects will be explored.

Theory

Raman scattering is the basis of the two Raman techniques. A molecule must have polarizability to Raman scatter and its symmetry must be even (or gerade) for it to have polarizability[2]. Furthermore, the more electrons a molecule has gererally increases its polarizability. Polarizability (α) is a measure of an applied electronic field's (E) ability to generate a dipole moment (μ) in the molecule.[5] In other words, it is an alteration of a molecule's electron cloud. Mathematically, this can be determined by the following equation:

$$\mu = \alpha E \tag{1.5.3.1}$$

To help provide a better visualization of how Raman spectroscopy works, a generic diagram can be seen in Figure 2. A sample is irradiated with monochromatic laser light; which is then scattered by the sample. The scattered light passes through a filter to remove any stray light that may have also been scattered by the sample.[2] The filtered light is then dispersed by the diffraction grating and collected on the detector. This set-up works for both the non-resonance and resonance Raman techniques.

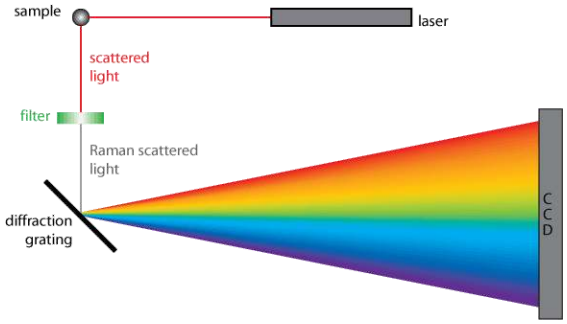


Figure 1: Simplified diagram of how a Raman spectrometer works. Images used with permission from www.doitpoms.ac.uk

Non-resonance Raman scattering occurs when the radiation interacts with a molecule resulting in polarization of the molecule's electrons.[4] The increase in energy from the radiation excites the electrons to an unstable virtual state; therefore, the interaction is almost immediately discontinued and the radiation is emitted (scattered) at a slightly different energy than the incident radiation.[4]

Resonance Raman scattering occurs in a similar fashion. However, the incident radiation is at a frequency near the frequency of an electronic transition of the molecule of interest. This provides enough energy to excite the electrons to a higher electronic state. Figure 1 provides a visual depiction of what non-resonance and resonance Raman scattering looks like in terms of energy levels.

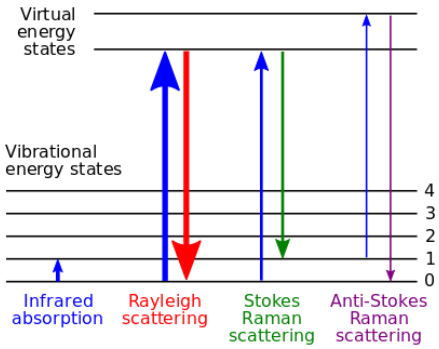


Figure 2: Diagram depicting the different processes for non-resonance and resonance Raman spectroscopy. Notice that fluorescence is more likely to be a problem with resonance Raman than with non-resonance. Image used with permisison from Wikipedia (Credit: Moxfyre).

Advantages of Non-Resonance and Resonance Raman

Instrumental techniques each have certain strengths that make them better suited for some jobs as oppose to others. Non-resonance is a good example of this notion. It is considered better suited for analyzing water containing samples due to water's low polarizability. Non-resonance and resonance Raman each have the capability to analyze samples in the gaseous, liquid, or solid state. Their non-destructive nature makes it a great candidate for doing analysis of delicate materials. Archeologists and art historians even find resonance Raman spectroscopy useful for studying and authentication of artifacts and artwork.[4]

Monochromatic light in the ultraviolet or near-infrared regions is generally used for both resonance and non-resonance Raman spectroscopy. A tunable laser is preferred for resonance Raman and can be an advantage. That is because only one laser is necessary to do analyses of multiples samples in which each one requires a different excitation wavelength.[4] This allows the user to switch out samples without having to switch out the lasers as well. It becomes a matter of just changing the setting on the tunable laser. If the laboratory is not equipped with a tunable laser, any laser that is available can be used to achieve the enhancement of the Raman signal. The only stipulation being that the laser available must have a frequency as near as possible to one of the analyte's electronic transitions.[2] Therefore, researchers conducting resonance Raman spectroscopy without a tunable laser are at the mercy of whatever laser they do have in the laboratory.

Resonance Raman spectroscopy has greater sensitivity compared to its non-resonance counterpart. It is capable of analyzing samples with concentrations as low as 10^{-8} M. Non-resonance Raman can analyze samples with concentrations no lower than 0.1 M. Resonance Raman spectroscopy produces a spectrum with relatively few lines. The reason being that the technique only augments Raman signals affiliated with chromophores in the analyte.[2,4] This makes the technique particularly useful for analysis of larger molecules like biomolecules.

Fluorescence Disadvantage

Fluorescence is a problem for both Resonance Raman techniques, particularly when using sources in the visible range.[2] Non-resonance Raman signals are generally weak and can be easily overwhelmed by fluorescence signals.[6] In addition, fluorescence has a longer excited state lifetime compared to Raman scattering, causing an inability to detect Raman signals.[2,6] Even when the analyte is not a fluorescent molecule, the signal could be a result of the sample matrix content (i.e. solvent or contaminants). Resonance Raman is particularly at risk of inducing fluorescence because it uses sources at frequencies near to that of a molecule's electronic transition. The radiation is more likely to absorb resulting in fluorescence as a possible mechanism for the electrons return to the ground state. Thus, highly fluorescent molecules should be avoided when using Raman spectroscopy; especially resonance Raman. Figure 3 is a general illustration of how a fluorescence signal can overwhelm Raman signals.

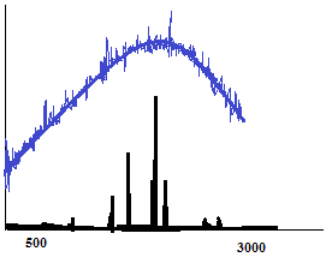


***Figure 3**: Two generic Raman spectra overlaid. The blue Raman spectrum represents one obtained via excitation source in the visible range. The black Raman spectrum represents one obtained via excitation source in the near-infrared range. The black Raman signals are free of fluorescence interference.*

There are techniques that spectroscopists use to avoid fluorescence interference. For instance, background subtraction could be done. Another example is to use near-infrared radiation to excite the sample as a means to overcome fluorescence.[6] A more elaborate method was used by Matousek et al. They took advantage of the differences in excitation lifetimes for Raman and fluorescence. It required implementing shifted excitation Raman difference spectroscopy (SERDS) in conjunction with a device known as a Kerr gate to successfully obtain a resonance Raman spectrum of the rhodamine 6G dye.[6] SERDS is a technique that uses two excitation wavelengths to produce two Raman spectra. The excitation wavelengths have a difference in value that corresponds to the bandwidth of the Raman signal.[6] The two spectra are subtracted from each other and the difference spectra is recreated by means of mathematical processes.[6]

A Kerr gate can be used to remove fluorescence from a Raman signal based on their different lifetimes.[6] The device consists of a couple of crossed polarizers, Kerr medium, and an additional laser to provide a gating pulse.[7] Now consider a sample that has been irradiated resulting in fluorescence and Raman scattering. The fluorescence and Raman scatter would pass through the crossed polarizer and then through the Kerr medium (Matousek et al. used carbon disulfide as the Kerr medium). The Kerr gate is referred to as being open when a laser pulse (the gating pulse) strikes the Kerr medium as the fluorescence and Raman scattered light pass through.[7] Furthermore, the gate remains open for a length of time corresponding to the lifetime of the Raman scatter,[7] The interaction of the gating pulse with the Kerr medium causes the light to become anisotropic and transmit beyond the Kerr medium.[7] The light then goes from being polarized in a linear direction to elliptical polarization. However, Raman scattered light can be selectively switched back to linear polarization by selecting the appropriate propagation length for Kerr medium transmission; or by altering the degree of anisotropy.[7] The Raman scattered light is then allowed to pass through the second crossed polarizer and on to the spectrometer. Any fluorescence that passes through the Kerr medium is prevented from entering the spectrometer due to its inability to transmit through the second crossed polarizer on account of its new elliptical polarization. Figure 4 should assist with the visualization of such process.

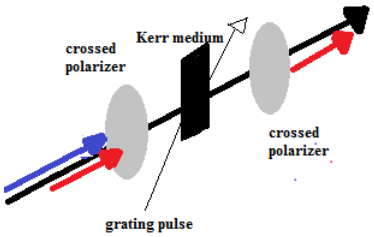


Figure 4: This is an illustration of a Kerr gate. The thick black arrow represents the direction of the signal produced. The blue and red arrows are fluorescence and Raman scattering, respectively. All other components are labeled in the figure.

Conclusions

This module was meant to provide an introduction to the similarities and differences between non-resonance and resonance Raman spectroscopy. Notice that they each have their own advantages making both of them powerful analytical techniques. Non-resonance Raman is more advantageous when compared to IR spectroscopy. However, resonance Raman appears to have the upper hand when compared to its non-resonance counterpart. The important thing is to choose the technique that is most appropriate for the work to be done.

Problems

1. What does Dr. Nivens' quote mean and what can be done to avoid the problem?
2. Archeology and art preservation were mentioned as fields in which Raman spectroscopy is useful due to the following characteristics: non-destructive to sample, qualitative analysis, and quantitative analysis. Name an additional area/field that could benefit from Raman due to these characteristics and why.
3. Does non-resonance Raman or resonance Raman have a better limit of detection?
4. What is polarizability?
5. You are working on a project that is trying to determine if lycopene is absorbed better via supplements or diet. You only have a Raman spectrometer available to conduct your analysis. Thus you decide to determine the amount absorbed in the body by subtracting the amount excreted in urine from the total intake. In general, would it be better to detect lycopene in your biological sample using non-resonance or resonance Raman spectroscopy and why?

References

1. Efremov, E.; Ariese, F.; Gooijer, C. “Achievements in resonance Raman spectroscopy: A Review of a technique with a distinct analytical chemistry potential” *Analytica Chimica Acta*, 606, **2008**, 119-134.
2. Smith, W.; Dent, G. Introduction, Basic Theory, and Principles and Resonance Raman Scattering. *Modern Raman Spectroscopy*, John Wiley & Sons, Ltd, England, 2005; 1-7 & 93-97.
3. Schmitt, M.; Popp, J. “Raman spectroscopy at the beginning of the twenty-first century” *J. Raman Spectrosc.*, 37, **2006**, 20-28.
4. Krishnan, R. S.; Shankar, R. K. “Raman effect: History of the discovery” *J. Raman Spectrosc.*, 10, **1981**, 1-8.
5. Ball, D.W. “Theory of Raman Spectroscopy” *Spectroscopy*, 16 (11), **2001**, 32.
6. Matousek, P.; Towrie, M.; Parker, A. W. “Fluorescence background suppression in Raman spectroscopy using combined Kerr gated and shifted excitation Raman difference techniques” *J. Raman Spectrosc.*, 33, **2002**, 238-242.

Solutions

1. "Fluorescence is the enemy of Raman" refers to the fact that fluorescence induced during Raman spectroscopy will inhibit detection of Raman signals. One way to avoid such a problem is to use an excitation source that is in the ultra-violet or near-infrared range.
2. Answers will vary, but here is an example: Forensic science is a field that could benefit for the indicated characteristics of Raman spectroscopy. The non-destructive nature will insure that precious evidence is not damage or destroyed during analysis. The evidence can then be preserved for additional testing. The qualitative and quantitative factors could provide information to investigators as to what is present in their evidence (i.e. bodily fluids, drugs, accelerants, etc.).
3. Resonance Raman is capable of analyte detection at concentrations as low as 10^{-8} M. The limit of detection is much higher for non-resonance Raman.
4. Polarizability measures the capability of an applied electric field to cause a dipole moment.
5. The sample will most likely contain a multitude of things because it is biological. Resonance Raman would be the better choice because lycopene contains chromophores which are targeted for excitation in that technique. Thus the spectra will not be cluttered by all the other contents in the biological sample.

1.5.3: Resonant vs. Nonresonant Raman Spectroscopy is shared under a CC BY 4.0 license and was authored, remixed, and/or curated by LibreTexts.

- **Resonant vs. Nonresonant Raman Spectroscopy** is licensed CC BY 4.0.

1.6: Current Applications of IR and Raman Spectroscopy

1.6: Current Applications of IR and Raman Spectroscopy is shared under a not declared license and was authored, remixed, and/or curated by LibreTexts.

1.7: Atomic Absorption Spectroscopy

Guystav Kirchoff and Robert Bunsen first used atomic absorption—along with atomic emission—in 1859 and 1860 as a means for identify atoms in flames and hot gases. Although atomic emission continued to develop as an analytical technique, progress in atomic absorption languished for almost a century. Modern atomic absorption spectroscopy has its beginnings in 1955 as a result of the independent work of A. C. Walsh and C. T. J. Alkemade [(a) Walsh, A. *Anal. Chem.* **1991**, *63*, 933A–941A; (b) Koirtyohann, S. R. *Anal. Chem.* **1991**, *63*, 1024A–1031A; (c) Slavin, W. *Anal. Chem.* **1991**, *63*, 1033A–1038A]. Commercial instruments were in place by the early 1960s, and the importance of atomic absorption as an analytical technique soon was evident.

Instrumentation

Atomic absorption spectrophotometers use the same single-beam or double-beam optics described earlier for molecular absorption spectrophotometers (see Figure 10.3.2 and Figure 10.3.3). There is, however, an important additional need in atomic absorption spectroscopy: we first must covert the analyte into free atoms. In most cases the analyte is in solution form. If the sample is a solid, then we must bring the analyte into solution before the analysis. When analyzing a lake sediment for Cu, Zn, and Fe, for example, we bring the analytes into solution as Cu^{2+}, Zn^{2+}, and Fe^{3+} by extracting them with a suitable reagent. For this reason, only the introduction of solution samples is considered in this chapter.

> What reagent we choose to use to bring an analyte into solution depends on our research goals. If we need to know the total amount of metal in the sediment, then we might try a microwave digestion using a mixture of concentrated acids, such as HNO_3, HCl, and HF. This destroys the sediment's matrix and brings everything into solution. On the other hand, if our interest is biologically available metals, we might extract the sample under milder conditions using, for example, a dilute solution of HCl or CH_3COOH at room temperature.

Atomization

The process of converting an analyte to a free gaseous atom is called ***atomization***. Converting an aqueous analyte into a free atom requires that we strip away the solvent, volatilize the analyte, and, if necessary, dissociate the analyte into free atoms. Desolvating an aqueous solution of $CuCl_2$, for example, leaves us with solid particulates of $CuCl_2$. Converting the particulate $CuCl_2$ to gas phases atoms of Cu and Cl requires thermal energy.

$$\mathrm{CuCl_2}(aq) \rightarrow \mathrm{CuCl_2}(s) \rightarrow \mathrm{Cu}(g) + 2\mathrm{Cl}(g)$$

There are two common atomization methods: flame atomization and electrothermal atomization, although a few elements are atomized using other methods.

Flame Atomizer

Figure 10.4.1 shows a typical flame atomization assembly with close-up views of several key components. In the unit shown here, the aqueous sample is drawn into the assembly by passing a high-pressure stream of compressed air past the end of a capillary tube immersed in the sample. When the sample exits the nebulizer it strikes a glass impact bead, which converts it into a fine aerosol mist within the spray chamber. The aerosol mist is swept through the spray chamber by the combustion gases—compressed air and acetylene in this case—to the burner head where the flame's thermal energy desolvates the aerosol mist to a dry aerosol of small, solid particulates. The flame's thermal energy then volatilizes the particles, producing a vapor that consists of molecular species, ionic species, and free atoms.

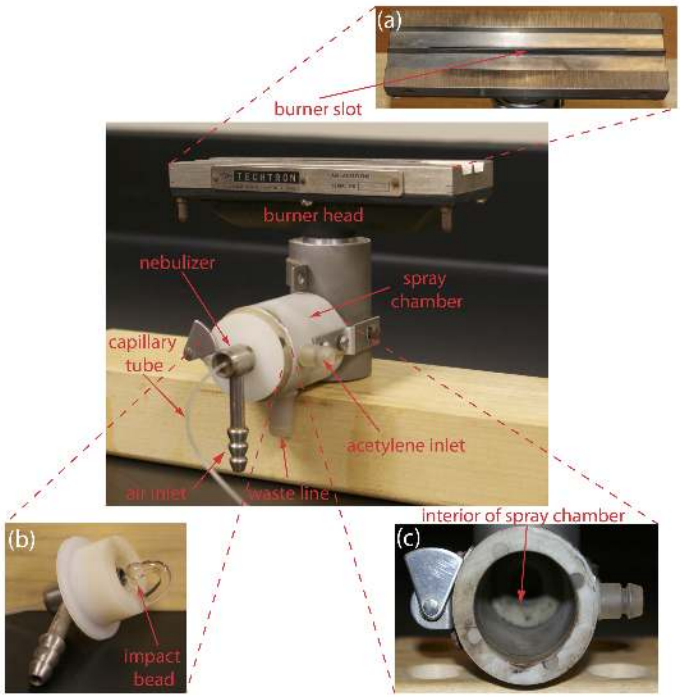


Figure 10.4.1 . Flame atomization assembly with expanded views of (a) the burner head showing the burner slot where the flame is located; (b) the nebulizer's impact bead; and (c) the interior of the spray chamber. Although the unit shown here is from an instrument dating to the 1970s, the basic components of a modern flame AA spectrometer are the same.

Burner. The slot burner in Figure 10.4.1 a provides a long optical pathlength and a stable flame. Because absorbance is directly proportional to pathlength, a long pathlength provides greater sensitivity. A stable flame minimizes uncertainty due to fluctuations in the flame.

The burner is mounted on an adjustable stage that allows the entire assembly to move horizontally and vertically. Horizontal adjustments ensure the flame is aligned with the instrument's optical path. Vertical adjustments change the height within the flame from which absorbance is monitored. This is important because two competing processes affect the concentration of free atoms in the flame. The more time an analyte spends in the flame the greater the atomization efficiency; thus, the production of free atoms increases with height. On the other hand, a longer residence time allows more opportunity for the free atoms to combine with oxygen to form a molecular oxide. As seen in Figure 10.4.2 , for a metal this is easy to oxidize, such as Cr, the concentration of free atoms is greatest just above the burner head. For a metal, such as Ag, which is difficult to oxidize, the concentration of free atoms increases steadily with height.

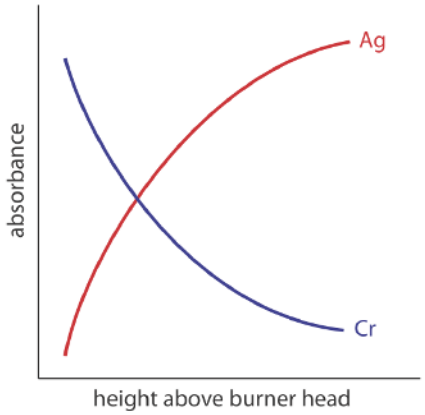


Figure 10.4.2 . Absorbance versus height profiles for Ag and Cr in flame atomic absorption spectroscopy.

Flame. The flame's temperature, which affects the efficiency of atomization, depends on the fuel–oxidant mixture, several examples of which are listed in Table 10.4.1 . Of these, the air–acetylene and the nitrous oxide–acetylene flames are the most

popular. Normally the fuel and oxidant are mixed in an approximately stoichiometric ratio; however, a fuel-rich mixture may be necessary for easily oxidized analytes.

Table 10.4.1 . Fuels and Oxidants Used for Flame Combustion

fuel	oxidant	temperature range (^{o}C)
natural gas	air	1700–1900
hydrogen	air	2000–2100
acetylene	air	2100–2400
acetylene	nitrous oxide	2600–2800
acetylene	oxygen	3050–3150

Figure 10.4.3 shows a cross-section through the flame, looking down the source radiation's optical path. The primary combustion zone usually is rich in gas combustion products that emit radiation, limiting is useful- ness for atomic absorption. The interzonal region generally is rich in free atoms and provides the best location for measuring atomic absorption. The hottest part of the flame typically is 2–3 cm above the primary combustion zone. As atoms approach the flame's secondary combustion zone, the decrease in temperature allows for formation of stable molecular species.

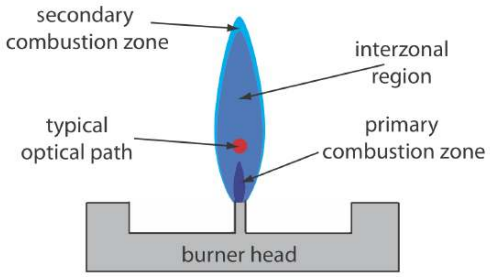


Figure 10.4.3 . Profile of typical flame using a slot burner. The relative size of each zone depends on many factors, including the choice of fuel and oxidant, and their relative proportions.

Sample Introduction. The most common means for introducing a sample into a flame atomizer is a continuous aspiration in which the sample flows through the burner while we monitor absorbance. Continuous aspiration is sample intensive, typically requiring from 2–5 mL of sample.

Flame microsampling allows us to introduce a discrete sample of fixed volume, and is useful if we have a limited amount of sample or when the sample's matrix is incompatible with the flame atomizer. For example, continuously aspirating a sample that has a high concentration of dissolved solids—sea water, for example, comes to mind—may build-up a solid de- posit on the burner head that obstructs the flame and that lowers the absorbance. Flame microsampling is accomplished using a micropipet to place 50–250 µL of sample in a Teflon funnel connected to the nebulizer, or by dipping the nebulizer tubing into the sample for a short time. Dip sampling usually is accomplished with an automatic sampler. The signal for flame microsampling is a transitory peak whose height or area is proportional to the amount of analyte that is injected.

Advantages and Disadvantages of Flame Atomization. The principal advantage of flame atomization is the reproducibility with which the sample is introduced into the spectrophotometer; a significant disadvantage is that the efficiency of atomization is quite poor. There are two reasons for poor atomization efficiency. First, the majority of the aerosol droplets produced during nebulization are too large to be carried to the flame by the combustion gases. Consequently, as much as 95% of the sample never reaches the flame, which is the reason for the waste line shown at the bottom of the spray chamber in Figure 10.4.1 . A second reason for poor atomization efficiency is that the large volume of combustion gases significantly dilutes the sample. Together, these contributions to the efficiency of atomization reduce sensitivity because the analyte's concentration in the flame may be a factor of 2.5×10^{-6} less than that in solution [Ingle, J. D.; Crouch, S. R. *Spectrochemical Analysis*, Prentice-Hall: Englewood Cliffs, NJ, 1988; p. 275].

Electrothermal Atomizers

A significant improvement in sensitivity is achieved by using the resistive heating of a graphite tube in place of a flame. A typical electrothermal atomizer, also known as a ***graphite furnace***, consists of a cylindrical graphite tube approximately 1–3 cm in length and 3–8 mm in diameter. As shown in Figure 10.4.4 , the graphite tube is housed in an sealed assembly that has an optically transparent window at each end. A continuous stream of inert gas is passed through the furnace, which protects the graphite tube from oxidation and removes the gaseous products produced during atomization. A power supply is used to pass a current through the graphite tube, resulting in resistive heating.

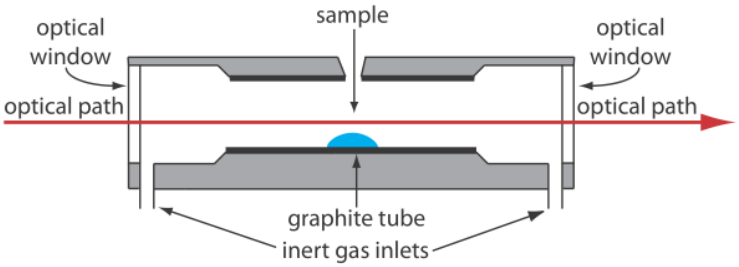


Figure 10.4.4 . Diagram showing a cross-section of an electrothermal analyzer.

Samples of between 5–50 μL are injected into the graphite tube through a small hole at the top of the tube. Atomization is achieved in three stages. In the first stage the sample is dried to a solid residue using a current that raises the temperature of the graphite tube to about 110°C. In the second stage, which is called ashing, the temperature is increased to between 350–1200°C. At these temperatures organic material in the sample is converted to CO_2 and H_2O, and volatile inorganic materials are vaporized. These gases are removed by the inert gas flow. In the final stage the sample is atomized by rapidly increasing the temperature to between 2000–3000°C. The result is a transient absorbance peak whose height or area is proportional to the absolute amount of analyte injected into the graphite tube. Together, the three stages take approximately 45–90 s, with most of this time used for drying and ashing the sample.

Electrothermal atomization provides a significant improvement in sensitivity by trapping the gaseous analyte in the small volume within the graphite tube. The analyte's concentration in the resulting vapor phase is as much as **1000 ×** greater than in a flame atomization [Parsons, M. L.; Major, S.; Forster, A. R. *Appl. Spectrosc.* **1983**, *37*, 411–418]. This improvement in sensitivity—and the resulting improvement in detection limits—is offset by a significant decrease in precision. Atomization efficiency is influenced strongly by the sample's contact with the graphite tube, which is difficult to control reproducibly.

Miscellaneous Atomization Methods

A few elements are atomized by using a chemical reaction to produce a volatile product. Elements such as As, Se, Sb, Bi, Ge, Sn, Te, and Pb, for example, form volatile hydrides when they react with $NaBH_4$ in the presence of acid. An inert gas carries the volatile hydride to either a flame or to a heated quartz observation tube situated in the optical path. Mercury is determined by the cold-vapor method in which it is reduced to elemental mercury with $SnCl_2$. The volatile Hg is carried by an inert gas to an unheated observation tube situated in the instrument's optical path.

Quantitative Applications

Atomic absorption is used widely for the analysis of trace metals in a variety of sample matrices. Using Zn as an example, there are standard atomic absorption methods for its determination in samples as diverse as water and wastewater, air, blood, urine, muscle tissue, hair, milk, breakfast cereals, shampoos, alloys, industrial plating baths, gasoline, oil, sediments, and rocks.

Developing a quantitative atomic absorption method requires several considerations, including choosing a method of atomization, selecting the wavelength and slit width, preparing the sample for analysis, minimizing spectral and chemical interferences, and selecting a method of standardization. Each of these topics is considered in this section.

Developing a Quantitative Method

Flame or Electrothermal Atomization? The most important factor in choosing a method of atomization is the analyte's concentration. Because of its greater sensitivity, it takes less analyte to achieve a given absorbance when using electrothermal atomization. Table 10.4.2 , which compares the amount of analyte needed to achieve an absorbance of 0.20 when using flame

atomization and electrothermal atomization, is useful when selecting an atomization method. For example, flame atomization is the method of choice if our samples contain 1–10 mg Zn^{2+}/L, but electrothermal atomization is the best choice for samples that contain 1–10 μg Zn^{2+}/L.

Table 10.4.2 . Concentration of Analyte (in mg/L) That Yields an Absorbance of 0.20

element	flame atomization	electrothermal atomization
Ag	1.5	0.0035
Al	40	0.015
As	40	0.050
Ca	0.8	0.003
Cd	0.6	0.001
Co	2.5	0.021
Cr	2.5	0.0075
Cu	1.5	0.012
Fe	2.5	0.006
Hg	70	0.52
Mg	0.15	0.00075
Mn	1	0.003
Na	0.3	0.00023
Ni	2	0.024
Pb	5	0.080
Pt	70	0.29
Sn	50	0.023
Zn	0.3	0.00071

Source: Varian Cookbook, SpectraAA Software Version 4.00 Pro.
As: 10 mg/L by hydride vaporization; Hg: 11.5 mg/L by cold-vapor; and Sn:18 mg/L by hydride vaporization

Selecting the Wavelength and Slit Width. The source for atomic absorption is a hollow cathode lamp that consists of a cathode and anode enclosed within a glass tube filled with a low pressure of an inert gas, such as Ne or Ar (Figure 10.4.5). Applying a potential across the electrodes ionizes the filler gas. The positively charged gas ions collide with the negatively charged cathode, sputtering atoms from the cathode's surface. Some of the sputtered atoms are in the excited state and emit radiation characteristic of the metal(s) from which the cathode is manufactured. By fashioning the cathode from the metallic analyte, a hollow cathode lamp provides emission lines that correspond to the analyte's absorption spectrum.

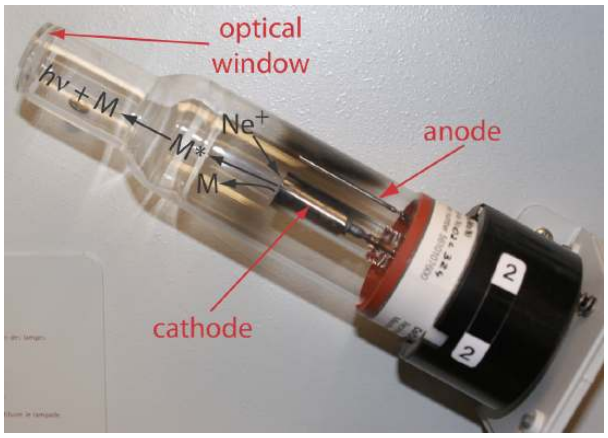


Figure 10.4.5 . Photo of a typical multielemental hollow cathode lamp. The cathode in this lamp is fashioned from an alloy of Co, Cr, Cu, Fe, Mn, and Ni, and is surrounded by a glass shield that isolates it from the anode. The lamp is filled with Ne gas. Also shown is the process that leads to atomic emission. Note the black deposit of sputtered metal on the outer wall of the hollow cathode lamp. See the text for additional details.

Because atomic absorption lines are narrow, we need to use a line source instead of a continuum source (compare, for example, Figure 10.2.4 with Figure 10.2.6). The effective bandwidth when using a continuum source is roughly 1000× larger than an atomic absorption line; thus, $P_T \approx P_0$, $\%T \approx 100$, and $A \approx 0$. Because a hollow cathode lamp is a line source, P_T and P_0 have different values giving a $\%T < 100$ and $A > 0$.

Each element in a hollow cathode lamp provides several atomic emission lines that we can use for atomic absorption. Usually the wavelength that provides the best sensitivity is the one we choose to use, although a less sensitive wavelength may be more appropriate for a sample that has higher concentration of analyte. For the Cr hollow cathode lamp in Table 10.4.3 , the best sensitivity is obtained using a wavelength of 357.9 nm.

Table 10.4.3 . Atomic Emission Lines for a Cr Hollow Cathode Lamp

wavelength (nm)	slit width (nm)	mg Cr/L giving $A = 0.20$	P_0 (relative)
357.9	0.2	2.5	40
425.4	0.2	12	85
429.0	0.5	20	100
520.5	0.2	1500	15
520.8	0.2	500	20

Another consideration is the emission line's intensity. If several emission lines meet our requirements for sensitivity, we may wish to use the emission line with the largest relative P_0 because there is less uncertainty in measuring P_0 and P_T. When analyzing a sample that is ≈10 mg Cr/L, for example, the first three wavelengths in Table 10.4.3 provide an appropriate sensitivity; the wavelengths of 425.4 nm and 429.0 nm, however, have a greater P_0 and will provide less uncertainty in the measured absorbance.

The emission spectrum for a hollow cathode lamp includes, in addition to the analyte's emission lines, additional emission lines from impurities present in the metallic cathode and from the filler gas. These additional lines are a potential source of stray radiation that could result in an instrumental deviation from Beer's law. The monochromator's slit width is set as wide as possible to improve the throughput of radiation and narrow enough to eliminate these sources of stray radiation.

Preparing the Sample. Flame and electrothermal atomization require that the analyte is in solution. Solid samples are brought into solution by dissolving in an appropriate solvent. If the sample is not soluble it is digested, either on a hot-plate or by microwave, using HNO_3, H_2SO_4, or $HClO_4$. Alternatively, we can extract the analyte using a Soxhlet extractor. Liquid samples are analyzed directly or the analytes extracted if the matrix is in- compatible with the method of atomization. A serum sample, for instance, is

difficult to aspirate when using flame atomization and may produce an unacceptably high background absorbance when using electrothermal atomization. A liquid–liquid extraction using an organic solvent and a chelating agent frequently is used to concentrate analytes. Dilute solutions of Cd^{2+}, Co^{2+}, Cu^{2+}, Fe^{3+}, Pb^{2+}, Ni^{2+}, and Zn^{2+}, for example, are concentrated by extracting with a solution of ammonium pyrrolidine dithiocarbamate in methyl isobutyl ketone.

Minimizing Spectral Interference. A spectral interference occurs when an analyte's absorption line overlaps with an interferent's absorption line or band. Because they are so narrow, the overlap of two atomic absorption lines seldom is a problem. On the other hand, a molecule's broad absorption band or the scattering of source radiation is a potentially serious spectral interference.

An important consideration when using a flame as an atomization source is its effect on the measured absorbance. Among the products of combustion are molecular species that exhibit broad absorption bands and particulates that scatter radiation from the source. If we fail to compensate for these spectral interferences, then the intensity of transmitted radiation is smaller than expected. The result is an apparent increase in the sample's absorbance. Fortunately, absorption and scattering of radiation by the flame are corrected by analyzing a blank.

Spectral interferences also occur when components of the sample's matrix other than the analyte react to form molecular species, such as oxides and hydroxides. The resulting absorption and scattering constitutes the sample's background and may present a significant problem, particularly at wavelengths below 300 nm where the scattering of radiation becomes more important. If we know the composition of the sample's matrix, then we can prepare our samples using an identical matrix. In this case the background absorption is the same for both the samples and the standards. Alternatively, if the background is due to a known matrix component, then we can add that component in excess to all samples and standards so that the contribution of the naturally occurring interferent is insignificant. Finally, many interferences due to the sample's matrix are eliminated by increasing the atomization temperature. For example, switching to a higher temperature flame helps prevents the formation of interfering oxides and hydroxides.

If the identity of the matrix interference is unknown, or if it is not possible to adjust the flame or furnace conditions to eliminate the interference, then we must find another method to compensate for the background interference. Several methods have been developed to compensate for matrix interferences, and most atomic absorption spectrophotometers include one or more of these methods.

One of the most common methods for ***background correction*** is to use a continuum source, such as a D_2 lamp. Because a D_2 lamp is a continuum source, absorbance of its radiation by the analyte's narrow absorption line is negligible. Only the background, therefore, absorbs radiation from the D_2 lamp. Both the analyte and the background, on the other hand, absorb the hollow cathode's radiation. Subtracting the absorbance for the D_2 lamp from that for the hollow cathode lamp gives a corrected absorbance that compensates for the background interference. Although this method of background correction is effective, it does assume that the background absorbance is constant over the range of wavelengths passed by the monochromator. If this is not true, then subtracting the two absorbances underestimates or overestimates the background.

> Other methods of background correction have been developed, including Zeeman effect background correction and Smith–Hieftje background correction, both of which are included in some commercially available atomic absorption spectrophotometers. Consult the chapter's additional resources for additional information.

Minimizing Chemical Interferences. The quantitative analysis of some elements is complicated by chemical interferences that occur during atomization. The most common chemical interferences are the formation of nonvolatile compounds that contain the analyte and ionization of the analyte.

One example of the formation of a nonvolatile compound is the effect of $\mathbf{PO_4^{3-}}$ or Al^{3+} on the flame atomic absorption analysis of Ca^{2+}. In one study, for example, adding 100 ppm Al^{3+} to a solution of 5 ppm Ca^{2+} decreased calcium ion's absorbance from 0.50 to 0.14, while adding 500 ppm $\mathbf{PO_4^{3-}}$ to a similar solution of Ca^{2+} decreased the absorbance from 0.50 to 0.38. These interferences are attributed to the formation of nonvolatile particles of $Ca_3(PO_4)_2$ and an Al–Ca–O oxide [Hosking, J. W.; Snell, N. B.; Sturman, B. T. *J. Chem. Educ.* **1977**, *54*, 128–130].

When using flame atomization, we can minimize the formation of non-volatile compounds by increasing the flame's temperature by changing the fuel-to-oxidant ratio or by switching to a different combination of fuel and oxidant. Another approach is to add a

releasing agent or a protecting agent to the sample. A ***releasing agent*** is a species that reacts preferentially with the interferent, releasing the analyte during atomization. For example, Sr^{2+} and La^{3+} serve as releasing agents for the analysis of Ca^{2+} in the presence of PO_4^{3-} or Al^{3+}. Adding 2000 ppm $SrCl_2$ to the Ca^{2+}/ PO_4^{3-} and to the Ca^{2+}/Al^{3+} mixtures described in the previous paragraph increased the absorbance to 0.48. A ***protecting agent*** reacts with the analyte to form a stable volatile complex. Adding 1% w/w EDTA to the Ca^{2+}/ PO_4^{3-} solution described in the previous paragraph increased the absorbance to 0.52.

An ionization interference occurs when thermal energy from the flame or the electrothermal atomizer is sufficient to ionize the analyte

$$M(s) \rightleftharpoons M^+(aq) + e^- \tag{1.7.1}$$

where M is the analyte. Because the absorption spectra for M and M^+ are different, the position of the equilibrium in reaction 1.7.1 affects the absorbance at wavelengths where M absorbs. To limit ionization we add a high concentration of an ***ionization suppressor***, which is a species that ionizes more easily than the analyte. If the ionization suppressor's concentration is sufficient, then the increased concentration of electrons in the flame pushes reaction 1.7.1 to the left, preventing the analyte's ionization. Potassium and cesium frequently are used as an ionization suppressor because of their low ionization energy.

Standardizing the Method. Because Beer's law also applies to atomic absorption, we might expect atomic absorption calibration curves to be linear. In practice, however, most atomic absorption calibration curves are nonlinear or linear over a limited range of concentrations. Nonlinearity in atomic absorption is a consequence of instrumental limitations, including stray radiation from the hollow cathode lamp and the variation in molar absorptivity across the absorption line. Accurate quantitative work, therefore, requires a suitable means for computing the calibration curve from a set of standards.

When possible, a quantitative analysis is best conducted using external standards. Unfortunately, matrix interferences are a frequent problem, particularly when using electrothermal atomization. For this reason the method of standard additions often is used. One limitation to this method of standardization, however, is the requirement of a linear relationship between absorbance and concentration.

> Most instruments include several different algorithms for computing the calibration curve. The instrument in my lab, for example, includes five algorithms. Three of the algorithms fit absorbance data using linear, quadratic, or cubic polynomial functions of the analyte's concentration. It also includes two algorithms that fit the concentrations of the standards to quadratic functions of the absorbance.

Representative Method 10.4.1: Determination of Cu and Zn in Tissue Samples

The best way to appreciate the theoretical and the practical details discussed in this section is to carefully examine a typical analytical method. Although each method is unique, the following description of the determination of Cu and Zn in biological tissues provides an instructive example of a typical procedure. The description here is based on Bhattacharya, S. K.; Goodwin, T. G.; Crawford, A. J. *Anal. Lett.* **1984**, *17*, 1567–1593, and Crawford, A. J.; Bhattacharya, S. K. Varian Instruments at Work, Number AA–46, April 1985.

Description of Method.

Copper and zinc are isolated from tissue samples by digesting the sample with HNO_3 after first removing any fatty tissue. The concentration of copper and zinc in the supernatant are determined by atomic absorption using an air-acetylene flame.

Procedure.

Tissue samples are obtained by a muscle needle biopsy and dried for 24–30 h at 105°C to remove all traces of moisture. The fatty tissue in a dried sample is removed by extracting overnight with anhydrous ether. After removing the ether, the sample is dried to obtain the fat-free dry tissue weight (FFDT). The sample is digested at 68°C for 20–24 h using 3 mL of 0.75 M HNO_3. After centrifuging at 2500 rpm for 10 minutes, the supernatant is transferred to a 5-mL volumetric flask. The digestion is repeated two more times, for 2–4 hours each, using 0.9-mL aliquots of 0.75 M HNO_3. These supernatants are added to the 5-mL volumetric flask, which is diluted to volume with 0.75 M HNO_3. The concentrations of Cu and Zn in the diluted supernatant are determined by flame atomic absorption spectroscopy using an air-acetylene flame and external standards. Copper is analyzed at a wavelength of

324.8 nm with a slit width of 0.5 nm, and zinc is analyzed at 213.9 nm with a slit width of 1.0 nm. Background correction using a D_2 lamp is necessary for zinc. Results are reported as µg of Cu or Zn per gram of FFDT.

Questions.

1. Describe the appropriate matrix for the external standards and for the blank?

    The matrix for the standards and the blank should match the matrix of the samples; thus, an appropriate matrix is 0.75 M HNO_3. Any interferences from other components of the sample matrix are minimized by background correction.

2. Why is a background correction necessary for the analysis of Zn, but not for the analysis of Cu?

    Background correction compensates for background absorption and scattering due to interferents in the sample. Such interferences are most severe when using a wavelength less than 300 nm. This is the case for Zn, but not for Cu.

3. A Cu hollow cathode lamp has several emission lines, the properties of which are shown in the following table. Explain why this method uses the line at 324.8 nm.

wavelength (nm)	slit width (nm)	mg Cu/L for A = 0.20	P_0 (relative)
217.9	0.2	15	3
218.2	0.2	15	3
222.6	0.2	60	5
244.2	0.2	400	15
249.2	0.5	200	24
324.8	0.5	1.5	100
327.4	0.5	3	87

    With 1.5 mg Cu/L giving an absorbance of 0.20, the emission line at 324.8 nm has the best sensitivity. In addition, it is the most intense emission line, which decreases the uncertainty in the measured absorbance.

Example 10.4.1

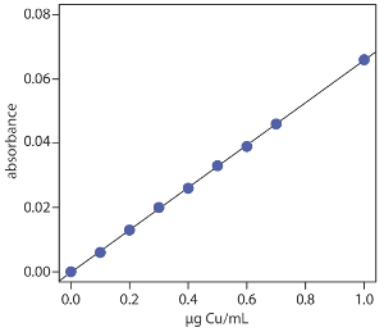
To evaluate the method described in Representative Method 10.4.1, a series of external standard is prepared and analyzed, providing the results shown here [Crawford, A. J.; Bhattacharya, S. K. “Microanalysis of Copper and Zinc in Biopsy-Sized Tissue Specimens by Atomic Absorption Spectroscopy Using a Stoichiometric Air-Acetylene Flame,” Varian Instruments at Work, Number AA–46, April 1985].

µg Cu/mL	absorbance	µg Cu/mL	absorbance
0.000	0.000	0.500	0.033
0.100	0.006	0.600	0.039
0.200	0.013	0.700	0.046
0.300	0.020	1.00	0.066
0.400	0.026		

A bovine liver standard reference material is used to evaluate the method’s accuracy. After drying and extracting the sample, a 11.23-mg FFDT tissue sample gives an absorbance of 0.023. Report the amount of copper in the sample as µg Cu/g FFDT.

Solution

Linear regression of absorbance versus the concentration of Cu in the standards gives the calibration curve shown below and the following calibration equation.



$$A = -0.0002 + 0.0661 \times \frac{\mu g\ Cu}{mL}$$

Substituting the sample's absorbance into the calibration equation gives the concentration of copper as 0.351 µg/mL. The concentration of copper in the tissue sample, therefore, is

$$\frac{\frac{0.351 \mu g\ Cu}{mL} \times 5.000\ mL}{0.01123\ g\ sample} = 156\ \mu g\ Cu/g\ FDT$$

Evaluation of Atomic Absorption Spectroscopy

Scale of Operation

Atomic absorption spectroscopy is ideally suited for the analysis of trace and ultratrace analytes, particularly when using electrothermal atomization. For minor and major analytes, sample are diluted before the analysis. Most analyses use a macro or a meso sample. The small volume requirement for electrothermal atomization or for flame microsampling, however, makes practical the analysis of micro and ultramicro samples.

Accuracy

If spectral and chemical interferences are minimized, an accuracy of 0.5–5% is routinely attainable. When the calibration curve is nonlinear, accuracy is improved by using a pair of standards whose absorbances closely bracket the sample's absorbance and assuming that the change in absorbance is linear over this limited concentration range. Determinate errors for electrothermal atomization often are greater than those obtained with flame atomization due to more serious matrix interferences.

Precision

For an absorbance greater than 0.1–0.2, the relative standard deviation for atomic absorption is 0.3–1% for flame atomization and 1–5% for electrothermal atomization. The principle limitation is the uncertainty in the concentration of free analyte atoms that result from variations in the rate of aspiration, nebulization, and atomization for a flame atomizer, and the consistency of injecting samples for electrothermal atomization.

Sensitivity

The sensitivity of a flame atomic absorption analysis is influenced by the flame's composition and by the position in the flame from which we monitor the absorbance. Normally the sensitivity of an analysis is optimized by aspirating a standard solution of analyte and adjusting the fuel-to-oxidant ratio, the nebulizer flow rate, and the height of the burner, to give the greatest absorbance. With electrothermal atomization, sensitivity is influenced by the drying and ashing stages that precede atomization. The temperature and time at each stage is optimized for each type of sample.

Sensitivity also is influenced by the sample's matrix. We already noted, for example, that sensitivity is decreased by a chemical interference. An increase in sensitivity may be realized by adding a low molecular weight alcohol, ester, or ketone to the solution, or by using an organic solvent.

Selectivity

Due to the narrow width of absorption lines, atomic absorption provides excellent selectivity. Atomic absorption is used for the analysis of over 60 elements at concentrations at or below the level of μg/L.

Time, Cost, and Equipment

The analysis time when using flame atomization is short, with sample throughputs of 250–350 determinations per hour when using a fully automated system. Electrothermal atomization requires substantially more time per analysis, with maximum sample throughputs of 20–30 determinations per hour. The cost of a new instrument ranges from between $10,000– $50,000 for flame atomization, and from $18,000–$70,000 for electrothermal atomization. The more expensive instruments in each price range include double-beam optics, automatic samplers, and can be programmed for multielemental analysis by allowing the wavelength and hollow cathode lamp to be changed automatically.

This page titled 1.7: Atomic Absorption Spectroscopy is shared under a CC BY-NC-SA 4.0 license and was authored, remixed, and/or curated by David Harvey.

- **10.4: Atomic Absorption Spectroscopy** by David Harvey is licensed CC BY-NC-SA 4.0.

1.8: Emission Spectroscopy

An analyte in an excited state possesses an energy, E_2, that is greater than its energy when it is in a lower energy state, E_1. When the analyte returns to its lower energy state—a process we call relaxation—the excess energy, ΔE

$$\Delta E = E_2 - E_1$$

is released. Figure 10.1.4 shows a simplified picture of this process.

The amount of time an analyte, A, spends in its excited state—what we call the excited state's ***lifetime***—is short, typically 10^{-5}–10^{-9} s for an electronic excited state and 10–15 s for a vibrational excited state. Relaxation of the analyte's excited state, A^*, occurs through several mechanisms, including collisions with other species in the sample, photochemical reactions, and the emission of photons. In the first process, which we call vibrational relaxation or nonradiative relaxation, the excess energy is released as heat.

$$A^* \longrightarrow A + \text{heat}$$

Relaxation by a photochemical reaction may involve simple decomposition

$$A^* \longrightarrow X + Y$$

or a reaction between A^* and another species

$$A^* + Z \longrightarrow X + Y$$

In both cases the excess energy is used up in the chemical reaction or released as heat.

In the third mechanism, the excess energy is released as a photon of electromagnetic radiation.

$$A^* \longrightarrow A + h\nu$$

The release of a photon following thermal excitation is called emission and that following the absorption of a photon is called photoluminescence. In chemiluminescence and bioluminescence, excitation results from a chemical or a biochemical reaction, respectively. Spectroscopic methods based on photoluminescence are the subject of the next section and atomic emission is covered in Chapter 10.7.

This page titled 1.8: Emission Spectroscopy is shared under a CC BY-NC-SA 4.0 license and was authored, remixed, and/or curated by David Harvey.

- **10.5: Emission Spectroscopy** by David Harvey is licensed CC BY-NC-SA 4.0.

1.9: Photoluminescent Spectroscopy

Photoluminescence is divided into two categories: fluorescence and phosphorescence. A pair of electrons that occupy the same electronic ground state have opposite spins and are in a singlet spin state (Figure 10.6.1 a).

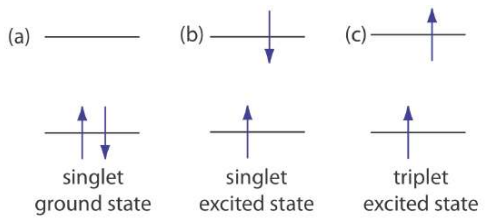


Figure 10.6.1 . Electron configurations for (a) a singlet ground state; (b) a singlet excited state; and (c) a triplet excited state.

When an analyte absorbs an ultraviolet or a visible photon, one of its valence electrons moves from the ground state to an excited state with a conservation of the electron's spin (Figure 10.6.1 b). Emission of a photon from a ***singlet excited state*** to the singlet ground state—or between any two energy levels with the same spin—is called ***fluorescence***. The probability of fluorescence is very high and the average lifetime of an electron in the excited state is only 10^{-5}–10^{-8} s. Fluorescence, therefore, rapidly decays once the source of excitation is removed.

In some cases an electron in a singlet excited state is transformed to a ***triplet excited state*** (Figure 10.6.1 c) in which its spin no is longer paired with the ground state. Emission between a triplet excited state and a singlet ground state—or between any two energy levels that differ in their respective spin states–is called ***phosphorescence***. Because the average lifetime for phosphorescence ranges from 10^{-4}–10^{4} s, phosphorescence may continue for some time after we remove the excitation source.

The use of molecular fluorescence for qualitative analysis and for semi-quantitative analysis dates to the early to mid 1800s, with more accurate quantitative methods appearing in the 1920s. Instrumentation for fluorescence spectroscopy using a filter or a monochromator for wavelength selection appeared in, respectively, the 1930s and 1950s. Although the discovery of phosphorescence preceded that of fluorescence by almost 200 years, qualitative and quantitative applications of molecular phosphorescence did not receive much attention until after the development of fluorescence instrumentation.

> As you might expect, the persistence of long-lived phosphorescence made it more noticeable.

Fluorescence and Phosphorescence Spectra

To appreciate the origin of fluorescence and phosphorescence we must consider what happens to a molecule following the absorption of a photon. Let's assume the molecule initially occupies the lowest vibrational energy level of its electronic ground state, which is the singlet state labeled S_0 in Figure 10.6.2 . Absorption of a photon excites the molecule to one of several vibrational energy levels in the first excited electronic state, S_1, or the second electronic excited state, S_2, both of which are singlet states. Relaxation to the ground state occurs by a number of mechanisms, some of which result in the emission of a photon and others that occur without the emission of a photon. These relaxation mechanisms are shown in Figure 10.6.2 . The most likely relaxation pathway from any excited state is the one with the shortest lifetime.

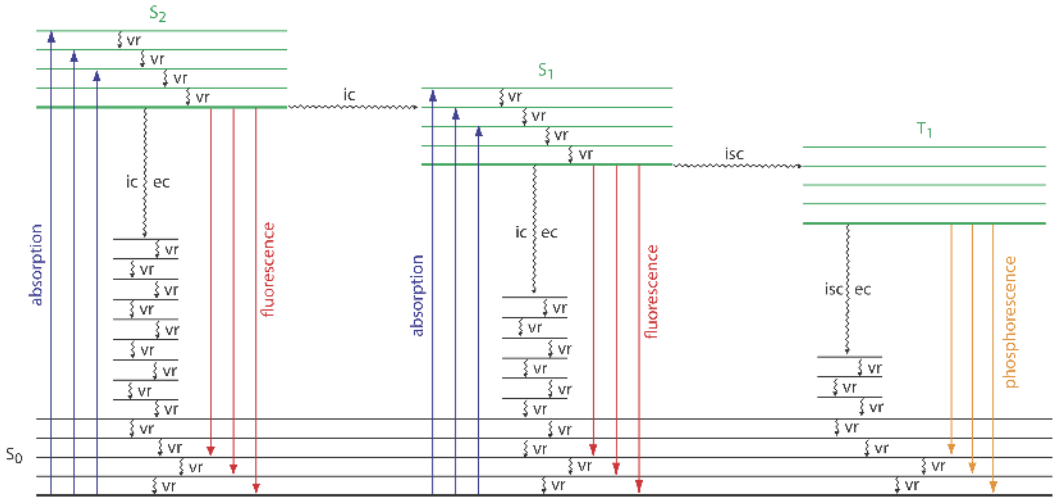


Figure 10.6.2 . Energy level diagram for a molecule that shows pathways for the deactivation of an excited state: ***vr*** is vibrational relaxation; ***ic*** is internal conversion; ***ec*** is external conversion; and ***isc*** is an intersystem crossing. The lowest vibrational energy for each electronic state is indicated by the thicker line. The electronic ground state is shown in black and the three electronic excited states are shown in green. The absorption, fluorescence, and phosphorescence of photons also are shown.

Radiationless Deactivation

When a molecule relaxes without emitting a photon we call the process ***radiationless deactivation***. One example of radiationless deactivation is ***vibrational relaxation***, in which a molecule in an excited vibrational energy level loses energy by moving to a lower vibrational energy level in the same electronic state. Vibrational relaxation is very rapid, with an average lifetime of $<10^{-12}$ s. Because vibrational relaxation is so efficient, a molecule in one of its excited state's higher vibrational energy levels quickly returns to the excited state's lowest vibrational energy level.

Another form of radiationless deactivation is an ***internal conversion*** in which a molecule in the ground vibrational level of an excited state passes directly into a higher vibrational energy level of a lower energy electronic state of the same spin state. By a combination of internal conversions and vibrational relaxations, a molecule in an excited electronic state may return to the ground electronic state without emitting a photon. A related form of radiationless deactivation is an ***external conversion*** in which excess energy is transferred to the solvent or to another component of the sample's matrix.

> Let's use Figure 10.6.2 to illustrate how a molecule can relax back to its ground state without emitting a photon. Suppose our molecule is in the highest vibrational energy level of the second electronic excited state. After a series of vibrational relaxations brings the molecule to the lowest vibrational energy level of S_2, it undergoes an internal conversion into a higher vibrational energy level of the first excited electronic state. Vibrational relaxations bring the molecule to the lowest vibrational energy level of S_1. Following an internal conversion into a higher vibrational energy level of the ground state, the molecule continues to undergo vibrational relaxation until it reaches the lowest vibrational energy level of S_0.

A final form of radiationless deactivation is an ***intersystem crossing*** in which a molecule in the ground vibrational energy level of an excited electronic state passes into one of the higher vibrational energy levels of a lower energy electronic state with a different spin state. For example, an intersystem crossing is shown in Figure 10.6.2 between the singlet excited state S_1 and the triplet excited state T_1.

Relaxation by Fluorescence

Fluorescence occurs when a molecule in an excited state's lowest vibrational energy level returns to a lower energy electronic state by emitting a photon. Because molecules return to their ground state by the fastest mechanism, fluorescence is observed only if it is a more efficient means of relaxation than a combination of internal conversions and vibrational relaxations.

A quantitative expression of fluorescence efficiency is the fluorescent ***quantum yield***, Φ_f, which is the fraction of excited state molecules that return to the ground state by fluorescence. The fluorescent quantum yields range from 1 when every molecule in an excited state undergoes fluorescence, to 0 when fluorescence does not occur.

The intensity of fluorescence, I_f, is proportional to the amount of radiation absorbed by the sample, $P_0 - P_T$, and the fluorescent quantum yield

$$I_f = k\Phi_f (P_0 - P_T) \tag{1.9.1}$$

where k is a constant that accounts for the efficiency of collecting and detecting the fluorescent emission. From Beer's law we know that

$$\frac{P_T}{P_0} = 10^{-\varepsilon bC} \tag{1.9.2}$$

where C is the concentration of the fluorescing species. Solving Equation 1.9.2 for P_T and substituting into Equation 1.9.1 gives, after simplifying

$$I_f = k\Phi_f P_0 \left(1 - 10^{-\varepsilon bC}\right) \tag{1.9.3}$$

When $\varepsilon bC < 0.01$, which often is the case when the analyte's concentration is small, Equation 1.9.3 simplifies to

$$I_f = 2.303 k\Phi_f \varepsilon bC P_0 = k' P_0 \tag{1.9.4}$$

where k' is a collection of constants. The intensity of fluorescence, therefore, increases with an increase in the quantum efficiency, the source's incident power, and the molar absorptivity and the concentration of the fluorescing species.

Fluorescence generally is observed when the molecule's lowest energy absorption is a $\pi \rightarrow \pi^*$ transition, although some $n \rightarrow \pi^*$ transitions show weak fluorescence. Many unsubstituted, nonheterocyclic aromatic compounds have a favorable fluorescence quantum yield, although substitutions on the aromatic ring can effect Φ_f significantly. For example, the presence of an electron-withdrawing group, such as $-NO_2$, decreases Φ_f, while adding an electron-donating group, such as –OH, increases Φ_f. Fluorrescence also increases for aromatic ring systems and for aromatic molecules with rigid planar structures. Figure 10.6.3 shows the fluorescence of quinine under a UV lamp.



Figure 10.6.3 . Tonic water, which contains quinine, is fluorescent when placed under a UV lamp. Source: Splarka (commons.Wikipedia.org).

A molecule's fluorescent quantum yield also is influenced by external variables, such as temperature and solvent. Increasing the temperature generally decreases Φ_f because more frequent collisions between the molecule and the solvent increases external conversion. A decrease in the solvent's viscosity decreases Φ_f for similar reasons. For an analyte with acidic or basic functional groups, a change in pH may change the analyte's structure and its fluorescent properties.

As shown in Figure 10.6.2 , fluorescence may return the molecule to any of several vibrational energy levels in the ground electronic state. Fluorescence, therefore, occurs over a range of wavelengths. Because the change in energy for fluorescent emission generally is less than that for absorption, a molecule's fluorescence spectrum is shifted to higher wavelengths than its absorption spectrum.

Relaxation by Phosphorescence

A molecule in a triplet electronic excited state's lowest vibrational energy level normally relaxes to the ground state by an intersystem crossing to a singlet state or by an external conversion. Phosphorescence occurs when the molecule relaxes by emitting a photon. As shown in Figure 10.6.2 , phosphorescence occurs over a range of wavelengths, all of which are at lower energies than the molecule's absorption band. The intensity of phosphorescence, I_p, is given by an equation similar to Equation 1.9.4 for fluorescence

$$I_P = 2.303k\Phi_P\varepsilon bCP_0 \tag{1.9.5}$$

$$= k'P_0 \tag{1.9.6}$$

where Φ_p is the ***phosphorescent quantum yield***.

Phosphorescence is most favorable for molecules with $n \rightarrow \pi^*$ transitions, which have a higher probability for an intersystem crossing than $\pi \rightarrow \pi^*$ transitions. For example, phosphorescence is observed with aromatic molecules that contain carbonyl groups or heteroatoms. Aromatic compounds that contain halide atoms also have a higher efficiency for phosphorescence. In general, an increase in phosphorescence corresponds to a decrease in fluorescence.

Because the average lifetime for phosphorescence can be quite long, ranging from 10^{-4}–10^4 s, the phosphorescent quantum yield usually is quite small. An improvement in Φ_p is realized by decreasing the efficiency of external conversion. This is accomplished in several ways, including lowering the temperature, using a more viscous solvent, depositing the sample on a solid substrate, or trapping the molecule in solution. Figure 10.6.4 shows an example of phosphorescence.

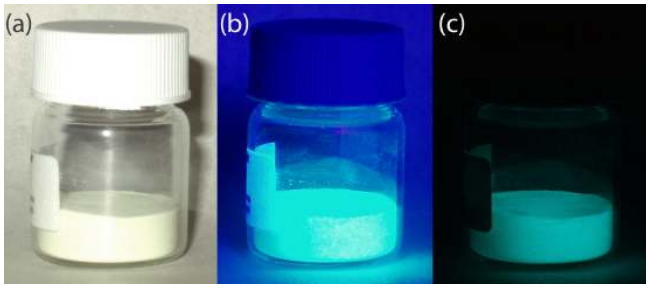


Figure 10.6.4 . An europium doped strontium silicate-aluminum oxide powder under (a) natural light, (b) a long-wave UV lamp, and (c) in total darkness. The photo taken in total darkness shows the phosphorescent emission. Source: modified from Splarka (commons.Wikipedia.org).

Excitation Versus Emission Spectra

Photoluminescence spectra are recorded by measuring the intensity of emitted radiation as a function of either the excitation wavelength or the emission wavelength. An ***excitation spectrum*** is obtained by monitoring emission at a fixed wavelength while varying the excitation wavelength. When corrected for variations in the source's intensity and the detector's response, a sample's excitation spectrum is nearly identical to its absorbance spectrum. The excitation spectrum provides a convenient means for selecting the best excitation wavelength for a quantitative or qualitative analysis.

In an ***emission spectrum*** a fixed wavelength is used to excite the sample and the intensity of emitted radiation is monitored as function of wavelength. Although a molecule has a single excitation spectrum, it has two emission spectra, one for fluorescence and one for phosphorescence. Figure 10.6.5 shows the UV absorption spectrum and the UV fluorescence emission spectrum for quinine.

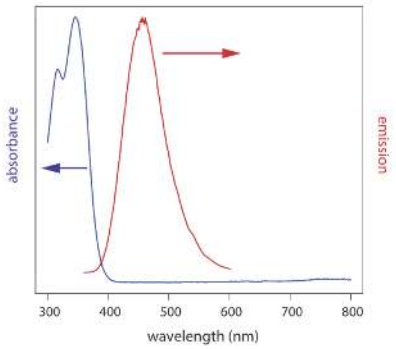


Figure 10.6.5 . Absorbance spectrum and fluorescence emission spectrum for quinine in 0.05 M H_2SO_4. The emission spectrum uses an excitation wavelength of 350 nm with a bandwidth of 20 nm. Both spectra are normalized so that the maximum absorbance is 1.00 and the maximum emission is 1.00. The actual maximum absorbance is 0.444 and the actual maximum emission is 126747. Source: data from Daniel Scott, Department of Chemistry & Biochemistry, DePauw University.

Instrumentation

The basic instrumentation for monitoring fluorescence and phosphorescence—a source of radiation, a means of selecting a narrow band of radiation, and a detector—are the same as those for absorption spectroscopy. The unique demands of fluorescence and phosphorescence, however, require some modifications to the instrument designs seen earlier in Figure 10.3.1 (filter photometer), Figure 10.3.2 (single-beam spectrophotometer), Figure 10.3.3 (double-beam spectrophotometer), and Figure 10.3.4 (diode array spectrometer). The most important difference is that the detector cannot be placed directly across from the source. Figure 10.6.6 shows why this is the case. If we place the detector along the source's axis it receives both the transmitted source radiation, P_T, and the fluorescent, I_f, or phosphorescent, I_p, radiation. Instead, we rotate the director and place it at 90º to the source.

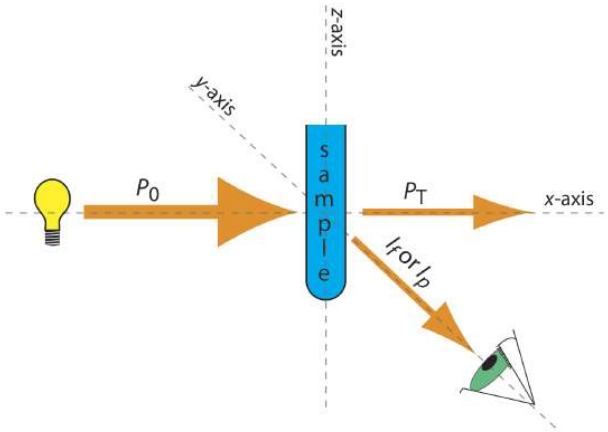


Figure 10.6.6 . Schematic diagram showing the orientation of the source and the detector when measuring fluorescence and phosphorescence. Contrast this to Figure 10.2.7, which shows the orientation for absorption spectroscopy.

Instruments for Measuring Fluorescence

Figure 10.6.7 shows the basic design of an instrument for measuring fluorescence, which includes two wavelength selectors, one for selecting the source's excitation wavelength and one for selecting the analyte's emission wavelength. In a ***fluorimeter*** the excitation and emission wavelengths are selected using absorption or interference filters. The excitation source for a fluorimeter usually is a low-pressure Hg vapor lamp that provides intense emission lines distributed throughout the ultraviolet and visible region. When a monochromator is used to select the excitation and the emission wavelengths, the instrument is called a ***spectrofluorometer***. With a monochromator the excitation source usually is a high-pressure Xe arc lamp, which has a continuous emission spectrum. Either instrumental design is appropriate for quantitative work, although only a spectrofluorometer can record an excitation or emission spectrum.

> A Hg vapor lamp has emission lines at 254, 312, 365, 405, 436, 546, 577, 691, and 773 nm.

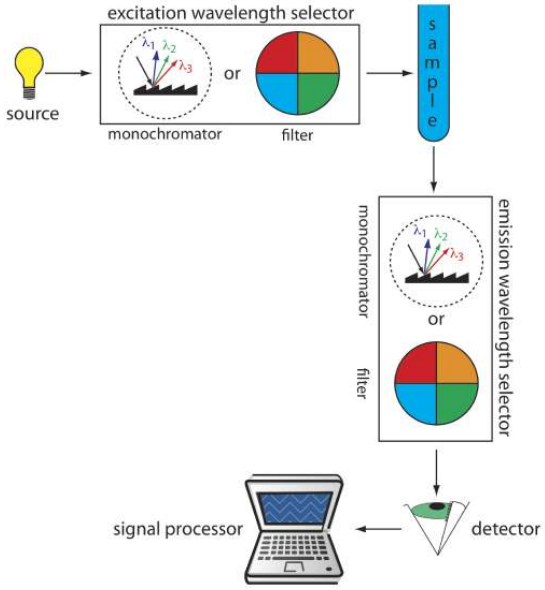


Figure 10.6.7 . Schematic diagram for measuring fluorescence showing the placement of the wavelength selectors for excitation and emission. When a filter is used the instrument is called a fluorimeter and when a monochromator is used the instrument is called a spectrofluorimeter.

The sample cells for molecular fluorescence are similar to those for molecular absorption (see Figure 10.3.6). Remote sensing using a fiber optic probe (see Figure 10.3.7) is possible using with either a fluorimeter or spectrofluorometer. An analyte that is fluorescent is monitored directly. For an analyte that is not fluorescent, a suitable fluorescent probe molecule is incorporated into the tip of the fiber optic probe. The analyte's reaction with the probe molecule leads to an increase or decrease in fluorescence.

Instruments for Measuring Phosphorescence

An instrument for molecular phosphorescence must discriminate between phosphorescence and fluorescence. Because the lifetime for fluorescence is shorter than that for phosphorescence, discrimination is achieved by incorporating a delay between exciting the sample and measuring the phosphorescent emission. Figure 10.6.8 shows how two out-of-phase choppers allow us to block fluorescent emission from reaching the detector when the sample is being excited and to prevent the source radiation from causing fluorescence when we are measuring the phosphorescent emission.

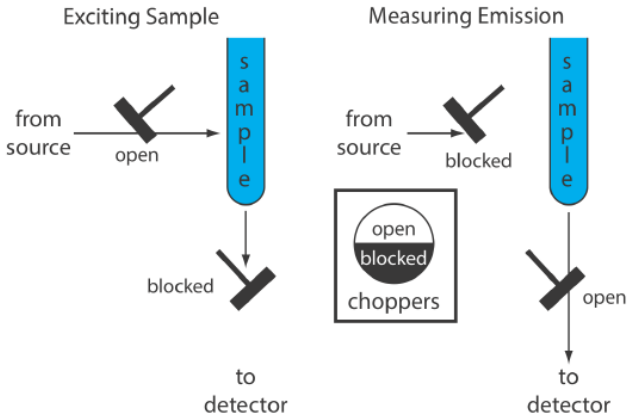


Figure 10.6.8 . Schematic diagram showing how choppers are used to prevent fluorescent emission from interfering with the measurement of phosphorescent emission.

Because phosphorescence is such a slow process, we must prevent the excited state from relaxing by external conversion. One way this is accomplished is by dissolving the sample in a suitable organic solvent, usually a mixture of ethanol, isopentane, and diethylether. The resulting solution is frozen at liquid-N_2 temperatures to form an optically clear solid. The solid matrix minimizes external conversion due to collisions between the analyte and the solvent. External conversion also is minimized by immobilizing the sample on a solid substrate, making possible room temperature measurements. One approach is to place a drop of a solution

that contains the analyte on a small disc of filter paper. After drying the sample under a heat lamp, the sample is placed in the spectrofluorometer for analysis. Other solid substrates include silica gel, alumina, sodium acetate, and sucrose. This approach is particularly useful for the analysis of thin layer chromatography plates.

Quantitative Applications

Molecular fluorescence and, to a lesser extent, phosphorescence are used for the direct or indirect quantitative analysis of analytes in a variety of matrices. A direct quantitative analysis is possible when the analyte's fluorescent or phosphorescent quantum yield is favorable. If the analyte is not fluorescent or phosphorescent, or if the quantum yield is unfavorable, then an indirect analysis may be feasible. One approach is to react the analyte with a reagent to form a product that is fluorescent or phosphorescent. Another approach is to measure a decrease in fluorescence or phosphores- cence when the analyte is added to a solution that contains a fluorescent or phosphorescent probe molecule. A decrease in emission is observed when the reaction between the analyte and the probe molecule enhances radiationless deactivation or results in a nonemitting product. The application of fluorescence and phosphorescence to inorganic and organic analytes are considered in this section.

Inorganic Analytes

Except for a few metal ions, most notably UO_2^+, most inorganic ions are not sufficiently fluorescent for a direct analysis. Many metal ions are determined indirectly by reacting with an organic ligand to form a fluorescent or, less commonly, a phosphorescent metal–ligand complex. One example is the reaction of Al^{3+} with the sodium salt of 2, 4, 3′-trihydroxyazobenzene-5′-sulfonic acid —also known as alizarin garnet R—which forms a fluorescent metal–ligand complex (Figure 10.6.9). The analysis is carried out using an excitation wavelength of 470 nm, with fluorescence monitored at 500 nm. Table 10.6.1 provides additional examples of chelating reagents that form fluorescent metal–ligand complexes with metal ions. A few inorganic nonmetals are determined by their ability to decrease, or quench, the fluorescence of another species. One example is the analysis for F^- based on its ability to quench the fluorescence of the Al^{3+}–alizarin garnet R complex.

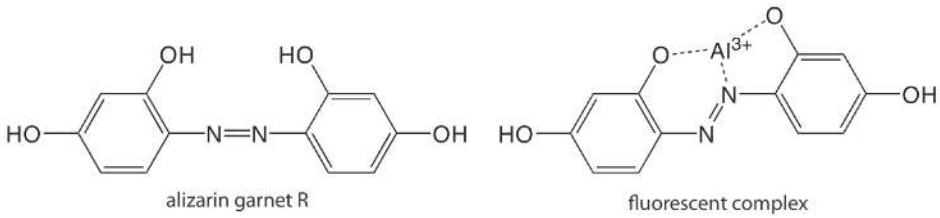


Figure 10.6.9 . Structure of alizarin garnet R and its metal–ligand complex with Al^{3+}.

Table 10.6.1 . Chelating Agents for the Fluorescent Analysis of Metal Ions

chelating agent	metal ions
8-hydroxyquinoline	Al^{3+}, Be^{2+}, Zn^{2+}, Li^+, Mg^{2+} (and others)
flavonal	Zr^{2+}, Sn^{4+}
benzoin	$B_4O_6^{2-}$, Zn^{2+}
2′, 3′, 4′, 5, 7 – pentahydroxylflavone	Be^{2+}
2-(*o*-hydroxyphenyl) benzoxazole	Cd^{2+}

Organic Analytes

As noted earlier, organic compounds that contain aromatic rings generally are fluorescent and aromatic heterocycles often are phosphorescent. Table 10.6.2 provides examples of several important biochemical, pharmaceutical, and environmental compounds that are analyzed quantitatively by fluorimetry or phosphorimetry. If an organic analyte is not naturally fluorescent or phosphorescent, it may be possible to incorporate it into a chemical reaction that produces a fluorescent or phosphorescent product. For example, the enzyme creatine phosphokinase is determined by using it to catalyze the formation of creatine from phosphocreatine. Reacting the creatine with ninhydrin produces a fluorescent product of unknown structure.

Table 10.6.2 . Examples of Naturally Photoluminescent Organic Analytes

class	compounds (F = fluorescence, P = phosphorescence)
aromatic amino acids	phenylalanine (F) tyrosine (F) tryptophan (F, P)
vitamins	vitamin A (F) vitamin B2 (F) vitamin B6 (F) vitamin B12 (F) vitamin E (F) folic acid (F)
catecholamines	dopamine (F) norepinephrine (F)
pharmaceuticals and drugs	quinine (F) salicylic acid (F, P) morphine (F) barbiturates (F) LSD (F) codeine (P) caffeine (P) sulfanilamide (P)
environmental pollutants	pyrene (F) benzo[a]pyrene (F) organothiophosphorous pesticides (F) carbamate insecticides (F) DDT (P)

Standardizing the Method

From Equation 1.9.4 and Equation 1.9.6 we know that the intensity of fluorescence or phosphorescence is a linear function of the analyte's concentration provided that the sample's absorbance of source radiation ($A = \varepsilon bC$) is less than approximately 0.01. Calibration curves often are linear over four to six orders of magnitude for fluorescence and over two to four orders of magnitude for phosphorescence. For higher concentrations of analyte the calibration curve becomes nonlinear because the assumptions that led to Equation 1.9.4 and Equation 1.9.6 no longer apply. Nonlinearity may be observed for smaller concentrations of analyte fluorescent or phosphorescent contaminants are present. As discussed earlier, quantum efficiency is sensitive to temperature and sample matrix, both of which must be con- trolled when using external standards. In addition, emission intensity depends on the molar absorptivity of the photoluminescent species, which is sensitive to the sample matrix.

Representative Method 10.6.1: Determination of Quinine in Urine

The best way to appreciate the theoretical and the practical details discussed in this section is to carefully examine a typical analytical method. Although each method is unique, the following description of the determination of quinine in urine provides an instructive example of a typical procedure. The description here is based on Mule, S. J.; Hushin, P. L. *Anal. Chem.* **1971**, *43*, 708–711, and O'Reilly, J. E.; *J. Chem. Educ.* **1975**, *52*, 610–612. Figure 10.6.3 shows the fluorescence of the quinine in tonic water.

Description of the Method

Quinine is an alkaloid used to treat malaria. It is a strongly fluorescent compound in dilute solutions of H_2SO_4 ($\Phi_f = 0.55$). Quinine's excitation spectrum has absorption bands at 250 nm and 350 nm and its emission spectrum has a single emission band at 450 nm. Quinine is excreted rapidly from the body in urine and is determined by measuring its fluorescence following its extraction from the urine sample.

Procedure

Transfer a 2.00-mL sample of urine to a 15-mL test tube and use 3.7 M NaOH to adjust its pH to between 9 and 10. Add 4 mL of a 3:1 (v/v) mixture of chloroform and isopropanol and shake the contents of the test tube for one minute. Allow the organic and the aqueous (urine) layers to separate and transfer the organic phase to a clean test tube. Add 2.00 mL of 0.05 M H_2SO_4 to the organic phase and shake the contents for one minute. Allow the organic and the aqueous layers to separate and transfer the aqueous phase to the sample cell. Measure the fluorescent emission at 450 nm using an excitation wavelength of 350 nm. Determine the concentration of quinine in the urine sample using a set of external standards in 0.05 M H_2SO_4, prepared from a 100.0 ppm solution of quinine in 0.05 M H_2SO_4. Use distilled water as a blank.

Questions

1. Chloride ion quenches the intensity of quinine's fluorescent emission. For example, in the presence of 100 ppm NaCl (61 ppm Cl^-) quinine's emission intensity is only 83% of its emission intensity in the absence of chloride. The presence of 1000 ppm NaCl (610 ppm Cl^-) further reduces quinine's fluorescent emission to less than 30% of its emission intensity in the absence of chloride. The concentration of chloride in urine typically ranges from 4600–6700 ppm Cl^-. Explain how this procedure prevents an interference from chloride.

> The procedure uses two extractions. In the first of these extractions, quinine is separated from urine by extracting it into a mixture of chloroform and isopropanol, leaving the chloride ion behind in the original sample.

2. Samples of urine may contain small amounts of other fluorescent compounds, which will interfere with the analysis if they are carried through the two extractions. Explain how you can modify the procedure to take this into account?

> One approach is to prepare a blank that uses a sample of urine known to be free of quinine. Subtracting the blank's fluorescent signal from the measured fluorescence from urine samples corrects for the interfering compounds.

The fluorescent emission for quinine at 450 nm can be induced using an excitation frequency of either 250 nm or 350 nm. The fluorescent quantum efficiency is the same for either excitation wavelength. Quinine's absorption spectrum shows that ε_{250} is greater than ε_{350}. Given that quinine has a stronger absorbance at 250 nm, explain why its fluorescent emission intensity is greater when using 350 nm as the excitation wavelength.

> From Equation 1.9.4 we know that I_f is a function of the following terms: k, Φ_f, P_0, ε, b, and C. We know that Φ_f, b, and C are the same for both excitation wavelengths and that ε is larger for a wavelength of 250 nm; we can, therefore, ignore these terms. The greater emission intensity when using an excitation wavelength of 350 nm must be due to a larger value for P_0 or k . In fact, P_0 at 350 nm for a high-pressure Xe arc lamp is about 170% of that at 250 nm. In addition, the sensitivity of a typical photomultiplier detector (which contributes to the value of k) at 350 nm is about 140% of that at 250 nm.

Example 10.6.1

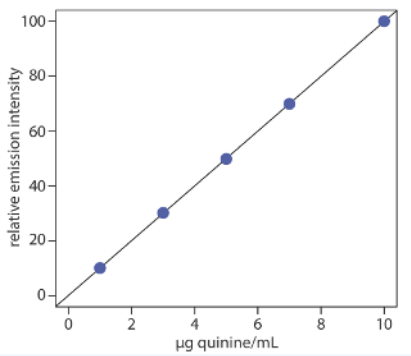
To evaluate the method described in Representative Method 10.6.1, a series of external standard are prepared and analyzed, providing the results shown in the following table. All fluorescent intensities are corrected using a blank prepared from a quinine-free sample of urine. The fluorescent intensities are normalized by setting I_f for the highest concentration standard to 100.

[quinine] (µg/mL)	I_f
1.00	10.11
3.00	30.20
5.00	49.84
7.00	69.89
10.00	100.0

After ingesting 10.0 mg of quinine, a volunteer provides a urine sample 24-h later. Analysis of the urine sample gives a relative emission intensity of 28.16. Report the concentration of quinine in the sample in mg/L and the percent recovery for the ingested quinine.

Solution

Linear regression of the relative emission intensity versus the concentration of quinine in the standards gives the calibration curve shown below and the following calibration equation.



$$I_f = 0.122 + 9.978 \times \frac{\text{g quinine}}{\text{mL}}$$

Substituting the sample's relative emission intensity into the calibration equation gives the concentration of quinine as 2.81 µg/mL. Because the volume of urine taken, 2.00 mL, is the same as the volume of 0.05 M H_2SO_4 used to extract the quinine, the concentration of quinine in the urine also is 2.81 µg/mL. The recovery of the ingested quinine is

$$\frac{\frac{2.81\ \mu\text{g quinine}}{\text{mL urine}} \times 2.00\ \text{mL urine} \times \frac{1\text{mg}}{1000\ \mu\text{g}}}{10.0\ \text{mg quinine ingested}} \times 100 = 0.0562\%$$

It can take 10–11 days for the body to completely excrete quinine so it is not surprising that such a small amount of quinine is recovered from this sample of urine.

Evaluation of Photoluminescence Spectroscopy

Scale of Operation

Photoluminescence spectroscopy is used for the routine analysis of trace and ultratrace analytes in macro and meso samples. Detection limits for fluorescence spectroscopy are influenced by the analyte's quantum yield. For an analyte with $\Phi_f > 0.5$, a picomolar detection limit is possible when using a high quality spectrofluorometer. For example, the detection limit for quinine sulfate, for which Φ is 0.55, generally is between 1 part per billion and 1 part per trillion. Detection limits for phosphorescence are somewhat higher, with typical values in the nanomolar range for low-temperature phosphorimetry and in the micromolar range for room-temperature phosphorimetry using a solid substrate.

Accuracy

The accuracy of a fluorescence method generally is between 1–5% when spectral and chemical interferences are insignificant. Accuracy is limited by the same types of problems that affect other optical spectroscopic methods. In addition, accuracy is affected by interferences that affect the fluorescent quantum yield. The accuracy of phosphorescence is somewhat greater than that for fluorescence.

Precision

The relative standard deviation for fluorescence usually is between 0.5–2% when the analyte's concentration is well above its detection limit. Precision usually is limited by the stability of the excitation source. The precision for phosphorescence often is limited by reproducibility in preparing samples for analysis, with relative standard deviations of 5–10% being common.

Sensitivity

From Equation 1.9.4 and Equation 1.9.6 we know that the sensitivity of a fluorescent or a phosphorescent method is affected by a number of parameters. We already have considered the importance of quantum yield and the effect of temperature and solution composition on Φ_f and Φ_p. Besides quantum yield, sensitivity is improved by using an excitation source that has a greater emission

intensity, P_0, at the desired wavelength, and by selecting an excitation wavelength for which the analyte has a greater molar absorptivity, ε. Another approach for improving sensitivity is to increase the volume from which emission is monitored. Figure 10.6.10 shows how rotating a monochromator's slits from their usual vertical orientation to a horizontal orientation increases the sampling volume. The result can in- crease the emission from the sample by $5-30\times$.

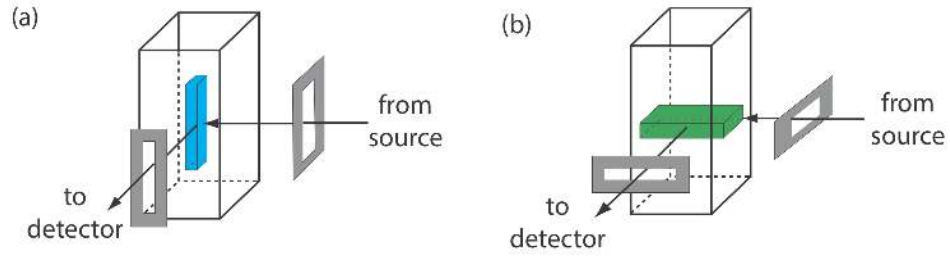


Figure 10.6.10 . Use of slit orientation to change the volume from which fluorescence is measured: (a) vertical slit orientation; (b) horizontal slit orientation. Suppose the slit's dimensions are 0.1 mm × 3 mm. In (a) the dimensions of the sampling volume are 0.1 mm × 0.1 mm × 3 mm, or 0.03 mm^3. For (b) the dimensions of the sampling volume are 0.1 mm × 3 mm × 3 mm, or 0.9 mm^3, a 30-fold increase in the sampling volume.

Selectivity

The selectivity of fluorescence and phosphorescence is superior to that of absorption spectrophotometry for two reasons: first, not every compound that absorbs radiation is fluorescent or phosphorescent; and, second, selectivity between an analyte and an interferent is possible if there is a difference in either their excitation or their emission spectra. The total emission intensity is a linear sum of that from each fluorescent or phosphorescent species. The analysis of a sample that contains *n* analytes, therefore, is accomplished by measuring the total emission intensity at *n* wavelengths.

Time, Cost, and Equipment

As with other optical spectroscopic methods, fluorescent and phosphorescent methods provide a rapid means for analyzing samples and are capable of automation. Fluorimeters are relatively inexpensive, ranging from several hundred to several thousand dollars, and often are satisfactory for quantitative work. Spectrofluorometers are more expensive, with models often exceeding $50,000.

This page titled 1.9: Photoluminescent Spectroscopy is shared under a CC BY-NC-SA 4.0 license and was authored, remixed, and/or curated by David Harvey.

- **10.6: Photoluminescent Spectroscopy** by David Harvey is licensed CC BY-NC-SA 4.0.

1.10: Atomic Emission Spectroscopy

The focus of this section is on the emission of ultraviolet and visible radiation following the thermal excitation of atoms. Atomic emission spectroscopy has a long history. Qualitative applications based on the color of flames were used in the smelting of ores as early as 1550 and were more fully developed around 1830 with the observation of atomic spectra generated by flame emission and spark emission [Dawson, J. B. *J. Anal. At. Spectrosc.* **1991**, *6*, 93–98]. Quantitative applications based on the atomic emission from electric sparks were developed by Lockyer in the early 1870 and quantitative applications based on flame emission were pioneered by Lundegardh in 1930. Atomic emission based on emission from a plasma was introduced in 1964.

> For an on-line introduction to much of the material in this section, see Atomic Emission Spectroscopy (AES) by Tomas Spudich and Alexander Scheeline, a resource that is part of the Analytical Sciences Digital Library.

Atomic Emission Spectra

Atomic emission occurs when a valence electron in a higher energy atomic orbital returns to a lower energy atomic orbital. Figure 10.7.1 shows a portion of the energy level diagram for sodium, which consists of a series of discrete lines at wavelengths that correspond to the difference in energy between two atomic orbitals.

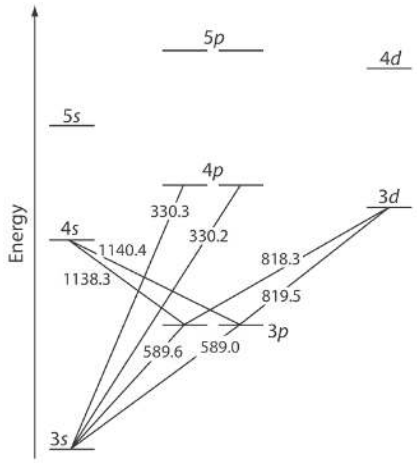


Figure 10.7.1 . Valence shell energy level diagram for sodium. The wavelengths corresponding to several transitions are shown. Note that this is the same energy level diagram as Figure 10.2.5.

The intensity of an atomic emission line, I_e, is proportional to the number of atoms, N^*, that populate the excited state,

$$I_e = kN^* \tag{1.10.1}$$

where k is a constant that accounts for the efficiency of the transition. If a system of atoms is in thermal equilibrium, the population of excited state i is related to the total concentration of atoms, N, by the Boltzmann distribution. For many elements at temperatures of less than 5000 K the Boltzmann distribution is approximated as

$$N^* = N\left(\frac{g_i}{g_0}\right)e^{-E_i/kT} \tag{1.10.2}$$

where g_i and g_0 are statistical factors that account for the number of equivalent energy levels for the excited state and the ground state, E_i is the energy of the excited state relative to a ground state energy, E_0, k is Boltzmann's constant (1.3807×10^{-23} J/K), and T is the temperature in Kelvin. From Equation 1.10.2 we expect that excited states with lower energies have larger populations and more intense emission lines. We also expect emission intensity to increase with temperature.

Equipment

An atomic emission spectrometer is similar in design to the instrumentation for atomic absorption. In fact, it is easy to adapt most flame atomic absorption spectrometers for atomic emission by turning off the hollow cathode lamp and monitoring the difference between the emission intensity when aspirating the sample and when aspirating a blank. Many atomic emission spectrometers,

however, are dedicated instruments designed to take advantage of features unique to atomic emission, including the use of plasmas, arcs, sparks, and lasers as atomization and excitation sources, and an enhanced capability for multielemental analysis.

Atomization and Excitation

Atomic emission requires a means for converting into a free gaseous atom an analyte that is present in a solid, liquid, or solution sample. The same source of thermal energy used for atomization usually serves as the excitation source. The most common methods are flames and plasmas, both of which are useful for liquid or solution samples. Solid samples are analyzed by dissolving in a solvent and using a flame or plasma atomizer.

Flame Sources

Atomization and excitation in flame atomic emission is accomplished with the same nebulization and spray chamber assembly used in atomic absorption (Figure 10.4.1). The burner head consists of a single or multiple slots, or a Meker-style burner. Older atomic emission instruments often used a total consumption burner in which the sample is drawn through a capillary tube and injected directly into the flame.

> A Meker burner is similar to the more common Bunsen burner found in most laboratories; it is designed to allow for higher temperatures and for a larger diameter flame.

Plasma Sources

A ***plasma*** is a hot, partially ionized gas that contains an abundant concentration of cations and electrons. The plasma used in atomic emission is formed by ionizing a flowing stream of argon gas, producing argon ions and electrons. A plasma's high temperature results from resistive heating as the electrons and argon ions move through the gas. Because a plasma operates at a much higher temperature than a flame, it provides for a better atomization efficiency and a higher population of excited states.

A schematic diagram of the inductively coupled plasma source (ICP) is shown in Figure 10.7.2 . The ICP torch consists of three concentric quartz tubes, surrounded at the top by a radio-frequency induction coil. The sample is mixed with a stream of Ar using a nebulizer, and is carried to the plasma through the torch's central capillary tube. Plasma formation is initiated by a spark from a Tesla coil. An alternating radio-frequency current in the induction coil creates a fluctuating magnetic field that induces the argon ions and the electrons to move in a circular path. The resulting collisions with the abundant unionized gas give rise to resistive heating, providing temperatures as high as 10000 K at the base of the plasma, and between 6000 and 8000 K at a height of 15–20 mm above the coil, where emission usually is measured. At these high temperatures the outer quartz tube must be thermally isolated from the plasma. This is accomplished by the tangential flow of argon shown in the schematic diagram.

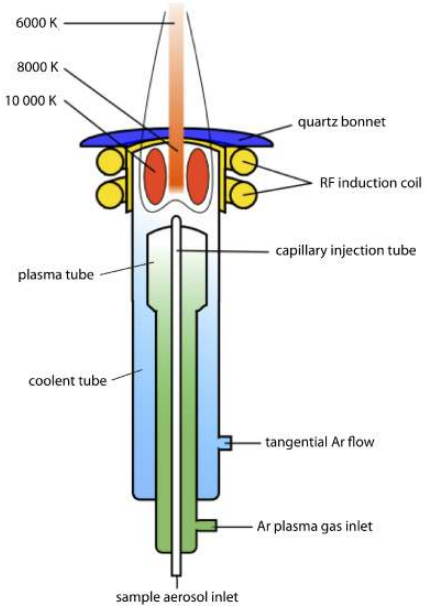


Figure 10.7.2 . Schematic diagram of an inductively coupled plasma torch.

Multielemental Analysis

Atomic emission spectroscopy is ideally suited for a multielemental analysis because all analytes in a sample are excited simultaneously. If the instrument includes a scanning monochromator, we can program it to move rapidly to an analyte's desired wavelength, pause to record its emission intensity, and then move to the next analyte's wavelength. This sequential analysis allows for a sampling rate of 3–4 analytes per minute.

Another approach to a multielemental analysis is to use a multichannel instrument that allows us to monitor simultaneously many analytes. A simple design for a multichannel spectrometer, shown in Figure 10.7.3 , couples a monochromator with multiple detectors that are positioned in a semicircular array around the monochromator at positions that correspond to the wavelengths for the analytes.

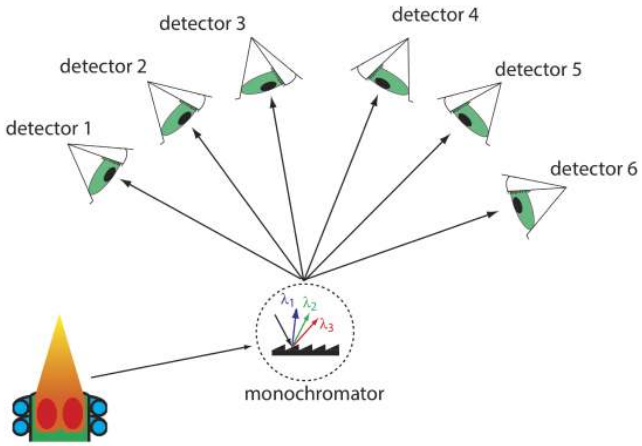


Figure 10.7.3 . Schematic diagram of a multichannel atomic emission spectrometer for the simultaneous analysis of several elements. Instruments may contain as many as 48–60 detectors.

Quantitative Applications

Atomic emission is used widely for the analysis of trace metals in a variety of sample matrices. The development of a quantitative atomic emission method requires several considerations, including choosing a source for atomization and excitation, selecting a wavelength and slit width, preparing the sample for analysis, minimizing spectral and chemical interferences, and selecting a method of standardization.

Choice of Atomization and Excitation Source

Except for the alkali metals, detection limits when using an ICP are significantly better than those obtained with flame emission (Table 10.7.1). Plasmas also are subject to fewer spectral and chemical interferences. For these reasons a plasma emission source is usually the better choice.

Table \(\PageIndex{1}). Detection Limits for Atomic Emission

element	detection limit (µg/mL): flame emission	detection limit (µg/mL): ICP
Ag	2	0.2
Al	3	0.2
As	2000	2
Ca	0.1	0.0001
Cd	300	0.07
Co	5	0.1
Cr	1	0.08
Fe	10	0.09
Hg	150	1
K	0.01	30
Li	0.001	0.02
Mg	1	0.02
Mn	1	0.01
Na	0.01	0.1
Ni	10	0.2
Pb	0.2	1
Pt	2000	0.9
Sn	100	3
Zn	1000	0.1

Source: Parsons, M. L.; Major, S.; Forster, A. R.; App. Spectrosc. 1983, 37, 411–418.

Selecting the Wavelength and Slit Width

The choice of wavelength is dictated by the need for sensitivity and the need to avoid interferences from the emission lines of other constituents in the sample. Because an analyte's atomic emission spectrum has an abundance of emission lines—particularly when using a high temperature plasma source—it is inevitable that there will be some overlap between emission lines. For example, an analysis for Ni using the atomic emission line at 349.30 nm is complicated by the atomic emission line for Fe at 349.06 nm.

A narrower slit width provides better resolution, but at the cost of less radiation reaching the detector. The easiest approach to selecting a wavelength is to record the sample's emission spectrum and look for an emission line that provides an intense signal and is resolved from other emission lines.

Preparing the Sample

Flame and plasma sources are best suited for samples in solution and in liquid form. Although a solid sample can be analyzed by directly inserting it into the flame or plasma, they usually are first brought into solution by digestion or extraction.

Minimizing Spectral Interferences

The most important spectral interference is broad, background emission from the flame or plasma and emission bands from molecular species. This background emission is particularly severe for flames because the temperature is insufficient to break down refractory compounds, such as oxides and hydroxides. Background corrections for flame emission are made by scanning over the emission line and drawing a baseline (Figure 10.7.4). Because a plasma's temperature is much higher, a background interference

due to molecular emission is less of a problem. Although emission from the plasma's core is strong, it is insignificant at a height of 10–30 mm above the core where measurements normally are made.

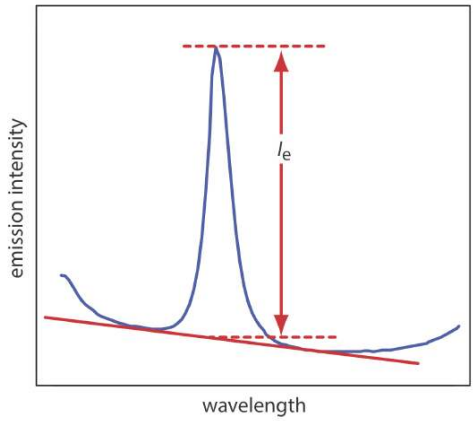


Figure 10.7.4 . Method for correcting an analyte's emission for the flame's background emission.

Minimizing Chemical Interferences

Flame emission is subject to the same types of chemical interferences as atomic absorption; they are minimized using the same methods: by adjusting the flame's composition and by adding protecting agents, releasing agents, or ionization suppressors. An additional chemical interference results from ***self-absorption***. Because the flame's temperature is greatest at its center, the concentration of analyte atoms in an excited state is greater at the flame's center than at its outer edges. If an excited state atom in the flame's center emits a photon, then a ground state atom in the cooler, outer regions of the flame may absorb the photon, which decreases the emission intensity. For higher concentrations of analyte self-absorption may invert the center of the emission band (Figure 10.7.5).

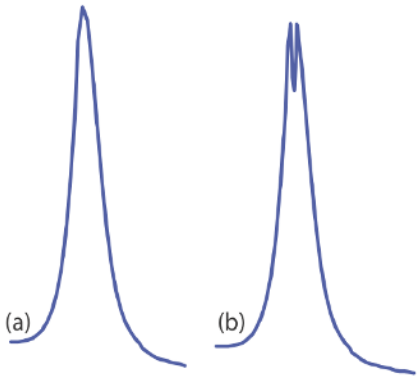


Figure 10.7.5 . Atomic emission lines for (a) a low concentration of analyte, and (b) a high concentration of analyte showing the effect of self-absorption.

Chemical interferences when using a plasma source generally are not significant because the plasma's higher temperature limits the formation of nonvolatile species. For example, $\mathbf{PO_4^{3-}}$ is a significant interferent when analyzing samples for Ca^{2+} by flame emission, but has a negligible effect when using a plasma source. In addition, the high concentration of electrons from the ionization of argon minimizes ionization interferences.

Standardizing the Method

From Equation 1.10.1 we know that emission intensity is proportional to the population of the analyte's excited state, N^*. If the flame or plasma is in thermal equilibrium, then the excited state population is proportional to the analyte's total population, N, through the Boltzmann distribution (Equation 1.10.2).

A calibration curve for flame emission usually is linear over two to three orders of magnitude, with ionization limiting linearity when the analyte's concentrations is small and self-absorption limiting linearity at higher concentrations of analyte. When using a

plasma, which suffers from fewer chemical interferences, the calibration curve often is linear over four to five orders of magnitude and is not affected significantly by changes in the matrix of the standards.

Emission intensity is affected significantly by many parameters, including the temperature of the excitation source and the efficiency of atomization. An increase in temperature of 10 K, for example, produces a 4% increase in the fraction of Na atoms in the 3*p* excited state, an uncertainty in the signal that may limit the use of external standards. The method of internal standards is used when the variations in source parameters are difficult to control. To compensate for changes in the temperature of the excitation source, the internal standard is selected so that its emission line is close to the analyte's emission line. In addition, the internal standard should be subject to the same chemical interferences to compensate for changes in atomization efficiency. To accurately correct for these errors the analyte and internal standard emission lines are monitored simultaneously.

Representative Method 10.7.1: Determination of Sodium in a Salt Substitute

The best way to appreciate the theoretical and the practical details discussed in this section is to carefully examine a typical analytical method. Although each method is unique, the following description of the determination of sodium in salt substitutes provides an instructive example of a typical procedure. The description here is based on Goodney, D. E. *J. Chem. Educ.* **1982**, *59*, 875–876.

Description of Method

Salt substitutes, which are used in place of table salt for individuals on low-sodium diets, replaces NaCl with KCl. Depending on the brand, fumaric acid, calcium hydrogen phosphate, or potassium tartrate also are present. Although intended to be sodium-free, salt substitutes contain small amounts of NaCl as an impurity. Typically, the concentration of sodium in a salt substitute is about 100 μg/g The exact concentration of sodium is determined by flame atomic emission. Because it is difficult to match the matrix of the standards to that of the sample, the analysis is accomplished by the method of standard additions.

Procedure

A sample is prepared by placing an approximately 10-g portion of the salt substitute in 10 mL of 3 M HCl and 100 mL of distilled water. After the sample has dissolved, it is transferred to a 250-mL volumetric flask and diluted to volume with distilled water. A series of standard additions is prepared by placing 25-mL portions of the diluted sample into separate 50-mL volumetric flasks, spiking each with a known amount of an approximately 10 mg/L standard solution of Na^+, and diluting to volume. After zeroing the instrument with an appropriate blank, the instrument is optimized at a wavelength of 589.0 nm while aspirating a standard solution of Na^+. The emission intensity is measured for each of the standard addition samples and the concentration of sodium in the salt substitute is reported in μg/g.

Questions

1. Potassium ionizes more easily than sodium. What problem might this present if you use external standards prepared from a stock solution of 10 mg Na/L instead of using a set of standard additions?

> Because potassium is present at a much higher concentration than is sodium, its ionization suppresses the ionization of sodium. Normally suppressing ionization is a good thing because it increases emission intensity. In this case, however, the difference between the standard's matrix and the sample's matrix means that the sodium in a standard experiences more ionization than an equivalent amount of sodium in a sample. The result is a determinate error.

2. One way to avoid a determinate error when using external standards is to match the matrix of the standards to that of the sample. We could, for example, prepare external standards using reagent grade KCl to match the matrix to that of the sample. Why is this not a good idea for this analysis?

> Sodium is a common contaminant in many chemicals. Reagent grade KCl, for example, may contain 40–50 μg Na/g. This is a significant source of sodium, given that the salt substitute contains approximately 100 μg Na/g.

3. Suppose you decide to use an external standardization. Given the previous questions, is the result of your analysis likely to underestimate or to overestimate the amount of sodium in the salt substitute?

> The solid black line in Figure 10.7.6 shows the ideal calibration curve, assuming we match the standard's matrix to the sample's matrix, and that we do so without adding any additional sodium. If we prepare the external standards without adding KCl, the emission for each standard decreases due to increased ionization. This is shown by the lower of the two

dashed red lines. Preparing the standards by adding reagent grade KCl increases the concentration of sodium due to its contamination. Because we underestimate the actual concentration of sodium in the standards, the resulting calibration curve is shown by the other dashed red line. In both cases, the sample's emission results in our overestimating the concentration of sodium in the sample.

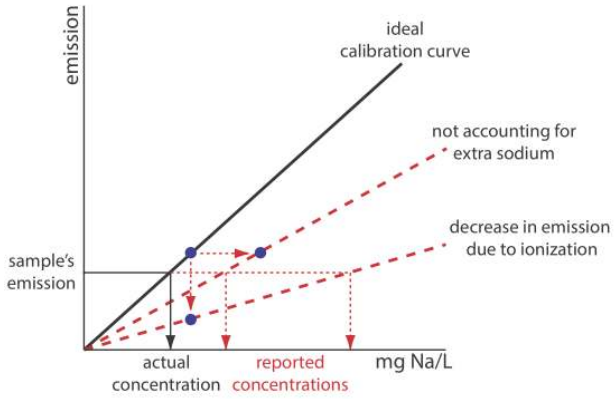


Figure 10.7.6 . External standards calibration curves for the flame atomic emission analysis of Na in a salt substitute. The solid black line shows the ideal calibration curve assuming we match the matrix of the samples and the standards using pure KCl. The lower of the two dashed red lines shows the effect of failing to add KCl to the external standards, which decreases emission. The other dashed red line shows the effect of using KCl that is contaminated with NaCl, which causes us to underestimate the concentration of Na in the standards. In both cases, the result is a positive determinate error in the analysis of samples.

4. One problem with analyzing salt samples is their tendency to clog the aspirator and burner assembly. What effect does this have on the analysis?

Clogging the aspirator and burner assembly decreases the rate of aspiration, which decreases the analyte's concentration in the flame. The result is a decrease in the emission intensity and a negative determinate error.

Example 10.7.1

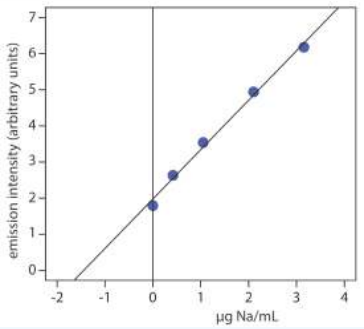
To evaluate the method described in Representative Method 10.7.1, a series of standard additions is prepared using a 10.0077-g sample of a salt substitute. The results of a flame atomic emission analysis of the standards is shown here [Goodney, D. E. *J. Chem. Educ.* **1982**, *59*, 875–876].

added Na (µg/mL)	I_e (arb. units)
0.000	1.79
0.420	2.63
1.051	3.54
2.102	4.94
3.153	6.18

What is the concentration of sodium, in µg/g, in the salt substitute.

Solution

Linear regression of emission intensity versus the concentration of added Na gives the standard additions calibration curve shown below, which has the following calibration equation.



$$I_e = 1.97 + 1.37 \times \frac{\mu g\ Na}{mL}$$

The concentration of sodium in the sample is the absolute value of the calibration curve's *x*-intercept. Substituting zero for the emission intensity and solving for sodium's concentration gives a result of 1.44 μgNa/mL. The concentration of sodium in the salt substitute is

$$\frac{\frac{1.44\ \mu g\ Na}{mL} \times \frac{50.00\ mL}{25.00\ mL} \times 250.0\ mL}{10.0077\ g\ sample} = 71.9\ \mu g\ Na/g$$

Evaluation of Atomic Emission Spectroscopy

Scale of Operation

The scale of operations for atomic emission is ideal for the direct analysis of trace and ultratrace analytes in macro and meso samples. With appropriate dilutions, atomic emission can be applied to major and minor analytes.

Accuracy

When spectral and chemical interferences are insignificant, atomic emission can achieve quantitative results with accuracies of 1–5%. For flame emission, accuracy frequently is limited by chemical interferences. Because the higher temperature of a plasma source gives rise to more emission lines, accuracy when using plasma emission often is limited by stray radiation from overlapping emission lines.

Precision

For samples and standards in which the analyte's concentration exceeds the detection limit by at least a factor of 50, the relative standard deviation for both flame and plasma emission is about 1–5%. Perhaps the most important factor that affect precision is the stability of the flame's or the plasma's temperature. For example, in a 2500 K flame a temperature fluctuation of ± 2.5 K gives a relative standard deviation of 1% in emission intensity. Significant improvements in precision are realized when using internal standards.

Sensitivity

Sensitivity is influenced by the temperature of the excitation source and the composition of the sample matrix. Sensitivity is optimized by aspirating a standard solution of analyte and maximizing the emission by adjusting the flame's composition and the height from which we monitor the emission. Chemical interferences, when present, decrease the sensitivity of the analysis. Because the sensitivity of plasma emission is less affected by the sample matrix, a calibration curve prepared using standards in a matrix of distilled water is possible even for samples that have more complex matrices.

Selectivity

The selectivity of atomic emission is similar to that of atomic absorption. Atomic emission has the further advantage of rapid sequential or simultaneous analysis of multiple analytes.

Time, Cost, and Equipment

Sample throughput with atomic emission is rapid when using an automated system that can analyze multiple analytes. For example, sampling rates of 3000 determinations per hour are possible using a multichannel ICP, and sampling rates of 300 determinations per hour when using a sequential ICP. Flame emission often is accomplished using an atomic absorption spectrometer, which typically costs between $10,000–$50,000. Sequential ICP's range in price from $55,000–$150,000, while an ICP capable of simultaneous multielemental analysis costs between $80,000–$200,000. Combination ICP's that are capable of both sequential and simultaneous analysis range in price from $150,000–$300,000. The cost of Ar, which is consumed in significant quantities, can not be overlooked when considering the expense of operating an ICP.

This page titled 1.10: Atomic Emission Spectroscopy is shared under a CC BY-NC-SA 4.0 license and was authored, remixed, and/or curated by David Harvey.

- **10.7: Atomic Emission Spectroscopy** by David Harvey is licensed CC BY-NC-SA 4.0.

1.11: Nuclear Magnetic Resonance Spectrometry

1.11: Nuclear Magnetic Resonance Spectrometry is shared under a not declared license and was authored, remixed, and/or curated by LibreTexts.

1.11.1: Additional Readings on NMR

1.11.1: Additional Readings on NMR is shared under a not declared license and was authored, remixed, and/or curated by LibreTexts.

1.11.2: Applications of NMR

1.11.2: Applications of NMR is shared under a not declared license and was authored, remixed, and/or curated by LibreTexts.

1.12: Spectroscopy Based on Scattering

The blue color of the sky during the day and the red color of the sun at sunset are the result of light scattered by small particles of dust, molecules of water, and other gases in the atmosphere. The efficiency of a photon's scattering depends on its wavelength. We see the sky as blue during the day because violet and blue light scatter to a greater extent than other, longer wavelengths of light. For the same reason, the sun appears red at sunset because red light is less efficiently scattered and is more likely to pass through the atmosphere than other wavelengths of light. The scattering of radiation has been studied since the late 1800s, with applications beginning soon thereafter. The earliest quantitative applications of scattering, which date from the early 1900s, used the elastic scattering of light by colloidal suspensions to determine the concentration of colloidal particles.

Origin of Scattering

If we send a focused, monochromatic beam of radiation with a wavelength λ through a medium of particles with dimensions $< 1.5\lambda$, the radiation scatters in all directions. For example, visible radiation of 500 nm is scattered by particles as large as 750 nm in the longest dimension. Two general categories of scattering are recognized. In elastic scattering, radiation is first absorbed by the particles and then emitted without undergoing a change in the radiation's energy. When the radiation emerges with a change in energy, the scattering is inelastic. Only elastic scattering is considered in this text.

Elastic scattering is divided into two types: Rayleigh, or small-particle scattering, and large-particle scattering. Rayleigh scattering occurs when the scattering particle's largest dimension is less than 5% of the radiation's wavelength. The intensity of the scattered radiation is proportional to its frequency to the fourth power, ν^4—which accounts for the greater scattering of blue light than red light—and is distributed symmetrically (Figure 10.8.1 a). For larger particles, scattering increases in the forward direction and decreases in the backward direction as the result of constructive and destructive interferences (Figure 10.8.1 b).

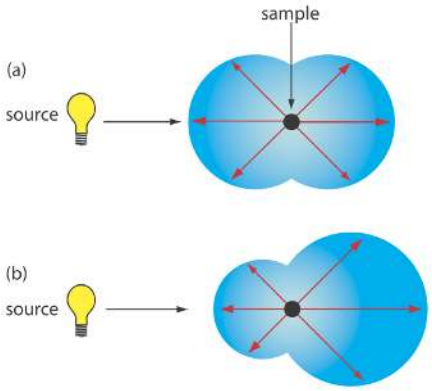


Figure 10.8.1 . Distribution of radiation for (a) Rayleigh, or small-particle scattering, and (b) large-particle scattering.

Turbidimetry and Nephelometry

Turbidimetry and nephelometry are two techniques that rely on the elastic scattering of radiation by a suspension of colloidal particles. In ***turbidimetry*** the detector is placed in line with the source and the decrease in the radiation's transmitted power is measured. In ***nephelometry*** the scattered radiation is measured at an angle of 90^o to the source. The similarity of turbidimetry to absorbance spectroscopy and of nephelometry to fluorescence spectroscopy is evident in the instrumental designs shown in Figure 10.8.2 . In fact, we can use a UV/Vis spectrophotometer for turbidimetry and we can use a spectrofluorometer for nephelometry.

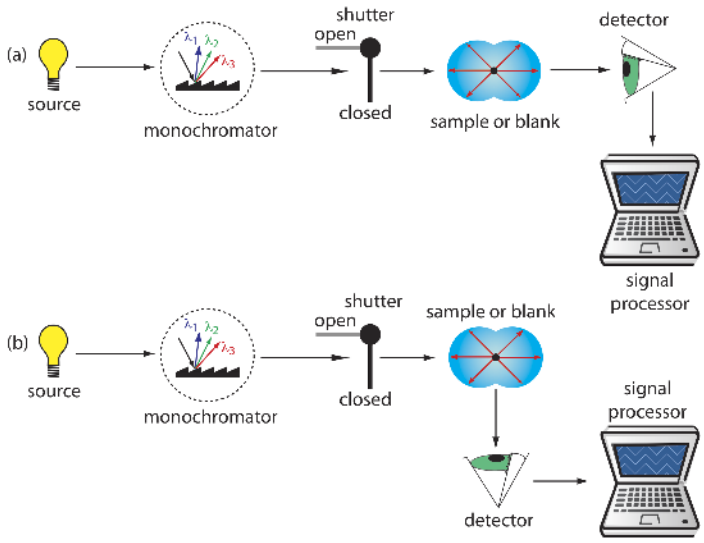


Figure 10.8.2 . Schematic diagrams for (a) a turbimeter, and (b) a nephelometer.

Turbidimetry or Nephelometry?

When developing a scattering method the choice between using turbidimetry or using nephelometry is determined by two factors. The most important consideration is the intensity of the scattered radiation relative to the intensity of the source's radiation. If the solution contains a small concentration of scattering particles, then the intensity of the transmitted radiation, I_T, is approximately the same as the intensity of the source's radiation, I_0. As we learned earlier in the section on molecular absorption, there is substantial uncertainty in determining a small difference between two intense signals. For this reason, nephelometry is a more appropriate choice for a sample that contains few scattering particles. Turbidimetry is a better choice when the sample contains a high concentration of scattering particles.

A second consideration in choosing between turbidimetry and nephelometry is the size of the scattering particles. For nephelometry, the intensity of scattered radiation at 90^o increases when the particles are small and Rayleigh scattering is in effect. For larger particles, as shown in Figure 10.8.1 , the intensity of scattering decreases at 90^o. When using an ultraviolet or a visible source of radiation, the optimum particle size is 0.1–1 μm. The size of the scattering particles is less important for turbidimetry where the signal is the relative decrease in transmitted radiation. In fact, turbidimetric measurements are feasible even when the size of the scattering particles results in an increase in reflection and refraction, although a linear relationship between the signal and the concentration of scattering particles may no longer hold.

Determining Concentration by Turbidimetry

For turbidimetry the measured transmittance, T, is the ratio of the intensity of source radiation transmitted by the sample, I_T, to the intensity of source radiation transmitted by a blank, I_0.

$$T = \frac{I_T}{I_0}$$

The relationship between transmittance and the concentration of the scattering particles is similar to that given by Beer's law

$$-\log T = kbC \tag{1.12.1}$$

where C is the concentration of the scattering particles in mass per unit volume (w/v), b is the pathlength, and k is a constant that depends on several factors, including the size and shape of the scattering particles and the wavelength of the source radiation. The exact relationship is established by a calibration curve prepared using a series of standards that contain known concentrations of analyte. As with Beer's law, Equation 1.12.1 may show appreciable deviations from linearity.

Determining Concentration by Nephelometry

For nephelometry the relationship between the intensity of scattered radiation, I_S, and the concentration of scattering particles is

$$I_s = kI_0C \tag{1.12.2}$$

where k is an empirical constant for the system and I_0 is the intensity of the source radiation. The value of k is determined from a calibration curve prepared using a series of standards that contain known concentrations of analyte.

Selecting a Wavelength for the Incident Radiation

The choice of wavelength is based primarily on the need to minimize potential interferences. For turbidimetry, where the incident radiation is transmitted through the sample, a monochromator or filter allow us to avoid wavelengths that are absorbed instead of scattered by the sample. For nephelometry, the absorption of incident radiation is not a problem unless it induces fluorescence from the sample. With a nonfluorescent sample there is no need for wavelength selection and a source of white light may be used as the incident radiation. For both techniques, other considerations in choosing a wavelength including the intensity of scattering, the trans- ducer's sensitivity (many common photon transducers are more sensitive to radiation at 400 nm than at 600 nm), and the source's intensity.

Preparing the Sample for Analysis

Although Equation 1.12.1 and Equation 1.12.2 relate scattering to the concentration of the scattering particles, the intensity of scattered radiation also is influenced by the size and the shape of the scattering particles. Samples that contain the same number of scattering particles may show significantly different values for $-\log T$ or I_S depending on the average diameter of the particles. For a quantitative analysis, therefore, it is necessary to maintain a uniform distribution of particle sizes throughout the sample and between samples and standards.

Most turbidimetric and nephelometric methods rely on precipitation reaction to form the scattering particles. As we learned in Chapter 8, a precipitate's properties, including particle size, are determined by the conditions under which it forms. To maintain a reproducible distribution of particle sizes between samples and standards, it is necessary to control parameters such as the concentration of reagents, the order of adding reagents, the pH and temperature, the agitation or stirring rate, the ionic strength, and the time between the precipitate's initial formation and the measurement of transmittance or scattering. In many cases a surface-active agent—such as glycerol, gelatin, or dextrin—is added to stabilize the precipitate in a colloidal state and to prevent the coagulation of the particles.

Applications

Turbidimetry and nephelometry are used to determine the clarity of water. The primary standard for measuring clarity is formazin, an easily prepared, stable polymer suspension (Figure 10.8.3) [Hach, C. C.; Bryant, M. "Turbidity Standards," Technical Information Series, Booklet No. 12, Hach Company: Loveland, CO, 1995]. A stock standard of formazin is prepared by combining a 1g/100mL solution of hydrazine sulfate, $N_2H_4 \cdot H_2SO_4$, with a 10 g/100 mL solution of hexamethylenetetramine to produce a suspension of particles that is defined as 4000 nephelometric turbidity units (NTU). A set of external standards with NTUs between 0 and 40 is prepared by diluting the stock standard. This method is readily adapted to the analysis of the clarity of orange juice, beer, and maple syrup.

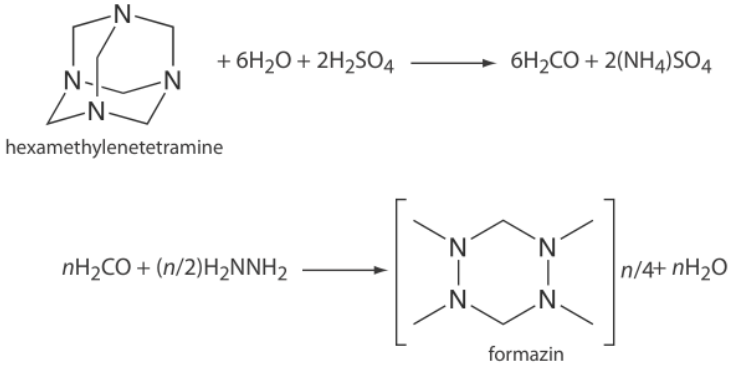


Figure 10.8.3 . Scheme for preparing formazin for use as a turbidity standard.

A number of inorganic cations and anions are determined by precipitating them under well-defined conditions. The transmittance or scattering of light, as defined by Equation 1.12.1 or Equation 1.12.2, is proportional to the concentration of the scattering particles, which, in turn, is related by the stoichiometry of the precipitation reaction to the analyte's concentration. Several examples of analytes determined in this way are listed in Table 10.8.1 .

Table 10.8.1 . Examples of Analytes Determined by Turbidimetry or Nephelometry

analyte	precipitant	precipitate
Ag^+	NaCl	AgCl
Ca^{2+}	$Na_2C_2O_4$	CaC_2O_4
Cl^-	$AgNO_3$	AgCl
CN^-	$AgNO_3$	AgCN
CO_3^{2-}	$BaCl_2$	$BaCO_3$
F^-	$CaCl_2$	CaF_2
SO_4^{2-}	$BaCl_2$	$BaSO_4$

Representative Method 10.8.1: Turbidimetric Determination of Sulfate in Water

The best way to appreciate the theoretical and the practical details discussed in this section is to carefully examine a typical analytical method. Although each method is unique, the following description of the determination of sulfate in water provides an instructive example of a typical procedure. The description here is based on Method 4500–SO42—C in *Standard Methods for the Analysis of Water and Wastewater*, American Public Health Association: Washington, D. C. 20th Ed., 1998.

Description of Method

Adding $BaCl_2$ to an acidified sample precipitates SO_4^{2-} as $BaSO_4$. The concentration of SO_4^{2-} is determined either by turbidimetry or by nephelometry using an incident source of radiation of 420 nm. External standards that contain know concentrations of SO_4^{2-} are used to standardize the method.

Procedure

Transfer a 100-mL sample to a 250-mL Erlenmeyer flask along with 20.00 mL of an appropriate buffer. For a sample that contains more than 10 mg SO_4^{2-}/L, the buffer's composition is 30 g of $MgCl_2 \cdot 6H_2O$, 5 g of $CH_3COONa \cdot 3H_2O$, 1.0 g of KNO_3, and 20 mL of glacial CH_3COOH per liter. The buffer for a sample that contain less than 10 mg SO_4^{2-}/L is the same except for the addition of 0.111 g of Na_2SO_4 per L.

Place the sample and the buffer on a magnetic stirrer operated at the same speed for all samples and standards. Add a spoonful of 20–30 mesh $BaCl_2$, using a measuring spoon with a capacity of 0.2–0.3 mL, to precipitate the SO_4^{2-} as BaSO4. Begin timing when the $BaCl_2$ is added and stir the suspension for 60 ± 2 s. When the stirring is complete, allow the solution to sit without stirring for 5.0± 0.5 min before measuring its transmittance or its scattering.

Prepare a calibration curve over the range 0–40 mg SO_4^{2-}/L by diluting a stock standard that is 100-mg SO_4^{2-}/L. Treat each standard using the procedure described above for the sample. Prepare a calibration curve and use it to determine the amount of sulfate in the sample.

Questions

1. What is the purpose of the buffer?

    If the precipitate's particles are too small, I_T is too small to measure reliably. Because rapid precipitation favors the formation of micro-crystalline particles of $BaSO_4$, we use conditions that favor the precipitate's growth over the nucleation of new particles. The buffer's high ionic strength and its acidity favor the precipitate's growth and prevent the formation of microcrystalline $BaSO_4$.

2. Why is it important to use the same stirring rate and time for the samples and standards?

    How fast and how long we stir the sample after we add $BaCl_2$ influences the size of the precipitate's particles.

3. Many natural waters have a slight color due to the presence of humic and fulvic acids, and may contain suspended matter (Figure 10.8.4). Explain why these might interfere with the analysis for sulfate. For each interferent, suggest a way to minimize its effect on the analysis.



Figure 10.8.4 . Waterfall on the River Swale in Richmond, England. The river, which flows out of the moors in the Yorkshire Dales, is brown in color as the result of organic matter that leaches from the peat found in the moors.

Suspended matter in a sample contributes to scattering and, therefore, results in a positive determinate error. We can eliminate this interference by filtering the sample prior to its analysis. A sample that is colored may absorb some of the source's radiation, leading to a positive determinate error. We can compensate for this interference by taking a sample through the analysis without adding $BaCl_2$. Because no precipitate forms, we use the transmittance of this sample blank to correct for the interference.

4. Why is Na_2SO_4 added to the buffer for samples that contain less than 10 mg SO_4^{2-}/L?

The uncertainty in a calibration curve is smallest near its center. If a sample has a high concentration of SO_4^{2-}, we can dilute it so that its concentration falls near the middle of the calibration curve. For a sample with a small concentration of SO_4^{2-}, the buffer increases the concentration of sulfate by

$$\frac{0.111\text{ g }Na_2SO_4}{\text{L}} \times \frac{96.06\text{ g }SO_4^{2-}}{142.04\text{ g }Na_2SO_4} \times \frac{1000\text{ mg}}{\text{g}} \times \frac{20.00\text{ mL}}{250.0\text{ mL}} = 6.00\text{ mg }SO_4^{2-}/\text{L}$$

After using the calibration curve to determine the amount of sulfate in the sample as analyzed, we subtract 6.00 mg SO_4^{2-}/L to determine the amount of sulfate in the original sample.

Example 10.8.1

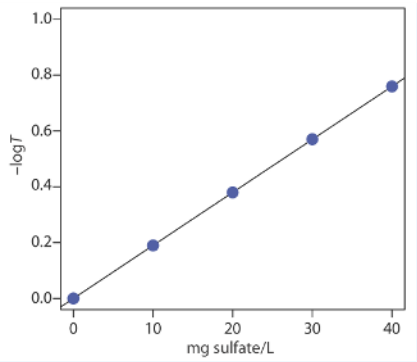
To evaluate the method described in Representative Method 10.8.1, a series of external standard was prepared and analyzed, providing the results shown in the following table.

mg SO_4^{2-}/L	transmittance
0.00	1.00
10.00	0.646
20.00	0.417
30.00	0.269
40.00	0.174

Analysis of a 100.0-mL sample of a surface water gives a transmittance of 0.538. What is the concentration of sulfate in the sample?

Solution

Linear regression of –log$T$ versus concentration of SO_4^{2-} gives the calibration curve shown below, which has the following calibration equation.



$$-\log T = -1.04 \times 10^{-5} + 0.0190 \times \frac{\text{mg } SO_4^{2-}}{\text{L}}$$

Substituting the sample's transmittance into the calibration curve's equation gives the concentration of sulfate in sample as 14.2 mg SO_4^{2-}/L.

This page titled 1.12: Spectroscopy Based on Scattering is shared under a CC BY-NC-SA 4.0 license and was authored, remixed, and/or curated by David Harvey.

- **10.8: Spectroscopy Based on Scattering** by David Harvey is licensed CC BY-NC-SA 4.0.

1.13: Neutron Activation Analysis

1.13: Neutron Activation Analysis is shared under a not declared license and was authored, remixed, and/or curated by LibreTexts.

1.14: Problems

1. Provide the missing information in the following table.

wavelength (m)	frequency (s^{-1})	wavenumber (cm^{-1})	energy (J)
4.50×10^{-9}			
	1.33×10^{15}		
		3215	
			7.20×10^{-19}

2. Provide the missing information in the following table.

[analyte] (M)	absorbance	%T	molar absorptivity (M^{-1} cm^{-1})	pathlength (cm)
1.40×10^{-4}			1120	1.00
	0.563		750	1.00
2.56×10^{-4}	0.225		456540	
1.55×10^{-3}	0.167		1550	5.00
		33.3		1.00
4.35×10^{-3}		21.2		
1.20×10^{-4}		81.3		10.00

3. A solution's transmittance is 35.0%. What is the transmittance if you dilute 25.0 mL of the solution to 50.0 mL?

4. A solution's transmittance is 85.0% when measured in a cell with a pathlength of 1.00 cm. What is the %T if you increase the pathlength to 10.00 cm?

5. The accuracy of a spectrophotometer is evaluated by preparing a solution of 60.06 ppm $K_2Cr_2O_7$ in 0.0050 M H_2SO_4, and measuring its absorbance at a wavelength of 350 nm in a cell with a pathlength of 1.00 cm. The expected absorbance is 0.640. What is the expected molar absorptivity of $K_2Cr_2O_7$ at this wavelength?

6. A chemical deviation to Beer's law may occur if the concentration of an absorbing species is affected by the position of an equilibrium reaction. Consider a weak acid, HA, for which K_a is 2×10^{-5}. Construct Beer's law calibration curves of absorbance versus the total concentration of weak acid (C_{total} = [HA] + [A^-]), using values for C_{total} of 1.0×10^{-5}, 3.0×10^{-5}, 5.0×10^{-5}, 7.0×10^{-5}, 9.0×10^{-5}, 11×10^{-5}, and 13×10^{-5} M for the following sets of conditions and comment on your results:

(a) $\varepsilon_{HA} = \varepsilon_{A^-} = 2000$ M^{-1} cm^{-1}; unbuffered solution.

(b) $\varepsilon_{HA} = 2000$ M^{-1} cm^{-1}; $\varepsilon_{A^-} = 500$ M^{-1} cm^{-1}; unbuffered solution.

(c) $\epsilon_{HA} = 2000$ M^{-1} cm^{-1}; $\epsilon_{A^-} = 500$ M^{-1} cm^{-1}; solution buffered to a pH of 4.5.

Assume a constant pathlength of 1.00 cm for all samples.

7. One instrumental limitation to Beer's law is the effect of polychromatic radiation. Consider a line source that emits radiation at two wavelengths, λ' and λ''. When treated separately, the absorbances at these wavelengths, A' and A'', are

$$A' = -\log \frac{P'_T}{P'_0} = \varepsilon' bC \qquad A'' = -\log \frac{P''_T}{P''_0} = \varepsilon'' bC$$

If both wavelengths are measured simultaneously the absorbance is

$$A = -\log \frac{(P_T' + P_T'')}{(P_0' + P_0'')}$$

(a) Show that if the molar absorptivities at λ' and λ'' are the same ($\varepsilon' = \varepsilon'' = \varepsilon$), then the absorbance is equivalent to

$$A = \varepsilon b C$$

(b) Construct Beer's law calibration curves over the concentration range of zero to 1×10^{-4} M using $\varepsilon' = 1000$ M^{-1} cm^{-1} and $\varepsilon'' = 1000$ M^{-1} cm^{-1}, and $\varepsilon' = 1000$ M^{-1} cm^{-1} and $\varepsilon'' = 100$ M^{-1} cm^{-1}. Assume a value of 1.00 cm for the pathlength and that $P_0' = P_0'' = 1$. Explain the difference between the two curves.

8. A second instrumental limitation to Beer's law is stray radiation. The following data were obtained using a cell with a pathlength of 1.00 cm when stray light is insignificant (P_{stray} = 0).

[analyte] (mM)	absorbance
0.00	0.00
2.00	0.40
4.00	0.80
6.00	1.20
8.00	1.60
10.00	3.00

Calculate the absorbance of each solution when P_{stray} is 5% of P_0, and plot Beer's law calibration curves for both sets of data. Explain any differences between the two curves. (*Hint*: Assume P_0 is 100).

9. In the process of performing a spectrophotometric determination of iron, an analyst prepares a calibration curve using a single-beam spectrophotometer similar to that shown in Figure 10.3.2. After preparing the calibration curve, the analyst drops and breaks the cuvette. The analyst acquires a new cuvette, measures the absorbance of the sample, and determines the %w/w Fe in the sample. Does the change in cuvette lead to a determinate error in the analysis? Explain.

10. The spectrophotometric methods for determining Mn in steel and for determining glucose use a chemical reaction to produce a colored spe- cies whose absorbance we can monitor. In the analysis of Mn in steel, colorless Mn^{2+} is oxidized to give the purple MnO_4^- ion. To analyze for glucose, which is also colorless, we react it with a yellow colored solution of the $Fe(CN)_6^{3-}$, forming the colorless $Fe(CN)_6^{4-}$ ion. The directions for the analysis of Mn do not specify precise reaction conditions, and samples and standards are treated separately. The conditions for the analysis of glucose, however, require that the samples and standards are treated simultaneously at exactly the same temperature and for exactly the same length of time. Explain why these two experimental procedures are so different.

11. One method for the analysis of Fe^{3+}, which is used with a variety of sample matrices, is to form the highly colored Fe^{3+}–thioglycolic acid complex. The complex absorbs strongly at 535 nm. Standardizing the method is accomplished using external standards. A 10.00-ppm Fe^{3+} working standard is prepared by transferring a 10-mL aliquot of a 100.0 ppm stock solution of Fe^{3+} to a 100-mL volumetric flask and diluting to volume. Calibration standards of 1.00, 2.00, 3.00, 4.00, and 5.00 ppm are prepared by transferring appropriate amounts of the 10.0 ppm working solution into separate 50-mL volumetric flasks, each of which contains 5 mL of thioglycolic acid, 2 mL of 20% w/v ammonium citrate, and 5 mL of 0.22 M NH_3. After diluting to volume and mixing, the absorbances of the external standards are measured against an appropriate blank. Samples are prepared for analysis by taking a portion known to contain approximately 0.1 g of Fe^{3+}, dissolving it in a minimum amount of HNO_3, and diluting to volume in a 1-L volumetric flask. A 1.00-mL aliquot of this solution is transferred to a 50-mL volumetric flask, along with 5 mL of thioglycolic acid, 2 mL of 20% w/v ammonium citrate, and 5 mL of 0.22 M NH_3 and diluted to volume. The absorbance of this solution is used to determine the concentration of $Fe3^+$ in the sample.

(a) What is an appropriate blank for this procedure?

(b) Ammonium citrate is added to prevent the precipitation of Al^{3+}. What is the effect on the reported concentration of iron in the sample if there is a trace impurity of Fe^{3+} in the ammonium citrate?

(c) Why does the procedure specify that the sample contain approximately 0.1 g of Fe^{3+}?

(d) Unbeknownst to the analyst, the 100-mL volumetric flask used to prepare the 10.00 ppm working standard of Fe^{3+} has a volume that is significantly smaller than 100.0 mL. What effect will this have on the reported concentration of iron in the sample?

12. A spectrophotometric method for the analysis of iron has a linear calibration curve for standards of 0.00, 5.00, 10.00, 15.00, and 20.00 mg Fe/L. An iron ore sample that is 40–60% w/w is analyzed by this method. An approximately 0.5-g sample is taken, dissolved in a minimum of concentrated HCl, and diluted to 1 L in a volumetric flask using distilled water. A 5.00 mL aliquot is removed with a pipet. To what volume—10, 25, 50, 100, 250, 500, or 1000 mL—should it be diluted to minimize the uncertainty in the analysis? Explain.

13. Lozano-Calero and colleagues developed a method for the quantitative analysis of phosphorous in cola beverages based on the formation of the blue-colored phosphomolybdate complex, $(NH_4)_3[PO_4(MoO_3)_{12}]$ [Lozano-Calero, D.; Martín-Palomeque, P.; Madueño-Loriguillo, S. *J. Chem. Educ.* **1996**, *73*, 1173–1174]. The complex is formed by adding $(NH_4)_6Mo_7O_{24}$ to the sample in the presence of a reducing agent, such as ascorbic acid. The concentration of the complex is determined spectrophotometrically at a wavelength of 830 nm, using an external standards calibration curve.

In a typical analysis, a set of standard solutions that contain known amounts of phosphorous is prepared by placing appropriate volumes of a 4.00 ppm solution of P_2O_5 in a 5-mL volumetric flask, adding 2 mL of an ascorbic acid reducing solution, and diluting to volume with distilled water. Cola beverages are prepared for analysis by pouring a sample into a beaker and allowing it to stand for 24 h to expel the dissolved CO_2. A 2.50-mL sample of the degassed sample is transferred to a 50-mL volumetric flask and diluted to volume. A 250-µL aliquot of the diluted sample is then transferred to a 5-mL volumetric flask, treated with 2 mL of the ascorbic acid reducing solution, and diluted to volume with distilled water.

(a) The authors note that this method can be applied only to noncol- ored cola beverages. Explain why this is true.

(b) How might you modify this method so that you can apply it to any cola beverage?

(c) Why is it necessary to remove the dissolved gases?

(d) Suggest an appropriate blank for this method?

(e) The author's report a calibration curve of

$$A = -0.02 + (0.72\ \text{ppm}^{-1}) \times C_{P_2O_5}$$

A sample of Crystal Pepsi, analyzed as described above, yields an absorbance of 0.565. What is the concentration of phosphorous, reported as ppm P, in the original sample of Crystal Pepsi?

> Crystal Pepsi was a colorless, caffeine-free soda produced by PepsiCo. It was available in the United States from 1992 to 1993.

14. EDTA forms colored complexes with a variety of metal ions that may serve as the basis for a quantitative spectrophotometric method of analysis. The molar absorptivities of the EDTA complexes of Cu^{2+}, Co^{2+}, and Ni^{2+} at three wavelengths are summarized in the following table (all values of ε are in M^{-1} cm^{-1}).

metal ion	$\varepsilon_{462.9}$	$\varepsilon_{732.0}$	$\varepsilon_{378.7}$
Co^{2+}	15.8	2.11	3.11
Cu^{2+}	2.32	95.2	7.73
Ni^{2+}	1.79	3.03	13.5

Using this information determine the following, assuming a pathlength, *b*, of 1.00 cm for all measurements:

(a) The concentration of Cu^{2+} in a solution that has an absorbance of 0.338 at a wavelength of 732.0 nm.

(b) The concentrations of Cu^{2+} and Co^{2+} in a solution that has an absorbance of 0.453 at a wavelength of 732.0 nm and 0.107 at a wavelength of 462.9 nm.

(c) The concentrations of Cu^{2+}, Co^{2+}, and Ni^{2+} in a sample that has an absorbance of 0.423 at a wavelength of 732.0 nm, 0.184 at a wavelength of 462.9 nm, and 0.291 at a wavelength of 378.7 nm.

15. The concentration of phenol in a water sample is determined by using steam distillation to separate the phenol from non-volatile impurities, followed by reacting the phenol in the distillate with 4-aminoantipyrine and $K_3Fe(CN)_6$ at pH 7.9 to form a colored antipyrine dye. A phenol standard with a concentration of 4.00 ppm has an absorbance of 0.424 at a wavelength of 460 nm using a 1.00 cm cell. A water sample is steam distilled and a 50.00-mL aliquot of the distillate is placed in a 100-mL volumetric flask and diluted to volume with distilled water. The absorbance of this solution is 0.394. What is the concentration of phenol (in parts per million) in the water sample?

16. Saito describes a quantitative spectrophotometric procedure for iron based on a solid-phase extraction using bathophenanthroline in a poly(vinyl chloride) membrane [Saito, T. *Anal. Chim. Acta* **1992**, *268*, 351–355]. In the absence of Fe^{2+} the membrane is colorless, but when immersed in a solution of Fe^{2+} and I^-, the membrane develops a red color as a result of the formation of an Fe^{2+}–bathophenanthroline complex. A calibration curve determined using a set of external standards with known concentrations of Fe^{2+} gave a standardization relationship of

$$A = (8.60 \times 10^3\ \mathrm{M^{-1}}) \times [\mathrm{Fe^{2+}}]$$

What is the concentration of iron, in mg Fe/L, for a sample with an absorbance of 0.100?

17. In the DPD colorimetric method for the free chlorine residual, which is reported as mg Cl_2/L, the oxidizing power of free chlorine converts the colorless amine N,N-diethyl-*p*-phenylenediamine to a colored dye that absorbs strongly over the wavelength range of 440–580 nm. Analysis of a set of calibration standards gave the following results.

mg Cl_2/L	absorbance
0.00	0.000
0.50	0.270
1.00	0.543
1.50	0.813
2.00	1.084

A sample from a public water supply is analyzed to determine the free chlorine residual, giving an absorbance of 0.113. What is the free chlorine residual for the sample in mg Cl_2/L?

18. Lin and Brown described a quantitative method for methanol based on its effect on the visible spectrum of methylene blue [Lin, J.; Brown, C. W. *Spectroscopy* **1995**, *10(5)*, 48–51]. In the absence of methanol, methylene blue has two prominent absorption bands at 610 nm and 663 nm, which correspond to the monomer and the dimer, respectively. In the presence of methanol, the intensity of the dimer's absorption band decreases, while that for the monomer increases. For concentrations of methanol between 0 and 30% v/v, the ratio of the two absorbance, A_{663}/A_{610}, is a linear function of the amount of methanol. Use the following standardization data to determine the %v/v methanol in a sample if A_{610} is 0.75 and A_{663} is 1.07.

%v/v methanol	A_{663}/A_{610}	%v/v methanol	A_{663}/A_{610}
0.0	1.21	20.0	1.62
5.0	1.29	25.0	1.74
10.0	1.42	30.0	1.84
15.0	1.52		

19. The concentration of the barbiturate barbital in a blood sample is determined by extracting 3.00 mL of blood with 15 mL of $CHCl_3$. The chloroform, which now contains the barbital, is extracted with 10.0 mL of 0.45 M NaOH (pH ≈ 13). A 3.00-mL sample of the aqueous extract is placed in a 1.00-cm cell and an absorbance of 0.115 is measured. The pH of the sample in the absorption cell is then adjusted to approximately 10 by adding 0.50 mL of 16% w/v NH_4Cl, giving an absorbance of 0.023. When 3.00 mL of a standard barbital solution with a concentration of 3 mg/100 mL is taken through the same procedure, the absorbance at pH 13 is 0.295 and the absorbance at a pH of 10 is 0.002. Report the mg barbital/100 mL in the sample.

20. Jones and Thatcher developed a spectrophotometric method for analyzing analgesic tablets that contain aspirin, phenacetin, and caffeine [Jones, M.; Thatcher, R. L. *Anal. Chem.* **1951**, *23*, 957–960]. The sample is dissolved in $CHCl_3$ and extracted with an aqueous solution of $NaHCO_3$ to remove the aspirin. After the extraction is complete, the chloroform is transferred to a 250-mL volumetric flask and diluted to volume with $CHCl_3$. A 2.00-mL portion of this solution is then diluted to volume in a 200-mL volumetric flask with $CHCl_3$. The absorbance of the final solution is measured at wavelengths of 250 nm and 275 nm, at which the absorptivities, in $ppm^{-1}\ cm^{-1}$, for caffeine and phenacetin are

analyte	ε_{250}	ε_{275}
caffeine	0.0131	0.0485
phenacetin	0.0702	0.0159

Aspirin is determined by neutralizing the $NaHCO_3$ in the aqueous solution and extracting the aspirin into $CHCl_3$. The combined extracts are diluted to 500 mL in a volumetric flask. A 20.00-mL portion of the solution is placed in a 100-mL volumetric flask and diluted to volume with $CHCl_3$. The absorbance of this solution is measured at 277 nm, where the absorptivity of aspirin is 0.00682 $ppm^{-1}\ cm^{-1}$. An analgesic tablet treated by this procedure is found to have absorbances of 0.466 at 250 nm, 0.164 at 275 nm, and 0.600 at 277 nm when using a cell with a 1.00 cm pathlength. Report the milligrams of aspirin, caffeine, and phenacetin in the analgesic tablet.

21. The concentration of SO_2 in a sample of air is determined by the *p*-rosaniline method. The SO_2 is collected in a 10.00-mL solution of $HgCl_4^{2-}$, where it reacts to form $Hg(SO_3)_2$, by pulling air through the solution for 75 min at a rate of 1.6 L/min. After adding *p*-rosaniline and formaldehyde, the colored solution is diluted to 25 mL in a volumetric flask. The absorbance is measured at 569 nm in a 1-cm cell, yielding a value of 0.485. A standard sample is prepared by substituting a 1.00-mL sample of a standard solution that contains the equivalent of 15.00 ppm SO_2 for the air sample. The absorbance of the standard is found to be 0.181. Report the concentration of SO_2 in the air in mg SO_2/L. The density of air is 1.18 g/liter.

22. Seaholtz and colleagues described a method for the quantitative analysis of CO in automobile exhaust based on the measurement of infrared radiation at 2170 cm^{-1} [Seaholtz, M. B.; Pence, L. E.; Moe, O. A. Jr. *J. Chem. Educ.* **1988**, *65*, 820–823]. A calibration curve is prepared by filling a 10-cm IR gas cell with a known pressure of CO and measuring the absorbance using an FT-IR, giving a calibration equation of

$$A = -1.1 \times 10^{-4} + (9.9 \times 10^{-4}) \times P_{CO}$$

Samples are prepared by using a vacuum manifold to fill the gas cell. After measuring the total pressure, the absorbance at 2170 cm^{-1} is measured. Results are reported as %CO (P_{CO}/P_{total}). The analysis of five exhaust samples from a 1973 coupe gives the following results.

P_{total} (torr)	absorbance
595	0.1146
354	0.0642
332	0.0591
233	0.0412
143	0.0254

Determine the %CO for each sample, and report the mean and the 95% confidence interval.

23. Figure 10.3.8 shows an example of a disposable IR sample card made using a thin sheet of polyethylene. To prepare an analyte for analysis, it is dissolved in a suitable solvent and a portion of the sample placed on the IR card. After the solvent evaporates, leaving the analyte behind as a thin film, the sample's IR spectrum is obtained. Because the thickness of the polyethylene film is not uniform, the primary application of IR cards is for a qualitative analysis. Zhao and Malinowski reported how an internal standardization with KSCN can be used for a quantitative IR analysis of polystyrene [Zhao, Z.; Malinowski, E. R. *Spectroscopy* **1996**, *11(7)*, 44–49]. Polystyrene is monitored at 1494 cm^{-1} and KSCN at 2064 cm^{-1}. Standard solutions are prepared by placing weighed portions of polystyrene in a 10-mL volumetric flask and diluting to volume with a solution of 10 g/L KSCN in methyl isobutyl ketone. A typical set of results is shown here.

g polystyrene	0.1609	0.3290	0.4842	0.6402	0.8006
A_{1494}	0.0452	0.1138	0.1820	0.3275	0.3195
A_{2064}	0.1948	0.2274	0.2525	0.3580	0.2703

When a 0.8006-g sample of a poly(styrene/maleic anhydride) copolymer is analyzed, the following results are obtained.

replicate	A_{1494}	A_{2064}
1	0.2729	0.3582
2	0.2074	0.2820
3	0.2785	0.3642

What is the %w/w polystyrene in the copolymer? Given that the reported %w/w polystyrene is 67%, is there any evidence for a determinate error at $\alpha = 0.05$?

24. The following table lists molar absorptivities for the Arsenazo complexes of copper and barium [Grossman, O.; Turanov, A. N. *Anal. Chim. Acta* **1992**, *257*, 195–202]. Suggest appropriate wavelengths for analyzing mixtures of copper and barium using their Arsenzao complexes.

wavelength (nm)	ε_{Cu} (M^{-1} cm^{-1})	ε_{Ba} (M^{-1} cm^{-1})
595	11900	7100
600	15500	7200
607	18300	7400
611	19300	6900
614	19300	7000
620	17800	7100
626	16300	8400
635	10900	9900
641	7500	10500
645	5300	10000
650	3500	8600
655	2200	6600
658	1900	6500
665	1500	3900
670	1500	2800
680	1800	1500

25. Blanco and colleagues report several applications of multiwavelength linear regression analysis for the simultaneous determination of two-component mixtures [Blanco, M.; Iturriaga, H.; Maspoch, S.; Tarin, P. *J. Chem. Educ.* **1989**, *66*, 178–180]. For each of the following, determine the molar concentration of each analyte in the mixture.

(a) Titanium and vanadium are determined by forming complexes with H_2O_2. Results for a mixture of Ti(IV) and V(V) and for stan-dards of 63.1 ppm Ti(IV) and 96.4 ppm V(V) are listed in the following table.

wavelength (nm)	$A_{Ti(V)\ Std}$	$A_{V(V)\ Std}$	A_{mix}
390	0.895	0.326	0.651
430	0.884	0.497	0.743
450	0.694	0.528	0.665
470	0.481	0.512	0.547
510	0.173	0.374	0.314

(b) Copper and zinc are determined by forming colored complexes with 2-pyridyl-azo-resorcinol (PAR). The absorbances for PAR, a mixture of Cu^{2+} and Zn^{2+}, and standards of 1.00 ppm Cu^{2+} and 1.00 ppm Zn^{2+} are listed in the following table. Note that you must correct the absorbances for the each metal for the contribution from PAR.

wavelength (nm)	A_{PAR}	$A_{Cu\ Std}$	$A_{Zn\ Std}$	A_{mix}
480	0.211	0.698	0.971	0.656
496	0.137	0.732	1.018	0.668
510	0.100	0.732	0.891	0.627
526	0.072	0.602	0.672	0.498
540	0.056	0.387	0.306	0.290

26. The stoichiometry of a metal–ligand complex, ML_n, is determined by the method of continuous variations. A series of solutions is prepared in which the combined concentrations of M and L are held constant at 5.15×10^{-4} M. The absorbances of these solutions are measured at a wavelength where only the metal–ligand complex absorbs. Using the following data, determine the formula of the metal–ligand complex.

mole fraction of M	mole fraction of L	absorbance
1.0	0.0	0.001
0.9	0.1	0.126
0.8	0.2	0.260
0.7	0.3	0.389
0.6	0.4	0.515
0.5	0.5	0.642
0.4	0.6	0.775
0.3	0.7	0.771
0.2	0.8	0.513
0.1	0.9	0.253
0.0	1.0	0.000

27. The stoichiometry of a metal–ligand complex, ML_n, is determined by the mole-ratio method. A series of solutions are prepared in which the metal's concentration is held constant at 3.65×10^{-4} M and the ligand's concentration is varied from 1×10^{-4} M to 1×10^{-3} M. Using the following data, determine the stoichiometry of the metal-ligand complex.

[ligand] (M)	absorbance	[ligand] (M)	absorbance
1.0×10^{-4}	0.122	6.0×10^{-4}	0.752
2.0×10^{-4}	0.251	7.0×10^{-4}	0.873
3.0×10^{-4}	0.376	8.0×10^{-4}	0.937
4.0×10^{-4}	0.496	9.0×10^{-4}	0.962
5.0×10^{-4}	0.625	1.0×10^{-3}	1.002

28. The stoichiometry of a metal–ligand complex, ML_n, is determined by the slope-ratio method. Two sets of solutions are prepared. For the first set of solutions the metal's concentration is held constant at 0.010 M and the ligand's concentration is varied. The following data are obtained at a wavelength where only the metal–ligand complex absorbs.

[ligand] (M)	absorbance
1.0×10^{-5}	0.012
2.0×10^{-5}	0.029
3.0×10^{-5}	0.042
4.0×10^{-5}	0.055
5.0×10^{-5}	0.069

For the second set of solutions the concentration of the ligand is held constant at 0.010 M, and the concentration of the metal is varied, yielding the following absorbances.

[metal] (M)	absorbance
1.0×10^{-5}	0.040
2.0×10^{-5}	0.085
3.0×10^{-5}	0.125
4.0×10^{-5}	0.162
5.0×10^{-5}	0.206

Using this data, determine the stoichiometry of the metal-ligand complex.

29. Kawakami and Igarashi developed a spectrophotometric method for nitrite based on its reaction with 5, 10, 15, 20-tetrakis(4-aminophenyl) porphrine (TAPP). As part of their study they investigated the stoichiometry of the reaction between TAPP and NO_2^-. The following data are derived from a figure in their paper [Kawakami, T.; Igarashi, S. *Anal. Chim. Acta* **1996**, *333*, 175–180].

[TAPP] (M)	[NO_2^-] (M)	absorbance
8.0×10^{-7}	0	0.227
8.0×10^{-7}	4.0×10^{-8}	0.223
8.0×10^{-7}	8.0×10^{-8}	0.211
8.0×10^{-7}	1.6×10^{-7}	0.191
8.0×10^{-7}	3.2×10^{-7}	0.152
8.0×10^{-7}	4.8×10^{-7}	0.127
8.0×10^{-7}	6.4×10^{-7}	0.107
8.0×10^{-7}	8.0×10^{-7}	0.092
8.0×10^{-7}	1.6×10^{-6}	0.058
8.0×10^{-7}	2.4×10^{-6}	0.045
8.0×10^{-7}	3.2×10^{-6}	0.037
8.0×10^{-7}	4.0×10^{-6}	0.034

What is the stoichiometry of the reaction?

30. The equilibrium constant for an acid–base indicator is determined by preparing three solutions, each of which has a total indicator concentration of 1.35×10^{-5} M. The pH of the first solution is adjusted until it is acidic enough to ensure that only the acid

form of the indicator is present, yielding an absorbance of 0.673. The absorbance of the second solution, whose pH is adjusted to give only the base form of the indicator, is 0.118. The pH of the third solution is adjusted to 4.17 and has an absorbance of 0.439. What is the acidity constant for the acid–base indicator?

31. The acidity constant for an organic weak acid is determined by measuring its absorbance as a function of pH while maintaining a constant total concentration of the acid. Using the data in the following table, determine the acidity constant for the organic weak acid.

pH	absorbance	pH	absorbance
1.53	0.010	4.88	0.193
2.20	0.010	5.09	0.227
3.66	0.035	5.69	0.288
4.11	0.072	7.20	0.317
4.35	0.103	7.78	0.317
4.75	0.169		

32. Suppose you need to prepare a set of calibration standards for the spectrophotometric analysis of an analyte that has a molar absorptivity of 1138 M^{-1} cm^{-1} at a wavelength of 625 nm. To maintain an acceptable precision for the analysis, the %T for the standards should be between 15% and 85%.

(a) What is the concentration for the most concentrated and for the least concentrated standard you should prepare, assuming a 1.00-cm sample cell.

(b) Explain how you will analyze samples with concentrations that are 10 μM, 0.1 mM, and 1.0 mM in the analyte.

33. When using a spectrophotometer whose precision is limited by the uncertainty of reading %T, the analysis of highly absorbing solutions can lead to an unacceptable level of indeterminate errors. Consider the analysis of a sample for which the molar absorptivity is $\mathbf{1.0 \times 10^4}$ M^{-1} cm^{-1} and for which the pathlength is 1.00 cm.

(a) What is the relative uncertainty in concentration for an analyte whose concentration is $\mathbf{2.0 \times 10^{-4}}$ M if s_T is ±0.002?

(b) What is the relative uncertainty in the concentration if the spectrophotometer is calibrated using a blank that consists of a $\mathbf{1.0 \times 10^{-4}}$ M solution of the analyte?

34. Hobbins reported the following calibration data for the flame atomic absorption analysis for phosphorous [Hobbins, W. B. "Direct Determination of Phosphorous in Aqueous Matricies by Atomic Absorption," Varian Instruments at Work, Number AA-19, February 1982].

mg P/L	absorbance
2130	0.048
4260	0.110
6400	0.173
8530	0.230

To determine the purity of a sample of Na_2HPO_4, a 2.469-g sample is dissolved and diluted to volume in a 100-mL volumetric flask. Analysis of the resulting solution gives an absorbance of 0.135. What is the purity of the Na_2HPO_4?

35. Bonert and Pohl reported results for the atomic absorption analysis of several metals in the caustic suspensions produced during the manufacture of soda by the ammonia-soda process [Bonert, K.; Pohl, B. "The Determination of Cd, Cr, Cu, Ni, and Pb in Concentrated $CaCl_2$/NaCl solutions by AAS," AA Instruments at Work (Varian) Number 98, November, 1990].

(a) The concentration of Cu is determined by acidifying a 200.0-mL sample of the caustic solution with 20 mL of concentrated HNO_3, adding 1 mL of 27% w/v H_2O_2, and boiling for 30 min. The resulting solution is diluted to 500 mL in a volumetric flask, filtered, and analyzed by flame atomic absorption using matrix matched standards. The results for a typical analysis are shown in the following table.

solution	mg Cu/L	absorbance
blank	0.000	0.007
standard 1	0.200	0.014
standard 2	0.500	0.036
standard 3	1.000	0.072
standard 4	2.000	0.146
sample		0.027

Determine the concentration of Cu in the caustic suspension.

(b) The determination of Cr is accomplished by acidifying a 200.0-mL sample of the caustic solution with 20 mL of concentrated HNO_3, adding 0.2 g of Na_2SO_3 and boiling for 30 min. The Cr is isolated from the sample by adding 20 mL of NH_3, producing a precipitate that includes the chromium as well as other oxides. The precipitate is isolated by filtration, washed, and transferred to a beaker. After acidifying with 10 mL of HNO_3, the solution is evaporated to dryness. The residue is redissolved in a combination of HNO_3 and HCl and evaporated to dryness. Finally, the residue is dissolved in 5 mL of HCl, filtered, diluted to volume in a 50-mL volumetric flask, and analyzed by atomic absorption using the method of standard additions. The atomic absorption results are summarized in the following table.

sample	mg Cr_{added}/L	absorbance
blank		0.001
sample		0.045
standard addition 1	0.200	0.083
standard addition 2	0.500	0.118
standard addition 3	1.000	0.192

Report the concentration of Cr in the caustic suspension.

36. Quigley and Vernon report results for the determination of trace metals in seawater using a graphite furnace atomic absorption spectrophotometer and the method of standard additions [Quigley, M. N.; Vernon, F. *J. Chem. Educ.* **1996**, *73*, 671–673]. The trace metals are first separated from their complex, high-salt matrix by coprecipitating with Fe^{3+}. In a typical analysis a 5.00-mL portion of 2000 ppm Fe^{3+} is added to 1.00 L of seawater. The pH is adjusted to 9 using NH_4OH, and the precipitate of $Fe(OH)_3$ allowed to stand overnight. After isolating and rinsing the precipitate, the $Fe(OH)_3$ and coprecipitated metals are dissolved in 2 mL of concentrated HNO_3 and diluted to volume in a 50-mL volumetric flask. To analyze for Mn^{2+}, a 1.00-mL sample of this solution is diluted to 100 mL in a volumetric flask. The following samples are injected into the graphite furnace and analyzed.

sample	absorbance
2.5-µL sample + 2.5 µL of 0 ppb Mn^{2+}	0.223
2.5-µL sample + 2.5 µL of 2.5 ppb Mn^{2+}	0.294
2.5-µL sample + 2.5 µL of 5.0 ppb Mn^{2+}	0.361

Report the ppb Mn^{2+} in the sample of seawater.

37. The concentration of Na in plant materials are determined by flame atomic emission. The material to be analyzed is prepared by grinding, homogenizing, and drying at 103°C. A sample of approximately 4 g is transferred to a quartz crucible and heated on a hot plate to char the organic material. The sample is heated in a muffle furnace at 550°C for several hours. After cooling to room temperature the residue is dissolved by adding 2 mL of 1:1 HNO_3 and evaporated to dryness. The residue is redissolved in 10 mL of 1:9 HNO_3, filtered and diluted to 50 mL in a volumetric flask. The following data are obtained during a typical analysis for the concentration of Na in a 4.0264-g sample of oat bran.

sample	mg Na/L	emission (arbitrary units)
blank	0.00	0.0
standard 1	2.00	90.3
standard 2	4.00	181
standard 3	6.00	272
standard 4	8.00	363
standard 5	10.00	448
sample		238

Report the concentration of µg Na/g sample.

38. Yan and colleagues developed a method for the analysis of iron based its formation of a fluorescent metal–ligand complex with the ligand 5-(4-methylphenylazo)-8-aminoquinoline [Yan, G.; Shi, G.; Liu, Y. *Anal. Chim. Acta* **1992**, *264*, 121–124]. In the presence of the surfactant cetyltrimethyl ammonium bromide the analysis is carried out using an excitation wavelength of 316 nm with emission monitored at 528 nm. Standardization with external standards gives the following calibration curve.

$$I_f = -0.03 + \left(1.594\ \text{mg}^{-1}\ \text{L}\right) \times \frac{\text{mg Fe}^{3+}}{\text{L}}$$

A 0.5113-g sample of dry dog food is ashed to remove organic materials, and the residue dissolved in a small amount of HCl and diluted to volume in a 50-mL volumetric flask. Analysis of the resulting solution gives a fluorescent emission intensity of 5.72. Determine the mg Fe/L in the sample of dog food.

39. A solution of 5.00×10^{-5} M 1,3-dihydroxynaphthelene in 2 M NaOH has a fluorescence intensity of 4.85 at a wavelength of 459 nm. What is the concentration of 1,3-dihydroxynaphthelene in a solution that has a fluorescence intensity of 3.74 under identical conditions?

40. The following data is recorded for the phosphorescent intensity of several standard solutions of benzo[a]pyrene.

[benzo[a]pyrene] (M)	emission intensity
0	0.00
1.00×10^{-5}	0.98
3.00×10^{-5}	3.22
6.00×10^{-5}	6.25
1.00×10^{-4}	10.21

What is the concentration of benzo[a]pyrene in a sample that yields a phosphorescent emission intensity of 4.97?

41. The concentration of acetylsalicylic acid, $C_9H_8O_4$, in aspirin tablets is determined by hydrolyzing it to the salicylate ion, $C_7H_5O_2^-$, and determining its concentration spectrofluorometrically. A stock standard solution is prepared by weighing 0.0774 g of

salicylic acid, $C_7H_6O_2$, into a 1-L volumetric flask and diluting to volume. A set of calibration standards is prepared by pipeting 0, 2.00, 4.00, 6.00, 8.00, and 10.00 mL of the stock solution into separate 100-mL volumetric flasks that contain 2.00 mL of 4 M NaOH and diluting to volume. Fluorescence is measured at an emission wavelength of 400 nm using an excitation wavelength of 310 nm with results shown in the following table.

mL of stock solution	emission intensity
0.00	0.00
2.00	3.02
4.00	5.98
6.00	9.18
8.00	12.13
10.00	14.96

Several aspirin tablets are ground to a fine powder in a mortar and pestle. A 0.1013-g portion of the powder is placed in a 1-L volumetric flask and diluted to volume with distilled water. A portion of this solution is filtered to remove insoluble binders and a 10.00-mL aliquot transferred to a 100-mL volumetric flask that contains 2.00 mL of 4 M NaOH. After diluting to volume the fluorescence of the resulting solution is 8.69. What is the %w/w acetylsalicylic acid in the aspirin tablets?

42. Selenium (IV) in natural waters is determined by complexing with ammonium pyrrolidine dithiocarbamate and extracting into $CHCl_3$. This step serves to concentrate the Se(IV) and to separate it from Se(VI). The Se(IV) is then extracted back into an aqueous matrix using HNO_3. After complexing with 2,3-diaminonaphthalene, the complex is extracted into cyclohexane. Fluorescence is measured at 520 nm following its excitation at 380 nm. Calibration is achieved by adding known amounts of Se(IV) to the water sample before beginning the analysis. Given the following results what is the concentration of Se(IV) in the sample.

[Se(IV)] added (nM)	emission intensity
0.00	323
2.00	597
4.00	862
6.00	1123

43. Fibrinogen is a protein that is produced by the liver and found in human plasma. Its concentration in plasma is clinically important. Many of the analytical methods used to determine the concentration of fibrinogen in plasma are based on light scattering following its precipitation. For example, da Silva and colleagues describe a method in which fibrino- gen precipitates in the presence of ammonium sulfate in a guanidine hydrochloride buffer [da Silva, M. P.; Fernandez-Romero, J. M.; Luque de Castro, M. D. *Anal. Chim. Acta* **1996**, *327*, 101–106]. Light scattering is measured nephelometrically at a wavelength of 340 nm. Analysis of a set of external calibration standards gives the following calibration equation

$$I_s = -4.66 + 9907.63C$$

where I_s is the intensity of scattered light and C is the concentration of fibrinogen in g/L. A 9.00-mL sample of plasma is collected from a patient and mixed with 1.00 mL of an anticoagulating agent. A 1.00-mL aliquot of this solution is diluted to 250 mL in a volumetric flask and is found to have a scattering intensity of 44.70. What is the concentration of fibrinogen, in gram per liter, in the plasma sample?

This page titled 1.14: Problems is shared under a CC BY-NC-SA 4.0 license and was authored, remixed, and/or curated by David Harvey.

- **10.9: Problems** by David Harvey is licensed CC BY-NC-SA 4.0.

1.15: Additional Resources

The following set of experiments introduce students to the applications of spectroscopy. Experiments are grouped into five categories: UV/Vis spectroscopy, IR spectroscopy, atomic absorption and atomic emission, fluorescence and phosphorescence, and signal averaging.

UV/Vis Spectroscopy

- Abney, J. R.; Scalettar, B. A. "Saving Your Students' Skin. Undergraduate Experiments That Probe UV Protection by Sunscreens and Sunglasses," *J. Chem. Educ.* **1998**, *75*, 757–760.
- Ainscough, E. W.; Brodie, A. M. "The Determination of Vanillin in Vanilla Extract," *J. Chem. Educ.* **1990**, *67*, 1070–1071.
- Allen, H. C.; Brauers, T.; Finlayson-Pitts, B. J. "Illustrating Deviations in the Beer-Lambert Law in an Instrumental Analysis Laboratory: Measuring Atmospheric Pollutants by Differential Optical Absorption Spectrometry," *J. Chem. Educ.* **1997**, *74*, 1459–1462.
- Blanco, M.; Iturriaga, H.; Maspoch, S.; Tarîn, P. "A Simple Method for Spectrophotometric Determination of Two-Components with Overlapped Spectra," *J. Chem. Educ.* **1989**, *66*, 178–180.
- Bonicamp, J. M.; Martin, K. L.; McBride, G. R.; Clark, R. W. "Beer's Law is Not a Straight Line: Amplification of Errors by Transformation," *Chem. Educator* **1999**, *4*, 81–88.
- Bruneau, E.; Lavabre, D.; Levy, G.; Micheau, J. C. "Quantitative Analysis of Continuous-Variation Plots with a Comparison of Several Methods," *J. Chem. Educ.* **1992**, *69*, 833–837.
- Cappas, C.; Hoffman, N.; Jones, J.; Young, S. "Determination of Concentrations of Species Whose Absorption Bands Overlap Extensively," *J. Chem. Educ.* **1991**, *68*, 300–303.
- Crisp, P. T.; Eckert, J. M.; Gibson, N. A. "The Determination of Anionic Surfactants in Natural and Waste Waters," *J. Chem. Educ.* **1983**, *60*, 236–238.
- Dilbeck, C. W.; Ganske, J. A. "Detection of NOx in Automobile Exhaust: An Applied Experiment in Atmospheric/Environmental Chemistry for the General Chemistry Laboratory," *Chem. Educator* **2008**, *13*, 1–5.
- Domínguez, A., Fernández, A.; González, N.; Iglesias, E.; Montenegro, L. "Determination of Critical Micelle Concentration of Some Surfactants by Three Techniques," *J. Chem. Educ.* **1997**, *74*, 1227– 1231.
- Gilbert, D. D. "Determining Optimum Spectral Bandwidth," *J. Chem. Educ.* **1991**, *68*, A278– A281.
- Han, J.; Story, T.; Han, G. "A Spectrophotometric Method for Quantitative Determination of Bromine Using Tris(2-carboxyethyl)phophine," *J. Chem. Educ.* **1999**, *76*, 976–977.
- Higginbotham, C.; Pike, C. F.; Rice, J, K. "Spectroscopy in Sol-Gel Matricies," *J. Chem. Educ.* **1998**, *75*, 461–464.
- Hill, Z. D.; MacCarthy, P. "Novel Approach to Job's Method," *J. Chem. Educ.* **1986**, *63*, 162–167.
- Ibañez, G. A.; Olivieri, A. C.; Escandar, G. M. "Determination of Equilibrium Constants of Metal Complexes from Spectrophotometric Measurements," *J. Chem. Educ.* **1999**, *76*, 1277–1281.
- Long, J. R.; Drago, R. S. "The Rigorous Evaluation of Spectrophotometric Data to Obtain an Equilibrium Constant," *J. Chem. Educ.* **1982**, *59*, 1037–1039.
- Lozano-Calero; D.; Martin-Palomeque, P. "Determination of Phosphorous in Cola Drinks," *J. Chem. Educ.* **1996**, *73*, 1173–1174.
- Maloney, K. M.; Quiazon, E. M.; Indralingam, R. "Measurement of Iron in Egg Yolk: An Instrumental Analysis Measurement Using Biochemical Principles," *J. Chem. Educ.* **2008**, *85*, 399–400.
- Mascotti, D. P.; Waner, M. J. "Complementary Spectroscopic Assays for Investigation Protein-Ligand Binding Activity: A Project for the Advanced Chemistry Laboratory," *J. Chem. Educ.* **2010**, *87*, 735– 738.
- McClain, R. L. "Construction of a Photometer as an Instructional Tool for Electronics and Instrumentation," *J. Chem. Educ.* **2014**, *91*, 747–750.
- McDevitt, V. L.; Rodriquez, A.; Williams, K. R. "Analysis of Soft Drinks: UV Spectrophotometry, Liquid Chromatography, and Capillary Electrophoresis," *J. Chem. Educ.* **1998**, *75*, 625–629.
- Mehra, M. C.; Rioux, J. "An Analytical Chemistry Experiment in Simultaneous Spectrophotometric Determination of Fe(III) and Cu(II) with Hexacyanoruthenate(II) Reagent," *J. Chem. Educ.* **1982**, *59*, 688–689.
- Mitchell-Koch, J. T.; Reid, K. R.; Meyerhoff, M. E. "Salicylate Detection by Complexation with Iron(III) and Optical Absorbance Spectroscopy," *J. Chem. Educ.* **2008**, *85*, 1658–1659.

- Msimanga, H. Z.; Wiese, J. “Determination of Acetaminophen in Analgesics by the Standard Addition Method: A Quantitative Analytical Chemistry Laboratory,” *Chem. Educator* **2005**, *10*, 1–7.
- Örstan, A.; Wojcik, J. F. “Spectroscopic Determination of Protein-Ligand Binding Constants,” *J. Chem. Educ.* **1987**, *64*, 814–816.
- Pandey, S.; Powell, J. R.; McHale, M. E. R.; Acree Jr., W. E. “Quantitative Determination of Cr(III) and Co(II) Using a Spectroscopic H-Point Standard Addition,” *J. Chem. Educ.* **1997**, *74*, 848–850.
- Parody-Morreale, A.; Cámara-Artigas, A.; Sánchez-Ruiz, J. M. “Spectrophotometric Determination of the Binding Constants of Succinate and Chloride to Glutamic Oxalacetic Transaminase,” *J. Chem. Educ.* **1990**, *67*, 988–990.
- Ravelo-Perez, L. M.; Hernández-Borges, J.; Rodríguez-Delgado, M. A.; Borges-Miquel, T. “Spectrophotometric Analysis of Lycopene in Tomatoes and Watermelons: A Practical Class,” *Chem. Educator* **2008**, *13*, 1–3.
- Russell, D. D.; Potts, J.; Russell, R. M.; Olson, C.; Schimpf, M. “Spectroscopic and Potentiometric Investigation of a Diprotic Acid: An Experimental Approach to Understanding Alpha Functions,” *Chem. Educator* **1999**, *4*, 68–72.
- Smith, E. T.; Matachek, J. R. “A Colorful Investigation of a Diprotic Acid: A General Chemistry Laboratory Exercise,” *Chem. Educator* **2002**, *7*, 359–363
- Tello-Solis, S. R. “Thermal Unfolding of Lysozyme Studied by UV Difference Spectroscopy,” *Chem. Educator* **2008**, *13*, 16–18.
- Tucker, S.; Robinson, R.; Keane, C.; Boff, M.; Zenko, M.; Batish, S.; Street, Jr., K. W. “Colorimetric Determination of pH,” *J. Chem. Educ.* **1989**, *66*, 769–771.
- Vitt, J. E. “Troubleshooting 101: An Instrumental Analysis Experiment,” *J. Chem. Educ.* **2008**, *85*, 1660–1662.
- Williams, K. R.; Cole, S. R.; Boyette, S. E.; Schulman, S. G. “The Use of Dristan Nasal Spray as the Unknown for Simultaneous Spectrophotometric Analysis of a Mixture,” *J. Chem. Educ.* **1990**, *67*, 535.
- Walmsley, F. “Aggregation in Dyes: A Spectrophotometric Study,” *J. Chem. Educ.* **1992**, *69*, 583. Wells, T. A. “Construction of a Simple Myoglobin-Based Optical Biosensor,” *Chem. Educator* **2007**, *12*, 1–3.
  Yarnelle, M. K.; West, K. J. “Modification of an Ultraviolet Spectrophotometric Determination of the Active Ingredients in APC Tablets,” *J. Chem. Educ.* **1989**, *66*, 601–602.

IR Spectroscopy

- Dragon, S.; Fitch, A. “Infrared Spectroscopy Determination of Lead Binding to Ethylenediaminetetraacetic Acid,” *J. Chem. Educ.* **1998**, *75*, 1018–1021.
- Frohlich, H. “Using Infrared Spectroscopy Measurements to Study Intermolecular Hydrogen Bonding,” *J. Chem. Educ.* **1993**, *70*, A3–A6.
- Garizi, N.; Macias, A.; Furch, T.; Fan, R.; Wagenknecht, P.; Singmaster, K. A. “Cigarette Smoke Analysis Using an Inexpensive Gas-Phase IR Cell,” *J. Chem. Educ.* **2001**, *78*, 1665–1666.
- Indralingam, R.; Nepomuceno, A. I. “The Use of Disposable IR Cards for Quantitative Analysis Using an Internal Standard,” *J. Chem. Educ.* **2001**, *78*, 958–960.
- Mathias, L. J.; Hankins, M. G.; Bertolucci, C. M.; Grubb, T. L.; Muthiah, J. “Quantitative Analysis by FTIR: Thin Films of Copolymers of Ethylene and Vinyl Acetate,” *J. Chem. Educ.* **1992**, *69*, A217– A219.
- Schuttlefield, J. D.; Grassian, V. H. “ATR-FTIR Spectroscopy in the Undergraduate Chemistry Laboratory. Part I: Fundamentals and Examples,” *J. Chem. Educ.* **2008**, *85*, 279–281.
- Schuttlefield, J. D.; Larsen, S. C.; Grassian, V. H. “ATR-FTIR Spectroscopy in the Undergraduate Chemistry Laboratory. Part II: A Physical Chemistry Laboratory Experiment on Surface Adsorption,” *J. Chem. Educ.* **2008**, *85*, 282–284.
- Seasholtz, M. B.; Pence, L. E.; Moe Jr., O. A. “Determination of Carbon Monoxide in Automobile Exhaust by FTIR Spectroscopy,” *J. Chem. Educ.* **1988**, *65*, 820–823.

Atomic Absorption and Atomic Emission Spectroscopy

- Amarasiriwardena, D. “Teaching analytical atomic spectroscopy advances in an environmental chemistry class using a project-based laboratory approach: investigation of lead and arsenic distributions in a lead arsenate contaminated apple orchard,” *Anal. Bioanal. Chem.* **2007**, *388*, 307–314.
- Bazzi, A.; Bazzi, J.; Deng, Y.’ Ayyash, M. “Flame Atomic Absorption Spectroscopic Determination of Iron in Breakfast Cereals: A Validated Experiment for the Analytical Chemistry Laboratory,” *Chem. Educator* **2014**, *19*, 283–286.

- Buffen, B. P. “Removal of Heavy Metals from Water: An Environmentally Significant Atomic Absorption Spectrometry Experiment,” *J. Chem. Educ.* **1999**, *76*, 1678–1679.
- Dockery, C. R.; Blew, M. J.; Goode, S. R. “Visualizing the Solute Vaporization Interference in Flame Atomic Absorption Spectroscopy,” *J. Chem. Educ.* **2008**, *85*, 854–858.
- Donas, M. K.; Whissel, G.; Dumas, A.; Golden, K. “Analyzing Lead Content in Ancient Bronze Coins by Flame Atomic Absorption Spectroscopy,” *J. Chem. Educ.* **2009**, *86*, 343–346.
- Finch, L. E.; Hillyer, M. M.; Leopold, M. C. “Quantitative Analysis of Heavy Metals in Children’s Toys and Jewelry: A Multi-Instrument, Multitechnique Exercise in Analytical Chemistry and Public Health,” *J. Chem. Educ.* **2015**, *92*, 849–854.
- Garrison, N.; Cunningham, M.; Varys, D.; Schauer, D. J. “Discovering New Biosorbents with Atomic Absorption Spectroscopy: An Undergraduate Laboratory Experiment,” *J. Chem. Educ.* **2014**, *91*, 583–585.
- Gilles de Pelichy, L. D.; Adams, C.; Smith, E. T. “Analysis of the Essential Nutrient Strontium in Marine Aquariums by Atomic Absorption Spectroscopy,” *J. Chem. Educ.* **1997**, *74*, 1192–1194.
- Hoskins, L. C.; Reichardt, P. B.; Stolzberg, R. J. “Determination of the Extraction Constant for Zinc Pyrrolidinecarbodithioate,” *J. Chem. Educ.* **1981**, *58*, 580–581.
- Kooser, A. S.; Jenkins, J. L.; Welch, L. E. “Inductively Coupled Plasma-Atomic Emission Spectroscopy: Two Laboratory Activities for the Undergraduate Instrumental Analysis Course,” *J. Chem. Educ.* **2003**, *80*, 86–88.
- Kostecka, K. S. “Atomic Absorption Spectroscopy of Calcium in Foodstuffs in Non-Science-Major Courses,” *J. Chem. Educ.* **2000**, *77*, 1321–1323.
- Kristian, K. E.; Friedbauer, S.; Kabashi, D.; Ferencz, K. M.; Barajas, J. C.; O’Brien, K. “A Simplified Digestion Protocol for the Analysis of Hg in Fish by Cold Vapor Atomic Absorption Spectroscopy,” *J. Chem. Educ.* **2015**, *92*, 698–702.
- Lehman, T. A.; Everett, W. W. “Solubility of Lead Sulfate in Water and in Sodium Sulfate Solutions,” *J. Chem. Educ.* **1982**, *59*, 797.
- Markow, P. G. “Determining the Lead Content of Paint Chips,” *J. Chem. Educ.* **1996**, *73*, 178–179.
- Masina, M. R.; Nkosi, P. A.; Rasmussen, P. W.; Shelembe, J. S.; Tyobeka, T. E. “Determination of Metal Ions in Pineapple Juice and Effluent of a Fruit Canning Industry,” *J. Chem. Educ.* **1989**, *66*, 342–343.
- Quigley, M. N. “Determination of Calcium in Analgesic Tablets using Atomic Absorption Spectrophotometry,” *J. Chem. Educ.* **1994**, *71*, 800.
- Quigley, M. N.; Vernon, F. “Determination of Trace Metal Ion Concentrations in Seawater,” *J. Chem. Educ.* **1996**, *73*, 671–675.
- Quigley, M. N.; Vernon, F. “A Matrix Modification Experiment for Use in Electrothermal Atomic Absorption Spectrophotometry,” *J. Chem. Educ.* **1996**, *73*, 980–981.
- Palkendo, J. A.; Kovach, J.; Betts, T. A. “Determination of Wear Metals in Used Motor Oil by Flame Atomic Absorption Spectroscopy,” *J. Chem. Educ.* **2014**, *91*, 579–582.
- Rheingold, A. L.; Hues, S.; Cohen, M. N. “Strontium and Zinc Content in Bones as an Indication of Diet,” *J. Chem. Educ*. **1983**, *60*, 233–234.
- Rocha, F. R. P.; Nóbrega, J. A. “Effects of Solution Physical Properties on Copper and Chromium Signals in Flame Atomic Absorption Spectrometry,” *J. Chem. Educ.* **1996**, *73*, 982–984.

Fluorescence and Phosphorescence Spectroscopy

- Bigger, S. W.; Bigger, A. S.; Ghiggino, K. P. “*FluSpec*: A Simulated Experiment in Fluorescence Spectroscopy,” *J. Chem. Educ.* **2014**, *91*, 1081–1083.
- Buccigross, J. M.; Bedell, C. M.; Suding-Moster, H. L. “Fluorescent Measurement of TNS Binding to Calmodulin,” *J. Chem. Educ.* **1996**, *73*, 275–278.
- Henderleiter, J. A.; Hyslopo, R. M. “The Analysis of Riboflavin in Urine by Fluorescence,” *J. Chem. Educ.* **1996**, *73*, 563–564.
- Koenig, M. H.; Yi, E. P.; Sandridge, M. J.; Mathew, A. S.; Demas, J. N. “Open-Box Approach to Measuring Fluorescence Quenching Using an iPad Screen and Digital SLR Camera,” *J. Chem. Educ.* **2015**, *92*, 310–316.
- Lagoria, M. G.; Román, E. S. “How Does Light Scattering Affect Luminescence? Fluorescence Spectra and Quantum Yields in the Solid Form,” *J. Chem. Educ.* **2002**, *79*, 1362–1367.
- Richardson, D. P.; Chang, R. “Lecture Demonstrations of Fluorescence and Phosphorescence,” *Chem. Educator* **2007**, *12*, 272–274.

- Seixas de Melo, J. S.; Cabral, C.; Burrows, H. D. “Photochemistry and Photophysics in the Laboratory. Showing the Role of Radiationless and Radiative Decay of Excited States,” *Chem. Educator* **2007**, *12*, 1–6.
- Sheffield, M. C.; Nahir, T. M. “Analysis of Selenium in Brazil Nuts by Microwave Digestion and Fluorescence Detection,” *J. Chem. Educ.* **2002**, *79*, 1345–1347.

Signal Averaging

- Blitz, J. P.; Klarup, D. G. “Signal-to-Noise Ratio, Signal Processing, and Spectral Information in the Instrumental Analysis Laboratory,” *J. Chem. Educ.* **2002**, *79*, 1358–1360.
- Stolzberg, R. J. “Introduction to Signals and Noise in an Instrumental Method Course,” *J. Chem. Educ.* **1983**, *60*, 171–172.
- Tardy, D. C. “Signal Averaging. A Signal-to-Noise Enhancement Experiment for the Advanced Chemistry Laboratory,” *J. Chem. Educ.* **1986**, *63*, 648–650.

The following sources provide additional information on spectroscopy in the following areas: general spectroscopy, Beer’s law, instrumentation, Fourier transforms, IR spectroscopy, atomic asorption and emission, luminescence, and applications.

General Spectroscopy

- Ball, D. W. “Units! Units! Units!” *Spectroscopy* **1995**, *10(8)*, 44–47.
- *A History of Analytical Chemistry, Laitinen, H. A.; Ewing, G. W, Eds. The Division of Analytical Chemistry of the American Chemical Society: Washington, D. C., 1977, p103–243.*
- Ingle, J. D.; Crouch, S. R. *Spectrochemical Analysis*, Prentice Hall, Englewood Cliffs, N. J.; 1988.
- Macomber, R. S. “A Unifying Approach to Absorption Spectroscopy at the Undergraduate Level,” *J. Chem. Educ.* **1997**, *74*, 65–67.
- Orchin, M.; Jaffe, H. H. *Symmetry, Orbitals and Spectra*, Wiley-Interscience: New York, 1971.
- Thomas, N. C. “The Early History of Spectroscopy,” *J. Chem. Educ.* **1991**, *68*, 631–633.

Beer’s Law

- Lykos, P. “The Beer-Lambert Law Revisited: A Development without Calculus,” *J. Chem. Educ.* **1992**, *69*, 730–732.
- Ricci, R. W.; Ditzler, M. A.; Nestor, L. P. “Discovering the Beer-Lambert Law,” *J. Chem. Educ.* **1994**, *71*, 983–985.

Instrumentation

• Altermose, I. R. “Evolution of Instrumentation for UV-Visible Spectrophotometry: Part I,” *J. Chem. Educ.* **1986**, *63*, A216–A223.

- Altermose, I. R. “Evolution of Instrumentation for UV-Visible Spectrophotometry: Part II,” *J. Chem. Educ.* **1986**, *63*, A262–A266.
- Grossman, W. E. L. “The Optical Characteristics and Production of Diffraction Gratings,” *J. Chem. Educ.* **1993**, *70*, 741–748.
- Jones, D. G. “Photodiode Array Detectors in UV-Vis Spectroscopy: Part I,” *Anal. Chem.* **1985**, *57*,1057A–1073A.
- Jones, D. G. “Photodiode Array Detectors in UV-Vis Spectroscopy: Part II,” *Anal. Chem.* **1985**, 11, 1207A–1214A.
- Palmer, C. “Diffraction Gratings,” *Spectroscopy*, **1995**, *10(2)*, 14–15.

Fourier Transforms

- Bracewell, R. N. “The Fourier Transform,” *Sci. American* **1989**, *260(6)*, 85–95.
- Glasser, L. “Fourier Transforms for Chemists: Part I. Introduction to the Fourier Transform,” *J. Chem. Educ.* **1987**, *64*, A228–A233.
- Glasser, L. “Fourier Transforms for Chemists: Part II. Fourier Transforms in Chemistry and Spectroscopy,” *J. Chem. Educ.* **1987**, *64*, A260–A266.
- Glasser, L. “Fourier Transforms for Chemists: Part III. Fourier Transforms in Data Treatment,” *J. Chem. Educ.* **1987**, *64*, A306–A313.
- Graff, D. K. “Fourier and Hadamard: Transforms in Spectroscopy,” *J. Chem. Educ.* **1995**, *72*, 304–309.
- Griffiths, P. R. *Chemical Fourier Transform Spectroscopy*, Wiley-Interscience: New York, 1975.
- *Transform Techniques in Chemistry, Griffiths, P. R. Ed., Plenum Press: New York, 1978.*
- Perkins, W. E. “Fourier Transform Infrared Spectroscopy: Part I. Instrumentation,” *J. Chem. Educ.* **1986**, *63*, A5–A10.
- Perkins, W. E. “Fourier Transform Infrared Spectroscopy: Part II. Advantages of FT-IR,” *J. Chem. Educ.* **1987**, *64*, A269–A271.

- Perkins, W. E. “Fourier Transform Infrared Spectroscopy: Part III. Applications,” *J. Chem. Educ.* **1987**, *64*, A296–A305.
- Strong III, F. C. “How the Fourier Transform Infrared Spectrophotometer Works,” *J. Chem. Educ.* **1979**, *56*, 681–684.

IR Spectroscopy.

- *Optical Spectroscopy: Sampling Techniques Manual, Harrick Scientific Corporation: Ossining, N. Y., 1987.*
- Leyden, D. E.; Shreedhara Murthy, R. S. “Surface-Selective Sampling Techniques in Fourier Transform Infrared Spectroscopy,” *Spectroscopy* **1987**, *2(2)*, 28–36.
- Porro, T. J.; Pattacini, S. C. “Sample Handling for Mid-Infrared Spectroscopy, Part I: Solid and Liquid Sampling,” *Spectroscopy* **1993**, *8(7)*, 40–47.
- Porro, T. J.; Pattacini, S. C. “Sample Handling for Mid-Infrared Spectroscopy, Part II: Specialized Techniques,” *Spectroscopy* **1993**, *8(8)*, 39–44.

Atomic Absorption and Emission

- Blades, M. W.; Weir, D. G. “Fundamental Studies of the Inductively Coupled Plasma,” *Spectroscopy* **1994**, *9*, 14–21.
- Greenfield, S. “Invention of the Annular Inductively Coupled Plasma as a Spectroscopic Source,” *J. Chem. Educ.* **2000**, *77*, 584–591.
- Hieftje, G. M. “Atomic Absorption Spectrometry - Has it Gone or Where is it Going?” *J. Anal. At. Spectrom.* **1989**, *4*, 117–122.
- Jarrell, R. F. “A Brief History of Atomic Emission Spectrochemical Analysis, 1666–1950,” *J. Chem. Educ.* **2000**, *77*, 573–576
- Koirtyohann, S. R. “A History of Atomic Absorption Spectrometry From an Academic Perspective,”*Anal. Chem.* **1991**, *63*, 1024A–1031A.
- L’Vov, B. V. “Graphite Furnace Atomic Absorption Spectrometry,” *Anal. Chem.* **1991**, *63*, 924A–931A.
- Slavin, W. “A Comparison of Atomic Spectroscopic Analytical Techniques,” *Spectroscopy*, **1991**, *6*, 16–21.
- Van Loon, J. C. *Analytical Atomic Absorption Spectroscopy*, Academic Press: New York, 1980.
- Walsh, A. “The Development of Atomic Absorption Methods of Elemental Analysis 1952–1962,” *Anal. Chem.* **1991**, *63*, 933A–941A.
- Welz, B. *Atomic Absorption Spectroscopy*, VCH: Deerfield Beach, FL, 1985.

Luminescence Spectroscopy

- Guilbault, G. G. *Practical Fluorescence*, Decker: New York, 1990.
- Schenk, G. “Historical Overview of Fluorescence Analysis to 1980,” *Spectroscopy* **1997**, *12*, 47–56.
- Vo-Dinh, T. *Room-Temperature Phosphorimetry for Chemical Analysis*, Wiley-Interscience: New York, 1984.
- Winefordner, J. D.; Schulman, S. G.; O’Haver, T. C. *Luminescence Spectroscopy in Analytical Chemistry*, Wiley-Interscience: New York, 1969.

Applications

- *Trace Analysis and Spectroscopic Methods for Molecules, Christian, G. D.; Callis, J. B. Eds., Wiley-Interscience: New York, 1986.*
- Vandecasteele, C.; Block, C. B. *Modern Methods for Trace Element Determination*, Wiley: Chichester, England, 1994.
- Skoog, D. A.; Holler, F. J.; Nieman, T. A. *Principles of Instrumental Analysis*, Saunders: Philadelphia, 1998.
- Van Loon, J. C. *Selected Methods of Trace Metal Analysis: Biological and Environmental Samples*, Wiley- Interscience: New York, 1985.

Gathered here are resources and experiments for analyzing multicomponent samples using mathematical techniques not covered in this textbook.

- Aberasturi, F.; Jimenez, A. I.; Jimenez, F.; Arias, J. J. “UV-Visible First-Derivative Spectrophotometry Applied to an Analysis of a Vitamin Mixture,” *J. Chem. Educ.* **2001**, *78*, 793–795.
- Afkhami, A.; Abbasi-Tarighat, M.; Bahram, M.; Abdollahi, H. “A new strategy for solving matrix effect in multivariate calibration standard addition data using combination of H-point curve isolation and H-point standard addition methods,” *Anal. Chim. Acta* **2008**, *613*, 144–151.
- Brown, C. W.; Obremski, R. J. “Multicomponent Quantitative Analysis,” *Appl. Spectrosc. Rev.* **1984**, *20*, 373–418.

- Charles, M. J.; Martin, N. W.; Msimanga, H. Z. “Simultaneous Determination of Aspirin, Salicylamide, and Caffeine in Pain Relievers by Target Factor Analysis,” *J. Chem. Educ.* **1997**, *74*, 1114–1117.
- Dado, G.; Rosenthal, J. “Simultaneous Determination of Cobalt, Copper, and Nickel by Multivariate Linear Regression,” *J. Chem. Educ.* **1990**, *67*, 797–800.
- DiTusa, M. R.; Schilt, A. A. “Selection of Wavelengths for Optimum Precision in Simultaneous Spectrophotometric Determinations,” *J. Chem. Educ.* **1985**, *62*, 541–542.
- Gómez, D. G.; de la Peña, A. M.; Mansilla, A. E.; Olivieri, A. C. “Spectrophotometric Analysis of Mixtures by Classical Least-Squares Calibration: An Advanced Experiment Introducing MATLAB,” *Chem. Educator* **2003**, *8*, 187–191.
- Harvey, D. T.; Bowman, A. “Factor Analysis of Multicomponent Samples,” *J. Chem. Educ.* **1990**, *67*, 470–472.
- Lucio-Gutierrez, J. R.; Salazar-Cavazos, M. L.; de Torres, N. W. “Chemometrics in the Teaching Lab. Quantification of a Ternary Mixture of Common Pharmaceuticals by First- and Second-Derivative IR Spectroscopy,” *Chem. Educator* **2004**, *9*, 234–238.
- Padney, S.; McHale, M. E. R.; Coym, K. S.; Acree Jr., W. E. “Bilinear Regression Analysis as a Means to Reduce Matrix Effects in Simultaneous Spectrophotometric Determination of Cr(III) and Co(II),” *J. Chem. Educ.* **1998**, *75*, 878–880.
- Raymond, M.; Jochum, C.; Kowalski, B. R. “Optimal Multicomponent Analysis Using the Generalized Standard Addition Method,” *J. Chem. Educ.* **1983**, *60*, 1072–1073.
- Ribone, M. E.; Pagani, A. P.; Olivieri, A. C.; Goicoechea, H. C. “Determination of the Active Principle in a Spectrophotometry and Principal Component Regression Analysis,” *J. Chem. Educ.* **2000**, *77*, 1330–1333.
- Rojas, F. S.; Ojeda, C. B. “Recent developments in derivative ultraviolet/visible absorption spectrophotometry: 2004–2008,” *Anal. Chim. Acta* **2009**, *635*, 22–44.

This page titled 1.15: Additional Resources is shared under a CC BY-NC-SA 4.0 license and was authored, remixed, and/or curated by David Harvey.

- **10.10: Additional Resources** by David Harvey is licensed CC BY-NC-SA 4.0.

1.16: Chapter Summary and Key Terms

Chapter Summary

The spectrophotometric methods of analysis covered in this chapter include those based on the absorption, emission, or scattering of electromagnetic radiation. When a molecule absorbs UV/Vis radiation it undergoes a change in its valence shell electron configuration. A change in vibrational energy results from the absorption of IR radiation. Experimentally we measure the fraction of radiation transmitted, T, by the sample. Instrumentation for measuring absorption requires a source of electromagnetic radiation, a means for selecting a wavelength, and a detector for measuring transmittance. Beer's law relates absorbance to both transmittance and to the concentration of the absorbing species ($A = -\log T = \varepsilon bC$).

In atomic absorption we measure the absorption of radiation by gas phase atoms. Samples are atomized using thermal energy from either a flame or a graphite furnace. Because the width of an atom's absorption band is so narrow, the continuum sources common for molecular absorption are not used. Instead, a hollow cathode lamp provides the necessary line source of radiation. Atomic absorption suffers from a number of spectral and chemical interferences. The absorption or scattering of radiation from the sample's matrix are important spectral interferences that are minimized by background correction. Chemical interferences include the formation of nonvolatile forms of the analyte and ionization of the analyte. The former interference is minimized by using a releasing agent or a protecting agent, and an ionization suppressor helps minimize the latter interference.

When a molecule absorbs radiation it moves from a lower energy state to a higher energy state. In returning to the lower energy state the molecule may emit radiation. This process is called photoluminescence. One form of photoluminescence is fluorescence in which the analyte emits a photon without undergoing a change in its spin state. In phosphorescence, emission occurs with a change in the analyte's spin state. For low concentrations of analyte, both fluorescent and phosphorescent emission intensities are a linear function of the analyte's concentration. Thermally excited atoms also emit radiation, forming the basis for atomic emission spectroscopy. Thermal excitation is achieved using either a flame or a plasma.

Spectroscopic measurements also include the scattering of light by a particulate form of the analyte. In turbidimetry, the decrease in the radiation's transmission through the sample is measured and related to the ana- lyte's concentration through an equation similar to Beer's law. In nephelometry we measure the intensity of scattered radiation, which varies linearly with the analyte's concentration.

Key Terms

absorbance
amplitude
background correction
chromophore
double-beam
electromagnetic spectrum
excitation spectrum
fiber-optic probe
fluorescence
frequency
interferometer
ionization suppressor
line source
mole-ratio method
nephelometry
phosphorescence
photoluminescence
polychromatic
relaxation
self-absorption
signal-to-noise ratio
slope-ratio method
spectrophotometer
transducer
turbidimetry
wavenumber

absorbance spectrum
attenuated total reflectance
Beer's law
continuum source
effective bandwidth
emission
external conversion
filter
fluorescent quantum yield
graphite furnace
internal conversion
Jacquinot's advantage
method of continuous variations
monochromatic
nominal wavelength
phosphorescent quantum yield
photon
protecting agent
releasing agent
signal averaging
single-beam
spectral searching
spectroscopy
transmittance
vibrational relaxation

absorptivity
atomization
chemiluminescence
dark current
electromagnetic radiation
emission spectrum
Fellgett's advantage
filter photometer
fluorimeter
interferogram
intersystem crossing
lifetime
molar absorptivity
monochromator
phase angle
photodiode array
plasma
radiationless deactivation
resolution
signal processor
singlet excited state
spectrofluorometer
stray radiation
triplet excited state
wavelength

This page titled 1.16: Chapter Summary and Key Terms is shared under a CC BY-NC-SA 4.0 license and was authored, remixed, and/or curated by David Harvey.

- **10.11: Chapter Summary and Key Terms** by David Harvey is licensed CC BY-NC-SA 4.0.

CHAPTER OVERVIEW

2: Chromatographic and Electrophoretic Methods

Drawing from an arsenal of analytical techniques—many of which were the subject of the preceding four chapters—analytical chemists design methods that detect increasingly smaller concentrations of analyte in increasingly more complex matrices. Despite the power of these analytical techniques, they often suffer from a lack of selectivity. For this reason, many analytical procedures include a step to separate the analyte from potential interferents. Although effective, each additional step in an analytical procedure increases the analysis time and the cost of the analysis, and introduces uncertainty. In this chapter we consider two analytical techniques that avoid these limitations by combining the separation and analysis: chromatography and electrophoresis.

2.1: Overview of Analytical Separations
2.2: General Theory of Column Chromatography
2.3: Optimizing Chromatographic Separations
2.4: Gas Chromatography
2.5: High-Performance Liquid Chromatography
2.5.1: HPLC Simulator
2.5.2: HPLC Method Development
2.6: Other Forms of Chromatography
2.7: Electrophoresis
2.8: Problems
2.9: Additional Resources
2.10: Chapter Summary and Key Terms

This page titled 2: Chromatographic and Electrophoretic Methods is shared under a CC BY-NC-SA 4.0 license and was authored, remixed, and/or curated by David Harvey.

2.1: Overview of Analytical Separations

In Chapter 7 we examined several methods for separating an analyte from potential interferents. For example, in a liquid–liquid extraction the analyte and interferent initially are present in a single liquid phase. We add a second, immiscible liquid phase and thoroughly mix them by shaking. During this process the analyte and interferents partition between the two phases to different extents, effecting their separation. After allowing the phases to separate, we draw off the phase enriched in analyte. Despite the power of liquid–liquid extractions, there are significant limitations.

Two Limitations of Liquid-Liquid Extractions

Suppose we have a sample that contains an analyte in a matrix that is incompatible with our analytical method. To determine the analyte's concentration we first separate it from the matrix using a simple liquid–liquid extraction. If we have several analytes, we may need to complete a separate extraction for each analyte. For a complex mixture of analytes this quickly becomes a tedious process. This is one limitation to a liquid–liquid extraction.

A more significant limitation is that the extent of a separation depends on the distribution ratio of each species in the sample. If the analyte's distribution ratio is similar to that of another species, then their separation becomes impossible. For example, let's assume that an analyte, *A*, and an interferent, *I*, have distribution ratios of, respectively, 5 and 0.5. If we use a liquid–liquid extraction with equal volumes of sample and extractant, then it is easy to show that a single extraction removes approximately 83% of the analyte and 33% of the interferent. Although we can remove 99% of the analyte with three extractions, we also remove 70% of the interferent. In fact, there is no practical combination of number of extractions or volumes of sample and extractant that produce an acceptable separation.

From Chapter 7 we know that the distribution ratio, *D*, for a solute, *S*, is

$$D = \frac{[S]_{ext}}{[S]_{samp}}$$

where $[S]_{ext}$ is its equilibrium concentration in the extracting phase and $[S]_{samp}$ is its equilibrium concentration in the sample. We can use the distribution ratio to calculate the fraction of *S* that remains in the sample, q_{samp}, after an extraction

$$q_{samp} = \frac{V_{samp}}{DV_{ext} + V_{samp}}$$

where V_{samp} is the volume of sample and V_{ext} is the volume of the extracting phase. For example, if D = 10, V_{samp} = 20, and V_{ext} = 5, the fraction of *S* remaining in the sample after the extraction is

$$q_{samp} = \frac{20}{10 \times 5 + 20} = 0.29$$

or 29%. The remaining 71% of the analyte is in the extracting phase.

A Better Way to Separate Mixtures

The problem with a liquid–liquid extraction is that the separation occurs in one direction only: from the sample to the extracting phase. Let's take a closer look at the liquid–liquid extraction of an analyte and an interferent with distribution ratios of, respectively, 5 and 0.5. Figure 12.1.1 shows that a single extraction using equal volumes of sample and extractant transfers 83% of the analyte and 33% of the interferent to the extracting phase. If the original concentrations of *A* and *I* are identical, then their concentration ratio in the extracting phase after one extraction is

$$\frac{[A]}{[I]} = \frac{0.83}{0.33} = 2.5$$

A single extraction, therefore, enriches the analyte by a factor of $2.5\times$. After completing a second extraction (Figure 12.1.1) and combining the two extracting phases, the separation of the analyte and the interferent, surprisingly, is less efficient.

$$\frac{[A]}{[I]} = \frac{0.97}{0.55} = 1.8$$

Figure 12.1.1 makes it clear why the second extraction results in a poorer overall separation: the second extraction actually favors the interferent!

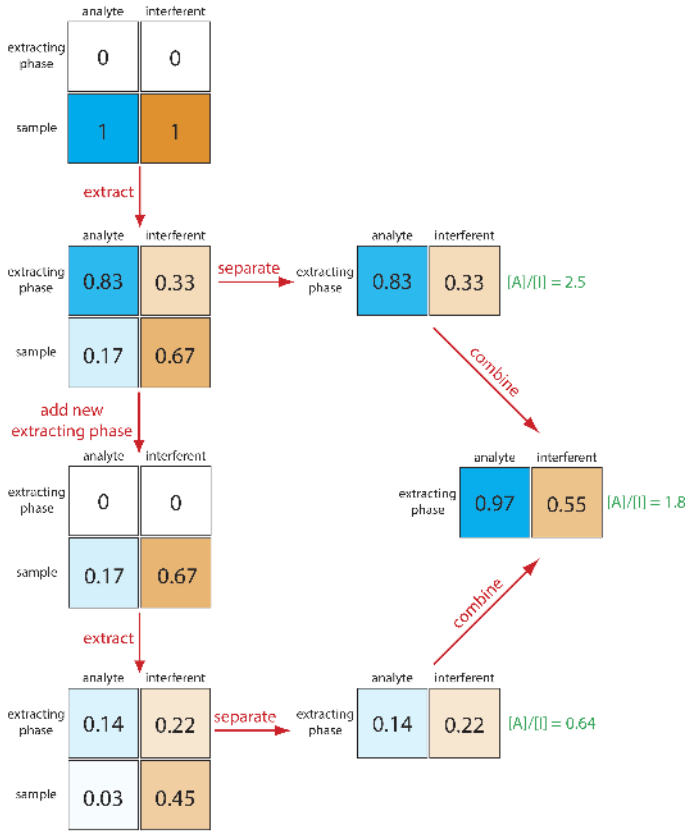


Figure 12.1.1 . Progress of a traditional liquid–liquid extraction using two identical extractions of a single sample using fresh portions of the extractant. The numbers give the fraction of analyte and interferent in each phase assuming equal volumes of sample and extractant and distribution ratios of 5 and 0.5 for the analyte and the interferent, respectively. The opacity of the colors equals the fraction of analyte and interferent present.

We can improve the separation by first extracting the solutes from the sample into the extracting phase and then extracting them back into a fresh portion of solvent that matches the sample's matrix (Figure 12.1.2). Because the analyte has the larger distribution ratio, more of it moves into the extractant during the first extraction and less of it moves back to the sample phase during the second extraction. In this case the concentration ratio in the extracting phase after two extractions is significantly greater.

$$\frac{[A]}{[I]} = \frac{0.69}{0.11} = 6.3$$

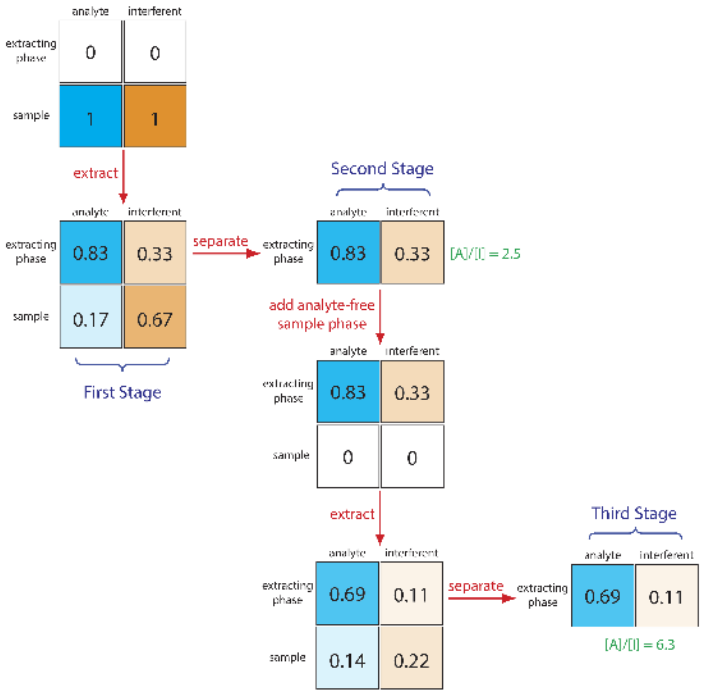


Figure 12.1.2 . Progress of a liquid–liquid extraction in which we first extract the solutes into the extracting phase and then extract them back into an analyte-free portion of the sample's phase. The numbers give the fraction of analyte and interferent in each phase assuming equal volumes of sample and extractant and distribution ratios of 5 and 0.5 for the analyte and the interferent, respectively. The opacity of the colors equals the fraction of analyte and interferent present.

Not shown in Figure 12.2 is that we can add a fresh portion of the extracting phase to the sample that remains after the first extraction (the bottom row of the first stage in Figure 12.2, beginning the process anew. As we increase the number of extractions, the analyte and the interferent each spread out in space over a series of stages. Because the interferent's distribution ratio is smaller than the analyte's, the interferent lags behind the analyte. With a sufficient number of extractions—that is, a sufficient number of stages—a complete separation of the analyte and interferent is possible. This process of extracting the solutes back and forth between fresh portions of the two phases, which we call a ***countercurrent extraction***, was developed by Craig in the 1940s [Craig, L. C. *J. Biol. Chem.* **1944**, *155*, 519–534]. The same phenomenon forms the basis of modern chromatography.

> See Appendix 16 for a more detailed consideration of the mathematics behind a countercurrent extraction.

Chromatographic Separations

In ***chromatography*** we pass a sample-free phase, which we call the ***mobile phase***, over a second sample-free ***stationary phase*** that remains fixed in space (Figure 12.1.3). We inject or place the sample into the mobile phase. As the sample moves with the mobile phase, its components partition between the mobile phase and the stationary phase. A component whose distribution ratio favors the stationary phase requires more time to pass through the system. Given sufficient time and sufficient stationary and mobile phase, we can separate solutes even if they have similar distribution ratios.

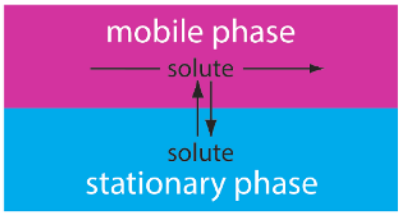


Figure 12.1.3 . In chromatography we pass a mobile phase over a stationary phase. When we inject a sample into the mobile phase, the sample's components both move with the mobile phase and partition into the stationary phase. The solute that spends the most time in the stationary phase takes the longest time to move through the system.

There are many ways in which we can identify a chromatographic separation: by describing the physical state of the mobile phase and the stationary phase; by describing how we bring the stationary phase and the mobile phase into contact with each other; or by describing the chemical or physical interactions between the solute and the stationary phase. Let's briefly consider how we might use each of these classifications.

> We can trace the history of chromatography to the turn of the century when the Russian botanist Mikhail Tswett used a column packed with calcium carbonate and a mobile phase of petroleum ether to separate colored pigments from plant extracts. As the sample moved through the column, the plant's pigments separated into individual colored bands. After effecting the separation, the calcium carbonate was removed from the column, sectioned, and the pigments recovered. Tswett named the technique chromatography, combining the Greek words for "color" and "to write." There was little interest in Tswett's technique until Martin and Synge's pioneering development of a theory of chromatography (see Martin, A. J. P.; Synge, R. L. M. "A New Form of Chromatogram Employing Two Liquid Phases," *Biochem. J.* **1941**, *35*, 1358–1366). Martin and Synge were awarded the 1952 Nobel Prize in Chemistry for this work.

Types of Mobile Phases and Stationary Phases

The mobile phase is a liquid or a gas, and the stationary phase is a solid or a liquid film coated on a solid substrate. We often name chromatographic techniques by listing the type of mobile phase followed by the type of stationary phase. In gas–liquid chromatography, for example, the mobile phase is a gas and the stationary phase is a liquid film coated on a solid substrate. If a technique's name includes only one phase, as in gas chromatography, it is the mobile phase.

Contact Between the Mobile Phase and the Stationary Phase

There are two common methods for bringing the mobile phase and the stationary phase into contact. In ***column chromatography*** we pack the stationary phase into a narrow column and pass the mobile phase through the column using gravity or by applying pressure. The stationary phase is a solid particle or a thin liquid film coated on either a solid particulate packing material or on the column's walls.

In ***planar chromatography*** the stationary phase is coated on a flat surface—typically, a glass, metal, or plastic plate. One end of the plate is placed in a reservoir that contains the mobile phase, which moves through the stationary phase by capillary action. In paper chromatography, for example, paper is the stationary phase.

Interaction Between the Solute and the Stationary Phase

The interaction between the solute and the stationary phase provides a third method for describing a separation (Figure 12.1.4). In ***adsorption chromatography***, solutes separate based on their ability to adsorb to a solid stationary phase. In ***partition chromatography***, the stationary phase is a thin liquid film on a solid support. Separation occurs because there is a difference in the equilibrium partitioning of solutes between the stationary phase and the mobile phase. A stationary phase that consists of a solid support with covalently attached anionic (e.g., $-SO_3^-$) or cationic (e.g., $-N(CH_3)_3^+$) functional groups is the basis for ion-exchange chromatography in which ionic solutes are attracted to the stationary phase by electrostatic forces. In size-exclusion chromatography the stationary phase is a porous particle or gel, with separation based on the size of the solutes. Larger solutes are unable to penetrate as deeply into the porous stationary phase and pass more quickly through the column.

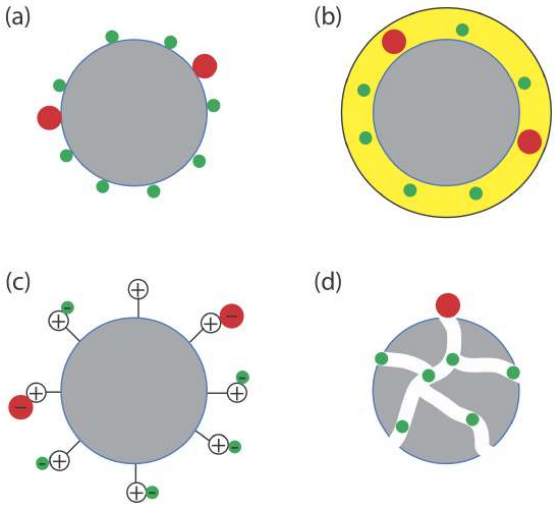


Figure 12.1.4 . Four examples of interactions between a solute and the stationary phase: (a) adsorption on a solid surface, (b) partitioning into a liquid phase, (c) ion-exchange, and (d) size exclusion. For each example, the smaller, green solute is more strongly retained than the larger, red solute.

There are other interactions that can serve as the basis of a separation. In affinity chromatography the interaction between an antigen and an antibody, between an enzyme and a substrate, or between a receptor and a ligand forms the basis of a separation. See this chapter's additional resources for some suggested readings.

Electrophoretic Separations

In chromatography, a separation occurs because there is a difference in the equilibrium partitioning of solutes between the mobile phase and the stationary phase. Equilibrium partitioning, however, is not the only basis for effecting a separation. In an electrophoretic separation, for example, charged solutes migrate under the influence of an applied potential. A separation occurs because of differences in the charges and the sizes of the solutes (Figure 12.1.5).

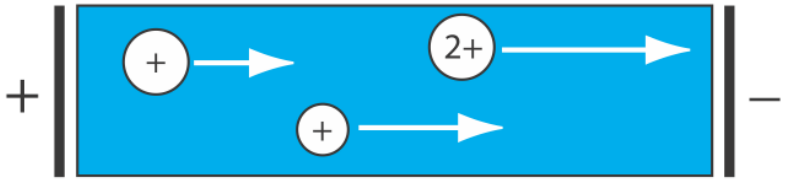


Figure 12.1.5 . Movement of charged solutes under the influence of an applied potential. The lengths of the arrows indicate the relative speed of the solutes. In general, a larger solute moves more slowly than a smaller solute of equal charge, and a solute with a larger charge move more quickly than a solute with a smaller charge.

This page titled 2.1: Overview of Analytical Separations is shared under a CC BY-NC-SA 4.0 license and was authored, remixed, and/or curated by David Harvey.

- **12.1: Overview of Analytical Separations** by David Harvey is licensed CC BY-NC-SA 4.0.

2.2: General Theory of Column Chromatography

Of the two methods for bringing the stationary phase and the mobile phases into contact, the most important is column chromatography. In this section we develop a general theory that we may apply to any form of column chromatography.

Figure 12.2.1 provides a simple view of a liquid–solid column chromatography experiment. The sample is introduced as a narrow band at the top of the column. Ideally, the solute's initial concentration profile is rectangular (Figure 12.2.2 a). As the sample moves down the column, the solutes begin to separate (Figure 12.2.1 b,c) and the individual solute bands begin to broaden and develop a Gaussian profile (Figure 12.2.2 b,c). If the strength of each solute's interaction with the stationary phase is sufficiently different, then the solutes separate into individual bands (Figure 12.2.1 d and Figure 12.2.2 d).

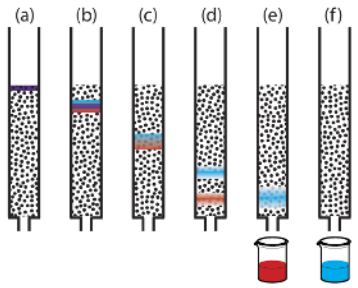


Figure 12.2.1 . Progress of a column chromatographic separation of a two-component mixture. In (a) the sample is layered on top of the stationary phase. As mobile phase passes through the column, the sample separates into two solute bands (b–d). In (e) and (f), we collect each solute as it elutes from the column.

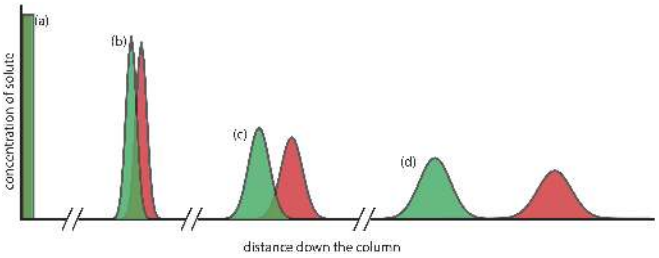


Figure 12.2.2 . An alternative view of the separation in Figure 12.2.1 showing the concentration of each solute as a function of distance down the column.

We can follow the progress of the separation by collecting fractions as they elute from the column (Figure 12.2.1 e,f), or by placing a suitable detector at the end of the column. A plot of the detector's response as a function of elution time, or as a function of the volume of mobile phase, is known as a ***chromatogram*** (Figure 12.2.3), and consists of a peak for each solute.

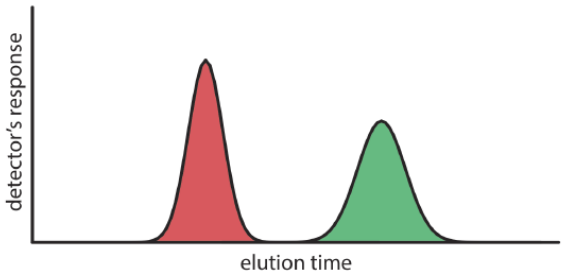


Figure 12.2.3 . Chromatogram for the separation shown in Figure 12.2.1 and Figure 12.2.2 , showing the detector's response as a function of the elution time.

> There are many possible detectors that we can use to monitor the separation. Later sections of this chapter describe some of the most popular.

We can characterize a chromatographic peak's properties in several ways, two of which are shown in Figure 12.2.4 . ***Retention time***, t_r, is the time between the sample's injection and the maximum response for the solute's peak. A chromatographic peak's ***baseline width***, w, as shown in Figure 12.2.4 , is determined by extending tangent lines from the inflection points on either side of the peak through the baseline. Although usually we report t_r and w using units of time, we can report them using units of volume by multiplying each by the mobile phase's velocity, or report them in linear units by measuring distances with a ruler.

> For example, a solute's retention volume, V_r, is $t_r \times u$ where u is the mobile phase's velocity through the column.

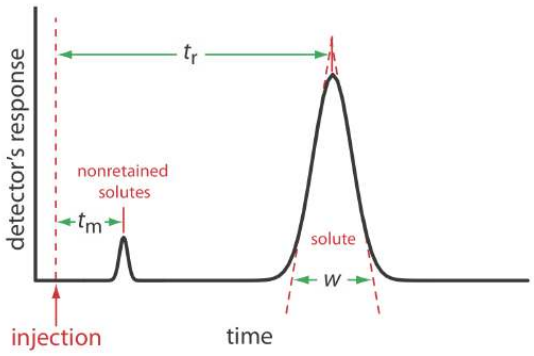


Figure 12.2.4 . Chromatogram showing a solute's retention time, t_r, and baseline width, w, and the column's void time, t_m, for nonretained solutes.

In addition to the solute's peak, Figure 12.2.4 also shows a small peak that elutes shortly after the sample is injected into the mobile phase. This peak contains all ***nonretained solutes***, which move through the column at the same rate as the mobile phase. The time required to elute the nonretained solutes is called the column's ***void time***, t_m.

Chromatographic Resolution

The goal of chromatography is to separate a mixture into a series of chromatographic peaks, each of which constitutes a single component of the mixture. The ***resolution*** between two chromatographic peaks, R_{AB}, is a quantitative measure of their separation, and is defined as

$$R_{AB} = \frac{t_{t,B} - t_{t,A}}{0.5\,(w_B + w_A)} = \frac{2\Delta t_r}{w_B + w_A} \tag{2.2.1}$$

where B is the later eluting of the two solutes. As shown in Figure 12.2.5 , the separation of two chromatographic peaks improves with an increase in R_{AB}. If the areas under the two peaks are identical—as is the case in Figure 12.2.5 —then a resolution of 1.50 corresponds to an overlap of only 0.13% for the two elution profiles. Because resolution is a quantitative measure of a separation's success, it is a useful way to determine if a change in experimental conditions leads to a better separation.

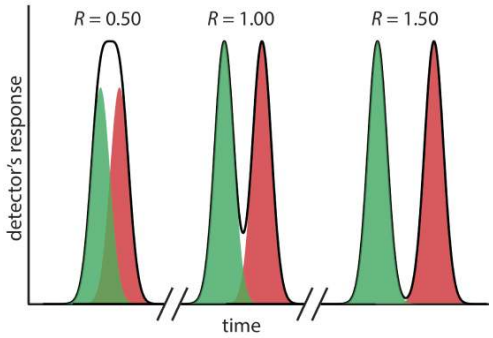


Figure 12.2.5 . Three examples that show the relationship between resolution and the separation of a two component mixture. The green peak and the red peak are the elution profiles for the two components. The chromatographic peak— which is the sum of the two elution profiles—is shown by the solid black line.

Example 12.2.1

In a chromatographic analysis of lemon oil a peak for limonene has a retention time of 8.36 min with a baseline width of 0.96 min. γ-Terpinene elutes at 9.54 min with a baseline width of 0.64 min. What is the resolution between the two peaks?

Solution

Using Equation 2.2.1 we find that the resolution is

$$R_{AB} = \frac{2\Delta t_r}{w_B + w_A} = \frac{2(9.54\text{ min} - 8.36\text{ min})}{0.64\text{ min} + 0.96\text{ min}} = 1.48$$

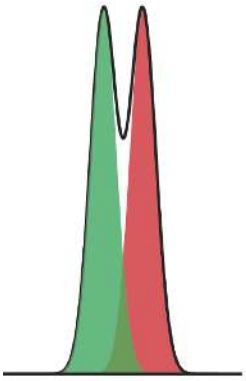


Figure 12.2.6 . Chromatogram for Exercise 12.2.1 .

? Exercise 12.2.1

Figure 12.2.6 shows the separation of a two-component mixture. What is the resolution between the two components? Use a ruler to measure Δt_r, w_A, and w_B in millimeters.

Answer

Because the relationship between elution time and distance is proportional, we can measure Δt_r, w_A, and w_B using a ruler. My measurements are 8.5 mm for Δt_r, and 12.0 mm each for w_A and w_B. Using these values, the resolution is

$$R_{AB} = \frac{2\Delta t_t}{w_A + w_B} = \frac{2(8.5\text{ mm})}{12.0\text{ mm} + 12.0\text{ mm}} = 0.70$$

Your measurements for Δt_r, w_A, and w_B will depend on the relative size of your monitor or printout; however, your value for the resolution should be similar to the answer above.

Equation 2.2.1 suggests that we can improve resolution by increasing Δt_r, or by decreasing w_A and w_B (Figure 12.2.7). To increase Δt_r we can use one of two strategies. One approach is to adjust the separation conditions so that both solutes spend less time in the mobile phase—that is, we increase each *solute's retention factor*—which provides more time to effect a separation. A second approach is to increase *selectivity* by adjusting conditions so that only one solute experiences a significant change in its retention time. The baseline width of a solute's peak depends on the solutes movement within and between the mobile phase and the stationary phase, and is governed by several factors that collectively we call *column efficiency*. We will consider each of these approaches for improving resolution in more detail, but first we must define some terms.

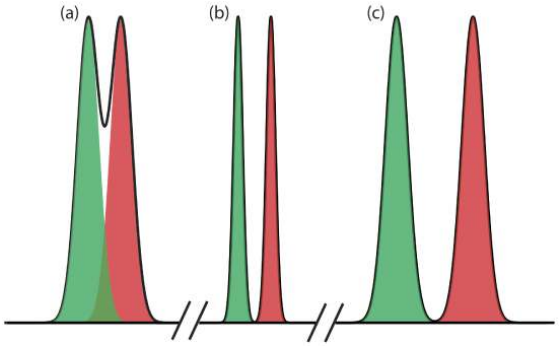


Figure 12.2.7 . Two method for improving chromatographic resolution: (a) original chromatogram; (b) chromatogram after decreasing w_A and w_B by 4×; and (c) chromatogram after increasing Δt_r by 2×.

Solute Retention Factor

Let's assume we can describe a solute's distribution between the mobile phase and stationary phase using the following equilibrium reaction

$$S_m \rightleftharpoons S_s$$

where S_m is the solute in the mobile phase and S_s is the solute in the stationary phase. Following the same approach we used in Chapter 7.7 for liquid–liquid extractions, the equilibrium constant for this reaction is an equilibrium partition coefficient, K_D.

$$K_D = \frac{[S_s]}{[S_m]}$$

This is not a trivial assumption. In this section we are, in effect, treating the solute's equilibrium between the mobile phase and the stationary phase as if it is identical to the equilibrium in a liquid–liquid extraction. You might question whether this is a reasonable assumption. There is an important difference between the two experiments that we need to consider. In a liquid–liquid extraction, which takes place in a separatory funnel, the two phases remain in contact with each other at all times, allowing for a true equilibrium. In chromatography, however, the mobile phase is in constant motion. A solute that moves into the stationary phase from the mobile phase will equilibrate back into a different portion of the mobile phase; this does not describe a true equilibrium.

So, we ask again: Can we treat a solute's distribution between the mobile phase and the stationary phase as an equilibrium process? The answer is yes, if the mobile phase velocity is slow relative to the kinetics of the solute's movement back and forth between the two phase. In general, this is a reasonable assumption.

In the absence of any additional equilibrium reactions in the mobile phase or the stationary phase, K_D is equivalent to the distribution ratio, D,

$$D = \frac{[S_0]}{[S_m]} = \frac{(\text{mol S})_s/V_s}{(\text{mol S})_m/V_m} = K_D \tag{2.2.2}$$

where V_s and V_m are the volumes of the stationary phase and the mobile phase, respectively.

A conservation of mass requires that the total moles of solute remain constant throughout the separation; thus, we know that the following equation is true.

$$(\text{mol S})_{tot} = (\text{mol S})_m + (\text{mol S})_s \tag{2.2.3}$$

Solving Equation 2.2.3 for the moles of solute in the stationary phase and substituting into Equation 2.2.2 leaves us with

$$D = \frac{\{(\text{mol S})_{tot} - (\text{mol S})_m\}/V_s}{(\text{mol S})_m/V_m}$$

Rearranging this equation and solving for the fraction of solute in the mobile phase, f_m, gives

$$f_m = \frac{(\text{mol S})_m}{(\text{mol S})_{tot}} = \frac{V_m}{DV_s + V_m} \tag{2.2.4}$$

which is identical to the result for a liquid-liquid extraction (see Chapter 7). Because we may not know the exact volumes of the stationary phase and the mobile phase, we simplify Equation 2.2.4 by dividing both the numerator and the denominator by V_m; thus

$$f_m = \frac{V_m/V_m}{DV_s/V_m + V_m/V_m} = \frac{1}{DV_s/V_m + 1} = \frac{1}{1+k} \tag{2.2.5}$$

where k

$$k = D \times \frac{V_s}{V_m} \tag{2.2.6}$$

is the solute's ***retention factor***. Note that the larger the retention factor, the more the distribution ratio favors the stationary phase, leading to a more strongly retained solute and a longer retention time.

Other (older) names for the retention factor are capacity factor, capacity ratio, and partition ratio, and it sometimes is given the symbol k'. Keep this in mind if you are using other resources. Retention factor is the approved name from the IUPAC Gold

Book.

We can determine a solute's retention factor from a chromatogram by measuring the column's void time, t_m, and the solute's retention time, t_r (see Figure 12.2.4). Solving Equation 2.2.5 for k, we find that

$$k = \frac{1 - f_m}{f_m} \tag{2.2.7}$$

Earlier we defined f_m as the fraction of solute in the mobile phase. Assuming a constant mobile phase velocity, we also can define f_m as

$$f_m = \frac{\text{time spent in the mobile phase}}{\text{time spent in the stationary phase}} = \frac{t_m}{t_r}$$

Substituting back into Equation 2.2.7 and rearranging leaves us with

$$k = \frac{1 - \frac{t_m}{t_t}}{\frac{t_m}{t_r}} = \frac{t_t - t_m}{t_m} = \frac{t'_r}{t_m} \tag{2.2.8}$$

where t'_r is the ***adjusted retention time***.

Example 12.2.2

In a chromatographic analysis of low molecular weight acids, butyric acid elutes with a retention time of 7.63 min. The column's void time is 0.31 min. Calculate the retention factor for butyric acid.

Solution

$$k_{but} = \frac{t_r - t_m}{t_m} = \frac{7.63 \text{ min} - 0.31 \text{ min}}{0.31 \text{ min}} = 23.6$$

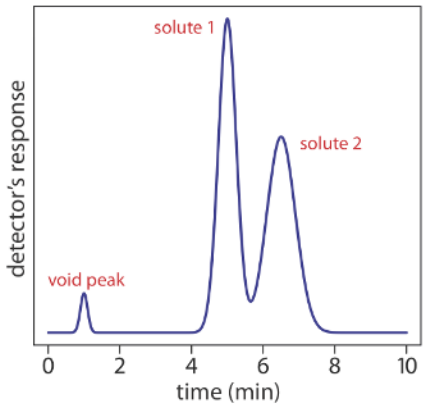


Figure 12.2.8 . Chromatogram for Exercise 12.2.2 .

Exercise 12.2.2

Figure 12.2.8 is the chromatogram for a two-component mixture. Determine the retention factor for each solute assuming the sample was injected at time t = 0.

Answer

Because the relationship between elution time and distance is proportional, we can measure t_m, $t_{r,1}$, and $t_{r,2}$ using a ruler. My measurements are 7.8 mm, 40.2 mm, and 51.5 mm, respectively. Using these values, the retention factors for solute A and solute B are

$$k_1 = \frac{t_{r1} - t_m}{t_m} = \frac{40.2 \text{ mm} - 7.8 \text{ mm}}{7.8 \text{ mm}} = 4.15$$

$$k_2 = \frac{t_{r2} - t_m}{t_m} = \frac{51.5 \text{ mm} - 7.8 \text{ mm}}{7.8 \text{ mm}} = 5.60$$

Your measurements for t_m, $t_{r,1}$, and $t_{r,2}$ will depend on the relative size of your monitor or printout; however, your value for the resolution should be similar to the answer above.

Selectivity

Selectivity is a relative measure of the retention of two solutes, which we define using a selectivity factor, α

$$\alpha = \frac{k_B}{k_A} = \frac{t_{r,B} - t_m}{t_{r,A} - t_m} \tag{2.2.9}$$

where solute A has the smaller retention time. When two solutes elute with identical retention time, $\alpha = 1.00$; for all other conditions $\alpha > 1.00$.

Example 12.2.3

In the chromatographic analysis for low molecular weight acids described in Example 12.2.2 , the retention time for isobutyric acid is 5.98 min. What is the selectivity factor for isobutyric acid and butyric acid?

Solution

First we must calculate the retention factor for isobutyric acid. Using the void time from Example 12.2.2 we have

$$k_{iso} = \frac{t_r - t_m}{t_m} = \frac{5.98 \text{ min} - 0.31 \text{ min}}{0.31 \text{ min}} = 18.3$$

The selectivity factor, therefore, is

$$\alpha = \frac{k_{but}}{k_{iso}} = \frac{23.6}{18.3} = 1.29$$

Exercise 12.2.3

Determine the selectivity factor for the chromatogram in Exercise 12.2.2 .

Answer

Using the results from Exercise 12.2.2 , the selectivity factor is

$$\alpha = \frac{k_2}{k_1} = \frac{5.60}{4.15} = 1.35$$

Your answer may differ slightly due to differences in your values for the two retention factors.

Column Efficiency

Suppose we inject a sample that has a single component. At the moment we inject the sample it is a narrow band of finite width. As the sample passes through the column, the width of this band continually increases in a process we call ***band broadening***. Column efficiency is a quantitative measure of the extent of band broadening.

See Figure 12.2.1 and Figure 12.2.2 . When we inject the sample it has a uniform, or rectangular concentration profile with respect to distance down the column. As it passes through the column, the band broadens and takes on a Gaussian concentration profile.

In their original theoretical model of chromatography, Martin and Synge divided the chromatographic column into discrete sections, which they called theoretical plates. Within each theoretical plate there is an equilibrium between the solute present in the

stationary phase and the solute present in the mobile phase [Martin, A. J. P.; Synge, R. L. M. *Biochem. J.* **1941**, *35*, 1358–1366]. They described column efficiency in terms of the number of ***theoretical plates***, *N*,

$$N = \frac{L}{H} \tag{2.2.10}$$

where *L* is the column's length and *H* is the height of a theoretical plate. For any given column, the column efficiency improves—and chromatographic peaks become narrower—when there are more theoretical plates.

If we assume that a chromatographic peak has a Gaussian profile, then the extent of band broadening is given by the peak's variance or standard deviation. The height of a theoretical plate is the peak's variance per unit length of the column

$$H = \frac{\sigma^2}{L} \tag{2.2.11}$$

where the standard deviation, σ, has units of distance. Because retention times and peak widths usually are measured in seconds or minutes, it is more convenient to express the standard deviation in units of time, τ, by dividing σ by the solute's average linear velocity, $\overline{u}$, which is equivalent to dividing the distance it travels, *L*, by its retention time, t_r.

$$\tau = \frac{\sigma}{\overline{u}} = \frac{\sigma t_r}{L} \tag{2.2.12}$$

For a Gaussian peak shape, the width at the baseline, *w*, is four times its standard deviation, τ.

$$w = 4\tau \tag{2.2.13}$$

Combining Equation 2.2.11, Equation 2.2.12, and Equation 2.2.13 defines the height of a theoretical plate in terms of the easily measured chromatographic parameters t_r and *w*.

$$H = \frac{Lw^2}{16t_r^2} \tag{2.2.14}$$

Combing Equation 2.2.14 and Equation 2.2.10 gives the number of theoretical plates.

$$N = 16\frac{t_r^2}{w^2} = 16\left(\frac{t_r}{w}\right)^2 \tag{2.2.15}$$

Example 12.2.4

A chromatographic analysis for the chlorinated pesticide Dieldrin gives a peak with a retention time of 8.68 min and a baseline width of 0.29 min. Calculate the number of theoretical plates? Given that the column is 2.0 m long, what is the height of a theoretical plate in mm?

Solution

Using Equation 2.2.15, the number of theoretical plates is

$$N = 16\frac{t_r^2}{w^2} = 16 \times \frac{(8.68\text{ min})^2}{(0.29\text{ min})^2} = 14300\text{ plates}$$

Solving Equation 2.2.10 for *H* gives the average height of a theoretical plate as

$$H = \frac{L}{N} = \frac{2.00\text{ m}}{14300\text{ plates}} \times \frac{1000\text{ mm}}{\text{m}} = 0.14\text{ mm/plate}$$

Exercise 12.2.4

For each solute in the chromatogram for Exercise 12.2.2 , calculate the number of theoretical plates and the average height of a theoretical plate. The column is 0.5 m long.

Answer

Because the relationship between elution time and distance is proportional, we can measure $t_{r,1}$, $t_{r,2}$, w_1, and w_2 using a ruler. My measurements are 40.2 mm, 51.5 mm, 8.0 mm, and 13.5 mm, respectively. Using these values, the number of theoretical plates for each solute is

$$N_1 = 16\frac{t_{r,1}^2}{w_1^2} = 16 \times \frac{(40.2\text{ mm})^2}{(8.0\text{ mm})^2} = 400\text{ theoretical plates}$$

$$N_2 = 16\frac{t_{r,2}^2}{w_2^2} = 16 \times \frac{(51.5\text{ mm})^2}{(13.5\text{ mm})^2} = 233\text{ theoretical plates}$$

The height of a theoretical plate for each solute is

$$H_1 = \frac{L}{N_1} = \frac{0.500\text{ m}}{400\text{ plates}} \times \frac{1000\text{ mm}}{\text{m}} = 1.2\text{ mm/plate}$$

$$H_2 = \frac{L}{N_2} = \frac{0.500\text{ m}}{233\text{ plates}} \times \frac{1000\text{ mm}}{\text{m}} = 2.15\text{ mm/plate}$$

Your measurements for $t_{r,1}$, $t_{r,2}$, w_1, and w_2 will depend on the relative size of your monitor or printout; however, your values for N and for H should be similar to the answer above.

It is important to remember that a theoretical plate is an artificial construct and that a chromatographic column does not contain physical plates. In fact, the number of theoretical plates depends on both the properties of the column and the solute. As a result, the number of theoretical plates for a column may vary from solute to solute.

Peak Capacity

One advantage of improving column efficiency is that we can separate more solutes with baseline resolution. One estimate of the number of solutes that we can separate is

$$n_c = 1 + \frac{\sqrt{N}}{4}\ln\frac{V_{max}}{V_{min}} \tag{2.2.16}$$

where n_c is the column's ***peak capacity***, and V_{min} and V_{max} are the smallest and the largest volumes of mobile phase in which we can elute and detect a solute [Giddings, J. C. *Unified Separation Science*, Wiley-Interscience: New York, 1991]. A column with 10 000 theoretical plates, for example, can resolve no more than

$$n_c = 1 + \frac{\sqrt{10000}}{4}\ln\frac{30\text{mL}}{1\text{mL}} = 86\text{ solutes}$$

if V_{min} and V_{max} are 1 mL and 30 mL, respectively. This estimate provides an upper bound on the number of solutes and may help us exclude from consideration a column that does not have enough theoretical plates to separate a complex mixture. Just because a column's theoretical peak capacity is larger than the number of solutes, however, does not mean that a separation is feasible. In most situations the practical peak capacity is less than the theoretical peak capacity because the retention characteristics of some solutes are so similar that a separation is impossible. Nevertheless, columns with more theoretical plates, or with a greater range of possible elution volumes, are more likely to separate a complex mixture.

The smallest volume we can use is the column's void volume. The largest volume is determined either by our patience—the maximum analysis time we can tolerate—or by our inability to detect solutes because there is too much band broadening.

Asymmetric Peaks

Our treatment of chromatography in this section assumes that a solute elutes as a symmetrical Gaussian peak, such as that shown in Figure 12.2.4 . This ideal behavior occurs when the solute's partition coefficient, K_D

$$K_D = \frac{[S_s]}{[S_m]}$$

is the same for all concentrations of solute. If this is not the case, then the chromatographic peak has an asymmetric peak shape similar to those shown in Figure 12.2.9 . The chromatographic peak in Figure 12.2.9 a is an example of ***peak tailing***, which occurs when some sites on the stationary phase retain the solute more strongly than other sites. Figure 12.2.9 b, which is an example of ***peak fronting*** most often is the result of overloading the column with sample.

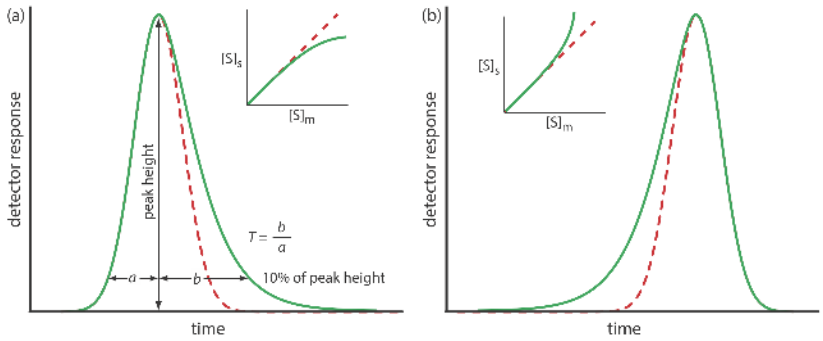


Figure 12.2.9 . Examples of asymmetric chromatographic peaks showing (a) peak tailing and (b) peak fronting. For both (a) and (b) the green chromatogram is the asymmetric peak and the red dashed chromatogram shows the ideal, Gaussian peak shape. The insets show the relationship between the concentration of solute in the stationary phase, $[S]_s$, and its concentration in the mobile phase, $[S]_m$. The dashed red lines show ideal behavior (K_D is constant for all conditions) and the green lines show nonideal behavior (K_D decreases or increases for higher total concentrations of solute). A quantitative measure of peak tailing, T, is shown in (a).

As shown in Figure 12.2.9 a, we can report a peak's asymmetry by drawing a horizontal line at 10% of the peak's maximum height and measuring the distance from each side of the peak to a line drawn vertically through the peak's maximum. The asymmetry factor, T, is defined as

$$T = \frac{b}{a}$$

The number of theoretical plates for an asymmetric peak shape is approximately

$$N \approx \frac{41.7 \times \frac{t_r^2}{(w_{0.1})^2}}{T + 1.25} = \frac{41.7 \times \frac{t_r^2}{(a+b)^2}}{T + 1.25}$$

where $w_{0.1}$ is the width at 10% of the peak's height [Foley, J. P.; Dorsey, J. G. *Anal. Chem.* **1983**, *55*, 730–737].

Asymmetric peaks have fewer theoretical plates, and the more asymmetric the peak the smaller the number of theoretical plates. For example, the following table gives values for N for a solute eluting with a retention time of 10.0 min and a peak width of 1.00 min.

b	a	T	N
0.5	0.5	1.00	1850
0.6	0.4	1.50	1520
0.7	0.3	2.33	1160
0.8	0.2	4.00	790

This page titled 2.2: General Theory of Column Chromatography is shared under a CC BY-NC-SA 4.0 license and was authored, remixed, and/or curated by David Harvey.

- **12.2: General Theory of Column Chromatography** by David Harvey is licensed CC BY-NC-SA 4.0.

2.3: Optimizing Chromatographic Separations

Now that we have defined the solute retention factor, selectivity, and column efficiency we are able to consider how they affect the resolution of two closely eluting peaks. Because the two peaks have similar retention times, it is reasonable to assume that their peak widths are nearly identical. If the number of theoretical plates is the same for all solutes—not strictly true, but not a bad assumption—then from equation 12.2.15, the ratio t_r/w is a constant. If two solutes have similar retention times, then their peak widths must be similar. Equation 12.2.1, therefore, becomes

$$R_{AB} = \frac{t_{r,B} - t_{r,A}}{0.5\,(w_B + w_A)} \approx \frac{t_{r,B} - t_{r,A}}{0.5\,(2w_B)} = \frac{t_{r,B} - t_{r,A}}{w_B} \tag{2.3.1}$$

where B is the later eluting of the two solutes. Solving equation 12.2.15 for w_B and substituting into Equation 2.3.1 leaves us with the following result.

$$R_{AB} = \frac{\sqrt{N_B}}{4} \times \frac{t_{r,B} - t_{r,A}}{t_{r,B}} \tag{2.3.2}$$

Rearranging equation 12.2.8 provides us with the following equations for the retention times of solutes A and B.

$$t_{r,A} = k_A t_\mathrm{m} + t_\mathrm{m} \quad \text{and} \quad t_{r,B} = k_B t_\mathrm{m} + t_\mathrm{m}$$

After substituting these equations into Equation 2.3.2 and simplifying, we have

$$R_{AB} = \frac{\sqrt{N_B}}{4} \times \frac{k_B - k_A}{1 + k_B}$$

Finally, we can eliminate solute A's retention factor by substituting in equation 12.2.9. After rearranging, we end up with the following equation for the resolution between the chromatographic peaks for solutes A and B.

$$R_{AB} = \frac{\sqrt{N_B}}{4} \times \frac{\alpha - 1}{\alpha} \times \frac{k_B}{1 + k_B} \tag{2.3.3}$$

In addition to resolution, another important factor in chromatography is the amount of time needed to elute a pair of solutes, which we can approximate using the retention time for solute B.

$$t_{r,s} = \frac{16 R_{AB}^2 H}{u} \times \left(\frac{\alpha}{\alpha - 1}\right)^2 \times \frac{(1 + k_B)^3}{k_B^2} \tag{2.3.4}$$

where u is the mobile phase's velocity.

> Although Equation 2.3.3 is useful for considering how a change in N, α, or k qualitatively affects resolution—which suits our purpose here—it is less useful for making accurate quantitative predictions of resolution, particularly for smaller values of N and for larger values of R. For more accurate predictions use the equation
>
> $$R_{AB} = \frac{\sqrt{N}}{4} \times (\alpha - 1) \times \frac{k_B}{1 + k_{avg}}$$
>
> where k_{avg} is $(k_A + k_B)/2$. For a derivation of this equation and for a deeper discussion of resolution in column chromatography, see Foley, J. P. "Resolution Equations for Column Chromatography," *Analyst*, **1991**, *116*, 1275-1279.

Equation 2.3.3 and Equation 2.3.4 contain terms that correspond to column efficiency, selectivity, and the solute retention factor. We can vary these terms, more or less independently, to improve resolution and analysis time. The first term, which is a function of the number of theoretical plates (for Equation 2.3.3) or the height of a theoretical plate (for Equation 2.3.4), accounts for the effect of column efficiency. The second term is a function of α and accounts for the influence of column selectivity. Finally, the third term in both equations is a function of k_B and accounts for the effect of solute B's retention factor. A discussion of how we can use these parameters to improve resolution is the subject of the remainder of this section.

Using the Retention Factor to Optimize Resolution

One of the simplest ways to improve resolution is to adjust the retention factor for solute *B*. If all other terms in Equation **2.3.3** remain constant, an increase in k_B will improve resolution. As shown by the green curve in Figure 12.3.1 , however, the improvement is greatest if the initial value of k_B is small. Once k_B exceeds a value of approximately 10, a further increase produces only a marginal improvement in resolution. For example, if the original value of k_B is 1, increasing its value to 10 gives an 82% improvement in resolution; a further increase to 15 provides a net improvement in resolution of only 87.5%.

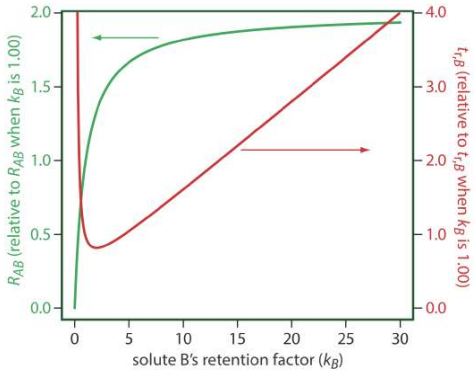


Figure 12.3.1 . Effect of k_B on the resolution for a pair of solutes, R_{AB}, and the retention time for the later eluting solute, $t_{r,B}$. The *y*-axes display the resolution and retention time relative to their respective values when k_B is 1.00.

Any improvement in resolution from increasing the value of k_B generally comes at the cost of a longer analysis time. The red curve in Figure 12.3.1 shows the relative change in the retention time for solute *B* as a function of its retention factor. Note that the minimum retention time is for $k_B = 2$. Increasing k_B from 2 to 10, for example, approximately doubles solute B's retention time.

> The relationship between retention factor and analysis time in Figure 12.3.1 works to our advantage if a separation produces an acceptable resolution with a large k_B. In this case we may be able to decrease k_B with little loss in resolution and with a significantly shorter analysis time.

To increase k_B without changing selectivity, α, any change to the chromatographic conditions must result in a general, nonselective increase in the retention factor for both solutes. In gas chromatography, we can accomplish this by decreasing the column's temperature. Because a solute's vapor pressure is smaller at lower temperatures, it spends more time in the stationary phase and takes longer to elute. In liquid chromatography, the easiest way to increase a solute's retention factor is to use a mobile phase that is a weaker solvent. When the mobile phase has a lower solvent strength, solutes spend proportionally more time in the stationary phase and take longer to elute.

Adjusting the retention factor to improve the resolution between one pair of solutes may lead to unacceptably long retention times for other solutes. For example, suppose we need to analyze a four-component mixture with baseline resolution and with a run-time of less than 20 min. Our initial choice of conditions gives the chromatogram in Figure 12.3.2 a. Although we successfully separate components 3 and 4 within 15 min, we fail to separate components 1 and 2. Adjusting conditions to improve the resolution for the first two components by increasing k_2 provides a good separation of all four components, but the run-time is too long (Figure 12.3.2 b). This problem of finding a single set of acceptable operating conditions is known as the ***general elution problem***.

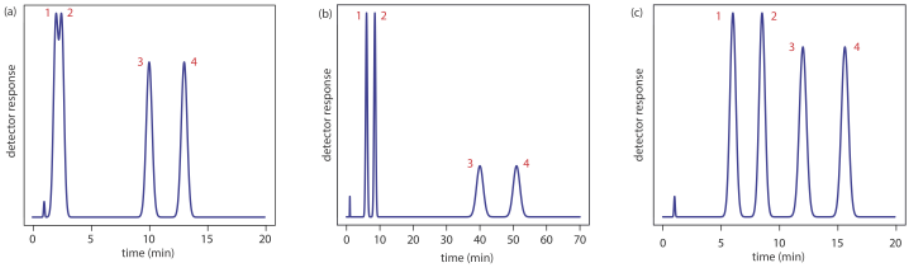


Figure 12.3.2 . Example showing the general elution problem in chromatography. See text for details.

One solution to the general elution problem is to make incremental adjustments to the retention factor as the separation takes place. At the beginning of the separation we set the initial chromatographic conditions to optimize the resolution for early eluting solutes. As the separation progresses, we adjust the chromatographic conditions to decrease the retention factor—and, therefore, to decrease the retention time—for each of the later eluting solutes (Figure 12.3.2 c). In gas chromatography this is accomplished by temperature programming. The column's initial temperature is selected such that the first solutes to elute are resolved fully. The temperature is then increased, either continuously or in steps, to bring off later eluting components with both an acceptable resolution and a reasonable analysis time. In liquid chromatography the same effect is obtained by increasing the solvent's eluting strength. This is known as a gradient elution. We will have more to say about each of these in later sections of this chapter.

Using Selectivity to Optimize Resolution

A second approach to improving resolution is to adjust the selectivity, α. In fact, for $\alpha \approx 1$ usually it is not possible to improve resolution by adjusting the solute retention factor, k_B, or the column efficiency, N. A change in α often has a more dramatic effect on resolution than a change in k_B. For example, changing α from 1.1 to 1.5, while holding constant all other terms, improves resolution by 267%. In gas chromatography, we adjust α by changing the stationary phase; in liquid chromatography, we change the composition of the mobile phase to adjust α.

To change α we need to selectively adjust individual solute retention factors. Figure 12.3.3 shows one possible approach for the liquid chromatographic separation of a mixture of substituted benzoic acids. Because the retention time of a compound's weak acid form and its weak base form are different, its retention time will vary with the pH of the mobile phase, as shown in Figure 12.3.3 a. The intersections of the curves in Figure 12.3.3 a show pH values where two solutes co-elute. For example, at a pH of 3.8 terephthalic acid and *p*-hydroxybenzoic acid elute as a single chromatographic peak.

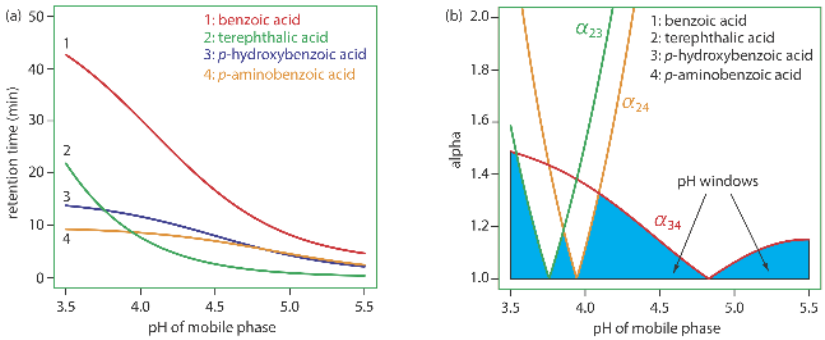


Figure 12.3.3 . Example showing how the mobile phase pH in liquid chromatography affects selectivity: (a) retention times for four substituted benzoic acids as a function of the mobile phase's pH; (b) alpha values for three pairs of solutes that are difficult to separate. See text for details. The mobile phase is an acetic acid/sodium acetate buffer and the stationary phase is a nonpolar hydrocarbon. Data from Harvey, D. T.; Byerly, S.; Bowman, A.; Tomlin, J. "Optimization of HPLC and GC Separations Using Response Surfaces," *J. Chem. Educ.* **1991**, *68*, 162–168.

Figure 12.3.3 a shows that there are many pH values where some separation is possible. To find the optimum separation, we plot a for each pair of solutes. The red, green, and orange curves in Figure 12.3.3 b show the variation in a with pH for the three pairs of solutes that are hardest to separate (for all other pairs of solutes, $\alpha > 2$ at all pH levels). The blue shading shows windows of pH values in which at least a partial separation is possible—this figure is sometimes called a window diagram—and the highest point in each window gives the optimum pH within that range. The best overall separation is the highest point in any window, which, for this example, is a pH of 3.5. Because the analysis time at this pH is more than 40 min (Figure 12.3.3 a), choosing a pH between 4.1–4.4 might produce an acceptable separation with a much shorter analysis time.

Let's use benzoic acid, C_6H_5COOH, to explain why pH can affect a solute's retention time. The separation uses an aqueous mobile phase and a nonpolar stationary phase. At lower pHs, benzoic acid predominately is in its weak acid form, C_6H_5COOH, and partitions easily into the nonpolar stationary phase. At more basic pHs, however, benzoic acid is in its weak base form, $C_6H_5COO^-$. Because it now carries a charge, its solubility in the mobile phase increases and its solubility in the nonpolar stationary phase decreases. As a result, it spends more time in the mobile phase and has a shorter retention time.

Although the usual way to adjust pH is to change the concentration of buffering agents, it also is possible to adjust pH by changing the column's temperature because a solute's pK_a value is pH-dependent; for a review, see Gagliardi, L. G.; Tascon, M.; Castells, C. B. "Effect of Temperature on Acid–Base Equilibria in Separation Techniques: A Review," *Anal. Chim. Acta*, **2015**, *889*, 35–57.

Using Column Efficiency to Optimize Resolution

A third approach to improving resolution is to adjust the column's efficiency by increasing the number of theoretical plates, *N*. If we have values for k_B and α, then we can use Equation 2.3.3 to calculate the number of theoretical plates for any resolution. Table 12.3.1 provides some representative values. For example, if α = 1.05 and k_B = 2.0, a resolution of 1.25 requires approximately 24 800 theoretical plates. If our column provides only 12 400 plates, half of what is needed, then a separation is not possible. How can we double the number of theoretical plates? The easiest way is to double the length of the column, although this also doubles the analysis time. A better approach is to cut the height of a theoretical plate, *H*, in half, providing the desired resolution without changing the analysis time. Even better, if we can decrease *H* by more than 50%, it may be possible to achieve the desired resolution with an even shorter analysis time by also decreasing k_B or α.

Table 12.3.1 . Minimum Number of Theoretical Plates to Achieve Desired Resolution for Selected Values of k_B and α

	R_{AB} = 1.00		R_{AB} = 1.25		R_{AB} = 1.50	
k_B	$\alpha = 1.05$	$\alpha = 1.10$	$\alpha = 1.05$	$\alpha = 1.10$	$\alpha = 1.05$	$\alpha = 1.10$
0.5	63500	17400	99200	27200	143000	39200
1.0	28200	7740	44100	12100	63500	17400
1.5	19600	5380	30600	8400	44100	12100
2.0	15900	4360	24800	6810	35700	9800
3.0	12500	3440	19600	5380	28200	7740
5.0	10200	2790	15900	4360	22900	6270
10.0	8540	2340	13300	3660	19200	5270

To decrease the height of a theoretical plate we need to understand the experimental factors that affect band broadening. There are several theoretical treatments of band broadening. We will consider one approach that considers four contributions: variations in path lengths, longitudinal diffusion, mass transfer in the stationary phase, and mass transfer in the mobile phase.

Multiple Paths: Variations in Path Length

As solute molecules pass through the column they travel paths that differ in length. Because of this difference in path length, two solute molecules that enter the column at the same time will exit the column at different times. The result, as shown in Figure 12.3.4 , is a broadening of the solute's profile on the column. The contribution of ***multiple paths*** to the height of a theoretical plate, H_p, is

$$H_p = 2\lambda d_p \tag{2.3.5}$$

where d_p is the average diameter of the particulate packing material and λ is a constant that accounts for the consistency of the packing. A smaller range of particle sizes and a more consistent packing produce a smaller value for λ. For a column without packing material, H_p is zero and there is no contribution to band broadening from multiple paths.

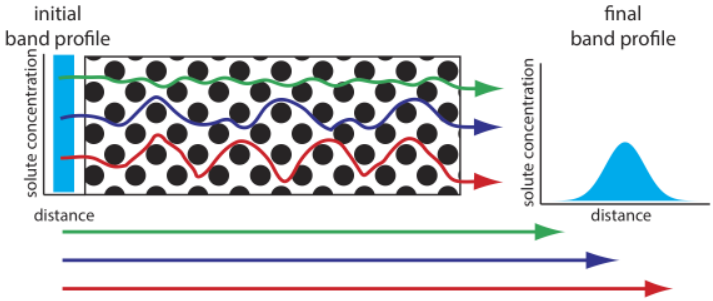


Figure 12.3.4 . The effect of multiple paths on a solute's band broadening. The solute's initial band profile is rectangular. As this band travels through the column, individual solute molecules travel different paths, three of which are shown by the meandering colored paths (the actual lengths of these paths are shown by the straight arrows at the bottom of the figure). Most solute molecules travel paths with lengths similar to that shown in blue, with a few traveling much shorter paths (green) or much longer paths (red). As a result, the solute's band profile at the end of the column is broader and Gaussian in shape.

An inconsistent packing creates channels that allow some solute molecules to travel quickly through the column. It also can creates pockets that temporarily trap some solute molecules, slowing their progress through the column. A more uniform packing minimizes these problems.

Longitudinal Diffusion

The second contribution to band broadening is the result of the solute's ***longitudinal diffusion*** in the mobile phase. Solute molecules are in constant motion, diffusing from regions of higher solute concentration to regions where the concentration of solute is smaller. The result is an increase in the solute's band width (Figure 12.3.5). The contribution of longitudinal diffusion to the height of a theoretical plate, H_d, is

$$H_d = \frac{2\gamma D_m}{u} \tag{2.3.6}$$

where D_m is the solute's diffusion coefficient in the mobile phase, u is the mobile phase's velocity, and γ is a constant related to the efficiency of column packing. Note that the effect of H_d on band broadening is inversely proportional to the mobile phase velocity: a higher velocity provides less time for longitudinal diffusion. Because a solute's diffusion coefficient is larger in the gas phase than in a liquid phase, longitudinal diffusion is a more serious problem in gas chromatography.

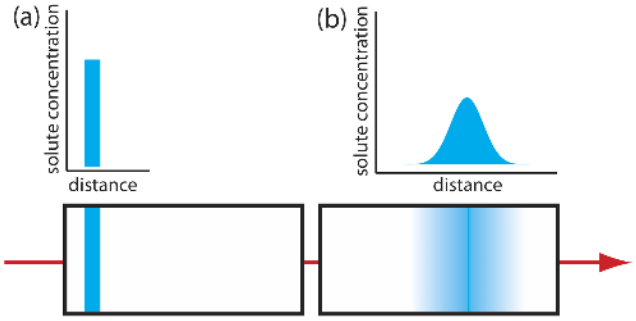


Figure 12.3.5 . The effect of longitudinal diffusion on a solute's band broadening. Two horizontal cross-sections through the column and the corresponding concentration versus distance profiles are shown, with (a) being earlier in time. The red arrow shows the direction in which the mobile phase is moving.

Mass Transfer

As the solute passes through the column it moves between the mobile phase and the stationary phase. We call this movement between phases ***mass transfer***. As shown in Figure 12.3.6 , band broadening occurs if the solute's movement within the mobile phase or within the stationary phase is not fast enough to maintain an equilibrium in its concentration between the two phases. On average, a solute molecule in the mobile phase moves down the column before it passes into the stationary phase. A solute molecule in the stationary phase, on the other hand, takes longer than expected to move back into the mobile phase. The

contributions of mass transfer in the stationary phase, H_s, and mass transfer in the mobile phase, H_m, are given by the following equations

$$H_s = \frac{qkd_f^2}{(1+k)^2 D_s} u \tag{2.3.7}$$

$$H_m = \frac{fn\left(d_p^2, d_c^2\right)}{D_m} u \tag{2.3.8}$$

where d_f is the thickness of the stationary phase, d_c is the diameter of the column, D_s and D_m are the diffusion coefficients for the solute in the stationary phase and the mobile phase, k is the solute's retention factor, and q is a constant related to the column packing material. Although the exact form of H_m is not known, it is a function of particle size and column diameter. Note that the effect of H_s and H_m on band broadening is directly proportional to the mobile phase velocity because a smaller velocity provides more time for mass transfer.

> The abbreviation *fn* in Equation **2.3.7** means "is a function of."

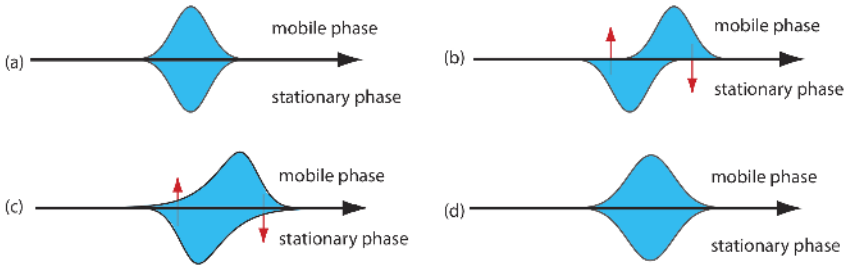


Figure 12.3.6 . Effect of mass transfer on band broadening: (a) Ideal equilibrium Gaussian profiles for the solute in the mobile phase and in the stationary phase. (b, c) If we allow the solute's band to move a small distance down the column, an equilibrium between the two phases no longer exits. The red arrows show the movement of solute—what we call the mass transfer of solute—from the stationary phase to the mobile phase, and from the mobile phase to the stationary phase. (d) Once equilibrium is reestablished, the solute's band is now broader.

Putting It All Together

The height of a theoretical plate is a summation of the contributions from each of the terms affecting band broadening.

$$H = H_p + H_d + H_s + H_m \tag{2.3.9}$$

An alternative form of this equation is the ***van Deemter equation***

$$H = A + \frac{B}{u} + Cu \tag{2.3.10}$$

which emphasizes the importance of the mobile phase's velocity. In the van Deemter equation, A accounts for the contribution of multiple paths (H_p), B/u accounts for the contribution of longitudinal diffusion (H_d), and Cu accounts for the combined contribution of mass transfer in the stationary phase and in the mobile phase (H_s and H_m).

There is some disagreement on the best equation for describing the relationship between plate height and mobile phase velocity [Hawkes, S. J. *J. Chem. Educ.* **1983**, *60*, 393–398]. In addition to the van Deemter equation, other equations include

$$H = \frac{B}{u} + (C_s + C_m)\, u$$

where C_s and C_m are the mass transfer terms for the stationary phase and the mobile phase and

$$H = Au^{1/3} + \frac{B}{u} + Cu$$

All three equations, and others, have been used to characterize chromatographic systems, with no single equation providing the best explanation in every case [Kennedy, R. T.; Jorgenson, J. W. *Anal. Chem.* **1989**, *61*, 1128–1135].

To increase the number of theoretical plates without increasing the length of the column, we need to decrease one or more of the terms in Equation 2.3.9. The easiest way to decrease H is to adjust the velocity of the mobile phase. For smaller mobile phase velocities, column efficiency is limited by longitudinal diffusion, and for higher mobile phase velocities efficiency is limited by the two mass transfer terms. As shown in Figure 12.3.7 —which uses the van Deemter equation—the optimum mobile phase velocity is the minimum in a plot of H as a function of u.

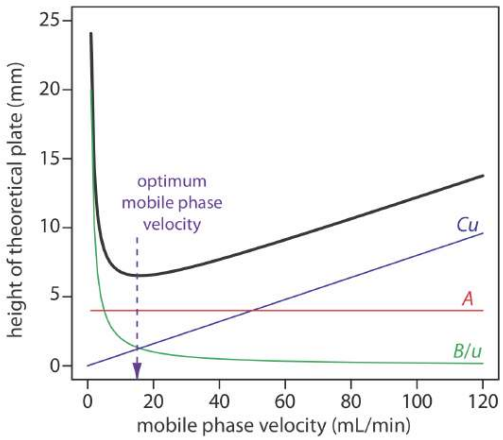


Figure 12.3.7 . Plot showing the relationship between the height of a theoretical plate, H, and the mobile phase's velocity, u, based on the van Deemter equation.

The remaining parameters that affect the terms in Equation 2.3.9 are functions of the column's properties and suggest other possible approaches to improving column efficiency. For example, both H_p and H_m are a function of the size of the particles used to pack the column. Decreasing particle size, therefore, is another useful method for improving efficiency.

> For a more detailed discussion of ways to assess the quality of a column, see Desmet, G.; Caooter, D.; Broeckhaven, K. "Graphical Data Represenation Methods to Assess the Quality of LC Columns," *Anal. Chem.* **2015**, *87*, 8593–8602.

Perhaps the most important advancement in chromatography columns is the development of open-tubular, or ***capillary columns***. These columns have very small diameters ($d_c \approx$ 50–500 μm) and contain no packing material ($d_p = 0$). Instead, the capillary column's interior wall is coated with a thin film of the stationary phase. Plate height is reduced because the contribution to H from H_p (Equation 2.3.5) disappears and the contribution from H_m (Equation 2.3.8) becomes smaller. Because the column does not contain any solid packing material, it takes less pressure to move the mobile phase through the column, which allows for longer columns. The combination of a longer column and a smaller height for a theoretical plate increases the number of theoretical plates by approximately $100\times$. Capillary columns are not without disadvantages. Because they are much narrower than packed columns, they require a significantly smaller amount of sample, which may be difficult to inject reproducibly. Another approach to improving resolution is to use thin films of stationary phase, which decreases the contribution to H from H_s (Equation 2.3.7).

> The smaller the particles, the more pressure is needed to push the mobile phase through the column. As a result, for any form of chromatography there is a practical limit to particle size.

This page titled 2.3: Optimizing Chromatographic Separations is shared under a CC BY-NC-SA 4.0 license and was authored, remixed, and/or curated by David Harvey.

- **12.3: Optimizing Chromatographic Separations** by David Harvey is licensed CC BY-NC-SA 4.0.

2.4: Gas Chromatography

In ***gas chromatography*** (GC) we inject the sample, which may be a gas or a liquid, into an gaseous mobile phase (often called the carrier gas). The mobile phase carries the sample through a packed or a capillary column that separates the sample's components based on their ability to partition between the mobile phase and the stationary phase. Figure 12.4.1 shows an example of a typical gas chromatograph, which consists of several key components: a supply of compressed gas for the mobile phase; a heated injector, which rapidly volatilizes the components in a liquid sample; a column, which is placed within an oven whose temperature we can control during the separation; and a detector to monitor the eluent as it comes off the column. Let's consider each of these components.



Figure 12.4.1 . Example of a typical gas chromatograph with insets showing the heated injection ports—note the symbol indicating that it is hot—and the oven that houses the column. This particular instrument is equipped with an autosampler for injecting samples, a capillary column, and a mass spectrometer (MS) as the detector. Note that the carrier gas is supplied by a tank of compressed gas.

Mobile Phase

The most common mobile phases for gas chromatography are He, Ar, and N_2, which have the advantage of being chemically inert toward both the sample and the stationary phase. The choice of carrier gas often is determined by the needs of instrument's detector. For a packed column the mobile phase velocity usually is 25–150 mL/min. The typical flow rate for a capillary column is 1–25 mL/min.

Chromatographic Columns

There are two broad classes of chromatographic columns: packed columns and capillary columns. In general, a packed column can handle larger samples and a capillary column can separate more complex mixtures.

Packed Columns

Packed columns are constructed from glass, stainless steel, copper, or aluminum, and typically are 2–6 m in length with internal diameters of 2–4 mm. The column is filled with a particulate solid support, with particle diameters ranging from 37–44 μm to 250–354 μm. Figure 12.4.2 shows a typical example of a packed column.

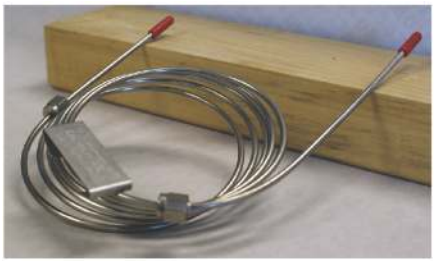


Figure 12.4.2 . Typical example of a packed column for gas chromatography. This column is made from stainless steel and is 2 m long with an internal diameter of 3.2 mm. The packing material in this column has a particle diameter of 149–177 μm. To put this in perspective, beach sand has a typical diameter of 700 μm and the diameter of fine grained sand is 250 μm.

The most widely used particulate support is diatomaceous earth, which is composed of the silica skeletons of diatoms. These particles are very porous, with surface areas ranging from 0.5–7.5 m^2/g, which provides ample contact between the mobile phase and the stationary phase. When hydrolyzed, the surface of a diatomaceous earth contains silanol groups (–SiOH), that serve as active sites for absorbing solute molecules in gas-solid chromatography (GSC).

In ***gas-liquid chromatography*** (GLC), we coat the packing material with a liquid mobile phase. To prevent uncoated packing material from adsorbing solutes, which degrades the quality of the separation, surface silanols are deactivated by reacting them with dimethyldichlorosilane and rinsing with an alcohol—typically methanol—before coating the particles with stationary phase.

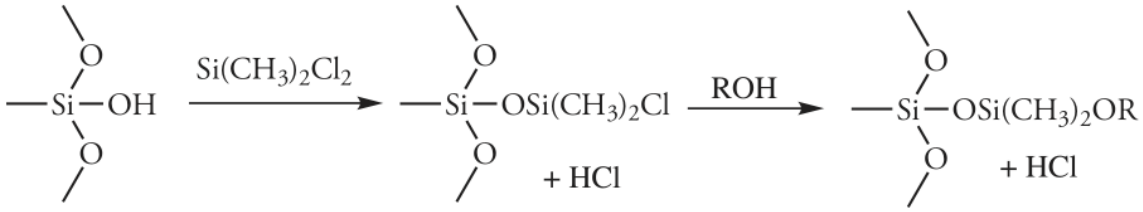


Figure 12.4.2 , for example, has approximately 1800 plates/m, or a total of approximately 3600 theoretical plates. If we assume a $V_{max}/V_{min} \approx 50$, then it has a peak capacity (equation 12.2.16) of

$$n_c = 1 + \frac{\sqrt{3600}}{4}\ln(50) \approx 60$$

Capillary Columns

A capillary, or ***open tubular column*** is constructed from fused silica and is coated with a protective polymer coating. Columns range from 15–100 m in length with an internal diameter of approximately 150–300 μm. Figure 12.4.3 shows an example of a typical capillary column.



Figure 12.4.3 . Typical example of a capillary column for gas chromatography. This column is 30 m long with an internal diameter of 247 μm. The interior surface of the capillary has a 0.25 μm coating of the liquid phase.

Capillary columns are of three principal types. In a ***wall-coated open tubular column*** (WCOT) a thin layer of stationary phase, typically 0.25 nm thick, is coated on the capillary's inner wall. In a ***porous-layer open tubular column*** (PLOT), a porous solid support—alumina, silica gel, and molecular sieves are typical examples—is attached to the capillary's inner wall. A ***support-coated open tubular column*** (SCOT) is a PLOT column that includes a liquid stationary phase. Figure 12.4.4 shows the differences between these types of capillary columns.

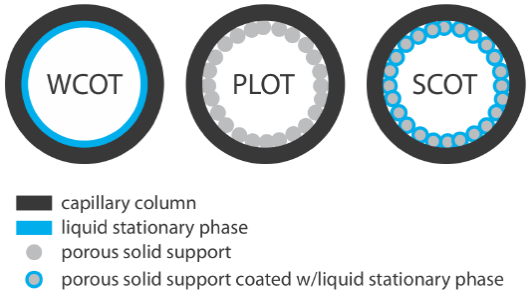


Figure 12.4.4 . Cross sections through the three types of capillary columns.

A capillary column provides a significant improvement in separation efficiency because it has more theoretical plates per meter and is longer than a packed column. For example, the capillary column in Figure 12.4.3 has almost 4300 plates/m, or a total of 129 000 theoretical plates. If we assume a $V_{max}/V_{min} \approx 50$, then it has a peak capacity of approximately 350. On the other hand, a packed column can handle a larger sample. Because of its smaller diameter, a capillary column requires a smaller sample, typically less than 10^{-2} μL.

Stationary Phases for Gas-Liquid Chromatography

Elution order in gas–liquid chromatography depends on two factors: the boiling point of the solutes, and the interaction between the solutes and the stationary phase. If a mixture's components have significantly different boiling points, then the choice of stationary phase is less critical. If two solutes have similar boiling points, then a separation is possible only if the stationary phase selectively interacts with one of the solutes. As a general rule, nonpolar solutes are separated more easily when using a nonpolar stationary phase, and polar solutes are easier to separate when using a polar stationary phase.

There are several important criteria for choosing a stationary phase: it must not react with the solutes, it must be thermally stable, it must have a low volatility, and it must have a polarity that is appropriate for the sample's components. Table 12.4.1 summarizes the properties of several popular stationary phases.

Table 12.4.1 . Selected Examples of Stationary Phases for Gas-Liquid Chromatography

stationary phase	polarity	trade name	temperature limit (°C)	representative applications
squalane	nonpolar	Squalane	150	low-boiling aliphatics hydrocarbons
Apezion L	nonpolar	Apezion L	300	amides, fatty acid methyl esters, terpenoids
polydimethyl siloxane	slightly polar	SE-30	300–350	alkaloids, amino acid derivatives, drugs, pesticides, phenols, steroids
phenylmethyl polysiloxane (50% phenyl, 50% methyl)	moderately polar	OV-17	375	alkaloids, drugs, pesticides, polyaromatic hydrocarbons, polychlorinated biphenyls
trifluoropropylmethyl polysiloxane (50% trifluoropropyl, 50% methyl)	moderately polar	OV-210	275	alkaloids, amino acid derivatives, drugs, halogenated compounds, ketones
cyanopropylphenylmethyl polysiloxane (50%cyanopropyl, 50% phenylmethyl)	polar	OV-225	275	nitriles, pesticides, steroids
polyethylene glycol	polar	Carbowax 20M	225	aldehydes, esters, ethers, phenols

Many stationary phases have the general structure shown in Figure 12.4.5 a. A stationary phase of polydimethyl siloxane, in which all the –R groups are methyl groups, $–CH_3$, is nonpolar and often makes a good first choice for a new separation. The order of elution when using polydimethyl siloxane usually follows the boiling points of the solutes, with lower boiling solutes eluting first. Replacing some of the methyl groups with other substituents increases the stationary phase's polarity and provides greater selectivity. For example, replacing 50% of the $–CH_3$ groups with phenyl groups, $–C_6H_5$, produces a slightly polar stationary phase. Increasing polarity is provided by substituting trifluoropropyl, $–C_3H_6CF$, and cyanopropyl, $–C_3H_6CN$, functional groups, or by using a stationary phase of polyethylene glycol (Figure 12.4.5 b).

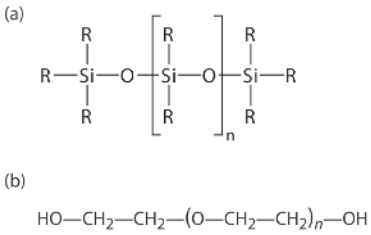


Figure 12.4.5 . General structures of common stationary phases: (a) substituted polysiloxane; (b) polyethylene glycol.

An important problem with all liquid stationary phases is their tendency to elute, or ***bleed*** from the column when it is heated. The temperature limits in Table 12.4.1 minimize this loss of stationary phase. Capillary columns with bonded or cross-linked stationary phases provide superior stability. A bonded stationary phase is attached chemically to the capillary's silica surface. Cross-linking, which is done after the stationary phase is in the capillary column, links together separate polymer chains to provide greater stability.

Another important consideration is the thickness of the stationary phase. From equation 12.3.7 we know that separation efficiency improves with thinner films of stationary phase. The most common thickness is 0.25 μm, although a thicker films is useful for highly volatile solutes, such as gases, because it has a greater capacity for retaining such solutes. Thinner films are used when separating low volatility solutes, such as steroids.

A few stationary phases take advantage of chemical selectivity. The most notable are stationary phases that contain chiral functional groups, which are used to separate enantiomers [Hinshaw, J. V. *LC*.*GC* **1993**, *11*, 644–648].

Sample Introduction

Three factors determine how we introduce a sample to the gas chromatograph. First, all of the sample's constituents must be volatile. Second, the analytes must be present at an appropriate concentration. Finally, the physical process of injecting the sample must not degrade the separation. Each of these needs is considered in this section.

Preparing a Volatile Sample

Not every sample can be injected directly into a gas chromatograph. To move through the column, the sample's constituents must be sufficiently volatile. A solute of low volatility, for example, may be retained by the column and continue to elute during the analysis of subsequent samples. A nonvolatile solute will condense at the top of the column, degrading the column's performance.

We can separate a sample's volatile analytes from its nonvolatile components using any of the extraction techniques described in Chapter 7. A liquid–liquid extraction of analytes from an aqueous matrix into methylene chloride or another organic solvent is a common choice. Solid-phase extractions also are used to remove a sample's nonvolatile components.

An attractive approach to isolating analytes is a ***solid-phase microextraction*** (SPME). In one approach, which is illustrated in Figure 12.4.6 , a fused-silica fiber is placed inside a syringe needle. The fiber, which is coated with a thin film of an adsorbent material, such as polydimethyl siloxane, is lowered into the sample by depressing a plunger and is exposed to the sample for a predetermined time. After withdrawing the fiber into the needle, it is transferred to the gas chromatograph for analysis.

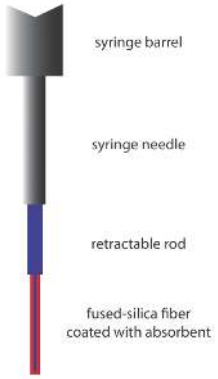


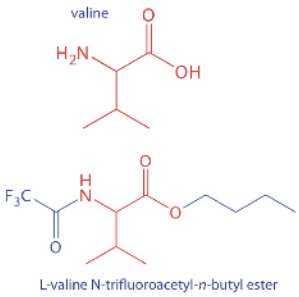
Figure 12.4.6 . Schematic diagram of a solid-phase microextraction device. The absorbent is shown in red.

Two additional methods for isolating volatile analytes are a purge-and-trap and headspace sampling. In a ***purge-and-trap***, we bubble an inert gas, such as He or N_2, through the sample, releasing—or purging—the volatile compounds. These compounds are carried by the purge gas through a trap that contains an absorbent material, such as Tenax, where they are retained. Heating the trap and back-flushing with carrier gas transfers the volatile compounds to the gas chromatograph. In ***headspace sampling*** we place the sample in a closed vial with an overlying air space. After allowing time for the volatile analytes to equilibrate between the sample and the overlying air, we use a syringe to extract a portion of the vapor phase and inject it into the gas chromatograph. Alternatively, we can sample the headspace with an SPME.

Thermal desorption is a useful method for releasing volatile analytes from solids. We place a portion of the solid in a glass-lined, stainless steel tube. After purging with carrier gas to remove any O_2 that might be present, we heat the sample. Volatile analytes are swept from the tube by an inert gas and carried to the GC. Because volatilization is not a rapid process, the volatile analytes often are concentrated at the top of the column by cooling the column inlet below room temperature, a process known as ***cryogenic focusing***. Once volatilization is complete, the column inlet is heated rapidly, releasing the analytes to travel through the column.

> The reason for removing O_2 is to prevent the sample from undergoing an oxidation reaction when it is heated.

To analyze a nonvolatile analyte we must convert it to a volatile form. For example, amino acids are not sufficiently volatile to analyze directly by gas chromatography. Reacting an amino acid, such as valine, with 1-butanol and acetyl chloride produces an esterified amino acid. Subsequent treatment with trifluoroacetic acid gives the amino acid's volatile N-trifluoroacetyl-*n*-butyl ester derivative.



L-valine N-trifluoroacetyl-*n*-butyl ester

Adjusting the Analyte's Concentration

In an analyte's concentration is too small to give an adequate signal, then we must concentrate the analyte before we inject the sample into the gas chromatograph. A side benefit of many extraction methods is that they often concentrate the analytes. Volatile organic materials isolated from an aqueous sample by a purge-and-trap, for example, are concentrated by as much as 1000×.

If an analyte is too concentrated, it is easy to overload the column, resulting in peak fronting (see Figure 12.2.7) and a poor separation. In addition, the analyte's concentration may exceed the detector's linear response. Injecting less sample or diluting the sample with a volatile solvent, such as methylene chloride, are two possible solutions to this problem.

Injecting the Sample

In Chapter 12.3 we examined several explanations for why a solute's band increases in width as it passes through the column, a process we called band broadening. We also introduce an additional source of band broadening if we fail to inject the sample into the minimum possible volume of mobile phase. There are two principal sources of this precolumn band broadening: injecting the sample into a moving stream of mobile phase and injecting a liquid sample instead of a gaseous sample. The design of a gas chromatograph's injector helps minimize these problems.

An example of a simple injection port for a packed column is shown in Figure 12.4.7 . The top of the column fits within a heated injector block, with carrier gas entering from the bottom. The sample is injected through a rubber septum using a microliter syringe, such as the one shown in in Figure 12.4.8 . Injecting the sample directly into the column minimizes band broadening because it mixes the sample with the smallest possible amount of carrier gas. The injector block is heated to a temperature at least 50°C above the boiling point of the least volatile solute, which ensures a rapid vaporization of the sample's components.

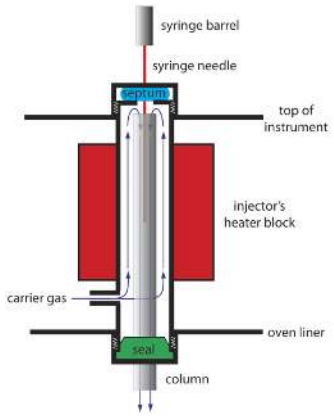


Figure 12.4.7 . Schematic diagram of a heated GC injector port for use with packed columns. The needle pierces a rubber septum and enters into the top of the column, which is located within a heater block.



Figure 12.4.8 . Example of a syringe for injecting samples into a gas chromatograph. This syringe has a maximum capacity of 10 µL with graduations every 0.1 µL.

Because a capillary column's volume is significantly smaller than that for a packed column, it requires a different style of injector to avoid overloading the column with sample. Figure 12.4.9 shows a schematic diagram of a typical split/splitless injector for use with a capillary column.

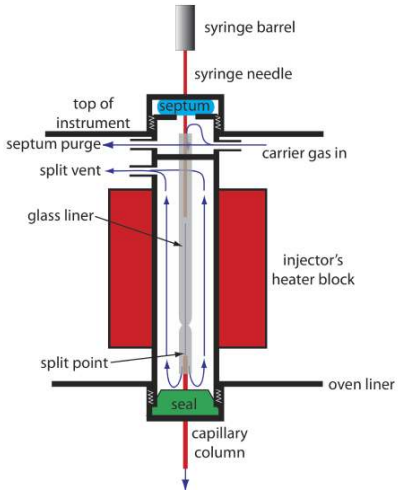


Figure 12.4.9 . Schematic diagram of a split/splitless injection port for use with capillary columns. The needle pierces a rubber septum and enters into a glass liner, which is located within a heater block. In a split injection the split vent is open; the split vent is closed for a splitless injection.

In a ***split injection*** we inject the sample through a rubber septum using a microliter syringe. Instead of injecting the sample directly into the column, it is injected into a glass liner where it mixes with the carrier gas. At the split point, a small fraction of the carrier gas and sample enters the capillary column with the remainder exiting through the split vent. By controlling the flow rate of the carrier gas as it enters the injector, and its flow rate through the septum purge and the split vent, we can control the fraction of sample that enters the capillary column, typically 0.1–10%.

> For example, if the carrier gas flow rate is 50 mL/min, and the flow rates for the septum purge and the split vent are 2 mL/min and 47 mL/min, respectively, then the flow rate through the column is 1 mL/min (= 50 – 2 – 47). The ratio of sample entering the column is 1/50, or 2%.

In a ***splitless injection***, which is useful for trace analysis, we close the split vent and allow all the carrier gas that passes through the glass liner to enter the column—this allows virtually all the sample to enters the column. Because the flow rate through the injector is low, significant precolumn band broadening is a problem. Holding the column's temperature approximately 20–25°C below the solvent's boiling point allows the solvent to condense at the entry to the capillary column, forming a barrier that traps the solutes. After allowing the solutes to concentrate, the column's temperature is increased and the separation begins.

For samples that decompose easily, an ***on-column injection*** may be necessary. In this method the sample is injected directly into the column without heating. The column temperature is then increased, volatilizing the sample with as low a temperature as is practical.

Temperature Control

Control of the column's temperature is critical to attaining a good separation when using gas chromatography. For this reason the column is placed inside a thermostated oven (see Figure 12.4.1). In an ***isothermal*** separation we maintain the column at a constant temperature. To increase the interaction between the solutes and the stationary phase, the temperature usually is set slightly below that of the lowest-boiling solute.

One difficulty with an isothermal separation is that a temperature that favors the separation of a low-boiling solute may lead to an unacceptably long retention time for a higher-boiling solute. ***Temperature programming*** provides a solution to this problem. At the beginning of the analysis we set the column's initial temperature below that for the lowest-boiling solute. As the separation progresses, we slowly increase the temperature at either a uniform rate or in a series of steps.

Detectors for Gas Chromatography

The final part of a gas chromatograph is the detector. The ideal detector has several desirable features: a low detection limit, a linear response over a wide range of solute concentrations (which makes quantitative work easier), sensitivity for all solutes or selectivity for a specific class of solutes, and an insensitivity to a change in flow rate or temperature.

Thermal Conductivity Detector (TCD)

One of the earliest gas chromatography detectors takes advantage of the mobile phase's thermal conductivity. As the mobile phase exits the column it passes over a tungsten-rhenium wire filament (see Figure 12.4.10 . The filament's electrical resistance depends on its temperature, which, in turn, depends on the thermal conductivity of the mobile phase. Because of its high thermal conductivity, helium is the mobile phase of choice when using a ***thermal conductivity detector*** (TCD).

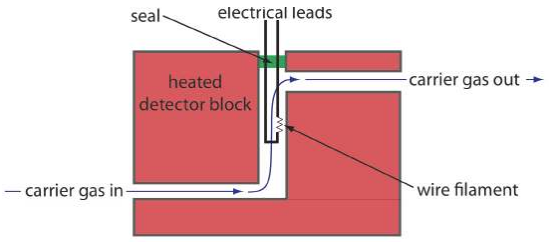


Figure 12.4.10 . Schematic diagram of a thermal conductivity detector showing one cell of a matched pair. The sample cell takes the carrier gas as it elutes from the column. A source of carrier gas that bypasses the column passes through a reference cell.

> Thermal conductivity, as the name suggests, is a measure of how easily a substance conducts heat. A gas with a high thermal conductivity moves heat away from the filament—and, thus, cools the filament—more quickly than does a gas with a low thermal conductivity.

When a solute elutes from the column, the thermal conductivity of the mobile phase in the TCD cell decreases and the temperature of the wire filament, and thus it resistance, increases. A reference cell, through which only the mobile phase passes, corrects for any time-dependent variations in flow rate, pressure, or electrical power, all of which affect the filament's resistance.

Because all solutes affect the mobile phase's thermal conductivity, the thermal conductivity detector is a universal detector. Another advantage is the TCD's linear response over a concentration range spanning 10^4–10^5 orders of magnitude. The detector also is non-

destructive, which allows us to recover analytes using a postdetector cold trap. One significant disadvantage of the TCD detector is its poor detection limit for most analytes.

Flame Ionization Detector (FID)

The combustion of an organic compound in an H_2/air flame results in a flame that contains electrons and organic cations, presumably CHO^+. Applying a potential of approximately 300 volts across the flame creates a small current of roughly 10^{-9} to 10^{-12} amps. When amplified, this current provides a useful analytical signal. This is the basis of the popular ***flame ionization detector,*** a schematic diagram of which is shown in Figure 12.4.11 .

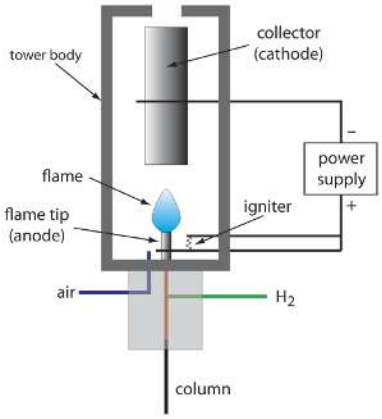


Figure 12.4.11 . Schematic diagram of a flame ionization detector. The eluent from the column mixes with H_2 and is burned in the presence of excess air. Combustion produces a flame that contains electrons and the cation $CHO^{+\cdot}$ Applying a potential between the flame's tip and the collector gives a current that is proportional to the concentration of cations in the flame.

Most carbon atoms—except those in carbonyl and carboxylic groups—generate a signal, which makes the FID an almost universal detector for organic compounds. Most inorganic compounds and many gases, such as H_2O and CO_2, are not detected, which makes the FID detector a useful detector for the analysis of organic analytes in atmospheric and aqueous environmental samples. Advantages of the FID include a detection limit that is approximately two to three orders of magnitude smaller than that for a thermal conductivity detector, and a linear response over 10^6–10^7 orders of magnitude in the amount of analyte injected. The sample, of course, is destroyed when using a flame ionization detector.

Electron Capture Detector (ECD)

The ***electron capture detector*** is an example of a selective detector. As shown in Figure 12.4.12 , the detector consists of a β-emitter, such as ^{63}Ni. The emitted electrons ionize the mobile phase, usually N_2, generating a standing current between a pair of electrodes. When a solute with a high affinity for capturing electrons elutes from the column, the current decreases, which serves as the signal. The ECD is highly selective toward solutes with electronegative functional groups, such as halogens and nitro groups, and is relatively insensitive to amines, alcohols, and hydrocarbons. Although its detection limit is excellent, its linear range extends over only about two orders of magnitude.

> A β-particle is an electron.

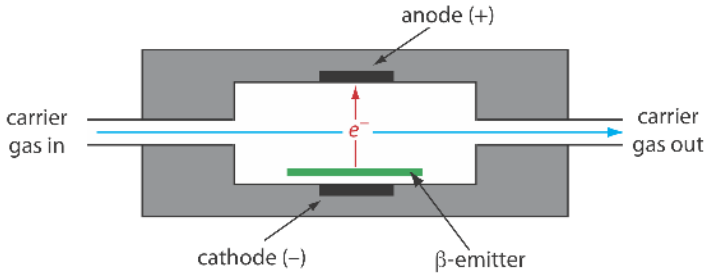


Figure 12.4.12 . Schematic diagram showing an electron capture detector.

Mass Spectrometer (MS)

A ***mass spectrometer*** is an instrument that ionizes a gaseous molecule using sufficient energy that the resulting ion breaks apart into smaller ions. Because these ions have different mass-to-charge ratios, it is possible to separate them using a magnetic field or an electrical field. The resulting mass spectrum contains both quantitative and qualitative information about the analyte. Figure 12.4.13 shows a mass spectrum for toluene.

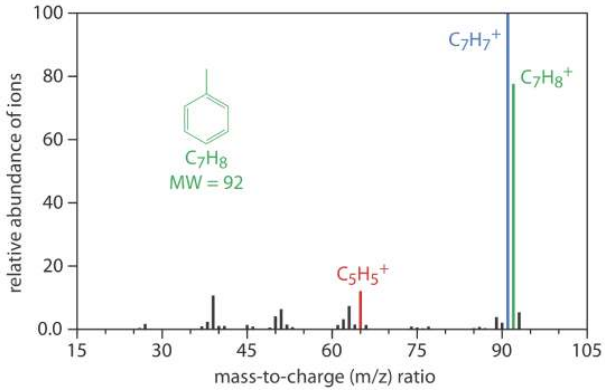


Figure 12.4.13 . Mass spectrum for toluene highlighting the molecular ion in green (m/z=92), and two fragment ions in blue (m/z=91) and in red (m/z= 65). A mass spectrum provides both quantitative and qualitative information: the height of any peak is proportional to the amount of toluene in the mass spectrometer and the fragmentation pattern is unique to toluene.

Figure 12.4.14 shows a block diagram of a typical gas chromatography-mass spectrometer (GC–MS) instrument. The effluent from the column enters the mass spectrometer's ion source in a manner that eliminates the majority of the carrier gas. In the ionization chamber the remaining molecules—a mixture of carrier gas, solvent, and solutes—undergo ionization and fragmentation. The mass spectrometer's mass analyzer separates the ions by their mass-to-charge ratio and a detector counts the ions and displays the mass spectrum.

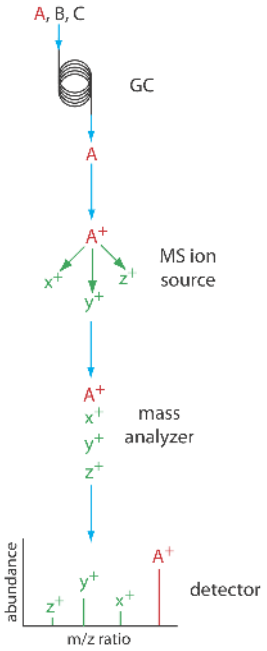


Figure 12.4.14 . Block diagram of GC– MS. A three component mixture enters the GC. When component A elutes from the column, it enters the MS ion source and ionizes to form the parent ion and several fragment ions. The ions enter the mass analyzer, which separates them by their mass-to-charge ratio, providing the mass spectrum shown at the detector.

There are several options for monitoring a chromatogram when using a mass spectrometer as the detector. The most common method is to continuously scan the entire mass spectrum and report the total signal for all ions that reach the detector during each scan. This total ion scan provides universal detection for all analytes. We can achieve some degree of selectivity by monitoring one

or more specific mass-to-charge ratios, a process called selective-ion monitoring. A mass spectrometer provides excellent detection limits, typically 25 fg to 100 pg, with a linear range of 10^5 orders of magnitude. Because we continuously record the mass spectrum of the column's eluent, we can go back and examine the mass spectrum for any time increment. This is a distinct advantage for GC–MS because we can use the mass spectrum to help identify a mixture's components.

> For more details on mass spectrometry see Introduction to Mass Spectrometry by Michael Samide and Olujide Akinbo, a resource that is part of the Analytical Sciences Digital Library.

Other Detectors

Two additional detectors are similar in design to a flame ionization detector. In the flame photometric detector, optical emission from phosphorous and sulfur provides a detector selective for compounds that contain these elements. The thermionic detector responds to compounds that contain nitrogen or phosphorous.

A Fourier transform infrared spectrophotometer (FT–IR) also can serve as a detector. In GC–FT–IR, effluent from the column flows through an optical cell constructed from a 10–40 cm Pyrex tube with an internal diameter of 1–3 mm. The cell's interior surface is coated with a reflecting layer of gold. Multiple reflections of the source radiation as it is transmit- ted through the cell increase the optical path length through the sample. As is the case with GC–MS, an FT–IR detector continuously records the column eluent's spectrum, which allows us to examine the IR spectrum for any time increment.

> See Section 10.3 for a discussion of FT-IR spectroscopy and instrumentation.

Quantitative Applications

Gas chromatography is widely used for the analysis of a diverse array of samples in environmental, clinical, pharmaceutical, biochemical, forensic, food science and petrochemical laboratories. Table 12.4.2 provides some representative examples of applications.

Table 12.4.2 . Representative Applications of Gas Chromatography

area	applications
environmental analysis	green house gases (CO_2, CH_4, NO_x) in air pesticides in water, wastewater, and soil vehicle emissions trihalomethanes in drinking water
clinical analysis	drugs blood alcohols
forensic analysis	analysis of arson accelerants detection of explosives
consumer products	volatile organics in spices and fragrances trace organics in whiskey monomers in latex paint
petrochemical and chemical industry	purity of solvents refinery gas composition of gasoline

Quantitative Calculations

In a GC analysis the area under the peak is proportional to the amount of analyte injected onto the column. A peak's area is determined by integration, which usually is handled by the instrument's computer or by an electronic integrating recorder. If two peak are resolved fully, the determination of their respective areas is straightforward.

Before electronic integrating recorders and computers, two methods were used to find the area under a curve. One method used a manual planimeter; as you use the planimeter to trace an object's perimeter, it records the area. A second approach for finding a peak's area is the cut-and-weigh method. The chromatogram is recorded on a piece of paper and each peak of interest is cut out and weighed. Assuming the paper is uniform in thickness and density of fibers, the ratio of weights for two peaks is the same as the ratio of areas. Of course, this approach destroys your chromatogram.

Overlapping peaks, however, require a choice between one of several options for dividing up the area shared by the two peaks (Figure 12.4.15). Which method we use depends on the relative size of the two peaks and their resolution. In some cases, the use of peak heights provides more accurate results [(a) Bicking, M. K. L. Chromatography Online, April 2006; (b) Bicking, M. K. L. Chromatography Online, June 2006].

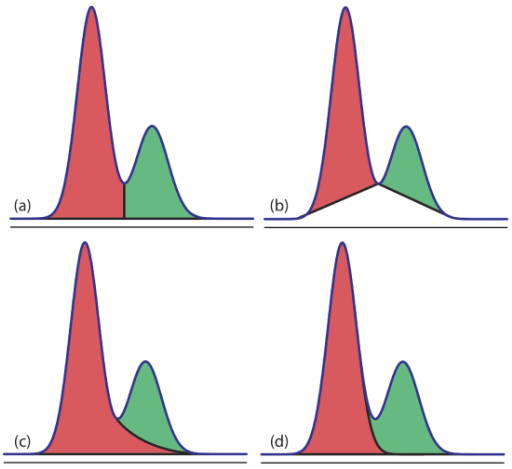


Figure 12.4.15 . Four methods for determining the areas under two overlapping chromatographic peaks: (a) the drop method; (b) the valley method; (c) the exponential skim method; and (d) the Gaussian skim method. Other methods for determining areas also are available.

For quantitative work we need to establish a calibration curve that relates the detector's response to the analyte's concentration. If the injection volume is identical for every standard and sample, then an external standardization provides both accurate and precise results. Unfortunately,even under the best conditions the relative precision for replicate injections may differ by 5%; often it is substantially worse. For quantitative work that requires high accuracy and precision, the use of internal standards is recommended.

To review the method of internal standards, see Chapter 5.3.

Example 12.4.1

Marriott and Carpenter report the following data for five replicate injections of a mixture that contains 1% v/v methyl isobutyl ketone and 1% v/v *p*-xylene in dichloromethane [Marriott, P. J.; Carpenter, P. D. *J. Chem. Educ.* **1996**, *73*, 96–99].

injection	peak	peak area (arb. units)
I	1	48075
	2	78112
II	1	85829
	2	135404
III	1	84136
	2	132332
IV	1	71681
	2	112889
V	1	58054
	2	91287

Assume that *p*-xylene (peak 2) is the analyte, and that methyl isobutyl ketone (peak 1) is the internal standard. Determine the 95% confidence interval for a single-point standardization with and without using the internal standard.

Solution

For a single-point external standardization we ignore the internal standard and determine the relationship between the peak area for *p*-xylene, A_2, and the concentration, C_2, of *p*-xylene.

$$A_2 = kC_2$$

Substituting the known concentration for *p*-xylene (1% v/v) and the appropriate peak areas, gives the following values for the constant *k*.

$$78112 \quad 135404 \quad 132332 \quad 112889 \quad 91287$$

The average value for *k* is 110 000 with a standard deviation of 25 100 (a relative standard deviation of 22.8%). The 95% confidence interval is

$$\mu = \overline{X} \pm \frac{ts}{\sqrt{n}} = 111000 \pm \frac{(2.78)(25100)}{\sqrt{5}} = 111000 \pm 31200$$

For an internal standardization, the relationship between the analyte's peak area, A_2, the internal standard's peak area, A_1, and their respective concentrations, C_2 and C_1, is

$$\frac{A_2}{A_1} = k\frac{C_2}{C_1}$$

Substituting in the known concentrations and the appropriate peak areas gives the following values for the constant *k*.

$$1.5917 \quad 1.5776 \quad 1.5728 \quad 1.5749 \quad 1.5724$$

The average value for *k* is 1.5779 with a standard deviation of 0.0080 (a relative standard deviation of 0.507%). The 95% confidence interval is

$$\mu = \overline{X} \pm \frac{ts}{\sqrt{n}} = 1.5779 \pm \frac{(2.78)(0.0080)}{\sqrt{5}} = 1.5779 \pm 0.0099$$

Although there is a substantial variation in the individual peak areas for this set of replicate injections, the internal standard compensates for these variations, providing a more accurate and precise calibration.

? Exercise 12.4.1

Figure 12.4.16 shows chromatograms for five standards and for one sample. Each standard and sample contains the same concentration of an internal standard, which is 2.50 mg/mL. For the five standards, the concentrations of analyte are 0.20 mg/mL, 0.40 mg/mL, 0.60 mg/mL, 0.80 mg/mL, and 1.00 mg/mL, respectively. Determine the concentration of analyte in the sample by (a) ignoring the internal standards and creating an external standards calibration curve, and by (b) creating an internal standard calibration curve. For each approach, report the analyte's concentration and the 95% confidence interval. Use peak heights instead of peak areas.

Answer

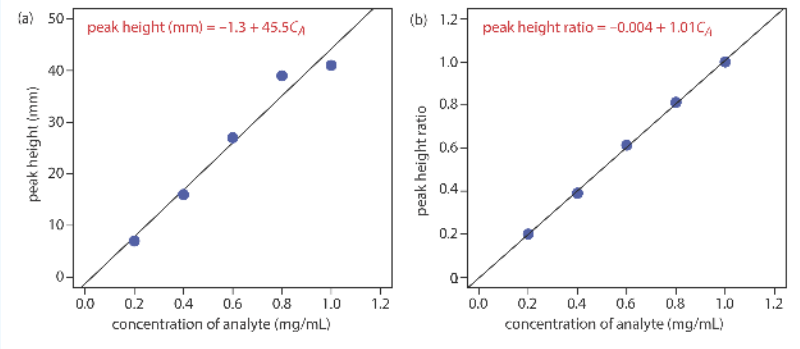
The following table summarizes my measurements of the peak heights for each standard and the sample, and their ratio (although your absolute values for peak heights will differ from mine, depending on the size of your monitor or printout, your relative peak height ratios should be similar to mine).

[standard] (mg/mL)	peak height of standard (mm)	peak height of analyte (mm)	peak height ratio
0.20	35	7	0.20
0.40	41	16	0.39
0.60	44	27	0.61
0.80	48	39	0.81
1.00	41	41	1.00
sample	39	21	0.54

Figure (a) shows the calibration curve and the calibration equation when we ignore the internal standard. Substituting the sample's peak height into the calibration equation gives the analyte's concentration in the sample as 0.49 mg/mL. The 95% confidence interval is ±0.24 mg/mL. The calibration curve shows quite a bit of scatter in the data because of uncertainty in the injection volumes.

Figure (b) shows the calibration curve and the calibration equation when we include the internal standard. Substituting the sample's peak height ratio into the calibration equation gives the analyte's concentration in the sample as 0.54 mg/mL. The 95% confidence interval is ±0.04 mg/mL.

To review the use of Excel or R for regression calculations and confidence intervals, see Chapter 5.5.



The data for this exercise were created so that the analyte's actual concentration is 0.55 mg/mL. Given the resolution of my ruler's scale, my answer is pretty reasonable. Your measurements may be slightly different, but your answers should be close to the actual values.

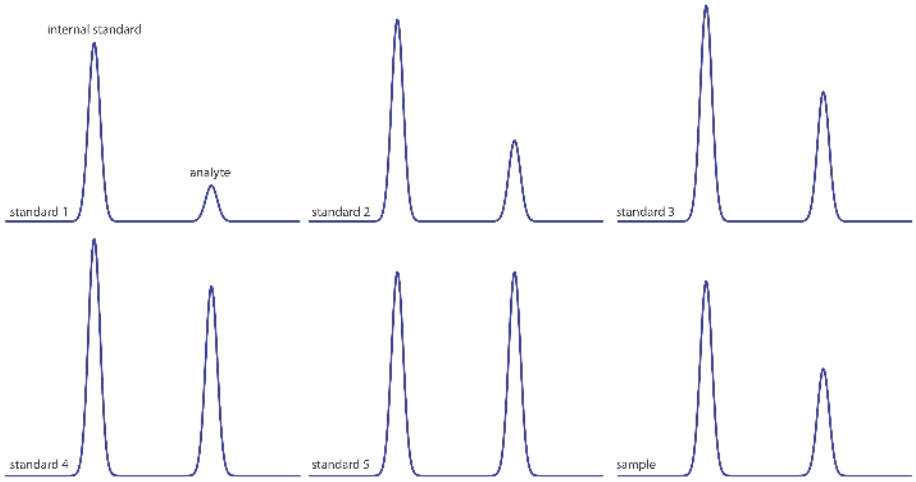


Figure 12.4.16 . Chromatograms for Practice Exercise 12.5.

Qualitative Applications

In addition to a quantitative analysis, we also can use chromatography to identify the components of a mixture. As noted earlier, when using an FT–IR or a mass spectrometer as the detector we have access to the eluent's full spectrum for any retention time. By interpreting the spectrum or by searching against a library of spectra, we can identify the analyte responsible for each chromatographic peak.

> In addition to identifying the component responsible for a particular chromatographic peak, we also can use the saved spectra to evaluate peak purity. If only one component is responsible for a chromatographic peak, then the spectra should be identical throughout the peak's elution. If a spectrum at the beginning of the peak's elution is different from a spectrum taken near the end of the peak's elution, then at least two components are co-eluting.

When using a nonspectroscopic detector, such as a flame ionization detector, we must find another approach if we wish to identify the components of a mixture. One approach is to spike a sample with the suspected compound and look for an increase in peak height. We also can compare a peak's retention time to the retention time for a known compound if we use identical operating conditions.

Because a compound's retention times on two identical columns are not likely to be the same—differences in packing efficiency, for example, will affect a solute's retention time on a packed column—creating a table of standard retention times is not possible. ***Kovat's retention index*** provides one solution to the problem of matching retention times. Under isothermal conditions, the adjusted retention times for normal alkanes increase logarithmically. Kovat defined the retention index, *I*, for a normal alkane as 100 times the number of carbon atoms. For example, the retention index is 400 for butane, C_4H_{10}, and 500 for pentane, C_5H_{12}. To determine the a compound's retention index, I_{cpd}, we use the following formula

$$I_{cpd} = 100 \times \frac{\log t'_{r,cpd} - \log t'_{r,x}}{\log t'_{r,x+1} - \log t'_{r,x}} + I_x \tag{2.4.1}$$

where $t'_{r,cpd}$ is the compound's adjusted retention time, $t'_{r,x}$ and $t'_{r,x+1}$ are the adjusted retention times for the normal alkanes that elute immediately before the compound and immediately after the compound, respectively, and I_x is the retention index for the normal alkane that elutes immediately before the compound. A compound's retention index for a particular set of chromatographic conditions—stationary phase, mobile phase, column type, column length, temperature, etc.—is reasonably consistent from day- to-day and between different columns and instruments.

> Tables of Kovat's retention indices are available; see, for example, the NIST Chemistry Webbook. A search for toluene returns 341 values of *I* for over 20 different stationary phases, and for both packed columns and capillary columns.

Example 12.4.2

In a separation of a mixture of hydrocarbons the following adjusted retention times are measured: 2.23 min for propane, 5.71 min for isobutane, and 6.67 min for butane. What is the Kovat's retention index for each of these hydrocarbons?

Solution

Kovat's retention index for a normal alkane is 100 times the number of carbons; thus, for propane, I = 300 and for butane, I = 400. To find Kovat's retention index for isobutane we use Equation 2.4.1.

$$I_{\text{isobutane}} = 100 \times \frac{\log(5.71) - \log(2.23)}{\log(6.67) - \log(2.23)} + 300 = 386$$

Exercise 12.4.2

When using a column with the same stationary phase as in Example 12.4.2 , you find that the retention times for propane and butane are 4.78 min and 6.86 min, respectively. What is the expected retention time for isobutane?

Answer

Because we are using the same column we can assume that isobutane's retention index of 386 remains unchanged. Using Equation 2.4.1, we have

$$386 = 100 \times \frac{\log x - \log(4.78)}{\log(6.86) - \log(4.78)} + 300$$

where x is the retention time for isobutane. Solving for x, we find that

$$0.86 = \frac{\log x - \log(4.78)}{\log(6.86) - \log(4.78)}$$

$$0.135 = \log x - 0.679$$

$$0.814 = \log x$$

$$x = 6.52$$

the retention time for isobutane is 6.5 min.

The best way to appreciate the theoretical and the practical details discussed in this section is to carefully examine a typical analytical method. Although each method is unique, the following description of the determination of trihalomethanes in drinking water provides an instructive example of a typical procedure. The description here is based on a Method 6232B in *Standard Methods for the Examination of Water and Wastewater*, 20th Ed., American Public Health Association: Washing- ton, DC, 1998.

Representative Method 12.4.1: Determination of Trihalomethanes in Drinking Water

Description of Method

Trihalomethanes, such as chloroform, $CHCl_3$, and bromoform, $CHBr_3$, are found in most chlorinated waters. Because chloroform is a suspected carcinogen, the determination of trihalomethanes in public drinking water supplies is of considerable importance. In this method the trihalomethanes $CHCl_3$, $CHBrCl_2$, $CHBr_2Cl$, and $CHBr_3$ are isolated using a liquid–liquid extraction with pentane and determined using a gas chromatograph equipped with an electron capture detector.

Procedure

Collect the sample in a 40-mL glass vial equipped with a screw-cap lined with a TFE-faced septum. Fill the vial until it overflows, ensuring that there are no air bubbles. Add 25 mg of ascorbic acid as a reducing agent to quench the further production of trihalomethanes. Seal the vial and store the sample at 4^{o}C for no longer than 14 days.

Prepare a standard stock solution for each trihalomethane by placing 9.8 mL of methanol in a 10-mL volumetric flask. Let the flask stand for 10 min, or until all surfaces wetted with methanol are dry. Weigh the flask to the nearest ±0.1 mg. Using a 100-µL syringe, add 2 or more drops of trihalomethane to the volumetric flask, allowing each drop to fall directly into the methanol. Reweigh the flask before diluting to volume and mixing. Transfer the solution to a 40-mL glass vial equipped with a TFE-lined screw-top and report the concentration in µg/mL. Store the stock solutions at –10 to –20°C and away from the light.

Prepare a multicomponent working standard from the stock standards by making appropriate dilutions of the stock solution with methanol in a volumetric flask. Choose concentrations so that calibration standards (see below) require no more than 20 µL of working standard per 100 mL of water.

Using the multicomponent working standard, prepare at least three, but preferably 5–7 calibration standards. At least one standard must be near the detection limit and the standards must bracket the expected concentration of trihalomethanes in the samples. Using an appropriate volumetric flask, prepare the standards by injecting at least 10 µL of the working standard below the surface of the water and dilute to volume. Gently mix each standard three times only. Discard the solution in the neck of the volumetric flask and then transfer the remaining solution to a 40-mL glass vial with a TFE-lined screw-top. If the standard has a headspace, it must be analyzed within 1 hr; standards without a headspace may be held for up to 24 hr.

Prepare an internal standard by dissolving 1,2-dibromopentane in hexane. Add a sufficient amount of this solution to pentane to give a final concentration of 30 µg 1,2-dibromopentane/L.

To prepare the calibration standards and samples for analysis, open the screw top vial and remove 5 mL of the solution. Recap the vial and weigh to the nearest ±0.1 mg. Add 2.00 mL of pentane (with the internal standard) to each vial and shake vigorously for 1 min. Allow the two phases to separate for 2 min and then use a glass pipet to transfer at least 1 mL of the pentane (the upper phase) to a 1.8-mL screw top sample vial equipped with a TFE septum, and store at 4°C until you are ready to inject them into the GC. After emptying, rinsing, and drying the sample's original vial, weigh it to the nearest ±0.1 mg and calculate the sample's weight to ±0.1 g. If the density is 1.0 g/mL, then the sample's weight is equivalent to its volume.

Inject a 1–5 µL aliquot of the pentane extracts into a GC equipped with a 2-mm ID, 2-m long glass column packed with a stationary phase of 10% squalane on a packing material of 80/100 mesh Chromosorb WAW. Operate the column at 67°C and a flow rate of 25 mL/min.

> A variety of other columns can be used. Another option, for example, is a 30-m fused silica column with an internal diameter of 0.32 mm and a 1 µm coating of the stationary phase DB-1. A linear flow rate of 20 cm/s is used with the following temperature program: hold for 5 min at 35°C; increase to 70°C at 10°C/min; increase to 200°C at 20°C/min.

Questions

1. A simple liquid–liquid extraction rarely extracts 100% of the analyte. How does this method account for incomplete extractions?

   Because we use the same extraction procedure for the samples and the standards, we reasonably expect that the extraction efficiency is the same for all samples and standards; thus, the relative amount of analyte in any two samples or standards is unaffected by an incomplete extraction.

2. Water samples are likely to contain trace amounts of other organic compounds, many of which will extract into pentane along with the trihalomethanes. A short, packed column, such as the one used in this method, generally does not do a particularly good job of resolving chromatographic peaks. Why do we not need to worry about these other compounds?

   An electron capture detector responds only to compounds, such as the trihalomethanes, that have electronegative functional groups. Because an electron capture detector will not respond to most of the potential interfering compounds, the chromatogram will have relatively few peaks other than those for the trihalomethanes and the internal standard.

3. Predict the order in which the four analytes elute from the GC column.

   Retention time should follow the compound's boiling points, eluting from the lowest boiling point to the highest boiling points. The expected elution order is $CHCl_3$ (61.2°C), $CHCl_2Br$ (90°C), $CHClBr_2$ (119°C), and $CHBr_3$ (149.1°C).

4. Although chloroform is an analyte, it also is an interferent because it is present at trace levels in the air. Any chloroform present in the laboratory air, for example, may enter the sample by diffusing through the sample vial's silicon septum. How can we determine whether samples are contaminated in this manner?

> A sample blank of trihalomethane-free water is kept with the samples at all times. If the sample blank shows no evidence for chloroform, then we can safely assume that the samples also are free from contamination.

5. Why is it necessary to collect samples without a headspace (a layer of air that overlays the liquid) in the sample vial?

> Because trihalomethanes are volatile, the presence of a headspace allows for the loss of analyte from the sample to the headspace, resulting in a negative determinate error.

6. In preparing the stock solution for each trihalomethane, the procedure specifies that we add two or more drops of the pure compound by dropping them into a volumetric flask that contains methanol. When preparing the calibration standards, however, the working standard must be injected below the surface of the methanol. Explain the reason for this difference.

> When preparing a stock solution, the potential loss of the volatile trihalomethane is unimportant because we determine its concentration by weight after adding it to the methanol and diluting to volume. When we prepare the calibration standard, however, we must ensure that the addition of trihalomethane is quantitative; thus, we inject it below the surface to avoid the potential loss of analyte.

Evaluation

Scale of Operation

Gas chromatography is used to analyze analytes present at levels ranging from major to ultratrace components. Depending on the detector, samples with major and minor analytes may need to be diluted before analysis. The thermal conductivity and flame ionization detectors can handle larger amounts of analyte; other detectors, such as an electron capture detector or a mass spectrometer, require substantially smaller amounts of analyte. Although the injection volume for gas chromatography is quite small—typically about a microliter—the amount of available sample must be sufficient that the injection is a representative subsample. For a trace analyte, the actual amount of injected analyte is often in the picogram range. Using Representative Method 12.4.1 as an example, a 3.0-μL injection of 1 μg/L $CHCl_3$ is equivalent to 15 pg of $CHCl_3$, assuming a 100% extraction efficiency.

Accuracy

The accuracy of a gas chromatographic method varies substantially from sample-to-sample. For routine samples, accuracies of 1–5% are common. For analytes present at very low concentration levels, for samples with complex matrices, or for samples that require significant processing before analysis, accuracy may be substantially poorer. In the analysis for trihalomethanes described in Representative Method 12.4.1, for example, determinate errors as large as ±25% are possible.

Precision

The precision of a gas chromatographic analysis includes contributions from sampling, sample preparation, and the instrument. The relative standard deviation due to the instrument typically is 1–5%, although it can be significantly higher. The principal limitations are detector noise, which affects the determination of peak area, and the reproducibility of injection volumes. In quantitative work, the use of an internal standard compensates for any variability in injection volumes.

Sensitivity

In a gas chromatographic analysis, sensitivity is determined by the detector's characteristics. Of particular importance for quantitative work is the detector's linear range; that is, the range of concentrations over which a calibration curve is linear. Detectors with a wide linear range, such as the thermal conductivity detector and the flame ionization detector, can be used to analyze samples over a wide range of concentrations without adjusting operating conditions. Other detectors, such as the electron capture detector, have a much narrower linear range.

Selectivity

Because it combines separation with analysis, chromatographic methods provide excellent selectivity. By adjusting conditions it usually is possible to design a separation so that the analytes elute by themselves, even when the mixture is complex. Additional

selectivity is obtained by using a detector, such as the electron capture detector, that does not respond to all compounds.

Time, Cost, and Equipment

Analysis time can vary from several minutes for samples that contain only a few constituents, to more than an hour for more complex samples. Preliminary sample preparation may substantially increase the analysis time. Instrumentation for gas chromatography ranges in price from inexpensive (a few thousand dollars) to expensive (>$50,000). The more expensive models are designed for capillary columns, include a variety of injection options, and use more sophisticated detectors, such as a mass spectrometer, or include multiple detectors. Packed columns typically cost <$200, and the cost of a capillary column is typically $300–$1000.

This page titled 2.4: Gas Chromatography is shared under a CC BY-NC-SA 4.0 license and was authored, remixed, and/or curated by David Harvey.

- **12.4: Gas Chromatography** by David Harvey is licensed CC BY-NC-SA 4.0.

2.5: High-Performance Liquid Chromatography

In ***high-performance liquid chromatography*** (HPLC) we inject the sample, which is in solution form, into a liquid mobile phase. The mobile phase carries the sample through a packed or capillary column that separates the sample's components based on their ability to partition between the mobile phase and the stationary phase. Figure 12.5.1 shows an example of a typical HPLC instrument, which has several key components: reservoirs that store the mobile phase; a pump for pushing the mobile phase through the system; an injector for introducing the sample; a column for separating the sample into its component parts; and a detector for monitoring the eluent as it comes off the column. Let's consider each of these components.

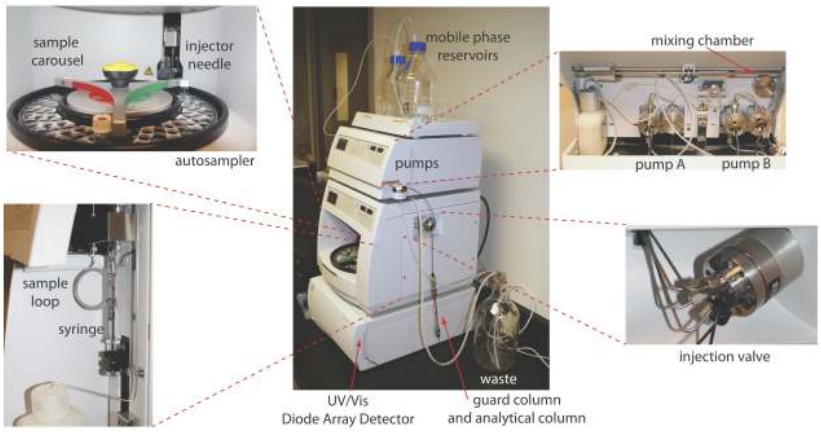


Figure 12.5.1 . Example of a typical high-performance liquid chromatograph with insets showing the pumps that move the mobile phase through the system and the plumbing used to inject the sample into the mobile phase. This particular instrument includes an autosampler. An instrument in which samples are injected manually does not include the features shown in the two left-most insets, and has a different style of loop injection valve.

A solute's retention time in HPLC is determined by its interaction with the stationary phase and the mobile phase. There are several different types of solute/stationary phase interactions, including liquid–solid adsorption, liquid–liquid partitioning, ion-exchange, and size-exclusion. This chapter deals exclusively with HPLC separations based on liquid–liquid partitioning. Other forms of liquid chromatography receive consideration in Chapter 12.6.

HPLC Columns

An HPLC typically includes two columns: an analytical column, which is responsible for the separation, and a guard column that is placed before the analytical column to protect it from contamination.

Analytical Columns

The most common type of HPLC column is a stainless steel tube with an internal diameter between 2.1 mm and 4.6 mm and a length between 30 mm and 300 mm (Figure 12.5.2). The column is packed with 3–10 μm porous silica particles with either an irregular or a spherical shape. Typical column efficiencies are 40000–60000 theoretical plates/m. Assuming a V_{max}/V_{min} of approximately 50, a 25-cm column with 50 000 plates/m has 12 500 theoretical plates and a peak capacity of 110.



Figure 12.5.2 . Typical packed column for HPLC. This particular column has an internal diameter of 4.6 mm and a length of 150 mm, and is packed with 5 μm particles coated with stationary phase.

Capillary columns use less solvent and, because the sample is diluted to a lesser extent, produce larger signals at the detector. These columns are made from fused silica capillaries with internal diameters from 44–200 μm and lengths of 50–250 mm. Capillary columns packed with 3–5 μm particles have been prepared with column efficiencies of up to 250 000 theoretical plates [Novotony, M. *Science*, **1989**, *246*, 51–57].

One limitation to a packed capillary column is the back pressure that develops when pumping the mobile phase through the small interstitial spaces between the particulate micron-sized packing material (Figure 12.5.3). Because the tubing and fittings that carry the mobile phase have pressure limits, a higher back pressure requires a lower flow rate and a longer analysis time. Monolithic columns, in which the solid support is a single, porous rod, offer column efficiencies equivalent to a packed capillary column while allowing for faster flow rates. A monolithic column—which usually is similar in size to a conventional packed column, although smaller, capillary columns also are available—is prepared by forming the mono- lithic rod in a mold and covering it with PTFE tubing or a polymer resin. Monolithic rods made of a silica-gel polymer typically have macropores with diameters of approximately 2 μm and mesopores—pores within the macropores—with diameters of approximately 13 nm [Cabrera, K. Chromatography Online, April 1, 2008].

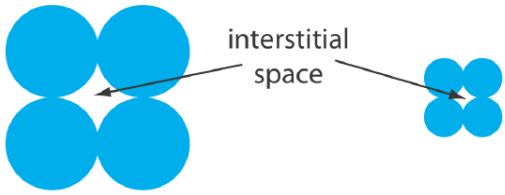


Figure 12.5.3 . The packing of smaller particles creates smaller interstitial spaces than the packing of larger particles. Although reducing particle size by **2×** increases efficiency by a factor of 1.4, it also produces a 4-fold increase in back pressure.

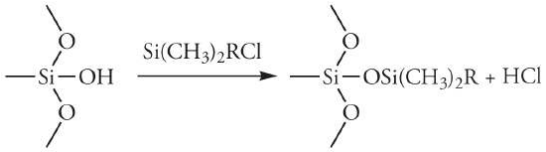
Guard Columns

Two problems tend to shorten the lifetime of an analytical column. First, solutes that bind irreversibly to the stationary phase degrade the column's performance by decreasing the amount of stationary phase available for effecting a separation. Second, particulate material injected with the sample may clog the analytical column. To minimize these problems we place a guard column before the analytical column. A Guard column usually contains the same particulate packing material and stationary phase as the analytical column, but is significantly shorter and less expensive—a length of 7.5 mm and a cost one-tenth of that for the corresponding analytical column is typical. Because they are intended to be sacrificial, guard columns are replaced regularly.

> If you look closely at Figure 12.5.1 , you will see the small guard column just above the analytical column.

Stationary Phases for Liquid-Liquid Chromatography

In liquid–liquid chromatography the stationary phase is a liquid film coated on a packing material, typically 3–10 μm porous silica particles. Because the stationary phase may be partially soluble in the mobile phase, it may elute, or bleed from the column over time. To prevent the loss of stationary phase, which shortens the column's lifetime, it is bound covalently to the silica particles. ***Bonded stationary phases*** are created by reacting the silica particles with an organochlorosilane of the general form $Si(CH_3)_2RCl$, where R is an alkyl or substituted alkyl group.



To prevent unwanted interactions between the solutes and any remaining –SiOH groups, $Si(CH_3)_3Cl$ is used to convert unreacted sites to $-SiOSi(CH_3)_3$; such columns are designated as end-capped.

The properties of a stationary phase depend on the organosilane's alkyl group. If R is a polar functional group, then the stationary phase is polar. Examples of polar stationary phases include those where R contains a cyano ($-C_2H_4CN$), a diol ($-C_3H_6OCH_2CHOHCH_2OH$), or an amino ($-C_3H_6NH_2$) functional group. Because the stationary phase is polar, the mobile phase is a nonpolar or a moderately polar solvent. The combination of a polar stationary phase and a nonpolar mobile phase is called ***normal-phase chromatography***.

In ***reversed-phase chromatography***, which is the more common form of HPLC, the stationary phase is nonpolar and the mobile phase is polar. The most common nonpolar stationary phases use an organochlorosilane where the R group is an *n*-octyl (C_8) or *n*-

octyldecyl (C_{18}) hydrocarbon chain. Most reversed-phase separations are carried out using a buffered aqueous solution as a polar mobile phase, or using other polar solvents, such as methanol and acetonitrile. Because the silica substrate may undergo hydrolysis in basic solutions, the pH of the mobile phase must be less than 7.5.

> It seems odd that the more common form of liquid chromatography is identified as reverse-phase instead of normal phase. You might recall that one of the earliest examples of chromatography was Mikhail Tswett's separation of plant pigments using a polar column of calcium carbonate and a nonpolar mobile phase of petroleum ether. The assignment of normal and reversed, therefore, is all about precedence.

Mobile Phases

The elution order of solutes in HPLC is governed by polarity. For a normal-phase separation, a solute of lower polarity spends proportionally less time in the polar stationary phase and elutes before a solute that is more polar. Given a particular stationary phase, retention times in normal-phase HPLC are controlled by adjusting the mobile phase's properties. For example, if the resolution between two solutes is poor, switching to a less polar mobile phase keeps the solutes on the column for a longer time and provides more opportunity for their separation. In reversed-phase HPLC the order of elution is the opposite that in a normal-phase separation, with more polar solutes eluting first. Increasing the polarity of the mobile phase leads to longer retention times. Shorter retention times require a mobile phase of lower polarity.

Choosing a Mobile Phase: Using the Polarity Index

There are several indices that help in selecting a mobile phase, one of which is the polarity index [Snyder, L. R.; Glajch, J. L.; Kirkland, J. J. *Practical HPLC Method Development*, Wiley-Inter- science: New York, 1988]. Table 12.5.1 provides values of the polarity index, P', for several common mobile phases, where larger values of P' correspond to more polar solvents. Mixing together two or more mobile phases—assuming they are miscible—creates a mobile phase of intermediate polarity. For example, a binary mobile phase made by combining solvent *A* and solvent *B* has a polarity index, P'_{AB}, of

$$P'_{AB} = \Phi_A P'_A + \Phi_B P'_B \tag{2.5.1}$$

where P'_A and P'_B are the polarity indices for solvents *A* and *B*, and Φ_A and Φ_B are the volume fractions for the two solvents.

Table 12.5.1 . Properties of HPLC Mobile Phases

mobile phase	polarity index (P')	UV cutoff (nm)
cyclohexane	0.04	210
n-hexane	0.1	210
carbon tetrachloride	1.6	265
i-propyl ether	2.4	220
toluene	2.4	286
diethyl ether	2.8	218
tetrahydrofuran	4.0	220
ethanol	4.3	210
ethyl acetate	4.4	255
dioxane	4.8	215
methanol	5.1	210
acetonitrile	5.8	190
water	10.2	—

Example 12.5.1

A reversed-phase HPLC separation is carried out using a mobile phase of 60% v/v water and 40% v/v methanol. What is the mobile phase's polarity index?

Solution

Using Equation 2.5.1 and the values in Table 12.5.1 , the polarity index for a 60:40 water–methanol mixture is

$$P'_{AB} = \Phi_{\text{water}} P'_{\text{water}} + \Phi_{\text{methanol}} P'_{\text{methanol}}$$

$$P'_{AB} = 0.60 \times 10.2 + 0.40 \times 5.1 = 8.2$$

Exercise 12.5.1

Suppose you need a mobile phase with a polarity index of 7.5. Explain how you can prepare this mobile phase using methanol and water.

Answer

If we let *x* be the fraction of water in the mobile phase, then 1 – *x* is the fraction of methanol. Substituting these values into Equation 2.5.1 and solving for *x*

$$7.5 = 10.2x + 5.1(1 - x)$$

$$7.5 = 10.2x + 5.1 - 5.1x$$

$$2.4 = 5.1x$$

gives *x* as 0.47. The mobile phase is 47% v/v water and 53% v/v methanol.

As a general rule, a two unit change in the polarity index corresponds to an approximately 10-fold change in a solute's retention factor. Here is a simple example. If a solute's retention factor, *k*, is 22 when using water as a mobile phase (P' = 10.2), then switching to a mobile phase of 60:40 water–methanol (P' = 8.2) decreases *k* to approximately 2.2. Note that the retention factor becomes smaller because we are switching from a more polar mobile phase to a less polar mobile phase in a reversed-phase separation.

Choosing a Mobile Phase: Adjusting Selectivity

Changing the mobile phase's polarity index changes a solute's retention factor. As we learned in Chapter 12.3, however, a change in *k* is not an effective way to improve resolution when the initial value of *k* is greater than 10. To effect a better separation between two solutes we must improve the selectivity factor, α. There are two common methods for increasing α: adding a reagent to the mobile phase that reacts with the solutes in a secondary equilibrium reaction or switching to a different mobile phase.

Taking advantage of a secondary equilibrium reaction is a useful strategy for improving a separation [(a) Foley, J. P. *Chromatography*, **1987**, *7*, 118–128; (b) Foley, J. P.; May, W. E. Anal. Chem. 1987, 59, 102–109; (c) Foley, J. P.; May, W. E. Anal. Chem. 1987, 59, 110–115]. Figure 12.3.3, which we considered earlier in this chapter, shows the reversed-phase separation of four weak acids—benzoic acid, terephthalic acid, *p*-aminobenzoic acid, and *p*-hydroxybenzoic acid—on a nonpolar C_{18} column using an aqueous buffer of acetic acid and sodium acetate as the mobile phase. The retention times for these weak acids are shorter when using a less acidic mobile phase because each solute is present in an anionic, weak base form that is less soluble in the nonpolar stationary phase. If the mobile phase's pH is sufficiently acidic, the solutes are present as neutral weak acids that are more soluble in the stationary phase and take longer to elute. Because the weak acid solutes do not have identical pK_a values, the pH of the mobile phase has a different effect on each solute's retention time, allowing us to find the optimum pH for effecting a complete separation of the four solutes.

> Acid–base chemistry is not the only example of a secondary equilibrium reaction. Other examples include ion-pairing, complexation, and the interaction of solutes with micelles. We will consider the last of these in Chapter 12.7 when we discuss

micellar electrokinetic capillary chromatography.

In Example 12.5.1 we learned how to adjust the mobile phase's polarity by blending together two solvents. A polarity index, however, is just a guide, and binary mobile phase mixtures with identical polarity indices may not resolve equally a pair of solutes. Table 12.5.2 , for example, shows retention times for four weak acids in two mobile phases with nearly identical values for P'. Although the order of elution is the same for both mobile phases, each solute's retention time is affected differently by the choice of organic solvent. If we switch from using acetonitrile to tetrahydrofuran, for example, we find that benzoic acid elutes more quickly and that *p*-hydroxybenzoic acid elutes more slowly. Although we can resolve fully these two solutes using mobile phase that is 16% v/v acetonitrile, we cannot resolve them if the mobile phase is 10% tetrahydrofuran.

Table 12.5.2 . Retention Times for Four Weak Acids in Mobile Phases With Similar Polarity Indexes

retention time (min)	16% acetonitrile (CH_3CN) 84% pH 4.11 aqueous buffer (P' = 9.5)	10% tetrahydrofuran (THF) 90% pH 4.11 aqueous buffer (P' = 9.6)
$t_{r,\,BA}$	5.18	4.01
$t_{r,\,PH}$	1.67	2.91
$t_{r,\,PA}$	1.21	1.05
$t_{r,\,TP}$	0.23	0.54

Key: BA is benzoic acid; PH is *p*-hydroxybenzoic acid; PA is *p*-aminobenzoic acid; TP is terephthalic acid
Source: Harvey, D. T.; Byerly, S.; Bowman, A.; Tomlin, J. "Optimization of HPLC and GC Separations Using Re- sponse Surfaces," *J. Chem. Educ.* **1991**, *68*, 162–168.

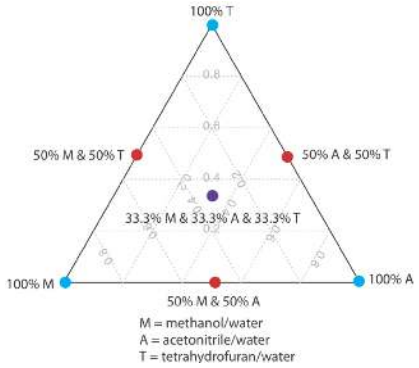


Figure 12.5.4 . Solvent triangle for optimizing a reversed-phase HPLC separation. The three blue circles show mobile phases consisting of an organic solvent and water. The three red circles are binary mobile phases created by combining equal volumes of the pure mobile phases. The ternary mobile phase shown by the purple circle contains all three of the pure mobile phases.

One strategy for finding the best mobile phase is to use the solvent triangle shown in Figure 12.5.4 , which allows us to explore a broad range of mobile phases with only seven experiments. We begin by adjusting the amount of acetonitrile in the mobile phase to produce the best possible separation within the desired analysis time. Next, we use Table 12.5.3 to estimate the composition of methanol/H_2O and tetrahydrofuran/H_2O mobile phases that will produce similar analysis times. Four additional mobile phases are prepared using the binary and ternary mobile phases shown in Figure 12.5.4 . When we examine the chromatograms from these seven mobile phases we may find that one or more provides an adequate separation, or we may identify a region within the solvent triangle where a separation is feasible. Figure 12.5.5 shows a resolution map for the reversed-phase separation of benzoic acid, terephthalic acid, *p*-aminobenzoic acid, and *p*-hydroxybenzoic acid on a nonpolar C_{18} column in which the maximum desired analysis time is set to 6 min [Harvey, D. T.; Byerly, S.; Bowman, A.; Tomlin, J. *J. Chem. Educ.* **1991**, *68*, 162–168]. The areas in blue, green, and red show mobile phase compositions that do not provide baseline resolution. The unshaded area represents mobile phase compositions where a separation is possible.

The choice to start with acetonitrile is arbitrary—we can just as easily choose to begin with methanol or with tetrahydrofuran.

Table 12.5.3 . Composition of Mobile Phases With Approximately Equal Solvent Strengths

%v/v CH_3OH	% v/v CH_3CN	%v/v THF
0	0	0
10	6	4
20	14	10
30	22	16
40	32	24
50	40	30
6	50	36
70	60	44
80	72	52
90	87	62
100	99	71

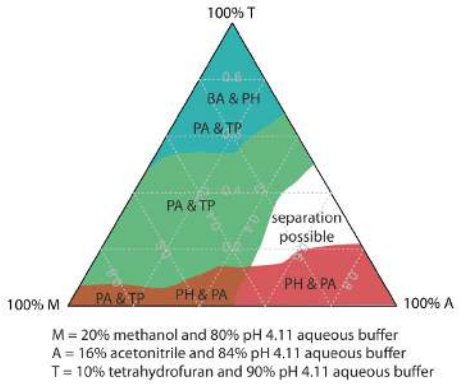


Figure 12.5.5 . Resolution map for the separation of benzoic acid (BA), terephthalic acid (TP), *p*-aminobenzoic acid (PA), and *p*-hydroxybenzoic acid (PH) on a nonpolar C_{18} column subject to a maximum analysis time of 6 min. The shaded areas represent regions where a separation is not possible, with the unresolved solutes identified. A separation is possible in the unshaded area. See Harvey, D. T.; Byerly, S.; Bowman, A.; Tomlin, J. "Optimization of HPLC and GC Separations Using Response Surfaces," *J. Chem. Educ.* **1991**, *68*, 162–168 for details on the mathematical model used to generate the resolution map.

Choosing a Mobile Phase: Isocratic and Gradient Elutions

A separation using a mobile phase that has a fixed composition is an ***isocratic elution***. One difficulty with an isocratic elution is that an appropriate mobile phase strength for resolving early-eluting solutes may lead to unacceptably long retention times for late-eluting solutes. Optimizing the mobile phase for late-eluting solutes, on the other hand, may provide an inadequate separation of early-eluting solutes. Changing the mobile phase's composition as the separation progresses is one solution to this problem. For a reversed-phase separation we use an initial mobile phase that is more polar. As the separation progresses, we adjust the composition of mobile phase so that it becomes less polar (see Figure 12.5.6). Such separations are called ***gradient elutions***.

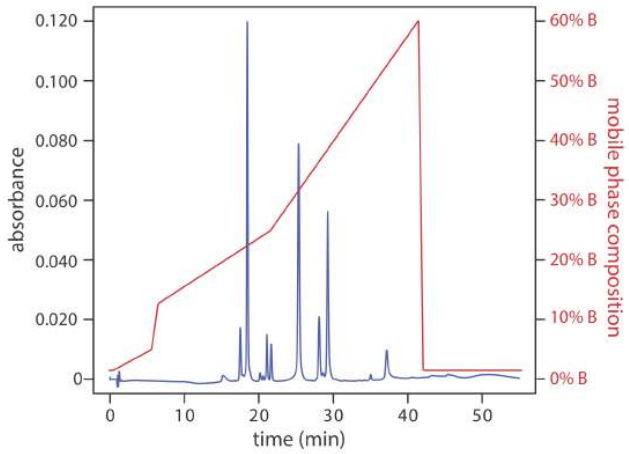


Figure 12.5.6 . Gradient elution separation of a mixture of flavonoids. Mobile phase A is an aqueous solution of 0.1% formic acid and mobile phase B is 0.1% formic acid in acetonitrile. The initial mobile phase is 98% A and 2% B. The percentage of mobile phase B increases in four steps: from 2% to 5% over 5 min, beginning at 0.5 min; from 5% to 12% over 1 min, beginning at 5.5 min; from 12% to 25% over 15 min, beginning at 6.5 min; and from 25% to 60% over 20 min, beginning at 21.5 min. Data provided by Christopher Schardon, Kyle Meinhardt, and Michelle Bushey, Department of Chemistry, Trinty University.

HPLC Plumbing

In a gas chromatograph the pressure from a compressed gas cylinder is sufficient to push the mobile phase through the column. Pushing a liquid mobile phase through a column, however, takes a great deal more effort, generating pressures in excess of several hundred atmospheres. In this section we consider the basic plumbing needed to move the mobile phase through the column and to inject the sample into the mobile phase.

Moving the Mobile Phase

A typical HPLC includes between 1–4 reservoirs for storing mobile phase solvents. The instrument in Figure 12.5.1 , for example, has two mobile phase reservoirs that are used for an isocratic elution or a gradient elution by drawing solvents from one or both reservoirs.

Before using a mobile phase solvent we must remove dissolved gases, such as N_2 and O_2, and small particulate matter, such as dust. Because there is a large drop in pressure across the column—the pressure at the column's entrance is as much as several hundred atmospheres, but it is atmospheric pressure at the column's exit—gases dissolved in the mobile phase are released as gas bubbles that may interfere with the detector's response. Degassing is accomplished in several ways, but the most common are the use of a vacuum pump or sparging with an inert gas, such as He, which has a low solubility in the mobile phase. Particulate materials, which may clog the HPLC tubing or column, are removed by filtering the solvents.

> Bubbling an inert gas through the mobile phase releases volatile dissolved gases. This process is called sparging.

The mobile phase solvents are pulled from their reservoirs by the action of one or more pumps. Figure 12.5.7 shows a close-up view of the pumps for the instrument in Figure 12.5.1 . The working pump and the equilibrating pump each have a piston whose back and forth movement maintains a constant flow rate of up to several mL/min and provides the high output pressure needed to push the mobile phase through the chromatographic column. In this particular instrument, each pump sends its mobile phase to a mixing chamber where they combine to form the final mobile phase. The relative speed of the two pumps determines the mobile phase's final composition.

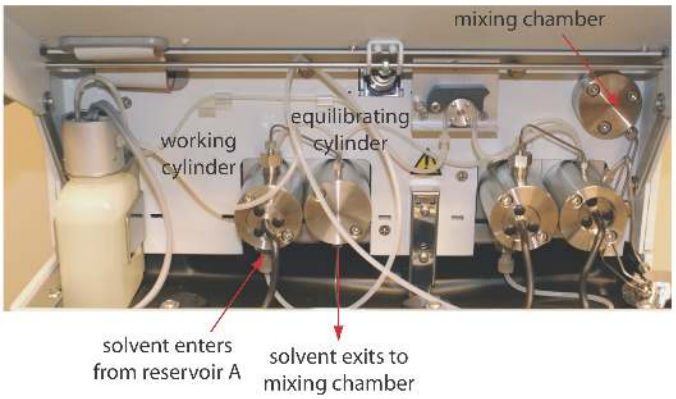


Figure 12.5.7 . Close-up view of the pumps for the instrument shown in Figure 12.5.1 . The working cylinder and the equilibrating cylinder for the pump on the left take solvent from reservoir A and send it to the mixing chamber. The pump on the right moves solvent from reservoir B to the mixing chamber. The mobile phase's flow rate is determined by the combined speeds of the two pumps. By changing the relative speeds of the two pumps, different binary mobile phases can be prepared.

The back and forth movement of a reciprocating pump creates a pulsed flow that contributes noise to the chromatogram. To minimize these pulses, each pump in Figure 12.5.7 has two cylinders. During the working cylinder's forward stoke it fills the equilibrating cylinder and establishes flow through the column. When the working cylinder is on its reverse stroke, the flow is maintained by the piston in the equilibrating cylinder. The result is a pulse-free flow.

There are other possible ways to control the mobile phase's composition and flow rate. For example, instead of the two pumps in Figure 12.5.7 , we can place a solvent proportioning valve before a single pump. The solvent proportioning value connects two or more solvent reservoirs to the pump and determines how much of each solvent is pulled during each of the pump's cycles. Another approach for eliminating a pulsed flow is to include a pulse damper between the pump and the column. A pulse damper is a chamber filled with an easily compressed fluid and a flexible diaphragm. During the piston's forward stroke the fluid in the pulse damper is compressed. When the piston withdraws to refill the pump, pressure from the expanding fluid in the pulse damper maintains the flow rate.

Injecting the Sample

The operating pressure within an HPLC is sufficiently high that we cannot inject the sample into the mobile phase by inserting a syringe through a septum, as is possible in gas chromatography. Instead, we inject the sample using a ***loop injector***, a diagram of which is shown in Figure 12.5.8 . In the load position a sample loop—which is available in a variety of sizes ranging from 0.5 μL to 5 mL—is isolated from the mobile phase and open to the atmosphere. The sample loop is filled using a syringe with a capacity several times that of the sample loop, with excess sample exiting through the waste line. After loading the sample, the injector is turned to the inject position, which redirects the mobile phase through the sample loop and onto the column.

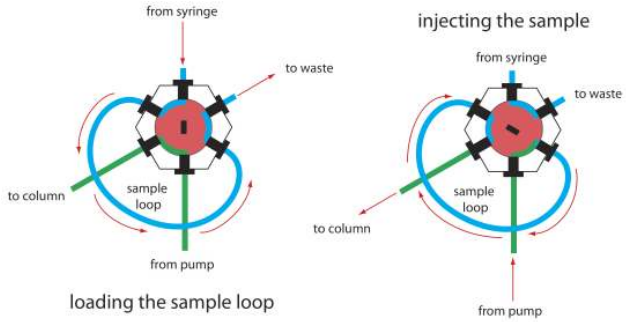


Figure 12.5.8 . Schematic diagram of a manual loop injector. In the load position the flow of mobile phase from the pump to the column (shown in green) is isolated from the sample loop, which is filled using a syringe (shown in blue). Rotating the inner valve (shown in red) to the inject position directs the mobile phase through the sample loop and onto the column.

The instrument in Figure 12.5.1 uses an autosampler to inject samples. Instead of using a syringe to push the sample into the sample loop, the syringe draws sample into the sample loop.

Detectors for HPLC

Many different types of detectors have been use to monitor HPLC separations, most of which use the spectroscopic techniques from Chapter 10 or the electrochemical techniques from Chapter 11.

Spectroscopic Detectors

The most popular HPLC detectors take advantage of an analyte's UV/Vis absorption spectrum. These detectors range from simple designs, in which the analytical wavelength is selected using appropriate filters, to a modified spectrophotometer in which the sample compartment includes a flow cell. Figure 12.5.9 shows the design of a typical flow cell when using a diode array spectrometer as the detector. The flow cell has a volume of 1–10 μL and a path length of 0.2–1 cm.

To review the details of how we measure absorbance, see Chapter 10.2. More information about different types of instruments, including the diode array spectrometer, is in Chapter 10.3.

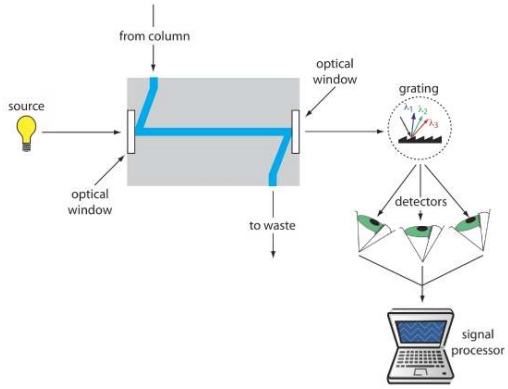


Figure 12.5.9 . Schematic diagram of a flow cell for a detector equipped with a diode array spectrometer.

When using a UV/Vis detector the resulting chromatogram is a plot of absorbance as a function of elution time (see Figure 12.5.10). If the detector is a diode array spectrometer, then we also can display the result as a three-dimensional chromatogram that shows absorbance as a function of wavelength and elution time. One limitation to using absorbance is that the mobile phase cannot absorb at the wavelengths we wish to monitor. Table 12.5.1 lists the minimum useful UV wavelength for several common HPLC solvents. Absorbance detectors provide detection limits of as little as 100 pg–1 ng of injected analyte.

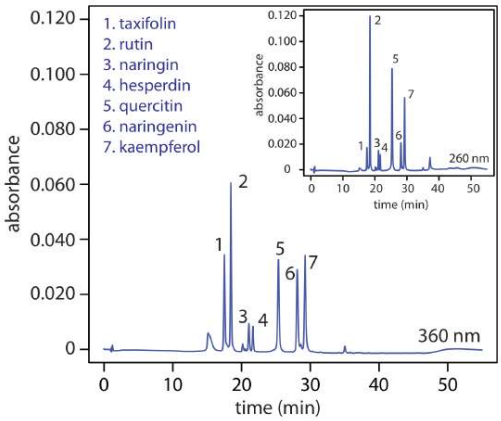


Figure 12.5.10 . HPLC separation of a mixture of flavonoids with UV/Vis detection at 360 nm and, in the inset, at 260 nm. The choice of wavelength affects each analyte's signal. By carefully choosing the wavelength, we can enhance the signal for the analytes of greatest interest. Data provided by Christopher Schardon, Kyle Meinhardt, and Michelle Bushey, Department of Chemistry, Trinty University.

If an analyte is fluorescent, we can place the flow cell in a spectrofluorimeter. As shown in Figure 12.5.11 , a fluorescence detector provides additional selectivity because only a few of a sample's components are fluorescent. Detection limits are as little as 1–10 pg of injected analyte.

> See Chapter 10.6 for a review of fluorescence spectroscopy and spectrofluorimeters.

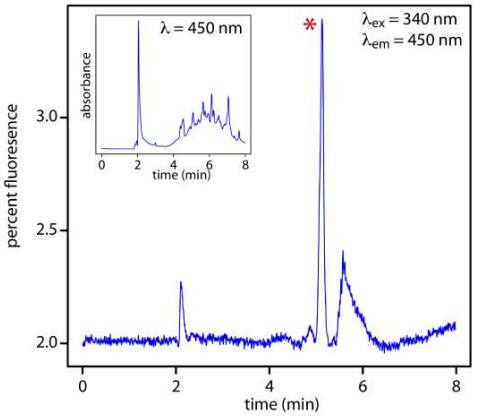


Figure 12.5.11 . HPLC chromatogram for the determination of riboflavin in urine using fluorescence detection with exci-tation at a wavelength of 340 nm and detection at 450 nm. The peak corresponding to riboflavin is marked with a red asterisk (*). The inset shows the same chromatogram when using a less-selective UV/Vis detector at a wavelength of 450 nm. Data provided by Jason Schultz, Jonna Berry, Kaelene Lundstrom, and Dwight Stoll, Department of Chemistry, Gustavus Adolphus College.

Electrochemical Detectors

Another common group of HPLC detectors are those based on electrochemical measurements such as amperometry, voltammetry, coulometry, and conductivity. Figure 12.5.12 , for example, shows an amperometric flow cell. Effluent from the column passes over the working electrode—held at a constant potential relative to a downstream reference electrode—that completely oxidizes or reduces the analytes. The current flowing between the working electrode and the auxiliary electrode serves as the analytical signal. Detection limits for amperometric electrochemical detection are from 10 pg–1 ng of injected analyte.

> See Chapter 11.4 for a review of amperometry.

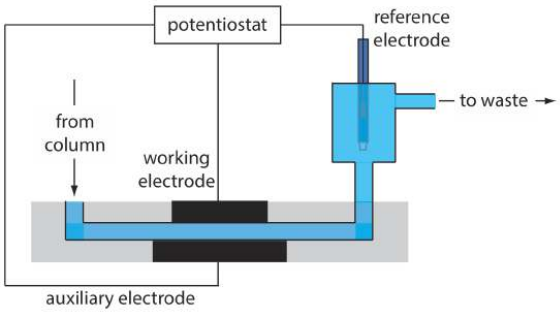


Figure 12.5.12 . Schematic diagram showing a flow cell for an amperometric electrochemical detector.

Other Detectors

Several other detectors have been used in HPLC. Measuring a change in the mobile phase's refractive index is analogous to monitoring the mobile phase's thermal conductivity in gas chromatography. A refractive index detector is nearly universal, responding to almost all compounds, but has a relatively poor detection limit of 0.1–1 μg of injected analyte. An additional limitation of a refractive index detector is that it cannot be used for a gradient elution unless the mobile phase components have identical refractive indexes.

Another useful detector is a mass spectrometer. Figure 12.5.13 shows a block diagram of a typical HPLC–MS instrument. The effluent from the column enters the mass spectrometer's ion source using an interface the removes most of the mobile phase, an essential need because of the incompatibility between the liquid mobile phase and the mass spectrometer's high vacuum environment. In the ionization chamber the remaining molecules—a mixture of the mobile phase components and solutes—undergo ionization and fragmentation. The mass spectrometer's mass analyzer separates the ions by their mass-to-charge ratio (m/z). A detector counts the ions and displays the mass spectrum.

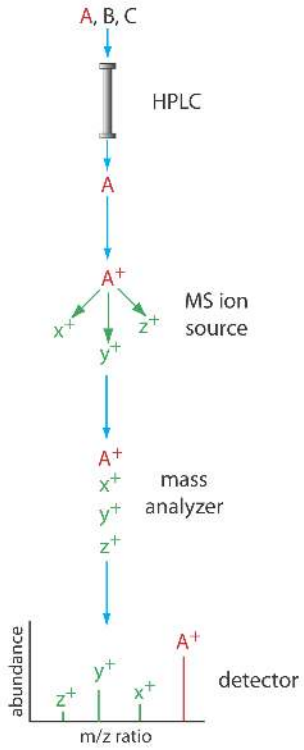


Figure 12.5.13 . Block diagram of an HPLC–MS. A three component mixture enters the HPLC. When component A elutes from the column, it enters the MS ion source and ionizes to form the parent ion and several fragment ions. The ions enter the mass analyzer, which separates them by their mass-to-charge ratio, providing the mass spectrum shown at the detector.

There are several options for monitoring the chromatogram when using a mass spectrometer as the detector. The most common method is to continuously scan the entire mass spectrum and report the total signal for all ions reaching the detector during each scan. This total ion scan provides universal detection for all analytes. As seen in Figure 12.5.14 , we can achieve some degree of selectivity by monitoring only specific mass-to-charge ratios, a process called selective-ion monitoring.

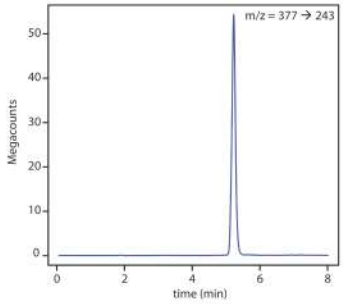


Figure 12.5.14 . HPLC–MS/MS chromatogram for the determination of riboflavin in urine. An initial parent ion with an m/z ratio of 377 enters a second mass spectrometer where it undergoes additional 20 ionization; the fragment ion with an m/z ratio of 243 provides the signal. The selectivity of this detector is evident when you compare this chromatogram to the one in Figure 12.5.11 , which uses fluoresence deterction. Data provided by Jason Schultz, Jonna Berry, Kaelene Lundstrom, and Dwight Stoll, Department of Chemistry, Gustavus Adolphus College.

The advantages of using a mass spectrometer in HPLC are the same as for gas chromatography. Detection limits are very good, typically 0.1–1 ng of injected analyte, with values as low as 1–10 pg for some samples. In addition, a mass spectrometer provides

qualitative, structural information that can help to identify the analytes. The interface between the HPLC and the mass spectrometer is technically more difficult than that in a GC–MS because of the incompatibility of a liquid mobile phase with the mass spectrometer's high vacuum requirement.

> For more details on mass spectrometry see Introduction to Mass Spectrometry by Michael Samide and Olujide Akinbo, a resource that is part of the Analytical Sciences Digital Library.

Quantitative Applications

High-performance liquid chromatography is used routinely for both qualitative and quantitative analyses of environmental, pharmaceutical, industrial, forensic, clinical, and consumer product samples.

Preparing Samples for Analysis

Samples in liquid form are injected into the HPLC after a suitable clean-up to remove any particulate materials, or after a suitable extraction to remove matrix interferents. In determining polyaromatic hydrocarbons (PAH) in wastewater, for example, an extraction with CH_2Cl_2 serves the dual purpose of concentrating the analytes and isolating them from matrix interferents. Solid samples are first dissolved in a suitable solvent or the analytes of interest brought into solution by extraction. For example, an HPLC analysis for the active ingredients and the degradation products in a pharmaceutical tablet often begins by extracting the powdered tablet with a portion of mobile phase. Gas samples are collected by bubbling them through a trap that contains a suitable solvent. Organic isocyanates in industrial atmospheres are collected by bubbling the air through a solution of 1-(2-methoxyphenyl)piperazine in toluene. The reaction between the isocyanates and 1-(2-methoxyphenyl)piperazine both stabilizes them against degradation before the HPLC analysis and converts them to a chemical form that can be monitored by UV absorption.

Quantitative Calculations

A quantitative HPLC analysis is often easier than a quantitative GC analysis because a fixed volume sample loop provides a more precise and accurate injection. As a result, most quantitative HPLC methods do not need an internal standard and, instead, use external standards and a normal calibration curve.

> An internal standard is necessary when using HPLC–MS because the interface between the HPLC and the mass spectrometer does not allow for a reproducible transfer of the column's eluent into the MS's ionization chamber.

Example 12.5.2

The concentration of polynuclear aromatic hydrocarbons (PAH) in soil is determined by first extracting the PAHs with methylene chloride. The extract is diluted, if necessary, and the PAHs separated by HPLC using a UV/Vis or fluorescence detector. Calibration is achieved using one or more external standards. In a typical analysis a 2.013-g sample of dried soil is extracted with 20.00 mL of methylene chloride. After filtering to remove the soil, a 1.00-mL portion of the extract is removed and diluted to 10.00 mL with acetonitrile. Injecting 5 µL of the diluted extract into an HPLC gives a signal of 0.217 (arbitrary units) for the PAH fluoranthene. When 5 µL of a 20.0-ppm fluoranthene standard is analyzed using the same conditions, a signal of 0.258 is measured. Report the parts per million of fluoranthene in the soil.

Solution

For a single-point external standard, the relationship between the signal, S, and the concentration, C, of fluoranthene is

$$S = kC$$

Substituting in values for the standard's signal and concentration gives the value of k as

$$k = \frac{S}{C} = \frac{0.258}{20.0 \text{ ppm}} = 0.0129 \text{ ppm}^{-1}$$

Using this value for k and the sample's HPLC signal gives a fluoranthene concentration of

$$C = \frac{S}{k} = \frac{0.217}{0.0129\ \text{ppm}^{-1}} = 16.8\ \text{ppm}$$

for the extracted and diluted soil sample. The concentration of fluoranthene in the soil is

$$\frac{16.8\ \text{g/mL} \times \frac{10.00\ \text{mL}}{1.00\ \text{mL}} \times 20.00\ \text{mL}}{2.013\ \text{g sample}} = 1670\ \text{ppm fluoranthene}$$

Exercise 12.5.2

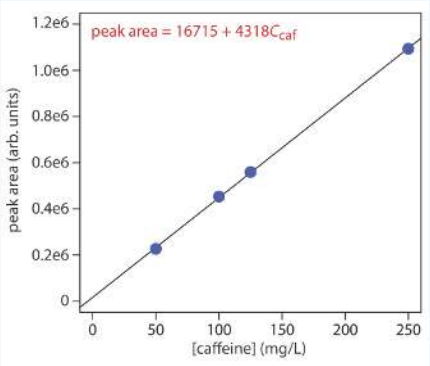
The concentration of caffeine in beverages is determined by a reversed-phase HPLC separation using a mobile phase of 20% acetonitrile and 80% water, and using a nonpolar C_8 column. Results for a series of 10-µL injections of caffeine standards are in the following table.

[caffeine] (mg/L)	peak area (arb. units)
50.0	226724
100.0	453762
125.0	559443
250.0	1093637

What is the concentration of caffeine in a sample if a 10-µL injection gives a peak area of 424195? The data in this problem comes from Kusch, P.; Knupp, G. "Simultaneous Determination of Caffeine in Cola Drinks and Other Beverages by Reversed-Phase HPTLC and Reversed-Phase HPLC," *Chem. Educator*, **2003**, *8*, 201–205.

Answer

The figure below shows the calibration curve and calibration equation for the set of external standards. Substituting the sample's peak area into the calibration equation gives the concentration of caffeine in the sample as 94.4 mg/L.



The best way to appreciate the theoretical and the practical details discussed in this section is to carefully examine a typical analytical method. Although each method is unique, the following description of the determination of fluoxetine in serum provides an instructive example of a typical procedure. The description here is based on Smyth, W. F. *Analytical Chemistry of Complex Matricies*, Wiley Teubner: Chichester, England, 1996, pp. 187–189.

Representative Method 12.5.1: Determination of Fluoxetine in Serum

Description of Method

Fluoxetine is another name for the antidepressant drug Prozac. The determination of fluoxetine in serum is an important part of monitoring its therapeutic use. The analysis is complicated by the complex matrix of serum samples. A solid-phase extraction

followed by an HPLC analysis using a fluorescence detector provides the necessary selectivity and detection limits.

Procedure

Add a known amount of the antidepressant protriptyline, which serves as an internal standard, to each serum sample and to each external standard. To remove matrix interferents, pass a 0.5-mL aliquot of each serum sample or standard through a C_{18} solid-phase extraction cartridge. After washing the cartridge to remove the interferents, elute the remaining constituents, including the analyte and the internal standard, by washing the cartridge with 0.25 mL of a 25:75 v/v mixture of 0.1 M $HClO_4$ and acetonitrile. Inject a 20-µL aliquot onto a 15-cm × 4.6-mm column packed with a 5 µm C_8-bonded stationary phase. The isocratic mobile phase is 37.5:62.5 v/v acetonitrile and water (that contains 1.5 g of tetramethylammonium perchlorate and 0.1 mL of 70% v/v $HClO_4$). Monitor the chromatogram using a fluorescence detector set to an excitation wave- length of 235 nm and an emission wavelength of 310 nm.

Questions

1. The solid-phase extraction is important because it removes constitutions in the serum that might interfere with the analysis. What types of interferences are possible?

> Blood serum, which is a complex mixture of compounds, is approximately 92% water, 6–8% soluble proteins, and less than 1% each of various salts, lipids, and glucose. A direct injection of serum is not advisable for three reasons. First, any particulate materials in the serum will clog the column and restrict the flow of mobile phase. Second, some of the compounds in the serum may absorb too strongly to the stationary phase, degrading the column's performance. Finally, although an HPLC can separate and analyze complex mixtures, an analysis is difficult if the number of constituents exceeds the column's peak capacity.

2. One advantage of an HPLC analysis is that a loop injector often eliminates the need for an internal standard. Why is an internal standard used in this analysis? What assumption(s) must we make when using the internal standard?

> An internal standard is necessary because of uncertainties introduced during the solid-phase extraction. For example, the volume of serum transferred to the solid-phase extraction cartridge, 0.5 mL, and the volume of solvent used to remove the analyte and internal standard, 0.25 mL, are very small. The precision and accuracy with which we can measure these volumes is not as good as when we use larger volumes. For example, if we extract the analyte into a volume of 0.24 mL instead of a volume of 0.25 mL, then the analyte's concentration increases by slightly more than 4%. In addition, the concentration of eluted analytes may vary from trial-to-trial due to variations in the amount of solution held up by the cartridge. Using an internal standard compensates for these variation. To be useful we must assume that the analyte and the internal standard are retained completely during the initial loading, that they are not lost when the cartridge is washed, and that they are extracted completely during the final elution.

3. Why does the procedure monitor fluorescence instead of monitoring UV absorption?

> Fluorescence is a more selective technique for detecting analytes. Many other commonly prescribed antidepressants (and their metabolites) elute with retention times similar to that of fluoxetine. These compounds, however, either do not fluoresce or are only weakly fluorescent.

4. If the peaks for fluoxetine and protriptyline are resolved insufficiently, how might you alter the mobile phase to improve their separation?

> Decreasing the amount of acetonitrile and increasing the amount of water in the mobile will increase retention times, providing more time to effect a separation.

Evaluation

With a few exceptions, the scale of operation, accuracy, precision, sensitivity, selectivity, analysis time, and cost for an HPLC method are similar to GC methods. Injection volumes for an HPLC method usually are larger than for a GC method because HPLC columns have a greater capacity. Because it uses a loop injection, the precision of an HPLC method often is better than a GC method. HPLC is not limited to volatile analytes, which means we can analyze a broader range of compounds. Capillary GC columns, on the other hand, have more theoretical plates, and can separate more complex mixtures.

This page titled 2.5: High-Performance Liquid Chromatography is shared under a CC BY-NC-SA 4.0 license and was authored, remixed, and/or curated by David Harvey.

- **12.5: High-Performance Liquid Chromatography** by David Harvey is licensed CC BY-NC-SA 4.0.

2.5.1: HPLC Simulator

An Excel-based HPLC simulator may be downloaded from the University of Geneva.

2.5.1: HPLC Simulator is shared under a not declared license and was authored, remixed, and/or curated by LibreTexts.

2.5.2: HPLC Method Development

Experimental Design Approach in HPLC Method Development: Application for the Simultaneous Determination of Sacubitril and Valsartan in Presence of Their Impurities and Investigation of Degradation Kinetics. Bahia A. Moussa, Hanaa M. A. Hashem, Marianne A. Mahrouse & Sally T. Mahmoud, *Chromatographia* (2018) 81:139-156. DOI 10.1007/s10337-017-3425-9.

The final publication is available at link.springer.com.

Questions for discussion:

1. Looking at the target analytes, can you predict the order of elution? Why or why not?
2. What is the intended use of the method under development?
3. What is novel about the work described in this paper? Is any specialinstrumentation used?
4. What is "face-centered composite" design? (Look it up.)
5. Why is it important to identify the degradation products? How were they identified?
6. Can you offer any critiques of the work? (Pretend you're a peer reviewer reading the draft.)

2.5.2: HPLC Method Development is shared under a not declared license and was authored, remixed, and/or curated by LibreTexts.

2.6: Other Forms of Chromatography

At the beginning of Section 12.5, we noted that there are several different types of solute/stationary phase interactions in liquid chromatography, but limited our discussion to liquid–liquid chromatography. In this section we turn our attention to liquid chromatography techniques in which partitioning occurs by liquid–solid adsorption, ion-exchange, and size exclusion.

Liquid-Solid Chromatography

In ***liquid–solid adsorption chromatography*** (LSC) the column packing also serves as the stationary phase. In Tswett's original work the stationary phase was finely divided $CaCO_3$, but modern columns employ porous 3–10 μm particles of silica or alumina. Because the stationary phase is polar, the mobile phase usually is a nonpolar or a moderately polar solvent. Typical mobile phases include hexane, isooctane, and methylene chloride. The usual order of elution—from shorter to longer retention times—is

olefins < aromatic hydrocarbons < ethers < esters, aldehydes, ketones < alcohols, amines < amide < carboxylic acids

Nonpolar stationary phases, such as charcoal-based absorbents, also are used. For most samples, liquid–solid chromatography does not offer any special advantages over liquid–liquid chromatography. One exception is the analysis of isomers, where LSC excels.

Ion-Exchange Chromatography

In ***ion-exchange chromatography*** (IEC) the stationary phase is a cross-linked polymer resin, usually divinylbenzene cross-linked polystyrene, with covalently attached ionic functional groups (see Figure 12.6.1 and Table 12.6.1). The counterions to these fixed charges are mobile and are displaced by ions that compete more favorably for the exchange sites. Ion-exchange resins are divided into four categories: strong acid cation exchangers; weak acid cation exchangers; strong base anion exchangers; and weak base anion exchangers.

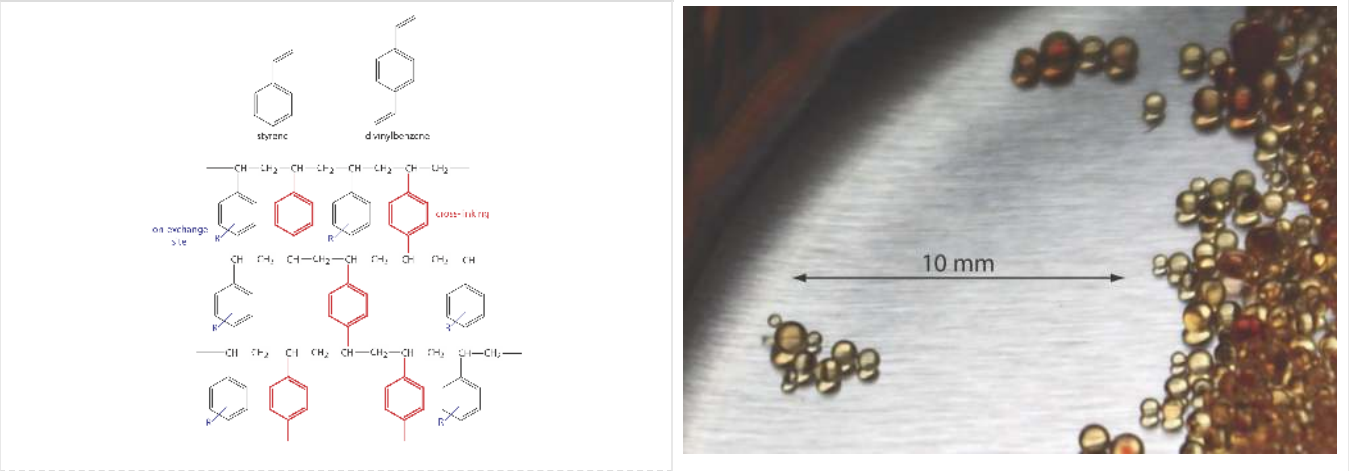


Figure 12.6.1 . Structures of styrene, divinylbenzene, and a styrene–divinylbenzene co-polymer modified for use as an ion-exchange resin are shown on the left. The ion-exchange sites, indicated by R and shown in blue, are mostly in the *para* position and are not necessarily bound to all styrene units. The cross-linking is shown in red. The photo on the right shows an example of the polymer beads. These beads are approximately 0.30–0.85 mm in diameter. Resins for use in ion-exchange chromatography typically are 5–11 μm in diameter.

Table 12.6.1 . Examples of Common Ion-Exchange Resins

type	functional group	examples
strong acid cation exchanger	sulfonic acid	$-SO_3^-$ $-CH_2CH_2SO_3^-$
weak acid cation exchanger	carboxylic acid	$-COO^-$ $-CH_2COO^-$
strong base anion exchanger	quaternary amine	$-CH_2N(CH_3)_3^+$ $-CH_2CH_2N(CH_2CH_3)_3^+$
weak base anion exchanger	amine	$-NH_4^+$ $-CH_2CH_2NH(CH_2CH_3)_3^+$

Strong acid cation exchangers include a sulfonic acid functional group that retains it anionic form—and thus its capacity for ion-exchange—in strongly acidic solutions. The functional groups for a weak acid cation exchanger, on the other hand, are fully protonated at pH levels less then 4 and lose their exchange capacity. The strong base anion exchangers include a quaternary amine, which retains a positive charge even in strongly basic solutions. Weak base anion exchangers remain protonated only at pH levels that are moderately basic. Under more basic conditions a weak base anion exchanger loses a proton and its exchange capacity.

The ion-exchange reaction of a monovalent cation, M^+, exchange site is

$$-SO_3^-H^+(s) + M^+(aq) \rightleftharpoons -SO_3^-M^+(s) + H^+(aq)$$

The equilibrium constant for this ion-exchange reaction, which we call the selectivity coefficient, *K*, is

$$K = \frac{\{-SO_3^-M^+\}\,[H^+]}{\{-SO_3^-H^+\}\,[M^+]} \tag{2.6.1}$$

where we use curly brackets, { }, to indicate a surface concentration instead of a solution concentration.

> We don't usually think about a solid's concentration. There is a good reason for this. In most cases, a solid's concentration is a constant. If you break a piece of chalk into two parts, for example, the mass and the volume of each piece retains the same proportional relationship as in the original piece of chalk. When we consider an ion binding to a reactive site on the solid's surface, however, the fraction of sites that are bound, and thus the concentration of bound sites, can take on any value between 0 and some maximum value that is proportional to the density of reactive sites.

Rearranging Equation 2.6.1 shows us that the distribution ratio, *D*, for the exchange reaction

$$D = \frac{\text{amount of } M^+ \text{ in the stationary phase}}{\text{amount of } M^+ \text{ in the mobile phase}}$$

$$D = \frac{\{-SO_3^-M^+\}}{[M^+]} = K \times \frac{\{-SO_3^-H^+\}}{[H^+]} \tag{2.6.2}$$

is a function of the concentration of H^+ and, therefore, the pH of the mobile phase.

An ion-exchange resin's selectivity is somewhat dependent on whether it includes strong or weak exchange sites and on the extent of cross-linking. The latter is particularly important as it controls the resin's permeability, and, therefore, the accessibility of exchange sites. An approximate order of selectivity for a typical strong acid cation exchange resin, in order of decreasing *D*, is

$$Al^{3+} > Ba^{2+} > Pb^{2+} > Ca^{2+} > Ni^{2+} > Cd^{2+} > Cu^{2+} > Co^{2+} > Zn^{2+} > Mg^{2+} > Ag^+ > K^+ > NH_4^+ > Na^+ > H^+ > Li^+$$

Note that highly charged cations bind more strongly than cations of lower charge, and that for cations of similar charge, those with a smaller hydrated radius (see Table 6.9.1 in Chapter 6), or that are more polarizable, bind more strongly. For a strong base anion exchanger the general elution order is

$$SO_4^{2-} > I^- > HSO_4^- > NO_3^- > Br^- > NO_2^- > Cl^- > HCO_3^- > CH3COO^- > OH^- > F^-$$

Anions of higher charge and of smaller hydrated radius bind more strongly than anions with a lower charge and a larger hydrated radius.

The mobile phase in IEC usually is an aqueous buffer, the pH and ionic composition of which determines a solute's retention time. Gradient elutions are possible in which the mobile phase's ionic strength or pH is changed with time. For example, an IEC separation of cations might use a dilute solution of HCl as the mobile phase. Increasing the concentration of HCl speeds the elution rate for more strongly retained cations because the higher concentration of H^+ allows it to compete more successfully for the ion-exchange sites.

> From Equation 2.6.2, a cation's distribution ratio, *D*, becomes smaller when the concentration of H^+ in the mobile phase increases.

An ion-exchange resin is incorporated into an HPLC column either as 5–11 μm porous polymer beads or by coating the resin on porous silica particles. Columns typically are 250 mm in length with internal diameters ranging from 2–5 mm.

Measuring the conductivity of the mobile phase as it elutes from the column serves as a universal detector for cationic and anionic analytes. Because the mobile phase contains a high concentration of ions—a mobile phase of dilute HCl, for example, contains significant concentrations of H^+ and Cl^-—we need a method for detecting the analytes in the presence of a significant background conductivity.

To minimize the mobile phase's contribution to conductivity, an ***ion-suppressor column*** is placed between the analytical column and the detector. This column selectively removes mobile phase ions without removing solute ions. For example, in cation-exchange chromatography using a dilute solution of HCl as the mobile phase, the suppressor column contains a strong base anion-exchange resin. The exchange reaction

$$H^+(aq) + Cl^-(aq) + \text{Resin}^+OH^-(s) \rightleftharpoons \text{Resin}^+\,Cl^-(s) + H_2O(l)$$

replaces the mobile phase ions H^+ and Cl^- with H_2O. A similar process is used in anion-exchange chromatography where the suppressor column contains a cation-exchange resin. If the mobile phase is a solution of Na_2CO_3, the exchange reaction

$$2Na^+(aq) + CO_3^{2-}(aq) + 2\,\text{Resin}^-\,H^+(s) \rightleftharpoons 2\,\text{Resin}^-\,Na^+(s) + H_2CO_3(aq)$$

replaces a strong electrolyte, Na_2CO_3, with a weak electrolyte, H_2CO_3.

Ion-suppression is necessary when the mobile phase contains a high concentration of ions. ***Single-column ion chromatography***, in which an ion-suppressor column is not needed, is possible if the concentration of ions in the mobile phase is small. Typically the stationary phase is a resin with a low capacity for ion-exchange and the mobile phase is a very dilute solution of methane sulfonic acid for cationic analytes, or potassium benzoate or potassium hydrogen phthalate for anionic analytes. Because the background conductivity is sufficiently small, it is possible to monitor a change in conductivity as the analytes elute from the column.

A UV/Vis absorbance detector can be used if the analytes absorb ultraviolet or visible radiation. Alternatively, we can detect indirectly analytes that do not absorb in the UV/Vis if the mobile phase contains a UV/Vis absorbing species. In this case, when a solute band passes through the detector, a decrease in absorbance is measured at the detector.

Ion-exchange chromatography is an important technique for the analysis of anions and cations in water. For example, an ion-exchange chromatographic analysis for the anions F^-, Cl^-, Br^-, NO_2^-, NO_3^-, PO_4^{3-}, and SO_4^{2-} takes approximately 15 minutes (Figure 12.6.2). A complete analysis of the same set of anions by a combination of potentiometry and spectrophotometry requires 1–2 days. Ion-exchange chromatography also is used for the analysis of proteins, amino acids, sugars, nucleotides, pharmaceuticals, consumer products, and clinical samples.

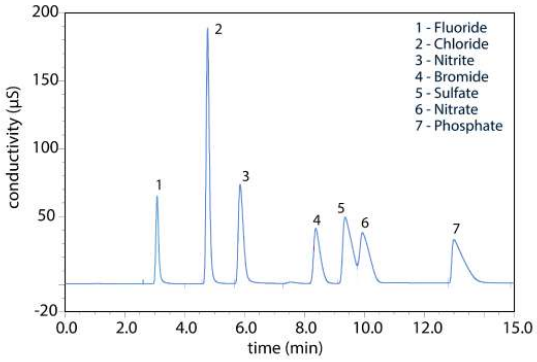


Figure 12.6.2 . Ion-exchange chromatographic analysis of water from Big Walnut Creek in Putnam County, Indiana. Data provided by Jeanette Pope, Department of Geosciences, DePauw University.

Size-Exclusion Chromatography

We have considered two classes of micron-sized stationary phases in this section: silica particles and cross-linked polymer resin beads. Both materials are porous, with pore sizes ranging from approximately 5–400 nm for silica particles, and from 5 nm to 100 µm for divinylbenzene cross-linked polystyrene resins. In ***size-exclusion chromatography***—which also is known by the terms molecular-exclusion or gel permeation chromatography—the separation of solutes depends upon their ability to enter into the pores of the stationary phase. Smaller solutes spend proportionally more time within the pores and take longer to elute from the column.

A stationary phase's size selectivity extends over a finite range. All solutes significantly smaller than the pores move through the column's entire volume and elute simultaneously, with a retention volume, V_r, of

$$V_r = V_i + V_o \tag{2.6.3}$$

where V_i is the volume of mobile phase occupying the stationary phase's pore space and V_o is volume of mobile phase in the remainder of the column. The largest solute for which Equation 2.6.3 holds is the column's inclusion limit, or permeation limit. Those solutes too large to enter the pores elute simultaneously with an retention volume of

$$V_r = V_o \tag{2.6.4}$$

Equation 2.6.4 defines the column's ***exclusion limit***.

For a solute whose size is between the inclusion limit and the exclusion limit, the amount of time it spends in the stationary phase's pores is proportional to its size. The retention volume for these solutes is

$$V_r = DV_i + V_o \tag{2.6.5}$$

where D is the solute's distribution ratio, which ranges from 0 at the exclusion limit to 1 at the inclusion limit. Equation 2.6.5 assumes that size-exclusion is the only interaction between the solute and the stationary phase that affects the separation. For this reason, stationary phases using silica particles are deactivated as described earlier, and polymer resins are synthesized without exchange sites.

Size-exclusion chromatography provides a rapid means for separating larger molecules, including polymers and biomolecules. A stationary phase for proteins that consists of particles with 30 nm pores has an inclusion limit of 7500 g/mol and an exclusion limit of 1.2×10^6 g/mol. Mixtures of proteins that span a wider range of molecular weights are separated by joining together in series several columns with different inclusion and exclusion limits.

Another important application of size-exclusion chromatography is the estimation of a solute's molecular weight (MW). Calibration curves are prepared using a series of standards of known molecular weight and measuring each standard's retention volume. As shown in Figure 12.6.3 , a plot of log(MW) versus V_r is roughly linear between the exclusion limit and the inclusion limit. Because a solute's retention volume is influenced by both its size and its shape, a reasonably accurate estimation of molecular weight is possible only if the standards are chosen carefully to minimize the effect of shape.

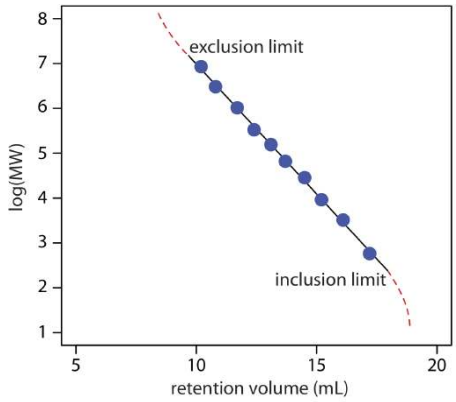


Figure 12.6.3 . Calibration curve for the determination of molecular weight by size-exclusion chromatography. The data shown here are adapted from Rouessac, F.; Rouessac, A. *Chemical Analysis: Modern Instrumentation Methods and Techniques*, Wiley: Chichester, England, 2004, p 141.

Size-exclusion chromatography is carried out using conventional HPLC instrumentation, replacing the HPLC column with an appropriate size-exclusion column. A UV/Vis detector is the most common means for obtaining the chromatogram.

Supercritical Fluid Chromatography

Although there are many analytical applications of gas chromatography and liquid chromatography, they can not separate and analyze all types of samples. Capillary column GC separates complex mixtures with excellent resolution and short analysis times. Its application is limited, however, to volatile analytes or to analytes made volatile by a suitable derivatization reaction. Liquid chromatography separates a wider range of solutes than GC, but the most common detectors—UV, fluorescence, and electrochemical— have poorer detection limits and smaller linear ranges than GC detectors, and are not as universal in their selectivity.

For some samples, ***supercritical fluid chromatography*** (SFC) provides a useful alternative to gas chromatography and liquid chromatography. The mobile phase in supercritical fluid chromatography is a gas held at a temperature and pressure that exceeds its critical point (Figure 12.6.4). Under these conditions the mobile phase is neither a gas nor a liquid. Instead, the mobile phase is a supercritical fluid.

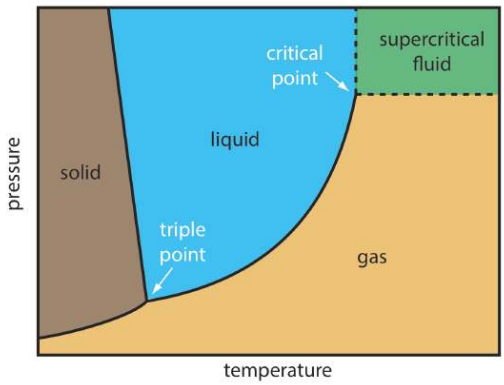


Figure 12.6.4 . Phase diagram showing the combinations of temperature and pres- sure for which a compound is in its solid state, its liquid state, and its gas state. For pressures and temperatures above the critical point, the compound is a supercritical fluid with properties intermediate between a gas and a liquid. Click here to see an interesting video demonstration of supercritical fluids from Nottingham Science City at the University of Nottingham.

Some properties of a supercritical fluid, as shown in Table 12.6.2 , are similar to a gas; other properties, however, are similar to a liquid. The viscosity of a supercritical fluid, for example, is similar to a gas, which means we can move a supercritical fluid through a capillary column or a packed column without the high pressures needed in HPLC. Analysis time and resolution, although not as good as in GC, usually are better than in conventional HPLC. The density of a supercritical fluid, on the other hand, is much closer to that of a liquid, which explains why supercritical fluids are good solvents. In terms of its separation power, a mobile phase in SFC behaves more like the liquid mobile phase in HPLC than the gaseous mobile phase in GC.

Table 12.6.2 . Typical Properties of Gases, Liquids, and Supercritical Fluids

phase	density (g/cm^3)	viscosity ($g\ cm^{-1}\ s^{-1}$)	diffusion coefficient ($cm^2\ s^{-1}$)
gas	$\approx 10^{-3}$	$\approx 10^{-4}$	≈ 0.1
supercritical fluid	$\approx 0.1 - 1$	$\approx 10^{-4} - 10^{-3}$	$\approx 10^{-4} - 10^{-3}$
liquid	≈ 1	$\approx 10^{-2}$	$\approx 10^{-3}$

The most common mobile phase for supercritical fluid chromatography is CO_2. Its low critical temperature of 31.1°C and its low critical pressure of 72.9 atm are relatively easy to achieve and maintain. Although supercritical CO_2 is a good solvent for nonpolar organics, it is less useful for polar solutes. The addition of an organic modifier, such as methanol, improves the mobile phase's elution strength. Other common mobile phases and their critical temperatures and pressures are listed in Table 12.6.3 .

Table 12.6.3 . Critical Points for Selected Supercritical Fluids

compound	critical temperature (°C)	critical pressure (atm)
carbon dioxide	31.3	72.9
ethane	32.4	48.3
nitrous oxide	36.5	71.4
ammonia	132.3	111.3
diethyl ether	193.6	36.3
isopropanol	235.3	47.0
methanol	240.5	78.9
ethanol	243.4	63.0
water	374.4	226.8

The instrumentation for supercritical fluid chromatography essentially is the same as that for a standard HPLC. The only important additions are a heated oven for the column and a pressure restrictor downstream from the column to maintain the critical pressure. Gradient elutions are accomplished by changing the applied pressure over time. The resulting change in the mobile phase's density affects its solvent strength. Detection is accomplished using standard GC detectors or HPLC detectors. Supercritical fluid chromatography has many applications in the analysis of polymers, fossil fuels, waxes, drugs, and food products.

This page titled 2.6: Other Forms of Chromatography is shared under a CC BY-NC-SA 4.0 license and was authored, remixed, and/or curated by David Harvey.

- **12.6: Other Forms of Chromatography** by David Harvey is licensed CC BY-NC-SA 4.0.

2.7: Electrophoresis

Electrophoresis is a class of separation techniques in which we separate analytes by their ability to move through a conductive medium—usually an aqueous buffer—in response to an applied electric field. In the absence of other effects, cations migrate toward the electric field's negatively charged cathode. Cations with larger charge-to-size ratios—which favors ions of greater charge and of smaller size—migrate at a faster rate than larger cat- ions with smaller charges. Anions migrate toward the positively charged anode and neutral species do not experience the electrical field and remain stationary.

> As we will see shortly, under normal conditions even neutral species and anions migrate toward the cathode.

There are several forms of electrophoresis. In slab gel electrophoresis the conducting buffer is retained within a porous gel of agarose or polyacrylamide. Slabs are formed by pouring the gel between two glass plates separated by spacers. Typical thicknesses are 0.25–1 mm. Gel electrophoresis is an important technique in biochemistry where it frequently is used to separate DNA fragments and proteins. Although it is a powerful tool for the qualitative analysis of complex mixtures, it is less useful for quantitative work.

In ***capillary electrophoresis*** the conducting buffer is retained within a capillary tube with an inner diameter that typically is 25–75 μm. The sample is injected into one end of the capillary tube, and as it migrates through the capillary the sample's components separate and elute from the column at different times. The resulting ***electropherogram*** looks similar to a GC or an HPLC chromatogram, and provides both qualitative and quantitative information. Only capillary electrophoretic methods receive further consideration in this section.

Theory of Electrophoresis

In capillary electrophoresis we inject the sample into a buffered solution retained within a capillary tube. When an electric field is applied across the capillary tube, the sample's components migrate as the result of two types of actions: electrophoretic mobility and electroosmotic mobility. ***Electrophoretic mobility*** is the solute's response to the applied electrical field in which cations move toward the negatively charged cathode, anions move toward the positively charged anode, and neutral species remain stationary. The other contribution to a solute's migration is ***electroosmotic flow***, which occurs when the buffer moves through the capillary in response to the applied electrical field. Under normal conditions the buffer moves toward the cathode, sweeping most solutes, including the anions and neutral species, toward the negatively charged cathode.

Electrophoretic Mobility

The velocity with which a solute moves in response to the applied electric field is called its ***electrophoretic velocity***, ν_{ep}; it is defined as

$$\nu_{ep} = \mu_{ep} E \tag{2.7.1}$$

where μ_{ep} is the solute's electrophoretic mobility, and E is the magnitude of the applied electrical field. A solute's electrophoretic mobility is defined as

$$\mu_{ep} = \frac{q}{6\pi\eta r} \tag{2.7.2}$$

where q is the solute's charge, η is the buffer's viscosity, and r is the solute's radius. Using Equation 2.7.1 and Equation 2.7.2 we can make several important conclusions about a solute's electrophoretic velocity. Electrophoretic mobility and, therefore, electrophoretic velocity, increases for more highly charged solutes and for solutes of smaller size. Because q is positive for a cation and negative for an anion, these species migrate in opposite directions. A neutral species, for which q is zero, has an electrophoretic velocity of zero.

Electroosmotic Mobility

When an electric field is applied to a capillary filled with an aqueous buffer we expect the buffer's ions to migrate in response to their electrophoretic mobility. Because the solvent, H_2O, is neutral we might reasonably expect it to remain stationary. What we

observe under normal conditions, however, is that the buffer moves toward the cathode. This phenomenon is called the electroosmotic flow.

Electroosmotic flow occurs because the walls of the capillary tubing carry a charge. The surface of a silica capillary contains large numbers of silanol groups (–SiOH). At a pH level greater than approximately 2 or 3, the silanol groups ionize to form negatively charged silanate ions ($–SiO^-$). Cations from the buffer are attracted to the silanate ions. As shown in Figure 12.7.1 , some of these cations bind tightly to the silanate ions, forming a fixed layer. Because the cations in the fixed layer only partially neutralize the negative charge on the capillary walls, the solution adjacent to the fixed layer—which is called the diffuse layer—contains more cations than anions. Together these two layers are known as the double layer. Cations in the diffuse layer migrate toward the cathode. Because these cations are solvated, the solution also is pulled along, producing the electroosmotic flow.

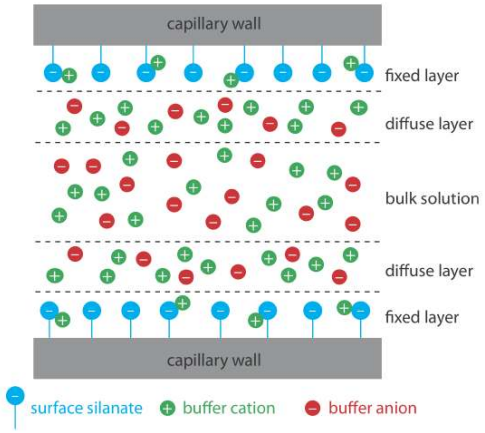


Figure 12.7.1 . Schematic diagram showing the origin of the double layer within a capillary tube. Although the net charge within the capillary is zero, the distribution of charge is not. The walls of the capillary have an excess of negative charge, which decreases across the fixed layer and the diffuse layer, reaching a value of zero in bulk solution.

> The anions in the diffuse layer, which also are solvated, try to move toward the anode. Because there are more cations than anions, however, the cations win out and the electroosmotic flow moves in the direction of the cathode.

The rate at which the buffer moves through the capillary, what we call its ***electroosmotic flow velocity***, ν_{eof}, is a function of the applied electric field, E, and the buffer's electroosmotic mobility, μ_{eof}.

$$\nu_{eof} = \mu_{eof} E \tag{2.7.3}$$

Electroosmotic mobility is defined as

$$\mu_{eof} = \frac{\varepsilon \zeta}{4\pi\eta} \tag{2.7.4}$$

where ϵ is the buffer dielectric constant, ζ is the zeta potential, and η is the buffer's viscosity.

The ***zeta potential***—the potential of the diffuse layer at a finite distance from the capillary wall—plays an important role in determining the electroosmotic flow velocity. Two factors determine the zeta potential's value. First, the zeta potential is directly proportional to the charge on the capillary walls, with a greater density of silanate ions corresponding to a larger zeta potential. Below a pH of 2 there are few silanate ions and the zeta potential and the electroosmotic flow velocity approach zero. As the pH increases, both the zeta potential and the electroosmotic flow velocity increase. Second, the zeta potential is directly proportional to the thickness of the double layer. Increasing the buffer's ionic strength provides a higher concentration of cations, which decreases the thickness of the double layer and decreases the electroosmotic flow.

> The definition of zeta potential given here admittedly is a bit fuzzy. For a more detailed explanation see Delgado, A. V.; González-Caballero, F.; Hunter, R. J.; Koopal, L. K.; Lyklema, J. "Measurement and Interpretation of Electrokinetic Phenomena," *Pure. Appl. Chem.* **2005**, *77*, 1753–1805. Although this is a very technical report, Sections 1.3–1.5 provide a good introduction to the difficulty of defining the zeta potential and of measuring its value.

The electroosmotic flow profile is very different from that of a fluid moving under forced pressure. Figure 12.7.2 compares the electroosmotic flow profile with the hydrodynamic flow profile in gas chromatography and liquid chromatography. The uniform, flat profile for electroosmosis helps minimize band broadening in capillary electrophoresis, improving separation efficiency.

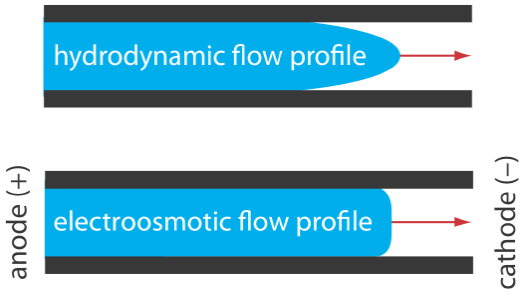


Figure 12.7.2 . Comparison of hydrodynamic flow and electroosmotic flow. The nearly uniform electroosmotic flow profile means that the electroosmotic flow velocity is nearly constant across the capillary.

Total Mobility

A solute's total velocity, ν_{tot}, as it moves through the capillary is the sum of its electrophoretic velocity and the electroosmotic flow velocity.

$$\nu_{tot} = \nu_{ep} + \nu_{eof}$$

As shown in Figure 12.7.3 , under normal conditions the following general relationships hold true.

$$(\nu_{tot})_{cations} > \nu_{eof}$$

$$(\nu_{tot})_{neutrals} = \nu_{eof}$$

$$(\nu_{tot})_{anions} < \nu_{eof}$$

Cations elute first in an order that corresponds to their electrophoretic mobilities, with small, highly charged cations eluting before larger cations of lower charge. Neutral species elute as a single band with an elution rate equal to the electroosmotic flow velocity. Finally, anions are the last components to elute, with smaller, highly charged anions having the longest elution time.

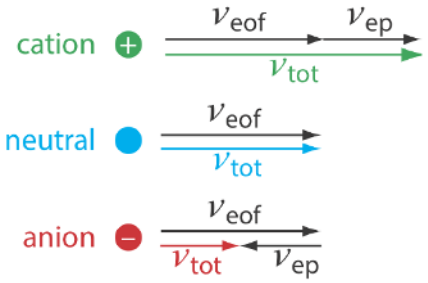


Figure 12.7.3 . Visual explanation for the general elution order in capillary electrophoresis. Each species has the same electroosmotic flow, ν_{eof}. Cations elute first because they have a positive electrophoretic velocity, ν_{ep}. Anions elute last because their negative electrophoretic velocity partially offsets the electroosmotic flow velocity. Neutrals elute with a velocity equal to the electroosmotic flow.

Migration Time

Another way to express a solute's velocity is to divide the distance it travels by the elapsed time

$$\nu_{tot} = \frac{l}{t_m} \tag{2.7.5}$$

where l is the distance between the point of injection and the detector, and t_m is the solute's migration time. To understand the experimental variables that affect migration time, we begin by noting that

$$\nu_{tot} = \mu_{tot} E = (\mu_{ep} + \mu_{eof}) E \tag{2.7.6}$$

Combining Equation 2.7.5 and Equation 2.7.6 and solving for t_m leaves us with

$$t_m = \frac{l}{(\mu_{ep} + \mu_{eof})\, E} \tag{2.7.7}$$

The magnitude of the electrical field is

$$E = \frac{V}{L} \tag{2.7.8}$$

where V is the applied potential and L is the length of the capillary tube. Finally, substituting Equation 2.7.8 into Equation 2.7.7 leaves us with the following equation for a solute's migration time.

$$t_m = \frac{lL}{(\mu_{ep} + \mu_{eof})\, V} \tag{2.7.9}$$

To decrease a solute's migration time—which shortens the analysis time—we can apply a higher voltage or use a shorter capillary tube. We can also shorten the migration time by increasing the electroosmotic flow, although this decreases resolution.

Efficiency

As we learned in Chapter 12.2, the efficiency of a separation is given by the number of theoretical plates, N. In capillary electrophoresis the number of theoretic plates is

$$N = \frac{l^2}{2Dt_m} = \frac{(\mu_{ep} + \mu_{eof})\, El}{2DL} \tag{2.7.10}$$

where D is the solute's diffusion coefficient. From Equation 2.7.10, the efficiency of a capillary electrophoretic separation increases with higher voltages. Increasing the electroosmotic flow velocity improves efficiency, but at the expense of resolution. Two additional observations deserve comment. First, solutes with larger electrophoretic mobilities—in the same direction as the electroosmotic flow—have greater efficiencies; thus, smaller, more highly charged cations are not only the first solutes to elute, but do so with greater efficiency. Second, efficiency in capillary electrophoresis is independent of the capillary's length. Theoretical plate counts of approximately 100 000–200 000 are not unusual.

> It is possible to design an electrophoretic experiment so that anions elute before cations—more about this later—in which smaller, more highly charged anions elute with greater efficiencies.

Selectivity

In chromatography we defined the selectivity between two solutes as the ratio of their retention factors. In capillary electrophoresis the analogous expression for selectivity is

$$\alpha = \frac{\mu_{ep,1}}{\mu_{ep,2}}$$

where $\mu_{ep,1}$ and $\mu_{ep,2}$ are the electrophoretic mobilities for the two solutes, chosen such that $\alpha \geq 1$. We can often improve selectivity by adjusting the pH of the buffer solution. For example, NH_4^+ is a weak acid with a pK_a of 9.75. At a pH of 9.75 the concentrations of NH_4^+ and NH_3 are equal. Decreasing the pH below 9.75 increases its electrophoretic mobility because a greater fraction of the solute is present as the cation NH_4^+. On the other hand, raising the pH above 9.75 increases the proportion of neutral NH_3, decreasing its electrophoretic mobility.

Resolution

The resolution between two solutes is

$$R = \frac{0.177(\mu_{ep,2} - \mu_{ep,1})\sqrt{V}}{\sqrt{D(\mu_{avg} + \mu_{eof}}} \tag{2.7.11}$$

where μ_{avg} is the average electrophoretic mobility for the two solutes. Increasing the applied voltage and decreasing the electroosmotic flow velocity improves resolution. The latter effect is particularly important. Although increasing electroosmotic

flow improves analysis time and efficiency, it de- creases resolution.

Instrumentation

The basic instrumentation for capillary electrophoresis is shown in Figure 12.7.4 and includes a power supply for applying the electric field, anode and cathode compartments that contain reservoirs of the buffer solution, a sample vial that contains the sample, the capillary tube, and a detector. Each part of the instrument receives further consideration in this section.

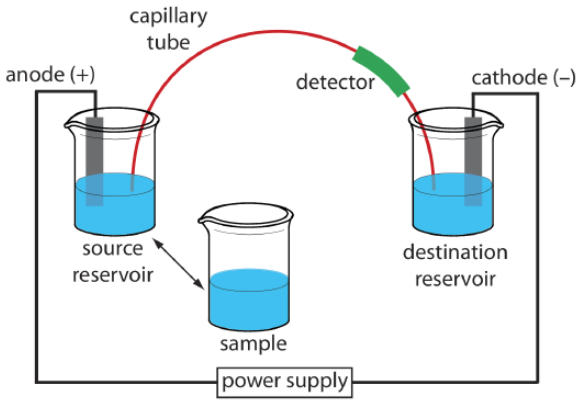


Figure 12.7.4 . Schematic diagram of the basic instrumentation for capillary electrophoresis. The sample and the source reservoir are switched when making injections.

Capillary Tubes

Figure 12.7.5 shows a cross-section of a typical capillary tube. Most capillary tubes are made from fused silica coated with a 15–35 μm layer of polyimide to give it mechanical strength. The inner diameter is typically 25–75 μm, which is smaller than the internal diameter of a capillary GC column, with an outer diameter of 200–375 μm.

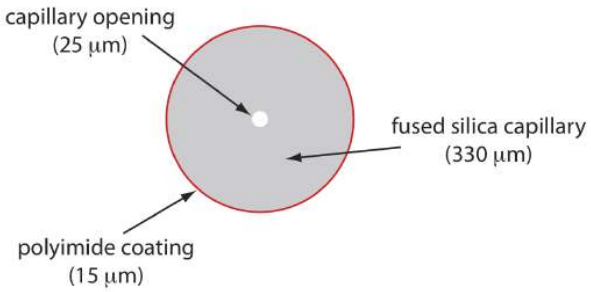


Figure 12.7.5 . Cross section of a capillary column for capillary electrophoresis. The dimensions shown here are typical and are scaled proportionally in this figure.

The capillary column's narrow opening and the thickness of its walls are important. When an electric field is applied to the buffer solution, current flows through the capillary. This current leads to the release of heat, which we call ***Joule heating***. The amount of heat released is proportional to the capillary's radius and to the magnitude of the electrical field. Joule heating is a problem because it changes the buffer's viscosity, with the solution at the center of the capillary being less viscous than that near the capillary walls. Because a solute's electrophoretic mobility depends on its viscosity (see Equation **2.7.2**), solute species in the center of the capillary migrate at a faster rate than those near the capillary walls. The result is an additional source of band broadening that degrades the separation. Capillaries with smaller inner diameters generate less Joule heating, and capillaries with larger outer diameters are more effective at dissipating the heat. Placing the capillary tube inside a thermostated jacket is another method for minimizing the effect of Joule heating; in this case a smaller outer diameter allows for a more rapid dissipation of thermal energy.

Injecting the Sample

There are two common methods for injecting a sample into a capillary electrophoresis column: hydrodynamic injection and electrokinetic injection. In both methods the capillary tube is filled with the buffer solution. One end of the capillary tube is placed in the destination reservoir and the other end is placed in the sample vial.

Hydrodynamic injection uses pressure to force a small portion of sample into the capillary tubing. A difference in pressure is applied across the capillary either by pressurizing the sample vial or by applying a vacuum to the destination reservoir. The volume of sample injected, in liters, is given by the following equation

$$V_{\text{inj}} = \frac{\Delta P d^4 \pi t}{128 \eta L} \times 10^3 \tag{2.7.12}$$

where ΔP is the difference in pressure across the capillary in pascals, d is the capillary's inner diameter in meters, t is the amount of time the pressure is applied in seconds, η is the buffer's viscosity in kg m^{-1} s^{-1}, and L is the length of the capillary tubing in meters. The factor of 10^3 changes the units from cubic meters to liters.

For a hydrodynamic injection we move the capillary from the source reservoir to the sample. The anode remains in the source reservoir. A hydrodynamic injection also is possible if we raise the sample vial above the destination reservoir and briefly insert the filled capillary.

Example 12.7.1

In a hydrodynamic injection we apply a pressure difference of 2.5×10^3 Pa (a $\Delta P \approx 0.02$ atm) for 2 s to a 75-cm long capillary tube with an internal diameter of 50 μm. Assuming the buffer's viscosity is 10^{-3} kg m^{-1} s^{-1}, what volume and length of sample did we inject?

Solution

Making appropriate substitutions into Equation 2.7.12 gives the sample's volume as

$$V_{inj} = \frac{\left(2.5 \times 10^3 \text{ kg m}^{-1} \text{ s}^{-2}\right)\left(50 \times 10^{-6} \text{ m}\right)^4 (3.14)(2 \text{ s})}{(128)\left(0.001 \text{ kg m}^{-1} \text{ s}^{-1}\right)(0.75 \text{ m})} \times 10^3 \text{L/m}^3$$

$$V_{inj} = 1 \times 10^{-9} \text{ L} = 1 \text{ nL}$$

Because the interior of the capillary is cylindrical, the length of the sample, l, is easy to calculate using the equation for the volume of a cylinder; thus

$$l = \frac{V_{\text{inj}}}{\pi r^2} = \frac{\left(1 \times 10^{-9} \text{ L}\right)\left(10^{-3} \text{ m}^3/\text{L}\right)}{(3.14)\left(25 \times 10^{-6} \text{ m}\right)^2} = 5 \times 10^{-4} \text{ m} = 0.5 \text{ mm}$$

Exercise 12.7.1

Suppose you need to limit your injection to less than 0.20% of the capillary's length. Using the information from Example 12.7.1 , what is the maximum injection time for a hydrodynamic injection?

Answer

The capillary is 75 cm long, which means that 0.20% of that sample's maximum length is 0.15 cm. To convert this to the maximum volume of sample we use the equation for the volume of a cylinder.

$$V_{inj} = l \pi r^2 = (0.15 \text{ cm})(3.14)\left(25 \times 10^{-4} \text{ cm}\right)^2 = 2.94 \times 10^{-6} \text{ cm}^3$$

Given that 1 cm^3 is equivalent to 1 mL, the maximum volume is 2.94×10^{-6} mL or 2.94×10^{-9} L. To find the maximum injection time, we first solve Equation 2.7.12 for t

$$t = \frac{128 V_{inj} \eta L}{P d^4 \pi} \times 10^{-3} \text{ m}^3/\text{L}$$

and then make appropriate substitutions.

$$t = \frac{(128)\left(2.94 \times 10^{-9}\ \text{L}\right)\left(0.001\ \text{kg m}^{-1}\ \text{s}^{-1}\right)(0.75\ \text{m})}{\left(2.5 \times 10^{3}\ \text{kg m}^{-1}\ \text{s}^{-2}\right)\left(50 \times 10^{-6}\ \text{m}\right)^{4}(3.14)} \times \frac{10^{-3}\ \text{m}^{3}}{\text{L}} = 5.8\ \text{s}$$

The maximum injection time, therefore, is 5.8 s.

In an ***electrokinetic injection*** we place both the capillary and the anode into the sample and briefly apply an potential. The volume of injected sample is the product of the capillary's cross sectional area and the length of the capillary occupied by the sample. In turn, this length is the product of the solute's velocity (see Equation 2.7.6) and time; thus

$$V_{inj} = \pi r^2 L = \pi r^2 (\mu_{ep} + \mu_{eof}) E' t \tag{2.7.13}$$

where r is the capillary's radius, L is the capillary's length, and E' is the effective electric field in the sample. An important consequence of Equation 2.7.13 is that an electrokinetic injection is biased toward solutes with larger electrophoretic mobilities. If two solutes have equal concentrations in a sample, we inject a larger volume—and thus more moles—of the solute with the larger μ_{ep}.

The electric field in the sample is different that the electric field in the rest of the capillary because the sample and the buffer have different ionic compositions. In general, the sample's ionic strength is smaller, which makes its conductivity smaller. The effective electric field is

$$E' = E \times \frac{\chi_{\text{buffer}}}{\chi_{\text{sample}}}$$

where χ_{buffer} and χ_{sample} are the conductivities of the buffer and the sample, respectively.

When an analyte's concentration is too small to detect reliably, it maybe possible to inject it in a manner that increases its concentration. This method of injection is called ***stacking***. Stacking is accomplished by placing the sample in a solution whose ionic strength is significantly less than that of the buffer in the capillary tube. Because the sample plug has a lower concentration of buffer ions, the effective field strength across the sample plug, E', is larger than that in the rest of the capillary.

We know from Equation 2.7.1 that electrophoretic velocity is directly proportional to the electrical field. As a result, the cations in the sample plug migrate toward the cathode with a greater velocity, and the anions migrate more slowly—neutral species are unaffected and move with the electroosmotic flow. When the ions reach their respective boundaries between the sample plug and the buffer, the electrical field decreases and the electrophoretic velocity of the cations decreases and that for the anions increases. As shown in Figure 12.7.6 , the result is a stacking of cations and anions into separate, smaller sampling zones. Over time, the buffer within the capillary becomes more homogeneous and the separation proceeds without additional stacking.

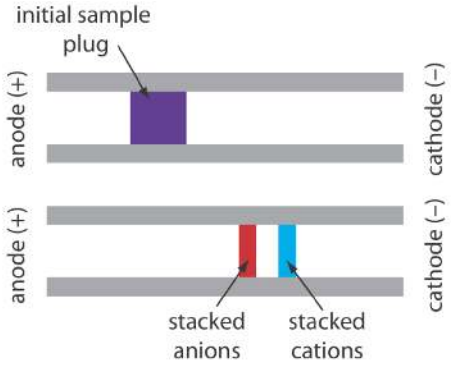


Figure 12.7.6 . The stacking of cations and anions. The top diagram shows the initial sample plug and the bottom diagram shows how the cations and anions are concentrated at opposite sides of the sample plug.

Applying the Electrical Field

Migration in electrophoresis occurs in response to an applied electric field. The ability to apply a large electric field is important because higher voltages lead to shorter analysis times (Equation 2.7.9), more efficient separations (Equation 2.7.10), and better

resolution (Equation 2.7.11). Because narrow bored capillary tubes dissipate Joule heating so efficiently, voltages of up to 40 kV are possible.

> Because of the high voltages, be sure to follow your instrument's safety guidelines.

Detectors

Most of the detectors used in HPLC also find use in capillary electrophoresis. Among the more common detectors are those based on the absorption of UV/Vis radiation, fluorescence, conductivity, amperometry, and mass spectrometry. Whenever possible, detection is done "on-column" before the solutes elute from the capillary tube and additional band broadening occurs.

UV/Vis detectors are among the most popular. Because absorbance is directly proportional to path length, the capillary tubing's small diameter leads to signals that are smaller than those obtained in HPLC. Several approaches have been used to increase the pathlength, including a Z-shaped sample cell and multiple reflections (see Figure 12.7.7). Detection limits are about 10^{-7} M.

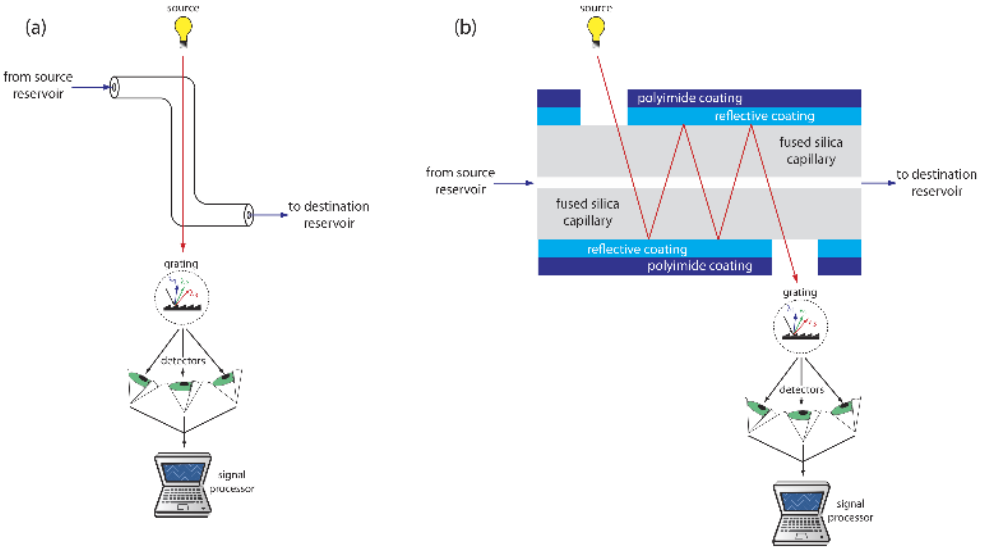


Figure 12.7.7 . Two approaches to on-column detection in capillary electrophoresis using a UV/Vis diode array spectrometer: (a) Z-shaped bend in capillary, and (b) multiple reflections.

Better detection limits are obtained using fluorescence, particularly when using a laser as an excitation source. When using fluorescence detection a small portion of the capillary's protective coating is removed and the laser beam is focused on the inner portion of the capillary tubing. Emission is measured at an angle of 90° to the laser. Because the laser provides an intense source of radiation that can be focused to a narrow spot, detection limits are as low as 10^{-16} M.

Solutes that do not absorb UV/Vis radiation or that do not undergo fluorescence can be detected by other detectors. Table 12.7.1 provides a list of detectors for capillary electrophoresis along with some of their important characteristics.

Table 12.7.1 . Characteristics of Detectors for Capillary Electrophoresis

detector	selectivity (universal or analyte must ...)	detection limited (moles injected)	detection limit (molarity)	on-column detection?
UV/Vis absorbance	have a UV/Vis chromophore	$10^{-13} - 10^{-16}$	$10^{-5} - 10^{-7}$	yes
indirect absorbancd	universal	$10^{-12} - 10^{-15}$	$10^{-4} - 10^{-6}$	yes
fluoresence	have a favorable quantum yield	$10^{-13} - 10^{-17}$	$10^{-7} - 10^{-9}$	yes
laser fluorescence	have a favorable quantum yield	$10^{-18} - 10^{-20}$	$10^{-13} - 10^{-16}$	yes
mass spectrometer	universal (total ion) selective (single ion)	$10^{-16} - 10^{-17}$	$10^{-8} - 10^{-10}$	no
amperometry	undergo oxidation or reduction	$10^{-18} - 10^{-19}$	$10^{-7} - 10^{-10}$	no
conductivity	universal	$10^{-15} - 10^{-16}$	$10^{-7} - 10^{-9}$	no
radiometric	be radioactive	$10^{-17} - 10^{-19}$	$10^{-10} - 10^{-12}$	yes

Capillary Electrophoresis Methods

There are several different forms of capillary electrophoresis, each of which has its particular advantages. Four of these methods are described briefly in this section.

Capillary Zone Electrophoresis (CZE)

The simplest form of capillary electrophoresis is ***capillary zone electrophoresis***. In CZE we fill the capillary tube with a buffer and, after loading the sample, place the ends of the capillary tube in reservoirs that contain additional buffer. Usually the end of the capillary containing the sample is the anode and solutes migrate toward the cathode at a velocity determined by their respective electrophoretic mobilities and the electroosmotic flow. Cations elute first, with smaller, more highly charged cations eluting before larger cations with smaller charges. Neutral species elute as a single band. Anions are the last species to elute, with smaller, more negatively charged anions being the last to elute.

We can reverse the direction of electroosmotic flow by adding an alkylammonium salt to the buffer solution. As shown in Figure 12.7.8 , the positively charged end of the alkyl ammonium ions bind to the negatively charged silanate ions on the capillary's walls. The tail of the alkyl ammonium ion is hydrophobic and associates with the tail of another alkyl ammonium ion. The result is a layer of positive charges that attract anions in the buffer. The migration of these solvated anions toward the anode reverses the electroosmotic flow's direction. The order of elution is exactly opposite that observed under normal conditions.

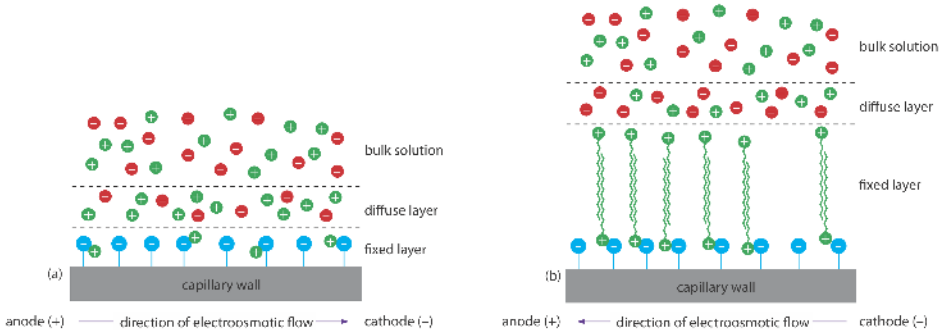


Figure 12.7.8 . Two modes of capillary zone electrophoresis showing (a) normal migration with electroosmotic flow toward the cathode and (b) reversed migration in which the electroosmotic flow is toward the anode.

Coating the capillary's walls with a nonionic reagent eliminates the electroosmotic flow. In this form of CZE the cations migrate from the anode to the cathode. Anions elute into the source reservoir and neutral species remain stationary.

Capillary zone electrophoresis provides effective separations of charged species, including inorganic anions and cations, organic acids and amines, and large biomolecules such as proteins. For example, CZE was used to separate a mixture of 36 inorganic and organic ions in less than three minutes [Jones, W. R.; Jandik, P. *J. Chromatog.* **1992**, *608*, 385–393]. A mixture of neutral species, of course, can not be resolved.

Micellar Electrokinetic Capillary Chromatography (MEKC)

One limitation to CZE is its inability to separate neutral species. ***Micellar electrokinetic capillary chromatography*** overcomes this limitation by adding a surfactant, such as sodium dodecylsulfate (Figure 12.7.9 a) to the buffer solution. Sodium dodecylsulfate, or SDS, consists of a long-chain hydrophobic tail and a negatively charged ionic functional group at its head. When the concentration of SDS is sufficiently large a micelle forms. A micelle consists of a spherical agglomeration of 40–100 surfactant molecules in which the hydrocarbon tails point inward and the negatively charged heads point outward (Figure 12.7.9 b).

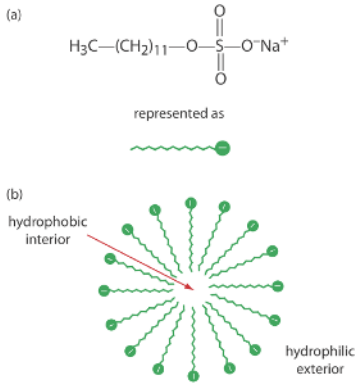


Figure 12.7.9 . (a) Structure of sodium dodecylsulfate and (b) cross section through a micelle showing its hydrophobic interior and its hydrophilic exterior.

Because micelles have a negative charge, they migrate toward the cathode with a velocity less than the electroosmotic flow velocity. Neutral species partition themselves between the micelles and the buffer solution in a manner similar to the partitioning of solutes between the two liquid phases in HPLC. Because there is a partitioning between two phases, we include the descriptive term chromatography in the techniques name. Note that in MEKC both phases are mobile.

The elution order for neutral species in MEKC depends on the extent to which each species partitions into the micelles. Hydrophilic neutrals are insoluble in the micelle's hydrophobic inner environment and elute as a single band, as they would in CZE. Neutral solutes that are extremely hy- drophobic are completely soluble in the micelle, eluting with the micelles as a single band. Those neutral species that exist in a partition equilibrium between the buffer and the micelles elute between the completely hydro- philic and completely hydrophobic neutral species. Those neutral species that favor the buffer elute before those favoring the micelles. Micellar electrokinetic chromatography is used to separate a wide variety of samples, including mixtures of pharmaceutical compounds, vitamins, and explosives.

Capillary Gel Electrophoresis (CGE)

In ***capillary gel electrophoresis*** the capillary tubing is filled with a polymeric gel. Because the gel is porous, a solute migrates through the gel with a velocity determined both by its electrophoretic mobility and by its size. The ability to effect a separation using size is helpful when the solutes have similar electrophoretic mobilities. For example, fragments of DNA of varying length have similar charge-to-size ratios, making their separation by CZE difficult. Because the DNA fragments are of different size, a CGE separation is possible.

The capillary used for CGE usually is treated to eliminate electroosmotic flow to prevent the gel from extruding from the capillary tubing. Samples are injected electrokinetically because the gel provides too much resistance for hydrodynamic sampling. The primary application of CGE is the separation of large biomolecules, including DNA fragments, proteins, and oligonucleotides.

Capillary Electrochromatography (CEC)

Another approach to separating neutral species is ***capillary electrochromatography***. In CEC the capillary tubing is packed with 1.5–3 μm particles coated with a bonded stationary phase. Neutral species separate based on their ability to partition between the stationary phase and the buffer, which is moving as a result of the electroosmotic flow; Figure 12.7.10 provides a representative example for the separation of a mixture of hydrocarbons. A CEC separation is similar to the analogous HPLC separation, but without the need for high pressure pumps. Efficiency in CEC is better than in HPLC, and analysis times are shorter.

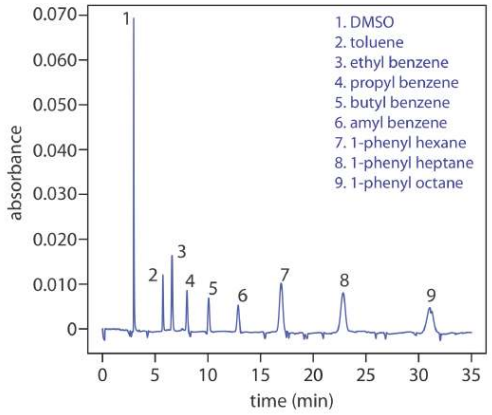


Figure 12.7.10 . Capillary electrochromatographic separation of a mixture of hydrocarbons in DMSO. The column contains a porous polymer of butyl methacrylate and lauryl acrylate (25%:75% mol:mol) with butane dioldacrylate as a crosslinker. Data provided by Zoe LaPier and Michelle Bushey, Department of Chemistry, Trinity University.

The best way to appreciate the theoretical and the practical details discussed in this section is to carefully examine a typical analytical method. Although each method is unique, the following description of the determination of a vitamin B complex by capillary zone electrophoresis or by micellar electrokinetic capillary chromatography provides an instructive example of a typical procedure. The description here is based on Smyth, W. F. *Analytical Chemistry of Complex Matrices*, Wiley Teubner: Chichester, England, 1996, pp. 154–156.

Representative Method 12.7.1: Determination of Vitamin B Complex by CZE or MEKC

Description of Method

The water soluble vitamins B_1 (thiamine hydrochloride), B_2 (riboflavin), B_3 (niacinamide), and B_6 (pyridoxine hydrochloride) are determined by CZE using a pH 9 sodium tetraborate-sodium dihydrogen phosphate buffer, or by MEKC using the same buffer with the addition of sodium dodecyl sulfate. Detection is by UV absorption at 200 nm. An internal standard of *o*-ethoxybenzamide is used to standardize the method.

Procedure

Crush a vitamin B complex tablet and place it in a beaker with 20.00 mL of a 50 % v/v methanol solution that is 20 mM in sodium tetraborate and 100.0 ppm in *o*-ethoxybenzamide. After mixing for 2 min to ensure that the B vitamins are dissolved, pass a 5.00-mL portion through a 0.45-μm filter to remove insoluble binders. Load an approximately 4 nL sample into a capillary column with an inner diameter of a 50 μm. For CZE the capillary column contains a 20 mM pH 9 sodium tetraborate-sodium dihydrogen phosphate buffer. For MEKC the buffer is also 150 mM in sodium dodecyl sulfate. Apply a 40 kV/m electrical field to effect both the CZE and MEKC separations.

Questions

1. Methanol, which elutes at 4.69 min, is included as a neutral species to indicate the electroosmotic flow. When using standard solutions of each vitamin, CZE peaks are found at 3.41 min, 4.69 min, 6.31 min, and 8.31 min. Examine the structures and pK_a information in Figure 12.7.11 and identify the order in which the four B vitamins elute.

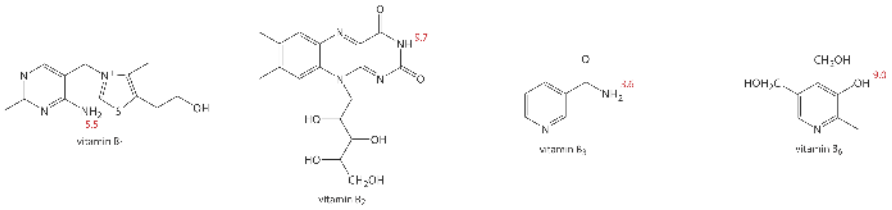


Figure 12.7.11 . Structures of the four water soluble B vitamins in their predominate forms at a pH of 9; pK_a values are shown in red.

At a pH of 9, vitamin B_1 is a cation and elutes before the neutral species methanol; thus it is the compound that elutes at 3.41 min. Vitamin B_3 is a neutral species at a pH of 9 and elutes with methanol at 4.69 min. The remaining two B vitamins are weak acids that partially ionize to weak base anions at a pH of 9. Of the two, vitamin B_6 is the stronger acid (a pK_a of 9.0 versus a pK_a of 9.7) and is present to a greater extent in its anionic form. Vitamin B_6, therefore, is the last of the vitamins to elute.

2. The order of elution when using MEKC is vitamin B_3 (5.58 min), vitamin B_6 (6.59 min), vitamin B_2 (8.81 min), and vitamin B_1 (11.21 min). What conclusions can you make about the solubility of the B vitamins in the sodium dodecylsulfate micelles? The micelles elute at 17.7 min.

The elution time for vitamin B_1 shows the greatest change, increasing from 3.41 min to 11.21 minutes. Clearly vitamin B_1 has the greatest solubility in the micelles. Vitamin B_2 and vitamin B3 have a more limited solubility in the micelles, and show only slightly longer elution times in the presence of the micelles. Interestingly, the elution time for vitamin B_6 decreases in the presence of the micelles.

3. For quantitative work an internal standard of *o*-ethoxybenzamide is added to all samples and standards. Why is an internal standard necessary?

Although the method of injection is not specified, neither a hydrodynamic injection nor an electrokinetic injection is particularly reproducible. The use of an internal standard compensates for this limitation.

Evaluation

When compared to GC and HPLC, capillary electrophoresis provides similar levels of accuracy, precision, and sensitivity, and it provides a comparable degree of selectivity. The amount of material injected into a capillary electrophoretic column is significantly smaller than that for GC and HPLC—typically 1 nL versus 0.1 µL for capillary GC and 1–100 µL for HPLC. Detection limits for capillary electrophoresis, however, are 100–1000 times poorer than that for GC and HPLC. The most significant advantages of capillary electrophoresis are improvements in separation efficiency, time, and cost. Capillary electrophoretic columns contain substantially more theoretical plates ($\approx 10^6$ plates/m) than that found in HPLC ($\approx 10^5$ plates/m) and capillary GC columns ($\approx 10^3$ plates/m), providing unparalleled resolution and peak capacity. Separations in capillary electrophoresis are fast and efficient. Furthermore, the capillary column's small volume means that a capillary electrophoresis separation requires only a few microliters of buffer, compared to 20–30 mL of mobile phase for a typical HPLC separation.

This page titled 2.7: Electrophoresis is shared under a CC BY-NC-SA 4.0 license and was authored, remixed, and/or curated by David Harvey.

- **12.7: Electrophoresis** by David Harvey is licensed CC BY-NC-SA 4.0.

2.8: Problems

1. The following data were obtained for four compounds separated on a 20-m capillary column.

compound	t_r (min)	w (min)
A	8.04	0.15
B	8.26	0.15
C	8.43	0.16

(a) Calculate the number of theoretical plates for each compound and the average number of theoretical plates for the column, in mm.

(b) Calculate the average height of a theoretical plate.

(c) Explain why it is possible for each compound to have a different number of theoretical plates.

2. Using the data from Problem 1, calculate the resolution and the selectivity factors for each pair of adjacent compounds. For resolution, use both equation 12.2.1 and equation 12.3.3, and compare your results. Discuss how you might improve the resolution between compounds B and C. The retention time for an nonretained solute is 1.19 min.

3. Use the chromatogram in Figure 12.8.1 , obtained using a 2-m column, to determine values for t_r, w, t'_r, k, N, and H.

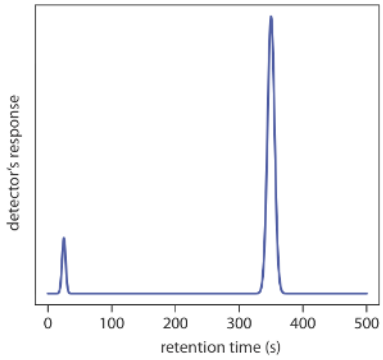


Figure 12.8.1 . Chromatogram for Problem 3.

4. Use the partial chromatogram in Figure 12.8.2 to determine the resolution between the two solute bands.

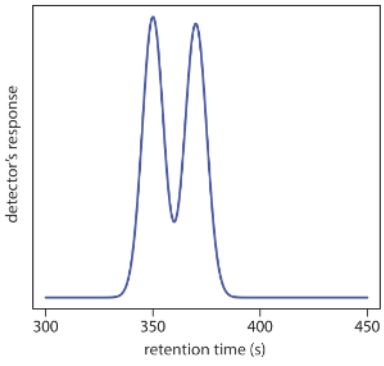


Figure 12.8.2 . Chromatogram for Problem 4.

5. The chromatogram in Problem 4 was obtained on a 2-m column with a column dead time of 50 s. Suppose you want to increase the resolution between the two components to 1.5. Without changing the height of a theoretical plate, what length column do you need? What height of a theoretical plate do you need to achieve a resolution of 1.5 without increasing the column's length?

6. Complete the following table.

N_B	α	k_B	R
100000	1.05	0.50	
10000	1.10		1.50
10000		4.0	1.00
	1.05	3.0	1.75

7. Moody studied the efficiency of a GC separation of 2-butanone on a dinonyl phthalate packed column [Moody, H. W. *J. Chem. Educ.* **1982**, *59*, 218–219]. Evaluating plate height as a function of flow rate gave a van Deemter equation for which *A* is 1.65 mm, *B* is 25.8 mm•mL min^{-1}, and *C* is 0.0236 mm•min mL^{-1}.

(a) Prepare a graph of *H* versus *u* for flow rates between 5 –120 mL/min.

(b) For what range of flow rates does each term in the Van Deemter equation have the greatest effect?

(c) What is the optimum flow rate and the corresponding height of a theoretical plate?

(d) For open-tubular columns the *A* term no longer is needed. If the *B* and *C* terms remain unchanged, what is the optimum flow rate and the corresponding height of a theoretical plate?

(e) Compared to the packed column, how many more theoretical plates are in the open-tubular column?

8. Hsieh and Jorgenson prepared 12–33 μm inner diameter HPLC columns packed with 5.44-μm spherical stationary phase particles [Hsieh, S.; Jorgenson, J. W. *Anal. Chem.* **1996**, *68*, 1212–1217]. To evaluate these columns they measured reduced plate height, *h*, as a function of reduced flow rate, *v*,

$$h = \frac{H}{d_p} \quad v = \frac{ud_p}{D_m}$$

where d_p is the particle diameter and D_m is the solute's diffusion coefficient in the mobile phase. The data were analyzed using van Deemter plots. The following table contains a portion of their results for norepinephrine.

internal diameter (μm)	A	B	C
33	0.63	1.32	0.10
33	0.67	1.30	0.08
23	0.40	1.34	0.09
23	0.58	1.11	0.09
17	0.31	1.47	0.11
17	0.40	1.41	0.11
12	0.22	1.53	0.11
12	0.19	1.27	0.12

(a) Construct separate van Deemter plots using the data in the first row and in the last row for reduced flow rates in the range 0.7–15. Determine the optimum flow rate and plate height for each case given d_p = 5.44 μm and D_m = $\mathbf{6.23 \times 10^{-6}}$ cm^2 s^{-1}.

(b) The *A* term in the van Deemter equation is strongly correlated with the column's inner diameter, with smaller diameter columns providing smaller values of *A*. Offer an explanation for this observation. *Hint: consider how many particles can fit across a capillary of each diameter.*

> When comparing columns, chromatographers often use dimensionless, reduced parameters. By including particle size and the solute's diffusion coefficient, the reduced plate height and reduced flow rate correct for differences between the packing material, the solute, and the mobile phase.

9. A mixture of *n*-heptane, tetrahydrofuran, 2-butanone, and *n*-propanol elutes in this order when using a polar stationary phase such as Carbowax. The elution order is exactly the opposite when using a nonpolar stationary phase such as polydimethyl siloxane. Explain the order of elution in each case.

10. The analysis of trihalomethanes in drinking water is described in Representative Method 12.4.1. A single standard that contains all four trihalomethanes gives the following results.

compound	concentration (ppb)	peak area
$CHCl_3$	1.30	1.35×10^4
$CHCl_2Br$	0.90	6.12×10^4
$CHClBr_2$	4.00	1.71×10^4
$CHBr_3$	1.20	1.52×10^4

Analysis of water collected from a drinking fountain gives areas of 1.56×10^4, 5.13×10^4, 1.49×10^4, and 1.76×10^4 for, respectively, $CHCl_3$, $CHCl_2Br$, $CHClBr_2$, and $CHBr_3$. All peak areas were corrected for variations in injection volumes using an internal standard of 1,2-dibromopentane. Determine the concentration of each of the trihalomethanes in the sample of water.

11. Zhou and colleagues determined the %w/w H_2O in methanol by capillary column GC using a polar stationary phase and a thermal conductivity detector [Zhou, X.; Hines, P. A.; White, K. C.; Borer, M. W. *Anal. Chem.* **1998**, *70*, 390–394]. A series of calibration standards gave the following results.

%w/w H_2O	peak height (arb. units)
0.00	1.15
0.0145	2.74
0.0472	6.33
0.0951	11.58
0.1757	20.43
0.2901	32.97

(a) What is the %w/w H_2O in a sample that has a peak height of 8.63?

(b) The %w/w H_2O in a freeze-dried antibiotic is determined in the following manner. A 0.175-g sample is placed in a vial along with 4.489 g of methanol. Water in the vial extracts into the methanol. Analysis of the sample gave a peak height of 13.66. What is the %w/w H_2O in the antibiotic?

12. Loconto and co-workers describe a method for determining trace levels of water in soil [Loconto, P. R.; Pan, Y. L.; Voice, T. C. *LC•GC* **1996**, *14*, 128–132]. The method takes advantage of the reaction of water with calcium carbide, CaC_2, to produce acetylene gas, C_2H_2. By carrying out the reaction in a sealed vial, the amount of acetylene produced is determined by sampling the headspace. In a typical analysis a sample of soil is placed in a sealed vial with CaC_2. Analysis of the headspace gives a blank corrected signal of 2.70×10^5. A second sample is prepared in the same manner except that a standard addition of 5.0 mg H_2O/g soil is added, giving a blank-corrected signal of 1.06×10^6. Determine the milligrams H_2O/g soil in the soil sample.

13. Van Atta and Van Atta used gas chromatography to determine the %v/v methyl salicylate in rubbing alcohol [Van Atta, R. E.; Van Atta, R. L. *J. Chem. Educ.* **1980**, *57*, 230–231]. A set of standard additions was prepared by transferring 20.00 mL of rubbing

alcohol to separate 25-mL volumetric flasks and pipeting 0.00 mL, 0.20 mL, and 0.50 mL of methyl salicylate to the flasks. All three flasks were diluted to volume using isopropanol. Analysis of the three samples gave peak heights for methyl salicylate of 57.00 mm, 88.5 mm, and 132.5 mm, respectively. Determine the %v/v methyl salicylate in the rubbing alcohol.

14. The amount of camphor in an analgesic ointment is determined by GC using the method of internal standards [Pant, S. K.; Gupta, P. N.; Thomas, K. M.; Maitin, B. K.; Jain, C. L. *LC•GC* **1990**, *8*, 322–325]. A standard sample is prepared by placing 45.2 mg of camphor and 2.00 mL of a 6.00 mg/mL internal standard solution of terpene hydrate in a 25-mL volumetric flask and diluting to volume with CCl_4. When an approximately 2-µL sample of the standard is injected, the FID signals for the two components are measured (in arbitrary units) as 67.3 for camphor and 19.8 for terpene hydrate. A 53.6-mg sample of an analgesic ointment is prepared for analysis by placing it in a 50-mL Erlenmeyer flask along with 10 mL of CCl_4. After heating to 50°C in a water bath, the sample is cooled to below room temperature and filtered. The residue is washed with two 5-mL portions of CCl_4 and the combined filtrates are collected in a 25-mL volumetric flask. After adding 2.00 mL of the internal standard solution, the contents of the flask are diluted to volume with CCl_4. Analysis of an approximately 2-µL sample gives FID signals of 13.5 for the terpene hydrate and 24.9 for the camphor. Report the %w/w camphor in the analgesic ointment.

15. The concentration of pesticide residues on agricultural products, such as oranges, is determined by GC-MS [Feigel, C. *Varian GC/MS Application Note*, Number 52]. Pesticide residues are extracted from the sample using methylene chloride and concentrated by evaporating the methylene chloride to a smaller volume. Calibration is accomplished using anthracene-d_{10} as an internal standard. In a study to determine the parts per billion heptachlor epoxide on oranges, a 50.0-g sample of orange rinds is chopped and extracted with 50.00 mL of methylene chloride. After removing any insoluble material by filtration, the methylene chloride is reduced in volume, spiked with a known amount of the internal standard and diluted to 10 mL in a volumetric flask. Analysis of the sample gives a peak–area ratio ($A_{analyte}/A_{intstd}$) of 0.108. A series of calibration standards, each containing the same amount of anthracene-d_{10} as the sample, gives the following results.

ppb heptachlor epoxide	$A_{analyte}/A_{intstd}$
20.0	0.065
60.0	0.153
200.0	0.637
500.0	1.554
1000.0	3.198

Report the nanograms per gram of heptachlor epoxide residue on the oranges.

16. The adjusted retention times for octane, toluene, and nonane on a particular GC column are 15.98 min, 17.73 min, and 20.42 min, respectively. What is the retention index for each compound?

17. The following data were collected for a series of normal alkanes using a stationary phase of Carbowax 20M.

alkane	t_r' (min)
pentane	0.79
hexane	1.99
heptane	4.47
octane	14.12
nonane	33.11

What is the retention index for a compound whose adjusted retention time is 9.36 min?

18. The following data were reported for the gas chromatographic analysis of *p*-xylene and methylisobutylketone (MIBK) on a capillary column [Marriott, P. J.; Carpenter, P. D. *J. Chem. Educ.* **1996**, *73*, 96–99].

injection mode	compound	t_r (min)	peak area (arb. units)	peak width (min)
split	MIBK	1.878	54285	0.028
	p-xylene	5.234	123483	0.044
splitless	MIBK	3.420	2493005	1.057
	p-xylene	5.795	3396656	1.051

Explain the difference in the retention times, the peak areas, and the peak widths when switching from a split injection to a splitless injection.

19. Otto and Wegscheider report the following retention factors for the reversed-phase separation of 2-aminobenzoic acid on a C_{18} column when using 10% v/v methanol as a mobile phase [Otto, M.; Wegscheider, W. *J. Chromatog.* **1983**, *258*, 11–22].

pH	*k*
2.0	10.5
3.0	16.7
4.0	15.8
5.0	8.0
6.0	2.2
7.0	1.8

Explain the effect of pH on the retention factor for 2-aminobenzene.

20. Haddad and associates report the following retention factors for the reversed-phase separation of salicylamide and caffeine [Haddad, P.; Hutchins, S.; Tuffy, M. *J. Chem. Educ.* **1983**, *60*, 166-168].

%v/v methanol	30%	35%	40%	45%	50%	55%
k_{sal}	2.4	1.6	1.6	1.0	0.7	0.7
k_{caff}	4.3	2.8	2.3	1.4	1.1	0.9

(a) Explain the trends in the retention factors for these compounds.

(b) What is the advantage of using a mobile phase with a smaller %v/v methanol? Are there any disadvantages?

21. Suppose you need to separate a mixture of benzoic acid, aspartame, and caffeine in a diet soda. The following information is available.

	t_r in aqueous mobile phase of pH			
compound	3.0	3.5	4.0	4.5
benzoic acid	7.4	7.0	6.9	4.4
aspartame	5.9	6.0	7.1	8.1
caffeine	3.6	3.7	4.1	4.4

(a) Explain the change in each compound's retention time.

(b) Prepare a single graph that shows retention time versus pH for each compound. Using your plot, identify a pH level that will yield an acceptable separation.

22. The composition of a multivitamin tablet is determined using an HPLC with a diode array UV/Vis detector. A 5-µL standard sample that contains 170 ppm vitamin C, 130 ppm niacin, 120 ppm niacinamide, 150 ppm pyridoxine, 60 ppm thiamine, 15 ppm folic acid, and 10 ppm riboflavin is injected into the HPLC, giving signals (in arbitrary units) of, respectively, 0.22, 1.35, 0.90, 1.37, 0.82, 0.36, and 0.29. The multivitamin tablet is prepared for analysis by grinding into a powder and transferring to a 125-mL Erlenmeyer flask that contains 10 mL of 1% v/v NH_3 in dimethyl sulfoxide. After sonicating in an ultrasonic bath for 2 min, 90 mL of 2% acetic acid is added and the mixture is stirred for 1 min and sonicated at 40°C for 5 min. The extract is then filtered through a 0.45-µm membrane filter. Injection of a 5-µL sample into the HPLC gives signals of 0.87 for vitamin C, 0.00 for niacin, 1.40 for niacinamide, 0.22 for pyridoxine, 0.19 for thiamine, 0.11 for folic acid, and 0.44 for riboflavin. Report the milligrams of each vitamin present in the tablet.

23. The amount of caffeine in an analgesic tablet was determined by HPLC using a normal calibration curve. Standard solutions of caffeine were prepared and analyzed using a 10-µL fixed-volume injection loop. Results for the standards are summarized in the following table.

concentration (ppm)	signal (arb. units)
50.0	8.354
100.0	16925
150.0	25218
200.0	33584
250.0	42002

The sample is prepared by placing a single analgesic tablet in a small beaker and adding 10 mL of methanol. After allowing the sample to dissolve, the contents of the beaker, including the insoluble binder, are quantitatively transferred to a 25-mL volumetric flask and diluted to volume with methanol. The sample is then filtered, and a 1.00-mL aliquot transferred to a 10-mL volumetric flask and diluted to volume with methanol. When analyzed by HPLC, the signal for caffeine is found to be 21 469. Report the milligrams of caffeine in the analgesic tablet.

24. Kagel and Farwell report a reversed-phase HPLC method for determining the concentration of acetylsalicylic acid (ASA) and caffeine (CAF) in analgesic tablets using salicylic acid (SA) as an internal standard [Kagel, R. A.; Farwell, S. O. *J. Chem. Educ.* **1983**, *60*, 163–166]. A series of standards was prepared by adding known amounts of ace- tylsalicylic acid and caffeine to 250-mL Erlenmeyer flasks and adding 100 mL of methanol. A 10.00-mL aliquot of a standard solution of salicylic acid was then added to each. The following results were obtained for a typical set of standard solutions.

	milligrams of		peak height ratios for	
standard	ASA	CAF	ASA/SA	CAF/SA
1	200.0	20.0	20.5	10.6
2	250.0	40.0	25.1	23.0
3	300.0	60.0	30.9	36.8

A sample of an analgesic tablet was placed in a 250-mL Erlenmeyer flask and dissolved in 100 mL of methanol. After adding a 10.00-mL portion of the internal standard, the solution was filtered. Analysis of the sample gave a peak height ratio of 23.2 for ASA and of 17.9 for CAF.

(a) Determine the milligrams of ASA and CAF in the tablet.

(b) Why is it necessary to filter the sample?

(c) The directions indicate that approximately 100 mL of methanol is used to dissolve the standards and samples. Why is it not necessary to measure this volume more precisely?

(d) In the presence of moisture, ASA decomposes to SA and acetic acid. What complication might this present for this analysis? How might you evaluate whether this is a problem?

25. Bohman and colleagues described a reversed-phase HPLC method for the quantitative analysis of vitamin A in food using the method of standard additions Bohman, O.; Engdahl, K. A.; Johnsson, H. *J. Chem. Educ.* **1982**, *59*, 251–252]. In a typical example, a 10.067-g sample of cereal is placed in a 250-mL Erlenmeyer flask along with 1 g of sodium ascorbate, 40 mL of ethanol, and 10 mL of 50% w/v KOH. After refluxing for 30 min, 60 mL of ethanol is added and the solution cooled to room temperature. Vitamin A is extracted using three 100-mL portions of hexane. The combined portions of hexane are evaporated and the residue containing vitamin A transferred to a 5-mL volumetric flask and diluted to volume with methanol. A standard addition is prepared in a similar manner using a 10.093-g sample of the cereal and spiking with 0.0200 mg of vitamin A. Injecting the sample and standard addition into the HPLC gives peak areas of, respectively, $\mathbf{6.77 \times 10^3}$ and $\mathbf{1.32 \times 10^4}$. Report the vitamin A content of the sample in milligrams/100 g cereal.

26. Ohta and Tanaka reported on an ion-exchange chromatographic method for the simultaneous analysis of several inorganic anions and the cations Mg^{2+} and Ca^{2+} in water [Ohta, K.; Tanaka, K. *Anal. Chim. Acta* **1998**, *373*, 189–195]. The mobile phase includes the ligand 1,2,4-benzenetricarboxylate, which absorbs strongly at 270 nm. Indirect detection of the analytes is possible because its absorbance decreases when complexed with an anion.

(a) The procedure also calls for adding the ligand EDTA to the mobile phase. What role does the EDTA play in this analysis?

(b) A standard solution of 1.0 mM $NaHCO_3$, 0.20 mM $NaNO_2$, 0.20 mM $MgSO_4$, 0.10 mM $CaCl_2$, and 0.10 mM $Ca(NO_3)_2$ gives the following peak areas (arbitrary units).

ion	$\mathbf{HCO_3^-}$	Cl^-	$\mathbf{NO_2^-}$	$\mathbf{NO_3^-}$
peak area	373.5	322.5	264.8	262.7
ion	Ca^{2+}	Mg^{2+}	$\mathbf{SO_4^{2-}}$	
peak area	458.9	352.0	341.3	

Analysis of a river water sample (pH of 7.49) gives the following results.

ion	$\mathbf{HCO_3^-}$	Cl^-	$\mathbf{NO_2^-}$	$\mathbf{NO_3^-}$
peak area	310.0	403.1	3.97	157.6
ion	Ca^{2+}	Mg^{2+}	$\mathbf{SO_4^{2-}}$	
peak area	734.3	193.6	324.3	

Determine the concentration of each ion in the sample.

(c) The detection of $\mathbf{HCO_3^-}$ actually gives the total concentration of carbonate in solution ($[\mathbf{CO_3^{2-}}]+[\mathbf{HCO_3^-}]+[H_2CO_3]$). Given that the pH of the water is 7.49, what is the actual concentration of $\mathbf{HCO_3^-}$?

(d) An independent analysis gives the following additional concentrations for ions in the sample: $[Na^+]$ = 0.60 mM; $[\mathbf{NH_4^+}]$ = 0.014 mM; and $[K^+]$ = 0.046 mM. A solution's ion balance is defined as the ratio of the total cation charge to the total anion charge. Determine the charge balance for this sample of water and comment on whether the result is reasonable.

27. The concentrations of Cl^-, $\mathbf{NO_2^-}$, and $\mathbf{SO_4^{2-}}$ are determined by ion chromatography. A 50-µL standard sample of 10.0 ppm Cl^-, 2.00 ppm $\mathbf{NO_2^-}$, and 5.00 ppm $\mathbf{SO_4^{2-}}$ gave signals (in arbitrary units) of 59.3, 16.1, and 6.08 respectively. A sample of effluent from a wastewater treatment plant is diluted tenfold and a 50-µL portion gives signals of 44.2 for Cl^-, 2.73 for $\mathbf{NO_2^-}$, and 5.04 for $\mathbf{SO_4^{2-}}$. Report the parts per million for each anion in the effluent sample.

28. A series of polyvinylpyridine standards of different molecular weight was analyzed by size-exclusion chromatography, yielding the following results.

formula weight	retention volume (mL)
600000	6.42
100000	7.98
30000	9.30
3000	10.94

When a preparation of polyvinylpyridine of unknown formula weight is analyzed, the retention volume is 8.45 mL. Report the average formula weight for the preparation.

29. Diet soft drinks contain appreciable quantities of aspartame, benzoic acid, and caffeine. What is the expected order of elution for these compounds in a capillary zone electrophoresis separation using a pH 9.4 buffer given that aspartame has pK_a values of 2.964 and 7.37, benzoic acid has a pK_a of 4.2, and the pK_a for caffeine is less than 0. Figure 12.8.3 provides the structures of these compounds.

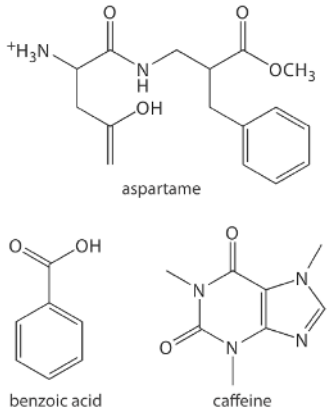


Figure 12.8.3
. Structures for the compounds in Problem 29.

30. Janusa and coworkers describe the determination of chloride by CZE [Janusa, M. A.; Andermann, L. J.; Kliebert, N. M.; Nannie, M. H. *J. Chem. Educ.* **1998**, *75*, 1463–1465]. Analysis of a series of external standards gives the following calibration curve.

$$\text{area} = -883 + 5590 \times \text{ppm } Cl^-$$

A standard sample of 57.22% w/w Cl^- is analyzed by placing 0.1011-g portions in separate 100-mL volumetric flasks and diluting to volume. Three unknowns are prepared by pipeting 0.250 mL, 0.500 mL, an 0.750 mL of the bulk unknown in separate 50-mL volumetric flasks and diluting to volume. Analysis of the three unknowns gives areas of 15 310, 31 546, and 47 582, respectively. Evaluate the accuracy of this analysis.

31. The analysis of NO_3^- in aquarium water is carried out by CZE using IO_4^- as an internal standard. A standard solution of 15.0 ppm NO_3^- and 10.0 ppm IO_4^- gives peak heights (arbitrary units) of 95.0 and 100.1, respectively. A sample of water from an aquarium is diluted 1:100 and sufficient internal standard added to make its concentration 10.0 ppm in IO_4^-. Analysis gives signals of 29.2 and 105.8 for NO_3^- and IO_4^-, respectively. Report the ppm NO_3^- in the sample of aquarium water.

32. Suggest conditions to separate a mixture of 2-aminobenzoic acid (pK_{a1} = 2.08, pK_{a2} = 4.96), benzylamine (pK_a = 9.35), and 4-methylphenol (pK_{a2} = 10.26) by capillary zone electrophoresis. Figure ***PageIndex4*** provides the structures of these compounds.

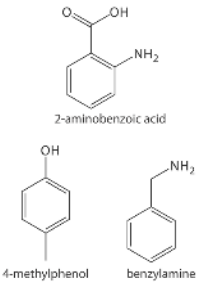


Figure 12.8.4 . Structures for the compounds in Problem 32.

33. McKillop and associates examined the electrophoretic separation of some alkylpyridines by CZE [McKillop, A. G.; Smith, R. M.; Rowe, R. C.; Wren, S. A. C. *Anal. Chem.* **1999**, *71*, 497–503]. Separations were carried out using either 50-µm or 75-µm inner diameter capillaries, with a total length of 57 cm and a length of 50 cm from the point of injection to the detector. The run buffer was a pH 2.5 lithium phosphate buffer. Separations were achieved using an applied voltage of 15 kV. The electroosmotic mobility, μ_{eof}, as measured using a neutral marker, was found to be $\mathbf{6.398 \times 10^{-5}}$ $cm^2\ V^{-1}\ s^{-1}$. The diffusion coefficient for alkylpyridines is $\mathbf{1.0 \times 10^{-5}}$ $cm^2\ s^{-1}$.

(a) Calculate the electrophoretic mobility for 2-ethylpyridine given that its elution time is 8.20 min.

(b) How many theoretical plates are there for 2-ethylpyridine?

(c) The electrophoretic mobilities for 3-ethylpyridine and 4-ethylpyridine are $\mathbf{3.366 \times 10^{-4}}$ $cm^2\ V^{-1}\ s^{-1}$ and $\mathbf{3.397 \times 10^{-4}}$ $\mathbf{cm^2\ V^{-1}\ s^{-1}}$, respectively. What is the expected resolution between these two alkylpyridines?

(d) Explain the trends in electrophoretic mobility shown in the following table.

alkylpyridine	μ_{ep} ($cm^2\ V^{-1}\ s^{-1}$)
2-methylpyridine	$\mathbf{3.581 \times 10^{-4}}$
2-ethylpyridine	$\mathbf{3.222 \times 10^{-4}}$
2-propylpyridine	$\mathbf{2.923 \times 10^{-4}}$
2-pentylpyridine	$\mathbf{2.534 \times 10^{-4}}$
2-hexylpyridine	$\mathbf{2.391 \times 10^{-4}}$

(e) Explain the trends in electrophoretic mobility shown in the following table.

alkylpyridine	μ_{ep} ($cm^2\ V^{-1}\ s^{-1}$)
2-ethylpyridine	$\mathbf{3.222 \times 10^{-4}}$
3-ethylpyridine	$\mathbf{3.366 \times 10^{-4}}$
4-ethylpyridine	$\mathbf{3.397 \times 10^{-4}}$

(f) The pK_a for pyridine is 5.229. At a pH of 2.5 the electrophoretic mobility of pyridine is $\mathbf{4.176 \times 10^{-4}}$ $cm^2\ V^{-1}\ s^{-1}$. What is the expected electrophoretic mobility if the run buffer's pH is 7.5?

This page titled 2.8: Problems is shared under a CC BY-NC-SA 4.0 license and was authored, remixed, and/or curated by David Harvey.

- **12.8: Problems** by David Harvey is licensed CC BY-NC-SA 4.0.

2.9: Additional Resources

The following set of experiments introduce students to the applications of chromatography and electrophoresis. Experiments are grouped into five categories: gas chromatography, high-performance liquid chromatography, ion-exchange chromatography, size-exclusion chromatography, and electrophoresis.

Gas Chromatography

- Bishop, R. D., Jr. "Using GC–MS to Determine Relative Reactivity Ratios," *J. Chem. Educ.* **1995**, *72*, 743–745.
- Elderd, D. M.; Kildahl, N. K.; Berka, L. H. "Experiments for Modern Introductory Chemistry: Identification of Arson Accelerants by Gas Chromatography," *J. Chem. Educ.* **1996**, *73*, 675–677.
- Fleurat-Lessard, P.; Pointet, K.; Renou-Gonnord, M.-F. "Quantitative Determination of PAHs in Diesel Engine Exhausts by GC–MS," *J. Chem. Educ.* **1999**, *76*, 962–965.
- Galipo, R. C.; Canhoto, A. J.; Walla, M. D.; Morgan, S. L. "Analysis of Volatile Fragrance and Flavor Compounds by Headspace Solid Phase Microextraction and GC–MS," *J. Chem. Educ.* **1999**, *76*, 245–248.
- Graham, R. C.; Robertson, J. K. "Analysis of Trihalomethanes in Soft Drinks," *J. Chem. Educ.* **1988**, *65*, 735–737.
- Heinzen, H.; Moyan, P.; Grompone, A. "Gas Chromatographic Determination of Fatty Acid Compositions," *J. Chem. Educ.* **1985**, *62*, 449–450.
- Kegley, S. E.; Hansen, K. J.; Cunningham, K. L. "Determination of Polychlorinated Biphenyls (PCBs) in River and Bay Sediments," *J. Chem. Educ.* **1996**, *73*, 558–562.
- Kostecka, K. S.; Rabah, A.; Palmer, C. F., Jr. "GC/MS Analysis of the Aromatic Composition of Gasoline," *J. Chem. Educ.* **1995**, *72*, 853–854.
- Quach, D. T.; Ciszkowski, N. A.; Finlayson-Pitts, B. J. "A New GC-MS Experiment for the Undergraduate Instrumental Analysis Laboratory in Environmental Chemistry: Methyl-t-butyl Ether and Benzene in Gasoline," *J. Chem. Educ.* **1998**, *75*, 1595–1598.
- Ramachandran, B. R.; Allen, J. M.; Halpern, A. M. "Air–Water Partitioning of Environmentally Important Organic Compounds," *J. Chem. Educ.* **1996**, *73*, 1058–1061.
- Rice, G. W. "Determination of Impurities in Whiskey Using Internal Standard Techniques," *J. Chem. Educ.* **1987**, *64*, 1055–1056.
- Rubinson, J. F.; Neyer-Hilvert, J. "Integration of GC-MS Instrumentation into the Undergraduate Laboratory: Separation and Identification of Fatty Acids in Commercial Fats and Oils," *J. Chem. Educ.* **1997**, *74*, 1106–1108.
- Rudzinski, W. E.; Beu, S. "Gas Chromatographic Determination of Environmentally Significant Pesticides," *J. Chem. Educ.* **1982**, *59*, 614–615.
- Sobel, R. M.; Ballantine, D. S.; Ryzhov, V. "Quantitation of Phenol Levels in Oil of Wintergreen Using Gas Chromatography–Mass Spectrometry with Selected Ion Monitoring," *J. Chem. Educ.* **2005**, *82*, 601–603.
- Welch, W. C.; Greco, T. G. "An Experiment in Manual Multiple Headspace Extraction for Gas Chromatography," *J. Chem. Educ.* **1993**, *70*, 333–335.
- Williams, K. R.; Pierce, R. E. "The Analysis of Orange Oil and the Aqueous Solubility of d-Limone," *J. Chem. Educ.* **1998**, *75*, 223–226.
- Wong, J. W.; Ngim, K. K.; Shibamoto, T.; Mabury, S. A.; Eiserich, J. P.; Yeo, H. C. H. "Determination of Formaldehyde in Cigarette Smoke," *J. Chem. Educ.* **1997**, *74*, 1100–1103.
- Yang, M. J.; Orton, M. L., Pawliszyn, J. "Quantitative Determination of Caffeine in Beverages Using a Combined SPME-GC/MS Method," *J. Chem. Educ.* **1997**, *74*, 1130–1132.

High-Performance Liquid Chromatography

- Batchelor, J. D.; Jones, B. T. "Determination of the Scoville Heat Value for Hot Sauces and Chilies: An HPLC Experiment," *J. Chem. Educ.* **2000**, *77*, 266–267.
- Beckers, J. L. "The Determination of Caffeine in Coffee: Sense or Nonsense?" *J. Chem. Educ.* **2004**, *81*, 90–93.
- Betts, T. A. "Pungency Quantitation of Hot Pepper Sauces Using HPLC," *J. Chem. Educ.* **1999**, *76*, 240–244.
- Bidlingmeyer, B. A.; Schmitz, S. "The Analysis of Artificial Sweeteners and Additives in Beverages by HPLC," *J. Chem. Educ.* **1991**, *68*, A195–A200.

- Bohman, O.; Engdahl, K.-A.; Johnsson, H. “High Performance Liquid Chromatography of Vitamin A: A Quantitative Determination,” *J. Chem. Educ.* **1982**, *59*, 251–252.
- Brenneman, C. A.; Ebeler, S. E. “Chromatographic Separations Using Solid-Phase Extraction Cartridges: Separation of Wine Phenolics,” *J. Chem. Educ.* **1999**, *76*, 1710–1711.
- Cantwell, F. F.; Brown, D. W. “Liquid Chromatographic Determination of Nitroanilines,” *J. Chem. Educ.* **1981**, *58*, 820–823.
- DiNunzio, J. E. “Determination of Caffeine in Beverages by High Performance Liquid Chromatography,” *J. Chem. Educ.* **1985**, *62*, 446–447.
- Ferguson, G. K. “Quantitative HPLC Analysis of an Analgesic/Caffeine Formulation: Determination of Caffeine,” *J. Chem. Educ.* **1998**, *75*, 467–469.
- Ferguson, G. K. “Quantitative HPLC Analysis of a Psychotherapeutic Medication: Simultaneous Determination of Amitriptyline Hydrochloride and Perphenazine,” *J. Chem. Educ.* **1998**, *75*, 1615–1618.
- Goodney, D. E. “Analysis of Vitamin C by High-Pressure Liquid Chromatography,” *J. Chem. Educ.* **1987**, *64*, 187–188.
- Guevremont, R.; Quigley, M. N. “Determination of Paralytic Shellfish Poisons Using Liquid Chromatography,” *J. Chem. Educ.* **1994**, *71*, 80–81.
- Haddad, P.; Hutchins, S.; Tuffy, M. “High Performance Liquid Chromatography of Some Analgesic Compounds,” *J. Chem. Educ.* **1983**, *60*, 166–168.
- Huang, J.; Mabury, S. A.; Sagebiel, J. C. “Hot Chili Peppers: Extraction, Cleanup, and Measurement of Capscaicin,” *J. Chem. Educ.* **2000**, *77*, 1630–1631.
- Joeseph, S. M.; Palasota, J. A. “The Combined Effect of pH and Percent Methanol on the HPLC Separation of Benzoic Acid and Phenol,” *J. Chem. Educ.* **2001**, *78*, 1381–1383.
- Lehame, S. “The Separation of Copper, Iron, and Cobalt Tetramethylene Dithiocarbamates by HPLC,” *J. Chem. Educ.* **1986**, *63*, 727–728.
- Luo, P.; Luo, M. Z.; Baldwin, R. P. “Determination of Sugars in Food Products,” *J. Chem. Educ.* **1993**, *70*, 679–681.
- Mueller, B. L.; Potts, L. W. “HPLC Analysis of an Asthma Medication,” *J. Chem. Educ.* **1988**, *65*, 905–906.
- Munari, M.; Miurin, M.; Goi, G. “Didactic Application to Riboflavin HPLC Analysis,” *J. Chem. Educ.* **1991**, *68*, 78–79.
- Orth, D. L. “HPLC Determination of Taurine in Sports Drinks,” *J. Chem. Educ.* **2001**, *78*, 791– 792.
- Remcho, V. T.; McNair, H. M.; Rasmussen, H. T. “HPLC Method Development with the Photodiode Array Detector,” *J. Chem. Educ.* **1992**, *69*, A117–A119.
- Richardson, W. W., III; Burns, L. “HPLC of the Polypeptides in a Hydrolyzate of Egg-White Lysozyme,” *J. Chem. Educ.* **1988**, *65*, 162–163.
- Silveira, A., Jr.; Koehler, J. A.; Beadel, E. F., Jr.; Monore, P. A. “HPLC Analysis of Chlorophyll a, Chlorophyll b, and β-Carotene in Collard Greens,” *J. Chem. Educ.* **1984**, *61*, 264–265.
- Siturmorang, M.; Lee, M. T. B.; Witzeman, L. K.; Heineman, W. R. “Liquid Chromatography with Electrochemical Detection (LC-EC): An Experiment Using 4-Aminophenol,” *J. Chem. Educ.* **1998**, *75*, 1035–1038.
- Sottofattori, E.; Raggio, R.; Bruno, O. “Milk as a Drug Analysis Medium: HPLC Determination of Isoniazid,” *J. Chem. Educ.* **2003**, *80*, 547–549.
- Strohl, A. N. “A Study of Colas: An HPLC Experiment,” *J. Chem. Educ.* **1985**, *62*, 447–448.
- Tran, C. D.; Dotlich, M. “Enantiomeric Separation of Beta-Blockers by High Performance Liquid Chromatography,” *J. Chem. Educ.* **1995**, *72*, 71–73.
- Van Arman, S. A.; Thomsen, M. W. “HPLC for Undergraduate Introductory Laboratories,” *J. Chem. Educ.* **1997**, *74*, 49–50.
- Wingen, L. M.; Low, J. C.; Finlayson-Pitts, B. J. “Chromatography, Absorption, and Fluorescence: A New Instrumental Analysis Experiment on the Measurement of Polycyclic Aromatic Hydrocarbons in Cigarette Smoke,” *J. Chem. Educ.* **1998**, *75*, 1599–1603.

Ion-Exchange Chromatography

- Bello, M. A.; Gustavo González, A. “Determination of Phosphate in Cola Beverages Using Nonsuppressed Ion Chromatography,” *J. Chem. Educ.* **1996**, *73*, 1174–1176.
- Kieber, R. J.; Jones, S. B. “An Undergraduate Laboratory for the Determination of Sodium, Potassium, and Chloride,” *J. Chem. Educ.* **1994**, *71*, A218–A222.
- Koubek, E.; Stewart, A. E. “The Analysis of Sulfur in Coal,” *J. Chem. Educ.* **1992**, *69*, A146–A148.

- Sinniah, K.; Piers, K. “Ion Chromatography: Analysis of Ions in Pond Water,” *J. Chem. Educ.* **2001**, *78*, 358–362.
- Xia, K.; Pierzynski, G. “Competitive Sorption between Oxalate and Phosphate in Soil: An Environmental Chemistry Laboratory Using Ion Chromatography,” *J. Chem. Educ.* **2003**, *80*, 71–75.

Size-Exchange Chromatography

- Brunauer, L. S.; Davis, K. K. “Size Exclusion Chromatography: An Experiment for High School and Community College Chemistry and Biotechnology Laboratory Programs,” *J. Chem. Educ.* **2008**, *85*, 683–685.
- Saiz, E.; Tarazona, M. P. “Size-Exclusion Chromatography Using Dual Detection,” *Chem. Educator* **2000**, *5*, 324–328.

Electrophoresis

- Almarez, R. T.; Kochis, M. “Microscale Capillary Electrophoresis: A Complete Instrumentation Experiment for Chemistry Students at the Undergraduate Junior or Senior Level,” *J. Chem. Educ.* **2003**, *80*, 316–319.
- Beckers, J. L. “The Determination of Caffeine in Coffee: Sense or Nonsense?” *J. Chem. Educ.* **2004**, *81*, 90–93.
- Beckers, J. L. “The Determination of Vanillin in a Vanilla Extract,” *J. Chem. Educ.* **2005**, *82*, 604– 606.
- Boyce, M. “Separation and Quantification of Simple Ions by Capillary Zone Electrophoresis,” *J. Chem. Educ.* **1999**, *76*, 815–819.
- Conradi, S.; Vogt, C.; Rohde, E. “Separation of Enatiomeric Barbiturates by Capillary Electrophoresis Using a Cyclodextrin-Containing Run Buffer,” *J. Chem. Educ.* **1997**, *74*, 1122–1125.
- Conte, E. D.; Barry, E. F.; Rubinstein, H. “Determination of Caffeine in Beverages by Capillary Zone Electrophoresis,” *J. Chem. Educ.* **1996**, *73*, 1169–1170.
- Demay, S.; Martin-Girardeau, A.; Gonnord, M.-F. “Capillary Electrophoretic Quantitative Analysis of Anions in Drinking Water,” *J. Chem. Educ.* **1999**, *76*, 812–815.
- Emry, R.; Cutright, R. D.; Wright, J.; Markwell, J. “Candies to Dye for: Cooperative, Open-Ended Student Activities to Promote Understanding of Electrophoretic Fractionation,” *J. Chem. Educ.* **2000**, *77*, 1323–1324.
- Gardner, W. P.; Girard, J. E. “Analysis of Common Household Cleaner-Disinfectants by Capillary Electrophoresis,” *J. Chem. Educ.* **2000**, *77*, 1335–1338.
- Gruenhagen, J. A.; Delaware, D.; Ma, Y. “Quantitative Analysis of Non-UV-Absorbing Cations in Soil Samples by High-Performance Capillary Electrophoresis,” *J. Chem. Educ.* **2000**, *77*, 1613–1616.
- Hage, D. S.; Chattopadhyay, A.; Wolfe, C. A. C.; Grundman, J.; Kelter, P. B. “Determination of Nitrate and Nitrite in Water by Capillary Electrophoresis,” *J. Chem. Educ.* **1998**, *75*, 1588–1590.
- Herman, H. B.; Jezorek, J. R.; Tang, Z. “Analysis of Diet Tonic Water Using Capillary Electrophoresis,” *J. Chem. Educ.* **2000**, *77*, 743–744.
- Janusa, M. A.; Andermann, L. J.; Kliebert, N. M.; Nannie, M. H. “Determination of Chloride Concentration Using Capillary Electrophoresis,” *J. Chem. Educ.* **1998**, *75*, 1463–1465.
- McDevitt, V. L.; Rodríguez, A.; Williams, K. R. “Analysis of Soft Drinks: UV Spectrophotometry, Liquid Chromatography, and Capillary Electrophoresis,” *J. Chem. Educ.* **1998**, *75*, 625–629.
- Palmer, C. P. “Demonstrating Chemical and Analytical Concepts in the Undergraduate Laboratory Using Capillary Electrophoresis and Micellar Electrokinetic Chromatography,” *J. Chem. Educ.* **1999**, *76*, 1542–1543.
- Pursell, C. J.; Chandler, B.; Bushey, M. M. “Capillary Electrophoresis Analysis of Cations in Water Samples,” *J. Chem. Educ.* **2004**, *81*, 1783–1786.
- Solow, M. “Weak Acid p*K*a Determination Using Capillary Zone Electrophoresis,” *J. Chem. Educ.* **2006**, *83*, 1194–1195.
- Thompson, L.; Veening, H.; Strain, T. G. “Capillary Electrophoresis in the Undergraduate Instrumental Analysis Laboratory: Determination of Common Analgesic Formulations,” *J. Chem. Educ.* **1997**, *74*, 1117–1121.
- Vogt, C.; Conradi, S.; Rhode, E. “Determination of Caffeine and Other Purine Compounds in Food and Pharmaceuticals by Micellar Electrokinetic Chromatography” *J. Chem. Educ.* **1997**, *74*, 1126– 1130.
- Weber, P. L.; Buck, D. R. “Capillary Electrophoresis: A Fast and Simple Method for the Determination of the Amino Acid Composition of Proteins,” *J. Chem. Educ.* **1994**, *71*, 609–612.
- Welder, F.; Colyer, C. L. “Using Capillary Electrophoresis to Determine the Purity of Acetylsalicylic Acid Synthesized in the Undergraduate Laboratory,” *J. Chem. Educ.* **2001**, *78*, 1525–1527.

- Williams, K. R.; Adhyaru, B.; German, I.; Russell, T. “Determination of a Diffusion Coefficient by Capillary Electrophoresis,” *J. Chem. Educ.* **2002**, *79*, 1475–1476.

The following texts provide a good introduction to the broad field of separations, including chromatography and electrophoresis.

- Giddings, J. C. *Unified Separation Science*, Wiley-Interscience: New York 1991.
- Karger, B. L.; Snyder, L. R.; Harvath, C. *An Introduction to Separation Science*, Wiley-Interscience: New York, 1973
- Miller, J. M. *Separation Methods in Chemical Analysis*, Wiley-Interscience: New York, 1975.
- Poole, C. F. *The Essence of Chromatography*, Elsevier: Amsterdam, 2003.

A more recent discussion of peak capacity is presented in the following papers.

- Chester, T. L. “Further Considerations of Exact Equations for Peak Capacity in Isocratic Liquid Chromatography,” *Anal. Chem.* **2014**, *86*, 7239–7241.
- Davis, J. M.; Stoll, D. R.; Carr, P. W. “Dependence of Effective Peak Capacity in Comprehensive Two-Dimensional Separations on the Distribution of Peak Capacity between the Two Dimensions,” *Anal. Chem.* **2008**, *80*, 8122–8134.
- Li, X.; Stoll, D. R.; Carr, P. W. “Equation for Peak Capacity Estimation in Two-Dimensional Liquid Chromatography,” *Anal. Chem.* **2009**, *81*, 845–850.
- Shen, Y.; Lee, M. “General Equation for Peak Capacity in Column Chromatography,” *Anal. Chem*. **1998**, *70*, 3853–3856.

The following references may be consulted for more information on gas chromatography.

- Grob, R. L., ed, *Modern Practice of Gas Chromatography*, Wiley-Interscience: New York, 1972.
- Hinshaw, J. V. “A Compendium of GC Terms and Techniques,” *LC•GC* **1992**, *10*, 516–522.
- Ioffe, B. V.; Vitenberg, A. G. *Head-Space Analysis and Related Methods in Gas Chromatography*, Wiley-Interscience: New York, 1982.
- Kitson, F. G.; Larsen, B. S.; McEwen, C. N. *Gas Chromatography and Mass Spectrometry: A Practical Guide*, Academic Press: San Diego, 1996.
- McMaster, M. C. *GC/MS: A Practical User’s Guide*, Wiley-Interscience: Hoboken, NJ, 2008.

The following references provide more information on high-performance liquid chromatography.

- Dorschel, C. A.; Ekmanis, J. L.; Oberholtzer, J. E.; Warren, Jr. F. V.; Bidlingmeyer, B. A. “LC Detectors,” *Anal. Chem.* **1989**, *61*, 951A–968A.
- Ehlert, S.; Tallarek, U. “High-pressure liquid chromatography in lab-on-a-chip devices,” *Anal. Bioanal. Chem.* **2007**, *388*, 517–520.
- Francois, I.; Sandra, K.; Sandra, P. “Comprehensive liquid chromatography: Fundamental aspects and practical considerations—A review,” *Anal. Chim. Acta* **2009**, *641*, 14–31.
- Harris, C. M. “Shrinking the LC Landscape,” *Anal. Chem.* **2003**, *75*, 64A–69A.
- Meyer, V. R. *Pitfalls and Errors of HPLC in Pictures*, Wiley-VCH: Weinheim, Germany, 2006.
- Pozo, O. J.; Van Eenoo, P.; Deventer, K.; Delbeke, F. T. “Detection and characterization of anabolic steroids in doping analysis by LC–MS,” *Trends Anal. Chem.* **2008**, *27*, 657–671.
- Scott, R. P. W. “Modern Liquid Chromatography,” *Chem. Soc. Rev.* **1992**, *21*, 137–145.
- Simpson, C. F., ed. *Techniques in Liquid Chromatography*, Wiley-Hayden: Chichester, England; 1982.
- Snyder, L. R.; Glajch, J. L.; Kirkland, J. J. *Practical HPLC Method Development*, Wiley-Interscience: New York,1988.
- van de Merbel, N. C. “Quantitative determination of endogenous compounds in biological samples using chromatographic techniques,” *Trends Anal. Chem.* **2008**, *27*, 924–933.
- Yeung, E. S. “Chromatographic Detectors: Current Status and Future Prospects,” *LC•GC* **1989**, *7*, 118–128.

The following references may be consulted for more information on ion chromatography.

- Shpigun, O. A.; Zolotov, Y. A. *Ion Chromatography in Water Analysis*, Ellis Horwood: Chichester, England, 1988.
- Smith, F. C. Jr.; Chang, R. C. *The Practice of Ion Chromatography*, Wiley-Interscience: New York, 1983.

The following references may be consulted for more information on supercritical fluid chromatography.

- Palmieri, M. D. “An Introduction to Supercritical Fluid Chromatography. Part I: Principles and Applications,” *J. Chem. Educ.* **1988**, *65*, A254–A259.
- Palmieri, M. D. “An Introduction to Supercritical Fluid Chromatography. Part II: Applications and Future Trends,” *J. Chem. Educ.* **1989**, *66*, A141–A147.

The following references may be consulted for more information on capillary electrophoresis.

- Baker, D. R. *Capillary Electrophoresis*, Wiley-Interscience: New York, 1995.
- Copper, C. L. “Capillary Electrophoresis: Part I. Theoretical and Experimental Background,” *J. Chem. Educ.* **1998**, *75*, 343–347.
- Copper, C. L.; Whitaker, K. W. “Capillary Electrophoresis: Part II. Applications,” *J. Chem. Educ.* **1998**, *75*, 347–351.
- DeFrancesco, L. “Capillary Electrophoresis: Finding a Niche,” *Today’s Chemist at Work*, February 2002, 59–64.
- Ekins, R. P. “Immunoassay, DNA Analysis, and Other Ligand Binding Assay Techniques: From Electropherograms to Multiplexed, Ultrasensative Microarrays on a Chip,” *J. Chem. Educ.* **1999**, *76*, 769– 780.
- Revermann, T.; Götz, S.; Künnemeyer, J.; Karst, U. “Quantitative analysis by microchip capillary electrophoresis—current limitations and problem-solving strategies,” *Analyst* **2008**, *133*, 167–174.
- Timerbaev, A. R. “Capillary electrophoresis coupled to mass spectrometry for biospeciation analysis: critical evaluation,” *Trends Anal. Chem.* **2009**, *28*, 416–425.
- Unger, K. K.; Huber, M.; Hennessy, T. P.; Hearn, M. T. W.; Walhagen, K. “A Critical Appraisal of Capillary Electrochromatography,” *Anal. Chem.* **2002**, *74*, 200A–207A.
- Varenne, A.; Descroix, S. “Recent strategies to improve resolution in capillary electrophoresis—A review,” *Anal. Chim. Acta* **2008**, *628*, 9–23.
- Vetter, A. J.; McGowan, G. J. “The Escalator—An Analogy for Explaining Electroosmotic Flow,” J. Chem. Educ. 2001, 78, 209–211.
- Xu, Y. “Tutorial: Capillary Electrophoresis,” *Chem. Educator*, **1996**, *1(2)*, 1–14.

The application of spreadsheets and computer programs for modeling chromatography is described in the following papers.

- Abbay, G. N.; Barry, E. F.; Leepipatpiboon, S.; Ramstad, T.; Roman, M. C.; Siergiej, R. W.; Snyder, L. R.; Winniford, W. L. “Practical Applications of Computer Simulation for Gas Chromatography Method Development,” *LC•GC* **1991**, *9*, 100–114.
- Drouen, A.; Dolan, J. W.; Snyder, L. R.; Poile, A.; Schoenmakers, P. J. “Software for Chromatographic Method Development,” *LC•GC* **1991**, *9*, 714–724.
- Kevra, S. A.; Bergman, D. L.; Maloy, J. T. “A Computational Introduction to Chromatographic Bandshape Analysis,” *J. Chem. Educ.* **1994**, *71*, 1023–1028.
- Rittenhouse, R. C. “HPLC for Windows: A Computer Simulation of High-Performance Liquid Chromatography,” *J. Chem. Educ.* **1995**, *72*, 1086–1087.
- Shalliker, R. A.; Kayillo, S.; Dennis, G. R. “Optimizing Chromatographic Separations: An Experiment Using an HPLC Simulator,” *J. Chem. Educ.* **2008**, *85*, 1265–1268.
- Sundheim, B. R. “Column Operations: A Spreadsheet Model,” *J. Chem. Educ.* **1992**, *69*, 1003– 1005.

The following papers discuss column efficiency, peak shapes, and overlapping chromatographic peaks.

- Bildingmeyer, B. A.; Warren, F. V., Jr. “Column Efficiency Measurement,” *Anal. Chem.* **1984**, *56*, 1583A–1596A.
- Hawkes, S. J. “Distorted Chromatographic Peaks,” *J. Chem. Educ.* **1994**, *71*, 1032–1033.
- Hinshaw, J. “Pinning Down Tailing Peaks,” *LC•GC* **1992**, *10*, 516–522.
- Meyer, V. K. “Chromatographic Integration Errors: A Closer Look at a Small Peak,” *LC•GC North America* **2009**, *27*, 232–244.
- Reid, V. R.; Synovec, R. E. “High-speed gas chromatography: The importance of instrumentation optimization and the elimination of extra-column band broadening,” *Talanta* **2008**, *76*, 703–717.

This page titled 2.9: Additional Resources is shared under a CC BY-NC-SA 4.0 license and was authored, remixed, and/or curated by David Harvey.

- **12.9: Additional Resources** by David Harvey is licensed CC BY-NC-SA 4.0.

2.10: Chapter Summary and Key Terms

Chapter Summary

Chromatography and electrophoresis are powerful analytical techniques that both separate a sample into its components and provide a means for determining each component's concentration. Chromatographic separations utilize the selective partitioning of the sample's components between a stationary phase that is immobilized within a column and a mobile phase that passes through the column.

The effectiveness of a chromatographic separation is described by the resolution between two chromatographic bands and is a function of each component's retention factor, the column's efficiency, and the column's selectivity. A solute's retention factor is a measure of its partitioning into the stationary phase, with larger retention factors corresponding to more strongly retained solutes. The column's selectivity for two solutes is the ratio of their retention factors, providing a relative measure of the column's ability to retain the two solutes. Column efficiency accounts for those factors that cause a solute's chromatographic band to increase in width during the separation. Column efficiency is defined in terms of the number of theoretical plates and the height of a theoretical plate, the later of which is a function of a number of parameters, most notably the mobile phase's flow rate. Chromatographic separations are optimized by increasing the number of theoretical plates, by increasing the column's selectivity, or by increasing the solute retention factor.

In gas chromatography the mobile phase is an inert gas and the stationary phase is a nonpolar or polar organic liquid that either is coated on a particulate material and packed into a wide-bore column, or coated on the walls of a narrow-bore capillary column. Gas chromatography is useful for the analysis of volatile components.

In high-performance liquid chromatography the mobile phase is either a nonpolar solvent (normal phase) or a polar solvent (reversed-phase). A stationary phase of opposite polarity, which is bonded to a particulate material, is packed into a wide-bore column. HPLC is applied to a wider range of samples than GC; however, the separation efficiency for HPLC is not as good as that for capillary GC.

Together, GC and HPLC account for the largest number of chromatographic separations. Other separation techniques, however, find special- ized applications: of particular importance are ion-exchange chromatography for separating anions and cations; size-exclusion chromatography for separating large molecules; and supercritical fluid chromatography for the analysis of samples that are not easily analyzed by GC or HPLC.

In capillary zone electrophoresis a sample's components are separated based on their ability to move through a conductive medium under the influence of an applied electric field. Positively charged solutes elute first, with smaller, more highly charged cations eluting before larger cations of lower charge. Neutral species elute without undergoing further separation. Finally, anions elute last, with smaller, more negatively charged anions being the last to elute. By adding a surfactant, neutral species can be separated by micellar electrokinetic capillary chromatography. Electrophoretic separations also can take advantage of the ability of polymeric gels to separate solutes by size (capillary gel electrophoresis), and the ability of solutes to partition into a stationary phase (capillary electrochromatography). In comparison to GC and HPLC, capillary electrophoresis provides faster and more efficient separations.

Key Terms

adjusted retention time	adsorption chromatography	band broadening
baseline width	bleed	bonded stationary phase
capillary column	capillary electrochromatography	capillary electrophoresis
capillary gel electrophoresis	capillary zone electrophoresis	chromatogram
chromatography	column chromatography	counter-current extraction
cryogenic focusing	electrokinetic injection	electroosmotic flow
electroosmotic flow velocity	electron capture detector	electropherogram
electrophoresis	electrophoretic mobility	electrophoretic velocity
exclusion limit	flame ionization detector	fronting
gas chromatography	gas–liquid chromatography	gas–solid chromatography
general elution problem	guard column	gradient elution
headspace sampling	high-performance liquid chromatography	hydrodynamic injection
inclusion limit	ion-exchange chromatography	ion suppressor column
isocratic elution	isothermal	Joule heating
Kovat's retention index	liquid–solid adsorption chromatography	longitudinal diffusion
loop injector	mass spectrometer	mass spectrum
mass transfer	micelle	micellar electrokinetic capillary chromatography
mobile phase	monolithic column	
nonretained solutes	normal-phase chromatography	multiple paths
open tubular column	packed columns	on-column injection
peak capacity	planar chromatography	partition chromatography
porous-layer open tubular column	purge-and-trap	polarity index
retention factor	retention time	resolution
selectivity factor	single-column ion chromatography	reversed-phase chromatography
split injection	splitless injection	solid-phase microextraction
stationary phase	supercritical fluid chromatography	stacking
tailing	temperature programming	support-coated open tubular column
thermal conductivity detector	van Deemter equation	theoretical plate
wall-coated open-tubular column	zeta potential	void time

This page titled 2.10: Chapter Summary and Key Terms is shared under a CC BY-NC-SA 4.0 license and was authored, remixed, and/or curated by David Harvey.

- **12.10: Chapter Summary and Key Terms** by David Harvey is licensed CC BY-NC-SA 4.0.

CHAPTER OVERVIEW

3: Mass Spectrometry

Mass spectrometry is an analytic method that employs ionization and mass analysis of compounds in order to determine the mass, formula and structure of the compound being analyzed. A mass analyzer is the component of the mass spectrometer that takes ionized masses and separates them based on charge to mass ratios and outputs them to the detector where they are detected and later converted to a digital output.

3.1: Accelerator Mass Spectroscopy
3.2: Fragmentation Patterns in Mass Spectra
3.3: GC/MS Combination- Shockwave
3.4: How the Mass Spectrometer Works
3.5: Introductory Mass Spectrometry
3.5.1: Fragmentation
3.5.2: High Resolution vs Low Resolution
3.5.3: Introduction to Mass Spectrometry
3.5.4: Isotopes- 13C
3.5.5: Isotopes- Br and Cl
3.5.6: Molecular Ions
3.5.7: Molecular Ion and Nitrogen
3.5.8: The Mass Spectrometry Experiment
3.6: MALDI-TOF
3.7: Mass Spectra
3.7.1: Interpreting a Mass Spectrum
3.7.2: Mass Spectrometry - Fragmentation Patterns
3.7.3: Mass Spectroscopy- Quizzes
3.8: Mass Spectra Interpretation- ALDEHYDES
3.9: Mass Spectrometers (Instrumentation)
3.9.1: Electrospray Ionization Mass Spectrometry
3.9.2: Injection Stage
3.9.3: Mass Analyzers (Mass Spectrometry)
3.10: Mass Spectrometry- Isotope Effects
3.11: Organic Compounds Containing Halogen Atoms
3.12: Selected Ion Monitoring- Shockwave
3.13: The Mass Spectra of Elements
3.14: The Molecular Ion (M^+) Peak
3.15: The M+1 Peak
3.16: Current Applications of Mass Spectrometry

Thumbnail: SIMS mass spectrometer, model IMS 3f. (GNU Free Documentation Licenses; CAMECA Archives).

3: Mass Spectrometry is shared under a not declared license and was authored, remixed, and/or curated by LibreTexts.

3.1: Accelerator Mass Spectroscopy

Accelerator Mass Spectroscopy (AMS) is a highly sensitive technique that is useful in isotopic analysis of specific elements in small samples (1mg or less of sample containing 10^6 atoms or less of the isotope of interest).[1]

Accelerator Mass Spectroscopy

AMS requires a particle accelerator, originally used in nuclear physics research, which limits its widespread use due to high costs and technical complexity. Fortunately, UC Davis researchers have access to the Lawrence Livermore National Laboratory Center for Accelerator Mass Spectrometry (CAMS LLNL), one of over 180 AMS research facilities in the world. AMS is distinct from conventional Mass Spectrometry (MS) because it accelerates ions to extremely high energies (millions of electron volts) compared to the thousands of electron volts in MS (1keV=1.6×10^{-16} J). This allows AMS to resolve ambiguities that arise in MS due to atomic and molecular ions of the same mass. AMS is most widely used for isotope studies of ^{14}C, which has applications in a variety of fields such as radiocarbon dating, climate studies, and biomedical analysis.[2] Some of the most fascinating applications of AMS range from exposure dating of surface rocks, ^{14}C labeled drug tracer studies, and even radiocarbon dating of artifacts such as the Shroud of Turin and the Dead Sea Scrolls.[3]

Theory

In conventional atomic mass spectrometry, samples are atomized and ionized, separated by their mass-to-charge ratio, then measured and/or counted by a detector. Rare isotopes such as ^{14}C present a challenge to conventional MS due to their low natural abundance and high background levels. Researchers were challenged by isobaric interference (interference from equal mass isotopes of different elements exemplified by ^{14}N in ^{14}C analysis), isotopic interference (interference from equal mass to charge isotopes of different elements), and molecular interference (interference from equal mass to charge molecules, such as $^{12}CH_2^-$, ^{12}CD, or $^{13}CH^-$ in ^{14}C analysis). Most AMS systems employ an electrostatic tandem accelerator that has a direct improvement in background rejection, resulting in a 10^8 time increase in the sensitivity of isotope ratio measurements. As the natural abundance of ^{14}C in modern carbon is 10^{-12} (isotopic ratio of ^{14}C:^{12}C), a sensitivity of 10^{-15} is a prerequisite for ^{14}C analysis.

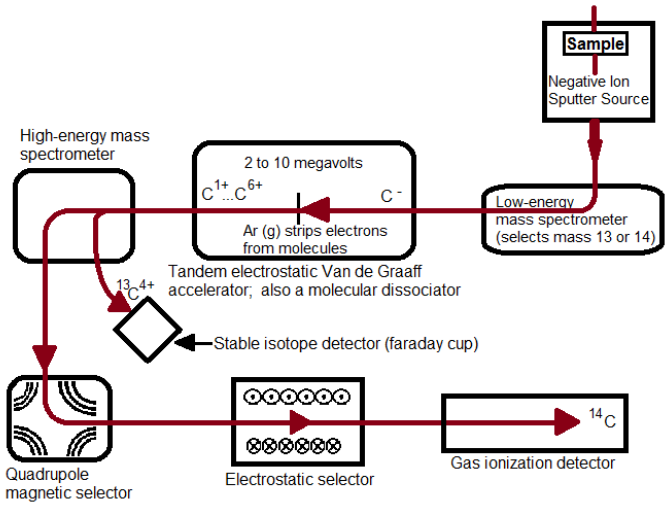


Figure 1. A schematic of the AMS system at Lawrence Livermore National Laboratory Center for Accelerator Mass Spectrometry.

Figure 1, above, starts with a negative ion sputter source, which commonly consists of a stream of Cesium ions (Cs^+) with energies of 2-3 keV focused on the surface of a solid sample in order to transfer enough energy to the target material to produce free atoms and ions of the sample material. This process, called sputtering, separates neutral, as well as positive and negative ions from the sample surface. The sample is held at a negative potential, and negatively charged ions are accelerated away from the sample, resulting in a beam of negative ions (Figure 2, below). Cs^+ is particularly useful in ^{14}C studies because it does not form a negative ion from ^{14}N, thereby eliminating isobar interference.[4] It is important to have a beam of negative ions entering the accelerator because the negative ions are attacted to the high -voltage terminal which results in their net acceleration.

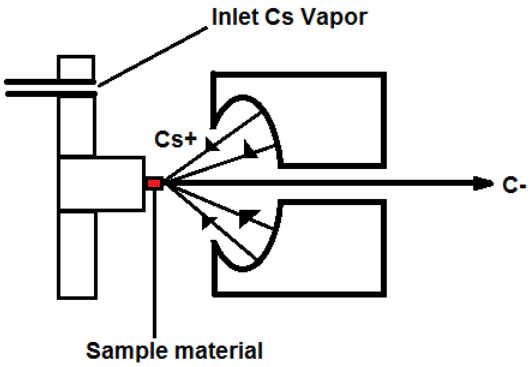


Figure 2. Cs sputter ion source.

The low energy (~5-10 keV) diverging beam that leaves the ion source is accelerated, focused and transported to the accelerator by the injector system.[2] CAMS LLNL employs a low-energy mass spectrometer that selects for the desired atomic mass[5] that separates ions by their mass to charge ratio (^{12}C, ^{13}C, and ^{14}C ions pass through separately). Most AMS systems use sequential injection, a process that switches between stable and rare isotopes via the application of varying voltages to the electrically insulated vacuum chamber of the analyzer magnet. In sequential injection, typical injection repetition rates are 10 sec^{-1} to minimize variations in the electrical load.[2] This process allows the development of more versatile systems, allowing for analysis of a wide range of isotopes.[1] The alternative to sequential injection is simultaneous injection, a process adopted in accelerators dedicated to ^{14}C analysis. A recombinator is used following sequential injection, which is a sequence of magnetic analyzers and quadrupole lenses that focus the stable and rare isotopes so they recombine and enter the accelerator together.

The traditional accelerator was first developed in the early 1930s for nuclear physics research. In 1939, UC Berkeley scientists Luis Alvarez and Robert Cornog were the first to use AMS in the detection of ^{3}He in nature using the 88-inch Berkeley cylclotron.[5] Now, over 70 years later, cyclotrons have been replaced by an accelerator type with greater energy stability: the tandem electrostatic accelerator. An electrostatic accelerator works by accellerating particles though a magnetic field generated by high voltages using a mechanic transport system that continuously transports charges from ground to the insulated high-voltage terminal. All tandem accelerators with a maximum terminal voltage above 5 MV use such a mechanical system.[2] The negative ions that enter the accelerator are attracted to the high-voltage terminal, which is what accellerates theCAMS LLNL employs a tandem Van de Graaff accelerator, in which a second acceleration of millions of volts is applied. In all tandem accelerators, atoms are stripped at the high-voltage terminal using either a thin Carbon foil or Argon gas. Stripping is the process in which two or more electrons are removed. The Van de Graaff accelerator removes at least four electrons. It is preferrable to remove at least three electrons because by this process that molecular isobars of ^{14}C (such as $^{12}CH_2^-$, ^{12}CD, or $^{13}CH^-$) are destroyed due to the high instability of their positively charged forms, and atomic C^+ ions such as $^{12}C^+$, $^{13}C^+$, and $^{14}C^+$ are separated due to their different mass to charge ratios.[4] The negative ions are changed to positively charged ions and are thus accelerated back to the ground potential in the high-energy part of the accelerator. Transmission through a foil changes with time due to radiation damage and foil thickening, thus gas strippers are used in all modern analyzers due to their increased transmission stability.[2]

Magnetic lenses focus the high energy particles leaving the accelerator into a magnetic dipole, (the high energy analyzing magnet). Stable isotopes can be collected at off-axis beam stops where secondary focusing lenses and additional analyzing equipment remove unwanted ions and molecular fragments to eliminate background. At CAMS LLNL, a magnetic quadrupole lens focuses the desired isotope and charge state to a high-energy mass spectrometer which passes $^{12}C^+$ and $^{13}C^+$ into Faraday cups and further focuses and stabilizes ^{14}C in a quadrupole/electrostatic cylindrical analyzer that leads to a gas ionization detector.[5] The magnetic quadrupole and electrostatic selectors coupled together ensure high selectivity and sensitivity, respectively. Other detectors commonly found in AMS systems include surface barrier, time-of-flight, gas filled magnets, and x-ray detectors.

Interpretation

Rare isotopes analyzed by AMS are always measured as a ratio of a stable, more abundant (but not too abundant) isotope. For example, the ratio in ^{14}C studies is generally shown as $^{14}C/^{13}C$. Less abundant isotopes are preferable in AMS because the decreased flux of ions reduces background and wear on the instrument, which is of particular concern due to the quick deterioration of particle detectors (performance deteriorates at rates higher than a few thousand particles per second[1]).

Applications

Common radioisotope elements measured with AMS and their applications are shown in Table 1[4], below. Because ^{14}C analysis is by far the most popular application of AMS, the methods discussed below are all techniques used involving ^{14}C.

***Table 1**. Radioisotope elements generally measured with AMS and their applications.*

Element (Common Isotope)	Radioisotope with AMS	Natural abundance	Half-life (yr)	Study application
Hydrogen (^{1}H)	3H	trace	12.33	Biological/biomedical Nutritional trace
Beryllium (^{9}Be)	10Be	trace	1,510,000	Geochronology Hydrogeological study Exposure dating
Carbon (^{12}C)	14C	1 x10-10%	5730	Biological/biomedical Nutritional trace
Aluminum (^{27}Al)	26Al	trace, synthetic	720,000	Biological/biomedical Exposure dating
Chlorine (^{35}Cl)	36Cl	7x10−11%	301,000	Earth Science Hydrogeological study Exposure dating Migration of nuclear waste
Calcium (^{40}Ca)	41Ca	trace, synthetic	116,000	Biological/biomedical Nuclear weapon testing
Nickel (58Ni)	59Ni	trace, synthetic	112,000	Nutritional trace
Iodine (127I)	129I	trace, synthetic	15,700,000	Biological/biomedical Migration of nuclear waste Environmental study

Radiocarbon dating is an analytical method based on the rate of decay of ^{14}C, a radioactive carbon isotope formed in the atmosphere by the reaction between neutrons from cosmic rays and ^{14}N (neutron + ^{14}N = ^{14}C + proton).[2] Resultant ^{14}C atoms are taken up by plants in the form of $^{14}CO_2$, then transferred to animals though the food chain. When animals and plants die, they cease to uptake ^{14}C, and a steady decay of ^{14}C continues in their tissues over time. ^{14}C atoms decay via electron emission (β radiation) to form ^{14}N, a process which has a half life of 5,730 years.[5] Radiocarbon levels in the atmosphere change according to complex patterns which are affected by a variety of fluctuations ranging from the sun's solar activity and the earth's magnetic field, to ocean ventilation rate and climate. ^{14}C analysis of tree rings, corals, lake sediments, ice cores, and other sources has led to a detailed record of ^{14}C variations through time, allowing researchers to establish an official radiocarbon calibration curve (also referred to as a radiocarbon clock) dating back 26,000 calendar years. In the 1960s, nuclear weapons testing released large amounts of neutrons into the atmosphere, nearly doubling ^{14}C activity.[2] Samples taken after this time period can be radiocarbon dated using a ^{14}C bomb curve like the peak shown below in Figure 3, can retrieve very precise dates (within 1 year at the steepest part of the curve).

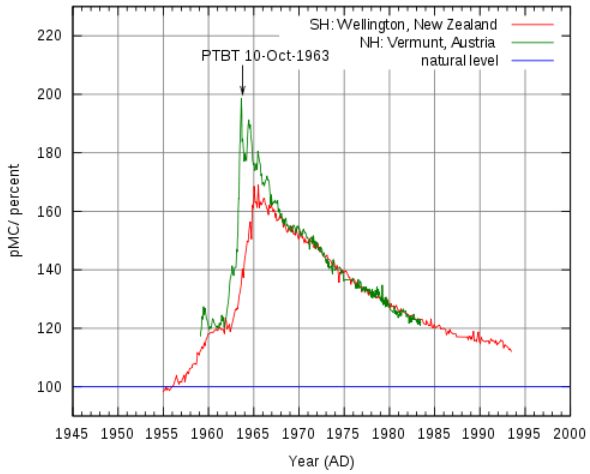


Figure 3. The New Zealand curve (red) is representative of atmospheric ^{14}C in the Southern Hemisphere, and the Austrian curve is representative of the Northern Hemisphere.

^{14}C analysis provides valuable information in the radiocarbon dating of the world's most priceless artifacts. One such example of the monumental impact of ^{14}C AMS is the radiocarbon dating of the Dead Sea Scrolls to dates from 300 BC to AD 61 by labs in Zurich and Arizona. AMS has also contributed greatly to environmental and atmospheric studies by providing information regarding particle composition and origin. In the biochemical field, synthesized ^{14}C labeled compounds can be administered as a tracer dose for in-vivo human metabolic and drug studies which require AMS analysis of graphitized biological samples.

AMS is a highly sensitive method for isotopic analysis that has numerous key applications that are only growing with advances in technology. High costs and technical complexities that arise with the use of a particle accelerator are the only limits to the widespread use of AMS. Recent times have seen the emergence of commercially available compact accelerators that use as low as 200 kV for radiocarbon dating and biomedical applications, and as particle accelerators become more commonplace, modifications to the instrument have also broadened the number of isotopes the instrument can measure.

References

1. Tuniz, C., Bird, J. R., Fink, D. and G. F. Herzog, *Accelerator Mass Spectrometry*. CRC PRess: Boca Raton, 1998; p 371.
2. Hellborg, R.; Skog, G., Accelerator mass spectrometry. *Mass Spectrometry Reviews* **2008,** *27* (5), 398-427.
3. Gove, H. E., *From Heroshima to the Iceman*. Institute of Physics Publishing: London, 1999; p 225.
4. Kim, S.. Graphitization for biological, biomedical, and environmental carbon-14-accelerator mass spectrometry applications: Optimization and characterization. Ph.D. dissertation, University of California, Davis, United States -- California. Retrieved February 28, 2011, from Dissertations & Theses @ University of California.(Publication No. AAT 3379582).
5. https://www.llnl.gov/str/Holloway.htmlc

Contributors

- Laura McWade

3.1: Accelerator Mass Spectroscopy is shared under a not declared license and was authored, remixed, and/or curated by LibreTexts.

3.2: Fragmentation Patterns in Mass Spectra

This page looks at how fragmentation patterns are formed when organic molecules are fed into a mass spectrometer, and how you can get information from the mass spectrum.

The formation of molecular ions

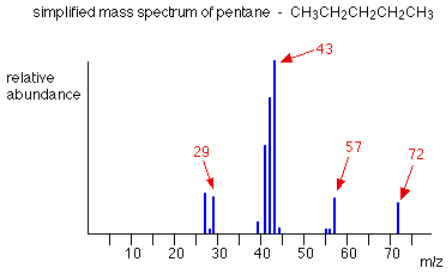
When the vaporized organic sample passes into the ionization chamber of a mass spectrometer, it is bombarded by a stream of electrons. These electrons have a high enough energy to knock an electron off an organic molecule to form a positive ion. This ion is called the **molecular ion - or sometimes the parent ion.** The molecular ion is often given the symbol M^+ or $M^{\cdot+}$- the dot in this second version represents the fact that somewhere in the ion there will be a single unpaired electron. That's one half of what was originally a pair of electrons - the other half is the electron which was removed in the ionization process.

Fragmentation

The molecular ions are energetically unstable, and some of them will break up into smaller pieces. The simplest case is that a molecular ion breaks into two parts - one of which is another positive ion, and the other is an uncharged free radical.

$$M^{\cdot+} \rightarrow X^+ + Y^{\cdot} \tag{3.2.1}$$

The uncharged free radical won't produce a line on the mass spectrum. Only charged particles will be accelerated, deflected and detected by the mass spectrometer. These uncharged particles will simply get lost in the machine - eventually, they get removed by the vacuum pump. The ion, X^+, will travel through the mass spectrometer just like any other positive ion - and will produce a line on the stick diagram. All sorts of fragmentations of the original molecular ion are possible - and that means that you will get a whole host of lines in the mass spectrum. For example, the mass spectrum of pentane looks like this:



It's important to realize that the pattern of lines in the mass spectrum of an organic compound tells you something quite different from the pattern of lines in the mass spectrum of an element. With an element, each line represents a different isotope of that element. With a compound, each line represents a different fragment produced when the molecular ion breaks up.

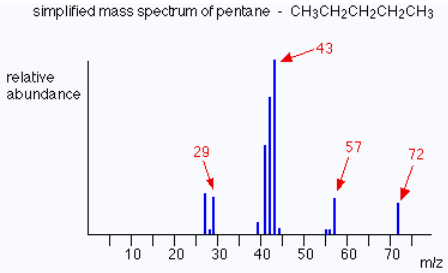
In the stick diagram showing the mass spectrum of pentane, the line produced by the heaviest ion passing through the machine (at m/z = 72) is due to the molecular ion. The tallest line in the stick diagram (in this case at m/z = 43) is called the **base peak**. This is usually given an arbitrary height of 100, and the height of everything else is measured relative to this. The base peak is the tallest peak because it represents the commonest fragment ion to be formed - either because there are several ways in which it could be produced during fragmentation of the parent ion, or because it is a particularly stable ion.

Using fragmentation patterns

This section will ignore the information you can get from the molecular ion (or ions). That is covered in three other pages which you can get at via the mass spectrometry menu. You will find a link at the bottom of the page.

Example 3.2.1: Mass Spectrum of Pentane

Let's have another look at the mass spectrum for pentane:



What causes the line at m/z = 57?

Solution

How many carbon atoms are there in this ion? There can't be 5 because 5 x 12 = 60. What about 4? 4 x 12 = 48. That leaves 9 to make up a total of 57. How about $C_4H_9^+$ then?

$C_4H_9^+$ would be $[CH_3CH_2CH_2CH_2]^+$, and this would be produced by the following fragmentation:



The methyl radical produced will simply get lost in the machine.

The line at m/z = 43 can be worked out similarly. If you play around with the numbers, you will find that this corresponds to a break producing a 3-carbon ion:



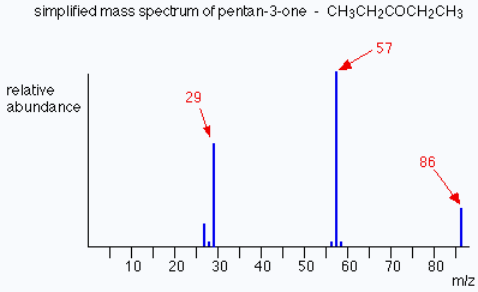
The line at m/z = 29 is typical of an ethyl ion, $[CH_3CH_2]^+$:



The other lines in the mass spectrum are more difficult to explain. For example, lines with m/z values 1 or 2 less than one of the easy lines are often due to loss of one or more hydrogen atoms during the fragmentation process.

Example 3.2.2: Pentan-3-one

This time the base peak (the tallest peak - and so the commonest fragment ion) is at m/z = 57. But this isn't produced by the same ion as the same m/z value peak in pentane.

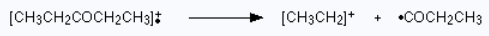


If you remember, the m/z = 57 peak in pentane was produced by $[CH_3CH_2CH_2CH_2]^+$. If you look at the structure of pentan-3-one, it's impossible to get that particular fragment from it.

Work along the molecule mentally chopping bits off until you come up with something that adds up to 57. With a small amount of patience, you'll eventually find $[CH_3CH_2CO]^+$ - which is produced by this fragmentation:



You would get exactly the same products whichever side of the CO group you split the molecular ion. The m/z = 29 peak is produced by the ethyl ion - which once again could be formed by splitting the molecular ion either side of the CO group.



Peak heights and the stability of ions

The more stable an ion is, the more likely it is to form. The more of a particular sort of ion that's formed, the higher its peak height will be. We'll look at two common examples of this.

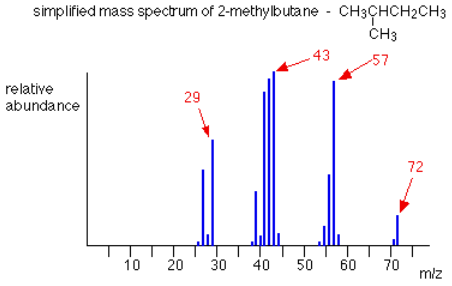
Examples involving carbocations (carbonium ions)

Summarizing the most important conclusion from the page on carbocations:

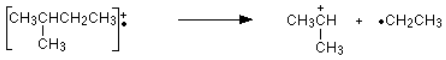
Order of stability of carbocations

primary < secondary < tertiary

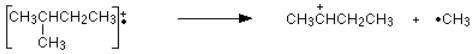
Applying the logic of this to fragmentation patterns, it means that a split which produces a secondary carbocation is going to be more successful than one producing a primary one. A split producing a tertiary carbocation will be more successful still. Let's look at the mass spectrum of 2-methylbutane. 2-methylbutane is an isomer of pentane - isomers are molecules with the same molecular formula, but a different spatial arrangement of the atoms.



Look first at the very strong peak at m/z = 43. This is caused by a different ion than the corresponding peak in the pentane mass spectrum. This peak in 2-methylbutane is caused by:



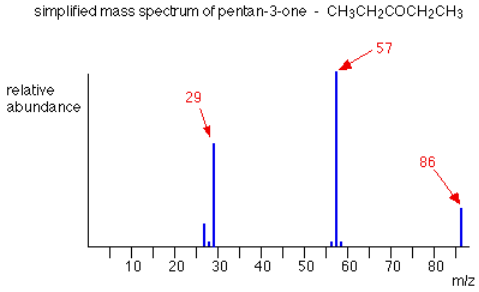
The ion formed is a secondary carbocation - it has two alkyl groups attached to the carbon with the positive charge. As such, it is relatively stable. The peak at m/z = 57 is much taller than the corresponding line in pentane. Again a secondary carbocation is formed - this time, by:



You would get the same ion, of course, if the left-hand CH_3 group broke off instead of the bottom one as we've drawn it. In these two spectra, this is probably the most dramatic example of the extra stability of a secondary carbocation.

Examples involving acylium ions, $[RCO]^+$

Ions with the positive charge on the carbon of a carbonyl group, C=O, are also relatively stable. This is fairly clearly seen in the mass spectra of ketones like pentan-3-one.



The base peak, at m/z=57, is due to the $[CH_3CH_2CO]^+$ ion. We've already discussed the fragmentation that produces this.

Using mass spectra to distinguish between compounds

Suppose you had to suggest a way of distinguishing between pentan-2-one and pentan-3-one using their mass spectra.

pentan-2-one		$CH_3COCH_2CH_2CH_3$
pentan-3-one		$CH_3CH_2COCH_2CH_3$

Each of these is likely to split to produce ions with a positive charge on the CO group. In the pentan-2-one case, there are two different ions like this:

- $[CH_3CO]^+$
- $[COCH_2CH_2CH_3]^+$

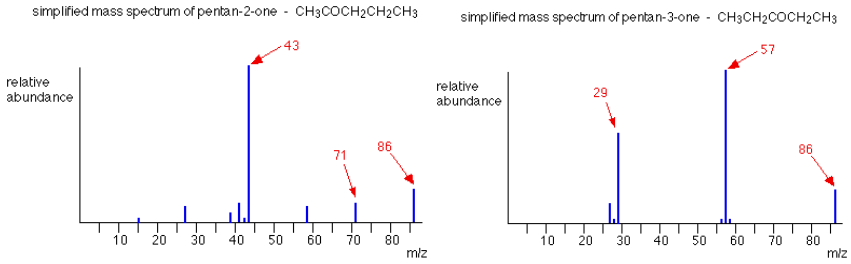
That would give you strong lines at m/z = 43 and 71.

With pentan-3-one, you would only get one ion of this kind:

- $[CH_3CH_2CO]^+$

In that case, you would get a strong line at 57. You don't need to worry about the other lines in the spectra - the 43, 57 and 71 lines give you plenty of difference between the two. The 43 and 71 lines are missing from the pentan-3-one spectrum, and the 57 line is missing from the pentan-2-one one.

The two mass spectra look like this:



Computer matching of mass spectra

As you've seen, the mass spectrum of even very similar organic compounds will be quite different because of the different fragmentations that can occur. Provided you have a computer data base of mass spectra, any unknown spectrum can be computer analysed and simply matched against the data base.

Contributors

- Jim Clark (Chemguide.co.uk)

This page titled 3.2: Fragmentation Patterns in Mass Spectra is shared under a CC BY-NC 4.0 license and was authored, remixed, and/or curated by Jim Clark.

3.3: GC/MS Combination- Shockwave

Contributors

- Thomas Chasteen, Department of Chemistry, Sam Houston State University

3.3: GC/MS Combination- Shockwave is shared under a not declared license and was authored, remixed, and/or curated by LibreTexts.

3.4: How the Mass Spectrometer Works

This page describes how a mass spectrum is produced using a mass spectrometer.

How a mass spectrometer works

If something is moving and you subject it to a sideways force, instead of moving in a straight line, it will move in a curve - deflected out of its original path by the sideways force. Suppose you had a cannonball traveling past you and you wanted to deflect it as it went by you. All you've got is a jet of water from a hose-pipe that you can squirt at it. Frankly, its not going to make a lot of difference! Because the cannonball is so heavy, it will hardly be deflected at all from its original course. But suppose instead, you tried to deflect a table tennis ball traveling at the same speed as the cannonball using the same jet of water. Because this ball is so light, you will get a huge deflection.

The amount of deflection you will get for a given sideways force depends on the mass of the ball. If you knew the speed of the ball and the size of the force, you could calculate the mass of the ball if you knew what sort of curved path it was deflected through. The less the deflection, the heavier the ball. You can apply exactly the same principle to atomic sized particles.

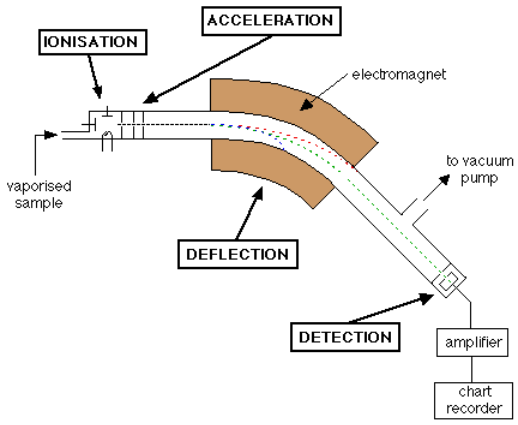
An outline of what happens in a mass spectrometer

Atoms can be deflected by magnetic fields - provided the atom is first turned into an ion. Electrically charged particles are affected by a magnetic field although electrically neutral ones aren't.

The sequence is :

- **Stage 1: Ionization**: The atom is ionised by knocking one or more electrons off to give a positive ion. This is true even for things which you would normally expect to form negative ions (chlorine, for example) or never form ions at all (argon, for example). Mass spectrometers always work with positive ions.
- **Stage 2: Acceleration:** The ions are accelerated so that they all have the same kinetic energy.
- **Stage 3: Deflection:** The ions are then deflected by a magnetic field according to their masses. The lighter they are, the more they are deflected. The amount of deflection also depends on the number of positive charges on the ion - in other words, on how many electrons were knocked off in the first stage. The more the ion is charged, the more it gets deflected.
- **Stage 4: Detection**: The beam of ions passing through the machine is detected electrically.

A full diagram of a mass spectrometer



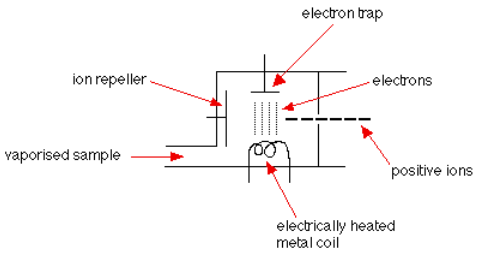
Understanding what's going on

The need for a vacuum

It's important that the ions produced in the ionization chamber have a free run through the machine without hitting air molecules.

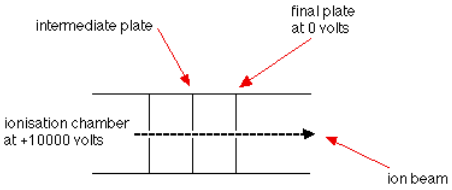
Ionization

The vaporized sample passes into the ionization chamber. The electrically heated metal coil gives off electrons which are attracted to the electron trap which is a positively charged plate.



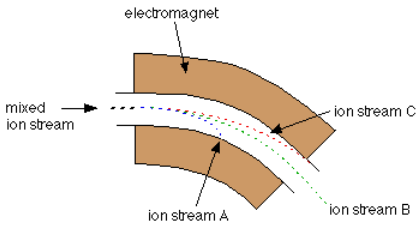
The particles in the sample (atoms or molecules) are therefore bombarded with a stream of electrons, and some of the collisions are energetic enough to knock one or more electrons out of the sample particles to make positive ions. Most of the positive ions formed will carry a charge of +1 because it is much more difficult to remove further electrons from an already positive ion. These positive ions are persuaded out into the rest of the machine by the ion repeller which is another metal plate carrying a slight positive charge.

Acceleration



The positive ions are repelled away from the very positive ionization chamber and pass through three slits, the final one of which is at 0 volts. The middle slit carries some intermediate voltage. All the ions are accelerated into a finely focused beam.

Deflection



Different ions are deflected by the magnetic field by different amounts. The amount of deflection depends on:

- the mass of the ion. Lighter ions are deflected more than heavier ones.
- the charge on the ion. Ions with 2 (or more) positive charges are deflected more than ones with only 1 positive charge.

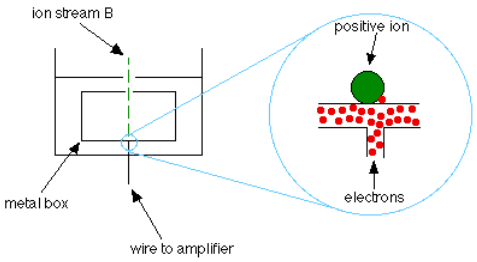
These two factors are combined into the mass/charge ratio. Mass/charge ratio is given the symbol m/z (or sometimes m/e). For example, if an ion had a mass of 28 and a charge of 1+, its mass/charge ratio would be 28. An ion with a mass of 56 and a charge of 2+ would also have a mass/charge ratio of 28.

In the last diagram, ion stream A is most deflected - it will contain ions with the smallest mass/charge ratio. Ion stream C is the least deflected - it contains ions with the greatest mass/charge ratio.

It makes it simpler to talk about this if we assume that the charge on all the ions is 1+. Most of the ions passing through the mass spectrometer will have a charge of 1+, so that the mass/charge ratio will be the same as the mass of the ion. Assuming 1+ ions, stream A has the lightest ions, stream B the next lightest and stream C the heaviest. Lighter ions are going to be more deflected than heavy ones.

Detection

Only ion stream B makes it right through the machine to the ion detector. The other ions collide with the walls where they will pick up electrons and be neutralised. Eventually, they get removed from the mass spectrometer by the vacuum pump.



When an ion hits the metal box, its charge is neutralized by an electron jumping from the metal on to the ion (right hand diagram). That leaves a space amongst the electrons in the metal, and the electrons in the wire shuffle along to fill it. A flow of electrons in the wire is detected as an electric current which can be amplified and recorded. The more ions arriving, the greater the current.

Detecting the other ions

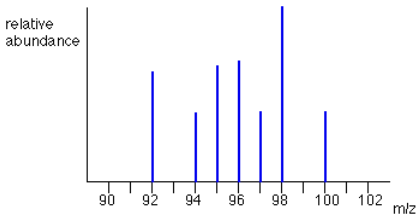
How might the other ions be detected - those in streams A and C which have been lost in the machine?

Remember that stream A was most deflected - it has the smallest value of m/z (the lightest ions if the charge is 1+). To bring them on to the detector, you would need to deflect them less - by using a smaller magnetic field (a smaller sideways force). To bring those with a larger m/z value (the heavier ions if the charge is +1) on to the detector you would have to deflect them more by using a larger magnetic field.

If you vary the magnetic field, you can bring each ion stream in turn on to the detector to produce a current which is proportional to the number of ions arriving. The mass of each ion being detected is related to the size of the magnetic field used to bring it on to the detector. The machine can be calibrated to record current (which is a measure of the number of ions) against m/z directly. The mass is measured on the ^{12}C scale.

What the mass spectrometer output looks like

The output from the chart recorder is usually simplified into a "stick diagram". This shows the relative current produced by ions of varying mass/charge ratio. The stick diagram for molybdenum looks like this:



You may find diagrams in which the vertical axis is labeled as either "relative abundance" or "relative intensity". Whichever is used, it means the same thing. The vertical scale is related to the current received by the chart recorder - and so to the number of ions arriving at the detector: the greater the current, the more abundant the ion.

As you will see from the diagram, the commonest ion has a mass/charge ratio of 98. Other ions have mass/charge ratios of 92, 94, 95, 96, 97 and 100. That means that molybdenum consists of 7 different isotopes. Assuming that the ions all have a charge of 1+, that means that the masses of the 7 isotopes on the carbon-12 scale are 92, 94, 95, 96, 97, 98 and 100.

Contributors

- Jim Clark (Chemguide.co.uk)

This page titled 3.4: How the Mass Spectrometer Works is shared under a CC BY-NC 4.0 license and was authored, remixed, and/or curated by Jim Clark.

SECTION OVERVIEW

3.5: Introductory Mass Spectrometry

Topic hierarchy

3.5.1: Fragmentation

3.5.2: High Resolution vs Low Resolution

3.5.3: Introduction to Mass Spectrometry

3.5.4: Isotopes- 13C

3.5.5: Isotopes- Br and Cl

3.5.6: Molecular Ions

3.5.7: Molecular Ion and Nitrogen

3.5.8: The Mass Spectrometry Experiment

This page titled 3.5: Introductory Mass Spectrometry is shared under a CC BY-NC 3.0 license and was authored, remixed, and/or curated by Chris Schaller.

3.5.1: Fragmentation

When molecules go through a mass spectrometer, some of them arrive intact at the detector, but many of them break into pieces in a variety of different ways. To establish a charge on a molecule, an electron had to be removed; removal of that electron is effected through a collision, usually with a high-energy electron. During that collision, energy is transferred from the high-energy electron to the molecule, and that energy has to go somewhere. Part of it gets partitioned into various bond vibrations, so bonds start to vibrate quite a lot, until some of them snap completely. The molecular ion breaks apart and forms a fragment ion.

Some fragment ions are very common in mass spectrometry. These ions are seen frequently for either of two reasons:

- there is not a pathway available to break the ion down.
- the ion is relatively stable, so it forms easily.

Fragmentations occur through well-defined pathways or mechanisms. A mechanism is a step-by-step series of events that happens in a reaction. It is important to understand how reactions happen, but we will look at fragmentations when we study radical reactions.

However, it is useful to know what factors make cations stable.

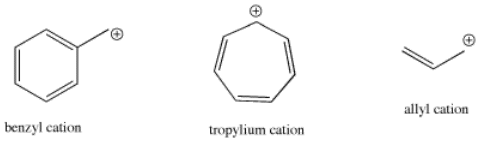
Some Common Ions

There are a number of ions commonly seen in mass spectrometry that tell you a little bit about the structure. Just like with anions, there are a couple of common factors influence cation stability:

- Electronegativity plays a role. More electronegative atoms are less likely to be cations.
- Polarizability also plays a role. More polarizable atoms are more likely to be cations.

However, in most cases, we will be looking at carbon with a positive charge, and there are additional factors to distinguish between them

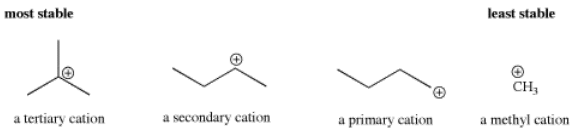
- Delocalization stabilizes a cation by spreading out the charge onto two or more different atoms.
- In Lewis structure terms, the easiest way to delocalize charge is via resonance.
- Resonance can involve other carbons, like in allyl and benzyl cations.



- Resonance can also involve other atoms, like in acylium or iminium cations.



- Delocalization can also be accomplished through inductive effects. The trend in carbocations is that the more substituents on teh carbocation, the greater the stability.
- Tertiary cations, with three substituents on the carbocation, are more stable than secondary cations, with two substituents on the carbocation. Secondary cations are more stable than primary ones. Primary cations are more stable than methyl cations.



Molecular orbital calculations suggest that the cation is stabilized through interaction with neighboring C-H bonds in the alkyl groups. Specifically, a C-H sigma bonding orbital has symmetry similar to the empty p orbital on the positive carbon. The lobes on the two orbitals can overlap such that they are in phase, and that allows electrons to be donated from the C-H bond to the central, electron-deficient carbon. Formally, there is a bonding interaction and an antibonding interaction between these two orbitals. Since

one of these orbitals is empty, the antibonding combination remains unoccupied. The bonding combination is populated, however, and since it is lower in energy than either the p orbital or the C-H sigma bond (all bonding combinations are lower in energy than the orbitals that combine to form them), there is a net decrease in energy.

Problem MS8.

Draw as many resonance structures as you can that help explain teh stability of the following cations:

a) allyl cation b) benzyl cation c) tropylium cation d) an acylium ion e) an iminium ion

Contributor

Chris P Schaller, Ph.D., (College of Saint Benedict / Saint John's University)

This page titled 3.5.1: Fragmentation is shared under a CC BY-NC 3.0 license and was authored, remixed, and/or curated by Chris Schaller.

3.5.2: High Resolution vs Low Resolution

Two common categories of mass spectrometry are high resolution mass spectrometry (HRMS) and low resolution mass spectrometry (LRMS). Not all mass spectrometers simply measure molecular weights as whole numbers. High resolution mass spectrometers can measure mass so accurately that they can detect the minute differences in mass between two compounds that, on a regular low-resolution instrument, would appear to be identical.

The reason is because atomic masses are not exact multiples of the mass of a proton, as we might usually think.

- An atom of ^{12}C weighs 12.00000 amu.
- An atom of ^{16}O weighs 15.9949 amu.
- An atom of ^{14}N weighs 14.0031 amu.
- An atom of ^{1}H weighs 1.00783 amu.

As a result, on a high resolution mass spectrometer, 2-octanone, $C_8H_{16}O$, has a molecular weight of 128.12018 instead of 128. Naphthalene, $C_{10}H_8$, has a molecular weight of 128.06264. Thus a high resolution mass spectrometer can supply an exact molecular formula for a compound because of the unique combination of masses that result.

- In LRMS, the molecular weight is determined to the nearest amu. The type of instrument used here is more common because it is less expensive and easier to maintain.
- In HRMS, the molecular weight in amu is determined to several decimal places. That precision allows the molecular formula to be narrowed down to only a few possibilities.

HRMS relies on the fact that the mass of an individual atom does not correspond to an integral number of atomic mass units.

Problem MS7.

Calculate the high-resolution molecular weights for the following formulae.

1. $C_{12}H_{20}O$ and $C_{11}H_{16}O_2$
2. $C_6H_{13}N$ and $C_5H_{11}N_2$

Contributor

Chris P Schaller, Ph.D., (College of Saint Benedict / Saint John's University)

This page titled 3.5.2: High Resolution vs Low Resolution is shared under a CC BY-NC 3.0 license and was authored, remixed, and/or curated by Chris Schaller.

3.5.3: Introduction to Mass Spectrometry

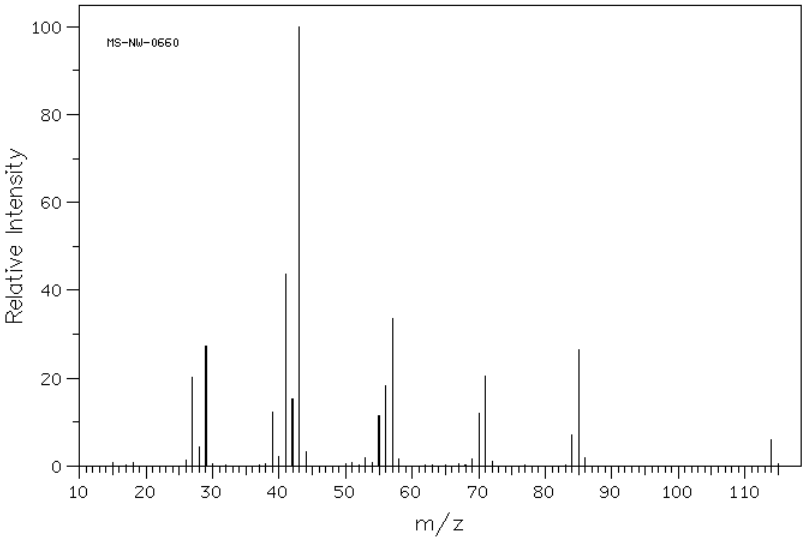


Figure MS1. Mass spectrum of hexane. Source: SDBSWeb : http://riodb01.ibase.aist.go.jp/sdbs/ (National Institute of Advanced Industrial Science and Technology of Japan, 22 August 2008)

- The y-axis is usually labeled "abundance" or "relative intensity". This axis shows how the relative ratios of molecules in the sample that have a particular mass.
- The x-axis is labeled "m/z" and corresponds to molecular mass. The designation m/z refers to the fact that this technique really measures the ratio of an ion's mass to its charge.
- A mass spectrum does not show the results from one molecule, but from millions of molecules. Because it is displaying results for a population of molecules, more than one mass is shown
- Many of the molecules in the sample fall apart during the experiment.
- A mass spectrum is a bar graph showing the weights of entire molecules as well as smaller pieces of molecules. The entire molecule must have the largest mass, the one farthest to the right, because if a molecule falls into pieces the pieces would be smaller than the whole.

Problem MS1.

The following figure shows the mass spectrum of a saturated hydrocarbon (containing only carbon and hydrogen with only single bonds between carbons, not double bonds).



1. Draw five different structures that would have the molecular weight of this compound.
2. Choose four smaller m/z values from the spectrum and draw one structure for each of them. Note that these fragments will not have complete Lewis structures.

Contributor

- Chris P Schaller, Ph.D., (College of Saint Benedict / Saint John's University)

This page titled 3.5.3: Introduction to Mass Spectrometry is shared under a CC BY-NC 3.0 license and was authored, remixed, and/or curated by Chris Schaller.

3.5.4: Isotopes- 13C

Isotopomers or isotopic isomers are isomers with isotopic atoms, having the same number of each isotope of each element but differing in their positions.

Isotopomers

If you look closely at the mass spectrum of an organic compound, 2-butanone, you see a line at m/z 72, which corresponds to 4 carbons, an oxygen and 8 hydrogens.

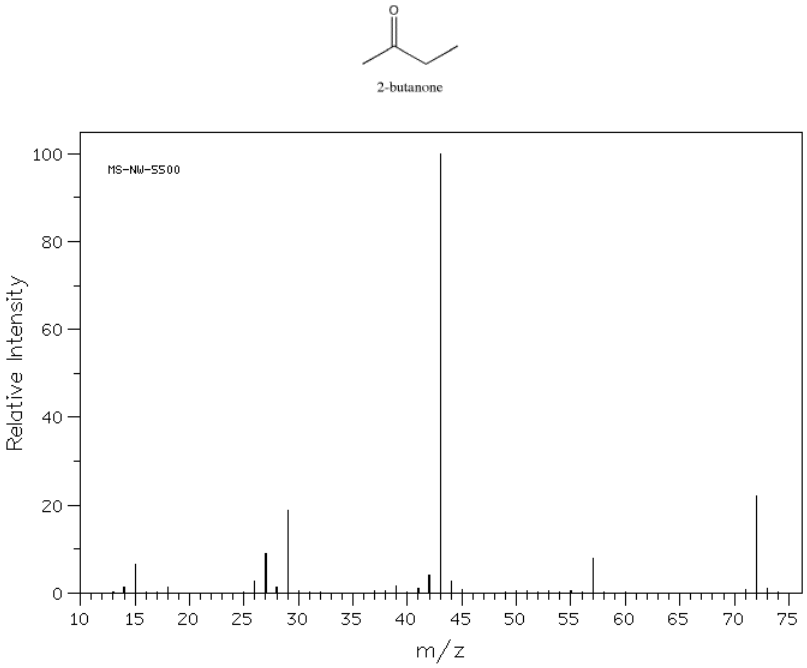


Figure MS3. Mass spectrum of 2-butanone. Source: SDBSWeb : http://riodb01.ibase.aist.go.jp/sdbs/ (National Institute of Advanced Industrial Science and Technology of Japan, 22 August 2008)

- Usually, whole numbers are used for molecular weights in mass spectrometry.
- The atomic masses in the periodic table, out to 4 decimal places, are the average masses including different possible isotopes.
- Because mass spectrometry examines individual molecules, individual atomic masses are needed, not average ones. Usually that means using a whole number.

In addition, there are a number of other lines at lower values of m/z; these correspond to the masses of smaller pieces of those 2-butanone molecules that fall apart during the experiment. We won't look too closely at how those arise until we get to radical reactions later in the course. However, we will look at some factors that make cations stable later in this chapter.

If you look closely at the mass spectrum of 2-butanone, you'll also see another little peak at m/z 73. This is referred to as the M+1 peak (one greater than the molecular ion), and it arises because of ^{13}C. This compound is referred to as an isotopomer; that means the same compound with a different isotope.

- ^{12}C is about 99% abundant; 99% of carbon atoms have a mass of 12 amu.
- ^{13}C is about 1% abundant; 1% of carbon atoms have a mass of 13 amu.
- Compounds that contain a ^{13}C atom have a mass one larger than expected.

The chance that a molecule in a sample contains a ^{13}C atom is related to the number of carbons present. If there is just one carbon atom in the molecule, it has a 1% chance of being a ^{13}C. That means the M+1 peak would be only 1/100th as tall as M+, the peak for the molecular ion.

- The M+1 peak from a ^{13}C atom is very small.
- The more carbons there are in a molecule, the bigger the M+1 peak.

- If there are 10 carbon atoms in the molecule, there is a 10% chance of a ^{13}C atom being present. The M+1 peak is about 1/10th the size of the M+ peak.
- If there are 100 carbons in the molecule, there is a very good chance that a ^{13}C atom is present. At that point, the M+1 peak is actually much larger than the M+. peak

Contributor

- Chris P Schaller, Ph.D., (College of Saint Benedict / Saint John's University)

This page titled 3.5.4: Isotopes- 13C is shared under a CC BY-NC 3.0 license and was authored, remixed, and/or curated by Chris Schaller.

3.5.5: Isotopes- Br and Cl



bromoethane

Figure MS5. Mass spectrum of chlorobenzene.

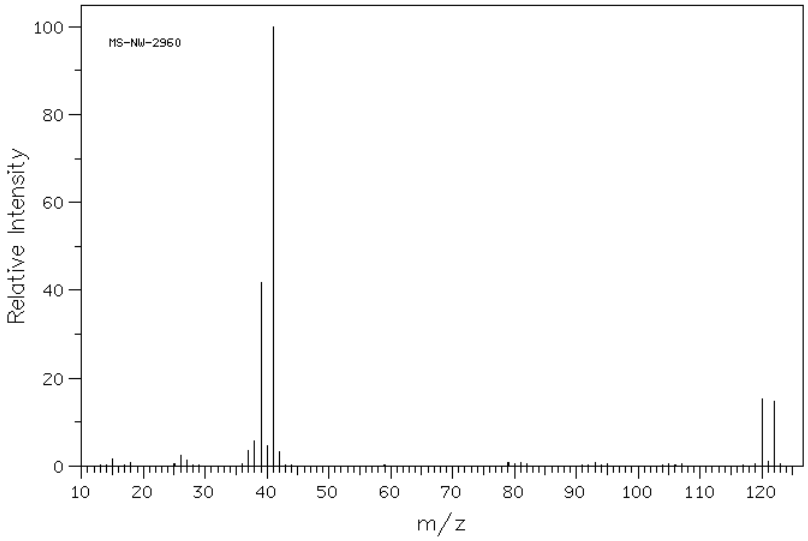
Source: SDBSWeb : http://riodb01.ibase.aist.go.jp/sdbs/ (National Institute of Advanced Industrial Science and Technology of Japan, 22 August 2008)

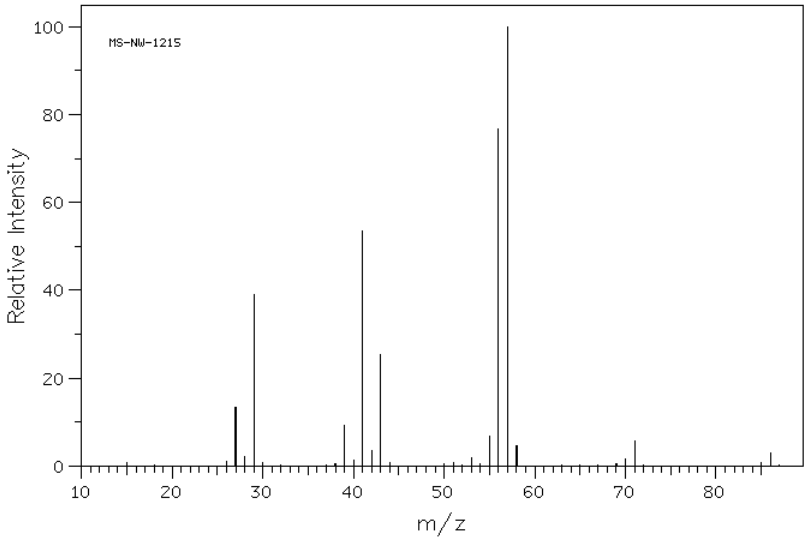
- Chlorinated compounds show an M+2 peak that is 1/3 as large as the M+ peak.

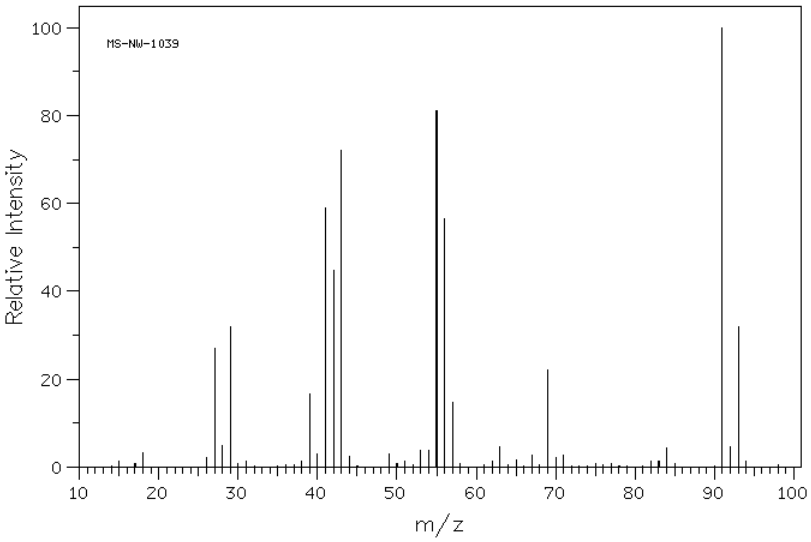
Note also that halogens are easily lost during mass spectrometry. If you subtract the mass of the halogen from the molecular ion mass, you will often find a peak that corresponds to the remainder of the structure.

Problem MS4.

Draw one possible structure for the compound in each of the following mass spectra.





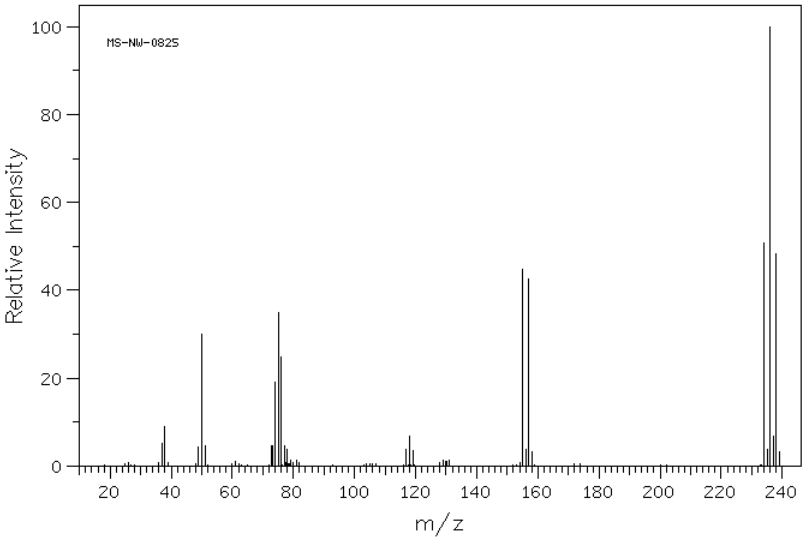


Source: SDBSWeb : http://riodb01.ibase.aist.go.jp/sdbs/ (National Institute of Advanced Industrial Science and Technology of Japan, 25 August 2008)

Problem MS5.

In the following mass spectrum, more than one halogen atom is present.

1. What is a possible structure of the compound?
2. Show why this pattern of molecular ions is observed.



Source: SDBSWeb : http://riodb01.ibase.aist.go.jp/sdbs/ (National Institute of Advanced Industrial Science and Technology of Japan, 25 August 2008)

Contributor

Chris P Schaller, Ph.D., (College of Saint Benedict / Saint John's University)

This page titled 3.5.5: Isotopes- Br and Cl is shared under a CC BY-NC 3.0 license and was authored, remixed, and/or curated by Chris Schaller.

3.5.6: Molecular Ions

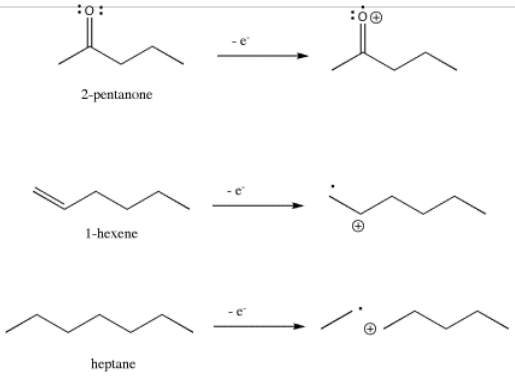
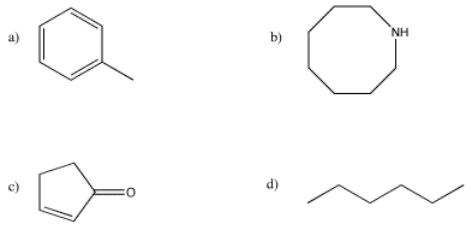


Figure MS4. Ionization in three different organic compounds.

Problem MS3.

Draw an equation for the formation of a molecular ion from each of the following compounds.



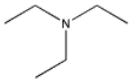
Contributor

Chris P Schaller, Ph.D., (College of Saint Benedict / Saint John's University)

This page titled 3.5.6: Molecular Ions is shared under a CC BY-NC 3.0 license and was authored, remixed, and/or curated by Chris Schaller.

3.5.7: Molecular Ion and Nitrogen

Molecular Weight: Even or Odd?



triethylamine

Figure MS6. Mass spectrum of triethylamine. Source: SDBSWeb : http://riodb01.ibase.aist.go.jp/sdbs/ (National Institute of Advanced Industrial Science and Technology of Japan, 22 August 2008)

This phenomenon is a result of the fact that the most common elements in organic compounds, carbon and oxygen, have even atomic weights (12 and 16, respectively), so any number of carbons and oxygens will have even weights. The most common isotope of hydrogen has an odd molecular weight, but because carbon and oxygen both have even valences (carbon forms four bonds and oxygen forms two), there is always an even number of hydrogen atoms in an organic compound containing those elements, so they also add up to an even numbered weight.

Nitrogen has an even atomic weight (14), so any number of nitrogen atoms will add up to an even molecular weight. Nitrogen, however, has an odd valence (it forms three bonds), and as a result there will be an odd number of hydrogens in a nitrogenous compound, and the molecular weight will be odd because of the presence of an extra hydrogen.

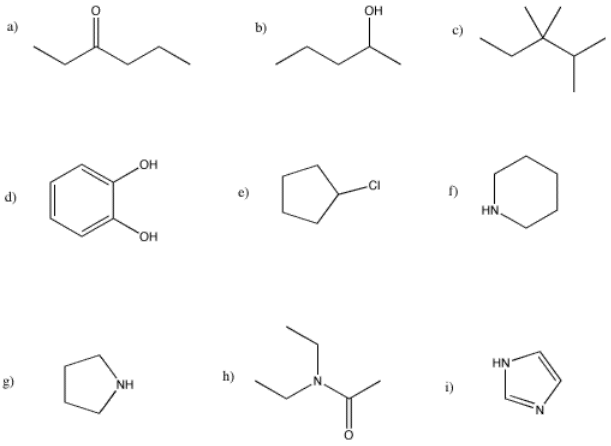
Of course, if there are two nitrogens in a molecule, there will be two extra hydrogens, so the molecular weight will actually be even. That means the rule about molecular weight and nitrogen should really be expressed as:

- odd numbers of nitrogen atoms in a molecule in an odd molecular weight.

What about those other atoms that sometimes show up in organic chemistry, such as the halogens? Halogens all have odd molecular weights (19 amu for fluorine, 35 or 37 for chlorine, 79 or 81 for bromine, and X for iodine). However, halogens all have a valence of 1, just like hydrogen. As a result, to add a halogen to methane, we would need to erase one of the hydrogen atoms and replace it with the halogen. Since we are just substituting one odd numbered atomic weight for another, the total weight remains even.

Problem MS6.

Calculate molecular weights for the following compounds.



Contributor

Chris P Schaller, Ph.D., (College of Saint Benedict / Saint John's University)

This page titled 3.5.7: Molecular Ion and Nitrogen is shared under a CC BY-NC 3.0 license and was authored, remixed, and/or curated by Chris Schaller.

3.5.8: The Mass Spectrometry Experiment

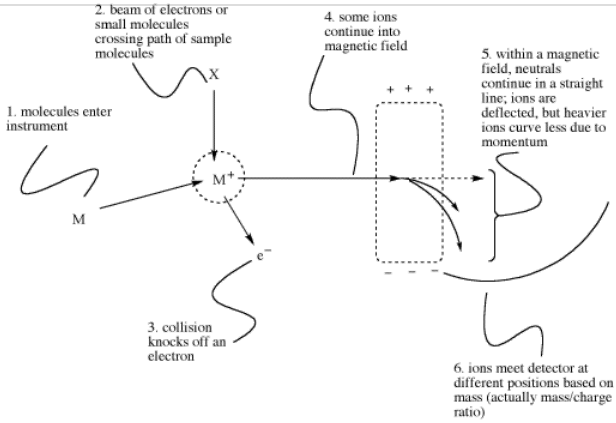


Figure MS2. A very approximate schematic of a typical mass spectrometry experiment.

Mass spectrometry only works with ions, not with neutral molecules. That means a neutral molecules must become charged in order to do this experiment. It is common to generate a cation from the molecule by removing one electron. The electron is knocked off the molecule in a collision. The collision can be caused in two different ways:

- The molecule can be sent through a stream of high-energy electrons. This method is called electron ionization.
- The molecule is sent through a stream of small molecules, such as ammonia or methane. This method is called chemical ionization.
- Electron ionization frequently results in the molecule falling to pieces because of the high energy of the electrons.
- Chemical ionization results in a "softer" collision because momentum can be dissipated through various bonds in both colliding molecules. Chemical ionization results in less fragmentation of the target molecule.
- However, after chemical ionization, the ionizing molecule sometimes sticks to the target molecule, leading to a greater "molecular" mass. For example, if ammonia is used for ionization, an extra mass may be observed at 17 amu higher than expected.

The reason the x-axis on a mass spectrum is labeled m/z (mass-to-charge ratio) is to acknowledge that there are really two factors contributing to the experiment.

Contributor

Chris P Schaller, Ph.D., (College of Saint Benedict / Saint John's University)

This page titled 3.5.8: The Mass Spectrometry Experiment is shared under a CC BY-NC 3.0 license and was authored, remixed, and/or curated by Chris Schaller.

3.6: MALDI-TOF

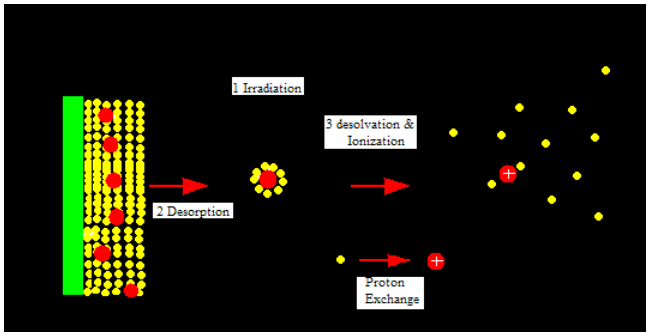
Proteins and peptides have been characterized by high pressure liquid chromatography (HPLC) or SDS PAGE by generating peptide maps. These peptide maps have been used as fingerprints of protein or as a tool to know the purity of a known protein in a known sample. Mass spectrometry gives a peptide map when proteins are digested with amino end specific, carboxy end specific, or amino acid specific digestive enzymes. This peptide map can be used to search a sequence database to find a good match from the existing database. This is because the more accurately the peptide masses are known, the less chance there is of bad matches.

Introduction

Electron spray ionization coupled to triple quadrupole (TSQ) and ion trap mass spectrometers (ITMS) and matrix assisted laser desorption ionization (MALDI) coupled to time of flight (TOF) analyzers have been successful for obtaining very accurate mass measurements. TOF, TSQ, and ITMS can give mass accuracies better than 0.1. MALDI-TOF mass spectra (MS) is a good tool for screening peptide masses of tryptic digests. This method is more effective because it requires relatively less intense sample preparation since the matrix is less susceptible to interferences caused by salts and detergents. Secondly MALDI-TOF-MS generates peptides containing only one charge and show only one peak in spectrum which facilitates data interpretation.

Schematic and Theory of MALDI

MALDI is a very sensitive technique for determining the mass of proteins, peptides, or polymers. Protein masses are identity of proteins and thus help in proteomics. Thus MALDI allows protein identification. MALDI sample preparation is relatively fast and easy. It is a first choice when it comes to protein study. Proteins, peptides, and polymers are fragile and tend to fragment when ionized by other ionization techniques.



MALDI is attached to a time of flight (TOF) analyzer which measures time it takes for the molecules to travel a fixed distance. MALDI is a soft ionization technique in which a short laser pulse, instead of continuous laser, of nitrogen gas usually around 237 nm is used to ionize molecules. A protein or peptide sample is placed on a target plate and mixed with an appropriate matrix on the target plate. The mixture of sample and matrix crystallizes due to the vacuum environment and then is irradiated with a short laser pulse. The sample molecules and the matrix now enter gas phase. This leads to release of matrix, samples molecules, and ions from the target plate. The ions then accelerate in TOF analyzer because they are subject to equal electric field. TOF is a field-free flight tube. The ions travel in a strait and linear direction to the detector. The mass to charge ration (m/z) of the sample ions can be calculated using the equation T= C1$(m/z)^{0.5}$ +C2. C1 and C2 are instrumental constants which can be determined with compounds of known mass. This equation is derived from the fact that potential energy equals kinetic energy.

$$KE = \frac{1}{2}mv^2 \quad (1)$$

$$v = \sqrt{\frac{2KE}{m}} \quad (2)$$

Since velocity is distance/time $v = d/t$ substitute it in equation 2 and solve for t to get eq. 3

$$t = m^{1/2} * d/(2KE)^{1/2} \text{ eq.3}$$

The distance the molecules travel and their kinetic energy is constant. So it is replaced by C1. Furthermore since the relationship between the t and $m^{1/2}$ is linear an intercept of C2 is added to get equation of a line.

$$t = C1(m/z)^{1/2} + C2 \quad \text{eq.4}$$

Sample preparation

Biomolecules such as proteins, peptides, sugars, and large organic molecules such as polymers, dendrimers and other macro molecules can be analyzed using MALDI. Sample preparation for MALDI is very simple; however, it is one of the most crucial steps in the MALDI analysis process. MALDI is more tolerant to sample contaminants, but contaminants can seriously disturb incorporation of sample molecules with growing matrix crystals. This results in bad spots on the target plate, leading to low signal to noise ratio, resolution, and sensitivity.

Samples can be prepared in two different ways. One removes the contaminants before applying them on to the matrix and one removes the contaminants after the sample is spotted on to the target plate either before or after adding the matrix.

Miniaturized chromatographic set-up is used for the first approach, while some scientists have cleaned in-gel digest of proteins using reverse phase(RP) HPLC microcolumns packed with different types of RP-HPLC beads (1). Now tips are also packed with RP or ion-exchange resin to remove salts and detergents from protein mixtures, and their effectiveness is shown by their recent commercialization. Tips and columns effectively remove MALDI contaminants and give small volume of sample, this can result in possible highly sensitive MALDI analysis of the samples.

Purification of biological samples on target plates involves synthetic membranes or surfaces. Membranes go on top of the target plate and the biological samples are spotted on top of the membranes. Biological samples interact with the membrane through strong hydrophobic forces. This enables samples to remain on the membrane while the buffers and salts are washed away. Then the MALDI-matrix solution is added to the purified samples on the target plate, ready for analysis. Perfluorosulfonated ionomer films, polyethylene membranes, nonporous polyurethane membranes, and C8 and C18 extraction disks are examples of membranes that have been used successfully in the past for biological mixtures. Self-assembled monolayers (SAMs) of octadecyl mercaptan on gold-sputtered disposable MALDI probe tips have been used to concentrate the sample and to act as a purification device. However, it is unfeasible because it requires overnight sample incubation to fully concentrate at the probe tip.

Matrix

The function of the matrix is adsorborption of energy from laser pulse, and then transfer to sample“thereby causing desorption of the analyte molecules in an expanding plume, to ionize the desorbed analyte molecules and to prevent aggregation of the analyte molecules”(2). The matrix molecules for MALDI are chosen on the basis on fulfillment of requirement that matrix molecules must be able to absorb ultraviolet wavelength of usually 237nm, low volatility and ability to transfer protons to the sample molecules. For proteins samples typical MALDI matrix consist of cinnamic acid and hydroxylated benzoic acid derivatives.

2,5-dihydroxybenzoic acid is more tolerant to the sample contaminants because it excludes them during crystallization process(3). The use of specially prepared thin matrix layers uses fast evaporation setup, which not only improves the sensitivity and resolution, but also allows the samples to be extensively washed, removing salts and detergents. Since the sensitivity depends on the concentration of the sample on the target plate, samples can be concentrated using PR-HPLC or bead-peptide concentration. In bead-peptide concentration RP-chromatographic beads are added to the proteins or peptide samples, and these samples preferentially bind to the beads through hydrophobic interactions while the contaminants like salts and chaotrophes do not. After a short incubation, the peptide-bead solution is harvested using pellets from a centrifugation, and dried in speed vacuum concentrator. In both cases, highly concentrated pellets of peptide-bound beads are obtained, which can be transferred to MALDI and left to dry. Because the beads are hydrophobic in nature, they form a cluster in highly concentrated spot (<1mm^2) on MALDI target plate after drying. Peptides elute on the target plate by a small volume of aqueous/organic MALDI-matrix solution and become incorporated into the growing matrix crystals at the same time. This process allows 10 to 100 fmol to be enough to be loaded on to the gels.

Sensitivity

Sensitivity of MALDI depends on sample preparation and the preparation of sample/matrix layer. They must be optimized by trial and error according to sample size, type, and previous history. Preparing a very thin matrix layer and applying of sample so that the sample is on the outer layer of matrix, give a sensitivity level of low attomole (10^-18). This method makes it possible for “… removal of salts present in the analyte solution by a sample washing procedure away from the sample very simply” (4). Small

matrix spots using nanoliter volumes of matrix and analyte solution, combined purification, concentration, and application procedures have also given similar sensitivities (5). In this method, matrix is adsorbed to nanoliter bed volume reversed-phase column prepared in an Eppendorf GeLoder tip. Then the column is washed and the sample is eluted with a few nanoliter volume of matrix onto the target plate.

Sensitivity is reduced with increasing molecular weight. The sensitivity is two to three magnitudes lower for proteins than it is for peptides. So the sensitivity of proteins is in the femtomole range.

Structural Information

Structural information of proteins can be determined by digesting proteins with specific endoprotease like trypsin, AspN, and GluC. MALDI is one of the best spectrometric techniques for direct analysis of peptide mixtures. Signals of peptides are suppressed because there is a competition for charge or optimal position in the matrix. Therefore signal intensity does not necessarily reflect the quantities of different peptides in the mixtures. Complete sequences can be obtained from a combination of spectra recorded in different modes, like positive and negative, matrices, and different enzyme digestion.

Sequence information is also possible to get from PSD. This is possible by controlling the voltage of the reflector, which results in different m/z ranges on the detector and generates a PSD spectrum. A large sample amount is required since only a small fraction goes under PSD. Additionally, the fragmentation can not be controlled since different site of a peptide can get fragmented. This makes it very had to get complete sequences of a peptide. Alternatively, collision cells are included to the flight tube in MALDI-TOF by some manufacturers, to have controlled fragmentation by collision-induced dissociation.

Large amounts of in-source fragmentation occurs before initiation of the acceleration voltage called in-source decay in delayed extraction equipped MALDI-TOF, which only yield long regions of sequence-specific ions (6). C-terminal sequence ladders can be generated by digestion of peptides with carboxypepsidase and N-terminal sequence ladders can be obtained by Edman degradation using low percentage of phenyltiocarbamate rather than phenyoisothiocarbamate in the coupling reaction. These ladders in the mixtures of peptides can be an alternative to sequence-specific fragment ions. This process often gives a lot of sequence information.

Secondary protein modifications can also be determined using MALDI-TOF-MS. The steps involved in determining secondary modifications are measuring mass of the intact protein, knowing the protein’s primary sequence, and generating site-specific information by direct mass spectrometric peptide mapping of a mixture derived by proteolytic cleavage of the proteins. In tandem (TOF/TOF) configurations, MALDI instruments can provide protein sequence data, as well.

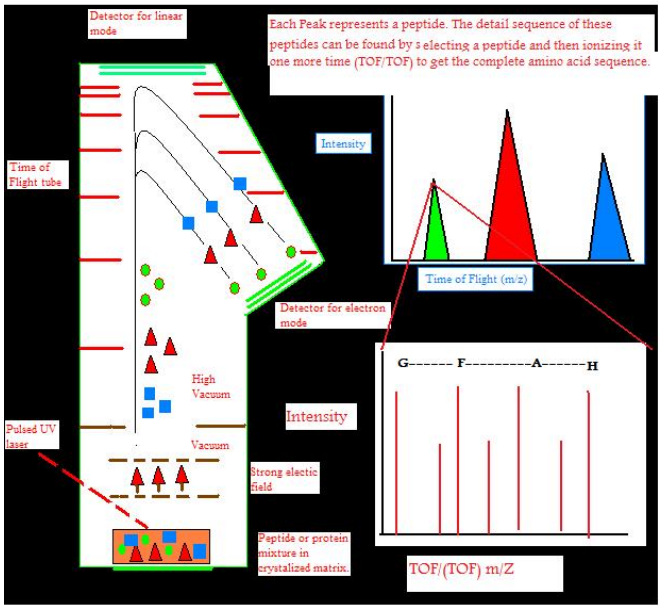
In tandem mass spectrometry, an ion of a particular mass is selected (that's the first stage of the analysis) and fragmented. Its constituent fragment ions are then mass-analyzed a second time (that's the tandem stage) to reveal data about the molecule's structure or sequence; single-stage TOF instruments lack this capability (though some fragmentation does occur via "post-source decay" as the ions traverse the flight tube).

Some companies offer tandem MALDI instruments based on hybrid mass analyzer configurations. Applied Biosystems' QSTAR, for instance, couples an optional MALDI source with a quadrupole-time-of-flight mass analyzer, as does Waters Corporation's MALDI Q-Tof Premier.

TOF analyzer

Modes

Ions can travel in a linear fashion and be detected by the detector at the opposite end as an ion source. This is called linear TOF. It is different from a reflectron TOF, in which ions are reflected to electrostatic mirror and detected by another detector. Linear TOF spectrum is limited in resolution leading to low mass accuracy. This is because initially different amount of kinetic energy can be attained by the ions with the same charge. This leads to different (m/z) ratio of ions which have different initial velocities. This is partially corrected by reflectron TOF. High energy ions penetrate deeper into the reflectron, taking longer distance and time, while low energy ions do not penetrate as deep into the reflectron and take a shorter path and time. This leads to correction of different times of ions with the same mass and charge. This leads to an increase of resolution to 10,000.



The amount of energy put into ions by the laser initially can also be corrected by a technique called delayed extraction (DE) in which acceleration voltage is applied slightly after the laser pulse. DE TOF increases resolution to 2000.

RE TOF can give full isotopic resolution for molecules up to 15 kDa. However 12C-only ion peak will have very low intensity for molecules bigger than 5kDa. Resolution is further decreased because each ion decays after acceleration and its time of flight can not be adjusted by RE TOF because decay has already occurred. These ions are not detected in RE TOF. However, these ions can be detected in linear TOF, but resolution still decreases because linear TOF has no way of correcting different energy inputs to an ion with the same mass and charge. It is better to use linear mode to get spectra and determine isotopically averaged mass for molecules bigger than 5-10 kDa. Resolution depends on the size of the molecules in a sample. The greater the size that the sample molecule has, the lower the resolution of it.

MALDI-TOF can only be compared to ESI because they are two ways of directly analyzing proteins, peptides, and polymers. MALDI-TOF samples can be reanalyzed while ESI samples can not because ESI is connected to LC column, and the analysis is limited to the width of the chromatographic peak. MALDI-TOF can scan 10 spectras for a peak 10 seconds wide per second, while it takes ESI almost 15 second. MALDI-TOF-MS generates mostly ions +/- 1 charge while ESI generates a charge for every 8-10 amino acids. That means ESI spectra are considerably more complex than MALDI spectra. Coulombic repulsion increases as the charge increase, leading to data deviation, and in MALDI spectra, this repulsion does not occur. However, multiple charges in ESI give better resolution because the higher the mass to charge ratio, the harder it is to get good resolution. In general MALDI is faster than ESI, and enables higher throughput. But ESI is more sensitive.

References

1. Proteomics in functional genomics : protein structure analysis / edited by P. Jollès and H. Jörnva
2. Fey SJ et al. (1997) Proteome analysis of Saccharomyces cerevisiae: A methodological outline. Electrophoresis 18: 1361-1372
   2. Karas M. et al. (1998) Laser desorption ionization of proteins with molecular mass exceeding 10,000 daltons. Anal Chem 60: 2299-2301
3. Patterson SD, Aebersold R (1995) Mass spectrometric approaches for the identification of gel-separated proteins. Electrophoresis 16: 1791-1814
4. Vorm O. Roepstroff P, Mann M (1994) Improved resolution and very high sensitivity in MALDI-TOF of matrix surfaces made by fast evaporation. Anal Chem 66: 3281-3287
5. Jespersen S, Niessen WM, et al. (1994) Attomole detection of proteins by matrix assisted laser desorption/ionization mass spectrometry with the use of picoliter vials. Rapid Comm. Mass Spectrom 8: 581-584
6. Reiber DC, Grower TA, et al. (1998) Identifying proteins and matrix-assisted laser desorption/ionization in source fragmentation data combined with databaseresearching. Anal Chem 70: 673-678

Contributors

- Basir Syed

3.6: MALDI-TOF is shared under a not declared license and was authored, remixed, and/or curated by LibreTexts.

3.7: Mass Spectra

Gas Chromatography/Mass Spectrometry (GS/MS)

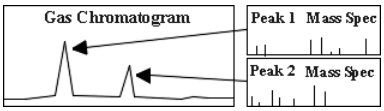
A mass spectrometer creates charged particles (ions) from molecules. It then analyzes those ions to provide information about the molecular weight of the compound and its chemical structure. There are many types of mass spectrometers and sample introduction techniques which allow a wide range of analyses. This discussion will focus on mass spectrometry as it's used in the powerful and widely used method of coupling Gas Chromatography (GC) with Mass Spectrometry (MS).



Pictured above is a GC/MS instrument used in the organic teaching labs.

Gas Chromatograph (GC)

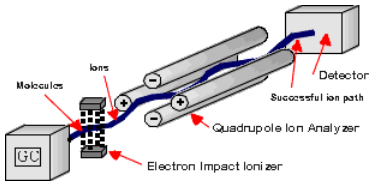
A mixture of compounds to be analysed is initially injected into the GC where the mixture is vaporized in a heated chamber. The gas mixture travels through a GC column, where the compounds become separated as they interact with the column. The chromatogram on the right shows peaks which result from this separation. Those separated compounds then immediately enter the mass spectrometer.



Mass Spectrometer (MS)

Below is a general schematic of a mass spectrometer. The blue line illustrates ions of a particular mass/charge ratio which reach the detector at a certain voltage combination. All mass spectrometers consist of three distinct regions:

1. Ionizer
2. Ion Analyzer
3. Detector



Ionizer

In the GC-MS discussed in this introduction, the charged particles (ions) required for mass analysis are formed by Electron Impact (EI) Ionization. The gas molecules exiting the GC are bombarded by a high-energy electron beam (70 eV). An electron which strikes a molecule may impart enough energy to remove another electron from that molecule. Methanol, for example, would undergo the following reaction in the ionizing region:

$$CH_3OH + 1\ \text{electron} \qquad CH_3OH^{+\bullet} + 2\ \text{electrons}$$

(note: the symbols +. indicate that a radical cation was formed)

EI Ionization usually produces singly charged ions containing one unpaired electron. A charged molecule which remains intact is called the molecular ion. Energy imparted by the electron impact and, more importantly, instability in a molecular ion can cause that ion to break into smaller pieces (fragments). The methanol ion may fragment in various ways, with one fragment carrying the charge and one fragment remaining uncharged. For example:

$$CH_3OH^{+\bullet}\text{(molecular ion)} \qquad CH_2OH^{+}\text{(fragment ion)} + H^{\bullet}$$

or

$$CH_3OH^{+\bullet}\text{(molecular ion)} \qquad CH_3^{+}\text{(fragment ion)} + {}^{\bullet}OH$$

Ion Analyzer

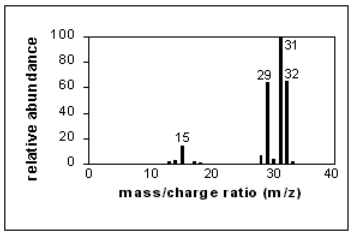
Molecular ions and fragment ions are accelerated by manipulation of the charged particles through the mass spectrometer. Uncharged molecules and fragments are pumped away. The quadrupole mass analyzer in this example uses positive (+) and negative (-) voltages to control the path of the ions. Ions travel down the path based on their mass to charge ratio (m/z). EI ionization produces singly charged particles, so the charge (z) is one. Therefore an ion's path will depend on its mass. If the (+) and (-) rods shown in the mass spectrometer schematic were 'fixed' at a particular rf/dc voltage ratio, then one particular m/z would travel the successful path shown by the solid line to the detector. However, voltages are not fixed, but are scanned so that ever increasing masses can find a successful path through the rods to the detector.

Detector

There are many types of detectors, but most work by producing an electronic signal when struck by an ion. Timing mechanisms which integrate those signals with the scanning voltages allow the instrument to report which m/z strikes the detector. The mass analyzer sorts the ions according to m/z and the detector records the abundance of each m/z. Regular calibration of the m/z scale is necessary to maintain accuracy in the instrument. Calibration is performed by introducing a well known compound into the instrument and "tweaking" the circuits so that the compound's molecular ion and fragment ions are reported accurately.

Interpreting spectra

A simple spectrum, that of methanol, is shown below. $CH_3OH^{+\bullet}$ (the molecular ion) and fragment ions appear in this spectrum.



Major peaks are shown in the table next to the spectrum. The x-axis of this bar graph is the increasing m/z ratio. The y-axis is the relative abundance of each ion, which is related to the number of times an ion of that m/z ratio strikes the detector. Assignment of relative abundance begins by assigning the most abundant ion a relative abundance of 100% (CH_2OH^+ in this spectrum). All other ions are shown as a percentage of that most abundant ion. For example, there is approximately 64% of the ion CHO^+ compared with the ion CH_2OH^+ in this spectrum. The y-axis may also be shown as abundance (not relative). Relative abundance is a way to directly compare spectra produced at different times or using different instruments.

ions	m/z
$CH_3OH^{+\bullet}$	32
$H_2C{=}OH^+$	31
$HC{\equiv}O^+$	29
H_3C^+	15

EI ionization introduces a great deal of energy into molecules. It is known as a "hard" ionization method. This is very good for producing fragments which generate information about the structure of the compound, but quite often the molecular ion does not appear or is a smaller peak in the spectrum.

Of course, real analyses are performed on compounds far more complicated than methanol Spectra interpretation can become complicated as initial fragments undergo further fragmentation, and as rearrangements occur. However, a wealth of information is contained in a mass spectrum and much can be determined using basic organic chemistry "common sense".

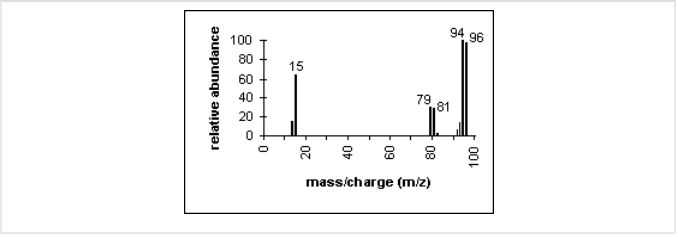
Following is some general information which will aid EI mass spectra interpretation

- **Molecular ion ($M^{\cdot+}$)**: If the molecular ion appears, it will be the highest mass in an EI spectrum (except for isotope peaks discussed below). This peak will represent the molecular weight of the compound. Its appearance depends on the stability of the compound. Double bonds, cyclic structures and aromatic rings stabilize the molecular ion and increase the probability of its appearance.
- **Reference Spectra**: Mass spectral patterns are reproducible. The mass spectra of many compounds have been published and may be used to identify unknowns. Instrument computers generally contain spectral libraries which can be searched for matches.
- **Fragmentation**: General rules of fragmentation exist and are helpful to predict or interpret the fragmentation pattern produced by a compound. Functional groups and overall structure determine how some portions of molecules will resist fragmenting, while other portions will fragment easily. A detailed discussion of those rules is beyond the scope of this introduction, and further information may be found in your organic textbook or in mass spectrometry reference books. A few brief examples by functional group are described (see Fragmentation Patterns).
- **Isotopes**: Isotopes occur in compounds analyzed by mass spectrometry in the same abundances that they occur in nature. A few of the isotopes commonly encountered in the analyses of organic compounds are below along with an example of how they can aid in peak identification.

Relative Isotope Abundance of Common Elements

Element	Isotope	Relative Abundance	Isotope	Relative Abundance	Isotope	Relative Abundance
Carbon	^{12}C	100	^{13}C	1.11		
Hydrogen	^{1}H	100	^{2}H	0.016		
Nitrogen	^{14}N	100	^{15}N	0.38		
Oxygen	^{16}O	100	^{17}O	0.04	^{18}O	0.20
Sulfur	^{32}S	100	^{33}S	0.78	^{34}S	4.40
Chlorine	^{35}Cl	100			^{37}Cl	32.5
Bromine	^{79}Br	100			^{81}Br	98.0

Methyl Bromide: An example of how isotopes can aid in peak identification.



The ratio of peaks containing ^{79}Br and its isotope ^{81}Br (100/98) confirms the presence of bromine in the compound.

Other Methods

An array of ionization methods and mass analyzers are available to meet the needs of many types of chemical analysis. A few are listed here with a highlight of their usefulness.

Sample introduction/ionization methods

Ionization method	Typical Analytes	Sample Introduction	Mass Range	Method Highlights
Electron Impact (EI)	Relatively small volatile	GC or liquid/solid probe	to 1,000 Daltons	Hard method versatile provides structure info
Chemical Ionization (CI)	Relatively small volatile	GC or liquid/solid probe	to 1,000 Daltons	Soft method molecular ion peak $[M+H]^+$
Electrospray (ESI)	Peptides Proteins nonvolatile	Liquid Chromatography or syringe	to 200,000 Daltons	Soft method ions often multiply charged
Fast Atom Bombardment (FAB)	Carbohydrates Organometallics Peptides nonvolatile	Sample mixed in viscous matrix	to 6,000 Daltons	Soft method but harder than ESI or MALDI
Matrix Assisted Laser Desorption (MALDI)	Peptides Proteins Nucleotides	Sample mixed in solid matrix	to 500,000 Daltons	Soft method very high mass

Mass Analyzers

Analyzer	System Highlights
Quadrupole	Unit mass resolution, fast scan, low cost
Sector (Magnetic and/or Electrostatic)	High resolution, exact mass
Time-of-Flight (TOF)	Theoretically, no limitation for m/z maximum, high throughput
Ion Cyclotron Resonance (ICR)	Very high resolution, exact mass, perform ion chemistry

Linked Systems

GC/MS:	Gas chromatography coupled to mass spectrometry
LC/MS:	Liquid chromatography coupled to electrospray ionization mass spectrometry

Outside Links

- A library of spectra can be found in the NIST WebBook, a data collection of the National Institute of Standards and Technology.
- Useful tools such as an exact mass calculator and a spectrum generator can be found in the MS Tools section of Scientific Instrument Services webpage.

- The JEOL Mass Spectrometry website contains tutorials, reference data and links to other sites.
- More general information and tutorials can be found in Scimedia, an educational resource.
- At the University of Arizona, the Wysocki Research Group studies surface-induced dissociation (SID) tandem mass spectrometry.
- Many more interesting and useful links can be found by following the site links in the above references.

Contributors

Dr. Linda Breci, Associate Director Arizona Proteomics Consortium University of Arizona

---

3.7: Mass Spectra is shared under a not declared license and was authored, remixed, and/or curated by LibreTexts.

3.7.1: Interpreting a Mass Spectrum

Here are a list of steps to follow when interpreting a mass spectrum. This simplified list will help you to interpret many spectra, however there are other mechanisms of fragmentation which cannot be covered in this brief tutorial.

Steps to interpret a mass spectrum

1. Look for the molecular ion peak.

- This peak (if it appears) will be the highest mass peak in the spectrum, except for isotope peaks.
- Nominal MW (meaning=rounded off) will be an even number for compounds containing only C, H, O, S, Si.
- Nominal MW will be an odd number if the compound also contains an odd number of N (1,3,...).

2. Try to calculate the molecular formula:

- The isotope peaks can be very useful, and are best explained with an example.
  - Carbon 12 has an isotope, carbon 13. Their abundances are ^{12}C=100%, ^{13}C=1.1%. This means that for every 100 $^{(12)}C$ atoms there are 1.1 $^{(13)}C$ atoms.
  - If a compound contains 6 carbons, then each atom has a 1.1% abundance of $^{(13)}C$.
  - Therefore, if the molecular ion peak is 100%, then the isotope peak (1 mass unit higher) would be 6x1.1%=6.6%.
  - If the molecular ion peak is not 100% then you can calculate the relative abundance of the isotope peak to the ion peak. For example, if the molecular ion peak were 34% and the isotope peak 2.3%: (2.3/34)x100 = 6.8%. 6.8% is the relative abundance of the isotope peak to the ion peak. Next, divide the relative abundance by the isotope abundance: 6.8/1.1=6 carbons.
- Follow this order when looking for information provided by isotopes: (A simplified table of isotopes is provided in the introduction, more detailed tables can be found in chemistry texts.)
  - Look for A+2 elements: O, Si, S, Cl, Br
  - Look for A+1 elements: C, N
  - "A" elements: H, F, P, I

3. Calculate the total number of rings plus double bonds:

- For the molecular formula: $C_xH_yN_zO_n$
  - rings + double bonds = x - (1/2)y + (1/2)z + 1

4. Postulate the molecular structure consistent with abundance and m/z of fragments.

- More information on specific fragmentation can be found in the quiz for each functional group.

Contributors

3.7.1: Interpreting a Mass Spectrum is shared under a not declared license and was authored, remixed, and/or curated by LibreTexts.

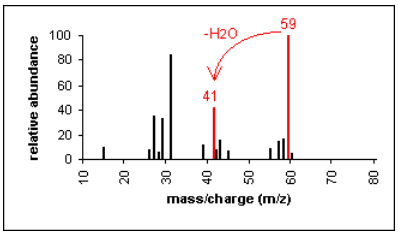
3.7.2: Mass Spectrometry - Fragmentation Patterns

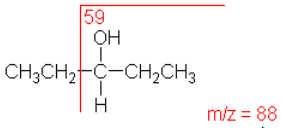
Following are examples of compounds listed by functional group, which demonstrate patterns which can be seen in mass spectra of compounds ionized by electron impact ionization. These examples do not provide information about the fragmentation mechanisms that cause these patterns. Additional information can be found in mass spectrometry reference books.

Alcohol

An alcohol's molecular ion is small or non-existent. Cleavage of the C-C bond next to the oxygen usually occurs. A loss of H_2O may occur as in the spectra below.

3-Pentanol ($C_5H_{12}O$) with MW = 88.15

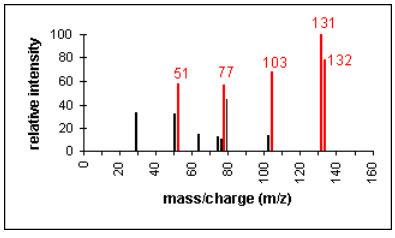


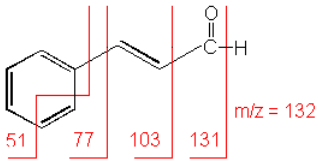


Aldehyde

Cleavage of bonds next to the carboxyl group results in the loss of hydrogen (molecular ion less 1) or the loss of CHO (molecular ion less 29).

3-Phenyl-2-propenal (C_9H_8O) with MW = 132.16

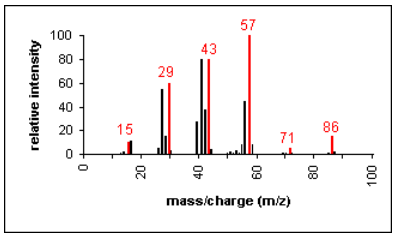


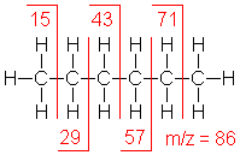


Alkane

Molecular ion peaks are present, possibly with low intensity. The fragmentation pattern contains clusters of peaks 14 mass units apart (which represent loss of (CH2)nCH3).

Hexane (C6H14) with MW = 86.18

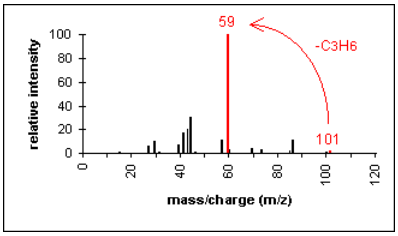


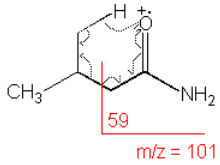


Amide

Primary amides show a base peak due to the McLafferty rearrangement.

3-Methylbutyramide ($C_5H_{11}NO$) with MW = 101.15

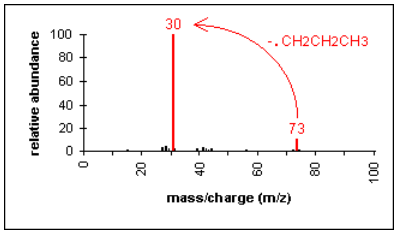


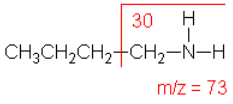


Amine

Molecular ion peak is an odd number. Alpha-cleavage dominates aliphatic amines.

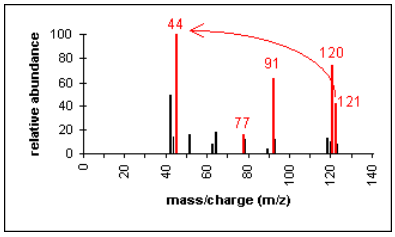
n-Butylamine (C4H11N) with MW = 73.13

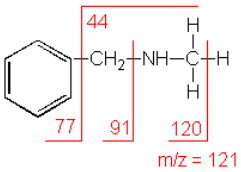




Another example is a secondary amine shown below. Again, the molecular ion peak is an odd number. The base peak is from the C-C cleavage adjacent to the C-N bond.

n-Methylbenzylamine ($C_8H_{11}N$) with MW = 121.18

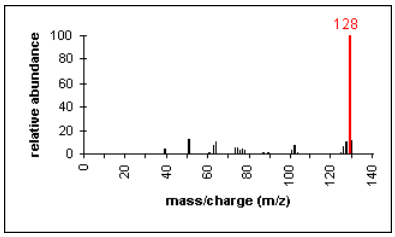


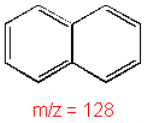


Aromatic

Molecular ion peaks are strong due to the stable structure.

Naphthalene ($C_{10}H_8$) with MW = 128.17

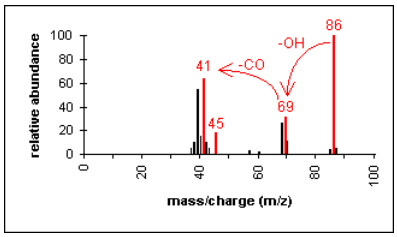


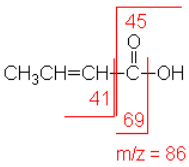


Carboxylic Acid

In short chain acids, peaks due to the loss of OH (molecular ion less 17) and COOH (molecular ion less 45) are prominent due to cleavage of bonds next to C=O.

2-Butenoic acid ($C_4H_6O_2$) with MW = 86.09

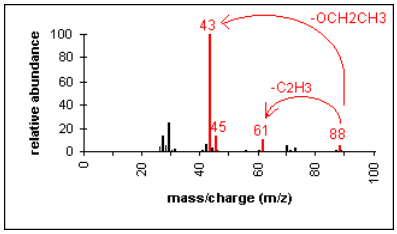


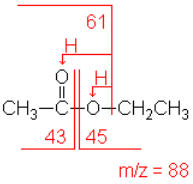


Ester

Fragments appear due to bond cleavage next to C=O (alkoxy group loss, -OR) and hydrogen rearrangements.

Ethyl acetate ($C_4H_8O_2$) with MW = 88.11

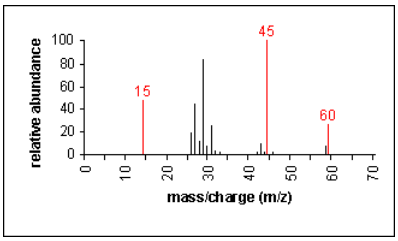


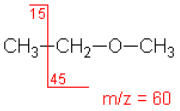


Ether

Fragmentation tends to occur alpha to the oxygen atom (C-C bond next to the oxygen).

Ethyl methyl ether (C_3H_8O) with MW = 60.10

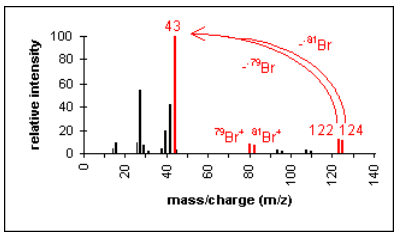


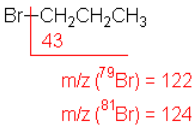


Halide

The presence of chlorine or bromine atoms is usually recognizable from isotopic peaks.

1-Bromopropane (C_3H_7Br) with MW = 123.00

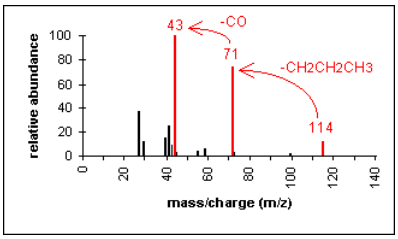


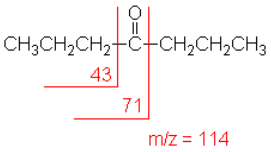


Ketone

Major fragmentation peaks result from cleavage of the C-C bonds adjacent to the carbonyl.

4-Heptanone ($C_7H_{14}O$) with MW = 114.19





Contributors

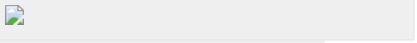
Dr. Linda Breci, Associate Director Arizona Proteomics Consortium University of Arizona

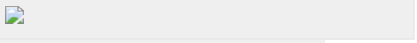
3.7.2: Mass Spectrometry - Fragmentation Patterns is shared under a not declared license and was authored, remixed, and/or curated by LibreTexts.

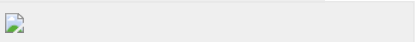
3.7.3: Mass Spectroscopy- Quizzes

1	Identify the molecular ion in this spectrum.	
		Hint
		Click on image to enlarge
	○	a) 45
	○	b) 46
	○	c) 47
2	For this same spectrum, choose the compound that the spectrum represents.	
		Hint Web Reference
		Click on image to enlarge
	○ **a)**	formic acid
	○ **b)**	1-propanol
	○ **c)**	ethanol
	○ **d)**	methanol
	○ **e)**	isopropyl alcohol
3	Find the alkyl ion series in the spectrum below. (Check the hint!)	
		Hint Web Reference
		Click on image to enlarge
	○ **a)**	15, 29, 43, 57
	○ **b)**	31, 45
	○ **c)**	none

4	Find the alkyl LOSS ion series in the same spectra shown below. (Check the hint!)	
		Hint Web Reference
		Click on image to enlarge 
	◯ **a)**	15, 29, 43, 57
	◯ **b)**	31, 45
	◯ **c)**	none
5	***For the same spectrum shown in the previous two questions, choose the compound that the spectrum represents.***	
		Hint Web Reference
		Click on image to enlarge 
	◯ **a)**	2-methyl-2-propanol
	◯ **b)**	1-butanol
	◯ **c)**	2-butanol
	◯ **d)**	1-pentanol
	◯ **e)**	2-methyl-1-propanol
6	***Identify the molecular ion in this spectrum.***	
		Hint Web Reference
		Click on image to enlarge 
	◯ **a)**	70
	◯ **b)**	71
	◯ **c)**	87
	◯ **d)**	88

7	***For the same spectrum, choose the compound that the spectrum represents.***	
		Hint Web Reference
		Click on image to enlarge 
	◯ **a)**	1-hexanol
	◯ **b)**	1-pentanol
	◯ **c)**	2-methyl-2-butanol
	◯ **d)**	2-pentanol
	◯ **e)**	1-butanol

8	***Choose the compound that this spectrum represents.***	
		Hint Web Reference
		Click on image to enlarge 
	◯ **a)**	2-methyl-2-butanol
	◯ **b)**	2-methyl-2-propanol
	◯ **c)**	2-butanol
	◯ **d)**	1-butanol
	◯ **e)**	2-methyl-1-propanol

9	***Choose the compound that this spectrum represents.***	
		Hint Web Reference
		Click on image to enlarge 
	◯ **a)**	2-pentanol

	◯ **b)**	2-methyl-2-propanol
	◯ **c)**	1-butanol
	◯ **d)**	2-methyl-1-propanol
	◯ **e)**	2-butanol

Contributors

3.7.3: Mass Spectroscopy- Quizzes is shared under a not declared license and was authored, remixed, and/or curated by LibreTexts.

3.8: Mass Spectra Interpretation- ALDEHYDES

ELECTRON IMPACT MASS SPECTROMETRY PRODUCED THE SPECTRA BELOW. MANY PEAKS ARE LABELLED TO AID INTERPRETATION: M/Z (RELATIVE ABUNDANCE). LOOK AT THE HINTS AND FOLLOW THE WEB REFERENCE LINK FOR

HELP. YOU WILL NEED A PERIODIC TABLE, A TABLE OF COMMON ISOTOPES (WHICH YOU CAN FIND IN THE WEB REFERENCE), A CALCULATOR, AND SCRATCH PAPER TO WORK THIS QUIZ.

2 ***For this same spectrum, choose the compound that the spectrum represents.***

Click on image to enlarge

- ◯ **a)** butanal
- ◯ **b)** propanal
- ◯ **c)** 2-propenal
- ◯ **d)** methoxy-ethene
- ◯ **e)** ethanediol

3. ***Find the alkyl ion series in the spectra below. (Check the hint!)***

Web Reference

		Click on image to enlarge
	◯ **a)**	15, 29, 43
	◯ **b)**	29, 43, 57
	◯ **c)**	none
4.	***Find the alkyl LOSS ion series in the same spectra shown below. (Check the hint!)***	
		Web Reference
		Click on image to enlarge
	◯ **a)**	15, 29, 43
	◯ **b)**	29, 43, 57
	◯ **c)**	none



5. ***For this same spectrum, choose the compound that the spectrum represents.***

Web Reference

Click on image to enlarge

- ◯ **a)** 2-propenal
- ◯ **b)** 2-methyl propanal
- ◯ **c)** pentanal
- ◯ **d)** 2-oxo-propanal
- ◯ **e)** butanal



6. ***Choose the compound that this spectrum represents.***

		Web Reference
		Click on image to enlarge
	○ **a)**	hexanal
	○ **b)**	3-methyl butanal
	○ **c)**	pentanal
	○ **d)**	2-methyl propanal
	○ **e)**	2,2-dimethyl propanal
7	***Choose the compound that this spectrum represents.***	
		Web Reference
		Click on image to enlarge
	○ **a)**	2-methyl propanal

	b)	butanal
	c)	2-oxo-propanal
	d)	2-propenal
	e)	pentanal
8	***Choose the compound that this spectrum represents.***	
		Web Reference
		Click on image to enlarge
	a)	2,2-dimethyl propanal
	b)	hexanal
	c)	2-oxo-propanal
	d)	3-methyl-butanal
	e)	pentanal

3.8: Mass Spectra Interpretation- ALDEHYDES is shared under a not declared license and was authored, remixed, and/or curated by LibreTexts.

3.9: Mass Spectrometers (Instrumentation)

3.9: Mass Spectrometers (Instrumentation) is shared under a not declared license and was authored, remixed, and/or curated by LibreTexts.

3.9.1: Electrospray Ionization Mass Spectrometry

Electrospray ionization is a soft ionization technique that is typically used to determine the molecular weights of proteins, peptides, and other biological macromolecules. Soft ionization is a useful technique when considering biological molecules of large molecular mass, such as the aformetioned, because this process does not fragment the macromolecules into smaller charged particles, rather it turns the macromolecule being ionized into small droplets. These droplets will then be further desolvated into even smaller droplets, which creates molecules with attached protons. These protonated and desolvated molecular ions will then be passed through the mass analyzer to the detector, and the mass of the sample can be determined.

Introduction

Electrospray ionization mass spectrometry is a desorption ionization method. Desorption ionization methods can be performed on solid or liquid samples, and allows for the sample to be nonvolatile or thermally unstable. This means that ionization of samples such as proteins, peptides, olgiopeptides, and some inorganic molecules can be performed. Electrospray ionization mass spectrometry requires that a molecule be of a fairly large mass. The instrument has a small mass range that it is able to detect, so therefore the mass of the unknown injected sample can easily be determined; as it must be in the range of the instrument. This quantitative analysis is done by considering the mass to charge ratios of the various peaks in the spectrum (Figure 1). The spectrum is shown with the mass-to-charge (m/z) ratio on the x-axis, and the relative intensity (%) of each peak shown on the y-axis. Calculations to determine the unknown mass, M_r, from the spectral data can then be performed using

$$p = \frac{m}{z} \tag{3.9.1.1}$$

$$p_1 = \frac{M_r + z_1}{z_1} \tag{3.9.1.2}$$

$$p_2 = \frac{M_r + (z_1 - 1)}{z_1 - 1} \tag{3.9.1.3}$$

where p_1 and p_2 are adjacent peaks. Peak p_1 comes before peak p_2 in the spectrum, and has a lower m/z value. The z_1 value represents the charge of peak one. It should be noted that as the m/z value increases, the number of protons attached to the molecular ion decreases. Figure 1 below illustrates these concepts. Electrospray ionization mass spectrometry research was pioneered by the analytical chemistry professor John Bennet Fenn, who shared the Nobel Prize in Chemistry with Koichi Tanaka in 2002 for his work on the subject.

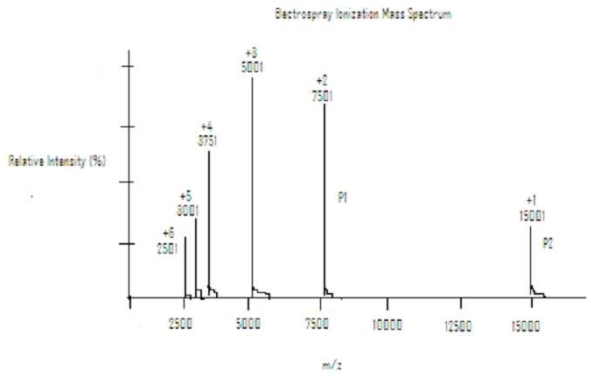


Figure 1. Mass Spectrum Example

Calculations for m/z in spectrum

$[M + 6H]^{6+}$ $[M + 5H]^{5+}$ $[M + 4H]^{4+}$

m/z = 15006/6 = 2501 m/z = 15005/5 = 3001 m/z = 15004/4 = 3751

$$[M + 3H]^{3+}\ [M + 2H]^{2+}\ [M + H]^{1+}$$

$$m/z = 15003/3 = 5001\ m/z = 15002/2 = 7501\ m/z = 15001/1 = 15001$$

Sample Preparation

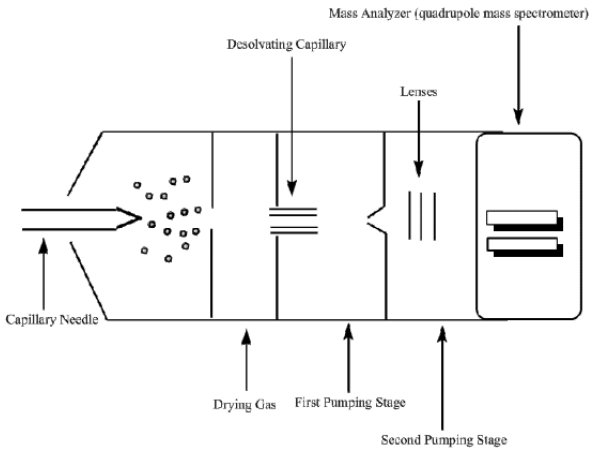
Samples for injection into the electrospray ionization mass spectrometer work the best if they are first purified. The reason purity in a sample is important is because this technique does not work well when mixtures are used as the analyte. For this reason a means of purification is often employed to inject a homogeneous sample into the capillary needle. High performance liquid chromatography, Capillary Electrophoresis, and Liquid-Solid Column Chromatography are methods of choice for this purpose. The chosen purification method is then attached to the capillary needle, and the sample can be introduced directly.

Advantages and Disadvantages

There are some clear advantages to using electrospray ionization mass spectrometry as an analytical method. One advantage is its ability to handle samples that have large masses. Another advantage is that this ionization method is one of the softest ionization methods available, therefore it has the ability to analyze biological samples that are defined by non-covalent interactions. A quadrupole mass analyzer can also be used for this method, which means that a sample's structure can be determined fairly easily. The m/z ratio range of the quadrupole instrument is fairly small, which means that the mass of the sample can be determined to with a high amount of accuracy. Finally, the sensitivity for this instrument is impressive and therefore can be useful in accurate quantitative and qualitative measurements.

Some disadvantages to electrospray ionization mass spectrometry are present as well. A major disadvantage is that this technique cannot analyze mixtures very well, and when forced to do so, the results are unreliable. The apparatus is also very difficult to clean and has a tendency to become overly contaminated with residues from previous experiments. Finally, the multiple charges that are attached to the molecular ions can make for confusing spectral data. This confusion is further fueled by use of a mixed sample, which is yet another reason why mixtures should be avoided when using an electrospray ionization mass spectrometer.

Apparatus



Capillary Needle

The capillary needle is the inlet into the apparatus for the liquid sample. Once in the capillary needle, the liquid sample is nebulized and charged. There is a large amount of pressure being applied to the capillary needle, which in effect nebulizes the liquid sample forming a mist. The stainless steel capillary needle is also surrounded by an electrode that retains a steady voltage of around 4000 volts. This applied voltage will place a charge on the droplets. Therefore, the mist that is ejected from the needle will be comprised of charged molecular ions.

Desolvating Capillary

The molecular ions are oxidized upon entering the desolvating capillary, and a continual voltage is applied to the gas chamber in which this capillary is located. Here the desolvation process begins, through the use of a dry gas or heat, and the desolvation process continues through various pumping stages as the molecular ion travels towards the mass analyzer. An example of a dry gas

would be an N_2 gas that has been dehydrated. The gas or heat then provides means of evaporation, or desolvation, for the ionized droplets. As the droplets become smaller in size, their electric field densities become more concentrated. The increase in electric field density causes the like charges to repel one another, which induces an increase in surface tension. The point where the droplet can no longer support this increase in surface tension is known as the Rayleigh limit. At this point, the droplet divides into smaller droplets of either positive or negative chrage. This process is refered to as either a coulombic explosion or the ions are described as exiting the droplet through the "Taylor cone". Once the molecular ions have reached the entrance to the mass analyzer, they have been effectively reduced through protonation.

Mass Analyzer

Mass Analyzers (Mass Spectrometry) are used to determine the mass-to-charge ratio (m/z), this ratio is used to differentiate between molecular ions that were formed in the desolvating capillary. In order for a mass-to-charge ratio to be determined, the mass analyzer must be able to separate even the smallest masses. The ability of the analyzer to resolve the mass peaks can be defined with the following equation;

$$R = \frac{m}{\Delta m} \tag{3.9.1.4}$$

This equation represents the mass of the first peak (m), divided by the difference between the neighboring peaks Δm. The better the resolution, the more useful the data. The mass analyzer must also be able to measure the ion currents produced by the multiply charged particles that are created in this process.

Mass analyzers use electrostatic lenses to direct the beam of molecular ions to the analyzer. A vacuum system is used to maintain a low pressure environment in order to prevent unwanted interactions between the molecular ions and any components that may be present in the atmosphere. These atmospheric components can effect the determined mass-to-charge ratio, so it is best to keep them to a minimum. The mass-to-charge ratio is then used to determine quantitative and qualitative properties of the liquid sample.

The mass analyzer used for electrospray ionization is a quadrupole mass spectrometer. A quadrupole mass spectrometer uses four charged rods, two negatively charged and two positively charged, that have alternating AC and DC currents. The rods are connected to both the positive terminal of the DC voltage and the negative terminal. Each pair of rods contains a negatively charged rod and a positively charged rod. The molecular ions are then sped through the chamber between these pairs of oppositely charged rods making use of a potential difference to do so. To maintain charge, and ultimately be readable by the detector, the molecular ions must travel through the quadrupole chamber without touching any of the four charged rods. If a molecular ion does run into one of the rods it will deem it neutral and undetectable.

Detector

The molecular ions pass through the mass analyzer to the detector. The detector most commonly used in conjunction with the quadrupole mass analyzer is a high energy dynode (HED), which is a electron multiplier with some slight variations. In an HED detector, the electrons are passed through the system at a high voltage and the electrons are measured at the end of the funnel shaped apparatus; otherwise known as the anode. A HED detector differs from the electron multiplier in that it operates at a much higher sensitivity for samples with a large mass than does the electron multiplier detector. Once the analog signal of the mass-to-charge ratio is recorded, it is then converted to a digital signal and a spectrum representing the data run can be analyzed.

References

1. Skoog, D.A.; Holler, F.J.; Crouch, S.R. Principles of Instrumental Analysis. Sixth Edition, Thomson Brooks/Cole, USA (2007).
2. Siuzdak, G. Mass Spectrometry for Biotechnology. Academic Press, Inc., USA (1996).
3. Chapman, J.R. Mass Spectrometry of Proteins and Peptides. Methods in Molecular Biology volume 146,Humana Press, Totowa, NJ (2000).
4. Snyder, A. P. Biochemical and Biotechnological Applications of Electrospray Ionization Mass Spectrometry. American Chemical Society, Washington, DC (1996).

Problems

Using the above spectrum, calculate the mass of the protein. For p_1, shown in spectrum, the m/z is 7501 and for p_2 the m/z is 15001. (Hint: Use the above equations, and the charge of p_1 for z_1)

Contributors

- Jennifer Murphy

3.9.1: Electrospray Ionization Mass Spectrometry is shared under a not declared license and was authored, remixed, and/or curated by LibreTexts.

3.9.2: Injection Stage

The principle components of a mass spectrometer are an inlet, ion source, mass analyzer, detector, and data analysis. The function of an inlet system is to introduce a small amount of sample into the ion source with minimal loss of vacuum. However, many mass spectrometers contain more than one inlet system to accommodate a variety of samples. These include batch inlets, direct probe inlets, and chromatographic and capillary electrophoretic inlet systems.

Batch Inlets

The batch inlet system is considered the most common and simplest inlet system. Normally, the inside of the system is lined with glass to elude losses of polar analytes by adsorption. This system externally volatizes the sample which leaks into an empty ionization region. Boiling points up to 500 degrees C of gaseous and liquid samples can be used on typical systems. The system's vacuum contains a sample pressure of 10^{-4} to 10^{-5} Torr. Liquids are introduced using a microliter syringe into a reservoir; gases are enclosed in a metering area that is confined between two valves before being expanded into a reservoir container. Liquids that have boiling points lower than 500 degrees C can not be used in the system because the reservoir and tubing need to be kept at high temperatures by ovens and heating tapes. This is to ensure that the liquid samples are transformed to the gaseous phase and then leaked through a metal or glass diaphragm containing pinholes to the ionization area.

Direct Probe Inlets

A direct probe inlet is for small quantities of sample, solids, and nonvolatile liquids. Solids and nonvolatile liquids are injected through a probe, or sample holder. The probe is inserted through a vacuum lock which is designed to limit the volume of air needed to pump from the system after the probe has been inserted into the ionization section. Unlike the batch inlet, the sample will need to be cooled and/or heated on the probe. The probe is placed extremely close (a few millimeters) to the ionization source, where the slit leads to the spectrometer, and the sample is held in place on the surface of a glass or aluminum capillary tube or a small cup. This position makes it possible for thermally unstable compounds to be analyzed before decomposition because of the low pressure in the ionization area which is in close proximity to the sample. Do to the probe, nonvolatile samples such as carbohydrates, steroids, and metal-organic species can be studied because the low pressures lead to increased concentrations of the nonvolatile samples. The principle sample requirement is attainment of an analyte partial pressure of at least 10^{-8} torr before the onset of decomposition.[1]

Chromatographic and Capillary Electrophoretic Inlets

Chromatographic systems and Capillary Electrophoretic units are often coupled with mass spectrometers in order to allow separation and identification of the components in the sample. If these systems and units are linked with a mass spectrometer, then other specialized inlets, electrokinetic and pressure injection, are required. Electrokinetic and pressure injection controls the amount of volume injected by the duration of the injection, which typically range between 5 to 50 nL.

Electrokinetic Injection

The electrokinetic injection method involves one end of the capillary and electrode in a small cup removed from the buffer. Ionic migration and electroosmotic flow of the sample in the capillary are a result of a voltage applied for a recorded time. After this voltage is applied, the capillary end and electrode are placed back into the regular buffer solution for the remainder of the separation. The electrokinetic Injection technique injects larger quantities of the mobile ions versus the slower moving ions.

Pressure Injection

The pressure injection method is similar to the electrokinetic injection because the capillary end and electrode are removed from the buffer and placed into a small cup. However, instead of a voltage being applied, a pressure difference drives the sample into the capillary. A vacuum is applied at the detector end which produces the potential difference by pressurizing the sample or elevating the sample end. Pressure injection does not discriminate because of ion mobility, but it cannot be used in gel-filled capillaries.[1]

References

1. Skoog, D., Holler, J., Crouch, S. Principles of Instrumental Analysis, 6th Ed.; Thomson Brooks/Cole: Belmont, 2007

3.9.2: Injection Stage is shared under a not declared license and was authored, remixed, and/or curated by LibreTexts.

3.9.3: Mass Analyzers (Mass Spectrometry)

Mass spectrometry is an analytic method that employs ionization and mass analysis of compounds to determine the mass, formula and structure of the compound being analyzed. A mass analyzer is the component of the mass spectrometer that takes ionized masses and separates them based on charge to mass ratios and outputs them to the detector where they are detected and later converted to a digital output.

Introduction

There are six general types of mass analyzers that can be used for the separation of ions in a mass spectrometry.

1. Quadrupole Mass Analyzer
2. Time of Flight Mass Analyzer
3. Magnetic Sector Mass Analyzer
4. Electrostatic Sector Mass Analyzer
5. Quadrupole Ion Trap Mass Analyzers
6. Ion Cyclotron Resonance

Quadrupole Mass Analyzer

The DC bias will cause all the charged molecules to accelerate and move away from the center line, the rate being proportional to their charge to mass ratio. If their course goes off too far they will hit the metal rods or the sides of the container and be absorbed. So the DC bias acts like the magnetic field B of the mass spec and can be tuned to specific charge to mass ratios hitting the detector.

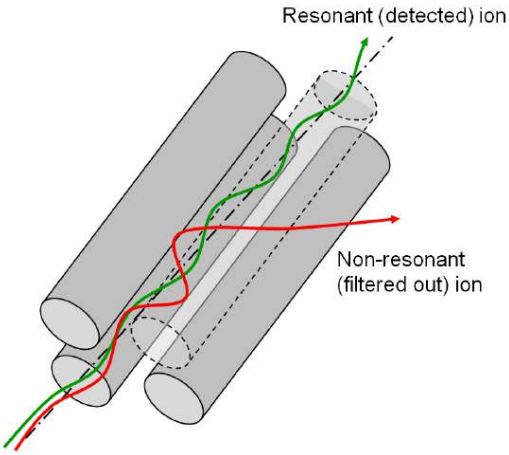


Figure 1: A quadrupole

The two sinusoidal electric fields at 90 orientation and 90 degrees degrees phase shift will cause an electric field which oscillates as a circle over time. So as the charged particles fly down toward the detector, they will be traveling in a spiral, the diameter of the spiral being determined by the charge to mass ratio of the molecule and the frequency and strength of the electric field. The combination of the DC bias and the circularly rotating electric field will be the charge particles will travel in a spiral which is curved. So by timing the peak of the curved spiral to coincide with the position of the detector at the end of the quadrupole, a great deal of selectivity to molecules charge to mass ratio can be obtained.

TOF (Time of Flight) Mass Analyzer

TOF Analyzers separate ions by time without the use of an electric or magnetic field. In a crude sense, TOF is similar to chromatography, except there is no stationary/ mobile phase, instead the separation is based on the kinetic energy and velocity of the ions.

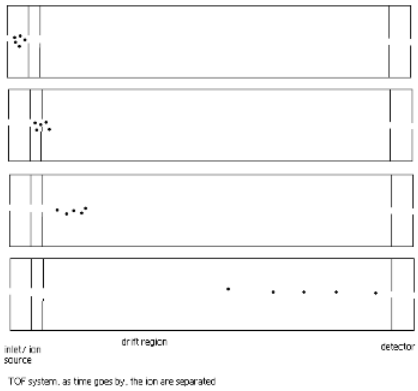


Figure 2: A TOF system. As time evolves, the ions (formed at the source) are separated.

Ions of the same charges have equal kinetic energies; kinetic energy of the ion in the flight tube is equal to the kinetic energy of the ion as it leaves the ion source:

$$KE = \frac{mv^2}{2} = zV \tag{1}$$

The time of flight, or time it takes for the ion to travel the length of the flight tube is:

$$T_f = \frac{L}{v} \tag{2}$$

- with L is the length of tube and
- v is the velocity of the ion

Substituting Equation 1 for kinetic energy in Equation 2 for time of flight:

$$T_f = L\sqrt{\frac{m}{z}}\sqrt{\frac{1}{2V}} \propto \sqrt{\frac{m}{z}} \tag{3}$$

During the analysis, L, length of tube, the Voltage from the ion source V are held constant, which can be used to say that time of flight is directly proportional to the root of the mass to charge ratio.

Unfortunately, at higher masses, resolution is difficult because flight time is longer. Also at high masses, not all of the ions of the same m/z values reach their ideal TOF velocities. To fix this problem, often a **reflectron** is added to the analyzer. The reflectron consists of a series of ring electrodes of very high voltage placed at the end of the flight tube. When an ion travels into the reflectron, it is reflected in the opposite direction due to the high voltage.

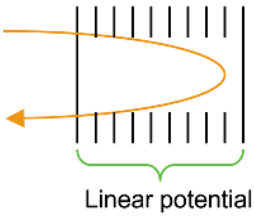


Figure 3: A reflection. Image used with permission from Wikipedia.

The reflectron increases resolution by narrowing the broadband range of flight times for a single m/z value. Faster ions travel further into the reflectrons, and slower ions travel less into the reflector. This way both slow and fast ions, of the same m/z value, reach the detector at the same time rather then at different times, narrowing the bandwidth for the output signal.

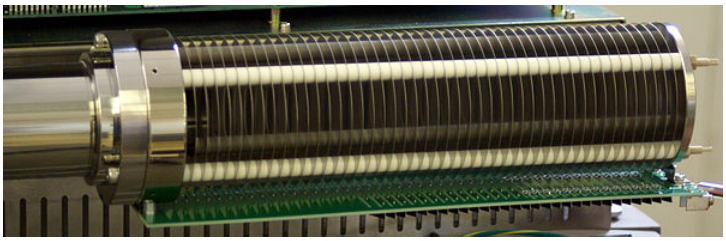


Figure 4. A photo of a reflectron. An ion mirror (right) attached to a flight tube (left) of the reflectron. Voltages applied to a stack of metal plates create the electric field reflecting the ions back to the flight tube. In this particular design, gaps between the mirror electrodes are too large. This can lead to a distortion of the field inside the mirror caused by a proximity of metal surface of the enveloping vacuum tube. Image used with permission from Wikipedia.

Magnetic Sector Mass Analyzer

Similar to time of flight (TOF) analyzer mentioned earlier,in magnetic sector analyzers ions are accelerated through a flight tube, where the ions are separated by charge to mass ratios. The difference between magnetic sector and TOF is that a magnetic field is used to separate the ions. As moving charges enter a magnetic field, the charge is deflected to a circular motion of a unique radius in a direction perpendicular to the applied magnetic field. Ions in the magnetic field experience two equal forces; force due to the magnetic field and centripetal force.

$$F_B = zvB = F_c = \frac{mv^2}{r} \tag{4}$$

The above equation can then be rearranged to give:

$$v = \frac{Bzr}{m} \tag{5}$$

If this equation is substituted into the kinetic energy equation:

$$KE = zV = \frac{mv^2}{2} \tag{6}$$

$$\frac{m}{z} = \frac{B^2r^2}{2V} \tag{7}$$

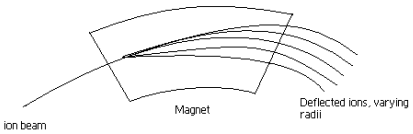


Figure 5: A magnetic sector separator.

Basically the ions of a certain m/z value will have a unique path radius which can be determined if both magnetic field magnitude B, and voltage difference V for region of acceleration are held constant. when similar ions pass through the magnetic field, they all will be deflected to the same degree and will all follow the same trajectory path. Those ions which are not selected by V and B values, will collide with either side of the flight tube wall or will not pass through the slit to the detector. Magnetic sector analyzers are used for mass focusing, they focus angular dispersions.

Electrostatic Sector Mass Analyzer

Is similar to time of flight analyzer in that it separates the ions while in flight, but it separates using an electric field. Electrostatic sector analyzer consists of two curved plates of equal and opposite potential. As the ion travels through the electric field, it is deflected and the force on the ion due to the electric field is equal to the centripetal force on the ion. Here the ions of the same kinetic energy are focused, and ions of different kinetic energies are dispersed.

\[KE = zV =\dfrac{mv^2}{2} \tag{8}]

$$F_E = zE = F_c = \frac{mv^2}{R} \tag{9}$$

Electrostatic sector analyzers are energy focusers, where an ion beam is focused for energy. Electrostatic and magnetic sector analyzers when employed individually are single focusing instruments. However when both techniques are used together, it is called a double focusing instrument., because in this instrument both the energies and the angular dispersions are focused.

Quadrupole Ion Trap Mass Analyzers

This analyzer employs similar principles as the quadrupole analyzer mentioned above, it uses an electric field for the separation of the ions by mass to charge ratios. The analyzer is made with a ring electrode of a specific voltage and grounded end cap electrodes. The ions enter the area between the electrodes through one of the end caps. After entry, the electric field in the cavity due to the electrodes causes the ions of certain m/z values to orbit in the space. As the radio frequency voltage increases, heavier mass ion orbits become more stabilized and the light mass ions become less stabilized, causing them to collide with the wall, and eliminating the possibility of traveling to and being detected by the detector.

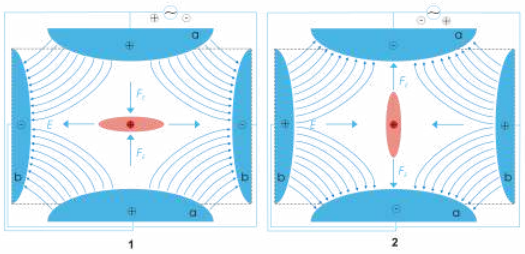


Figure 5: Scheme of a Quadrupole ion trap of classical setup with a particle of positive charge (dark red), surrounded by a cloud of similarly charged particles (light red). The electric field E (blue) is generated by a quadrupole of endcaps (a, positive) and a ring electrode (b). Picture 1 and 2 show two states during an AC cycle. Image used with permission from Wikipedia.

The quadrupole ion trap usually runs a mass selective ejection, where selectively it ejects the trapped ions in order of in creasing mass by gradually increasing the applied radio frequency voltage.

Ion Cyclotron Resonance (ICR)

ICR is an ion trap that uses a magnetic field in order to trap ions into an orbit inside of it. In this analyzer there is no separation that occurs rather all the ions of a particular range are trapped inside, and an applied external electric field helps to generate a signal. As mentioned earlier, when a moving charge enters a magnetic field, it experiences a centripetal force making the ion orbit. Again the force on the ion due to the magnetic field is equal to the centripetal force on the ion.

$$zvB = \frac{mv^2}{r} \tag{10}$$

Angular velocity of the ion perpendicular to the magnetic field can be substituted here $w_c = v/r$

$$zB = mw_c \tag{11}$$

$$w_c = \frac{zB}{m} \tag{12}$$

Frequency of the orbit depends on the charge and mass of the ions, not the velocity. If the magnetic field is held constant, the charge to mass ratio of each ion can be determined by measuring the angular velocity ω_c. The relationship is that, at high w_c, there is low m/z value, and at low ω_c, there is a high m/z value. Charges of opposite signs have the same angular velocity, the only difference is that they orbit in the opposite direction.

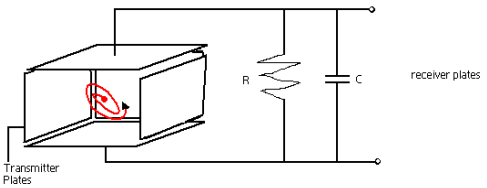


Figure 6: An ICR trap.

To generate an electric signal from the trapped ions, a vary electric field is applied to the ion trap

$$E = E_o \cos(\omega_c t) \tag{13}$$

When the ω_c in the electric field matches the ω_c of a certain ion, the ion absorbs energy making the velocity and orbiting radius of the ion increase. In this high energy orbit, as the ion oscillates between two plates, electrons accumulate at one of the plates over the other inducing an oscillating current, or current image. The current is directly proportional to the number of ions in the cell at a certain frequency.

In a Fourier Transform ICR, all of the ions within the cell are excited simultaneously so that the current image is coupled with the image of all of the individual ion frequencies. A Fourier transform is used to differential the summed signals to produce the desired results.

References

1. K. Downard, *Mass Spectrometry: A Foundation Course*, The Royal Society of Chemistry: UK 2004, Chapter 3
2. Skoog, Holler, Grouch, *Principles of Instrumental Analysis*, Thomson Brooks/Cole 2007, chapter 20
3. C. Herbert, R. Johnstone, *Mass Spectrometry Basics*, CRC Press LLC, 2003 chapter 25, 26, 39
4. E. De Hoffman, V. Stroobant, *Mass Spectrometry: Principles and Applications*, 2nd ed.;Wiley: England, 2001, chapter 2

Contributors

- Ommaima Khan

3.9.3: Mass Analyzers (Mass Spectrometry) is shared under a not declared license and was authored, remixed, and/or curated by LibreTexts.

3.10: Mass Spectrometry- Isotope Effects

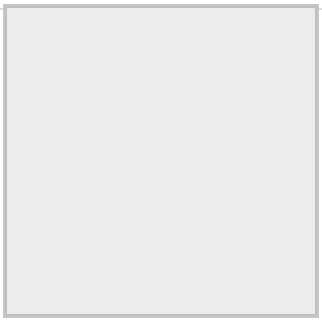


Figure 1 and the isotope abundance data from Table 1, we can see that there are 1.08 ^{13}C atoms for every 100 ^{12}C atoms, and the ^{13}C peak will be 1.08% as large as the ^{12}C peak.

The example above is simple, but the same methods can be applied to determine isotope peaks in more complicated molecules as well. The molecule $C_4Br_1O_2H_5$ has several isotope effects: ^{13}C, ^{2}H, ^{81}Br, ^{17}O, and ^{18}O all must be taken into account. First we will look at the $(M+1)^+$ peak in comparison with the M^+ peak. Only isotopes that will increase the value of M by 1 must be taken into consideration here – since ^{81}Br and ^{18}O would both increase M by 2, they can be ignored (the most abundant isotopes for Br and O are ^{79}Br and ^{16}O). Like the previous example, there are 1.08 ^{13}C atoms for every 100 ^{12}C atoms. However, there are 4 carbon atoms in our molecule, and any one of them being a ^{13}C atom would result in a molecule with mass (M+1). So it is necessary to multiply the probability of an atom being a ^{13}C atom by the number of C atoms in the molecule. Therefore, we have:

$$4C * 1.08 = 4.32 = \text{molecules with a } ^{13}C \text{ atom per 100 molecules}$$

We can repeat this analysis for ^{2}H and ^{17}O:

$$5H * 0.015 = 0.075 = \text{molecules with a } ^{2}H \text{ atom per 100 molecules}$$

$$2O * 0.04 = 0.08 = \text{molecules with a } ^{17}O \text{ atom per 100 molecules}$$

Any of the three isotopes, ^{13}C, ^{2}H, or ^{17}O occurring in our molecule would result in an $(M+1)^+$ peak. To get the ratio of $(M+1)^+/M^+$, we need to add all three probabilities:

$$4.32 + 0.075 + 0.08 = 4.475 = (M+1)^+ \text{ molecules per 100 } M^+ \text{ molecules}$$

We can say then that the $(M+1)^+$ peak is 4.475% as high as the M^+ peak.

A similar analysis can be easily repeated for $(M+2)^+$:

$$1Br * 98 = 98 = \text{molecules with an } ^{81}Br \text{ molecule per 100 molecules}$$

$$2O * 0.2 = 0.4 = \text{molecules with an } ^{18}O \text{ molecule per 100 molecules}$$

$$98 + 0.4 = 98.4 = (M+2)^+ \text{ molecules per 100 } M^+ \text{ molecules}$$

The $(M + 2)^+$ peak is therefore 98.4% as tall as the M^+ peak.

This method is useful because using isotopic differences, it is possible to differentiate two molecules of identical mass numbers.

References

1. Skoog, DA. Holler, FJ. Crouch, SR. Principles of Instrumental Analysis, 6th Edition. Thomson Brooks/Cole (2007).
2. Coursey, J. S., Schwab, D. J., Dragoset, R. A. (2001). Atomic Weights and Isotopic Compositions. National Institute of Standards and Technology, Gaithersburg, MD.

Outside Links

- http://en.wikipedia.org/wiki/Mass_spectrometer
  - This wikipedia page is about the Mass Spectrometer instrument.
- http://en.wikipedia.org/wiki/Mass_spectrum_analysis
  - This wikipedia page is more directly related to isotope effects, as it focuses on reading mass spectra.

- http://www.chem.uoa.gr/applets/AppletMS/Appl_MS2.htm
  - This applett is fun to play with. It generates isotope peaks in a specified mass fragment.

Problems

1. Predict the $(M+1)^+$ relative peak heights for meta-nitrobenzene.
2. Why would this method of looking at isotope ratios relating to peak heights make distinguishing molecules with Chlorine and Bromine from other molecules very easy?
3. Predict the $(M+4)^+$ relative peak heights for $C_3H_2SCl_2$
4. Predict the $(M+1)^+$ and $(M+2)^+$ relative peak heights for 1,1,1-tribromo-2-propene

Contributors

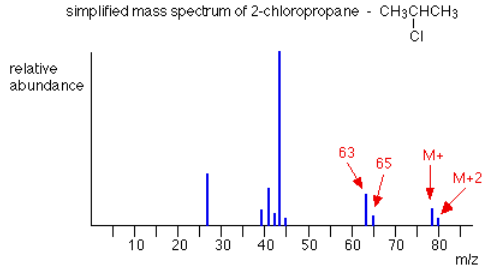
- Morgan Kelley (UCD)

3.10: Mass Spectrometry- Isotope Effects is shared under a not declared license and was authored, remixed, and/or curated by LibreTexts.

3.11: Organic Compounds Containing Halogen Atoms

This page explains how the M+2 peak in a mass spectrum arises from the presence of chlorine or bromine atoms in an organic compound. It also deals briefly with the origin of the M+4 peak in compounds containing two chlorine atoms.

One chlorine atom in a compound



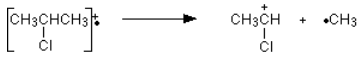
The molecular ion peaks (M+ and M+2) each contain one chlorine atom - but the chlorine can be either of the two chlorine isotopes, ^{35}Cl and ^{37}Cl.

The molecular ion containing the ^{35}Cl isotope has a relative formula mass of 78. The one containing ^{37}Cl has a relative formula mass of 80 - hence the two lines at m/z = 78 and m/z = 80.

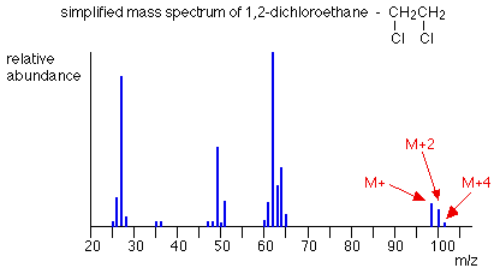
Notice that the peak heights are in the ratio of 3 : 1. That reflects the fact that chlorine contains 3 times as much of the ^{35}Cl isotope as the ^{37}Cl one. That means that there will be 3 times more molecules containing the lighter isotope than the heavier one.

So . . . if you look at the molecular ion region, and find two peaks separated by 2 m/z units and with a ratio of 3 : 1 in the peak heights, that tells you that the molecule contains 1 chlorine atom.

You might also have noticed the same pattern at m/z = 63 and m/z = 65 in the mass spectrum above. That pattern is due to fragment ions also containing one chlorine atom - which could either be ^{35}Cl or ^{37}Cl. The fragmentation that produced those ions was:



Two chlorine atoms in a compound



The lines in the molecular ion region (at m/z values of 98, 100 ands 102) arise because of the various combinations of chlorine isotopes that are possible. The carbons and hydrogens add up to 28 - so the various possible molecular ions could be:

$$28 + 35 + 35 = 98$$

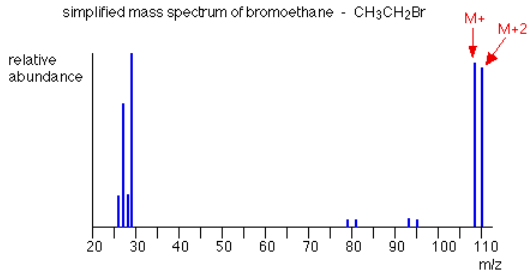
$$28 + 35 + 37 = 100$$

$$28 + 37 + 37 = 102$$

If you have the necessary math, you could show that the chances of these arrangements occurring are in the ratio of 9:6:1 - and this is the ratio of the peak heights. If you don't know the right bit of math, just learn this ratio! So . . . if you have 3 lines in the molecular ion region (M+, M+2 and M+4) with gaps of 2 m/z units between them, and with peak heights in the ratio of 9:6:1, the compound contains 2 chlorine atoms.

Compounds containing bromine atoms

Bromine has two isotopes, ^{79}Br and ^{81}Br in an approximately 1:1 ratio (50.5 : 49.5 if you want to be fussy!). That means that a compound containing 1 bromine atom will have two peaks in the molecular ion region, depending on which bromine isotope the molecular ion contains. Unlike compounds containing chlorine, though, the two peaks will be very similar in height.



The carbons and hydrogens add up to 29. The M+ and M+2 peaks are therefore at m/z values given by:

$$29 + 79 = 108$$

$$29 + 81 = 110$$

Hence, if two lines in the molecular ion region are observed with a gap of 2 m/z units between them and with almost equal heights, this suggests the presence of a bromine atom in the molecule.

Contributors

- Jim Clark (Chemguide.co.uk)

This page titled 3.11: Organic Compounds Containing Halogen Atoms is shared under a CC BY-NC 4.0 license and was authored, remixed, and/or curated by Jim Clark.

3.12: Selected Ion Monitoring- Shockwave

Contributors

- Thomas Chasteen, Department of Chemistry, Sam Houston State University

3.12: Selected Ion Monitoring- Shockwave is shared under a not declared license and was authored, remixed, and/or curated by LibreTexts.

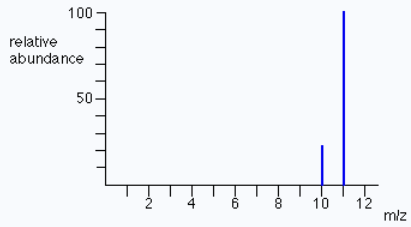
3.13: The Mass Spectra of Elements

This page looks at the information you can get from the mass spectrum of an element. It shows how you can find out the masses and relative abundances of the various isotopes of the element and use that information to calculate the relative atomic mass of the element. It also looks at the problems thrown up by elements with diatomic molecules - like chlorine, Cl_2.

The mass spectrum of monatomic elements

Monatomic elements include all those except for things like chlorine, Cl_2, with molecules containing more than one atom.

Example 3.13.1: The Mass Spectrum of Boron



The number of isotopes: The two peaks in the mass spectrum shows that there are 2 isotopes of boron - with relative isotopic masses of 10 and 11 on the ^{12}C scale.

The abundance of the isotopes: The relative sizes of the peaks gives you a direct measure of the relative abundances of the isotopes. The tallest peak is often given an arbitrary height of 100 - but you may find all sorts of other scales used. It doesn't matter in the least. You can find the relative abundances by measuring the lines on the stick diagram. In this case, the two isotopes (with their relative abundances) are:

boron-10		23
boron-11		100

Working out the relative atomic mass

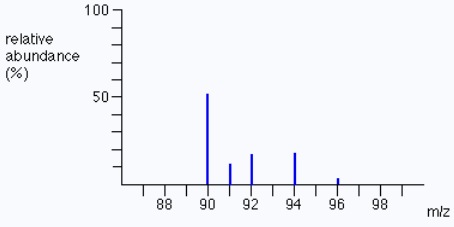
The relative atomic mass (RAM) of an element is given the symbol $\mathbf{A_r}$ and is defined as:

The relative atomic mass of an element is the weighted average of the masses of the isotopes on a scale on which a carbon-12 atom has a mass of exactly 12 units A "weighted average" allows for the fact that there won't be equal amounts of the various isotopes. The example coming up should make that clear.

> Suppose you had 123 typical atoms of boron. 23 of these would be ^{10}B and 100 would be ^{11}B.
>
> The total mass of these would be (23 x 10) + (100 x 11) = 1330
>
> The average mass of these 123 atoms would be 1330 / 123 = 10.8 (to 3 significant figures).
>
> 10.8 is the relative atomic mass of boron.

Notice the effect of the "weighted" average. A simple average of 10 and 11 is, of course, 10.5. Our answer of 10.8 allows for the fact that there are a lot more of the heavier isotope of boron - and so the "weighted" average ought to be closer to that.

Example 3.13.2: The Mass Spectrum of Zirconium



The number of isotopes: The 5 peaks in the mass spectrum shows that there are 5 isotopes of zirconium - with relative isotopic masses of 90, 91, 92, 94 and 96 on the ^{12}C scale.

The abundance of the isotopes: This time, the relative abundances are given as percentages. Again you can find these relative abundances by measuring the lines on the stick diagram. In this case, the 5 isotopes (with their relative percentage abundances) are:

zirconium-90		51.5
zirconium-91		11.2
zirconium-92		17.1
zirconium-94		17.4
zirconium-96		2.8

Working out the relative atomic mass

Suppose you had 100 typical atoms of zirconium. 51.5 of these would be ^{90}Zr, 11.2 would be ^{91}Zr and so on.

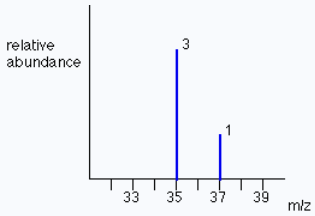
The total mass of these 100 typical atoms would be

$$(51.5 \times 90) + (11.2 \times 91) + (17.1 \times 92) + (17.4 \times 94) + (2.8 \times 96) = 9131.8$$

The average mass of these 100 atoms would be 9131.8 / 100 = 91.3 (to 3 significant figures). 91.3 is the relative atomic mass of zirconium.

Example 3.13.3: The Mass Spectrum of Chlorine

Chlorine is taken as typical of elements with more than one atom per molecule. We'll look at its mass spectrum to show the sort of problems involved. Chlorine has two isotopes, ^{35}Cl and ^{37}Cl, in the approximate ratio of 3 atoms of ^{35}Cl to 1 atom of ^{37}Cl. You might suppose that the mass spectrum would look like this:



You would be wrong! The problem is that chlorine consists of molecules, not individual atoms. When chlorine is passed into the ionization chamber, an electron is knocked off the molecule to give a molecular ion, Cl_2^+. These ions won't be particularly stable, and some will fall apart to give a chlorine atom and a Cl^+ ion. The term for this is fragmentation.

$$Cl_2^+ \rightarrow Cl + Cl^+ \qquad (3.13.1)$$

If the Cl atom formed is not then ionized in the ionization chamber, it simply gets lost in the machine - neither accelerated nor deflected.

The Cl^+ ions will pass through the machine and will give lines at 35 and 37, depending on the isotope and you would get exactly the pattern in the last diagram. The problem is that you will also record lines for the unfragmented Cl_2^+ ions.

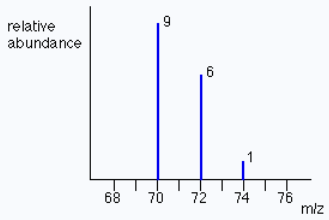
Think about the possible combinations of chlorine-35 and chlorine-37 atoms in a Cl_2^+ ion. Both atoms could be ^{35}Cl, both atoms could be ^{37}Cl, or you could have one of each sort. That would give you total masses of the Cl_2^+ ion of:

35 + 35 = 70

35 + 37 = 72

37 + 37 = 74

That means that you would get a set of lines in the m/z = 70 region looking like this:

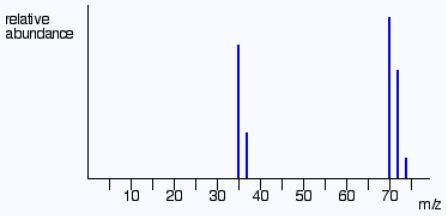


These lines would be in addition to the lines at 35 and 37.

The relative heights of the 70, 72 and 74 lines are in the ratio 9:6:1. If you know the right bit of math, it's very easy to show this. If not, don't worry. Just remember that the ratio is 9:6:1.

What you can't do is make any predictions about the relative heights of the lines at 35/37 compared with those at 70/72/74. That depends on what proportion of the molecular ions break up into fragments. That's why you've got the chlorine mass spectrum in two separate bits so far. You must realise that the vertical scale in the diagrams of the two parts of the spectrum isn't the same.

The overall mass spectrum looks like this:



Contributors

- Jim Clark (Chemguide.co.uk)

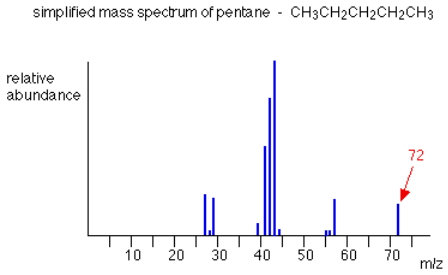
This page titled 3.13: The Mass Spectra of Elements is shared under a CC BY-NC 4.0 license and was authored, remixed, and/or curated by Jim Clark.

3.14: The Molecular Ion (M^+) Peak

This page explains how to find the relative formula mass (relative molecular mass) of an organic compound from its mass spectrum. It also shows how high resolution mass spectra can be used to find the molecular formula for a compound.

When the vaporised organic sample passes into the ionization chamber of a mass spectrometer, it is bombarded by a stream of electrons. These electrons have a high enough energy to knock an electron off an organic molecule to form a positive ion. This ion is called the molecular ion. The molecular ion is often given the symbol M^+ or $M^{\cdot+}$ - the dot in this second version represents the fact that somewhere in the ion there will be a single unpaired electron. That's one half of what was originally a pair of electrons - the other half is the electron which was removed in the ionization process. The molecular ions tend to be unstable and some of them break into smaller fragments. These fragments produce the familiar stick diagram. Fragmentation is irrelevant to what we are talking about on this page - all we're interested in is the molecular ion.

In the mass spectrum, the heaviest ion (the one with the greatest m/z value) is likely to be the molecular ion. A few compounds have mass spectra which don't contain a molecular ion peak, because all the molecular ions break into fragments. For example, in the mass spectrum of pentane, the heaviest ion has an m/z value of 72.



Because the largest m/z value is 72, that represents the largest ion going through the mass spectrometer - and you can reasonably assume that this is the molecular ion. The relative formula mass of the compound is therefore 72.

Finding the relative formula mass (relative molecular mass) from a mass spectrum is therefore trivial. Look for the peak with the highest value for m/z, and that value is the relative formula mass of the compound. There are, however, complications which arise because of the possibility of different isotopes (either of carbon or of chlorine or bromine) in the molecular ion. These cases are dealt with on separate pages.

Using a mass spectrum to find a molecular formula

So far we've been looking at m/z values in a mass spectrum as whole numbers, but it's possible to get far more accurate results using a high resolution mass spectrometer. You can use that more accurate information about the mass of the molecular ion to work out the molecular formula of the compound.

For normal calculation purposes, you tend to use rounded-off relative isotopic masses. For example, you are familiar with the atomic mass numbers (Z). To 4 decimal places, however, these are the relative isotopic masses.

Isotope	Z	Mass
^{1}H	1	1.0078
^{12}C	12	12.0000
^{14}N	14	14.0031
^{16}O	16	15.9949

The carbon value is 12.0000, of course, because all the other masses are measured on the carbon-12 scale which is based on the carbon-12 isotope having a mass of exactly 12.

Using these accurate values to find a molecular formula

Two simple organic compounds have a relative formula mass of 44 - propane, C_3H_8, and ethanal, CH_3CHO. Using a high resolution mass spectrometer, you could easily decide which of these you had. On a high resolution mass spectrometer, the molecular ion peaks for the two compounds give the following m/z values:

C_3H_8		44.0624
CH_3CHO		44.0261

You can easily check that by adding up numbers from the table of accurate relative isotopic masses above.

Example 3.14.1:

A gas was known to contain only elements from the following list:

^{1}H		1.0078
^{12}C		12.0000
^{14}N		14.0031
^{16}O		15.9949

The gas had a molecular ion peak at m/z = 28.0312 in a high resolution mass spectrometer. What was the gas?

Solution

After a bit of playing around, you might reasonably come up with 3 gases which had relative formula masses of approximately 28 and which contained the elements from the list. They are N_2, CO and C_2H_4. Working out their accurate relative formula masses gives:

N_2		28.0062
CO		27.9949
C_2H_4		28.0312

The gas is obviously C_2H_4.

Contributors

- Jim Clark (Chemguide.co.uk)

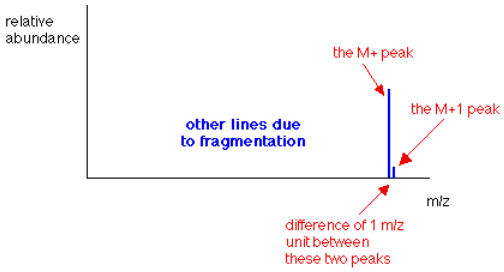
This page titled 3.14: The Molecular Ion (M^+) Peak is shared under a CC BY-NC 4.0 license and was authored, remixed, and/or curated by Jim Clark.

3.15: The M+1 Peak

This page explains how the M+1 peak in a mass spectrum can be used to estimate the number of carbon atoms in an organic compound.

What causes the M+1 peak?

If you had a complete (rather than a simplified) mass spectrum, you will find a small line 1 m/z unit to the right of the main molecular ion peak. This small peak is called the M+1 peak.

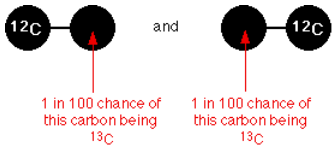


The carbon-13 isotope

The M+1 peak is caused by the presence of the ^{13}C isotope in the molecule. ^{13}C is a stable isotope of carbon - don't confuse it with the ^{14}C isotope which is radioactive. Carbon-13 makes up 1.11% of all carbon atoms. If you had a simple compound like methane, CH_4, approximately 1 in every 100 of these molecules will contain carbon-13 rather than the more common carbon-12. That means that 1 in every 100 of the molecules will have a mass of 17 (13 + 4) rather than 16 (12 + 4). The mass spectrum will therefore have a line corresponding to the molecular ion $[^{13}CH_4]^+$ as well as $[^{12}CH_4]^+$. The line at m/z = 17 will be much smaller than the line at m/z = 16 because the carbon-13 isotope is much less common. Statistically you will have a ratio of approximately 1 of the heavier ions to every 99 of the lighter ones. That's why the M+1 peak is much smaller than the M+ peak.

Using the M+1 peak

Imagine a compound containing 2 carbon atoms. Either of them has an approximately 1 in 100 chance of being ^{13}C.



There's therefore a 2 in 100 chance of the molecule as a whole containing one ^{13}C atom rather than a ^{12}C atom - which leaves a 98 in 100 chance of both atoms being ^{12}C. That means that the ratio of the height of the M+1 peak to the M+ peak will be approximately 2 : 98. That's pretty close to having an M+1 peak approximately 2% of the height of the M+ peak.

Using the relative peak heights to predict the number of carbon atoms

If you measure the peak height of the M+1 peak as a percentage of the peak height of the M+ peak, that gives you the number of carbon atoms in the compound. We've just seen that a compound with 2 carbons will have an M+1 peak approximately 2% of the height of the M+ peak. Similarly, you could show that a compound with 3 carbons will have the M+1 peak at about 3% of the height of the M+ peak. The approximations we are making won't hold with more than 2 or 3 carbons. The proportion of carbon atoms which are ^{13}C isn't 1% - it's 1.11%. And the approximation that a ratio of 2 : 98 is about 2% doesn't hold as the small number increases.

Consider a molecule with 5 carbons in it. You could work out that 5.55 (5 x 1.11) molecules will contain 1 ^{13}C to every 94.45 (100 - 5.55) which contain only ^{12}C atoms. If you convert that to how tall the M+1 peak is as a percentage of the M+ peak, you get an answer of 5.9% (5.55/94.45 x 100). That's close enough to 6% that you might assume wrongly that there are 6 carbon atoms. Above 3 carbon atoms, then, you shouldn't really be making the approximation that the height of the M+1 peak as a percentage of the height of the M+ peak tells you the number of carbons - you will need to do some fiddly sums!

Contributors

Jim Clark (Chemguide.co.uk)

This page titled 3.15: The M+1 Peak is shared under a CC BY-NC 4.0 license and was authored, remixed, and/or curated by Jim Clark.

3.16: Current Applications of Mass Spectrometry

3.16: Current Applications of Mass Spectrometry is shared under a not declared license and was authored, remixed, and/or curated by LibreTexts.

CHAPTER OVERVIEW

4: Electrochemical Methods

In Chapter 10 we examined several spectroscopic techniques that take advantage of the interaction between electromagnetic radiation and matter. In this chapter we turn our attention to electrochemical techniques in which the potential, current, or charge in an electrochemical cell serves as the analytical signal.

Although there are only three fundamental electrochemical signals, there are many possible experimental designs—too many, in fact, to cover adequately in an introductory textbook. The simplest division of electrochemical techniques is between bulk techniques, in which we measure a property of the solution in the electrochemical cell, and interfacial techniques, in which the potential, current, or charge depends on the species present at the interface between an electrode and the solution in which it sits. The measurement of a solution's conductivity, which is proportional to the total concentration of dissolved ions, is one example of a bulk electrochemical technique. A determination of pH using a pH electrode is an example of an interfacial electrochemical technique. Only interfacial electrochemical methods receive further consideration in this chapter.

- 4.1: Overview of Electrochemistry
- 4.2: Potentiometric Methods
- 4.3: Coulometric Methods
- 4.4: Voltammetric and Amperometric Methods
  - 4.4.1: Cyclic Voltammetry
  - 4.4.2: Anodic Stripping Voltammetry
- 4.5: Problems
- 4.6: Additional Resources
- 4.7: Chapter Summary and Key Terms

This page titled 4: Electrochemical Methods is shared under a CC BY-NC-SA 4.0 license and was authored, remixed, and/or curated by David Harvey.

4.1: Overview of Electrochemistry

The focus of this chapter is on analytical techniques that use a measurement of potential, current, or charge to determine an analyte's concentration or to characterize an analyte's chemical reactivity. Collectively we call this area of analytical chemistry ***electrochemistry*** because its originated from the study of the movement of electrons in an oxidation–reduction reaction.

Despite the difference in instrumentation, all electrochemical techniques share several common features. Before we consider individual examples in greater detail, let's take a moment to consider some of these similarities. As you work through the chapter, this overview will help you focus on similarities between different electrochemical methods of analysis. You will find it easier to understand a new analytical method when you can see its relationship to other similar methods.

Five Important Concepts

To understand electrochemistry we need to appreciate five important and interrelated concepts: (1) the electrode's potential determines the analyte's form at the electrode's surface; (2) the concentration of analyte at the electrode's surface may not be the same as its concentration in bulk solution; (3) in addition to an oxidation–reduction reaction, the analyte may participate in other chemical reactions; (4) current is a measure of the rate of the analyte's oxidation or reduction; and (5) we cannot control simultaneously current and potential.

> The material in this section—particularly the five important concepts—draws upon a vision for understanding electrochemistry outlined by Larry Faulkner in the article "Understanding Electrochemistry: Some Distinctive Concepts," *J. Chem. Educ.* **1983**, *60*, 262–264. See also, Kissinger, P. T.; Bott, A. W. "Electrochemistry for the Non-Electrochemist," *Current Separations*, **2002**, *20:2*, 51–53.

The Electrode's Potential Determines the Analyte's Form

In Chapter 6 we introduced the ladder diagram as a tool for predicting how a change in solution conditions affects the position of an equilibrium reaction. Figure 11.1.1 , for example, shows a ladder diagram for the Fe^{3+}/Fe^{2+} and the Sn^{4+}/Sn^{2+} equilibria. If we place an electrode in a solution of Fe^{3+} and Sn^{4+} and adjust its potential to +0.500 V, Fe^{3+} is reduced to Fe^{2+} but Sn^{4+} is not reduced to Sn^{2+}.

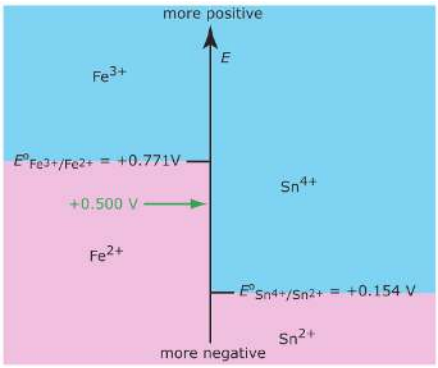


Figure 11.1.1 . Redox ladder diagram for Fe^{3+}/Fe^{2+} and for Sn^{4+}/Sn^{2+} redox couples. The areas in blue show the potential range where the oxidized forms are the predominate species; the reduced forms are the predominate species in the areas shown in pink. Note that a more positive potential favors the oxidized forms. At a potential of +0.500 V (green arrow) Fe^{3+} reduces to Fe^{2+}, but Sn^{4+} remains unchanged. You may wish to review the earlier treatment of oxidation–reduction reactions in Chapter 6.4 and the development of ladder diagrams for oxidation–reduction reactions in Chapter 6.6.

Interfacial Concentrations May Not Equal Bulk Concentrations

In Chapter 6 we introduced the Nernst equation, which provides a mathematical relationship between the electrode's potential and the concentrations of an analyte's oxidized and reduced forms in solution. For example, the Nernst equation for Fe^{3+} and Fe^{2+} is

$$E = E_{Fe^{3+}/Fe^{2+}} - \frac{RT}{nF}\ln\frac{[Fe^{2+}]}{[Fe^{3+}]} = \frac{0.05916}{1}\log\frac{[Fe^{2+}]}{[Fe^{3+}]} \quad (4.1.1)$$

where E is the electrode's potential and $E^\circ_{Fe^{3+}/Fe^{2+}}$ is the standard-state reduction potential for the reaction $Fe^{3+}(aq) \rightleftharpoons Fe^{2+}(aq) + e^-$. Because it is the potential of the electrode that determines the analyte's form at the electrode's surface, the concentration terms in Equation 4.1.1 are those of Fe^{2+} and Fe^{3+} at the electrode's surface, not their concentrations in bulk solution.

This distinction between a species' surface concentration and its bulk concentration is important. Suppose we place an electrode in a solution of Fe^{3+} and fix its potential at 1.00 V. From the ladder diagram in Figure 11.1.1 , we know that Fe^{3+} is stable at this potential and, as shown in Figure 11.1.2 a, the concentration of Fe^{3+} is the same at all distances from the electrode's surface. If we change the electrode's potential to +0.500 V, the concentration of Fe^{3+} at the electrode's surface decreases to approximately zero. As shown in Figure 11.1.2 b, the concentration of Fe^{3+} increases as we move away from the electrode's surface until it equals the concentration of Fe^{3+} in bulk solution. The resulting concentration gradient causes additional Fe^{3+} from the bulk solution to diffuse to the electrode's surface.

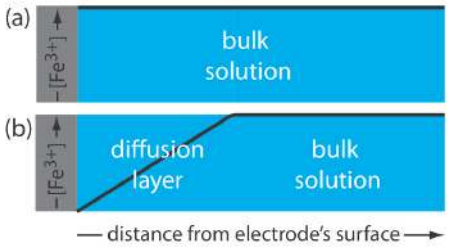


Figure 11.1.2 . Concentration of Fe^{3+} as a function of distance from the electrode's surface at (a) E = +1.00 V and (b) E = +0.500 V. The electrode is shown in gray and the solution in blue.

> We call the region of solution that contains this concentration gradient in Fe^{3+} the diffusion layer. We will have more to say about this in Chapter 11.4.

The Analyte May Participate in Other Reactions

Figure 11.1.1 and Figure 11.1.2 shows how the electrode's potential affects the concentration of Fe^{3+} and how the concentration of Fe^{3+} varies as a function of distance from the electrode's surface. The reduction of Fe^{3+} to Fe^{2+}, which is governed by Equation 4.1.1, may not be the only reaction that affects the concentration of Fe^{3+} in bulk solution or at the electrode's surface. The adsorption of Fe^{3+} at the electrode's surface or the formation of a metal–ligand complex in bulk solution, such as $Fe(OH)^{2+}$, also affects the concentration of Fe^{3+}.

Current is a Measure of Rate

The reduction of Fe^{3+} to Fe^{2+} consumes an electron, which is drawn from the electrode. The oxidation of another species, perhaps the solvent, at a second electrode is the source of this electron. Because the reduction of Fe^{3+} to Fe^{2+} consumes one electron, the flow of electrons between the electrodes—in other words, the current—is a measure of the rate at which Fe^{3+} is reduced. One important consequence of this observation is that the current is zero when the reaction $Fe^{3+}(aq) \rightleftharpoons Fe^{2+}(aq) + e^-$ is at equilibrium.

> The rate of the reaction $Fe^{3+}(aq) \rightleftharpoons Fe^{2+}(aq) + e^-$ is the change in the concentration of Fe^{3+} as a function of time.

We Cannot Control Simultaneously Both the Current and the Potential

If a solution of Fe^{3+} and Fe^{2+} is at equilibrium, the current is zero and the potential is given by Equation 4.1.1. If we change the potential away from its equilibrium position, current flows as the system moves toward its new equilibrium position. Although the initial current is quite large, it decreases over time, reaching zero when the reaction reaches equilibrium. The current, therefore, changes in response to the applied potential. Alternatively, we can pass a fixed current through the electrochemical cell, forcing the reduction of Fe^{3+} to Fe^{2+}. Because the concentrations of Fe^{3+} decreases and the concentration of Fe^{2+} increases, the potential, as given by Equation 4.1.1, also changes over time. In short, if we choose to control the potential, then we must accept the resulting current, and we must accept the resulting potential if we choose to control the current.

Controlling and Measuring Current and Potential

Electrochemical measurements are made in an electrochemical cell that consists of two or more electrodes and the electronic circuitry needed to control and measure the current and the potential. In this section we introduce the basic components of electrochemical instrumentation.

The simplest electrochemical cell uses two electrodes. The potential of one electrode is sensitive to the analyte's concentration, and is called the ***working electrode*** or the ***indicator electrode***. The second electrode, which we call the ***counter electrode***, completes the electrical circuit and provides a reference potential against which we measure the working electrode's potential. Ideally the counter electrode's potential remains constant so that we can assign to the working electrode any change in the overall cell potential. If the counter electrode's potential is not constant, then we replace it with two electrodes: a ***reference electrode*** whose potential remains constant and an ***auxiliary electrode*** that completes the electrical circuit.

Because we cannot control simultaneously the current and the potential, there are only three basic experimental designs: (1) we can measure the potential when the current is zero, (2) we can measure the potential while we control the current, and (3) we can measure the current while we control the potential. Each of these experimental designs relies on ***Ohm's law***, which states that the current, i, passing through an electrical circuit of resistance, R, generates a potential, E.

$$E = iR$$

Each of these experimental designs uses a different type of instrument. To help us understand how we can control and measure current and potential, *we will describe these instruments as if the analyst is operating them manually*. To do so the analyst observes a change in the current or the potential and manually adjusts the instrument's settings to maintain the desired experimental conditions. It is important to understand that modern electrochemical instruments provide an automated, electronic means for controlling and measuring current and potential, and that they do so by using very different electronic circuitry than that described here.

> This point bears repeating: It is important to understand that the experimental designs in Figure 11.1.3 , Figure 11.1.4 , and Figure 11.1.5 do not represent the electrochemical instruments you will find in today's analytical labs. For further information about modern electrochemical instrumentation, see this chapter's additional resources.

Potentiometers

To measure the potential of an electrochemical cell under a condition of zero current we use a ***potentiometer***. Figure 11.1.3 shows a schematic diagram for a manual potentiometer that consists of a power supply, an electrochemical cell with a working electrode and a counter electrode, an ammeter to measure the current that passes through the electrochemical cell, an adjustable, slide-wire resistor, and a tap key for closing the circuit through the electrochemical cell. Using Ohm's law, the current in the upper half of the circuit is

$$i_{\text{upper}} = \frac{E_{\text{PS}}}{R_{ab}}$$

where E_{PS} is the power supply's potential, and R_{ab} is the resistance between points a and b of the slide-wire resistor. In a similar manner, the current in the lower half of the circuit is

$$i_{\text{lower}} = \frac{E_{\text{cell}}}{R_{cb}}$$

where E_{cell} is the potential difference between the working electrode and the counter electrode, and R_{cb} is the resistance between the points c and b of the slide-wire resistor. When $i_{\text{upper}} = i_{\text{lower}} = 0$, no current flows through the ammeter and the potential of the electrochemical cell is

$$E_{\text{coll}} = \frac{R_{cb}}{R_{ab}} \times E_{\text{PS}} \tag{4.1.2}$$

To determine E_{cell} we briefly press the tap key and observe the current at the ammeter. If the current is not zero, then we adjust the slide wire resistor and remeasure the current, continuing this process until the current is zero. When the current is zero, we use

Equation 4.1.2 to calculate E_{cell}.

Using the tap key to briefly close the circuit through the electrochemical cell minimizes the current that passes through the cell and limits the change in the electrochemical cell's composition. For example, passing a current of 10^{-9} A through the electrochemical cell for 1 s changes the concentrations of species in the cell by approximately 10^{-14} moles. Modern potentiometers use operational amplifiers to create a high-impedance voltmeter that measures the potential while drawing a current of less than 10^{-9} A.

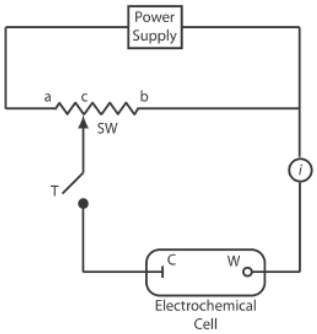


Figure 11.1.3 . Schematic diagram of a manual potentiometer: C is the counter electrode; W is the working electrode; SW is a slide-wire resistor; T is a tap key and *i* is an ammeter for measuring current.

Galvanostats

A ***galvanostat***, a schematic diagram of which is shown in Figure 11.1.4 , allows us to control the current that flows through an electrochemical cell. The current from the power supply through the working electrode is

$$i = \frac{E_{PS}}{R + R_{cell}}$$

where E_{PS} is the potential of the power supply, R is the resistance of the resistor, and R_{cell} is the resistance of the electrochemical cell. If $R >> R_{cell}$, then the current between the auxiliary and working electrodes

$$i = \frac{E_{PS}}{R} \approx \text{constant}$$

maintains a constant value. To monitor the working electrode's potential, which changes as the composition of the electrochemical cell changes, we can include an optional reference electrode and a high-impedance potentiometer.

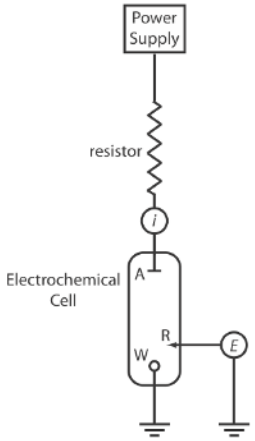


Figure 11.1.4 . Schematic diagram of a galvanostat: A is the auxiliary electrode; W is the working electrode; R is an optional reference electrode, *E* is a high-impedance potentiometer, and *i* is an ammeter. The working electrode and the optional reference electrode are connected to a ground.

Potentiostats

A ***potentiostat***, a schematic diagram of which is shown in Figure 11.1.5 , allows us to control the working electrode's potential. The potential of the working electrode is measured relative to a constant-potential reference electrode that is connected to the working

electrode through a high-impedance potentiometer. To set the working electrode's potential we adjust the slide wire resistor that is connected to the auxiliary electrode. If the working electrode's potential begins to drift, we adjust the slide wire resistor to return the potential to its initial value. The current flowing between the auxiliary electrode and the working electrode is measured with an ammeter. Modern potentiostats include waveform generators that allow us to apply a time-dependent potential profile, such as a series of potential pulses, to the working electrode.

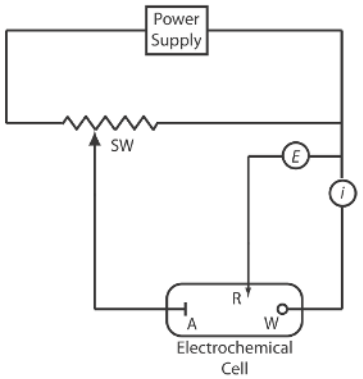


Figure 11.1.5 . Schematic diagram for a manual potentiostat: W is the working electrode; A is the auxiliary electrode; R is the reference electrode; SW is a slide-wire resistor, *E* is a high-impendance potentiometer; and *i* is an ammeter.

Interfacial Electrochemical Techniques

Because interfacial electrochemistry is such a broad field, let's use Figure 11.1.6 to organize techniques by the experimental conditions we choose to use (Do we control the potential or the current? How do we change the applied potential or applied current? Do we stir the solution?) and the analytical signal we decide to measure (Current? Potential?).

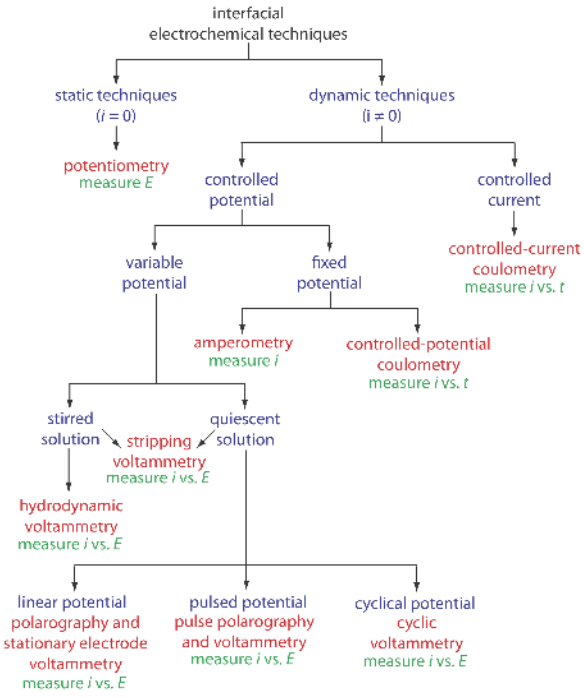


Figure 11.1.6 . Family tree that highlights the similarities and differences between a number of interfacial electrochemical techniques. The specific techniques are shown in red, the experimental conditions are shown in blue, and the analytical signals are shown in green.

At the first level, we divide interfacial electrochemical techniques into static techniques and dynamic techniques. In a static technique we do not allow current to pass through the electrochemical cell and, as a result, the concentrations of all species remain constant. Potentiometry, in which we measure the potential of an electrochemical cell under static conditions, is one of the most important quantitative electrochemical methods and is discussed in detail in Chapter 11.2.

Dynamic techniques, in which we allow current to flow and force a change in the concentration of species in the electrochemical cell, comprise the largest group of interfacial electrochemical techniques. Coulometry, in which we measure current as a function of time, is covered in Chapter 11.3. Amperometry and voltammetry, in which we measure current as a function of a fixed or variable potential, is the subject of Chapter 11.4.

This page titled 4.1: Overview of Electrochemistry is shared under a CC BY-NC-SA 4.0 license and was authored, remixed, and/or curated by David Harvey.

- **11.1: Overview of Electrochemistry** by David Harvey is licensed CC BY-NC-SA 4.0.

4.2: Potentiometric Methods

In potentiometry we measure the potential of an electrochemical cell under static conditions. Because no current—or only a negligible current—flows through the electrochemical cell, its composition remains unchanged. For this reason, potentiometry is a useful quantitative method of analysis. The first quantitative potentiometric applications appeared soon after the formulation, in 1889, of the Nernst equation, which relates an electrochemical cell's potential to the concentration of electroactive species in the cell [Stork, J. T. *Anal. Chem.* **1993**, *65*, 344A–351A].

> For an on-line introduction to much of the material in this section, see Analytical Electrochemistry: Potentiometry by Erin Gross, Richard S. Kelly, and Donald M. Cannon, Jr., a resource that is part of the Analytical Sciences Digital Library.

Potentiometry initially was restricted to redox equilibria at metallic electrodes, which limited its application to a few ions. In 1906, Cremer discovered that the potential difference across a thin glass membrane is a function of pH when opposite sides of the membrane are in contact with solutions that have different concentrations of H_3O^+. This discovery led to the development of the glass pH electrode in 1909. Other types of membranes also yield useful potentials. For example, in 1937 Kolthoff and Sanders showed that a pellet of AgCl can be used to determine the concentration of Ag^+. Electrodes based on membrane potentials are called ion-selective electrodes, and their continued development extends potentiometry to a diverse array of analytes.

Potentiometric Measurements

As shown in Figure 11.1.3, we use a potentiometer to determine the difference between the potential of two electrodes. The potential of one electrode—the working or indicator electrode—responds to the analyte's activity and the other electrode—the counter or reference electrode—has a known, fixed potential. In this section we introduce the conventions for describing potentiometric electrochemical cells, and the relationship between the measured potential and the analyte's activity.

> In Chapter 6 we noted that a chemical reaction's equilibrium position is a function of the activities of the reactants and products, not their concentrations. To be correct, we should write the Nernst equation in terms of activities. So why didn't we use activities in Chapter 9 when we calculated redox titration curves? There are two reasons for that choice. First, concentrations are always easier to calculate than activities. Second, in a redox titration we determine the analyte's concentration from the titration's end point, not from the potential at the end point. The only reasons for calculating a titration curve is to evaluate its feasibility and to help us select a useful indicator. In most cases, the error we introduce by assuming that concentration and activity are identical is too small to be a significant concern.
>
> In potentiometry we cannot ignore the difference between activity and concentration. Later in this section we will consider how we can design a potentiometric method so that we can ignore the difference between activity and concentration. See Chapter 6.9 to review our earlier discussion of activity and concentration.

Potentiometric Electrochemical Cells

A schematic diagram of a typical potentiometric electrochemical cell is shown in Figure 11.2.1 . The electrochemical cell consists of two half-cells, each of which contains an electrode immersed in a solution of ions whose activities determine the electrode's potential. A ***salt bridge*** that contains an inert electrolyte, such as KCl, connects the two half-cells. The ends of the salt bridge are fixed with porous frits, which allow the electrolyte's ions to move freely between the half-cells and the salt bridge. This movement of ions in the salt bridge completes the electrical circuit.

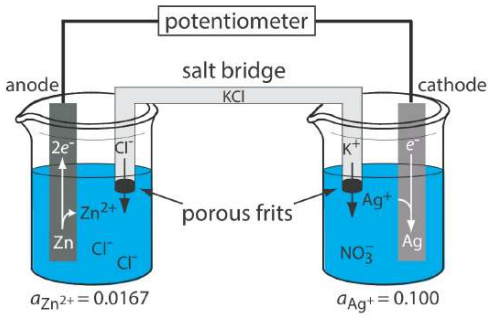


Figure 11.2.1 . Example of a potentiometric electrochemical cell. The activities of Zn^{2+} and Ag^{+} are shown below the two half-cells.

By convention, we identify the electrode on the left as the ***anode*** and assign to it the oxidation reaction; thus

$$\mathrm{Zn}(s) \rightleftharpoons \mathrm{Zn}^{2+}(aq) + 2e^{-}$$

The electrode on the right is the ***cathode***, where the reduction reaction occurs.

$$\mathrm{Ag}^{+}(aq) + e^{-} \rightleftharpoons \mathrm{Ag}(s)$$

The potential of the electrochemical cell in Figure 11.2.1 is for the reaction

$$\mathrm{Zn}(s) + 2\mathrm{Ag}^{+}(aq) \rightleftharpoons 2\mathrm{Ag}(s) + \mathrm{Zn}^{2+}(\mathrm{aq})$$

We also define potentiometric electrochemical cells such that the cathode is the indicator electrode and the anode is the reference electrode.

> The reason for separating the electrodes is to prevent the oxidation reaction and the reduction reaction from occurring at one of the electrodes. For example, if we place a strip of Zn metal in a solution of $AgNO_3$, the reduction of Ag^{+} to Ag occurs on the surface of the Zn at the same time as a potion of the Zn metal oxidizes to Zn^{2+}. Because the transfer of electrons from Zn to Ag^{+} occurs at the electrode's surface, we can not pass them through the potentiometer.

Shorthand Notation for Electrochemical Cells

Although Figure 11.2.1 provides a useful picture of an electrochemical cell, it is not a convenient way to represent it (Imagine having to draw a picture of each electrochemical cell you are using!). A more useful way to describe an electrochemical cell is a shorthand notation that uses symbols to identify different phases and that lists the composition of each phase. We use a vertical slash (|) to identify a boundary between two phases where a potential develops, and a comma (,) to separate species in the same phase or to identify a boundary between two phases where no potential develops. Shorthand cell notations begin with the anode and continue to the cathode. For example, we describe the electrochemical cell in Figure 11.2.1 using the following shorthand notation.

$$\mathrm{Zn}(s)\,|\mathrm{ZnCl_2}(aq, a_{\mathrm{Zn^{2+}}} = 0.0167)|\,|\mathrm{AgNO_3}(aq, a_{\mathrm{Ag^{+}}} = 0.100)|\,\mathrm{Ag}(s)$$

The double vertical slash (||) represents the salt bridge, the contents of which we usually do not list. Note that a double vertical slash implies that there is a potential difference between the salt bridge and each half-cell.

✔ Example 11.2.1

What are the anodic, the cathodic, and the overall reactions responsible for the potential of the electrochemical cell in Figure 11.2.2 ? Write the shorthand notation for the electrochemical cell.

Solution

The oxidation of Ag to Ag^{+} occurs at the anode, which is the left half-cell. Because the solution contains a source of Cl^{-}, the anodic reaction is

$$\mathrm{Ag}(s) + \mathrm{Cl}^{-}(aq) \rightleftharpoons \mathrm{AgCl}(s) + e^{-}$$

The cathodic reaction, which is the right half-cell, is the reduction of Fe^{3+} to Fe^{2+}.

$$Fe^{3+}(aq) + e^- \rightleftharpoons Fe^{2+}(aq)$$

The overall cell reaction, therefore, is

$$Ag(s) + Fe^{3+}(aq) + Cl^-(aq) \rightleftharpoons AgCl(s) + Fe^{2+}(aq)$$

The electrochemical cell's shorthand notation is

$$Ag(s)\,|HCl(aq, a_{Cl^-} = 0.100), AgCl(sat'd)|$$
$$|FeCl_2(aq, a_{Fe^{2+}} = 0.0100),\ Fe^{3+}(aq, a_{Fe^{3+}} = 0.0500)|\,Pt(s)$$

Note that the Pt cathode is an inert electrode that carries electrons to the reduction half-reaction. The electrode itself does not undergo reduction.

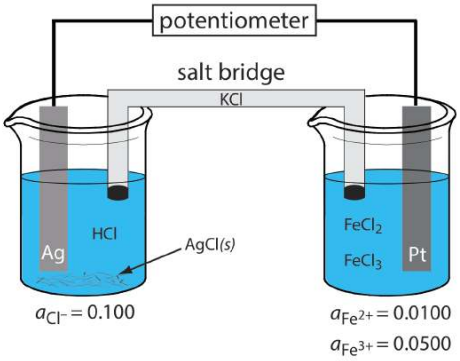


Figure 11.2.2 . Potentiometric electrochemical cell for Example 11.2.1 .

Exercise 11.2.1

Write the reactions occurring at the anode and the cathode for the potentiometric electrochemical cell with the following shorthand notation.

$$Pt(s)\,|\,H_2(g),\,H^+(aq)\,||\,Cu^{2+}(aq)\,|\,Cu(s)$$

Answer

The oxidation of H_2 to H^+ occurs at the anode

$$H_2(g) \rightleftharpoons 2H^+(aq) + 2e^-$$

and the reduction of Cu^{2+} to Cu occurs at the cathode.

$$Cu^{2+}(aq) + 2e^- \rightleftharpoons Cu(s)$$

The overall cell reaction, therefore, is

$$Cu^{2+}(aq) + H_2(g) \rightleftharpoons 2H^+(aq) + Cu(s)$$

Potential and Activity—The Nernst Equation

The potential of a potentiometric electrochemical cell is

$$E_{cell} = E_{cathode} - E_{anode} \tag{4.2.1}$$

where $E_{cathode}$ and E_{anode} are reduction potentials for the redox reactions at the cathode and the anode, respectively. Each reduction potential is given by the Nernst equation

$$E = E^\circ - \frac{RT}{nF}\ln Q$$

where E^o is the standard-state reduction potential, R is the gas constant, T is the temperature in Kelvins, n is the number of electrons in the redox reaction, F is Faraday's constant, and Q is the reaction quotient. At a temperature of 298 K (25°C) the Nernst equation is

$$E = E^\circ - \frac{0.05916}{n} \log Q \tag{4.2.2}$$

where E is in volts.

Using Equation 4.2.2, the potential of the anode and cathode in Figure 11.2.1 are

$$E_{\text{anode}} = E^\circ_{\text{Zn}^{2+}/\text{Zn}} - \frac{0.05916}{2} \log \frac{1}{a_{\text{Zn}^{2+}}}$$

$$E_{\text{anode}} = E^\circ_{\text{Ag}^{+}/\text{Ag}} - \frac{0.05916}{1} \log \frac{1}{a_{\text{Ag}^{+}}}$$

Even though an oxidation reaction is taking place at the anode, we define the anode's potential in terms of the corresponding reduction reaction and the standard-state reduction potential. See Chapter 6.4 for a review of using the Nernst equation in calculations.

Substituting E_{cathode} and E_{anode} into Equation 4.2.1, along with the activities of Zn^{2+} and Ag^+ and the standard-state reduction potentials, gives E_{cell} as

$$E_{\text{cell}} = \left(E^\circ_{\text{Ag}^{+}/\text{Ag}} - \frac{0.05916}{1} \log \frac{1}{a_{\text{Ag}^{+}}} \right) - \left(E^\circ_{\text{Zn}^{2+}/\text{Zn}} - \frac{0.05916}{2} \log \frac{1}{a_{\text{Zn}^{2+}}} \right)$$

$$E_{\text{cell}} = \left(0.7996 - \frac{0.05916}{1} \log \frac{1}{0.100} \right) - \left(-0.7618 - \frac{0.05916}{2} \log \frac{1}{0.0167} \right) = 1.555 \text{ V}$$

You will find values for the standard-state reduction potentials in Appendix 13.

Example 11.2.2

What is the potential of the electrochemical cell shown in Example 11.2.1 ?

Solution

Substituting E_{cathode} and E_{anode} into Equation 4.2.1, along with the concentrations of Fe^{3+}, Fe^{2+}, and Cl^- and the standard-state reduction potentials gives

$$E_{\text{cell}} = \left(E^\circ_{\text{Fe}^{3+}/\text{Fe}^{2+}} - \frac{0.05916}{1} \log \frac{a_{\text{Fe}^{2+}}}{a_{\text{Fe}^{3+}}} \right) - \left(E^\circ_{\text{AgCl/Ag}} - \frac{0.05916}{1} \log a_{\text{Cl}^-} \right)$$

$$E_{\text{cell}} = \left(0.771 - \frac{0.05916}{1} \log \frac{0.0100}{0.0500} \right) - \left(0.2223 - \frac{0.05916}{1} \log(0.100) \right) = 0.531 \text{ V}$$

Exercise 11.2.2

What is the potential for the electrochemical cell in Exercise 11.2.1 if the activity of H^+ in the anodic half-cell is 0.100, the fugacity of H_2 in the anodic half-cell is 0.500, and the activity of Cu^{2+} in the cathodic half-cell is 0.0500? Fugacity, f, is the equivalent term for the activity of a gas.

Answer

Making appropriate substitutions into Equation 4.2.1 and solving for E_{cell} gives its value as

$$E_{\text{cell}} = \left(E^{\circ}_{Cu^{2+}/Cu} - \frac{0.05916}{2}\log\frac{1}{a_{Cu^{2+}}}\right) - \left(E^{\circ}_{H^{+}/H_2} - \frac{0.05916}{2}\log\frac{f_{H_2}}{a^{2}_{H^{+}}}\right)$$

$$E_{\text{cell}} = \left(0.3419 - \frac{0.05916}{2}\log\frac{1}{0.0500}\right) - \left(0.0000 - \frac{0.05916}{2}\log\frac{0.500}{(0.100)^2}\right) = 0.3537 \text{ V}$$

In potentiometry, we assign the reference electrode to the anodic half-cell and assign the indicator electrode to the cathodic half-cell. Thus, if the potential of the cell in Figure 11.2.1 is +1.50 V and the activity of Zn^{2+} is 0.0167, then we can solve the following equation for a_{Ag^+}

$$1.50 \text{ V} = \left(0.7996 - \frac{0.05916}{1}\log\frac{1}{a_{Ag^+}}\right) - \left(-0.7618 - \frac{0.05916}{2}\log\frac{1}{0.0167}\right)$$

obtaining an activity of 0.0118.

Example 11.2.3

What is the activity of Fe^{3+} in an electrochemical cell similar to that in Example 11.2.1 if the activity of Cl^- in the left-hand cell is 1.0, the activity of Fe^{2+} in the right-hand cell is 0.015, and E_{cell} is +0.546 V?

Solution

Making appropriate substitutions into Equation 4.2.1

$$0.546 = \left(0.771 - \frac{0.05916}{1}\log\frac{0.0100}{a_{Fe^{3+}}}\right) - \left(0.2223 - \frac{0.05916}{1}\log(1.0)\right)$$

and solving for $a_{Fe^{3+}}$ gives its activity as 0.0135.

Exercise 11.2.3

What is the activity of Cu^{2+} in the electrochemical cell in Exercise 11.2.1 if the activity of H^+ in the anodic half-cell is 1.00 with a fugacity of 1.00 for H_2, and an E_{cell} of +0.257 V?

Answer

Making appropriate substitutions into Equation 4.2.1

$$0.257 \text{ V} = \left(0.3419 - \frac{0.05916}{2}\log\frac{1}{a_{Cu^{2+}}}\right) - \left(0.0000 - \frac{0.05916}{2}\log\frac{1.00}{(1.00)^2}\right)$$

and solving for $a_{Cu^{2+}}$ gives its activity as 1.35×10^{-3}.

Despite the apparent ease of determining an analyte's activity using the Nernst equation, there are several problems with this approach. One problem is that standard-state potentials are temperature-dependent and the values in reference tables usually are for a temperature of 25°C. We can overcome this problem by maintaining the electrochemical cell at 25°C or by measuring the standard-state potential at the desired temperature.

Another problem is that a standard-sate reduction potential may have a significant matrix effect. For example, the standard-state reduction potential for the Fe^{3+}/Fe^{2+} redox couple is +0.735 V in 1 M $HClO_4$, +0.70 V in 1 M HCl, and +0.53 V in 10 M HCl. The difference in potential for equimolar solutions of HCl and $HClO_4$ is the result of a difference in the activity coefficients for Fe^{3+} and Fe^{2+} in these two media. The shift toward a more negative potential with an increase in the concentration of HCl is the result of chloride's ability to form a stronger complex with Fe^{3+} than with Fe^{2+}. We can minimize this problem by replacing the standard-state potential with a matrix-dependent formal potential. Most tables of standard-state potentials, including those in Appendix 13, include selected formal potentials.

Finally, a more serious problem is the presence of additional potentials in the electrochemical cell not included in Equation 4.2.1. In writing the shorthand notation for an electrochemical cell we use a double slash (||) to indicate the salt bridge, suggesting a potential exists at the interface between each end of the salt bridge and the solution in which it is immersed. The origin of this potential is discussed in the following section.

Junction Potentials

A ***junction potential*** develops at the interface between two ionic solution if there is a difference in the concentration and mobility of the ions. Consider, for example, a porous membrane that separations a solution of 0.1 M HCl from a solution of 0.01 M HCl (Figure 11.2.3 a). Because the concentration of HCl on the membrane's left side is greater than that on the right side of the membrane, H^+ and Cl^- will diffuse in the direction of the arrows. The mobility of H^+, however, is greater than that for Cl^-, as shown by the difference in the lengths of their respective arrows. Because of this difference in mobility, the solution on the right side of the membrane develops an excess concentration of H^+ and a positive charge (Figure 11.2.3 b). Simultaneously, the solution on the membrane's left side develops a negative charge because there is an excess concentration of Cl^-. We call this difference in potential across the membrane a junction potential and represent it as E_j.

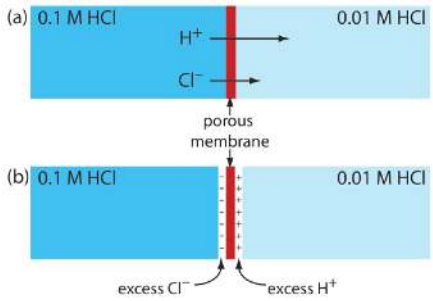


Figure 11.2.3 . Origin of the junction potential between a solution of 0.1 M HCl and a solution of 0.01 M HCl.

The magnitude of the junction potential depends upon the difference in the concentration of ions on the two sides of the interface, and may be as large as 30–40 mV. For example, a junction potential of 33.09 mV has been measured at the interface between solutions of 0.1 M HCl and 0.1 M NaCl [Sawyer, D. T.; Roberts, J. L., Jr. *Experimental Electrochemistry for Chemists*, Wiley-Interscience: New York, 1974, p. 22]. A salt bridge's junction potential is minimized by using a salt, such as KCl, for which the mobilities of the cation and anion are approximately equal. We also can minimize the junction potential by incorporating a high concentration of the salt in the salt bridge. For this reason salt bridges frequently are constructed using solutions that are saturated with KCl. Nevertheless, a small junction potential, generally of unknown magnitude, is always present.

When we measure the potential of an electrochemical cell, the junction potential also contributes to E_{cell}; thus, we rewrite Equation 4.2.1 as

$$E_{cell} = E_{cathode} - E_{anode} + E_j$$

to include its contribution. If we do not know the junction potential's actual value—which is the usual situation—then we cannot directly calculate the analyte's concentration using the Nernst equation. Quantitative analytical work is possible, however, if we use one of the standardization methods—external standards, the method of standard additions, or internal standards—discussed in Chapter 5.3.

Reference Electrodes

In a potentiometric electrochemical cell one of the two half-cells provides a fixed reference potential and the potential of the other half-cell responds the analyte's concentration. By convention, the reference electrode is the anode; thus, the short hand notation for a potentiometric electrochemical cell is

reference electrode || indicator electrode

and the cell potential is

$$E_{cell} = E_{ind} - E_{ref} + E_j$$

The ideal reference electrode provides a stable, known potential so that we can attribute any change in E_{cell} to the analyte's effect on the indicator electrode's potential. In addition, it should be easy to make and to use the reference electrode. Three common reference electrodes are discussed in this section.

Standard Hydrogen Electrode

Although we rarely use the ***standard hydrogen electrode*** (SHE) for routine analytical work, it is the reference electrode used to establish standard-state potentials for other half-reactions. The SHE consists of a Pt electrode immersed in a solution in which the activity of hydrogen ion is 1.00 and in which the fugacity of $H_2(g)$ is 1.00 (Figure 11.2.4). A conventional salt bridge connects the SHE to the indicator half-cell. The short hand notation for the standard hydrogen electrode is

$$\mathrm{Pt}(s),\ \mathrm{H_2}\,(g, f_{\mathrm{H_2}} = 1.00)\,|\,\mathrm{H^+}\,(aq, a_{\mathrm{H^+}} = 1.00)\,\|$$

and the standard-state potential for the reaction

$$\mathrm{H^+}(aq) + e^- = \frac{1}{2}\mathrm{H_2}(g)$$

is, by definition, 0.00 V at all temperatures. Despite its importance as the fundamental reference electrode against which we measure all other potentials, the SHE is rarely used because it is difficult to prepare and inconvenient to use.

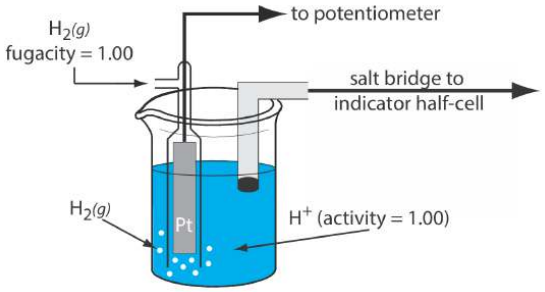


Figure 11.2.4 . Schematic diagram showing the standard hydrogen electrode.

Calomel Electrodes

A calomel reference electrode is based on the following redox couple between Hg_2Cl_2 and Hg (calomel is the common name for Hg_2Cl_2)

$$\mathrm{Hg_2Cl_2}(s) + 2e^- \rightleftharpoons 2\mathrm{Hg}(l) + 2\mathrm{Cl^-}(aq)$$

for which the potential is

$$E = E^\circ_{\mathrm{Hg_2Cl_2/Hg}} - \frac{0.05916}{2}\log\,(a_{\mathrm{Cl^-}})^2 = +0.2682\mathrm{V} - \frac{0.05916}{2}\log\,(a_{\mathrm{Cl^-}})^2$$

The potential of a calomel electrode, therefore, depends on the activity of Cl^- in equilibrium with Hg and Hg_2Cl_2.

As shown in Figure 11.2.5 , in a ***saturated calomel electrode*** (SCE) the concentration of Cl^- is determined by the solubility of KCl. The electrode consists of an inner tube packed with a paste of Hg, Hg_2Cl_2, and KCl, situated within a second tube that contains a saturated solution of KCl. A small hole connects the two tubes and a porous wick serves as a salt bridge to the solution in which the SCE is immersed. A stopper in the outer tube provides an opening for adding addition saturated KCl. The short hand notation for this cell is

$$\mathrm{Hg}(l)|\mathrm{Hg_2Cl_2}(s), \mathrm{KCl}(aq,\ \mathrm{sat'd}\ )\|$$

Because the concentration of Cl^- is fixed by the solubility of KCl, the potential of an SCE remains constant even if we lose some of the inner solution to evaporation. A significant disadvantage of the SCE is that the solubility of KCl is sensitive to a change in temperature. At higher temperatures the solubility of KCl increases and the electrode's potential decreases. For example, the potential of the SCE is +0.2444 V at 25°C and +0.2376 V at 35°C. The potential of a calomel electrode that contains an unsaturated solution of KCl is less dependent on the temperature, but its potential changes if the concentration, and thus the activity of Cl^-, increases due to evaporation.

For example, the potential of a calomel electrode is +0.280 V when the concentration of KCl is 1.00 M and +0.336 V when the concentration of KCl is 0.100 M. If the activity of Cl^- is 1.00, the potential is +0.2682 V.

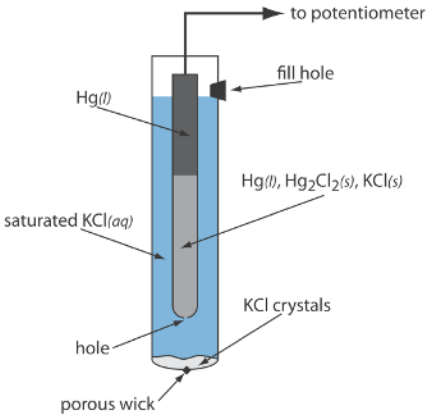


Figure 11.2.5 . Schematic diagram showing the saturated calomel electrode.

Silver/Silver Chloride Electrodes

Another common reference electrode is the ***silver/silver chloride electrode***, which is based on the reduction of AgCl to Ag.

$$\mathrm{AgCl}(s) + e^- \rightleftharpoons \mathrm{Ag}(s) + \mathrm{Cl}^-(aq)$$

As is the case for the calomel electrode, the activity of Cl^- determines the potential of the Ag/AgCl electrode; thus

$$E = E^\circ_{\mathrm{AgCl/Ag}} - 0.05916 \log a_{\mathrm{Cl}^-} = 0.2223 \text{ V} - 0.05916 \log a_{\mathrm{Cl}^-}$$

When prepared using a saturated solution of KCl, the electrode's potential is +0.197 V at 25°C. Another common Ag/AgCl electrode uses a solution of 3.5 M KCl and has a potential of +0.205 V at 25°C. As you might expect, the potential of a Ag/AgCl electrode using a saturated solution of KCl is more sensitive to a change in temperature than an electrode that uses an unsaturated solution of KCl.

A typical Ag/AgCl electrode is shown in Figure 11.2.6 and consists of a silver wire, the end of which is coated with a thin film of AgCl, immersed in a solution that contains the desired concentration of KCl. A porous plug serves as the salt bridge. The electrode's short hand notation is

$$\mathrm{Ag}(s) | \mathrm{Ag\,Cl}(s), \mathrm{KCl}\,(aq, a_{\mathrm{Cl}^-} = x) \|$$

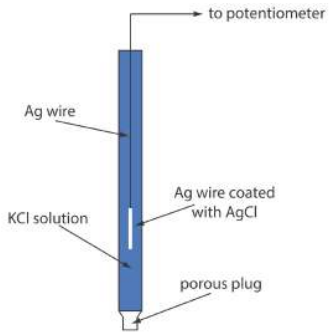


Figure 11.2.6 . Schematic diagram showing a Ag/AgCl electrode. Because the electrode does not contain solid KCl, this is an example of an unsaturated Ag/AgCl electrode.

Converting Potentials Between Reference Electrodes

The standard state reduction potentials in most tables are reported relative to the standard hydrogen electrode's potential of +0.00 V. Because we rarely use the SHE as a reference electrode, we need to convert an indicator electrode's potential to its equivalent value when using a different reference electrode. As shown in the following example, this is easy to do.

Example 11.2.4

The potential for an Fe^{3+}/Fe^{2+} half-cell is +0.750 V relative to the standard hydrogen electrode. What is its potential if we use a saturated calomel electrode or a saturated silver/silver chloride electrode?

Solution

When we use a standard hydrogen electrode the potential of the electrochemical cell is

$$E_{\text{cell}} = E_{\text{Fe}^{3+}/\text{Fe}^{2+}} - E_{\text{SHE}} = 0.750\ \text{V} - 0.000\ \text{V} = 0.750\ \text{V}$$

We can use the same equation to calculate the potential if we use a saturated calomel electrode

$$E_{\text{cell}} = E_{\text{Fe}^{3+}/\text{Fe}^{2+}} - E_{\text{SHE}} = 0.750\ \text{V} - 0.2444\ \text{V} = 0.506\ \text{V}$$

or a saturated silver/silver chloride electrode

$$E_{\text{cell}} = E_{\text{Fe}^{3+}/\text{Fe}^{2+}} - E_{\text{SHE}} = 0.750\ \text{V} - 0.197\ \text{V} = 0.553\ \text{V}$$

Figure 11.2.7 provides a pictorial representation of the relationship between these different potentials.

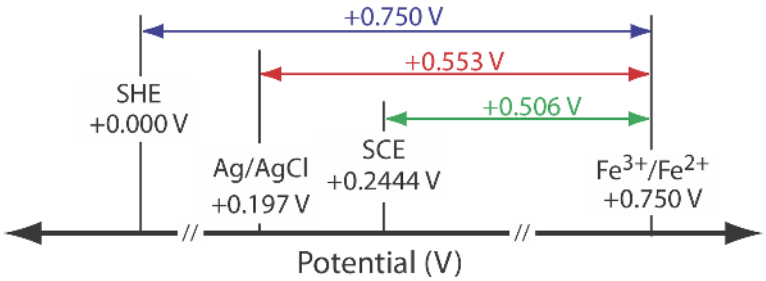


Figure 11.2.7 . Relationship between the potential of an Fe^{3+}/Fe^{2+} half-cell relative to the reference electrodes in Example 11.2.4 . The potential relative to a standard hydrogen electrode is shown in blue, the potential relative to a saturated silver/silver chloride electrode is shown in red, and the potential relative to a saturated calomel electrode is shown in green.

Exercise 11.2.4

The potential of a UO_2^+/U^{4+} half-cell is –0.0190 V relative to a saturated calomel electrode. What is its potential when using a saturated silver/silver chloride electrode or a standard hydrogen electrode?

Answer

When using a saturated calomel electrode, the potential of the electro- chemical cell is

$$E_{\text{cell}} = E_{\text{UO}_2^+/\text{U}^{4+}} - E_{\text{SCE}}$$

Substituting in known values

$$-0.0190\ \text{V} = E_{\text{UO}_2^+/\text{U}^{4+}} - 0.2444\ \text{V}$$

and solving for $E_{\text{UO}_2^+/\text{U}^{4+}}$ gives its value as +0.2254 V. The potential relative to the Ag/AgCl electrode is

$$E_{\text{cell}} = E_{\text{UO}_2^+/\text{U}^{4+}} - E_{\text{Ag/AgCl}} = 0.2254\ \text{V} - 0.197\ \text{V} = 0.028\ \text{V}$$

and the potential relative to the standard hydrogen electrode is

$$E_{\text{cell}} = E_{\text{UO}_2^+/\text{U}^{4+}} - E_{\text{SHE}} = 0.2254\ \text{V} - 0.000\ \text{V} = 0.2254\ \text{V}$$

Metallic Indicator Electrodes

In potentiometry, the potential of the indicator electrode is proportional to the analyte's activity. Two classes of indicator electrodes are used to make potentiometric measurements: metallic electrodes, which are the subject of this section, and ion-selective

electrodes, which are covered in the next section.

Electrodes of the First Kind

If we place a copper electrode in a solution that contains Cu^{2+}, the electrode's potential due to the reaction

$$Cu^{2+}(aq) + 2e^- \rightleftharpoons Cu(s)$$

is determined by the activity of Cu^{2+}.

$$E = E^\circ_{Cu^{2+}/Cu} - \frac{0.05916}{2}\log\frac{1}{a_{Cu^{2+}}} = +0.3419V - \frac{0.05916}{2}\log\frac{1}{a_{Cu^{2+}}}$$

If copper is the indicator electrode in a potentiometric electrochemical cell that also includes a saturated calomel reference electrode

$$SCE \| Cu^{2+}\,(aq, a_{Cu^{2+}} = x)\,|Cu(s)$$

then we can use the cell potential to determine an unknown activity of Cu^{2+} in the indicator electrode's half-cell

$$E_{cell} = E_{ind} - E_{SCE} + E_j = +0.3419V - \frac{0.05916}{2}\log\frac{1}{a_{Cu^{2+}}} - 0.2224V + E_j$$

An indicator electrode in which the metal is in contact with a solution containing its ion is called an ***electrode of the first kind***. In general, if a metal, M, is in a solution of M^{n+}, the cell potential is

$$E_{cell} = K - \frac{0.05916}{n}\log\frac{1}{a_{M^{n+}}} = K + \frac{0.05916}{n}\log a_{M^{n+}}$$

where K is a constant that includes the standard-state potential for the M^{n+}/M redox couple, the potential of the reference electrode, and the junction potential.

> Note that including E_j in the constant K means we do not need to know the junction potential's actual value; however, the junction potential must remain constant if K is to maintain a constant value.

For a variety of reasons—including the slow kinetics of electron transfer at the metal–solution interface, the formation of metal oxides on the electrode's surface, and interfering reactions—electrodes of the first kind are limited to the following metals: Ag, Bi, Cd, Cu, Hg, Pb, Sn, Tl, and Zn.

> Many of these electrodes, such as Zn, cannot be used in acidic solutions because they are easily oxidized by H^+.
>
> $$Zn(s) + 2H^+(aq) \rightleftharpoons H_2(g) + Zn^{2+}(aq)$$

Electrodes of the Second Kind

The potential of an electrode of the first kind responds to the activity of M^{n+}. We also can use this electrode to determine the activity of another species if it is in equilibrium with M^{n+}. For example, the potential of a Ag electrode in a solution of Ag^+ is

$$E = 0.7996V + 0.05916\log a_{Ag^+} \tag{4.2.3}$$

If we saturate the indicator electrode's half-cell with AgI, the solubility reaction

$$AgI(s) \rightleftharpoons Ag^+(aq) + I^-(aq)$$

determines the concentration of Ag^+; thus

$$a_{Ag^+} = \frac{K_{sp,AgI}}{a_{I^-}} \tag{4.2.4}$$

where $K_{sp,AgI}$ is the solubility product for AgI. Substituting Equation 4.2.4 into Equation 4.2.3

$$E = 0.7996 \text{ V} + 0.05916 \log \frac{K_{sp,\ AgI}}{a_{I^-}}$$

shows that the potential of the silver electrode is a function of the activity of I^-. If we incorporate this electrode into a potentiometric electrochemical cell with a saturated calomel electrode

$$\text{SCE} \| \text{AgI}(s),\ I^-\ (aq, a_{I^-} = x)\ | \text{Ag(s)}$$

then the cell potential is

$$E_{cell} = K - 0.05916 \log a_{I^-}$$

where K is a constant that includes the standard-state potential for the Ag^+/Ag redox couple, the solubility product for AgI, the reference electrode's potential, and the junction potential.

If an electrode of the first kind responds to the activity of an ion in equilibrium with M^{n+}, we call it an ***electrode of the second kind***. Two common electrodes of the second kind are the calomel and the silver/silver chloride reference electrodes.

> In an electrode of the second kind we link together a redox reaction and another reaction, such as a solubility reaction. You might wonder if we can link together more than two reactions. The short answer is yes. An electrode of the third kind, for example, links together a redox reaction and two other reactions. Such electrodes are less common and we will not consider them in this text.

Redox Electrodes

An electrode of the first kind or second kind develops a potential as the result of a redox reaction that involves the metallic electrode. An electrode also can serve as a source of electrons or as a sink for electrons in an unrelated redox reaction, in which case we call it a ***redox electrode.*** The Pt cathode in Figure 11.2.2 and Example 11.2.1 is a redox electrode because its potential is determined by the activity of Fe^{2+} and Fe^{3+} in the indicator half-cell. Note that a redox electrode's potential often responds to the activity of more than one ion, which limits its usefulness for direct potentiometry.

Membrane Electrodes

If metals were the only useful materials for constructing indicator electrodes, then there would be few useful applications of potentiometry. In 1906, Cremer discovered that the potential difference across a thin glass membrane is a function of pH when opposite sides of the membrane are in contact with solutions that have different concentrations of H_3O^+. The existence of this ***membrane potential*** led to the development of a whole new class of indicator electrodes, which we call ***ion-selective electrodes*** (ISEs). In addition to the glass pH electrode, ion-selective electrodes are available for a wide range of ions. It also is possible to construct a membrane electrode for a neutral analyte by using a chemical reaction to generate an ion that is monitored with an ion-selective electrode. The development of new membrane electrodes continues to be an active area of research.

Membrane Potentials

Figure 11.2.8 shows a typical potentiometric electrochemical cell equipped with an ion-selective electrode. The short hand notation for this cell is

$$\text{ref (sample)}\ \|[\text{A}]_{\text{samp}}\ (aq, a_A = x)\ |[\text{A}]_{\text{int}}\ (aq, a_A = y)\|\ \text{ref (internal)}$$

where the ion-selective membrane is represented by the vertical slash that separates the two solutions that contain analyte: the sample solution and the ion-selective electrode's internal solution. The potential of this electrochemical cell includes the potential of each reference electrode, a junction potential, and the membrane's potential

$$E_{cell} = E_{ref(int)} - E_{ref(samp)} + E_{mem} + E_j \tag{4.2.5}$$

where E_{mem} is the potential across the membrane and The notations ref(sample) and ref(internal) represent a reference electrode immersed in the sample and a reference electrode immersed in the ISE's internal solution. Because the junction potential and the potential of the two reference electrodes are constant, any change in E_{cell} reflects a change in the membrane's potential.

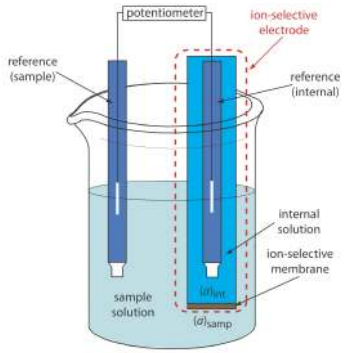


Figure 11.2.8 . Schematic diagram that shows a typical potentiometric cell with an ion-selective electrode. The ion-selective electrode's membrane separates the sample, which contains the analyte at an activity of $(a_A)_{samp}$, from an internal solution that contains the analyte with an activity of $(a_A)_{int}$.

The analyte's interaction with the membrane generates a membrane potential if there is a difference in its activity on the membrane's two sides. Current is carried through the membrane by the movement of either the analyte or an ion already present in the membrane's matrix. The membrane potential is given by the following Nernst-like equation

$$E_{mem} = E_{asym} - \frac{RT}{zF} \ln \frac{(a_A)_{int}}{(a_A)_{samp}} \tag{4.2.6}$$

where $(a_A)_{samp}$ is the analyte's activity in the sample, $(a_A)_{int}$ is the analyte's activity in the ion-selective electrode's internal solution, and z is the analyte's charge. Ideally, E_{mem} is zero when $(a_A)_{int} = (a_A)_{samp}$. The term E_{asym}, which is an ***asymmetry potential***, accounts for the fact that E_{mem} usually is not zero under these conditions.

> For now we simply note that a difference in the analyte's activity results in a membrane potential. As we consider different types of ion-selective electrodes, we will explore more specifically the source of the membrane potential.

Substituting Equation 4.2.6 into Equation 4.2.5, assuming a temperature of 25°C, and rearranging gives

$$E_{cell} = K + \frac{0.05916}{z} \log (a_A)_{samp} \tag{4.2.7}$$

where K is a constant that includes the potentials of the two reference electrodes, the junction potentials, the asymmetry potential, and the analyte's activity in the internal solution. Equation 4.2.7 is a general equation and applies to all types of ion-selective electrodes.

Selectivity of Membranes

A membrane potential results from a chemical interaction between the analyte and active sites on the membrane's surface. Because the signal depends on a chemical process, most membranes are not selective toward a single analyte. Instead, the membrane potential is proportional to the concentration of each ion that interacts with the membrane's active sites. We can rewrite Equation 4.2.7 to include the contribution to the potential of an interferent, I

$$E_{cell} = K + \frac{0.05916}{z_A} \log \left\{ a_A + K_{A,I} (a_I)^{z_A/z_I} \right\}$$

where z_A and z_I are the charges of the analyte and the interferent, and $K_{A,I}$ is a selectivity coefficient that accounts for the relative response of the interferent. The selectivity coefficient is defined as

$$K_{A,I} = \frac{(a_A)_e}{(a_I)_e^{z_A/z_I}} \tag{4.2.8}$$

where $(a_A)_e$ and $(a_I)_e$ are the activities of analyte and the interferent that yield identical cell potentials. When the selectivity coefficient is 1.00, the membrane responds equally to the analyte and the interferent. A membrane shows good selectivity for the analyte when $K_{A,I}$ is significantly less than 1.00.

Selectivity coefficients for most commercially available ion-selective electrodes are provided by the manufacturer. If the selectivity coefficient is not known, it is easy to determine its value experimentally by preparing a series of solutions, each of which contains the same activity of interferent, $(a_I)_{add}$, but a different activity of analyte. As shown in Figure 11.2.9 , a plot of cell potential versus the log of the analyte's activity has two distinct linear regions. When the analyte's activity is significantly larger than $K_{A,I} \times (a_I)_{add}$, the potential is a linear function of $\log(a_A)$, as given by Equation 4.2.7. If $K_{A,I} \times (a_I)_{add}$ is significantly larger than the analyte's activity, however, the cell's potential remains constant. The activity of analyte and interferent at the intersection of these two linear regions is used to calculate $K_{A,I}$.

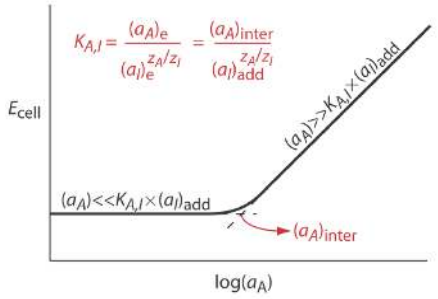


Figure 11.2.9 . Diagram showing the experimental determination of an ion-selective electrode's selectivity for an analyte. The activity of analyte that corresponds to the intersection of the two linear portions of the curve, $(a_A)_{inter}$, produces a cell potential identical to that of the interferent. The equation for the selectivity coefficient, $K_{A,I}$, is shown in red.

Example 11.2.5

Sokalski and co-workers described a method for preparing ion-selective electrodes with significantly improved selectivities [Sokalski, T.; Ceresa, A.; Zwicki, T.; Pretsch, E. *J. Am. Chem. Soc.* **1997**, *119*, 11347–11348]. For example, a conventional Pb^{2+} ISE has a $\log K_{Pb^{2+}/Mg^{2+}}$ of –3.6. If the potential for a solution in which the activity of Pb^{2+} is 4.1×10^{-12} is identical to that for a solution in which the activity of Mg^{2+} is 0.01025, what is the value of $\log K_{Pb^{2+}/Mg^{2+}}$ for their ISE?

Solution

Making appropriate substitutions into Equation 4.2.8, we find that

$$K_{Pb^{2+}/Mg^{2+}} = \frac{(a_{Pb^{2+}})_e}{(a_{Mg^{2+}})_e^{z_{Pb^{2+}}/z_{Mg^{2+}}}} = \frac{4.1 \times 10^{-12}}{(0.01025)^{+2/+2}} = 4.0 \times 10^{-10}$$

The value of $\log K_{Pb^{2+}/Mg^{2+}}$, therefore, is –9.40.

Exercise 11.2.5

A ion-selective electrode for NO_2^- has log$K_{A,I}$ values of –3.1 for F^-, –4.1 for SO_4^{2-}, –1.2 for I^-, and –3.3 for NO_3^-. Which ion is the most serious interferent and for what activity of this interferent is the potential equivalent to a solution in which the activity of NO_2^- is 2.75×10^{-4}?

Answer

The larger the value of $K_{A,I}$ the more serious the interference. Larger values for $K_{A,I}$ correspond to more positive (less negative) values for log$K_{A,I}$; thus, I^-, with a $K_{A,I}$ of 6.3×10^{-2}, is the most serious of these interferents. To find the activity of I^- that gives a potential equivalent to a NO_2^- activity of 2.75×10^{-4}, we note that

$$a_{NO_2^-} = K_{A,I} \times a_{I^-}$$

Making appropriate substitutions

$$2.75 \times 10^{-4} = (6.3 \times 10^{-2}) \times a_{I^-}$$

and solving for a_{I^-} gives its activity as 4.4×10^{-3}.

Glass Ion-Selective Electrodes

The first commercial ***glass electrodes*** were manufactured using Corning 015, a glass with a composition that is approximately 22% Na_2O, 6% CaO, and 72% SiO_2. When immersed in an aqueous solution for several hours, the outer approximately 10 nm of the membrane's surface becomes hydrated, resulting in the formation of negatively charged sites, —SiO^-. Sodium ions, Na^+, serve as counter ions. Because H^+ binds more strongly to —SiO^- than does Na^+, they displace the sodium ions

$$H^+ + -SiO^-Na^+ \rightleftharpoons -SiO^-H^+ + Na^+$$

explaining the membrane's selectivity for H^+. The transport of charge across the membrane is carried by the Na^+ ions. The potential of a glass electrode using Corning 015 obeys the equation

$$E_{cell} = K + 0.05916 \log a_{H^+} \tag{4.2.9}$$

over a pH range of approximately 0.5 to 9. At more basic pH values the glass membrane is more responsive to other cations, such as Na^+ and K^+.

Example 11.2.6

For a Corning 015 glass membrane, the selectivity coefficient K_{H^+/Na^+} is $\approx 10^{-11}$. What is the expected error if we measure the pH of a solution in which the activity of H^+ is 2×10^{-13} and the activity of Na^+ is 0.05?

Solution

A solution in which the actual activity of H^+, $(a_{H^+})_{act}$, is 2×10^{-13} has a pH of 12.7. Because the electrode responds to both H^+ and Na^+, the apparent activity of H^+, $(a_{H^+})_{app}$, is

$$(a_{H^+})_{app} = (a_{H^+})_{act} + (K_{H^+/Na^+} \times a_{Na^+}) = 2 \times 10^{-13} + (10^{-11} \times 0.05) = 7 \times 10^{-13}$$

The apparent activity of H^+ is equivalent to a pH of 12.2, an error of –0.5 pH units.

Replacing Na_2O and CaO with Li_2O and BaO extends the useful pH range of glass membrane electrodes to pH levels greater than 12.

Glass membrane pH electrodes often are available in a combination form that includes both the indicator electrode and the reference electrode. The use of a single electrode greatly simplifies the measurement of pH. An example of a typical combination electrode is shown in Figure 11.2.10 .

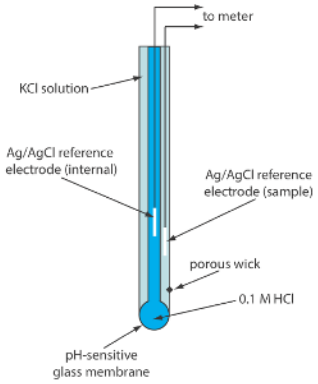


Figure 11.2.10 . Schematic diagram showing a combination glass electrode for measuring pH. The indicator electrode consists of a pH-sensitive glass membrane and an internal Ag/AgCl reference electrode in a solution of 0.1 M HCl. The sample's reference electrode is a Ag/AgCl electrode in a solution of KCl (which may be saturated with KCl or contain a fixed concentration of KCl). A porous wick serves as a salt bridge between the sample and its reference electrode.

The observation that the Corning 015 glass membrane responds to ions other than H^+ (see Example 11.2.6) led to the development of glass membranes with a greater selectivity for other cations. For example, a glass membrane with a composition of 11% Na_2O, 18% Al_2O_3, and 71% SiO_2 is used as an ion-selective electrode for Na^+. Other glass ion-selective electrodes have been developed for the analysis of Li^+, K^+, Rb^+, Cs^+, NH_4^+, Ag^+, and Tl^+. Table 11.2.1 provides several examples.

Table 11.2.1 . Representative Examples of Glass Membrane Ion-Selective Electrodes for Analytes Other Than H^+

analyte	membrane composition	selectivity coefficients
Na^+	11% Na_2O, 18% Al_2O_3, 71% SiO_2	$K_{Na^+/H^+} = 1000$ $K_{Na^+/K^+} = 0.001$ $K_{Na^+/Li^+} = 0.001$
Li^+	15% Li_2O, 25% Al_2O_3, 60% SiO_2	$K_{Li^+/Na^+} = 0.3$ $K_{Li^+/K^+} = 0.001$
K^+	27% Na_2O, 5% Al_2O_3, 68% SiO_2	$K_{K^+/Na^+} = 0.05$

Selectivity coefficients are approximate; values found experimentally may vary substantially from the listed values. See Cammann, K. *Working With Ion-Selective Electrodes*, Springer-Verlag: Berlin, 1977.

Because an ion-selective electrode's glass membrane is very thin—it is only about 50 μm thick—they must be handled with care to avoid cracks or breakage. Glass electrodes usually are stored in a storage buffer recommended by the manufacturer, which ensures that the membrane's outer surface remains hydrated. If a glass electrode dries out, it is reconditioned by soaking for several hours in a solution that contains the analyte. The composition of a glass membrane will change over time, which affects the electrode's performance. The average lifetime for a typical glass electrode is several years.

Solid-State Ion-Selective Electrodes

A s***olid-state ion-selective electrode*** has a membrane that consists of either a polycrystalline inorganic salt or a single crystal of an inorganic salt. We can fashion a polycrystalline solid-state ion-selective electrode by sealing a 1–2 mm thick pellet of AgS—or a mixture of AgS and a second silver salt or another metal sulfide—into the end of a nonconducting plastic cylinder, filling the cylinder with an internal solution that contains the analyte, and placing a reference electrode into the internal solution. Figure 11.2.11 shows a typical design.

> The NaCl in a salt shaker is an example of polycrystalline material because it consists of many small crystals of sodium chloride. The NaCl salt plates used in IR spectroscopy (see Chapter 10), on the other hand, are an example of a single crystal of sodium chloride.

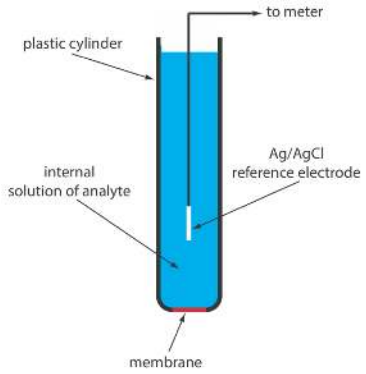


Figure 11.2.11 . Schematic diagram of a solid-state electrode. The internal solution contains a solution of analyte of fixed activity.

The membrane potential for a Ag_2S pellet develops as the result of a difference in the extent of the solubility reaction

$$Ag_2S(s) \rightleftharpoons 2Ag^+(aq) + S^{2-}(aq)$$

on the membrane's two sides, with charge carried across the membrane by Ag^+ ions. When we use the electrode to monitor the activity of Ag^+, the cell potential is

$$E_{cell} = K + 0.05916 \log a_{Ag^+}$$

The membrane also responds to the activity of S^{2-}, with a cell potential of

$$E_{cell} = K - \frac{0.05916}{2} \log a_{S^{2-}}$$

If we combine an insoluble silver salt, such as AgCl, with the Ag_2S, then the membrane potential also responds to the concentration of Cl^-, with a cell potential of

$$E_{cell} = K - 0.05916 \log a_{Cl^-}$$

By mixing Ag_2S with CdS, CuS, or PbS, we can make an ion-selective electrode that responds to the activity of Cd^{2+}, Cu^{2+}, or Pb^{2+}. In this case the cell potential is

$$E_{cell} = K + \frac{0.05916}{2} \ln a_{M^{2+}}$$

where $a_{M^{2+}}$ is the activity of the metal ion.

Table 11.2.2 provides examples of polycrystalline, Ag_2S-based solid-state ion-selective electrodes. The selectivity of these ion-selective electrodes depends on the relative solubility of the compounds. A Cl^- ISE using a Ag_2S/AgCl membrane is more selective for Br^- ($K_{Cl^-/Br^-} = 10^2$) and for I^- ($K_{Cl^-/I^-} = 10^6$) because AgBr and AgI are less soluble than AgCl. If the activity of Br^- is sufficiently high, AgCl at the membrane/solution interface is replaced by AgBr and the electrode's response to Cl^- decreases substantially. Most of the polycrystalline ion-selective electrodes listed in Table 11.2.2 operate over an extended range of pH levels. The equilibrium between S^{2-} and HS^- limits the analysis for S^{2-} to a pH range of 13–14.

11.2.2 . Representative Examples of Polycrystalline Solid-State Ion-Selective Electrodes

analyte	membrane composition	selectivity coefficients
Ag^+	Ag_2S	$K_{Ag^+/Cu^{2+}} = 10^{-6}$ $K_{Ag^+/Pb^{2+}} = 10^{-10}$ Hg^{2+} interferes
Cd^{2+}	CdS/Ag_2S	$K_{Cd^{2+}/Fe^{2+}} = 200$ $K_{Cd^{2+}/Pb^{2+}} = 6$ Ag^+, Hg^{2+}, and Cu^{2+} must be absent
Cu^{2+}	CuS/Ag_2S	$K_{Cu^{2+}/Fe^{3+}} = 10$ $K_{Cu^{2+}/Cu^+} = 10^{-6}$ Ag^+ and Hg^{2+} must be absent
Pb^{2+}	PbS/Ag_2S	$K_{Pb^{2+}/Fe^{3+}} = 1$ $K_{Pb^{2+}/Cd^{2+}} = 1$ Ag^+, Hg^{2+}, and Cu^{2+} must be absent
Br^-	$AgBr/Ag_2S$	$K_{Br^-/I^-} = 5000$ $K_{Br^-/Cl^-} = 0.005$ $K_{Br^-/OH^-} = 10^{-5}$ S^{2-} must be absent
Cl^-	$AgCl/Ag_2S$	$K_{Cl^-/I^-} = 10^6$ $K_{Cl^-/Br^-} = 100$ $K_{Cl^-/OH^-} = 0.01$ S^{2-} must be absent
I^-	AgI/Ag_2S	$K_{I^-/S^{2-}} = 30$ $K_{I^-/Br^-} = 10^{-4}$ $K_{I^-/Cl^-} = 10^{-6}$ $K_{I^-/OH^-} = 10^{-7}$
SCN^-	$AgSCN/Ag_2S$	$K_{SCN^-/I^-} = 10^3$ $K_{SCN^-/Br^-} = 100$ $K_{SCN^-/Cl^-} = 0.1 K_{SCN^-/OH^-} = 0.01$ S^{2-} must be absent
S^{2-}	Ag_2S	Hg^{2+} must be absent

Selectivity coefficients are approximate; values found experimentally may vary substantially from the listed values. See Cammann, K. *Working With Ion-Selective Electrodes*, Springer-Verlag: Berlin, 1977.

The membrane of a F^- ion-selective electrode is fashioned from a single crystal of LaF_3, which usually is doped with a small amount of EuF_2 to enhance the membrane's conductivity. Because EuF_2 provides only two F^- ions—compared to the three F^- ions in LaF_3—each EuF_2 produces a vacancy in the crystal's lattice. Fluoride ions pass through the membrane by moving into adjacent vacancies. As shown in Figure 11.2.11 , the LaF_3 membrane is sealed into the end of a non-conducting plastic cylinder, which contains a standard solution of F^-, typically 0.1 M NaF, and a Ag/AgCl reference electrode.

The membrane potential for a F^- ISE results from a difference in the solubility of LaF_3 on opposite sides of the membrane, with the potential given by

$$E_{cell} = K - 0.05916 \log a_{F^-}$$

One advantage of the F^- ion-selective electrode is its freedom from interference. The only significant exception is OH^- (K_{F^-/OH^-} = 0.1), which imposes a maximum pH limit for a successful analysis. Below a pH of 4 the predominate form of fluoride in solution is HF, which does not contribute to the membrane potential. For this reason, an analysis for fluoride is carried out at a pH greater than 4.

Example 11.2.7

What is the maximum pH that we can tolerate if we need to analyze a solution in which the activity of F^- is 1×10^{-5} with an error of less than 1%?

Solution

In the presence of OH^- the cell potential is

$$E_{cell} = K - 0.05916 \left\{ a_{F^-} + K_{F^-/OH^-} \times a_{OH^-} \right\}$$

To achieve an error of less than 1%, the term $K_{F^-/OH^-} \times a_{OH^-}$ must be less than 1% of a_{F^-}; thus

$$K_{F^-/OH^-} \times a_{OH^-} \leq 0.01 \times a_{F^-}$$

$$0.10 \times a_{OH^-} \leq 0.01 \times \left(1.0 \times 10^{-5}\right)$$

Solving for a_{OH^-} gives the maximum allowable activity for OH^- as 1×10^{-6}, which corresponds to a pH of less than 8.

Exercise 11.2.6

Suppose you wish to use the nitrite-selective electrode in Exercise 11.2.5 to measure the activity of NO_2^-. If the activity of NO_2^- is 2.2×10^{-4}, what is the maximum pH you can tolerate if the error due to OH^- must be less than 10%? The selectivity coefficient for OH^-, $K_{NO_2^-/OH^-}$, is 630. Do you expect the electrode to have a lower pH limit? Clearly explain your answer.

Answer

In the presence of OH^- the cell potential is

$$E_{cell} = K - 0.05916 \log \left\{ a_{NO_2^-} + K_{NO_2^-/OH^-} \times a_{OH^-} \right\}$$

To achieve an error of less than 10%, the term $K_{NO_2^-/OH^-} \times a_{OH^-}$ must be less than 1% of $a_{NO_2^-}$; thus

$$K_{NO_2^-/OH^-} \times a_{OH^-} \leq 0.10 \times a_{NO_2^-}$$

$$630 \times a_{OH^-} \leq 0.10 \times \left(2.2 \times 10^{-4}\right)$$

Solving for a_{OH^-} gives its maximum allowable activity as 3.5×10^{-8}, which corresponds to a pH of less than 6.54.

The electrode does have a lower pH limit. Nitrite is the conjugate weak base of HNO_2, a species to which the ISE does not respond. As shown by the ladder diagram below, at a pH of 4.15 approximately 10% of nitrite is present as HNO_2. A minimum pH of 4.5 is the usual recommendation when using a nitrite ISE. This corresponds to a NO_2^-/HNO_2 ratio of

$$pH = pK_a + \log \frac{[NO_2^-]}{[HNO_2]}$$

$$4.5 = 3.15 + \log \frac{[NO_2^-]}{[HNO_2]}$$

$$\frac{[NO_2^-]}{[HNO_2]} \approx 22$$

Thus, at a pH of 4.5 approximately 96% of nitrite is present as NO_2^-.

Unlike a glass membrane ion-selective electrode, a solid-state ISE does not need to be conditioned before it is used, and it may be stored dry. The surface of the electrode is subject to poisoning, as described above for a Cl^- ISE in contact with an excessive concentration of Br^-. If an electrode is poisoned, it can be returned to its original condition by sanding and polishing the crystalline membrane.

Poisoning simply means that the surface has been chemically modified, such as AgBr forming on the surface of a AgCl membrane.

Liquid-Based Ion-Selective Electrodes

Another class of ion-selective electrodes uses a hydrophobic membrane that contains a liquid organic complexing agent that reacts selectively with the analyte. Three types of organic complexing agents have been used: cation exchangers, anion exchangers, and neutral ionophores. A membrane potential exists if the analyte's activity is different on the two sides of the membrane. Current is carried through the membrane by the analyte.

An ***ionophore*** is a ligand whose exterior is hydrophobic and whose interior is hydrophilic. The crown ether shown here is one example of a neutral ionophore.



One example of a ***liquid-based ion-selective electrode*** is that for Ca^{2+}, which uses a porous plastic membrane saturated with the cation exchanger di-(*n*-decyl) phosphate. As shown in Figure 11.2.12 , the membrane is placed at the end of a non-conducting cylindrical tube and is in contact with two reservoirs. The outer reservoir contains di-(*n*-decyl) phosphate in di-*n*-octylphenylphosphonate, which soaks into the porous membrane. The inner reservoir contains a standard aqueous solution of Ca^{2+} and a Ag/AgCl reference electrode. Calcium ion-selective electrodes also are available in which the di-(*n*-decyl) phosphate is immobilized in a polyvinyl chloride (PVC) membrane that eliminates the need for the outer reservoir.

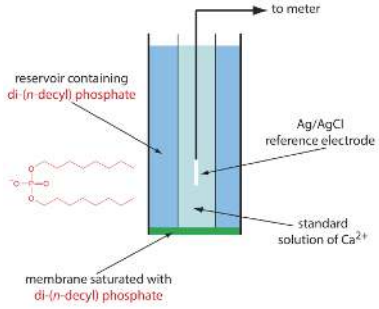


Figure 11.2.12 . Schematic diagram showing a liquid-based ion-selective electrode for Ca^{2+}. The structure of the cation exchanger, di-(*n*-decyl) phosphate, is shown in red.

The membrane potential for the Ca^{2+} ISE develops as the result of a difference in the extent of the complexation reaction

$$Ca^{2+}(aq) + 2\,(C_{10}H_{21}O)_2\,PO_2^-(mem) \rightleftharpoons Ca\,[(C_{10}H_{21}O)_2PO_2]_2\,(mem)$$

on the two sides of the membrane, where (*mem*) indicates a species that is present in the membrane. The cell potential for the Ca^{2+} ion-selective electrode is

$$E_{cell} = K + \frac{0.05916}{2}\log a_{Ca^{2+}}$$

The selectivity of this electrode for Ca^{2+} is very good, with only Zn^{2+} showing greater selectivity.

Table 11.2.3 lists the properties of several liquid-based ion-selective electrodes. An electrode using a liquid reservoir can be stored in a dilute solution of analyte and needs no additional conditioning before use. The lifetime of an electrode with a PVC membrane, however, is proportional to its exposure to aqueous solutions. For this reason these electrodes are best stored by covering the membrane with a cap along with a small amount of wetted gauze to maintain a humid environment. Before using the electrode it is conditioned in a solution of analyte for 30–60 minutes.

Table 11.2.3 . Representative Examples of Liquid-Based Ion-Selective Electrodes

analyte	membrane composition	selectivity coefficients
Ca^{2+}	di-(*n*-decyl) phosphate in PVC	$K_{Ca^{2+}/Zn^{2+}} = 1 - 5$ $K_{Ca^{2+}/Al^{3+}} = 0.90$ $K_{Ca^{2+}/Mn^{2+}} = 0.38$ $K_{Ca^{2+}/Cu^{2+}} = 0.070$ $K_{Ca^{2+}/Mg^{2+}} = 0.032$
K^+	valinomycin in PVC	$K_{K^+/Rb^+} = 1.9$ $K_{K^+/Cs^+} = 0.38$ $K_{K^+/Li^+} = 10^{-4}$
Li^+	ETH 149 in PVC	$K_{Li^+/H^+} = 1$ $K_{Li^+/Na^+} = 0.03$ $K_{Li^+/K^+} = 0.007$
NH_4^+	nonactin and monactin in PVC	$K_{NH_4^+/K^+} = 0.12$ $K_{NH_4^+/H^+} = 0.016$ $K_{NH_4^+/Li^+} = 0.0042$ $K_{NH_4^+/Na^+} = 0.002$
ClO_3^-	$Fe(o\text{-phen})_3^{3+}$ in *p*-nitrocymene with porous membrane	$K_{ClO_4^-/OH^-} = 1$ $K_{ClO_4^-/I^-} = 0.012$ $K_{ClO_4^-/NO_3^-} = 0.0015$ $K_{ClO_4^-/Br^-} = 5.6 \times 10^{-4}$ $K_{ClO_4^-/Cl^-} = 2.2 \times 10^{-4}$
NO_3^-	tetradodecyl ammonium nitrate in pVC	$K_{NO_3^-/Cl^-} = 0.006$ $K_{NO_3^-/F^-} = 9 \times 10^{-4}$

Selectivity coefficients are approximate; values found experimentally may vary substantially from the listed values. See Cammann, K. *Working With Ion-Selective Electrodes*, Springer-Verlag: Berlin, 1977.

Gas-Sensing Electrodes

A number of membrane electrodes respond to the concentration of a dissolved gas. The basic design of a ***gas-sensing electrode***, as shown in Figure 11.2.13 , consists of a thin membrane that separates the sample from an inner solution that contains an ion-selective electrode. The membrane is permeable to the gaseous analyte, but impermeable to nonvolatile components in the sample's matrix. The gaseous analyte passes through the membrane where it reacts with the inner solution, producing a species whose concentration is monitored by the ion-selective electrode. For example, in a CO_2 electrode, CO_2 diffuses across the membrane where it reacts in the inner solution to produce H_3O^+.

$$CO_2(aq) + 2H_2O(l) \rightleftharpoons HCO_3^-(aq) + H_3O^+(aq) \tag{4.2.10}$$

The change in the activity of H_3O^+ in the inner solution is monitored with a pH electrode, for which the cell potential is given by Equation 4.2.9. To find the relationship between the activity of H_3O^+ in the inner solution and the activity of CO_2 in the inner solution we rearrange the equilibrium constant expression for reaction 4.2.10; thus

$$a_{H_3O^+} = K_a \times \frac{a_{CO_2}}{a_{HCO_3^-}} \tag{4.2.11}$$

where K_a is the equilibrium constant. If the activity of HCO_3^- in the internal solution is sufficiently large, then its activity is not affected by the small amount of CO_2 that passes through the membrane. Substituting Equation 4.2.11 into Equation 4.2.9 gives

$$E_{cell} = K' + 0.05916 \log a_{co_2}$$

where K′ is a constant that includes the constant for the pH electrode, the equilibrium constant for reaction 4.2.10 and the activity of HCO_3^- in the inner solution.

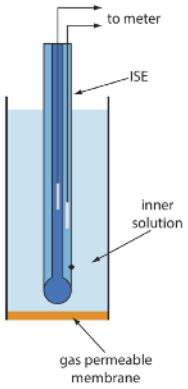


Figure 11.2.13 . Schematic diagram of a gas-sensing membrane electrode.

Table 11.2.4 lists the properties of several gas-sensing electrodes. The composition of the inner solution changes with use, and both the inner solution and the membrane must be replaced periodically. Gas-sensing electrodes are stored in a solution similar to the internal solution to minimize their exposure to atmospheric gases.

Table 11.2.4 . Representative Examples of Gas-Sensing Electrodes

analyte	inner solution	reaction in inner solution	ion-selective electrode
CO_2	10 mM $NaHCO_3$ 10 mM NaCl	$CO_2(aq) + 2H_2O(l) \rightleftharpoons HCO_3^-(aq) + H_3O^+(aq)$	glass pH ISE
HCN	10 mM $KAg(CN)_2$	$HCN(aq) + H_2O(l) \rightleftharpoons CN^-(aq) + H_3O^+(aq)$	Ag_2S solid-state ISE
HF	1 M H_3O^+	$HF(aq) + H_2O(l) \rightleftharpoons F^-(aq) + H_3O^+(aq)$	F^- solid-state ISE
H_2S	pH 5 citrate buffer	$H_2S(aq) + H_2O(l) \rightleftharpoons HS^-(aq) + H_3O^+(aq)$	Ag_2S solid state ISE
NH_3	10 mM NH_4Cl 0.1 M KNO_3	$NH_3(aq) + H_2O(l) \rightleftharpoons NH_4^+(aq) + OH^-(aq)$	glass pH ISE
NO_2	20 mM $NaNO_2$ 0.1 M KNO_3	$2NO_2(aq) + 3H_2O(l) \rightleftharpoons NO_3^-(aq) + NO_2^-(aq) + 2H_3O^+(aq)$	glass pH ISE
SO_2	1 mM $NaHSO_3$ pH 5	$SO_2(aq) + 2H_2O(l) \rightleftharpoons HSO_3^-(aq) + H_3O^+(aq)$	glass pH ISE

Source: Cammann, K. *Working With Ion-Selective Electrodes*, Springer-Verlag: Berlin, 1977.

Potentiometric Biosensors

The approach for developing gas-sensing electrodes can be modified to create potentiometric electrodes that respond to a biochemically important species. The most common class of potentiometric biosensors are ***enzyme electrodes***, in which we trap or immobilize an enzyme at the surface of a potentiometric electrode. The analyte's reaction with the enzyme produces a product whose concentration is monitored by the potentiometric electrode. Potentiometric biosensors also have been designed around other biologically active species, including antibodies, bacterial particles, tissues, and hormone receptors.

One example of an enzyme electrode is the urea electrode, which is based on the catalytic hydrolysis of urea by urease

$$CO(NH_2)_2(aq) + 2H_2O(l) \rightleftharpoons 2NH_4^+(aq) + CO_3^-(aq)$$

Figure 11.2.14 shows one version of the urea electrode, which modifies a gas-sensing NH_3 electrode by adding a dialysis membrane that traps a pH 7.0 buffered solution of urease between the dialysis membrane and the gas permeable membrane [(a) Papastathopoulos, D. S.; Rechnitz, G. A. *Anal. Chim. Acta* **1975**, *79*, 17–26; (b) Riechel, T. L. *J. Chem. Educ*. **1984**, *61*, 640–642].

An NH_3 electrode, as shown in Table 11.2.4 , uses a gas-permeable membrane and a glass pH electrode. The NH_3 diffuses across the membrane where it changes the pH of the internal solution.

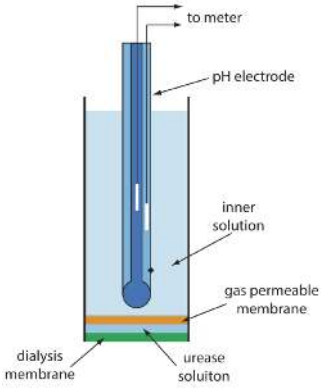


Figure 11.2.14 . Schematic diagram showing an enzyme-based potentiometric biosensor for urea. A solution of the enzyme urease is trapped between a dialysis membrane and a gas permeable membrane. Urea diffuses across the dialysis membrane and reacts with urease, producing NH_3 that diffuses across the gas permeable membrane. The resulting change in the internal solution's pH is measured with the pH electrode.

When immersed in the sample, urea diffuses through the dialysis membrane where it reacts with the enzyme urease to form the ammonium ion, $\mathbf{NH_4^+}$, which is in equilibrium with NH_3.

$$\mathbf{NH_4^+}(aq) + \mathbf{H_2O}(l) \rightleftharpoons \mathbf{H_3O^+}(aq) + \mathbf{NH_3}(aq)$$

The NH_3, in turn, diffuses through the gas permeable membrane where a pH electrode measures the resulting change in pH. The electrode's response to the concentration of urea is

$$E_{\text{cell}} = K - 0.05916 \log a_{\text{urea}} \tag{4.2.12}$$

Another version of the urea electrode (Figure 11.2.15) immobilizes the enzyme urease in a polymer membrane formed directly on the tip of a glass pH electrode [Tor, R.; Freeman, A. *Anal. Chem.* **1986**, *58*, 1042–1046]. In this case the response of the electrode is

$$\text{pH} = Ka_{\text{urea}} \tag{4.2.13}$$

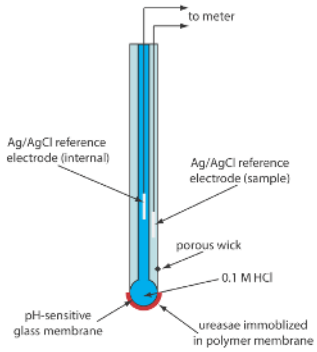


Figure 11.2.15 . Schematic diagram of an enzyme-based potentiometric biosensor for urea in which urease is immobilized in a polymer membrane coated onto the pH-sensitive glass membrane of a pH electrode.

Few potentiometric biosensors are available commercially. As shown in Figure 11.2.14 and Figure 11.2.15 , however, it is possible to convert an ion-selective electrode or a gas-sensing electrode into a biosensor. Several representative examples are described in Table 11.2.5 , and additional examples can be found in this chapter's additional resources.

Table 11.2.5 . Representative Examples of Potentiometric Biosensors

analyte	biologically active phase	substance determined
5′-AMP	AMP-deaminase (E)	NH_3
L-arginine	arginine and urease (E)	NH_3
asparagine	asparaginase (E)	NH_4^+
L-cysteine	*Proteus morganii* (B)	H_2S
L-glutamate	yellow squash (T)	CO_2
L-glutamine	*Sarcina flava* (B)	NH_3
oxalate	oxalate decarboxylase (E)	CO_2
penicillin	penicllinase (E)	H_3O^+
L-phenylalanine	L-amino acid oxidase/horseradish peroxidase (E)	I^-
sugars	bacteria from dental plaque (B)	H_3O^+
urea	urease (E)	NH_3 or H_3O^+

Source: Complied from Cammann, K. *Working With Ion-Selective Electrodes*, Springer-Verlag: Berlin, 1977 and Lunte, C. E.; Heineman, W. R. "Electrochemical techniques in Bioanalysis," in Steckham, E. ed. *Topics in Current Chemistry*, Vol. 143, Springer-Verlag: Berlin, 1988, p.8.
Abbreviations for biologically active phase: E = enzyme; B = bacterial particle; T = tissue.

Quantitative Applications

The potentiometric determination of an analyte's concentration is one of the most common quantitative analytical techniques. Perhaps the most frequent analytical measurement is the determination of a solution's pH, a measurement we will consider in more detail later in this section. Other areas where potentiometry is important are clinical chemistry, environmental chemistry, and potentiometric titrations. Before we consider representative applications, however, we need to examine more closely the relationship between cell potential and the analyte's concentration and methods for standardizing potentiometric measurements.

Activity and Concentration

The Nernst equation relates the cell potential to the analyte's activity. For example, the Nernst equation for a metallic electrode of the first kind is

$$E_{\text{cell}} = K + \frac{0.05916}{n} \log a_{M^{n+}} \tag{4.2.14}$$

where $a_{M^{n+}}$ is the metal ion's activity. When we use a potentiometric electrode, however, our goal is to determine the analyte's concentration. As we learned in Chapter 6, an ion's activity is the product of its concentration, $[M^{n+}]$, and a matrix-dependent activity coefficient, $\gamma_{Mn^{n+}}$.

$$a_{M^{n+}} = [M^{n+}]\,\gamma_{M^{n+}} \tag{4.2.15}$$

Substituting Equation 4.2.15 into Equation 4.2.14 and rearranging, gives

$$E_{\text{cell}} = K + \frac{0.05916}{n} \log \gamma_{M^{n+}} + \frac{0.05916}{n} \log [M^{n+}] \tag{4.2.16}$$

We can solve Equation 4.2.16 for the metal ion's concentration if we know the value for its activity coefficient. Unfortunately, if we do not know the exact ionic composition of the sample's matrix—which is the usual situation—then we cannot calculate the value of $\gamma_{Mn^{n+}}$. There is a solution to this dilemma. If we design our system so that the standards and the samples have an identical matrix, then the value of $\gamma_{Mn^{n+}}$ remains constant and Equation 4.2.16 simplifies to

$$E_{cell} = K' + \frac{0.05916}{n} \log [M^{n+}]$$

where K' includes the activity coefficient.

Quantitative Analysis Using External Standards

Before we can determine the concentration of analyte in a sample, we must standardize the electrode. If the electrode's response obeys the Nernst equation, then we can determine the constant K using a single external standard. Because a small deviation from the ideal slope of $\pm RT/nF$ or $\pm RT/zF$ is not unexpected, we usually use two or more external standards.

> To review the use of external standards, see Chapter 5.3.

In the absence of interferents, a calibration curve of E_{cell} versus $\log a_A$, where A is the analyte, is a straight-line. A plot of E_{cell} versus $\log[A]$, however, may show curvature at higher concentrations of analyte as a result of a matrix-dependent change in the analyte's activity coefficient. To maintain a consistent matrix we add a high concentration of an inert electrolyte to all samples and standards. If the concentration of added electrolyte is sufficient, then the difference between the sample's matrix and the matrix of the standards will not affect the ionic strength and the activity coefficient essentially remains constant. The inert electrolyte added to the sample and the standards is called a ***total ionic strength adjustment buffer*** (TISAB).

Example 11.2.8

The concentration of Ca^{2+} in a water sample is determined using the method of external standards. The ionic strength of the samples and the standards is maintained at a nearly constant level by making each solution 0.5 M in KNO_3. The measured cell potentials for the external standards are shown in the following table.

$[Ca^{2+}]$ (M)	E_{cell} (V)
1.00×10^{-5}	–0.125
5.00×10^{-5}	–0.103
1.00×10^{-4}	–0.093
5.00×10^{-4}	–0.072
1.00×10^{-3}	–0.063
5.00×10^{-3}	–0.043
1.00×10^{-2}	–0.033

What is the concentration of Ca^{2+} in a water sample if its cell potential is found to be –0.084 V?

Solution

Linear regression gives the calibration curve in Figure 11.2.16 , with an equation of

$$E_{cell} = 0.027 + 0.0303 \log [Ca^{2+}]$$

Substituting the sample's cell potential gives the concentration of Ca^{2+} as 2.17×10^{-4} M. Note that the slope of the calibration curve, which is 0.0303, is slightly larger than its ideal value of 0.05916/2 = 0.02958; this is not unusual and is one reason for using multiple standards.

> One reason that it is not unusual to find that the experimental slope deviates from its ideal value of 0.05916/n is that this ideal value assumes that the temperature is 25°C.

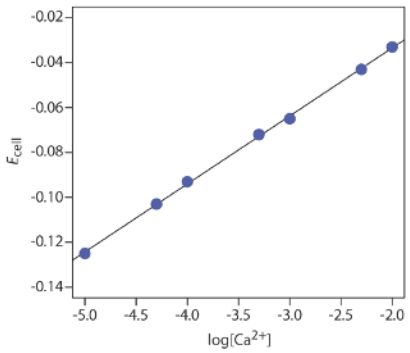


Figure 11.2.16 . Calibration curve for the data in Example 11.2.8 .

Quantitative Analysis Using the Method of Standard Additions

Another approach to calibrating a potentiometric electrode is the method of standard additions. First, we transfer a sample with a volume of V_{samp} and an analyte concentration of C_{samp} into a beaker and measure the potential, $(E_{cell})_{samp}$. Next, we make a standard addition by adding to the sample a small volume, V_{std}, of a standard that contains a known concentration of analyte, C_{std}, and measure the potential, (E_{cell})std. If V_{std} is significantly smaller than V_{samp}, then we can safely ignore the change in the sample's matrix and assume that the analyte's activity coefficient is constant. Example 11.2.9 demonstrates how we can use a one-point standard addition to determine the concentration of analyte in a sample.

To review the method of standard additions, see Chapter 5.3.

Example 11.2.9

The concentration of Ca^{2+} in a sample of sea water is determined using a Ca ion-selective electrode and a one-point standard addition. A 10.00-mL sample is transferred to a 100-mL volumetric flask and diluted to volume. A 50.00-mL aliquot of the sample is placed in a beaker with the Ca ISE and a reference electrode, and the potential is measured as –0.05290 V. After adding a 1.00-mL aliquot of a 5.00×10^{-2} M standard solution of Ca^{2+} the potential is –0.04417 V. What is the concentration of Ca^{2+} in the sample of sea water?

Solution

To begin, we write the Nernst equation before and after adding the standard addition. The cell potential for the sample is

$$(E_{cell})_{samp} = K + \frac{0.05916}{2} \log C_{samp}$$

and that following the standard addition is

$$(E_{cell})_{std} = K + \frac{0.05916}{2} \log \left\{ \frac{V_{samp}}{V_{tot}} C_{samp} + \frac{V_{std}}{V_{tot}} C_{std} \right\}$$

where V_{tot} is the total volume (V_{samp} + V_{std}) after the standard addition. Subtracting the first equation from the second equation gives

$$\Delta E = (E_{cell})_{std} - (E_{cell})_{samp} = \frac{0.05916}{2} \log \left\{ \frac{V_{samp}}{V_{tot}} C_{samp} + \frac{V_{std}}{V_{tot}} C_{std} \right\} - \frac{0.05916}{2} \log C_{samp}$$

Rearranging this equation leaves us with

$$\frac{2\Delta E_{cell}}{0.05916} = \log \left\{ \frac{V_{samp}}{V_{tot}} + \frac{V_{std} C_{std}}{V_{tot} C_{samp}} \right\}$$

Substituting known values for ΔE, V_{samp}, V_{std}, V_{tot} and C_{std},

$$\frac{2\times\{-0.04417-(-0.05290)\}}{0.05916} = \log\left\{\frac{50.00\text{ mL}}{51.00\text{ mL}} + \frac{(1.00\text{ mL})(5.00\times10^{-2}\text{M})}{(51.00\text{ mL})C_{\text{samp}}}\right\}$$

$$0.2951 = \log\left\{0.9804 + \frac{9.804\times10^{-4}}{C_{\text{samp}}}\right\}$$

and taking the inverse log of both sides gives

$$1.973 = 0.9804 + \frac{9.804 \times 10^{-4}}{C_{\text{samp}}}$$

Finally, solving for C_{samp} gives the concentration of Ca^{2+} as $\mathbf{9.88 \times 10^{-4}}$ M. Because we diluted the original sample of seawater by a factor of 10, the concentration of Ca^{2+} in the seawater sample is $\mathbf{9.88 \times 10^{-3}}$ M.

Free Ions Versus Complexed Ions

Most potentiometric electrodes are selective toward the free, uncomplexed form of the analyte, and do not respond to any of the analyte's complexed forms. This selectivity provides potentiometric electrodes with a significant advantage over other quantitative methods of analysis if we need to determine the concentration of free ions. For example, calcium is present in urine both as free Ca^{2+} ions and as protein-bound Ca^{2+} ions. If we analyze a urine sample using atomic absorption spectroscopy, the signal is proportional to the total concentration of Ca^{2+} because both free and bound calcium are atomized. Analyzing urine with a Ca^{2+} ISE, however, gives a signal that is a function of only free Ca^{2+} ions because the protein-bound Ca^{2+} can not interact with the electrode's membrane.

The best way to appreciate the theoretical and the practical details discussed in this section is to carefully examine a typical analytical method. Although each method is unique, the following description of the determination of F^- in toothpaste provides an instructive example of a typical procedure. The description here is based on Kennedy, J. H. *Analytical Chemistry—Practice*, Harcourt Brace Jaovanovich: San Diego, 1984, p. 117–118.

Representative Method 11.2.1: Determination of Fluoride in Toothpaste

Description of the Method

The concentration of fluoride in toothpastes that contains soluble F^- is determined with a F^- ion-selective electrode using a calibration curve prepared with external standards. Although the F^- ISE is very selective (only OH^- with a K_{F^-/OH^-} of 0.1 is a significant interferent), Fe^{3+} and Al^{3+} interfere with the analysis because they form soluble fluoride complexes that do not interact with the ion-selective electrode's membrane. This interference is minimized by reacting any Fe^{3+} and Al^{3+} with a suitable complexing agent.

Procedure

Prepare 1 L of a standard solution of 1.00% w/v SnF_2 and transfer it to a plastic bottle for storage. Using this solution, prepare 100 mL each of standards that contain 0.32%, 0.36%, 0.40%, 0.44% and 0.48% w/v SnF_2, adding 400 mg of malic acid to each solution as a stabilizer. Transfer the standards to plastic bottles for storage. Prepare a total ionic strength adjustment buffer (TISAB) by mixing 500 mL of water, 57 mL of glacial acetic acid, 58 g of NaCl, and 4 g of disodium DCTA (*trans*-1,2-cyclohexanetetraacetic acid) in a 1-L beaker, stirring until dissolved. Cool the beaker in a water bath and add 5 M NaOH until the pH is between 5–5.5. Transfer the contents of the beaker to a 1-L volumetric flask and dilute to volume. Prepare each external standard by placing approximately 1 g of a fluoride-free toothpaste, 30 mL of distilled water, and 1.00 mL of standard into a 50-mL plastic beaker and mix vigorously for two min with a stir bar. Quantitatively transfer the resulting suspension to a 100-mL volumetric flask along with 50 mL of TISAB and dilute to volume with distilled water. Store the entire external standard in a 250-mL plastic beaker until you are ready to measure the potential. Prepare toothpaste samples by obtaining an approximately 1-g portion and treating in the same manner as the standards. Measure the cell potential for the external standards and the samples using a F^- ion-selective electrode and an appropriate reference electrode. When measuring the potential, stir the solution and allow two to three minutes to reach a stable potential. Report the concentration of F^- in the toothpaste %w/w SnF_2.

Questions

1. The total ionic strength adjustment buffer serves several purposes in this procedure. Identify these purposes.

The composition of the TISAB has three purposes:

(a) The high concentration of NaCl (the final solutions are approximately 1 M NaCl) ensures that the ionic strength of each external standard and each sample is essentially identical. Because the activity coefficient for fluoride is the same in all solutions, we can write the Nernst equation in terms of fluoride's concentration instead of its activity.

(b) The combination of glacial acetic acid and NaOH creates an acetic acid/acetate buffer of pH 5–5.5. As shown in Figure 11.2.17 , the pH of this buffer is high enough to ensure that the predominate form of fluoride is F^- instead of HF. This pH also is sufficiently acidic that it avoids an interference from OH^- (see Example 4.2.8)).

(c) DCTA is added as a complexing agent for Fe^{3+} or Al^{3+}, preventing the formation of $\mathbf{FeF_6^{3-}}$ or $\mathbf{AlF_6^{3-}}$.

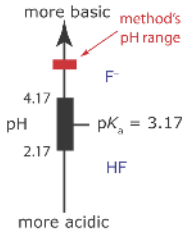


Figure 11.2.17 . Ladder diagram for HF/F^-. Maintaining a pH greater than 4.2 ensures that the only significant form of fluoride is F^-.

2. Why is a fluoride-free toothpaste added to the standard solutions?

Adding a fluoride-free toothpaste protects against any unaccounted for matrix effects that might influence the ion-selective electrode's response. This assumes, of course, that the matrices of the two toothpastes are otherwise similar.

3. The procedure specifies that the standards and the sample should be stored in plastic containers. Why is it a bad idea to store the solutions in glass containers?

The fluoride ion is capable of reacting with glass to form SiF_4.

4. Suppose your calibration curve has a slope of –57.98 mV for each 10-fold change in the concentration of F^-. The ideal slope from the Nernst equation is –59.16 mV per 10-fold change in concentration. What effect does this have on the quantitative analysis for fluoride in toothpaste?

No effect at all! This is why we prepare a calibration curve using multiple standards.

Measurement of pH

With the availability of inexpensive glass pH electrodes and pH meters, the determination of pH is one of the most common quantitative analytical measurements. The potentiometric determination of pH, however, is not without complications, several of which we discuss in this section.

One complication is confusion over the meaning of pH [Kristensen, H. B.; Saloman, A.; Kokholm, G. *Anal. Chem.* **1991**, *63*, 885A–891A]. The conventional definition of pH in most general chemistry textbooks is

$$\mathbf{pH = -\log [H^+]} \tag{4.2.17}$$

As we now know, pH actually is a measure of the activity of H^+.

$$\mathbf{pH = -\log a_{H^+}} \tag{4.2.18}$$

> Try this experiment—find several general chemistry textbooks and look up *pH* in each textbook's index. Turn to the appropriate pages and see how it is defined. Next, look up *activity* or *activity coefficient* in each textbook's index and see if these terms are indexed.

Equation 4.2.17 only approximates the true pH. If we calculate the pH of 0.1 M HCl using Equation 4.2.17, we obtain a value of 1.00; the solution's actual pH, as defined by Equation 4.2.18, is 1.1 [Hawkes, S. J. *J. Chem. Educ.* **1994**, *71*, 747–749]. The activity and the concentration of H^+ are not the same in 0.1 M HCl because the activity coefficient for H^+ is not 1.00 in this matrix. Figure 11.2.18 shows a more colorful demonstration of the difference between activity and concentration.

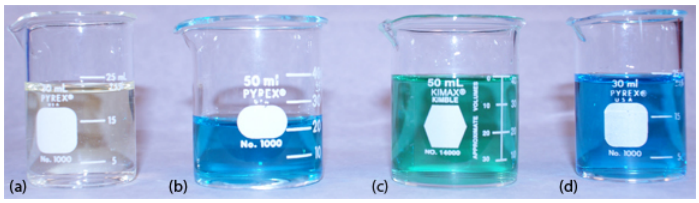


Figure 11.2.18 . A demonstration of the difference between activity and concentration using the indicator methyl green. The indicator is pale yellow in its acid form (beaker a: 1.0 M HCl) and is blue in its base form (beaker d: H_2O). In 10 mM HCl the indicator is in its base form (beaker b: 20 mL of 10 mM HCl with 3 drops of methyl green). Adding 20 mL of 5 M LiCl to this solution shifts the indicator's color to green (beaker c); although the concentration of HCl is cut in half to 5 mM, the activity of H^+ has increased as evidenced by the green color that is intermediate between the indicator's pale yellow, acid form and its blue, base form. The demonstration shown here is adapted from McCarty, C. G.; Vitz, E. "pH Paradoxes: Demonstrating That It Is Not True That pH ≡ –log[H^+]," *J. Chem. Educ.* **2006**, *83*, 752–757. This paper provides several additional demonstrations that illustrate the difference between concentration and activity.

A second complication in measuring pH is the uncertainty in the relationship between potential and activity. For a glass membrane electrode, the cell potential, $(E_{cell})_{samp}$, for a sample of unknown pH is

$$(E_{cell})_{samp} = K - \frac{RT}{F}\ln\frac{1}{a_{H^+}} = K - \frac{2.303RT}{F}pH_{samp} \tag{4.2.19}$$

where K includes the potential of the reference electrode, the asymmetry potential of the glass membrane, and any junction potentials in the electrochemical cell. All the contributions to K are subject to uncertainty, and may change from day-to-day, as well as from electrode-to-electrode. For this reason, before using a pH electrode we calibrate it using a standard buffer of known pH. The cell potential for the standard, $(E_{cell})_{std}$, is

$$(E_{ccll})_{std} = K - \frac{2.303RT}{F}pH_{std} \tag{4.2.20}$$

where pH_{std} is the standard's pH. Subtracting Equation 4.2.20 from Equation 4.2.19 and solving for pH_{samp} gives

$$pH_{samp} = pH_{std} - \frac{\{(E_{cell})_{samp} - (E_{cell})_{std}\}F}{2.303RT} \tag{4.2.21}$$

which is the operational definition of pH adopted by the International Union of Pure and Applied Chemistry [Covington, A. K.; Bates, R. B.; Durst, R. A. *Pure & Appl. Chem.* **1985**, *57*, 531–542].

Calibrating a pH electrode presents a third complication because we need a standard with an accurately known activity for H^+. Table 11.2.6 provides pH values for several primary standard buffer solutions accepted by the National Institute of Standards and Technology.

Table 11.2.6 . pH Values for Selected NIST Primary Standard Buffers

temp (°C)	saturated (at 25°C) KHC_4H4O_7 (tartrate)	0.05 m $KH_2C_6H_5O_7$ (citrate)	0.05 m $KHC_8H_4O_4$ (phthlate)	0.025 m KH_2PO_4, 0.025 m $NaHPO_4$	0.008695 m KH_2PO_4, 0.03043 m Na_2HPO_4	0.01 m $Na_4B_4O_7$	0.025 m $NaHCO_3$, 0.025 m Na_2CO_3
0	—	3.863	4.003	6.984	7.534	9.464	10.317
5	—	3.840	3.999	6.951	7.500	9.395	10.245
10	—	3.820	3.998	6.923	7.472	9.332	10.179
15	—	3.802	3.999	6.900	7.448	9.276	10.118
20	—	3.788	4.002	6.881	7.429	9.225	10.062
25	3.557	3.776	4.008	6.865	7.413	9.180	10.012
30	3.552	3.766	4.015	6.854	7.400	9.139	9.966
35	3.549	3.759	4.024	6.844	7.389	9.012	9.925
40	3.547	3.753	4.035	6.838	7.380	9.068	9.889
45	3.547	3.750	4.047	6.834	7.373	9.038	9.856
50	3.549	3.749	4.060	6.833	7.367	9.011	9.828

Source: Values taken from Bates, R. G. *Determination of pH: Theory and Practice*, 2nd ed. Wiley: New York, 1973. See also Buck, R. P., et. al."Measurement of pH. Definition, Standards, and Procedures," *Pure. Appl. Chem.* **2002**, *74*, 2169–2200. All concentrations are molal (m).

To standardize a pH electrode using two buffers, choose one near a pH of 7 and one that is more acidic or basic depending on your sample's expected pH. Rinse your pH electrode in deionized water, blot it dry with a laboratory wipe, and place it in the buffer with the pH closest to 7. Swirl the pH electrode and allow it to equilibrate until you obtain a stable reading. Adjust the "Standardize" or "Calibrate" knob until the meter displays the correct pH. Rinse and dry the electrode, and place it in the second buffer. After the electrode equilibrates, adjust the "Slope" or "Temperature" knob until the meter displays the correct pH.

Some pH meters can compensate for a change in temperature. To use this feature, place a temperature probe in the sample and connect it to the pH meter. Adjust the "Temperature" knob to the solution's temperature and calibrate the pH meter using the "Calibrate" and "Slope" controls. As you are using the pH electrode, the pH meter compensates for any change in the sample's temperature by adjusting the slope of the calibration curve using a Nernstian response of $2.303RT/F$.

Clinical Applications

Because of their selectivity for analytes in complex matricies, ion-selective electrodes are important sensors for clinical samples. The most common analytes are electrolytes, such as Na^+, K^+, Ca^{2+}, H^+, and Cl^-, and dissolved gases such as CO_2. For extracellular fluids, such as blood and urine, the analysis can be made *in vitro*. An *in situ* analysis, however, requires a much smaller electrode that we can insert directly into a cell. Liquid-based membrane microelectrodes with tip diameters smaller than 1 μm are constructed by heating and drawing out a hard-glass capillary tube with an initial diameter of approximately 1–2 mm (Figure 11.2.19). The microelectrode's tip is made hydrophobic by dipping into a solution of dichlorodimethyl silane, and an inner solution appropriate for the analyte and a Ag/AgCl wire reference electrode are placed within the microelectrode. The microelectrode is dipped into a solution of the liquid complexing agent, which through capillary action draws a small volume of the liquid complexing agent into the tip. Potentiometric microelectrodes have been developed for a number of clinically important analytes, including H^+, K^+, Na^+, Ca^{2+}, Cl^-, and I^- [Bakker, E.; Pretsch, E. *Trends Anal. Chem.* **2008**, *27*, 612–618].

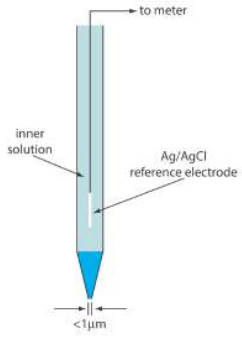


Figure 11.2.19 . Schematic diagram of a liquid-based ion-selective microelectrode.

Environmental Applications

Although ion-selective electrodes are used in environmental analysis, their application is not as widespread as in clinical analysis. Although standard potentiometric methods are available for the analysis of CN^-, F^-, NH_3, and NO_3^- in water and wastewater, other analytical methods generally provide better detection limits. One potential advantage of an ion-selective electrode is the ability to incorporate it into a flow cell for the continuous monitoring of wastewater streams.

Potentiometric Titrations

One method for determining the equivalence point of an acid–base titration is to use a pH electrode to monitor the change in pH during the titration. A potentiometric determination of the equivalence point is possible for acid–base, complexation, redox, and precipitation titrations, as well as for titrations in aqueous and nonaqueous solvents. Acid–base, complexation, and precipitation potentiometric titrations usually are monitored with an ion-selective electrode that responds the analyte, although an electrode that responds to the titrant or a reaction product also can be used. A redox electrode, such as a Pt wire, and a reference electrode are used for potentiometric redox titrations. More details about potentiometric titrations are found in Chapter 9.

Evaluation

Scale of Operation

The working range for most ion-selective electrodes is from a maximum concentration of 0.1–1 M to a minimum concentration of $10^{-5} - 10^{-11}$ M [(a) Bakker, E.; Pretsch, E. *Anal. Chem.* **2002**, *74*, 420A–426A; (b) Bakker, E.; Pretsch, E. *Trends Anal. Chem.* **2005**, *24*, 199–207]. This broad working range extends from major analytes to ultratrace analytes, and is significantly greater than many other analytical techniques. To use a conventional ion-selective electrode we need a minimum sample volume of several mL (a macro sample). Microelectrodes, such as the one shown in Figure 11.2.19 , are used with an ultramicro sample, although care is needed to ensure that the sample is representative of the original sample.

Accuracy

The accuracy of a potentiometric analysis is limited by the error in measuring E_{cell}. Several factors contribute to this measurement error, including the contribution to the potential from interfering ions, the finite current that passes through the cell while we measure the potential, differences between the analyte's activity coefficient in the samples and the standard solutions, and junction potentials. We can limit the effect of an interfering ion by including a separation step before the potentiometric analysis. Modern high impedance potentiometers minimize the amount of current that passes through the electrochemical cell. Finally, we can minimize the errors due to activity coefficients and junction potentials by matching the matrix of the standards to that of the sample. Even in the best circumstances, however, a difference of approximately ±1 mV for samples with equal concentrations of analyte is not unusual.

We can evaluate the effect of uncertainty on the accuracy of a potentiometric measurement by using a propagation of uncertainty. For a membrane ion-selective electrode the general expression for potential is

$$E_{cell} = K + \frac{RT}{zF}\ln[A]$$

where z is the analyte's, A, charge. From Table 4.3.1 in Chapter 4, the uncertainty in the cell potential, ΔE_{cell} is

$$\triangle E_{\text{cell}} = \frac{RT}{zF} \times \frac{\Delta[A]}{[A]}$$

Rearranging and multiplying through by 100 gives the percent relative error in concentration as

$$\%\ \text{relative error} = \frac{\Delta[A]}{[A]} \times 100 = \frac{\triangle E_{\text{cell}}}{RT/zF} \times 100 \tag{4.2.22}$$

The relative error in concentration, therefore, is a function of the measurement error for the electrode's potential, ΔE_{cell}, and the analyte's charge. Table 11.2.7 provides representative values for ions with charges of ±1 and ±2 at a temperature of 25ºC. Accuracies of 1–5% for monovalent ions and 2–10% for divalent ions are typical. Although Equation 4.2.22 applies to membrane electrodes, we can use if for a metallic electrode by replacing *z* with *n*.

Table 11.2.7 . Relationship Between the Uncertainty in Measuring E_{cell} and the Relative Error in the Analyte's Concentration

$\Delta E_{\text{cell}}(\pm\ \text{mV})$	% relative error when $z = \pm 1$	% relative error when $z = \pm 2$
0.1	±0.4	±0.8
0.5	±1.9	±3.9
1.0	±3.0	±7.8
1.5	±5.8	±11.1
2.0	±7.8	±15.6

Precision

Precision in potentiometry is limited by variations in temperature and the sensitivity of the potentiometer. Under most conditions—and when using a simple, general-purpose potentiometer—we can measure the potential with a repeatability of ±0.1 mV. Using Table 11.2.7 , this corresponds to an uncertainty of ±0.4% for monovalent analytes and ±0.8% for divalent analytes. The reproducibility of potentiometric measurements is about a factor of ten poorer.

Sensitivity

The sensitivity of a potentiometric analysis is determined by the term *RT*/*nF* or *RT*/*zF* in the Nernst equation. Sensitivity is best for smaller values of *n* or *z*.

Selectivity

As described earlier, most ion-selective electrodes respond to more than one analyte; the selectivity for the analyte, however, often is significantly greater than the sensitivity for the interfering ions. The manufacturer of an ion-selective usually provides an ISE's selectivity coefficients, which allows us to determine whether a potentiometric analysis is feasible for a given sample.

Time, Cost, and Equipment

In comparison to other techniques, potentiometry provides a rapid, relatively low-cost means for analyzing samples. The limiting factor when analyzing a large number of samples is the need to rinse the electrode between samples. The use of inexpensive, disposable ion-selective electrodes can increase a lab's sample throughput. Figure 11.2.20 shows one example of a disposable ISE for Ag^+ [Tymecki, L.; Zwierkowska, E.; Głąb, S.; Koncki, R. *Sens. Actuators B* **2003**, *96*, 482–488]. Commercial instruments for measuring pH or potential are available in a variety of price ranges, and includes portable models for use in the field.

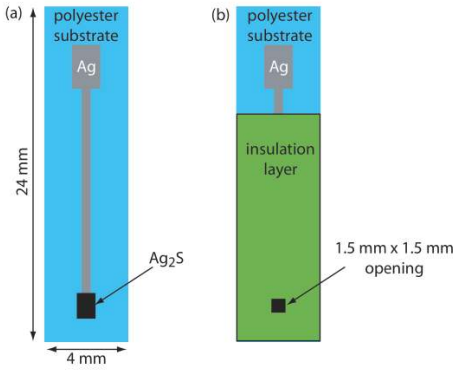


Figure 11.2.20 . Schematic diagram of a disposable ion-selective electrode created by screen-printing. In (a) a thin film of conducting silver is printed on a polyester substrate and a film of Ag_2S overlaid near the bottom. In (b) an insulation layer with a small opening is layered on top exposes a portion of the Ag_2S membrane that is immersed in the sample. The top of the polyester substrate remains uncoated, which allows us to connect the electrode to a potentiometer through the Ag film. The small inset shows the electrode's actual size.

This page titled 4.2: Potentiometric Methods is shared under a CC BY-NC-SA 4.0 license and was authored, remixed, and/or curated by David Harvey.

- **11.2: Potentiometric Methods** by David Harvey is licensed CC BY-NC-SA 4.0.

4.3: Coulometric Methods

In a potentiometric method of analysis we determine an analyte's concentration by measuring the potential of an electrochemical cell under static conditions in which no current flows and the concentrations of species in the electrochemical cell remain fixed. Dynamic techniques, in which current passes through the electrochemical cell and concentrations change, also are important electrochemical methods of analysis. In this section we consider coulometry. Voltammetry and amperometry are covered in Chapter 11.4.

Coulometry is based on an exhaustive electrolysis of the analyte. By exhaustive we mean that the analyte is oxidized or reduced completely at the working electrode, or that it reacts completely with a reagent generated at the working electrode. There are two forms of coulometry: ***controlled-potential coulometry***, in which we apply a constant potential to the electrochemical cell, and ***controlled-current coulometry***, in which we pass a constant current through the electrochemical cell.

During an electrolysis, the total charge, Q, in coulombs, that passes through the electrochemical cell is proportional to the absolute amount of analyte by ***Faraday's law***

$$Q = nFN_A \tag{4.3.1}$$

where n is the number of electrons per mole of analyte, F is Faraday's constant (96 487 C mol^{-1}), and N_A is the moles of analyte. A coulomb is equivalent to an A•sec; thus, for a constant current, i, the total charge is

$$Q = it_e \tag{4.3.2}$$

where t_e is the electrolysis time. If the current varies with time, as it does in controlled-potential coulometry, then the total charge is

$$Q = \int_0^{t_e} i(t)dt \tag{4.3.3}$$

In coulometry, we monitor current as a function of time and use either Equation 4.3.2 or Equation 4.3.3 to calculate Q. Knowing the total charge, we then use Equation 4.3.1 to determine the moles of analyte. To obtain an accurate value for N_A, all the current must oxidize or reduce the analyte; that is, coulometry requires 100% ***current efficiency*** or an accurate measurement of the current efficiency using a standard.

> Current efficiency is the percentage of current that actually leads to the analyte's oxidation or reduction.

Controlled-Potential Coulometry

The easiest way to ensure 100% current efficiency is to hold the working electrode at a constant potential where the analyte is oxidized or reduced completely and where no potential interfering species are oxidized or reduced. As electrolysis progresses, the analyte's concentration and the current decrease. The resulting current-versus-time profile for controlled-potential coulometry is shown in Figure 11.3.1 . Integrating the area under the curve (Equation 4.3.3) from t = 0 to $t = t_e$ gives the total charge. In this section we consider the experimental parameters and instrumentation needed to develop a controlled-potential coulometric method of analysis.

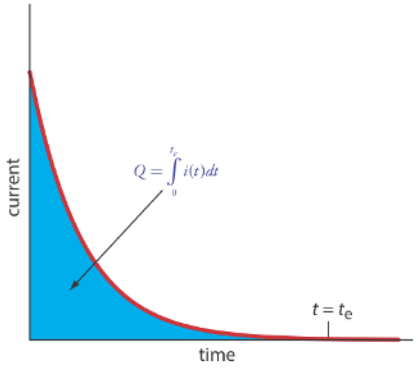


Figure 11.3.1 . Current versus time for a controlled-potential coulometric analysis. The measured current is shown by the red curve. The integrated area under the curve, shown in blue, is the total charge.

Selecting a Constant Potential

To understand how an appropriate potential for the working electrode is selected, let's develop a constant-potential coulometric method for Cu^{2+} based on its reduction to copper metal at a Pt working electrode.

$$Cu^{2+}(aq) + 2e^- \rightleftharpoons Cu(s) \tag{4.3.4}$$

Figure 11.3.2 shows a ladder diagram for an aqueous solution of Cu^{2+}. From the ladder diagram we know that reaction 4.3.4 is favored when the working electrode's potential is more negative than +0.342 V versus the standard hydrogen electrode. To ensure a 100% current efficiency, however, the potential must be sufficiently more positive than +0.000 V so that the reduction of H_3O^+ to H_2 does not contribute significantly to the total current flowing through the electrochemical cell.

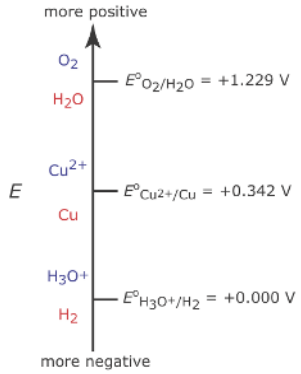


Figure 11.3.2 . Ladder diagram for an aqueous solution of Cu^{2+} showing steps for the reductions of O_2 to H_2O, of Cu^{2+} to Cu, and of H_3O^+ to H_2. For each step, the oxidized species is in blue and the reduced species is in red

We can use the Nernst equation for reaction 4.3.4 to estimate the minimum potential for quantitatively reducing Cu^{2+}.

$$E = E^\circ_{Cu^{2+}/Cu} - \frac{0.05916}{2} \log \frac{1}{[Cu^{2+}]} \tag{4.3.5}$$

So why are we using the concentration of Cu^{2+} in Equation 4.3.5 instead of its activity? In potentiometry we use activity because we use E_{cell} to determine the analyte's concentration. Here we use the Nernst equation to help us select an appropriate potential. Once we identify a potential, we can adjust its value as needed to ensure a quantitative reduction of Cu^{2+}. In addition, in coulometry the analyte's concentration is given by the total charge, not the applied potential.

If we define a quantitative electrolysis as one in which we reduce 99.99% of $^{Cu2+}$ to Cu, then the concentration of Cu^{2+} at t_e is

$$[Cu^{2+}]_{t_e} = 0.0001 \times [Cu^{2+}]_0 \tag{4.3.6}$$

where $[Cu^{2+}]_0$ is the initial concentration of Cu^{2+} in the sample. Substituting Equation 4.3.6 into Equation 4.3.5 allows us to calculate the desired potential.

$$E = E^\circ_{Cu^{2+}/Cu} - \frac{0.05916}{2} \log \frac{1}{0.0001 \times [Cu^{2+}]}$$

If the initial concentration of Cu^{2+} is 1.00×10^{-4} M, for example, then the working electrode's potential must be more negative than +0.105 V to quantitatively reduce Cu^{2+} to Cu. Note that at this potential H_3O^+ is not reduced to H_2, maintaining 100% current efficiency.

> Many controlled-potential coulometric methods for Cu^{2+} use a potential that is negative relative to the standard hydrogen electrode—see, for example, Rechnitz, G. A. *Controlled-Potential Analysis*, Macmillan: New York, 1963, p.49. Based on the ladder diagram in Figure 11.3.2 you might expect that applying a potential <0.000 V will partially reduce H_3O^+ to H_2, resulting in a current efficiency that is less than 100%. The reason we can use such a negative potential is that the reaction rate for the reduction of H_3O^+ to H_2 is very slow at a Pt electrode. This results in a significant ***overpotential***—the need to apply a potential more positive or a more negative than that predicted by thermodynamics—which shifts E^o for the H_3O^+/H_2 redox couple to a more negative value.

Minimizing Electrolysis Time

In controlled-potential coulometry, as shown in Figure 11.3.1 , the current decreases over time. As a result, the rate of electrolysis —recall from Chapter 11.1 that current is a measure of rate—becomes slower and an exhaustive electrolysis of the analyte may require a long time. Because time is an important consideration when designing an analytical method, we need to consider the factors that affect the analysis time.

We can approximate the current's change as a function of time in Figure 11.3.1 as an exponential decay; thus, the current at time t is

$$i_t = i_0 e^{-kt} \tag{4.3.7}$$

where i_0 is the current at $t = 0$ and k is a rate constant that is directly proportional to the area of the working electrode and the rate of stirring, and that is inversely proportional to the volume of solution. For an exhaustive electrolysis in which we oxidize or reduce 99.99% of the analyte, the current at the end of the analysis, t_e, is

$$i_{t_e} \leq 0.0001 \times i_0 \tag{4.3.8}$$

Substituting Equation 4.3.8 into Equation 4.3.7 and solving for t_e gives the minimum time for an exhaustive electrolysis as

$$t_e = -\frac{1}{k} \times \ln(0.0001) = \frac{9.21}{k}$$

From this equation we see that a larger value for k reduces the analysis time. For this reason we usually carry out a controlled-potential coulometric analysis in a small volume electrochemical cell, using an electrode with a large surface area, and with a high stirring rate. A quantitative electrolysis typically requires approximately 30–60 min, although shorter or longer times are possible.

Instrumentation

A three-electrode potentiostat is used to set the potential in controlled-potential coulometry (see Figure 11.1.5). The working electrodes is usually one of two types: a cylindrical Pt electrode manufactured from platinum-gauze (Figure 11.3.3), or a Hg pool electrode. The large overpotential for the reduction of H_3O^+ at Hg makes it the electrode of choice for an analyte that requires a negative potential. For example, a potential more negative than –1 V versus the SHE is feasible at a Hg electrode—but not at a Pt electrode—even in a very acidic solution. Because mercury is easy to oxidize, it is less useful if we need to maintain a potential that is positive with respect to the SHE. Platinum is the working electrode of choice when we need to apply a positive potential.



Figure 11.3.3 . Example of a cylindrical Pt-gauze electrode used in controlled-potential coulometry. The electrode shown here has a diameter of 13 mm and a height of 48 mm, and was fashioned from Pt wire with a diameter of approximately 0.15 mm. The electrode's surface has 360 openings/cm^2 and a total surface area of approximately 40 cm^2.

The auxiliary electrode, which often is a Pt wire, is separated by a salt bridge from the analytical solution. This is necessary to prevent the electrolysis products generated at the auxiliary electrode from reacting with the analyte and interfering in the analysis. A saturated calomel or Ag/AgCl electrode serves as the reference electrode.

The other essential need for controlled-potential coulometry is a means for determining the total charge. One method is to monitor the current as a function of time and determine the area under the curve, as shown in Figure 11.3.1 . Modern instruments use electronic integration to monitor charge as a function of time. The total charge at the end of the electrolysis is read directly from a digital readout.

Electrogravimetry

If the product of controlled-potential coulometry forms a deposit on the working electrode, then we can use the change in the electrode's mass as the analytical signal. For example, if we apply a potential that reduces Cu^{2+} to Cu at a Pt working electrode, the difference in the electrode's mass before and after electrolysis is a direct measurement of the amount of copper in the sample. As we learned in Chapter 8, we call an analytical technique that uses mass as a signal a gravimetric technique; thus, we call this ***electrogravimetry***.

Controlled-Current Coulometry

A second approach to coulometry is to use a constant current in place of a constant potential, which results in the current-versus-time profile shown in Figure 11.3.4 . Controlled-current coulometry has two advantages over controlled-potential coulometry. First, the analysis time is shorter because the current does not decrease over time. A typical analysis time for controlled-current coulometry is less than 10 min, compared to approximately 30–60 min for controlled-potential coulometry. Second, because the total charge simply is the product of current and time (Equation **4.3.2**), there is no need to integrate the current-time curve in Figure 11.3.4 .

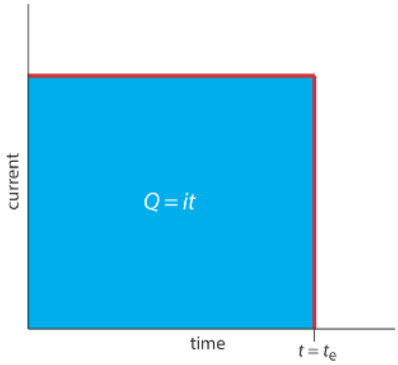


Figure 11.3.4 . Current versus time for a controlled-current coulometric analysis. The measured current is shown by the red curve. The integrated area under the curve, shown in blue, is the total charge.

Using a constant current presents us with two important experimental problems. First, during electrolysis the analyte's concentration—and, therefore, the current that results from its oxidation or reduction—decreases continuously. To maintain a

constant current we must allow the potential to change until another oxidation reaction or reduction reaction occurs at the working electrode. Unless we design the system carefully, this secondary reaction results in a current efficiency that is less than 100%. The second problem is that we need a method to determine when the analyte's electrolysis is complete. As shown in Figure 11.3.1 , in a controlled-potential coulometric analysis we know that electrolysis is complete when the current reaches zero, or when it reaches a constant background or residual current. In a controlled-current coulometric analysis, however, current continues to flow even when the analyte's electrolysis is complete. A suitable method for determining the reaction's endpoint, t_e, is needed.

Maintaining Current Efficiency

To illustrate why a change in the working electrode's potential may result in a current efficiency of less than 100%, let's consider the coulometric analysis for Fe^{2+} based on its oxidation to Fe^{3+} at a Pt working electrode in 1 M H_2SO_4.

$$Fe^{2+}(aq) \rightleftharpoons Fe^{3+}(aq) + e^-$$

Figure 11.3.5 shows the ladder diagram for this system. At the beginning of the analysis, the potential of the working electrode remains nearly constant at a level near its initial value.

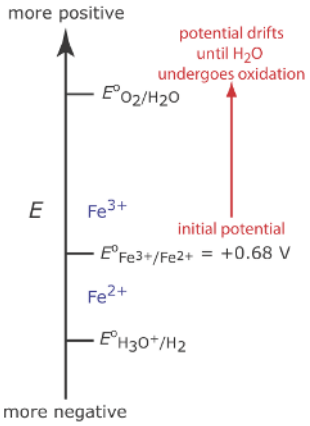


Figure 11.3.5 . Ladder diagram for the constant-current coulometric analysis of Fe^{2+}. The red arrow and text shows how the potential drifts to more positive values, decreasing the current efficiency.

As the concentration of Fe^{2+} decreases and the concentration of Fe^{3+} increases, the working electrode's potential shifts toward more positive values until the oxidation of H_2O begins.

$$2H_2O(l) \rightleftharpoons O_2(g) + 4H^+(aq) + 4e^-$$

Because a portion of the total current comes from the oxidation of H_2O, the current efficiency for the analysis is less than 100% and we cannot use Equation 4.3.1 to determine the amount of Fe^{2+} in the sample.

Although we cannot prevent the potential from drifting until another species undergoes oxidation, we can maintain a 100% current efficiency if the product of that secondary oxidation reaction both rapidly and quantitatively reacts with the remaining Fe^{2+}. To accomplish this we add an excess of Ce^{3+} to the analytical solution. As shown in Figure 11.3.6 , when the potential of the working electrode shifts to a more positive potential, Ce^{3+} begins to oxidize to Ce^{4+}

$$Ce^{3+}(aq) \rightleftharpoons Ce^{4+}(aq) + e^- \qquad (4.3.9)$$

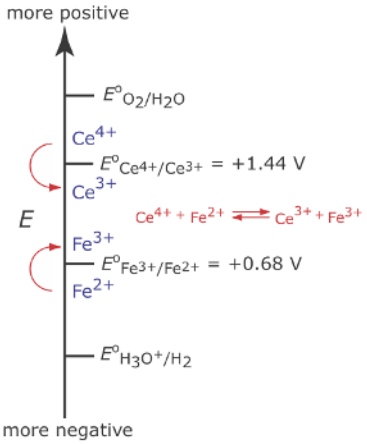


Figure 11.3.6 . Ladder diagram for the constant-current coulometric analysis of Fe^{2+} in the presence of a Ce^{3+} mediator. As the potential drifts to more positive values, we eventually reach a potential where Ce^{3+} undergoes oxidation. Because Ce^{4+}, the product of the oxidation of Ce^{3+}, reacts with Fe^{2+}, we maintain current efficiency.

The Ce^{4+} that forms at the working electrode rapidly mixes with the solution where it reacts with any available Fe^{2+}.

$$Ce^{4+}(aq) + Fe^{2+}(aq) \rightleftharpoons Ce^{3+}(aq) + Fe^{3+}(aq) \tag{4.3.10}$$

Combining reaction 4.3.9 and reaction 4.3.10 shows that the net reaction is the oxidation of Fe^{2+} to Fe^{3+}

$$Fe^{2+}(aq) \rightleftharpoons Fe^{3+}(aq) + e^-$$

which maintains a current efficiency of 100%. A species used to maintain 100% current efficiency is called a ***mediator***.

Endpoint Determination

Adding a mediator solves the problem of maintaining 100% current efficiency, but it does not solve the problem of determining when the analyte's electrolysis is complete. Using the analysis for Fe^{2+} in Figure 11.3.6 , when the oxidation of Fe^{2+} is complete current continues to flow from the oxidation of Ce^{3+}, and, eventually, the oxidation of H_2O. What we need is a signal that tells us when no more Fe^{2+} is present in the solution.

For our purposes, it is convenient to treat a controlled-current coulometric analysis as a reaction between the analyte, Fe^{2+}, and the mediator, Ce^{3+}, as shown by reaction 4.3.10. This reaction is identical to a redox titration; thus, we can use the end points for a redox titration—visual indicators and potentiometric or conductometric measurements—to signal the end of a controlled-current coulometric analysis. For example, ferroin provides a useful visual endpoint for the Ce^{3+} mediated coulometric analysis for Fe^{2+}, changing color from red to blue when the electrolysis of Fe^{2+} is complete.

> Reaction 4.3.10 is the same reaction we used in Chapter 9 to develop our understanding of redox titrimetry.

Instrumentation

Controlled-current coulometry normally is carried out using a two-electrode galvanostat, which consists of a working electrode and a counter electrode. The working electrode—often a simple Pt electrode—also is called the generator electrode since it is where the mediator reacts to generate the species that reacts with the analyte. If necessary, the counter electrode is isolated from the analytical solution by a salt bridge or a porous frit to prevent its electrolysis products from reacting with the analyte. Alternatively, we can generate the oxidizing agent or the reducing agent externally, and allow it to flow into the analytical solution. Figure 11.3.7 shows one simple method for accomplishing this. A solution that contains the mediator flows into a small-volume electrochemical cell with the products exiting through separate tubes. Depending upon the analyte, the oxidizing agent or the reducing reagent is delivered to the analytical solution. For example, we can generate Ce^{4+} using an aqueous solution of Ce^{3+}, directing the Ce^{4+} that forms at the anode to our sample.

Figure 11.1.4 shows an example of a manual galvanostat. Although a modern galvanostat uses very different circuitry, you can use Figure 11.1.4 and the accompanying discussion to understand how we can use the working electrode and the counter electrode to control the current. Figure 11.1.4 includes an optional reference electrode, but its presence or absence is not important if we are not interested in monitoring the working electrode's potential.

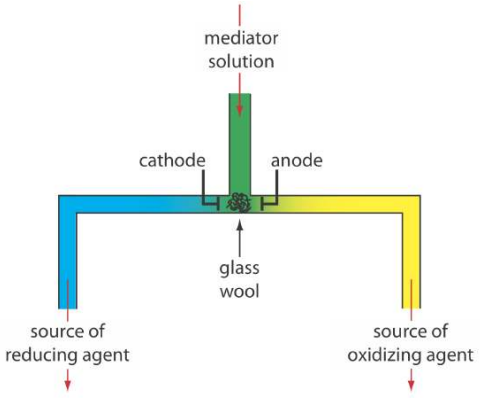


Figure 11.3.7 . One example of a device for the external generation of oxidizing agents and reducing agents for controlled-current coulometry. A solution containing the mediator flows into a small-volume electrochemical cell. The resulting oxidation products, which form at the anode, flow to the right and serve as an oxidizing agent. Reduction at the cathode generates a reducing agent.

There are two other crucial needs for controlled-current coulometry: an accurate clock for measuring the electrolysis time, t_e, and a switch for starting and stopping the electrolysis. An analog clock can record time to the nearest ±0.01 s, but the need to stop and start the electrolysis as we approach the endpoint may result in an overall uncertainty of ±0.1 s. A digital clock allows for a more accurate measurement of time, with an overall uncertainty of ±1 ms. The switch must control both the current and the clock so that we can make an accurate determination of the electrolysis time.

Coulometric Titrations

A controlled-current coulometric method sometimes is called a coulometric titration because of its similarity to a conventional titration. For example, in the controlled-current coulometric analysis for Fe^{2+} using a Ce^{3+} mediator, the oxidation of Fe^{2+} by Ce^{4+} (reaction 4.3.10) is identical to the reaction in a redox titration.

There are other similarities between controlled-current coulometry and titrimetry. If we combine Equation 4.3.1 and Equation 4.3.2 and solve for the moles of analyte, N_A, we obtain the following equation.

$$N_A = \frac{i}{nF} \times t_e \tag{4.3.11}$$

Compare Equation 4.3.11 to the relationship between the moles of analyte, N_A, and the moles of titrant, N_T, in a titration

$$N_A = N_T = M_T \times V_T$$

where M_T and V_T are the titrant's molarity and the volume of titrant at the end point. In constant-current coulometry, the current source is equivalent to the titrant and the value of that current is analogous to the titrant's molarity. Electrolysis time is analogous to the volume of titrant, and t_e is equivalent to the a titration's end point. Finally, the switch for starting and stopping the electrolysis serves the same function as a buret's stopcock.

For simplicity, we assumed above that the stoichiometry between the analyte and titrant is 1:1. The assumption, however, is not important and does not effect our observation of the similarity between controlled-current coulometry and a titration.

Quantitative Applications

Coulometry is used for the quantitative analysis of both inorganic and organic analytes. Examples of controlled-potential and controlled-current coulometric methods are discussed in the following two sections.

Controlled-Potential Coulometry

The majority of controlled-potential coulometric analyses involve the determination of inorganic cations and anions, including trace metals and halides ions. Table 11.3.1 summarizes several of these methods.

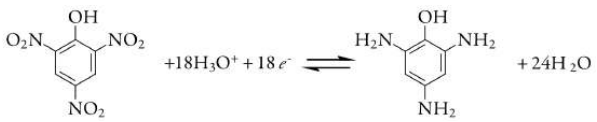
Table 11.3.1 . Representative Controlled-Potential Coulometric Analyses for Inorganic Ions

analyte	electrolytic reaction	electrode
antimony	$Sb(III) + 3e^- \rightleftharpoons Sb$	Pt
arsenic	$As(III) \rightleftharpoons As(V) + 2e^-$	Pt
cadmium	$Cd(II) + 2e^- \rightleftharpoons Cd$	Pt or Hg
cobalt	$Co(II) + 2e^- \rightleftharpoons Co$	Pt or Hg
copper	$Cu(II) + 2e^- \rightleftharpoons Cu$	Pt or Hg
halides (X^-)	$Ag + X^- \rightleftharpoons AgX + e^-$	Ag
iron	$Fe(II) \rightleftharpoons Fe(III) + e^-$	Pt
lead	$Pb(II) + 2e^- \rightleftharpoons Pb$	Pt or Hg
nickel	$Ni(II) + 2e^- \rightleftharpoons Ni$	Pt or Hg
plutonium	$Pu(III) \rightleftharpoons Pu(IV) + e^-$	Pt
silver	$Ag(I) + 1e^- \rightleftharpoons Ag$	Pt
tin	$Sn(II) + 2e^- \rightleftharpoons Sn$	Pt
uranium	$U(VI) + 2e^- \rightleftharpoons U(IV)$	Pt or Hg
zinc	$Zn(II) + 2e^- \rightleftharpoons Zn$	Pt or Hg

Source: Rechnitz, G. A. *Controlled-Potential Analysis*, Macmillan: New York, 1963.
Electrolytic reactions are written in terms of the change in the analyte's oxidation state. The actual species in solution depends on the analyte.

The ability to control selectivity by adjusting the working electrode's potential makes controlled-potential coulometry particularly useful for the analysis of alloys. For example, we can determine the composition of an alloy that contains Ag, Bi, Cd, and Sb by dissolving the sample and placing it in a matrix of 0.2 M H_2SO_4 along with a Pt working electrode and a Pt counter electrode. If we apply a constant potential of +0.40 V versus the SCE, Ag(I) deposits on the electrode as Ag and the other metal ions remain in solution. When electrolysis is complete, we use the total charge to determine the amount of silver in the alloy. Next, we shift the working electrode's potential to –0.08 V versus the SCE, depositing Bi on the working electrode. When the coulometric analysis for bismuth is complete, we determine antimony by shifting the working electrode's potential to –0.33 V versus the SCE, depositing Sb. Finally, we determine cadmium following its electrodeposition on the working electrode at a potential of –0.80 V versus the SCE.

We also can use controlled-potential coulometry for the quantitative analysis of organic compounds, although the number of applications is significantly less than that for inorganic analytes. One example is the six-electron reduction of a nitro group, $–NO_2$, to a primary amine, $–NH_2$, at a mercury electrode. Solutions of picric acid—also known as 2,4,6-trinitrophenol, or TNP, a close relative of TNT—is analyzed by reducing it to triaminophenol.



Another example is the successive reduction of trichloroacetate to dichloroacetate, and of dichloroacetate to monochloroacetate

$$Cl_3CCOO^-(aq) + H_3O^+(aq) + 2e^- \rightleftharpoons Cl_2HCCOO^-(aq) + Cl^-(aq) + H_2O(l)$$

$$Cl_2HCCOO^-(aq) + H_3O^+(aq) + 2e^- \rightleftharpoons ClH_2CCOO^-(aq) + Cl^-(aq) + H_2O(l)$$

We can analyze a mixture of trichloroacetate and dichloroacetate by selecting an initial potential where only the more easily reduced trichloroacetate reacts. When its electrolysis is complete, we can reduce dichloroacetate by adjusting the potential to a more negative potential. The total charge for the first electrolysis gives the amount of trichloroacetate, and the difference in total charge between the first electrolysis and the second electrolysis gives the amount of dichloroacetate.

Controlled-Current Coulometry (Coulometric Titrations)

The use of a mediator makes a coulometric titration a more versatile analytical technique than controlled-potential coulometry. For example, the direct oxidation or reduction of a protein at a working electrode is difficult if the protein's active redox site lies deep within its structure. A coulometric titration of the protein is possible, however, if we use the oxidation or reduction of a mediator to produce a solution species that reacts with the protein. Table 11.3.2 summarizes several controlled-current coulometric methods based on a redox reaction using a mediator.

Table 11.3.2 . Representative Examples of Coulometric Redox Titrations

mediator	electrochemically generated reagent and reaction	representative application
Ag^+	$\mathbf{Ag^+} \rightleftharpoons \mathbf{Ag^{2+}} + e^-$	$\mathbf{H_2C_2O_4}(aq) + 2\mathbf{Ag^{2+}}(aq) + 2H_2O(l) \rightleftharpoons 2CO_2(g) + 2\mathbf{Ag^+}(aq) + 2H_3O^+(aq)$
Br^-	$2\mathbf{Br^-} \rightleftharpoons \mathbf{Br_2} + 2e^-$	$\mathbf{H_2S}(aq) + \mathbf{Br_2}(aq) + 2H_2O(l) \rightleftharpoons S(s) + 2\mathbf{Br^-}(aq) + 2H_3O^+(aq)$
Ce^{3+}	$\mathbf{Ce^{3+}} \rightleftharpoons \mathbf{Ce^{4+}} + e^-$	$\mathbf{Fe(CN)_6^{4-}}(aq) + \mathbf{Ce^{4+}}(aq) \rightleftharpoons \mathbf{Fe(CN)_6^{3-}}(aq) + \mathbf{Ce^{3+}}(aq)$
Cl^-	$2\mathbf{Cl^-} \rightleftharpoons \mathbf{Cl_2} + 2e^-$	$\mathbf{Ti(I)}(aq) + \mathbf{Cl_2}(aq) \rightleftharpoons \mathbf{Ti(III)}(aq) + 2\mathbf{Cl^-}(aq)$
Fe^{3+}	$\mathbf{Fe^{3+}} + e^- \rightleftharpoons \mathbf{Fe^{2+}}$	$\mathbf{Cr_2O_7^{2-}}(aq) + 6\mathbf{Fe^{2+}}(aq) + 14H_3O^+(aq) \rightleftharpoons 2\mathbf{Cr^{3+}}(aq) + 6\mathbf{Fe^{3+}}(aq) + 21H_2O(l)$
I^-	$3\mathbf{I^-} \rightleftharpoons \mathbf{I_3^-} + 2e^-$	$2\mathbf{S_2O_3^{2-}}(aq) + \mathbf{I_3^-}(aq) \rightleftharpoons \mathbf{S_4O_6^{2-}}(aq) + 3\mathbf{I^-}(aq)$
Mn^{2+}	$\mathbf{Mn^{2+}} \rightleftharpoons \mathbf{Mn^{3+}} + e^-$	$\mathbf{As(III)}(aq) + 2\mathbf{Mn^{3+}}(aq) \rightleftharpoons \mathbf{As(V)}(aq) + 2\mathbf{Mn^{2+}}(aq)$

Note: The electrochemically generated reagent and the analyte are shown in **bold**.

For an analyte that is not easy to oxidize or reduce, we can complete a coulometric titration by coupling a mediator's oxidation or reduction to an acid–base, precipitation, or complexation reaction that involves the analyte. For example, if we use H_2O as a mediator, we can generate H_3O^+at the anode

$$6H_2O(l) \rightleftharpoons 4H_3O^+(aq) + O_2(g) + 4e^-$$

and generate OH^- at the cathode.

$$2H_2O(l) + 2e^- \rightleftharpoons 2OH^-(aq) + H_2(g)$$

If we carry out the oxidation or reduction of H_2O using the generator cell in Figure 11.3.7 , then we can selectively dispense H_3O^+ or OH^- into a solution that contains the analyte. The resulting reaction is identical to that in an acid–base titration. Coulometric acid–base titrations have been used for the analysis of strong and weak acids and bases, in both aqueous and non-aqueous matrices. Table 11.3.3 summarizes several examples of coulometric titrations that involve acid–base, complexation, and precipitation reactions.

Table 11.3.3 . Representative Coulometric Titrations Using Acid–Base, Complexation, and Precipitation Reactions

type of reaction	mediator	electrochemically generated reagent and reaction	representative application
acid-base	H_2O	$\mathbf{6H_2O \rightleftharpoons 4H_3O^+ + O_2 + e^-}$	$\mathbf{OH^-}(aq) + \mathbf{H_3O^+}(aq) \rightleftharpoons 2\mathbf{H_2O}(l)$
acid-base	H_2O	$\mathbf{2H_2O + 2e^- \rightleftharpoons 2OH^- + H_2}$	$\mathbf{H_3O^+}(aq) + \mathbf{OH^-}(aq) \rightleftharpoons 2\mathbf{H_2O}(l)$
complexation	$HgNH_3Y^{2-}$ (Y = EDTA)	$\mathbf{HgNH_3Y^{2-} + NH_4^+ + 2e^- \rightleftharpoons HY^{3-} + Hg + 2NH_3}$	$\mathbf{Ca^{2+}}(aq) + \mathbf{HY^{3-}}(aq) + \mathbf{H_2O}(l) \rightleftharpoons \mathbf{CaY^{2-}}(aq) + \mathbf{H_3O^+}(aq)$
complexation	Ag	$\mathbf{Ag \rightleftharpoons Ag^+ + e^-}$	$\mathbf{I^-}(aq) + \mathbf{Ag^+}(aq) \rightleftharpoons \mathbf{AgI}(s)$
precipitation	Hg	$\mathbf{2Hg \rightleftharpoons Hg_2^{2+} + 2e^-}$	$\mathbf{2Cl^-}(aq) + \mathbf{Hg_2^{2+}}(aq) \rightleftharpoons \mathbf{Hg_2Cl_2}(s)$
precipitation	$\mathbf{Fe(CN)_6^{3-}}$	$\mathbf{Fe(CN)_6^{3-} + e^- \rightleftharpoons Fe(CN)_6^{4-}}$	$\mathbf{3Zn^{2+}}(aq) + \mathbf{K^+}(aq) + 2\mathbf{Fe(CN)_6^{4-}}(aq) \rightleftharpoons \mathbf{K_2Zn_3[Fe(CN)_6]_2}(s)$

Note: The electrochemically generated reagent and the analyte are shown in **bold**.

In comparison to a conventional titration, a coulometric titration has two important advantages. The first advantage is that electrochemically generating a titrant allows us to use a reagent that is unstable. Although we cannot prepare and store a solution of a highly reactive reagent, such as Ag^{2+} or Mn^{3+}, we can generate them electrochemically and use them in a coulometric titration. Second, because it is relatively easy to measure a small quantity of charge, we can use a coulometric titration to determine an analyte whose concentration is too small for a conventional titration.

Quantitative Calculations

The absolute amount of analyte in a coulometric analysis is determined using Faraday's law (Equation 4.3.1) and the total charge given by Equation 4.3.2 or by Equation 4.3.3. The following example shows the calculations for a typical coulometric analysis.

Example 11.3.1

To determine the purity of a sample of $Na_2S_2O_3$, a sample is titrated coulometrically using I^- as a mediator and $\mathbf{I_3^-}$ as the titrant. A sample weighing 0.1342 g is transferred to a 100-mL volumetric flask and diluted to volume with distilled water. A 10.00-mL portion is transferred to an electrochemical cell along with 25 mL of 1 M KI, 75 mL of a pH 7.0 phosphate buffer, and several drops of a starch indicator solution. Electrolysis at a constant current of 36.45 mA requires 221.8 s to reach the starch indicator endpoint. Determine the sample's purity.

Solution

As shown in Table 11.3.2 , the coulometric titration of $\mathbf{S_2O_3^{2-}}$ with $\mathbf{I_3^-}$ is

$$2\mathbf{S_2O_3^{2-}}(aq) + \mathbf{I_3^-}(aq) \rightleftharpoons \mathbf{S_4O_6^{2-}}(aq) + 3\mathbf{I^-}(aq)$$

The oxidation of $\mathbf{S_2O_3^{2-}}$ to $\mathbf{S_4O_6^{2-}}$ requires one electron per $\mathbf{S_2O_3^{2-}}$ (n = 1). Combining Equation 4.3.1 and Equation 4.3.2, and solving for the moles and grams of $Na_2S_2O_3$ gives

$$N_A = \frac{it_e}{nF} = \frac{(0.03645\ \text{A})(221.8\ \text{s})}{\left(\frac{1\ \text{mol}\ e^-}{\text{mol}\ \text{Na}_2\text{S}_2\text{O}_3}\right)\left(\frac{96487\ \text{C}}{\text{mol}\ e^-}\right)} = 8.379 \times 10^{-5}\ \text{mol}\ \text{Na}_2\text{S}_2\text{O}_3$$

This is the amount of $Na_2S_2O_3$ in a 10.00-mL portion of a 100-mL sample; thus, there are 0.1325 grams of $Na_2S_2O_3$ in the original sample. The sample's purity, therefore, is

$$\frac{0.1325\ \text{g}\ \text{Na}_2\text{S}_2\text{O}_3}{0.1342\ \text{g sample}} \times 100 = 98.73\%\ \text{w/w}\ \text{Na}_2\text{S}_2\text{O}_3$$

Note that for Equation 4.3.1 and Equation 4.3.2 it does not matter whether $S_2O_3^{2-}$ is oxidized at the working electrode or is oxidized by I_3^-.

Exercise 11.3.1

To analyze a brass alloy, a 0.442-g sample is dissolved in acid and diluted to volume in a 500-mL volumetric flask. Electrolysis of a 10.00-mL sample at –0.3 V versus a SCE reduces Cu^{2+} to Cu, requiring a total charge of 16.11 C. Adjusting the potential to –0.6 V versus a SCE and completing the electrolysis requires 0.442 C to reduce Pb^{2+} to Pb. Report the %w/w Cu and Pb in the alloy.

Answer

The reduction of Cu^{2+} to Cu requires two electrons per mole of Cu (n = 2). Using Equation 4.3.1, we calculate the moles and the grams of Cu in the portion of sample being analyzed.

$$N_{Cu} = \frac{Q}{nF} = \frac{16.11\text{ C}}{\frac{2\text{ mol } e^-}{\text{mol Cu}} \times \frac{96487\text{ C}}{\text{mol } e^-}} = 8.348 \times 10^{-5}\text{ mol Cu}$$

$$8.348 \times 10^{-5}\text{ mol Cu} \times \frac{63.55\text{ g Cu}}{\text{mol Cu}} = 5.301 \times 10^{-3}\text{ g Cu}$$

This is the Cu from a 10.00 mL portion of a 500.0 mL sample; thus, the %/w/w copper in the original sample of brass is

$$\frac{5.301 \times 10^{-3}\text{ g Cu} \times \frac{500.0\text{ mL}}{10.00\text{ mL}}}{0.442\text{ g sample}} \times 100 = 60.0\%\text{ w/w Cu}$$

For lead, we follow the same process; thus

$$N_{Pb} = \frac{Q}{nF} = \frac{0.422\text{ C}}{\frac{2\text{ mol } e^-}{\text{mol Pb}} \times \frac{96487\text{ C}}{\text{mol } e^-}} = 2.19 \times 10^{-6}\text{ mol Pb}$$

$$2.19 \times 10^{-6}\text{ mol Pb} \times \frac{207.2\text{ g Pb}}{\text{mol Cu}} = 4.53 \times 10^{-4}\text{ g Pb}$$

$$\frac{4.53 \times 10^{-4}\text{ g Pb} \times \frac{500.0\text{ mL}}{10.00\text{ mL}}}{0.442\text{ g sample}} \times 100 = 5.12\%\text{ w/w Pb}$$

Representative Method 11.3.1: Determination of Dichromate by a Coulometric Redox Titration

The best way to appreciate the theoretical and the practical details discussed in this section is to carefully examine a typical analytical method. Although each method is unique, the following description of the determination of $Cr_2O_7^{2-}$ provides an instructive example of a typical procedure. The description here is based on Bassett, J.; Denney, R. C.; Jeffery, G. H.; Mendham, J. *Vogel's Textbook of Quantitative Inorganic Analysis*, Longman: London, 1978, p. 559–560.

Description of the Method

Thee concentration of $Cr_2O_7^{2-}$ in a sample is determined by a coulometric redox titration using Fe^{3+} as a mediator and electrogenerated Fe^{3+} as the titrant. The endpoint of the titration is determined potentiometrically.

Procedure

The electrochemical cell consists of a Pt working electrode and a Pt counter electrode placed in separate cells connected by a porous glass disk. Fill the counter electrode's cell with 0.2 M Na_2SO_4, keeping the level above that of the solution in the working electrode's cell. Connect a platinum electrode and a tungsten electrode to a potentiometer so that you can measure the working electrode's potential during the analysis. Prepare a mediator solution of approximately 0.3 M $NH_4Fe(SO_4)_2$. Add 5.00 mL of sample, 2 mL of 9 M H_2SO_4, and 10–25 mL of the mediator solution to the working electrode's cell, and add distilled water as needed to cover the electrodes. Bubble pure N_2 through the solution for 15 min to remove any O_2 that is present. Maintain the flow of N_2 during the electrolysis, turning if off momentarily when measuring the potential. Stir the solution using a magnetic stir bar.

Adjust the current to 15–50 mA and begin the titration. Periodically stop the titration and measure the potential. Construct a titration curve of potential versus time and determine the time needed to reach the equivalence point.

Questions

1. Is the platinum working electrode the cathode or the anode?

   Reduction of Fe^{3+} to Fe^{2+} occurs at the working electrode, making it the cathode in this electrochemical cell.

2. Why is it necessary to remove dissolved oxygen by bubbling N_2 through the solution?

   Any dissolved O_2 will oxidize Fe^{2+} back to Fe^{3+}, as shown by the following reaction.

   $$4Fe^{2+}(aq) + O_2 + 4H_3O^+(aq) \rightleftharpoons 4Fe^{3+}(aq) + 6H_2O(l)$$

   To maintain current efficiency, all the Fe^{2+} must react with $Cr_2O_7^{2-}$. The reaction of Fe^{2+} with O_2 means that more of the Fe^{3+} mediator is needed, increasing the time to reach the titration's endpoint. As a result, we report the presence of too much $Cr_2O_7^{2-}$.

3. What is the effect on the analysis if the $NH_4Fe(SO_4)_2$ is contaminated with trace amounts of Fe^{2+}? How can you compensate for this source of Fe^{2+}?

   There are two sources of Fe^{2+}: that generated from the mediator and that present as an impurity. Because the total amount of Fe^{2+} that reacts with $Cr_2O_7^{2-}$ remains unchanged, less Fe^{2+} is needed from the mediator. This decreases the time needed to reach the titration's end point. Because the apparent current efficiency is greater than 100%, the reported concentration of $Cr_2O_7^{2-}$ is too small. We can remove trace amount of Fe^{2+} from the mediator's solution by adding H_2O_2 and heating at 50–70°C until the evolution of O_2 ceases, converting the Fe^{2+} to Fe^{3+}. Alternatively, we can complete a blank titration to correct for any impurities of Fe^{2+} in the mediator.

4. Why is the level of solution in the counter electrode's cell maintained above the solution level in the working electrode's cell?

   This prevents the solution that contains the analyte from entering the counter electrode's cell. The oxidation of H_2O at the counter electrode produces O_2, which can react with the Fe^{2+} generated at the working electrode or the Cr^{3+} resulting from the reaction of Fe^{2+} and $Cr_2O_7^{2-}$. In either case, the result is a positive determinate error.

Characterization Applications

One useful application of coulometry is determining the number of electrons involved in a redox reaction. To make the determination, we complete a controlled-potential coulometric analysis using a known amount of a pure compound. The total charge at the end of the electrolysis is used to determine the value of *n* using Faraday's law (Equation 4.3.1).

Example 11.3.2

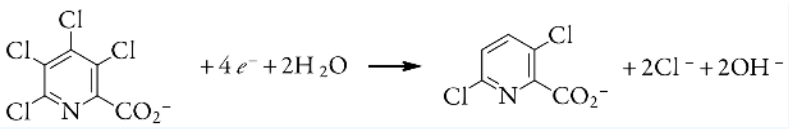
A 0.3619-g sample of tetrachloropicolinic acid, $C_6HNO_2Cl_4$, is dissolved in distilled water, transferred to a 1000-mL volumetric flask, and diluted to volume. An exhaustive controlled-potential electrolysis of a 10.00-mL portion of this solution at a spongy silver cathode requires 5.374 C of charge. What is the value of *n* for this reduction reaction?

Solution

The 10.00-mL portion of sample contains 3.619 mg, or 1.39×10^{-5} mol of tetrachloropicolinic acid. Solving Equation 4.3.1 for *n* and making appropriate substitutions gives

$$n = \frac{Q}{FN_A} = \frac{5.374\ \text{C}}{(96478\ \text{C/mol}\ e^-)\,(1.39 \times 10^{-5}\ \text{mol}\ C_6HNO_2Cl_4)} = 4.01\ \text{mol e}^-/\text{mol}\ C_6HNO_2Cl_4$$

Thus, reducing a molecule of tetrachloropicolinic acid requires four electrons. The overall reaction, which results in the selective formation of 3,6-dichloropicolinic acid, is



Evaluation

Scale of Operation

A coulometric method of analysis can analyze a small absolute amount of an analyte. In controlled-current coulometry, for example, the moles of analyte consumed during an exhaustive electrolysis is given by Equation 4.3.11. An electrolysis using a constant current of 100 μA for 100 s, for example, consumes only 1×10^{-7} mol of analyte if $n = 1$. For an analyte with a molecular weight of 100 g/mol, 1×10^{-7} mol of analyte corresponds to only 10 μg. The concentration of analyte in the electrochemical cell, however, must be sufficient to allow an accurate determination of the endpoint. When using a visual end point, the smallest concentration of analyte that can be determined by a coulometric titration is approximately 10^{-4} M. As is the case for a conventional titration, a coulometric titration using a visual end point is limited to major and minor analytes. A coulometric titration to a preset potentiometric endpoint is feasible even if the analyte's concentration is as small as 10^{-7} M, extending the analysis to trace analytes [Curran, D. J. "Constant-Current Coulometry," in Kissinger, P. T.; Heineman, W. R., eds., *Laboratory Techniques in Electroanalytical Chemistry*, Marcel Dekker Inc.: New York, 1984, pp. 539–568].

Accuracy

In controlled-current coulometry, accuracy is determined by the accuracy with which we can measure current and time, and by the accuracy with which we can identify the end point. The maximum measurement errors for current and time are about ±0.01% and ±0.1%, respectively. The maximum end point error for a coulometric titration is at least as good as that for a conventional titration, and is often better when using small quantities of reagents. Together, these measurement errors suggest that an accuracy of 0.1%–0.3% is feasible. The limiting factor in many analyses, therefore, is current efficiency. A current efficiency of more than 99.5% is fairly routine, and it often exceeds 99.9%.

In controlled-potential coulometry, accuracy is determined by current efficiency and by the determination of charge. If the sample is free of interferents that are easier to oxidize or reduce than the analyte, a current efficiency of greater than 99.9% is routine. When an interferent is present, it can often be eliminated by applying a potential where the exhaustive electrolysis of the interferents is possible without the simultaneous electrolysis of the analyte. Once the interferent is removed the potential is switched to a level where electrolysis of the analyte is feasible. The limiting factor in the accuracy of many controlled-potential coulometric methods of analysis is the determination of charge. With electronic integrators the total charge is determined with an accuracy of better than 0.5%.

If we cannot obtain an acceptable current efficiency, an electrogravimetric analysis is possible if the analyte—and only the analyte—forms a solid deposit on the working electrode. In this case the working electrode is weighed before beginning the electrolysis and reweighed when the electrolysis is complete. The difference in the electrode's weight gives the analyte's mass.

Precision

Precision is determined by the uncertainties in measuring current, time, and the endpoint in controlled-current coulometry or the charge in controlled-potential coulometry. Precisions of ±0.1–0.3% are obtained routinely in coulometric titrations, and precisions of ±0.5% are typical for controlled-potential coulometry.

Sensitivity

For a coulometric method of analysis, the calibration sensitivity is equivalent to nF in Equation 4.3.1. In general, a coulometric method is more sensitive if the analyte's oxidation or reduction involves a larger value of n.

Selectivity

Selectivity in controlled-potential and controlled-current coulometry is improved by adjusting solution conditions and by selecting the electrolysis potential. In controlled-potential coulometry, the potential is fixed by the potentiostat, and in controlled-current coulometry the potential is determined by the redox reaction with the mediator. In either case, the ability to control the electrolysis

potential affords some measure of selectivity. By adjusting pH or by adding a complexing agent, it is possible to shift the potential at which an analyte or interferent undergoes oxidation or reduction. For example, the standard-state reduction potential for Zn^{2+} is –0.762 V versus the SHE. If we add a solution of NH_3, forming $Zn(NH_3)_4^{2+}$, the standard state potential shifts to –1.04 V. This provides an additional means for controlling selectivity when an analyte and an interferent undergo electrolysis at similar potentials.

Time, Cost, and Equipment

Controlled-potential coulometry is a relatively time consuming analysis, with a typical analysis requiring 30–60 min. Coulometric titrations, on the other hand, require only a few minutes, and are easy to adapt to an automated analysis. Commercial instrumentation for both controlled-potential and controlled-current coulometry is available, and is relatively inexpensive. Low cost potentiostats and constant-current sources are available for approximately $1000.

This page titled 4.3: Coulometric Methods is shared under a CC BY-NC-SA 4.0 license and was authored, remixed, and/or curated by David Harvey.

- **11.3: Coulometric Methods** by David Harvey is licensed CC BY-NC-SA 4.0.

4.4: Voltammetric and Amperometric Methods

In ***voltammetry*** we apply a time-dependent potential to an electrochemical cell and measure the resulting current as a function of that potential. We call the resulting plot of current versus applied potential a ***voltammogram***, and it is the electrochemical equivalent of a spectrum in spectroscopy, providing quantitative and qualitative information about the species involved in the oxidation or reduction reaction [Maloy, J. T. *J. Chem. Educ.* **1983**, *60*, 285–289]. The earliest voltammetric technique is polarography, developed by Jaroslav Heyrovsky in the early 1920s—an achievement for which he was awarded the Nobel Prize in Chemistry in 1959. Since then, many different forms of voltammetry have been developed, a few of which are highlighted in Figure 11.1.6. Before examining these techniques and their applications in more detail, we must first consider the basic experimental design for voltammetry and the factors influencing the shape of the resulting voltammogram.

> For an on-line introduction to much of the material in this section, see Analytical Electrochemistry: The Basic Concepts by Richard S. Kelly, a resource that is part of the Analytical Sciences Digital Library.

Voltammetric Measurements

Although early voltammetric methods used only two electrodes, a modern voltammeter makes use of a three-electrode potentiostat, such as that shown in Figure 11.1.5. In voltammetry we apply a time-dependent potential excitation signal to the working electrode—changing its potential relative to the fixed potential of the reference electrode—and measure the current that flows between the working electrode and the auxiliary electrode. The auxiliary electrode generally is a platinum wire and the reference electrode usually is a SCE or a Ag/AgCl electrode.

> Figure 11.1.5 shows an example of a manual three-electrode potentiostat. Although a modern potentiostat uses very different circuitry, you can use Figure 11.1.5 and the accompanying discussion to understand how we can control the potential of working electrode and measure the resulting current.

For the working electrode we can choose among several different materials, including mercury, platinum, gold, silver, and carbon. The earliest voltammetric techniques used a mercury working electrode. Because mercury is a liquid, the working electrode usual is a drop suspended from the end of a capillary tube. In the ***hanging mercury drop electrode***, or HMDE, we extrude the drop of Hg by rotating a micrometer screw that pushes the mercury from a reservoir through a narrow capillary tube (Figure 11.4.1 a).

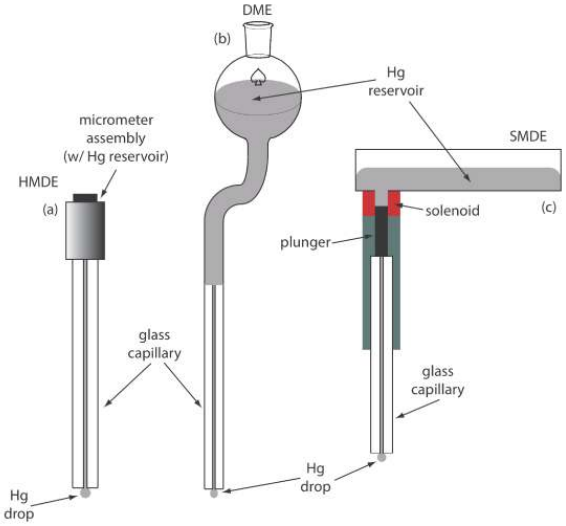


Figure 11.4.1 . Three examples of mercury electrodes: (a) hanging mercury drop electrode, or HMDE; (b) dropping mercury electrode, or DME; and (c) static mercury drop electrode, or SMDE.

In the ***dropping mercury electrode***, or DME, mercury drops form at the end of the capillary tube as a result of gravity (Figure 11.4.1 b). Unlike the HMDE, the mercury drop of a DME grows continuously—as mercury flows from the reservoir under the

influence of gravity—and has a finite lifetime of several seconds. At the end of its lifetime the mercury drop is dislodged, either manually or on its own, and is replaced by a new drop. The ***static mercury drop electrode***, or SMDE, uses a solenoid driven plunger to control the flow of mercury (Figure 11.4.1 c). Activation of the solenoid momentarily lifts the plunger, allowing mercury to flow through the capillary, forming a single, hanging Hg drop. Repeated activation of the solenoid produces a series of Hg drops. In this way the SMDE may be used as either a HMDE or a DME. There is one additional type of mercury electrode: the ***mercury film electrode***. A solid electrode—typically carbon, platinum, or gold—is placed in a solution of Hg^{2+} and held at a potential where the reduction of Hg^{2+} to Hg is favorable, depositing a thin film of mercury on the solid electrode's surface.

Mercury has several advantages as a working electrode. Perhaps its most important advantage is its high overpotential for the reduction of H_3O^+ to H_2, which makes accessible potentials as negative as –1 V versus the SCE in acidic solutions and –2 V versus the SCE in basic solutions (Figure 11.4.2). A species such as Zn^{2+}, which is difficult to reduce at other electrodes without simultaneously reducing H_3O^+, is easy to reduce at a mercury working electrode. Other advantages include the ability of metals to dissolve in mercury—which results in the formation of an ***amalgam***—and the ability to renew the surface of the electrode by extruding a new drop. One limitation to mercury as a working electrode is the ease with which it is oxidized. Depending on the solvent, a mercury electrode can not be used at potentials more positive than approximately –0.3 V to +0.4 V versus the SCE.

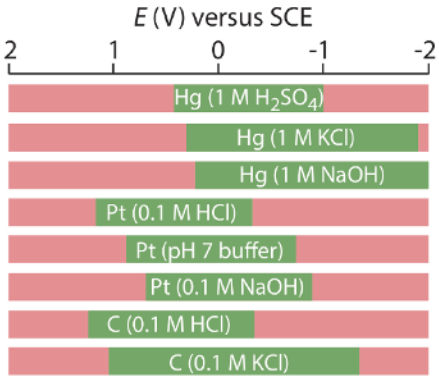


Figure 11.4.2 . Approximate potential windows for mercury, platinum, and carbon (graphite) electrodes in acidic, neutral, and basic aqueous solvents. The useful potential windows are shown in green; potentials in red result in the oxidation or the reduction of the solvent or the electrode. Complied from Adams, R. N. *Electrochemistry at Solid Electrodes*, Marcel Dekker, Inc.: New York, 1969 and Bard, A. J.; Faulkner, L. R. *Electro- chemical Methods*, John Wiley & Sons: New York, 1980.

Solid electrodes constructed using platinum, gold, silver, or carbon may be used over a range of potentials, including potentials that are negative and positive with respect to the SCE (Figure 11.4.2). For example, the potential window for a Pt electrode extends from approximately +1.2 V to –0.2 V versus the SCE in acidic solutions, and from +0.7 V to –1 V versus the SCE in basic solutions. A solid electrode can replace a mercury electrode for many voltammetric analyses that require negative potentials, and is the electrode of choice at more positive potentials. Except for the carbon paste electrode, a solid electrode is fashioned into a disk and sealed into the end of an inert support with an electrical lead (Figure 11.4.3). The carbon paste electrode is made by filling the cavity at the end of the inert support with a paste that consists of carbon particles and a viscous oil. Solid electrodes are not without problems, the most important of which is the ease with which the electrode's surface is altered by the adsorption of a solution species or by the formation of an oxide layer. For this reason a solid electrode needs frequent reconditioning, either by applying an appropriate potential or by polishing.

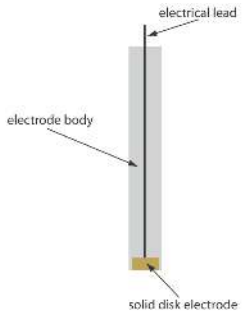


Figure 11.4.3 . Schematic showing a solid electrode. The electrode is fashioned into a disk and sealed in the end of an inert polymer support along with an electrical lead.

A typical arrangement for a voltammetric electrochemical cell is shown in Figure 11.4.4 . In addition to the working electrode, the reference electrode, and the auxiliary electrode, the cell also includes a N_2-purge line for removing dissolved O_2, and an optional stir bar. Electrochemical cells are available in a variety of sizes, allowing the analysis of solution volumes ranging from more than 100 mL to as small as 50 μL.

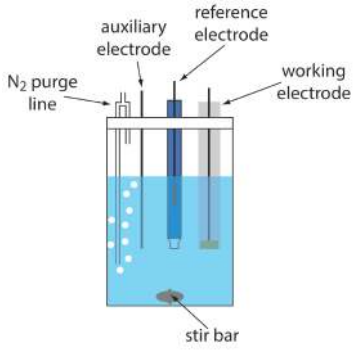


Figure 11.4.4 . Typical electrochemical cell for voltammetry.

Current In Voltammetry

When we oxidize an analyte at the working electrode, the resulting electrons pass through the potentiostat to the auxiliary electrode, reducing the solvent or some other component of the solution matrix. If we reduce the analyte at the working electrode, the current flows from the auxiliary electrode to the cathode. In either case, the current from the redox reactions at the working electrode and the auxiliary electrodes is called a ***faradaic current***. In this section we consider the factors affecting the magnitude of the faradaic current, as well as the sources of any non-faradaic currents.

Sign Conventions

Because the reaction of interest occurs at the working electrode, we describe the faradaic current using this reaction. A faradaic current due to the analyte's reduction is a ***cathodic current***, and its sign is positive. An ***anodic current*** results from the analyte's oxidation at the working electrode, and its sign is negative.

Influence of Applied Potential on the Faradaic Current

As an example, let's consider the faradaic current when we reduce $\mathbf{Fe(CN)_6^{3-}}$ to $\mathbf{Fe(CN)_6^{4-}}$ at the working electrode. The relationship between the concentrations of $\mathbf{Fe(CN)_6^{3-}}$, the concentration of $\mathbf{Fe(CN)_6^{4-}}$, and the potential is given by the Nernst equation

$$E = +0.356\ \text{V} - 0.05916 \log \frac{[\mathbf{Fe(CN)_6^{4-}}]_{x=0}}{[\mathbf{Fe(CN)_6^{3-}}]_{x=0}}$$

where +0.356V is the standard-statepotential for the $\mathbf{Fe(CN)_6^{3-}}$/$\mathbf{Fe(CN)_6^{4-}}$ redox couple, and x = 0 indicates that the concentrations of $\mathbf{Fe(CN)_6^{3-}}$- and $\mathbf{Fe(CN)_6^{4-}}$ are those at the surface of the working electrode. We use surface concentrations instead of bulk concentrations because the equilibrium position for the redox reaction

$$Fe(CN)_6^{3-}(aq) + e^- \rightleftharpoons Fe(CN)_6^{4-}(aq)$$

is established at the electrode's surface.

Let's assume we have a solution for which the initial concentration of $Fe(CN)_6^{3-}$ is 1.0 mM and that $Fe(CN)_6^{4-}$ is absent. Figure 11.4.5 shows the ladder diagram for this solution.

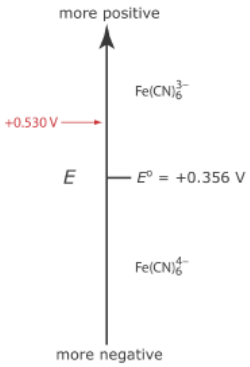


Figure 11.4.5 . Ladder diagram for the $Fe(CN)_6^{3-}/Fe(CN)_6^{4-}$ redox half-reaction.

If we apply a potential of +0.530 V to the working electrode, the concentrations of $Fe(CN)_6^{3-}$ and $Fe(CN)_6^{4-}$ at the surface of the electrode are unaffected, and no faradaic current is observed. If we switch the potential to +0.356 V some of the $Fe(CN)_6^{3-}$ at the electrode's surface is reduced to $Fe(CN)_6^{4-}$until we reach a condition where

$$[Fe(CN)_6^{3-}]_{x=0} = [Fe(CN)_6^{4-}]_{x=0} = 0.50 \text{ mM}$$

> This is the first of the five important principles of electrochemistry outlined in Chapter 11.1: the electrode's potential determines the analyte's form at the electrode's surface.

If this is all that happens after we apply the potential, then there would be a brief surge of faradaic current that quickly returns to zero, which is not the most interesting of results. Although the concentrations of $Fe(CN)_6^{3-}$ and $Fe(CN)_6^{4-}$ at the electrode surface are 0.50 mM, their concentrations in bulk solution remains unchanged.

> This is the second of the five important principles of electrochemistry outlined in Chapter 11.1: the analyte's concentration at the electrode may not be the same as its concentration in bulk solution.

Because of this difference in concentration, there is a concentration gradient between the solution at the electrode's surface and the bulk solution. This concentration gradient creates a driving force that transports $Fe(CN)_6^{4-}$ away from the electrode and that transports $Fe(CN)_6^{3-}$ to the electrode (Figure 11.4.6). As the $Fe(CN)_6^{3-}$ arrives at the electrode it, too, is reduced to $Fe(CN)_6^{4-}$. A faradaic current continues to flow until there is no difference between the concentrations of $Fe(CN)_6^{3-}$ and $Fe(CN)_6^{4-}$ at the electrode and their concentrations in bulk solution.

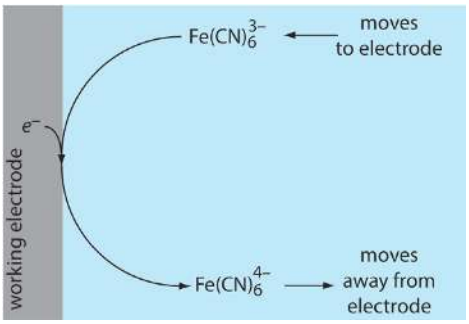


Figure 11.4.6 . Schematic diagram showing the transport of $Fe(CN)_6^{4-}$ away from the electrode's surface and the transport of $Fe(CN)_6^{3-}$ toward the electrode's surface following the reduction of $Fe(CN)_6^{3-}$ to $Fe(CN)_6^{4-}$.

Although the potential at the working electrode determines if a faradaic current flows, the magnitude of the current is determined by the rate of the resulting oxidation or reduction reaction. Two factors contribute to the rate of the electrochemical reaction: the rate at which the reactants and products are transported to and from the electrode—what we call ***mass transport***—and the rate at which electrons pass between the electrode and the reactants and products in solution.

> This is the fourth of the five important principles of electrochemistry outlined in Chapter 11.1: current is a measure of rate.

Influence of Mass Transport on the Faradaic Current

There are three modes of mass transport that affect the rate at which reactants and products move toward or away from the electrode surface: diffusion, migration, and convection. ***Diffusion*** occurs whenever the concentration of an ion or a molecule at the surface of the electrode is different from that in bulk solution. If we apply a potential sufficient to completely reduce $\mathbf{Fe(CN)_6^{3-}}$ at the electrode surface, the result is a concentration gradient similar to that shown in Figure 11.4.7 . The region of solution over which diffusion occurs is the ***diffusion layer***. In the absence of other modes of mass transport, the width of the diffusion layer, δ, increases with time as the $\mathbf{Fe(CN)_6^{3-}}$ must diffuse from an increasingly greater distance.

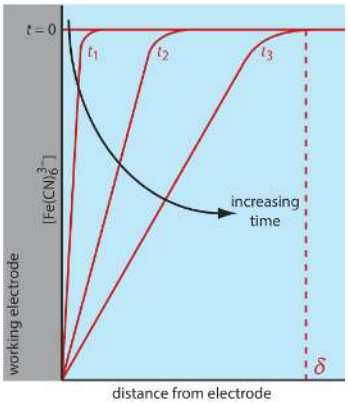


Figure 11.4.7 . Concentration gradients (in red) for $\mathbf{Fe(CN)_6^{3-}}$ following the application of a potential that completely reduces it to $\mathbf{Fe(CN)_6^{4-}}$. Before we apply the potential (t = 0) the concentration of $\mathbf{Fe(CN)_6^{3-}}$ is the same at all distances from the electrode's surface. After we apply the potential, its concentration at the electrode's surface decreases to zero and $\mathbf{Fe(CN)_6^{3-}}$ diffuses to the electrode from bulk solution. The longer we apply the potential, the greater the distance over which diffusion occurs. The dashed red line shows the extent of the diffusion layer at time t_3. These profiles assume that convection and migration do not contribute significantly to the mass transport of $\mathbf{Fe(CN)_6^{3-}}$.

Convection occurs when we mix the solution, which carries reactants toward the electrode and removes products from the electrode. The most common form of convection is stirring the solution with a stir bar; other methods include rotating the electrode and incorporating the electrode into a flow-cell.

The final mode of mass transport is ***migration***, which occurs when a charged particle in solution is attracted to or repelled from an electrode that carries a surface charge. If the electrode carries a positive charge, for example, an anion will move toward the electrode and a cation will move toward the bulk solution. Unlike diffusion and convection, migration affects only the mass transport of charged particles.

The movement of material to and from the electrode surface is a complex function of all three modes of mass transport. In the limit where diffusion is the only significant form of mass transport, the current in a voltammetric cell is equal to

$$i = \frac{nFAD\,(C_{\text{bulk}} - C_{x=0})}{\delta} \tag{4.4.1}$$

where n the number of electrons in the redox reaction, F is Faraday's constant, A is the area of the electrode, D is the diffusion coefficient for the species reacting at the electrode, C_{bulk} and $C_{x\,=\,0}$ are its concentrations in bulk solution and at the electrode surface, and δ is the thickness of the diffusion layer.

For Equation 4.4.1 to be valid, convection and migration must not interfere with the formation of a diffusion layer. We can eliminate migration by adding a high concentration of an inert supporting electrolyte. Because ions of similar charge equally are attracted to or repelled from the surface of the electrode, each has an equal probability of undergoing migration. A large excess of

an inert electrolyte ensures that few reactants or products experience migration. Although it is easy to eliminate convection by not stirring the solution, there are experimental designs where we cannot avoid convection, either because we must stir the solution or because we are using an electrochemical flow cell. Fortunately, as shown in Figure 11.4.8 , the dynamics of a fluid moving past an electrode results in a small diffusion layer—typically 1–10 μm in thickness—in which the rate of mass transport by convection drops to zero.

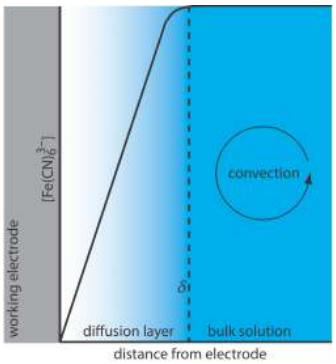


Figure 11.4.8 . Concentration gradient for $Fe(CN)_6^{3-}$ when stirring the solution. Diffusion is the only significant form of mass transport close to the electrode's surface. At distances greater than δ, convection is the only significant form of mass transport, maintaining a homogeneous solution in which the concentration of $Fe(CN)_6^{3-}$ at δ is the same as its concentration in bulk solution.

Effect of Electron Transfer Kinetics on the Faradaic Current

The rate of mass transport is one factor that influences the current in voltammetry. The ease with which electrons move between the electrode and the species that reacts at the electrode also affects the current. When electron transfer kinetics are fast, the redox reaction is at equilibrium. Under these conditions the redox reaction is ***electrochemically reversible*** and the Nernst equation applies. If the electron transfer kinetics are sufficiently slow, the concentration of reactants and products at the electrode surface—and thus the magnitude of the faradaic current—are not what is predicted by the Nernst equation. In this case the system is ***electrochemically irreversible***.

Charging Currents

In addition to the faradaic current from a redox reaction, the current in an electrochemical cell includes other, nonfaradaic sources. Suppose the charge on an electrode is zero and we suddenly change its potential so that the electrode's surface acquires a positive charge. Cations near the electrode's surface will respond to this positive charge by migrating away from the electrode; anions, on the other hand, will migrate toward the electrode. This migration of ions occurs until the electrode's positive surface charge and the negative charge of the solution near the electrode are equal. Because the movement of ions and the movement of electrons are indistinguishable, the result is a small, short-lived ***nonfaradaic current*** that we call the ***charging current***. Every time we change the electrode's potential, a transient charging current flows.

> The migration of ions in response to the electrode's surface charge leads to the formation of a structured electrode-solution interface that we call the ***electrical double layer***, or EDL. When we change an electrode's potential, the charging current is the result of a restructuring of the EDL. The exact structure of the electrical double layer is not important in the context of this text, but you can consult this chapter's additional resources for additional information.

Residual Current

Even in the absence of analyte, a small, measurable current flows through an electrochemical cell. This ***residual current*** has two components: a faradaic current due to the oxidation or reduction of trace impurities and a nonfaradaic charging current. Methods for discriminating between the analyte's faradaic current and the residual current are discussed later in this chapter.

Shape of Voltammograms

The shape of a voltammogram is determined by several experimental factors, the most important of which are how we measure the current and whether convection is included as a means of mass transport. As shown in Figure 11.4.9 , despite an abundance of

different voltammetric techniques, several of which are discussed in this chapter, there are only three common shapes for voltammograms.

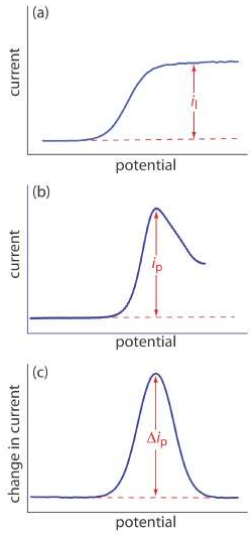


Figure 11.4.9 . The three common shapes for voltammograms. The dashed red line shows the residual current.

For the voltammogram in Figure 11.4.9 a, the current increases from a background residual current to a ***limiting current***, i_l. Because the faradaic current is inversely proportional to δ (Equation 4.4.1), a limiting current occurs only if the thickness of the diffusion layer remains constant because we are stirring the solution (see Figure 11.4.8). In the absence of convection the diffusion layer increases with time (see Figure 11.4.7). As shown in Figure 11.4.9 b, the resulting voltammogram has a ***peak current*** instead of a limiting current.

For the voltammograms in Figure 11.4.9 a and Figure 11.4.9 b, we measure the current as a function of the applied potential. We also can monitor the change in current, Δi, following a change in potential. The resulting voltammogram, shown in Figure 11.4.9 c, also has a peak current.

Quantitative and Qualitative Aspects of Voltammetry

Earlier we described a voltammogram as the electrochemical equivalent of a spectrum in spectroscopy. In this section we consider how we can extract quantitative and qualitative information from a voltammogram. For simplicity we will limit our treatment to voltammograms similar to Figure 11.4.9 a.

Determining Concentration

Let's assume that the redox reaction at the working electrode is

$$O + ne^- \rightleftharpoons R \tag{4.4.2}$$

where O is the analyte's oxidized form and R is its reduced form. Let's also assume that only O initially is present in bulk solution and that we are stirring the solution. When we apply a potential that results in the reduction of O to R, the current depends on the rate at which O diffuses through the fixed diffusion layer shown in Figure 11.4.7 . Using Equation 4.4.1, the current, i, is

$$i = K_O\left([O]_{\text{bulk}} - [O]_{x=0}\right) \tag{4.4.3}$$

where K_O is a constant equal to $nFAD_O/\delta$. When we reach the limiting current, i_l, the concentration of O at the electrode surface is zero and Equation 4.4.3 simplifies to

$$i_l = K_O[O]_{\text{bulk}} \tag{4.4.4}$$

Equation 4.4.4 shows us that the limiting current is a linear function of the concentration of O in bulk solution. To determine the value of K_O we can use any of the standardization methods covered in Chapter 5. Equations similar to Equation 4.4.4 can be developed for the other two types of voltammograms shown in Figure 11.4.9 .

Determining the Standard-State Potential

To extract the standard-state potential from a voltammogram, we need to rewrite the Nernst equation for reaction 4.4.2

$$E = E^{\circ}_{O/R} - \frac{0.05916}{n} \log \frac{[R]_{x=0}}{[O]_{x=0}} \tag{4.4.5}$$

in terms of current instead of the concentrations of O and R. We will do this in several steps. First, we substitute Equation 4.4.4 into Equation 4.4.3 and rearrange to give

$$[O]_{x=0} = \frac{i_l - i}{K_O} \tag{4.4.6}$$

Next, we derive a similar equation for $[R]_{x = 0}$, by noting that

$$i = K_R \left([R]_{x=0} - [R]_{\text{bulk}} \right)$$

Because the concentration of $[R]_{\text{bulk}}$ is zero—remember our assumption that the initial solution contains only O—we can simplify this equation

$$i = K_R [R]_{x=0}$$

and solve for $[R]_{x = 0}$.

$$[R]_{x=0} = \frac{i}{K_R} \tag{4.4.7}$$

Now we are ready to finish our derivation. Substituting Equation 4.4.7 and Equation 4.4.6 into Equation 4.4.5 and rearranging leaves us with

$$E = E^{\circ}_{O/R} - \frac{0.05916}{n} \log \frac{K_O}{K_R} - \frac{0.05916}{n} \log \frac{i}{i_l - i} \tag{4.4.8}$$

When the current, i, is half of the limiting current, i_l,

$$i = 0.5 \times i_l$$

we can simplify Equation 4.4.8 to

$$E_{1/2} = E^{\circ}_{O/R} - \frac{0.05916}{n} \log \frac{K_O}{K_R} \tag{4.4.9}$$

where $E_{1/2}$ is the half-wave potential (Figure 11.4.10). If K_O is approximately equal to K_R, which often is the case, then the half-wave potential is equal to the standard-state potential. Note that Equation 4.4.9 is valid only if the redox reaction is electrochemically reversible.

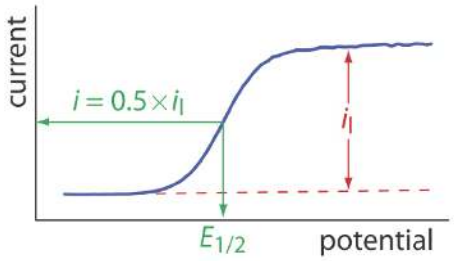


Figure 11.4.10 . Determination of the limiting current, i_l, and the half-wave potential, $E_{1/2}$, for the voltammogram in Figure 11.4.9 a.

Voltammetric Techniques

In voltammetry there are three important experimental parameters under our control: how we change the potential applied to the working electrode, when we choose to measure the current, and whether we choose to stir the solution. Not surprisingly, there are many different voltammetric techniques. In this section we consider several important examples.

Polarography

The first important voltammetric technique to be developed—***polarography***—uses the dropping mercury electrode shown in Figure 11.4.1 b as the working electrode. As shown in Figure 11.4.11 , the current is measured while applying a linear potential ramp.

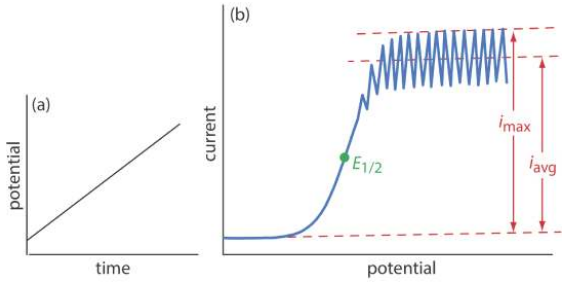


Figure 11.4.11 . Details of normal polarography: (a) the linear potential-excitation signal, and (b) the resulting voltammogram.

Although polarography takes place in an unstirred solution, we obtain a limiting current instead of a peak current. When a Hg drop separates from the glass capillary and falls to the bottom of the electrochemical cell, it mixes the solution. Each new Hg drop, therefore, grows into a solution whose composition is identical to the bulk solution. The oscillations in the current are a result of the Hg drop's growth, which leads to a time-dependent change in the area of the working electrode. The limiting current—which also is called the diffusion current—is measured using either the maximum current, i_{max}, or from the average current, i_{avg}. The relationship between the analyte's concentration, C_A, and the limiting current is given by the Ilkovic equations

$$i_{max} = 706nD^{1/2}m^{2/3}t^{1/6}C_A = K_{max}C_A$$

$$i_{avg} = 607nD^{1/2}m^{2/3}t^{1/6}C_A = K_{avg}C_A$$

where n is the number of electrons in the redox reaction, D is the analyte's diffusion coefficient, m is the flow rate of Hg, t is the drop's lifetime and K_{max} and K_{avg} are constants. The half-wave potential, $E_{1/2}$, provides qualitative information about the redox reaction.

Normal polarography has been replaced by various forms of ***pulse polarography***, several examples of which are shown in Figure 11.4.12 [Osteryoung, J. *J. Chem. Educ.* **1983**, *60*, 296–298]. Normal pulse polarography (Figure 11.4.12 a), for example, uses a series of potential pulses characterized by a cycle of time τ, a pulse-time of t_p, a pulse potential of ΔE_p, and a scan rate of $\Delta E/\Delta t$. Typical experimental conditions for normal pulse polarography are $\tau \approx 1\ s$, $t_p \approx 50$ ms, and $\Delta E/\Delta t \approx 2\ mV/s$. The initial value of $\Delta E_p \approx 2\ mV$, and it increases by ≈ 2 mV with each pulse. The current is sampled at the end of each potential pulse for approximately 17 ms before returning the potential to its initial value. The shape of the resulting voltammogram is similar to Figure 11.4.11 , but without the current oscillations. Because we apply the potential for only a small portion of the drop's lifetime, there is less time for the analyte to undergo oxidation or reduction and a smaller diffusion layer. As a result, the faradaic current in normal pulse polarography is greater than in the polarography, resulting in better sensitivity and smaller detection limits.

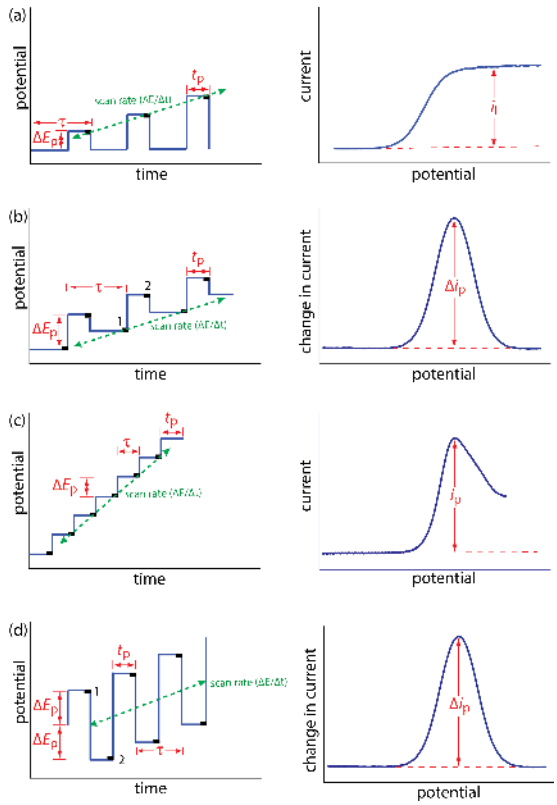


Figure 11.4.12 . Potential-excitation signals and voltammograms for (a) normal pulse polarography, (b) differential pulse polarography, (c) staircase polarography, and (d) square-wave polarography. The current is sampled at the time intervals shown by the black rectangles. When measuring a change in current, Δi, the current at point 1 is subtracted from the current at point 2. The symbols in the diagrams are as follows: τ is the cycle time; ΔE_p is a fixed or variable pulse potential relative to the beginning of the cycle; and t_p is the pulse time. The scan rate (change in potential per unit time) is shown by the dashed arrow.

In differential pulse polarography (Figure 11.4.12 b) the current is measured twice per cycle: for approximately 17 ms before applying the pulse and for approximately 17 ms at the end of the cycle. The difference in the two currents gives rise to the peak-shaped voltammogram. Typical experimental conditions for differential pulse polarography are $\tau \approx 1$ s, $t_p \approx 50$ ms, $\Delta E_p \approx 50$ mV, and $\Delta E/\Delta t \approx 2$ mV/s.

> The voltammogram for differential pulse polarography is approximately the first derivative of the voltammogram for normal pulse polarography. To see why this is the case, note that the change in current over a fixed change in potential, $\Delta i/\Delta E$, approximates the slope of the voltammogram for normal pulse polarography. You may recall that the first derivative of a function returns the slope of the function at each point. The first derivative of a sigmoidal function is a peak-shaped function.

Other forms of pulse polarography include staircase polarography (Figure 11.4.12 c) and square-wave polarography (Figure 11.4.12 d). One advantage of square-wave polarography is that we can make τ very small—perhaps as small as 5 ms, compared to 1 s for other forms of pulse polarography—which significantly decreases analysis time. For example, suppose we need to scan a potential range of 400 mV. If we use normal pulse polarography with a $\Delta E/\Delta t$ of 2 mV/cycle and a τ of 1 s/cycle, then we need 200 s to complete the scan. If we use square-wave polarography with a $\Delta E/\Delta t$ of 2 mV/cycle and a τ of 5 ms/cycle, we can complete the scan in 1 s. At this rate, we can acquire a complete voltammogram using a single drop of Hg!

Polarography is used extensively for the analysis of metal ions and inorganic anions, such as IO_3^- and NO_3^-. We also can use polarography to study organic compounds with easily reducible or oxidizable functional groups, such as carbonyls, carboxylic acids, and carbon-carbon double bonds.

Hydrodynamic Voltammetry

In polarography we obtain a limiting current because each drop of mercury mixes the solution as it falls to the bottom of the electrochemical cell. If we replace the DME with a solid electrode (see Figure 11.4.3), we can still obtain a limiting current if we mechanically stir the solution during the analysis, using either a stir bar or by rotating the electrode. We call this approach ***hydrodynamic voltammetry***.

Hydrodynamic voltammetry uses the same potential profiles as in polarography, such as a linear scan (Figure 11.4.11) or a differential pulse (Figure 11.4.12 b). The resulting voltammograms are identical to those for polarography, except for the lack of current oscillations from the growth of the mercury drops. Because hydrodynamic voltammetry is not limited to Hg electrodes, it is useful for analytes that undergo oxidation or reduction at more positive potentials.

Stripping Voltammetry

Another important voltammetric technique is ***stripping voltammetry***, which consists of three related techniques: anodic stripping voltammetry, cathodic stripping voltammetry, and adsorptive stripping voltammetry. Because anodic stripping voltammetry is the more widely used of these techniques, we will consider it in greatest detail.

Anodic stripping voltammetry consists of two steps (Figure 11.4.13). The first step is a controlled potential electrolysis in which we hold the working electrode—usually a hanging mercury drop or a mercury film electrode—at a cathodic potential sufficient to deposit the metal ion on the electrode. For example, when analyzing Cu^{2+} the deposition reaction is

$$\mathbf{Cu^{2+} + 2e^- \rightleftharpoons Cu(Hg)}$$

where Cu(Hg) indicates that the copper is amalgamated with the mercury. This step serves as a means of concentrating the analyte by transferring it from the larger volume of the solution to the smaller volume of the electrode. During most of the electrolysis we stir the solution to increase the rate of deposition. Near the end of the deposition time we stop the stirring—eliminating convection as a mode of mass transport—and allow the solution to become quiescent. Typical deposition times of 1–30 min are common, with analytes at lower concentrations requiring longer times.

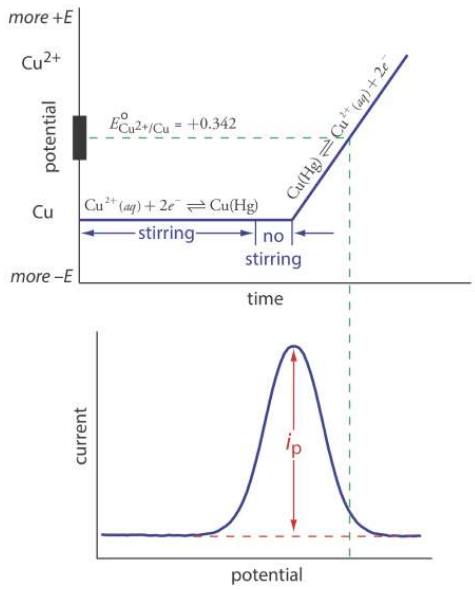


Figure 11.4.13 . Potential-excitation signal and voltammogram for anodic stripping voltammetry at a hanging mercury drop electrode or a mercury film electrode. Note the ladder diagram for copper in the upper figure.

In the second step, we scan the potential anodically—that is, toward a more positive potential. When the working electrode's potential is sufficiently positive, the analyte is stripped from the electrode, returning to solution in its oxidized form.

$$\mathbf{Cu(Hg) \rightleftharpoons\ Cu^{2+} + 2e^-}$$

Monitoring the current during the stripping step gives a peak-shaped voltammogram, as shown in Figure 11.4.13 . The peak current is proportional to the analyte's concentration in the solution. Because we are concentrating the analyte in the electrode, detection

limits are much smaller than other electrochemical techniques. An improvement of three orders of magnitude—the equivalent of parts per billion instead of parts per million—is routine.

Anodic stripping voltammetry is very sensitive to experimental conditions, which we must carefully control to obtain results that are accurate and precise. Key variables include the area of the mercury film or the size of the hanging Hg drop, the deposition time, the rest time, the rate of stirring, and the scan rate during the stripping step. Anodic stripping voltammetry is particularly useful for metals that form amalgams with mercury, several examples of which are listed in Table 11.4.1 .

Table 11.4.1 . Representative Examples of Analytes Determined by Stripping Voltammetry

anodic stripping voltammetry	cathodic stripping voltammetry	adsorptive stripping voltammetry
Bi^{3+}	Br^-	bilirubin
Cd^{2+}	Cl^-	codeine
Cu^{2+}	I^-	cocaine
Ga^{3+}	mercaptans (RSH)	digitoxin
In^{3+}	S^{2-}	dopamine
Pb^{2+}	SCN^-	heme
Tl^+		monesin
Sn^{2+}		testosterone
Zn^{2+}		

Source: Compiled from Peterson, W. M.; Wong, R. V. *Am. Lab.* November 1981, 116–128; Wang, J. *Am. Lab.* May 1985, 41–50.

The experimental design for cathodic stripping voltammetry is similar to anodic stripping voltammetry with two exceptions. First, the deposition step involves the oxidation of the Hg electrode to Hg_2^{2+}, which then reacts with the analyte to form an insoluble film at the surface of the electrode. For example, when Cl^- is the analyte the deposition step is

$$2Hg(l) + 2Cl^-(aq) \rightleftharpoons Hg_2Cl_2(s) + 2e^-$$

Second, stripping is accomplished by scanning cathodically toward a more negative potential, reducing Hg_2^{2+} back to Hg and returning the analyte to solution.

$$Hg_2Cl_2(s) + 2e^- \rightleftharpoons 2Hg(l) + 2Cl^-(aq)$$

Table 11.4.1 lists several analytes analyzed successfully by cathodic stripping voltammetry.

In adsorptive stripping voltammetry, the deposition step occurs without electrolysis. Instead, the analyte adsorbs to the electrode's surface. During deposition we maintain the electrode at a potential that enhances adsorption. For example, we can adsorb a neutral molecule on a Hg drop if we apply a potential of –0.4 V versus the SCE, a potential where the surface charge of mercury is approximately zero. When deposition is complete, we scan the potential in an anodic or a cathodic direction, depending on whether we are oxidizing or reducing the analyte. Examples of compounds that have been analyzed by absorptive stripping voltammetry also are listed in Table 11.4.1 .

Cyclic Voltammetry

In the voltammetric techniques consider to this point we scan the potential in one direction, either to more positive potentials or to more negative potentials. In ***cyclic voltammetry*** we complete a scan in both directions. Figure 11.4.14 a shows a typical potential-excitation signal. In this example, we first scan the potential to more positive values, resulting in the following oxidation reaction for the species *R*.

$$R \rightleftharpoons O + ne^-$$

When the potential reaches a predetermined switching potential, we reverse the direction of the scan toward more negative potentials. Because we generated the species *O* on the forward scan, during the reverse scan it reduces back to *R*.

$$O + ne^- \rightleftharpoons R$$

Cyclic voltammetry is carried out in an unstirred solution, which, as shown in Figure 11.4.14 b, results in peak currents instead of limiting currents. The voltammogram has separate peaks for the oxidation reaction and for the reduction reaction, each characterized by a peak potential and a peak current.

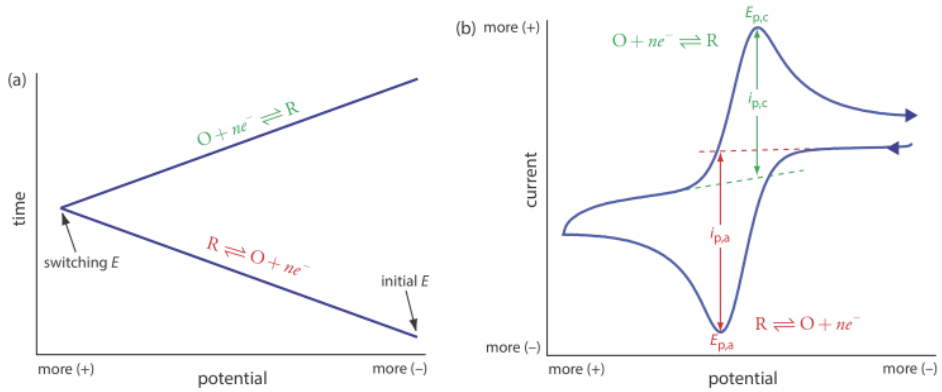


Figure 11.4.14 . Details for cyclic voltammetry. (a) One cycle of the triangular potential-excitation signal showing the initial potential and the switching potential. A cyclic voltammetry experiment can consist of one cycle or many cycles. Although the initial potential in this example is the negative switching potential, the cycle can begin with an intermediate initial potential and cycle between two limits. (b) The resulting cyclic voltammogram showing the measurement of the peak currents and peak potentials.

The peak current in cyclic voltammetry is given by the Randles-Sevcik equation

$$i_p = (2.69 \times 10^5)\, n^{3/2} A D^{1/2} \nu^{1/2} C_A$$

where n is the number of electrons in the redox reaction, A is the area of the working electrode, D is the diffusion coefficient for the electroactive species, ν is the scan rate, and C_A is the concentration of the electroactive species at the electrode. For a well-behaved system, the anodic and the cathodic peak currents are equal, and the ratio $i_{p,a}/i_{p,c}$ is 1.00. The half-wave potential, $E_{1/2}$, is midway between the anodic and cathodic peak potentials.

$$E_{1/2} = \frac{E_{p,a} + E_{p,c}}{2}$$

Scanning the potential in both directions provides an opportunity to explore the electrochemical behavior of species generated at the electrode. This is a distinct advantage of cyclic voltammetry over other voltammetric techniques. Figure 11.4.15 shows the cyclic voltammogram for the same redox couple at both a faster and a slower scan rate. At the faster scan rate, 11.4.15 a, we see two peaks. At the slower scan rate in Figure 11.4.15 b, however, the peak on the reverse scan disappears. One explanation for this is that the products from the reduction of *R* on the forward scan have sufficient time to participate in a chemical reaction whose products are not electroactive.

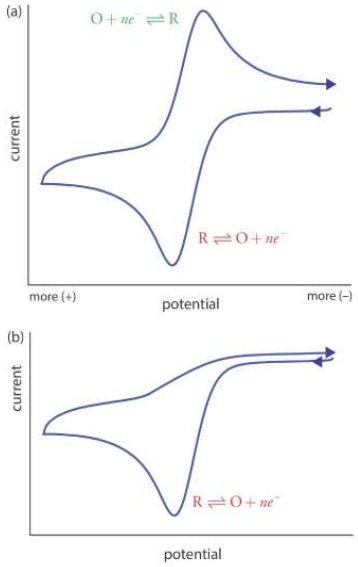


Figure 11.4.15 . Cyclic voltammograms for *R* obtained at (a) a faster scan rate and at (b) a slower scan rate. One of the principal uses of cyclic voltammetry is to study the chemical and electrochemical behavior of compounds. See this chapter's additional resources for further information.

Amperometry

The final voltammetric technique we will consider is ***amperometry***, in which we apply a constant potential to the working electrode and measure current as a function of time. Because we do not vary the potential, amperometry does not result in a voltammogram.

One important application of amperometry is in the construction of chemical sensors. One of the first amperometric sensors was developed in 1956 by L. C. Clark to measure dissolved O_2 in blood. Figure 11.4.16 shows the sensor's design, which is similar to a potentiometric membrane electrode. A thin, gas-permeable membrane is stretched across the end of the sensor and is separated from the working electrode and the counter electrode by a thin solution of KCl. The working electrode is a Pt disk cathode, and a Ag ring anode serves as the counter electrode. Although several gases can diffuse across the membrane, including O_2, N_2, and CO_2, only oxygen undergoes reduction at the cathode

$$\mathrm{O_2}(g) + 4\mathrm{H_3O^+}(aq) + 4e^- \rightleftharpoons 6\mathrm{H_2O}(l)$$

with its concentration at the electrode's surface quickly reaching zero. The concentration of O_2 at the membrane's inner surface is fixed by its diffusion through the membrane, which creates a diffusion profile similar to that in Figure 11.4.8 . The result is a steady-state current that is proportional to the concentration of dissolved oxygen. Because the electrode consumes oxygen,the sample is stirred to prevent the depletion of O_2 at the membrane's outer surface.

> The oxidation of the Ag anode is the other half-reaction.
>
> $$\mathrm{Ag}(s) + \mathrm{Cl^-}(aq) \rightleftharpoons \mathrm{AgCl}(s) + e^-$$

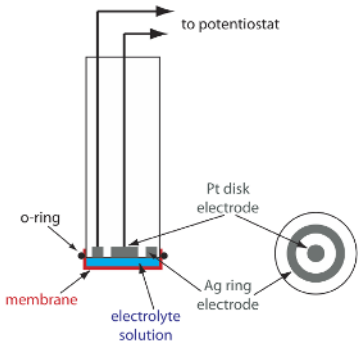


Figure 11.4.16 . Clark amperometric sensor for determining dissolved O_2. The diagram on the right is a cross-section through the electrode, which shows the Ag ring electrode and the Pt disk electrode.

Another example of an amperometric sensor is a glucose sensor. In this sensor the single membrane in Figure 11.4.16 is replaced with three membranes. The outermost membrane of polycarbonate is permeable to glucose and O_2. The second membrane contains an immobilized preparation of glucose oxidase that catalyzes the oxidation of glucose to gluconolactone and hydrogen peroxide.

$$\beta-\text{D}-\text{glucose}\ (aq)+\ \text{O}_2(aq)+\text{H}_2\text{O}(l)\rightleftharpoons\text{gluconolactone}\ (aq)+\ \text{H}_2\text{O}_2(aq)$$

The hydrogen peroxide diffuses through the innermost membrane of cellulose acetate where it undergoes oxidation at a Pt anode.

$$\text{H}_2\text{O}_2(aq)+2\text{OH}^-(aq)\rightleftharpoons\ \text{O}_2(aq)+2\text{H}_2\text{O}(l)+2e^-$$

Figure 11.4.17 summarizes the reactions that take place in this amperometric sensor. FAD is the oxidized form of flavin adenine nucleotide—the active site of the enzyme glucose oxidase—and $FADH_2$ is the active site's reduced form. Note that O_2 serves a mediator, carrying electrons to the electrode.

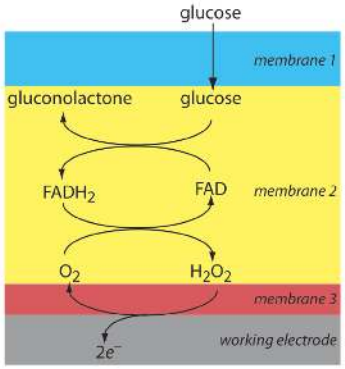


Figure 11.4.17 . Schematic showing the reactions by which an amperometric biosensor responds to glucose.

By changing the enzyme and mediator, it is easy to extend to the amperometric sensor in Figure 11.4.17 to the analysis of other analytes. For example, a CO_2 sensor has been developed using an amperometric O_2 sensor with a two-layer membrane, one of which contains an immobilized preparation of autotrophic bacteria [Karube, I.; Nomura, Y.; Arikawa, Y. *Trends in Anal. Chem.* **1995**, *14*, 295–299]. As CO_2 diffuses through the membranes it is converted to O_2 by the bacteria, increasing the concentration of O_2 at the Pt cathode.

Quantitative Applications

Voltammetry has been used for the quantitative analysis of a wide variety of samples, including environmental samples, clinical samples, pharmaceutical formulations, steels, gasoline, and oil.

Selecting the Voltammetric Technique

The choice of which voltammetric technique to use depends on the sample's characteristics, including the analyte's expected concentration and the sample's location. For example, amperometry is ideally suited for detecting analytes in flow systems, including the *in vivo* analysis of a patient's blood or as a selective sensor for the rapid analysis of a single analyte. The portability of amperometric sensors, which are similar to potentiometric sensors, also make them ideal for field studies. Although cyclic

voltammetry is used to determine an analyte's concentration, other methods described in this chapter are better suited for quantitative work.

Pulse polarography and stripping voltammetry frequently are interchangeable. The choice of which technique to use often depends on the analyte's concentration and the desired accuracy and precision. Detection limits for normal pulse polarography generally are on the order of 10^{-6} M to 10^{-7} M, and those for differential pulse polarography, staircase, and square wave polarography are between 10^{-7} M and 10^{-9} M. Because we concentrate the analyte in stripping voltammetry, the detection limit for many analytes is as little as 10^{-10} M to 10^{-12} M. On the other hand, the current in stripping voltammetry is much more sensitive than pulse polarography to changes in experimental conditions, which may lead to poorer precision and accuracy. We also can use pulse polarography to analyze a wider range of inorganic and organic analytes because there is no need to first deposit the analyte at the electrode surface.

Stripping voltammetry also suffers from occasional interferences when two metals, such as Cu and Zn, combine to form an intermetallic compound in the mercury amalgam. The deposition potential for Zn . is sufficiently negative that any Cu^{2+} in the sample also deposits into the mercury drop or film, leading to the formation of intermetallic compounds such as CuZn and $CuZn_2$. During the stripping step, zinc in the intermetallic compounds strips at potentials near that of copper, decreasing the current for zinc at its usual potential and increasing the apparent current for copper. It is possible to overcome this problem by adding an element that forms a stronger intermetallic compound with the interfering metal. Thus, adding Ga^{3+} minimizes the interference of Cu when analyzing for Zn by forming an intermetallic compound of Cu and Ga.

Correcting the Residual Current

In any quantitative analysis we must correct the analyte's signal for signals that arise from other sources. The total current, i_{tot}, in voltammetry consists of two parts: the current from the analyte's oxidation or reduction, i_A, and a background or residual current, i_r.

$$i_{tot} = i_A + i_r$$

The residual current, in turn, has two sources. One source is a faradaic current from the oxidation or reduction of trace interferents in the sample, i_{int}. The other source is the charging current, i_{ch}, that accompanies a change in the working electrode's potential.

$$i_r = i_{\text{int}} + i_{ch}$$

We can minimize the faradaic current due to impurities by carefully preparing the sample. For example, one important impurity is dissolved O_2, which undergoes a two-step reduction: first to H_2O_2 at a potential of –0.1 V versus the SCE, and then to H_2O at a potential of –0.9 V versus the SCE. Removing dissolved O_2 by bubbling an inert gas such as N_2 through the sample eliminates this interference. After removing the dissolved O_2, maintaining a blanket of N_2 over the top of the solution prevents O_2 from reentering the solution.

> The cell in Figure 11.4.4 shows a typical N_2 purge line.

There are two methods to compensate for the residual current. One method is to measure the total current at potentials where the analyte's faradaic current is zero and extrapolate it to other potentials. This is the method shown in Figure 11.4.9 . One advantage of extrapolating is that we do not need to acquire additional data. An important disadvantage is that an extrapolation assumes that any change in the residual current with potential is predictable, which may not be the case. A second, and more rigorous approach, is to obtain a voltammogram for an appropriate blank. The blank's residual current is then subtracted from the sample's total current.

Analysis for Single Components

The analysis of a sample with a single analyte is straightforward using any of the standardization methods discussed in Chapter 5.

✔ Example 11.4.1

The concentration of As(III) in water is determined by differential pulse polarography in 1 M HCl. The initial potential is set to –0.1 V versus the SCE and is scanned toward more negative potentials at a rate of 5 mV/s. Reduction of As(III) to As(0) occurs

at a potential of approximately –0.44 V versus the SCE. The peak currents for a set of standard solutions, corrected for the residual current, are shown in the following table.

[As(III)] (μM)	i_p (μM)
1.00	0.298
3.00	0.947
6.00	1.83
9.00	2.72

What is the concentration of As(III) in a sample of water if its peak current is 1.37 μA?

Solution

Linear regression gives the calibration curve shown in Figure 11.4.18 , with an equation of

$$i_p = 0.0176 + 3.01 \times [\text{As(III)}]$$

Substituting the sample's peak current into the regression equation gives the concentration of As(III) as 4.49 μM.

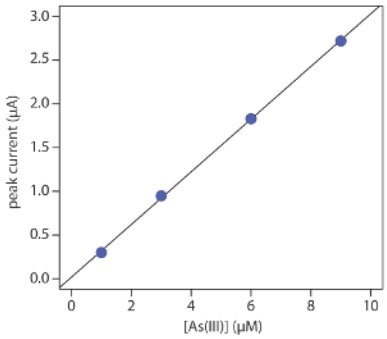


Figure 11.4.18 . Calibration curve for the data in Example 11.4.1 .

Exercise 11.4.1

The concentration of copper in a sample of sea water is determined by anodic stripping voltammetry using the method of standard additions. The analysis of a 50.0-mL sample gives a peak current of 0.886 μA. After adding a 5.00-μL spike of 10.0 mg/L Cu^{2+}, the peak current increases to 2.52 μA. Calculate the μg/L copper in the sample of sea water.

Answer

For anodic stripping voltammetry, the peak current, i_p, is a linear function of the analyte's concentration

$$i_p = K \times C_{\text{Cu}}$$

where K is a constant that accounts for experimental parameters such as the electrode's area, the diffusion coefficient for Cu^{2+}, the deposition time, and the rate of stirring. For the analysis of the sample before the standard addition we know that the current is

$$i_p = 0.886\ \mu\text{A} = K \times C_{\text{Cu}}$$

and after the standard addition the current is

$$i_p = 2.52\ \mu\text{A} = K\left\{C_{\text{Cu}} \times \frac{50.00\ \text{mL}}{50.005\ \text{mL}} + \frac{10.00\text{mgCu}}{\text{L}} \times \frac{0.005\ \text{mL}}{50.005\ \text{mL}}\right\}$$

where 50.005 mL is the total volume after we add the 5.00 μL spike. Solving each equation for K and combining leaves us with the following equation.

$$\frac{0.886\ \mu A}{C_{Cu}} = K = \frac{2.52\ \mu A}{C_{Cu} \times \frac{50.00\ mL}{50.005\ mL} + \frac{10.00\ mg\ Cu}{L} \times \frac{0.005\ mL}{50.005\ mL}}$$

Solving this equation for C_{Cu} gives its value as 5.42×10^{-4} mg Cu^{2+}/L, or 0.542 μg Cu^{2+}/L.

Multicomponent Analysis

Voltammetry is a particularly attractive technique for the analysis of samples that contain two or more analytes. Provided that the analytes behave independently, the voltammogram of a multicomponent mixture is a summation of each analyte's individual voltammograms. As shown in Figure 11.4.19 , if the separation between the half-wave potentials or between the peak potentials is sufficient, we can determine the presence of each analyte as if it is the only analyte in the sample. The minimum separation between the half-wave potentials or peak potentials for two analytes depends on several factors, including the type of electrode and the potential-excitation signal. For normal polarography the separation is at least ±0.2–0.3 V, and differential pulse voltammetry requires a minimum separation of ±0.04–0.05 V.

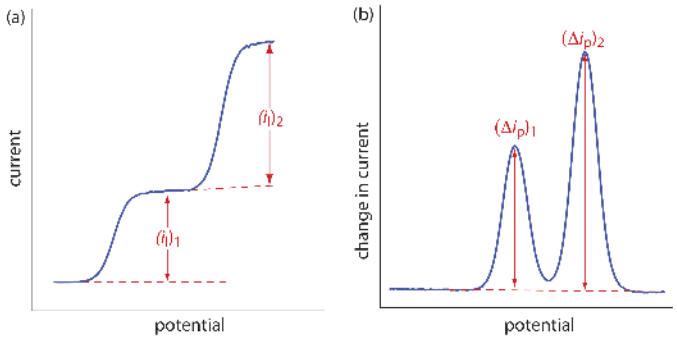


Figure 11.4.19 . Voltammograms for a sample that contains two analytes showing the measurement of (a) limiting currents, and (b) peak currents.

If the voltammograms for two analytes are not sufficiently separated, a simultaneous analysis may be possible. An example of this approach is outlined the following example.

Example 11.4.2

The differential pulse polarographic analysis of a mixture of indium and cadmium in 0.1 M HCl is complicated by the overlap of their respective voltammograms [Lanza P. *J. Chem. Educ.* **1990**, *67*, 704–705]. The peak potential for indium is at –0.557 V and that for cadmium is at –0.597 V. When a 0.800-ppm indium standard is analyzed, Δi_p (in arbitrary units) is 200.5 at –0.557 V and 87.5 at –0.597 V relative to a saturated Ag/AgCl reference electorde. A standard solution of 0.793 ppm cadmium has a Δi_p of 58.5 at –0.557 V and 128.5 at –0.597 V. What is the concentration of indium and cadmium in a sample if Δi_p is 167.0 at a potential of –0.557 V and 99.5 at a potential of –0.597V.

Solution

The change in current, Δi_p, in differential pulse polarography is a linear function of the analyte's concentration

$$\Delta i_p = k_A C_A$$

where k_A is a constant that depends on the analyte and the applied potential, and C_A is the analyte's concentration. To determine the concentrations of indium and cadmium in the sample we must first find the value of k_A for each analyte at each potential. For simplicity we will identify the potential of –0.557 V as E_1, and that for –0.597 V as E_2. The values of k_A are

$$k_{In,E_1} = \frac{200.5}{0.800\ ppm} = 250.6\ ppm^{-1}$$
$$k_{In,E_2} = \frac{87.5}{0.800\ ppm} = 109.4\ ppm^{-1}$$
$$k_{Cd E_1} = \frac{58.5}{0.793\ ppm} = 73.8\ ppm^{-1}$$
$$k_{Cd E_2} = \frac{128.5}{0.793\ ppm} = 162.0\ ppm^{-1}$$

Next, we write simultaneous equations for the current at the two potentials.

$$\Delta i_{E_1} = 167.0 = 250.6 \text{ ppm}^{-1} \times C_{\text{In}} + 73.8 \text{ ppm}^{-1} \times C_{\text{Cd}}$$
$$\Delta i_{E_2} = 99.5 = 109.4 \text{ ppm}^{-1} \times C_{\text{In}} + 162.0 \text{ ppm}^{-1} \times C_{\text{Cd}}$$

Solving the simultaneous equations, which is left as an exercise, gives the concentration of indium as 0.606 ppm and the concentration of cadmium as 0.205 ppm.

Environmental Samples

Voltammetry is one of several important analytical techniques for the analysis of trace metals in environmental samples, including groundwater, lakes, rivers and streams, seawater, rain, and snow. Detection limits at the parts-per-billion level are routine for many trace metals using differential pulse polarography, with anodic stripping voltammetry providing parts-per-trillion detection limits for some trace metals.

One interesting environmental application of anodic stripping voltammetry is the determination of a trace metal's chemical form within a water sample. Speciation is important because a trace metal's bioavailability, toxicity, and ease of transport through the environment often depends on its chemical form. For example, a trace metal that is strongly bound to colloidal particles generally is not toxic because it is not available to aquatic lifeforms. Unfortunately, anodic stripping voltammetry can not distinguish a trace metal's exact chemical form because closely related species, such as Pb^{2+} and $PbCl^{+}$, produce a single stripping peak. Instead, trace metals are divided into "operationally defined" categories that have environmental significance.

Operationally defined means that an analyte is divided into categories by the specific methods used to isolate it from the sample. There are many examples of operational definitions in the environmental literature. The distribution of trace metals in soils and sediments, for example, often is defined in terms of the reagents used to extract them; thus, you might find an operational definition for Zn^{2+} in a lake sediment as that extracted using 1.0 M sodium acetate, or that extracted using 1.0 M HCl.

Although there are many speciation schemes in the environmental literature, we will consider one proposed by Batley and Florence [see (a) Batley, G. E.; Florence, T. M. *Anal. Lett.* **1976**, *9*, 379–388; (b) Batley, G. E.; Florence, T. M. *Talanta* **1977**, *24*, 151–158; (c) Batley, G. E.; Florence, T. M. *Anal. Chem.* **1980**, *52*, 1962–1963; (d) Florence, T. M., Batley, G. E.; *CRC Crit. Rev. Anal. Chem.* **1980**, *9*, 219–296]. This scheme, which is outlined in Table 11.4.2 , combines anodic stripping voltammetry with ion-exchange and UV irradiation, dividing soluble trace metals into seven groups. In the first step, anodic stripping voltammetry in a pH 4.8 acetic acid buffer differentiates between labile metals and nonlabile metals. Only labile metals—those present as hydrated ions, weakly bound complexes, or weakly adsorbed on colloidal surfaces—deposit at the electrode and give rise to a signal. Total metal concentration are determined by ASV after digesting the sample in 2 M HNO_3 for 5 min, which converts all metals into an ASV-labile form.

Table 11.4.2 . Operational Speciation of Soluble Trace Metals

method	speciation of soluble metals						
ASV	labile metals			nonlabile or bound metals			
Ion-Exchange	removed	not removed		removed		not removed	
UV Irradiation		released	not released	released	not released	released	not released
Groups	I	II	III	IV	V	VI	VII
Group I: free metal ions; weaker labile organic complexes and inorganic complexes							
Group II: stronger labile organic complexes; labile metals absorbed on organic solids							
Group III: stronger labile inorganic complexes; labile metals absorbed on inorganic solids							
Group IV: weaker nonlabile organic complexes							
Group V: weaker nonlabile inorganic complexes							
Group VI: stronger nonlabile organic complexes; nonlabile metals absorbed on organic solids							
Group VII: stronger nonlabile inorganic complexes; nonlabile metals absorbed on inorganic solids							
Operational definitions of speciation from (a)Batley,G.E.;Florence,T.M.*Anal.Lett.***1976**,*9*,379–388; (b)Batley,G.E.;Florence,T.M.*Talanta***1977**,*24*,151–158; (c) Batley, G. E.; Florence, T. M. *Anal. Chem.* **1980**, *52*, 1962–1963; (d) Florence, T. M., Batley, G. E.; *CRC Crit. Rev. Anal. Chem.* **1980**, *9*, 219–296.							

A Chelex-100 ion-exchange resin further differentiates between strongly bound metals—usually metals bound to inorganic and organic solids, but also those tightly bound to chelating ligands—and more loosely bound metals. Finally, UV radiation differentiates between metals bound to organic phases and inorganic phases. The analysis of seawater samples, for example, suggests that cadmium, copper, and lead are present primarily as labile organic complexes or as labile adsorbates on organic colloids (Group II in Table 11.4.2).

Differential pulse polarography and stripping voltammetry are used to determine trace metals in airborne particulates, incinerator fly ash, rocks, minerals, and sediments. The trace metals, of course, are first brought into solution using a digestion or an extraction.

Amperometric sensors also are used to analyze environmental samples. For example, the dissolved O_2 sensor described earlier is used to determine the level of dissolved oxygen and the biochemical oxygen demand, or BOD, of waters and wastewaters. The latter test—which is a measure of the amount of oxygen required by aquatic bacteria as they decompose organic matter—is important when evaluating the efficiency of a wastewater treatment plant and for monitoring organic pollution in natural waters. A high BOD suggests that the water has a high concentration of organic matter. Decomposition of this organic matter may seriously deplete the level of dissolved oxygen in the water, adversely affecting aquatic life. Other amperometric sensors are available to monitor anionic surfactants in water, and CO_2, H_2SO_4, and NH_3 in atmospheric gases.

Clinical Samples

Differential pulse polarography and stripping voltammetry are used to determine the concentration of trace metals in a variety of clinical samples, including blood, urine, and tissue. The determination of lead in blood is of considerable interest due to concerns about lead poisoning. Because the concentration of lead in blood is so small, anodic stripping voltammetry frequently is the more appropriate technique. The analysis is complicated, however, by the presence of proteins that may adsorb to the mercury electrode, inhibiting either the deposition or stripping of lead. In addition, proteins may prevent the electrodeposition of lead through the formation of stable, nonlabile complexes. Digesting and ashing the blood sample mini- mizes this problem. Differential pulse polarography is useful for the routine quantitative analysis of drugs in biological fluids, at concentrations of less than 10^{-6} M [Brooks, M. A. “Application of Electrochemistry to Pharmaceutical Analysis,” Chapter 21 in Kissinger, P. T.; Heinemann, W. R., eds. *Laboratory Techniques in Electroanalytical Chemistry*, Marcel Dekker, Inc.: New York, 1984, pp 539–568.]. Amperometric sensors using enzyme catalysts also have many clinical uses, several examples of which are shown in Table 11.4.3 .

Table 11.4.3 . Representative Amperometric Biosensors

analyte	enzyme	species detected
choline	choline oxidase	H_2O_2
ethanol	alcohol oxidase	H_2O_2
formaldehyde	formaldehyde dehydrogenase	NADH
glucose	glucose oxidase	H_2O_2
glutamine	glutaminase, glutamine oxidase	H_2O_2
glycerol	glycerol dehydrogenase	NADH, O_2
lactate	lactate oxidase	H_2O_2
phenol	polyphenol oxidase	quinone
inorganic phosphorous	nucleoside phosphoylase	O_2

Source: Cammann, K.; Lemke, U.; Rohen, A.; Sander, J.; Wilken, H.; Winter, B. *Angew. Chem. Int. Ed. Engl.* **1991**, *30*, 516–539.

Miscellaneous Samples

In addition to environmental samples and clinical samples, differential pulse polarography and stripping voltammetry are used for the analysis of trace metals in other sample, including food, steels and other alloys, gasoline, gunpowder residues, and pharmaceuticals. Voltammetry is an important technique for the quantitative analysis of organics, particularly in the pharmaceutical industry where it is used to determine the concentration of drugs and vitamins in formulations. For example, voltammetric methods are available for the quantitative analysis of vitamin A, niacinamide, and riboflavin. When the compound of interest is not electroactive, it often can be derivatized to an electroactive form. One example is the differential pulse polarographic determination of sulfanilamide, which is converted into an electroactive azo dye by coupling with sulfamic acid and 1-napthol.

Representative Method 11.4.1: Determination of Chloropromazine in a Pharmaceutical Product

The best way to appreciate the theoretical and the practical details discussed in this section is to carefully examine a typical analytical method. Although each method is unique, the following description of the determination of chloropromazine in a pharmaceutical product provides an instructive example of a typical procedure. The description here is based on a method from Pungor, E. *A Practical Guide to Instrumental Analysis*, CRC Press: Boca Raton, FL, 1995, pp. 34–37.

Description of Method

Chlorpromazine, also is known by its trade name Thorazine, is an antipsychotic drug used in the treatment of schizophrenia. The amount of chlorpromazine in a pharmaceutical product is determined voltammetrically at a graphite working electrode in a unstirred solution, with calibration by the method of standard additions.

Procedure

Add 10.00 mL of an electrolyte solution consisting of 0.01 M HCl and 0.1 M KCl to the electrochemical cell. Place a graphite working electrode, a Pt auxiliary electrode, and a SCE reference electrode in the cell, and record the voltammogram from 0.2 V to 2.0 V at a scan rate of 50 mV/s. Weigh out an appropriate amount of the pharmaceutical product and dissolve it in a small amount of the electrolyte. Transfer the solution to a 100-mL volumetric flask and dilute to volume with the electrolyte. Filter a small amount of the diluted solution and transfer 1.00 mL of the filtrate to the voltammetric cell. Mix the contents of the voltammetric cell and allow the solution to sit for 10 s before recording the voltammogram. Return the potential to 0.2 V, add 1.00 mL of a chlorpromazine standard and record the voltammogram. Report the %w/w chlorpromazine in the formulation.

Questions

1. Is chlorpromazine undergoing oxidation or reduction at the graphite working electrode?

    Because we are scanning toward more positive potentials, we are oxidizing chlorpromazine.

2. Why does this procedure use a graphite electrode instead of a Hg electrode?

As shown in Figure 11.4.2 , the potential window for a Hg electrode extends from approximately –0.3 V to between –1V and –2 V, de- pending on the pH. Because we are scanning the potential from 0.2 V to 2.0 V, we cannot use a Hg electrode.

3. Many voltammetric procedures require that we first remove dissolved O_2 by bubbling N_2 through the solution. Why is this not necessary for this analysis?

Dissolved O_2 is a problem when we scan toward more negative potentials, because its reduction may produce a significant cathodic current. In this procedure we are scanning toward more positive potentials and generating anodic currents; thus, dissolved O_2 is not an interferent and does not need to be removed.

4. What is the purpose of recording a voltammogram in the absence of chlorpromazine?

This voltammogram serves as a blank, which provides a measurement of the residual current due to the electrolyte. Because the potential window for a graphite working electrode (see Figure 11.4.2) does not extend to 2.0 V, there is a measurable anodic residual current due to the solvent's oxidation. Having measured this residual current, we can subtract it from the total current in the presence of chlorpromazine.

5. Based on the description of this procedure, what is the shape of the resulting voltammogram. You may wish to review the three common shapes shown in Figure 11.4.9 .

Because the solution is unstirred, the voltammogram will have a peak current similar to that shown in Figure 11.4.9 b.

Characterization Applications

In the previous section we learned how to use voltammetry to determine an analyte's concentration in a variety of different samples. We also can use voltammetry to characterize an analyte's properties, including verifying its electrochemical reversibility, determining the number of electrons transferred during its oxidation or reduction, and determining its equilibrium constant in a coupled chemical reaction.

Electrochemical Reversibility and Determination of *n*

Earlier in this chapter we derived a relationship between $E_{1/2}$ and the standard-state potential for a redox couple (Equation 4.4.9), noting that a redox reaction must be electrochemically reversible. How can we tell if a redox reaction is reversible by looking at its voltammogram? For a reversible redox reaction Equation 4.4.8, which we repeat here, describes the relationship between potential and current for a voltammetric experiment with a limiting current.

$$E = E^{\circ}_{O/R} - \frac{0.05916}{n}\log\frac{K_O}{K_R} - \frac{0.05916}{n}\log\frac{i}{i_l - i}$$

If a reaction is electrochemically reversible, a plot of E versus $\log(i/i_l - i)$ is a straight line with a slope of $-0.05916/n$. In addition, the slope should yield an integer value for n.

Example 11.4.3

The following data were obtained from a linear scan hydrodynamic voltammogram of a reversible reduction reaction.

E (V vs. SCE)	current (μA)
–0.358	0.37
–0.372	0.95
–0.382	1.71
–0.400	3.48
–0.410	4.20
–0.435	4.97

The limiting current is 5.15 μA. Show that the reduction reaction is reversible, and determine values for n and for $E_{1/2}$.

Solution

Figure 11.4.20 shows a plot of E versus $\log(i/i_l–i)$. Because the result is a straight-line, we know the reaction is electrochemically reversible under the conditions of the experiment. A linear regression analysis gives the equation for the straight line as

$$E = -0.391\text{V} - 0.0300 \log \frac{i}{i_l - i}$$

From Equation 4.4.8, the slope is equivalent to –0.05916/n; solving for n gives a value of 1.97, or 2 electrons. From Equation 4.4.8 and Equation 4.4.9, we know that $E_{1/2}$ is the y-intercept for a plot of E versus $\log(i/i_l - i)$; thus, $E_{1/2}$ for the data in this example is –0.391 V versus the SCE.

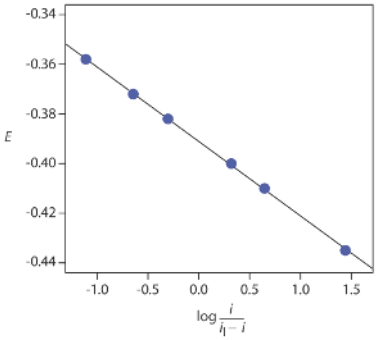


Figure 11.4.20 . Determination of electrochemical reversibility for the data in Example 11.4.3 .

We also can use cyclic voltammetry to evaluate electrochemical reversibility by looking at the difference between the peak potentials for the anodic and the cathodic scans. For an electrochemically reversible reaction, the following equation holds true.

$$\Delta E_p = E_{p,a} - E_{p,c} = \frac{0.05916 \text{ V}}{n}$$

As an example, for a two-electron reduction we expect a ΔE_p of approximately 29.6 mV. For an electrochemically irreversible reaction the value of ΔE_p is larger than expected.

Determining Equilibrium Constants for Coupled Chemical Reactions

Another important application of voltammetry is determining the equilibrium constant for a solution reaction that is coupled to a redox reaction. The presence of the solution reaction affects the ease of electron transfer in the redox reaction, shifting $E_{1/2}$ to a more negative or to a more positive potential. Consider, for example, the reduction of O to R

$$O + ne^- \rightleftharpoons R$$

the voltammogram for which is shown in Figure 11.4.21 . If we introduce a ligand, L, that forms a strong complex with O, then we also must consider the reaction

$$O + pL \rightleftharpoons OL_p$$

In the presence of the ligand, the overall redox reaction is

$$OL_p + ne^- \rightleftharpoons R + pL$$

Because of its stability, the reduction of the OL_p complex is less favorable than the reduction of O. As shown in Figure 11.4.21 , the resulting voltammogram shifts to a potential that is more negative than that for O. Furthermore, the shift in the voltammogram increases as we increase the ligand's concentration.

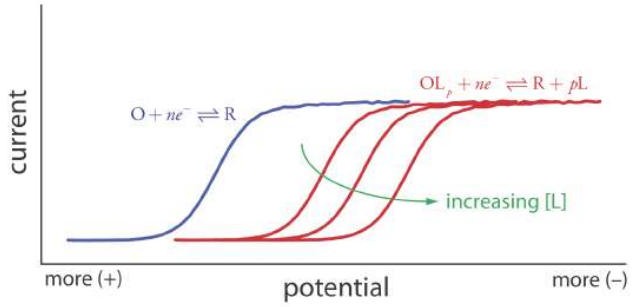


Figure 11.4.21 . Effect of a metal-ligand complexation reaction on a voltammogram. The voltammogram in blue is for the reduction of *O* in the absence of ligand. Adding the ligand shifts the potentials to more negative potentials, as shown by the voltammograms in red.

We can use this shift in the value of $E_{1/2}$ to determine both the stoichiometry and the formation constant for a metal-ligand complex. To derive a relationship between the relevant variables we begin with two equations: the Nernst equation for the reduction of *O*

$$E = E^{\circ}_{O/R} - \frac{0.05916}{n} \log \frac{[R]_{x=0}}{[O]_{x=0}} \tag{4.4.10}$$

and the stability constant, β_p for the metal-ligand complex at the electrode surface.

$$\beta_p = \frac{[OL_p]_{x=0}}{[O]_{x=0}[L]^p_{x=0}} \tag{4.4.11}$$

In the absence of ligand the half-wave potential occurs when $[R]_{x = 0}$ and $[O]_{x = 0}$ are equal; thus, from the Nernst equation we have

$$(E_{1/2})_{nc} = E^{\circ}_{O/R} \tag{4.4.12}$$

where the subscript "*nc*" signifies that the complex is not present.
When ligand is present we must account for its effect on the concentration of *O*. Solving Equation 4.4.1 for $[O]_{x = 0}$ and substituting into the Equation 4.4.10 gives

$$E = E^{\circ}_{O/R} - \frac{0.05916}{n} \log \frac{[R]_{x=0}[L]^p_{x=0}\beta_p}{[OL_p]_{x=0}} \tag{4.4.13}$$

If the formation constant is sufficiently large, such that essentially all *O* is present as the complex OL_p, then $[R]_{x = 0}$ and $[OL_p]_{x = 0}$ are equal at the half-wave potential, and Equation 4.4.13 simplifies to

$$(E_{1/2})_c = E^{\circ}_{O/R} - \frac{0.05916}{n} \log [L]^p_{x=0}\beta_p \tag{4.4.14}$$

where the subscript "*c*" indicates that the complex is present. Defining $\Delta E_{1/2}$ as

$$\triangle E_{1/2} = (E_{1/2})_c - (E_{1/2})_{nc} \tag{4.4.15}$$

and substituting Equation 4.4.12 and Equation 4.4.14 and expanding the log term leaves us with the following equation.

$$\Delta E_{1/2} = -\frac{0.05916}{n} \log \beta_p - \frac{0.05916p}{n} \log [L] \tag{4.4.16}$$

A plot of $\Delta E_{1/2}$ versus log[*L*] is a straight-line, with a slope that is a function of the metal-ligand complex's stoichiometric coefficient, *p*, and a *y*-intercept that is a function of its formation constant β_p.

Example 11.4.4

A voltammogram for the two-electron reduction (n = 2) of a metal, *M*, has a half-wave potential of –0.226 V versus the SCE. In the presence of an excess of ligand, *L*, the following half-wave potentials are recorded.

[L] (M)	$(E_{1/2})_c$ (V vs. SCE)
0.020	–0.494
0.040	–0.512
0.060	–0.523
0.080	–0.530
0.100	–0.536

Determine the stoichiometry of the metal-ligand complex and its formation constant.

Solution

We begin by calculating values of $\Delta E_{1/2}$ using Equation 4.4.15, obtaining the values in the following table.

[L] (M)	$\Delta E_{1/2}$ (V vs. SCE)
0.020	–0.268
0.040	–0.286
0.060	–0.297
0.080	–0.304
0.100	–0.310

Figure 11.4.22 shows the resulting plot of $\Delta E_{1/2}$ as a function of log[L]. A linear regression analysis gives the equation for the straight line as

$$\Delta E_{1/2} = -0.370\text{V} - 0.0601 \log [L]$$

From Equation 4.4.16 we know that the slope is equal to –0.05916p/n. Using the slope and n = 2, we solve for p obtaining a value of 2.03 ≈ 2. The complex's stoichiometry, therefore, is ML_2. We also know, from Equation 4.4.16, that the y-intercept is equivalent to –(0.05916/n)logβ_p. Solving for β_2 gives a formation constant of 3.2×10^{12}.

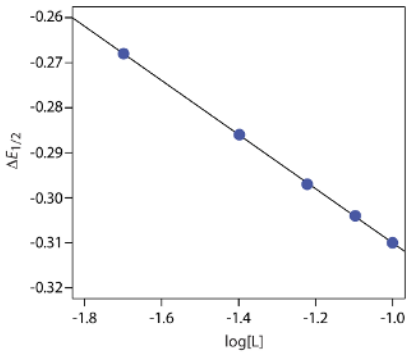


Figure 11.4.22 . Determination of the stoichiometry and formation constant for a metal-ligand complex using the data in Example 11.4.4 .

? Exercise 11.4.2

The voltammogram for 0.50 mM Cd^{2+} has an $E_{1/2}$ of –0.565 V versus an SCE. After making the solution 0.115 M in ethylenediamine, $E_{1/2}$ is –0.845 V, and $E_{1/2}$ is –0.873 V when the solution is 0.231 M in ethylenediamine. Determine the stoichiometry of the Cd^{2+}–ethylenediamine complex and its formation constant. The data in this problem comes from

Morinaga, K. "Polarographic Studies of Metal Complexes. V. Ethylenediamine Complexes of Cadmium, Nickel, and Zinc," *Bull. Chem. Soc. Japan* **1956**, *29*, 793–799.

Answer

For simplicity, we will use *en* as a shorthand notation for ethylenediamine. From the three half-wave potentials we have a $\Delta E_{1/2}$ of –0.280 V for 0.115 M en and a $\Delta E_{1/2}$ of –0.308 V for 0.231 M en. Using Equation 4.4.16 we write the following two equations.

$$-0.280 = -\frac{0.05916}{2}\log\beta_p - \frac{0.05916p}{2}\log(0.115)$$
$$-0.308 = -\frac{0.05916}{2}\log\beta_p - \frac{0.05916p}{2}\log(0.231)$$

To solve for the value of *p*, we first subtract the second equation from the first equation

$$0.028 = -\frac{0.05916p}{2}\log(0.115) - \left\{-\frac{0.05916p}{2}\log(0.231)\right\}$$

which eliminates the term with β_p. Next we solve this equation for *p*

$$0.028 = \left(2.778 \times 10^{-2}\right) \times p - \left(1.882 \times 10^{-2}\right) \times p = \left(8.96 \times 10^{-3}\right) \times p$$

obtaining a value of 3.1, or $p \approx 3$. Thus, the complex is $Cd(en)_3$. To find the formation complex, β_3, we return to Equation 4.4.16, using our value for *p*. Using the data for an en concentration of 0.115 M

$$-0.280 = -\frac{0.05916}{2}\log\beta_3 - \frac{0.05916 \times 3}{2}\log(0.115)$$
$$-0.363 = -\frac{0.05916}{2}\log\beta_3$$

gives a value for β_3 of 1.92×10^{12}. Using the data for an en concentration of 0.231 M gives a value of 2.10×10^{12}.

As suggested by Figure 11.4.15 , cyclic voltammetry is one of the most powerful electrochemical techniques for exploring the mechanism of coupled electrochemical and chemical reactions. The treatment of this aspect of cyclic voltammetry is beyond the level of this text, although you can consult this chapter's additional resources for additional information.

Evaluation

Scale of Operation

Detection levels at the parts-per-million level are routine. For some analytes and for some voltammetric techniques, lower detection limits are possible. Detection limits at the parts-per-billion and the part-per-trillion level are possible with stripping voltammetry. Although most analyses are carried out in conventional electrochemical cells using macro samples, the availability of microelectrodes with diameters as small as 2 μm, allows for the analysis of samples with volumes under 50 μL. For example, the concentration of glucose in 200-μm pond snail neurons was monitored successfully using an amperometric glucose electrode with a 2 mm tip [Abe, T.; Lauw, L. L.; Ewing, A. G. *J. Am. Chem. Soc.* **1991**, *113*, 7421–7423].

Accuracy

The accuracy of a voltammetric analysis usually is limited by our ability to correct for residual currents, particularly those due to charging. For an analyte at the parts-per-million level, an accuracy of ±1–3% is routine. Accuracy decreases for samples with significantly smaller concentrations of analyte.

Precision

Precision generally is limited by the uncertainty in measuring the limiting current or the peak current. Under most conditions, a precision of ±1–3% is reasonable. One exception is the analysis of ultratrace analytes in complex matrices by stripping voltammetry, in which the precision may be as poor as ±25%.

Sensitivity

In many voltammetric experiments, we can improve the sensitivity by adjusting the experimental conditions. For example, in stripping voltammetry we can improve sensitivity by increasing the deposition time, by increasing the rate of the linear potential scan, or by using a differential-pulse technique. One reason that potential pulse techniques are popular is that they provide an improvement in current relative to a linear potential scan.

Selectivity

Selectivity in voltammetry is determined by the difference between half-wave potentials or peak potentials, with a minimum difference of ±0.2–0.3 V for a linear potential scan and ±0.04–0.05 V for differential pulse voltammetry. We often can improve selectivity by adjusting solution conditions. The addition of a complexing ligand, for example, can substantially shift the potential where a species is oxidized or reduced to a potential where it no longer interferes with the determination of an analyte. Other solution parameters, such as pH, also can be used to improve selectivity.

Time, Cost, and Equipment

Commercial instrumentation for voltammetry ranges from <$1000 for simple instruments to >$20,000 for a more sophisticated instrument. In general, less expensive instrumentation is limited to linear potential scans. More expensive instruments provide for more complex potential-excitation signals using potential pulses. Except for stripping voltammetry, which needs a long deposition time, voltammetric analyses are relatively rapid.

This page titled 4.4: Voltammetric and Amperometric Methods is shared under a CC BY-NC-SA 4.0 license and was authored, remixed, and/or curated by David Harvey.

- **11.4: Voltammetric and Amperometric Methods** by David Harvey is licensed CC BY-NC-SA 4.0.

4.4.1: Cyclic Voltammetry

4.4.1: Cyclic Voltammetry is shared under a not declared license and was authored, remixed, and/or curated by LibreTexts.

4.4.2: Anodic Stripping Voltammetry

4.4.2: Anodic Stripping Voltammetry is shared under a not declared license and was authored, remixed, and/or curated by LibreTexts.

4.5: Problems

1. Identify the anode and the cathode for the following electrochemical cells, and identify the oxidation or the reduction reaction at each electrode.

(a) Pt| $FeCl_2$ (*aq*, 0.015), $FeCl_3$ (*aq*, 0.045) || $AgNO_3$ (*aq*, 0.1) | Ag

(b) Ag | AgBr(*s*), NaBr (*aq*, 1.0) || $CdCl_2$ (*aq*, 0.05) | Cd

(c) Pb | $PbSO_4$ (*s*), H_2SO_4 (*aq*, 1.5) || H_2SO_4 (*aq*, 2.0), $PbSO_4$ (*s*) | PbO_2

2. Calculate the potential for each electrochemical cell in problem 1. The values in parentheses are the activities of the associated species.

3. Calculate the activity of KI, *x*, in the following electrochemical cell if the potential is +0.294 V.

$$Ag \mid AgCl\ (s), NaCl\ (aq, 0.1) \parallel KI\ (aq, x), I_2\ (s) \mid Pt$$

4. What reaction prevents us from using Zn as an electrode of the first kind in an acidic solution? Which other metals do you expect to behave in the same manner as Zn when immersed in an acidic solution?

5. Creager and colleagues designed a salicylate ion-selective electrode using a PVC membrane impregnated with tetraalkylammonium salicylate [Creager, S. E.; Lawrence, K. D.; Tibbets, C. R. *J. Chem. Educ.* **1995**, *72*, 274–276]. To determine the ion-selective electrode's selectivity coefficient for benzoate, they prepared a set of salicylate calibration standards in which the concentration of benzoate was held constant at 0.10 M. Using the following data, determine the value of the selectivity coefficient.

[salicylate] (M)	potential (mV)
1.0	20.2
1.0×10^{-1}	73.5
1.0×10^{-2}	126
1.0×10^{-3}	168
1.0×10^{-4}	182
1.0×10^{-5}	182
1.0×10^{-6}	177

What is the maximum acceptable concentration of benzoate if you plan to use this ion-selective electrode to analyze a sample that contains as little as 10^{-5} M salicylate with an accuracy of better than 1%?

6. Watanabe and co-workers described a new membrane electrode for the determination of cocaine, a weak base alkaloid with a pK_a of 8.64 [Watanabe, K.; Okada, K.; Oda, H.; Furuno, K.; Gomita, Y.; Katsu, T. *Anal. Chim. Acta* **1995**, *316*, 371–375]. The electrode's response for a fixed concentration of cocaine is independent of pH in the range of 1–8, but decreases sharply above a pH of 8. Offer an explanation for this pH dependency.

7. Figure 11.2.14 shows a schematic diagram for an enzyme electrode that responds to urea by using a gas-sensing NH_3 electrode to measure the amount of ammonia released following the enzyme's reaction with urea. In turn, the NH_3 electrode uses a pH electrode to monitor the change in pH due to the ammonia. The response of the urea electrode is given by equation 11.2.12. Beginning with equation 11.2.19, which gives the potential of a pH electrode, show that equation 11.2.12 for the urea electrode is correct.

8. Explain why the response of an NH_3-based urea electrode (Figure 11.2.14 and equation 11.2.12) is different from the response of a urea electrode in which the enzyme is coated on the glass membrane of a pH electrode (Figure 11.2.15 and equation 11.2.13).

9. A potentiometric electrode for HCN uses a gas-permeable membrane, a buffered internal solution of 0.01 M $KAg(CN)_2$, and a Ag_2S ISE electrode that is immersed in the internal solution. Consider the equilibrium reactions that take place within the internal

solution and derive an equation that relates the electrode's potential to the concentration of HCN in the sample. To check your work, search on-line for US Patent 3859191 and consult Figure 2.

10. Mifflin and associates described a membrane electrode for the quantitative analysis of penicillin in which the enzyme penicillinase is immobilized in a polyacrylamide gel coated on the glass membrane of a pH electrode [Mifflin, T. E.; Andriano, K. M.; Robbins, W. B. *J. Chem. Educ.* **1984**, *61*, 638–639]. The following data were collected using a set of penicillin standards.

[penicillin] (M)	potential (mV)
1.0×10^{-2}	220
2.0×10^{-3}	204
1.0×10^{-3}	190
2.0×10^{-4}	153
1.0×10^{-4}	135
1.0×10^{-5}	96
1.0×10^{-6}	80

(a) Over what range of concentrations is there a linear response?

(b) What is the calibration curve's equation for this concentration range?

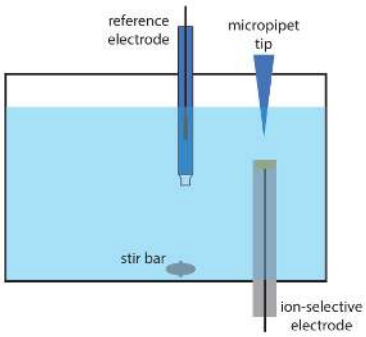
(c) What is the concentration of penicillin in a sample that yields a potential of 142 mV?

11. An ion-selective electrode can be placed in a flow cell into which we inject samples or standards. As the analyte passes through the cell, a potential spike is recorded instead of a steady-state potential. The concentration of K^+ in serum has been determined in this fashion using standards prepared in a matrix of 0.014 M NaCl [Meyerhoff, M. E.; Kovach, P. M. *J. Chem. Educ.* **1983**, *9*, 766–768].

$[K^+]$ (mM)	*E* (arb. units)	$[K^+]$ (mM)	*E* (arb. units)
0.10	25.5	0.60	58.7
0.20	37.2	0.80	64.0
0.40	50.8	1.00	66.8

A 1.00-mL sample of serum is diluted to volume in a 10-mL volumetric flask and analyzed, giving a potential of 51.1 (arbitrary units). Report the concentration of K^+ in the sample of serum.

12. Wang and Taha described an interesting application of potentiometry, which they call batch injection [Wang, J.; Taha, Z. *Anal. Chim. Acta* **1991**, *252*, 215–221]. As shown in the figure below, an ion-selective electrode is placed in an inverted position in a large volume tank, and a fixed volume of a sample or a standard solution is injected toward the electrode's surface using a micropipet. The response of the electrode is a spike in potential that is proportional to the analyte's concentration. The following data were collected using a pH electrode and a set of pH standards.



pH	potential (mV)
2.0	+300
3.0	+240
4.0	+168
5.0	+81
6.0	+35
8.0	–92
9.0	–168
10.0	–235
11.0	–279

Determine the pH of the following samples given the recorded peak potentials: tomato juice, 167 mV; tap water, –27 mV; coffee, 122 mV.

13. The concentration of NO_3^- in a water sample is determined by a one-point standard addition using a NO_3^- ion-selective electrode. A 25.00-mL sample is placed in a beaker and a potential of 0.102 V is measured. A 1.00-mL aliquot of a 200.0-mg/L standard solution of NO_3^- is added, after which the potential is 0.089 V. Report the mg NO_3^-/L in the water sample.

14. In 1977, when I was an undergraduate student at Knox College, my lab partner and I completed an experiment to determine the concentration of fluoride in tap water and the amount of fluoride in toothpaste. The data in this problem are from my lab notebook.

(a) To analyze tap water, we took three 25.0-mL samples and added 25.0 mL of TISAB to each. We measured the potential of each solution using a F^- ISE and an SCE reference electrode. Next, we made five 1.00-mL additions of a standard solution of 100.0 ppm F^- to each sample, and measured the potential after each addition, recording the potential three times.

mL of standard added	potential (mV), replicate 1	potential (mV), replicate 2	potential (mV), replicate 3
0.00	–79	–82	–83
1.00	–119	–119	–118
2.00	–133	–133	–133
3.00	–142	–142	–142
4.00	–149	–148	–148
5.00	–154	–153	–153

Report the parts-per-million of F^- in the tap water.

(b) To analyze the toothpaste, we measured 0.3619 g into a 100-mL volumetric flask, added 50.0 mL of TISAB, and diluted to volume with distilled water. After we ensured that the sample was thoroughly mixed, we transferred three 20.0-mL portions into separate beakers and measured the potential of each using a F^- ISE and an SCE reference electrode. Next, we made five 1.00-mL additions of a standard solution of 100.0 ppm F^- to each sample, and measured the potential after each addition, recording the potential three times.

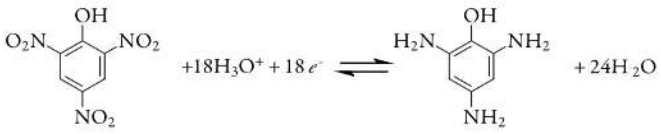
mL of standard added	potential (mV), replicate 1	potential (mV), replicate 2	potential (mV), replicate 3
0.00	–55	–54	–55
1.00	–82	–82	–83
2.00	–94	–94	–94
3.00	–102	–103	–102
4.00	–108	–108	–109
5.00	–112	–112	–113

Report the parts-per-million F^- in the toothpaste.

15. You are responsible for determining the amount of KI in iodized salt and decide to use an I^- ion-selective electrode. Describe how you would perform this analysis using external standards and how you would per-form this analysis using the method of standard additions.

16. Explain why each of the following decreases the analysis time in controlled-potential coulometry: a larger surface area for the working electrode; a smaller volume of solution; and a faster stirring rate.

17. The purity of a sample of picric acid, $C_6H_3N_3O_7$, is determined by controlled-potential coulometry, converting picric acid to triaminophenol, $C_6H_9N_3O$.



A 0.2917-g sample of picric acid is placed in a 1000-mL volumetric flask and diluted to volume. A 10.00-mL portion of this solution is transferred to a coulometric cell and sufficient water added so that the Pt cathode is immersed. An exhaustive electrolysis of the sample re-quires 21.67 C of charge. Report the purity of the picric acid.

18. The concentration of H_2S in the drainage from an abandoned mine is determined by a coulometric titration using KI as a mediator and I_3^- as the titrant.

$$H_2S(aq) + I_3^-(aq) + 2H_2O(l) \rightleftharpoons 2H_3O^+(aq) + 3I^-(aq) + S(s)$$

A 50.00-mL sample of water is placed in a coulometric cell, along with an excess of KI and a small amount of starch as an indicator. Electrolysis is carried out at a constant current of 84.6 mA, requiring 386 s to reach the starch end point. Report the concentration of H_2S in the sample in μg/mL.

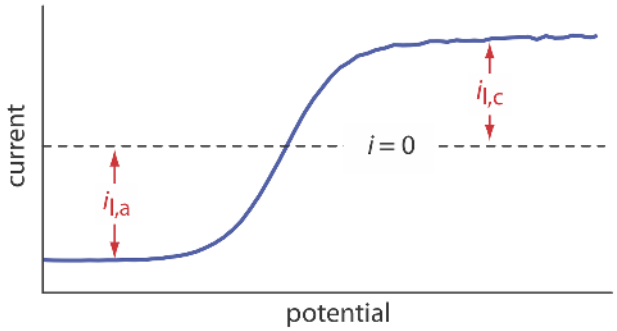
19. One method for the determination of a given mass of H_3AsO_3 is a coulometric titration using I_3^- as a titrant. The relevant standard-state reactions and potentials are summarized here

$$H_3AsO_4(aq) + 2H^+(aq) + 2e^- \rightleftharpoons H_3AsO_3(aq) + H_2O(l)$$
$$I_3^-(aq) + 2e^- \rightleftharpoons 3I^-(aq)$$

with standard state reduction potentials of, respectively, +0.559 V and +0.536 V. Explain why the coulometric titration is carried out in a neutral solution (pH ≈ 7) instead of in a strongly acidic solution (pH < 0).

20. The production of adiponitrile, $NC(CH_2)_4CN$, from acrylonitrile, CH_2=CHCN, is an important industrial process. A 0.594-g sample of acrylonitrile is placed in a 1-L volumetric flask and diluted to volume. An exhaustive controlled-potential electrolysis of a 1.00-mL portion of the diluted acrylonitrile requires 1.080 C of charge. What is the value of *n* for the reduction of acrylonitrile to adiponitrile?

21. The linear-potential scan hydrodynamic voltammogram for a mixture of Fe^{2+} and Fe^{3+} is shown in the figure below where $i_{l,a}$ and $i_{l,c}$ are the anodic and cathodic limiting currents.



(a) Show that the potential is given by

$$E = E^{\circ}_{Fe^{3+}/Fe^{2+}} - 0.05916 \log \frac{K_{Fe^{3+}}}{K_{Fe^{2+}}} - 0.05916 \log \frac{i - i_{l,a}}{i_{l,c} - i}$$

(b) What is the potential when i = 0 for a solution that is 0.100 mM Fe^{3+} and 0.050 mM Fe^{2+}?

22. The amount of sulfur in aromatic monomers is determined by differential pulse polarography. Standard solutions are prepared for analysis by dissolving 1.000 mL of the purified monomer in 25.00 mL of an electrolytic solvent, adding a known amount of sulfur, deaerating, and measuring the peak current. The following results were obtained for a set of calibration standards.

µg S added	peak current (µA)
0	0.14
28	0.70
56	1.23
112	2.41
168	3.42

Analysis of a 1.000-mL sample, treated in the same manner as the standards, gives a peak current of 1.77 µA. Report the mg S/mL in the sample.

23. The purity of a sample of $K_3Fe(CN)_6$ is determined using linear-potential scan hydrodynamic voltammetry at a glassy carbon electrode. The following data were obtained for a set of external calibration standards.

$[K_3Fe(CN)_6]$ (mM)	limiting current (µA)
2.0	127
4.0	252
6.0	376
8.0	500
10.0	624

A sample of impure $K_3Fe(CN)_6$ is prepared for analysis by diluting a 0.246-g portion to volume in a 100-mL volumetric flask. The limiting current for the sample is 444 μA. Report the purity of this sample of $K_3Fe(CN)_6$.

24. One method for determining whether an individual recently fired a gun is to look for traces of antimony in residue collected from the individual's hands. Anodic stripping voltammetry at a mercury film electrode is ideally suited for this analysis. In a typical analysis a sample is collected from a suspect using a cotton-tipped swab wetted with 5% v/v HNO_3. After returning to the lab, the swab is placed in a vial that contains 5.0 mL of 4 M HCl that is 0.02 M in hydrazine sulfate. After soaking the swab, a 4.0-mL portion of the solution is transferred to an electrochemical cell along with 100 μL of 0.01 M $HgCl_2$. After depositing the thin film of mercury and the antimony, the stripping step gives a peak current of 0.38 μA. After adding a standard addition of 100 μL of 5.00×10^2 ppb Sb, the peak current increases to 1.14 μA. How many nanograms of Sb were collected from the suspect's hand?

25. Zinc is used as an internal standard in an analysis of thallium by differential pulse polarography. A standard solution of 5.00×10^{-5} M Zn^{2+} and 2.50×10^{-5} M Tl^+ has peak currents of 5.71 μA and 3.19 μA, respectively. An 8.713-g sample of a zinc-free alloy is dissolved in acid, transferred to a 500-mL volumetric flask, and diluted to volume. A 25.0-mL portion of this solution is mixed with 25.0 mL of 5.00×10^{-4} M Zn^{2+}. Analysis of this solution gives peak currents of 12.3 μA and of 20.2 μA for Zn^{2+} and Tl^+, respectively. Report the %w/w Tl in the alloy.

26. Differential pulse voltammetry at a carbon working electrode is used to determine the concentrations of ascorbic acid and caffeine in drug formulations [Lau, O.; Luk, S.; Cheung, Y. *Analyst* **1989**, *114*, 1047–1051]. In a typical analysis a 0.9183-g tablet is crushed and ground into a fine powder. A 0.5630-g sample of this powder is transferred to a 100-mL volumetric flask, brought into solution, and diluted to volume. A 0.500-mL portion of this solution is then transferred to a voltammetric cell that contains 20.00 mL of a suitable supporting electrolyte. The resulting voltammogram gives peak currents of 1.40 μA and 3.88 μA for ascorbic acid and for caffeine, respectively. A 0.500-mL aliquot of a standard solution that contains 250.0 ppm ascorbic acid and 200.0 ppm caffeine is then added. A voltammogram of this solution gives peak currents of 2.80 μA and 8.02 μA for ascorbic acid and caffeine, respectively. Report the milligrams of ascorbic acid and milligrams of caffeine in the tablet.

27. Ratana-ohpas and co-workers described a stripping analysis method for determining tin in canned fruit juices [Ratana-ohpas, R.; Kanatharana, P.; Ratana-ohpas, W.; Kongsawasdi, W. *Anal. Chim. Acta* **1996**, *333*, 115–118]. Standards of 50.0 ppb Sn^{4+}, 100.0 ppb Sn^{4+}, and 150.0 ppb Sn^{4+} were analyzed giving peak currents (arbitrary units) of 83.0, 171.6, and 260.2, respectively. A 2.00-mL sample of lychee juice is mixed with 20.00 mL of 1:1 HCl/HNO_3. A 0.500-mL portion of this mixture is added to 10 mL of 6 M HCl and the volume adjusted to 30.00 mL. Analysis of this diluted sample gave a signal of 128.2 (arbitrary units). Report the parts-per-million Sn^{4+} in the original sample of lychee juice.

28. Sittampalam and Wilson described the preparation and use of an amperometric sensor for glucose [Sittampalam, G.; Wilson, G. S. *J. Chem. Educ.* **1982**, *59*, 70–73]. The sensor is calibrated by measuring the steady-state current when it is immersed in standard solutions of glucose. A typical set of calibration data is shown here.

[glucose] (mg/100 mL)	current (arb. units)
2.0	17.2
4.0	32.9
6.0	52.1
8.0	68.0
10.0	85.8

A 2.00-mL sample is diluted to 10 mL in a volumetric flask and a steady-state current of 23.6 (arbitrary units) is measured. What is the concentration of glucose in the sample in mg/100 mL?

29. Differential pulse polarography is used to determine the concentrations of lead, thallium, and indium in a mixture. Because the peaks for lead and thallium, and for thallium and indium overlap, a simultaneous analysis is necessary. Peak currents (in arbitrary units) at –0.385 V, –0.455 V, and –0.557 V are measured for a single standard solution, and for a sample, giving the results shown in the following table. Report the mg/mL of Pb^{2+}, Tl^+ and In^{3+} in the sample.

analyte	[standard] (μg/mL)	peak current at –0.385 V	peak current at –0.455 V	peak current at –0.557 V
Pb^{2+}	1.0	26.1	2.9	0
Tl^{+}	2.0	7.8	23.5	3.2
In^{3+}	0.4	0	0	22.9
sample		60.6	28.8	54.1

30. Abass and co-workers developed an amperometric biosensor for NH_4^+ that uses the enzyme glutamate dehydrogenase to catalyze the following reaction

$$\text{2 - oxyglutarate}\,(aq) + NH_4^+(aq) + \text{NADH}(aq) \rightleftharpoons \text{glutamate}\,(aq) + NAD^+(aq) + H_2O(l)$$

where NADH is the reduced form of nicotinamide adenine dinucleotide [Abass, A. K.; Hart, J. P.; Cowell, D. C.; Chapell, A. *Anal. Chim. Acta* **1988**, *373*, 1–8]. The biosensor actually responds to the concentration of NADH, however, the rate of the reaction depends on the concentration of NH_4^+. If the initial concentrations of 2-oxyglutarate and NADH are the same for all samples and standards, then the signal is proportional to the concentration of NH_4^+. As shown in the following table, the sensitivity of the method is dependent on pH.

pH	sensitivity (nA S^{-1} M^{-1})
6.2	1.67×10^3
6.75	5.00×10^3
7.3	9.33×10^3
7.7	1.04×10^4
8.3	1.27×10^4
9.3	2.67×10^3

Two possible explanations for the effect of pH on the sensitivity of this analysis are the acid–base chemistry of NH_4^+ and the acid–base chemistry of the enzyme. Given that the pK_a for NH_4^+ is 9.244, explain the source of this pH-dependent sensitivity.

31. The speciation scheme for trace metals in Table 11.4.2 divides them into seven operationally defined groups by collecting and analyzing two samples following each of four treatments, requiring a total of eight samples and eight measurements. After removing insoluble particulates by filtration (treatment 1), the solution is analyzed for the concentration of ASV labile metals and for the total concentration of metals. A portion of the filtered solution is then passed through an ion-exchange column (treatment 2), and the concentrations of ASV metal and of total metal are determined. A second portion of the filtered solution is irradiated with UV light (treatment 3), and the concentrations of ASV metal and of total metal are measured. Finally, a third portion of the filtered solution is irradiated with UV light and passed through an ion-exchange column (treatment 4), and the concentrations of ASV labile metal and of total metal again are determined. The groups that are included in each measurement are summarized in the following table.

treatment	groups removed by treatement	groups contributing to ASV-labile metals	groups contributing to total metals
1	none	I, II, III	I, II, III, IV, V, VI, VII
2	I, IV, V	II, III	II, III, V1, VII
3	none	I, II, III, IV, VI	I, II, III, IV, V, VI, VII
4	I, II, IV, V, VI	III	III, VII

(a) Explain how you can use these eight measurements to determine the concentration of metals present in each of the seven groups identified in Table 11.4.2.

(b) Batley and Florence report the following results for the speciation of cadmium, lead, and copper in a sample of seawater [Batley, G. E.; Florence, T. M. *Anal. Lett.* **1976**, *9*, 379–388]. Determine the speciation of each metal in comment on your results.

measurement treatement: ASV-labile or total	ppb Cd^{2+}	ppb Pb^{2+}	ppb Cu^{2+}
1: ASV-labile	0.24	0.39	0.26
2: total	0.28	0.50	0.40
2: ASV-labile	0.21	0.33	0.17
2: total	0.26	0.43	0.24
3: ASV-labile	0.26	0.37	0.33
3: total	0.28	0.5	0.43
4: ASV-labile	0.00	0.00	0.00
4: total	0.02	0.12	0.10

32. The concentration of Cu^{2+} in seawater is determined by anodic stripping voltammetry at a hanging mercury drop electrode after first releasing any copper bound to organic matter. To a 20.00-mL sample of seawater is added 1 mL of 0.05 M HNO_3 and 1 mL of 0.1% H_2O_2. The sample is irradiated with UV light for 8 hr and then diluted to volume in a 25-mL volumetric flask. Deposition of Cu^{2+} takes place at –0.3 V versus an SCE for 10 min, producing a peak current of 26.1 (arbitrary units). A second 20.00-mL sample of the seawater is treated identically, except that 0.1 mL of a 5.00 μM solution of Cu^{2+} is added, producing a peak current of 38.4 (arbitrary units). Report the concentration of Cu^{2+} in the seawater in mg/L.

33. Thioamide drugs are determined by cathodic stripping analysis [Davidson, I. E.; Smyth, W. F. Anal. Chem. 1977, 49, 1195–1198]. Deposition occurs at +0.05 V versus an SCE. During the stripping step the potential is scanned cathodically and a stripping peak is observed at –0.52 V. In a typical application a 2.00-mL sample of urine is mixed with 2.00 mL of a pH 4.78 buffer. Following a 2.00 min deposition, a peak current of 0.562 μA is measured. A 0.10-mL addition of a 5.00 μM solution of the drug is added to the same solution. A peak current of 0.837 μA is recorded using the same deposition and stripping conditions. Report the drug's molar concentration in the urine sample.

34. The concentration of vanadium (V) in sea water is determined by adsorptive stripping voltammetry after forming a complex with catechol [van der Berg, C. M. G.; Huang, Z. Q. *Anal. Chem.* **1984**, *56*, 2383–2386]. The catechol-V(V) complex is deposited on a hanging mercury drop electrode at a potential of –0.1 V versus a Ag/AgCl reference electrode. A cathodic potential scan gives a stripping peak that is proportional to the concentration of V(V). The following standard additions are used to analyze a sample of seawater.

$[V(V)]_{added}$ (M)	peak current (μA)
2.0×10^{-8}	24
4.0×10^{-8}	33
8.0×10^{-8}	52
1.2×10^{-7}	69
1.8×10^{-7}	97
2.8×10^{-7}	140

Determine the molar concentration of V (V) in the sample of sea water, assuming that the standard additions result in a negligible change in the sample's volume.

35. The standard-state reduction potential for Cu^{2+} to Cu is +0.342 V versus the SHE. Given that Cu^{2+} forms a very stable complex with the ligand EDTA, do you expect that the standard-state reduction potential for $Cu(EDTA)^{2-}$ is greater than +0.342 V, less than +0.342 V, or equal to +0.342 V? Explain your reasoning.

36. The polarographic half-wave potentials (versus the SCE) for Pb^{2+} and for Tl^{+} in 1 M HCl are, respectively, –0.44 V and –0.45 V. In an electrolyte of 1 M NaOH, however, the half-wave potentials are –0.76 V for Pb^{2+} and –0.48 V for Tl^{+}. Why does the change in electrolyte have such a significant effect on the half-wave potential for Pb^{2+}, but not on the half-wave potential for Tl^{+}?

37. The following data for the reduction of Pb^{2+} were collected by normal-pulse polarography.

potential (V vs. SCE)	current (μA)
–0.345	0.16
–0.370	0.98
–0.383	2.05
–0.393	3.13
–0.409	4.62
–0.420	5.16

The limiting current was 5.67 μA. Verify that the reduction reaction is reversible and determine values for n and $E_{1/2}$. The half-wave potentials for the normal-pulse polarograms of Pb^{2+} in the presence of several different concentrations of OH^{-} are shown in the following table.

$[OH^{-}]$ (M)	$E_{1/2}$ (V vs. SCE)	$[OH^{-}]$ (M)	$E_{1/2}$ (V vs. SCE)
0.050	–0.646	0.150	–0.689
0.100	–0.673	0.300	–0.715

Determine the stoichiometry of the Pb-hydroxide complex and its formation constant.

38. In 1977, when I was an undergraduate student at Knox College, my lab partner and I completed an experiment to study the voltammetric behavior of Cd^{2+} (in 0.1 M KNO_3) and Ni^{2+} (in 0.2 M KNO_3) at a dropping mercury electrode. The data in this problem are from my lab notebook. All potentials are relative to an SCE reference electrode.

potential for Cd^{2+} (V)	current for Cd^{2+} (μA)	potential for Ni^{2+} (V)	current for Ni^{2+} (μA)
–0.60	4.5	–1.07	1.90
–0.58	3.4	–1.05	1.75
–0.56	2.1	–1.03	1.50
–0.54	0.6	–1.02	1.25
–0.52	0.2	–1.00	1.00

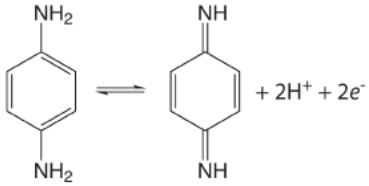
The limiting currents for Cd^{2+} was 4.8 μA and that for Ni^{2+} was 2.0 μA. Evaluate the electrochemical reversibility for each metal ion and comment on your results.

39. Baldwin and co-workers report the following data from a cyclic voltammetry study of the electrochemical behavior of *p*-phenylenediamine in a pH 7 buffer [Baldwin, R. P.; Ravichandran, K.; Johnson, R. K. *J. Chem. Educ.* **1984**, *61*, 820–823]. All

potentials are measured relative to an SCE.

scan rate (mV/s)	$E_{p,a}$ (V)	$E_{p,c}$ (V)	$i_{p,a}$ (mA)	$i_{p,c}$ (mA)
2	0.148	0.104	0.34	0.30
5	0.149	0.098	0.56	0.53
10	0.152	0.095	1.00	0.04
20	0.161	0.095	1.44	1.44
50	0.167	0.082	2.12	1.81
100	0.180	0.063	2.50	2.19

The initial scan is toward more positive potentials, leading to the oxidation reaction shown here.



Use this data to show that the reaction is electrochemically irreversible. A reaction may show electrochemical irreversibility because of slow electron transfer kinetics or because the product of the oxidation reaction participates in a chemical reaction that produces an nonelectroactive species. Based on the data in this problem, what is the likely source of *p*-phenylenediamine's electrochemical irreversibility?

This page titled 4.5: Problems is shared under a CC BY-NC-SA 4.0 license and was authored, remixed, and/or curated by David Harvey.

- **11.5: Problems** by David Harvey is licensed CC BY-NC-SA 4.0.

4.6: Additional Resources

The following set of experiments introduce students to the applications of electrochemistry. Experiments are grouped into four categories: general electrochemistry, preparation of electrodes, potentiometry, coulometry, and voltammetry and amperometry.

General Electrochemistry

- Chatmontree, A.; Chairam, S.; Supasorn, S.; Amatatongchai, M.; Jarujamrus, P; Tamuang, S.; Somsook E. “Student Fabriaction and Use of Simple, Low-Cost, Paper-Based Galvanic Cells to Investigate Electrochemistry,” *J. Chem. Educ.* **2015**, *92*, 1044–1048.
- Mills, K. V.; Herrick, R. S.; Guilmette, L. W.; Nestor, L. P.; Shafer, H.; Ditzler, M. A. “Introducing Undergraduate Students to Electrochemistry: A Two-Week Discovery Chemistry Experiment,” *J. Chem. Educ.* **2008**, *85*, 1116–119.

Preparation of Electrodes

- Christopoulos, T. K.; Diamandis, E. P. “Use of a Sintered Glass Crucible for Easy Construction of Liquid-Membrane Ion-Selective Electrodes,” *J. Chem. Educ.* **1988**, *65*, 648.
- Fricke, G. H.; Kuntz, M. J. “Inexpensive Solid-State Ion-Selective Electrodes for Student Use,” *J. Chem. Educ.* **1977**, *54*, 517–520.
- Inamdar, S. N.; Bhat, M. A.; Haram, S. K. “Construction of Ag/AgCl Reference Electrode form Used Felt-Tipped Pen Barrel for Undergraduate Laboratory,” *J. Chem. Educ.* **2009**, *86*, 355–356.
- Lloyd, B. W.; O’Brien, F. L.; Wilson, W. D. “Student Preparation and Analysis of Chloride and Calcium Ion Selective Electrodes,” *J. Chem. Educ.* **1976**, *53*, 328–330.
- Mifflin, T. E.; Andriano, K. M.; Robbins, W. B. “Determination of Penicillin Using an Immobilized Enzyme Electrode,” *J. Chem. Educ.* **1984**, *61*, 638–639.
- Palanivel, A.; Riyazuddin, P. “Fabrication of an Inexpensive Ion-Selective Electrode,” *J. Chem. Educ.* **1984**, *61*, 290.
- Ramaley, L; Wedge, P. J.; Crain, S. M. “Inexpensive Instrumental Analysis: Part 1. Ion-Selective Electrodes,” *J. Chem. Educ.* **1994**, *71*, 164–167.
- Selig, W. S. “Potentiometric Titrations Using Pencil and Graphite Sensors,” *J. Chem. Educ.* **1984**, *61*, 80–81.

Potentiometry

- Chan, W. H; Wong, M. S.; Yip, C. W. “Ion-Selective Electrode in Organic Analysis: A Salicylate Electrode,” *J. Chem. Educ.* **1986**, *63*, 915–916.
- Harris, T. M. “Potentiometric Measurement in a Freshwater Aquarium,” *J. Chem. Educ.* **1993**, *70*, 340–341.
- Kauffman, C. A.; Muza, A. L.; Porambo, M. W.; Marsh, A. L. “Use of a Commercial Silver-Silver Chloride Electrode for the Measurement of Cell Potentials to Determine Mean Ionic Activity Coefficients,” *Chem. Educator* **2010**, *15*, 178–180.
- Martínez-Fàbregas, E.; Alegret, S. “A Practical Approach to Chemical Sensors through Potentiometric Transducers: Determination of Urea in Serum by Means of a Biosensor,” *J. Chem. Educ.* **1994**, *71*, A67–A70.
- Moresco, H.; Sansón, P.; Seoane, G. “Simple Potentiometric Determination of Reducing Sugars,” *J. Chem. Educ.* **2008**, *85*, 1091–1093.
- Radic, N.; Komijenovic, J. “Potentiometric Determination of an Overall Formation Constant Using an Ion-Selective Membrane Electrode,” *J. Chem. Educ.* **1993**, *70*, 509–511.
- Riyazuddin, P.; Devika, D. “Potentiometric Acid–Base Titrations with Activated Graphite Electrodes,”*J. Chem. Educ.* **1997**, *74*, 1198–1199.

Coulometry

- Bertotti, M.; Vaz, J. M.; Telles, R. “Ascorbic Acid Determination in Natural Orange Juice,” *J. Chem. Educ.* **1995**, *72*, 445–447.
- Kalbus, G. E.; Lieu, V. T. “Dietary Fat and Health: An Experiment on the Determination of Iodine Number of Fats and Oils by Coulometric Titration,” *J. Chem. Educ.* **1991**, *68*, 64–65.
- Lötz, A. “A Variety of Electrochemical Methods in a Coulometric Titration Experiment,” *J. Chem. Educ.* **1998**, *75*, 775–777.
- Swim, J.; Earps, E.; Reed, L. M.; Paul, D. “Constant-Current Coulometric Titration of Hydrochloric Acid,” *J. Chem. Educ.* **1996**, *73*, 679–683.

Voltammetry and Amperometry

- Blanco-López, M. C.; Lobo-Castañón, M. J.; Miranda-Ordieres, A. J. "Homemade Bienzymatic-Amperometric Biosensor for Beverages Analysis," *J. Chem. Educ.* **2007**, *84*, 677–680.
- García-Armada, P.; Losada, J.; de Vicente-Pérez, S. "Cation Analysis Scheme by Differential Pulse Polarography," *J. Chem. Educ.* **1996**, *73*, 544–547.
- Herrera-Melián, J. A.; Doña-Rodríguez, J. M.; Hernández-Brito, J.; Pérez-Peña, J. "Voltammetric Determination of Ni and Co in Water Samples," *J. Chem. Educ.* **1997**, *74*, 1444–1445.
- King, D.; Friend, J.; Kariuki, J. "Measuring Vitamin C Content of Commercial Orange Juice Using a Pencil Lead Electrode," *J. Chem. Educ.* **2010**, *87*, 507–509.
- Marin, D.; Mendicuti, F. "Polarographic Determination of Composition and Thermodynamic Stability Constant of a Complex Metal Ion," *J. Chem. Educ.* **1988**, *65*, 916–918.
- Messersmith, S. J. "Cyclic Voltammetry Simulations with DigiSim Software: An Upper-Level Undergraduate Experiment," *J. Chem. Educ.* **2014**, *91*, 1498–1500.
- Sadik, O. A.; Brenda, S.; Joasil, P.; Lord, J. "Electropolymerized Conducting Polymers as Glucose Sensors," *J. Chem. Educ.* **1999**, *76*, 967–970.
- Sittampalam, G.; Wilson, G. S. "Amperometric Determination of Glucose at Parts Per Million Levels with Immobilized Glucose Oxidase," *J. Chem. Educ.* **1982**, *59*, 70–73.
- Town, J. L.; MacLaren, F.; Dewald, H. D. "Rotating Disk Voltammetry Experiment," *J. Chem. Educ.* **1991**, *68*, 352–354.
- Wang, J. "Sensitive Electroanalysis Using Solid Electrodes," *J. Chem. Educ.* **1982**, *59*, 691–692.
- Wang, J. "Anodic Stripping Voltammetry," *J. Chem. Educ.* **1983**, *60*, 1074–1075.
- Wang, J.; Maccà, C. "Use of Blood-Glucose Test Strips for Introducing Enzyme Electrodes and Modern Biosensors," *J. Chem. Educ.* **1996**, *73*, 797–800.
- Wang, Q.; Geiger, A.; Frias, R; Golden, T. D. "An Introduction to Electrochemistry for Undergraduates: Detection of Vitamin C (Ascorbic Acid) by Inexpensive Electrode Sensors," *Chem. Educator* **2000**, *5*, 58–60.

The following general references providing a broad introduction to electrochemistry.

- Adams, R. N. *Electrochemistry at Solid Surfaces*, Marcel Dekker: New York, 1969.
- Bard, A. J.; Faulkner, L. R. *Electrochemical Methods*, Wiley: New York, 1980.
- Faulkner, L. R. "Electrochemical Characterization of Chemical Systems" in Kuwana, T. E., ed. *Physical Methods in Modern Chemical Analysis*, Vol. 3, Academic Press: New York, 1983, pp. 137–248.
- Kissinger, P. T.; Heineman, W. R. *Laboratory Techniques in Electroanalytical Chemistry*, Marcel Dekker: New York, 1984.
- Lingane, J. J. *Electroanalytical Chemistry*, 2nd Ed., Interscience: New York, 1958.
- Sawyer, D. T.; Roberts, J. L., Jr. *Experimental Electrochemistry for Chemists*, Wiley-Interscience: New York, 1974.
- Vassos, B. H.; Ewing, G. W. *Electroanalytical Chemistry*, Wiley-Interscience: New York, 1983.

These short articles provide a good introduction to important principles of electrochemistry.

- Faulkner, L. R. "Understanding Electrochemistry: Some Distinctive Concepts," *J. Chem. Educ.* **1983**, *60*, 262–264.
- Huddle, P. A.; White, M. D.; Rogers, F. "Using a Teaching Model to Correct Known Misconceptions in Electrochemistry," *J. Chem. Educ.* **2000**, *77*, 104–110.
- Maloy, J. T. "Factors Affecting the Shape of Current-Potential Curves," *J. Chem. Educ.* **1983**, *60*, 285–289.
- Miles, D. T. "Run-D.M.C.: A Mnemonic Aid for Explaining Mass Transfer in Electrochemical Systems," *J. Chem. Educ.* **2013**, *90*, 1649–1653.
- Thompson, R. Q.; Craig, N. C. "Unified Electroanalytical Chemistry: Application of the Concept of Equilibrium," *J. Chem. Educ.* **2001**, *78*, 928–934.
- Zoski, C. G. "Charging Current Discrimination in Analytical Voltammetry," *J. Chem. Educ.* **1986**, *63*, 910–914.

Additional information on potentiometry and ion-selective electrodes can be found in the following sources.

- Bakker, E.; Diamond, D.; Lewenstam, A.; Pretsch, E. "Ions Sensors: Current Limits and New Trends," *Anal. Chim. Acta* **1999**, *393*, 11–18.
- Bates, R. G. *Determination of pH: Theory and Practice*, 2nd ed., Wiley: New York, 1973.

- Bobacka, J.; Ivaska, A.; Lewenstam, A. “Potentiometric Ion Sensors,” *Chem. Rev.* **2008**, *108*, 329–351.
- Buck, R. P. “Potentiometry: pH Measurements and Ion Selective Electrodes” in Weissberger, A., ed. *Physical Methods of Organic Chemistry*, Vol. 1, Part IIA, Wiley: New York, 1971, pp. 61–162.
- Cammann, K. *Working With Ion-Selective Electrodes*, Springer-Verlag: Berlin, 1977.
- Evans, A. P*otentiometry and Ion-Selective Electrodes*, Wiley: New York, 1987.
- Frant, M. S. “Where Did Ion Selective Electrodes Come From?” *J. Chem. Educ.* **1997**, *74*, 159–166.
- Light, T. S. “Industrial Use and Application of Ion-Selective Electrodes,” *J. Chem. Educ.* **1997**, *74*, 171–177.
- Rechnitz, G. A. “Ion and Bio-Selective Membrane Electrodes,” *J. Chem. Educ.* **1983**, *60*, 282–284.
- Ruzicka, J. “The Seventies—Golden Age for Ion-Selective Electrodes,” *J. Chem. Educ.* **1997**, *74*, 167– 170.
- Young, C. C. “Evolution of Blood Chemistry Analyzers Based on Ion Selective Electrodes,” *J. Chem. Educ.* **1997**, *74*, 177–182.

The following sources provide additional information on electrochemical biosensors.

- Alvarez-Icasa, M.; Bilitewski, U. “Mass Production of Biosensors,” *Anal. Chem.* **1993**, *65*, 525A– 533A.
- Meyerhoff, M. E.; Fu, B.; Bakker, E. Yun, J-H; Yang, V. C. “Polyion-Sensititve Membrane Electrodes for Biomedical Analysis,” *Anal. Chem.* **1996**, *68*, 168A–175A.
- Nicolini, C.; Adami, M; Antolini, F.; Beltram, F.; Sartore, M.; Vakula, S. “Biosensors: A Step to Bioelectronics,” *Phys. World*, May 1992, 30–34.
- Rogers, K. R.; Williams. L. R. “Biosensors for Environmental Monitoring: A Regulatory Perspective,” *Trends Anal. Chem.* **1995**, *14*, 289–294.
- Schultz, J. S. “Biosensors,” *Sci. Am.* August 1991, 64–69.
- Thompson, M.; Krull, U. “Biosensors and the Transduction of Molecular Recognition,” *Anal. Chem.* **1991**, *63*, 393A–405A.
- Vadgama, P. “Designing Biosensors,” *Chem. Brit.* **1992**, *28*, 249–252.

A good source covering the clinical application of electrochemistry is listed below.

- Wang, J. *Electroanalytical Techniques in Clinical Chemistry and Laboratory Medicine*, VCH: New York, 1998.

Coulometry is covered in the following texts.

- Rechnitz, G. A. *Controlled-Potential Analysis*, Macmillan: New York, 1963.
- Milner, G. W. C.; Philips, G. *Coulometry in Analytical Chemistry*, Pergamon: New York, 1967.

For a description of electrogravimetry, see the following resource.

- Tanaka, N. “Electrodeposition”, in Kolthoff, I. M.; Elving, P. J., eds. *Treatise on Analytical Chemistry, Part I: Theory and Practice*, Vol. 4, Interscience: New York, 1963.

The following sources provide additional information on polarography and pulse polarography.

- Flato, J. B. “The Renaissance in Polarographic and Voltammetric Analysis,” *Anal. Chem.* **1972**, *44(11)*, 75A–87A.
- Kolthoff, I. M.; Lingane, J. J. *Polarography*, Interscience: New York, 1952.
- Osteryoung, J. “Pulse Voltammetry,” *J. Chem. Educ.* **1983**, *60*, 296–298.

Additional Information on stripping voltammetry is available in the following text.

- Wang, J. *Stripping Analysis*, VCH Publishers: Deerfield Beach, FL, 1985.

The following papers discuss the numerical simulation of voltammetry.

- Bozzini, B. “A Simple Numerical Procedure for the Simulation of “Lifelike” Linear-Sweep Voltammo- grams,” *J. Chem. Educ.* **2000**, *77*, 100–103.
- Howard, E.; Cassidy, J. “Analysis with Microelectrodes Using Microsoft Excel Solver,” *J. Chem. Educ.* **2000**, *77*, 409–411.
- Kätelhön, E.; Compton, R. G. “Testing and Validating Electroanalytical Simulations,” *Analyst*, **2015**, *140*, 2592–2598.
- Messersmith, S. J. “Cyclic Voltammetry Simulations with DigiSim Software: An Upper-Level Undergraduate Experiment,” *J. Chem. Educ.* **2014**, *91*, 1498–1500.

Gathered together here are many useful resources for cyclic voltammetry, including experiments.

- Carriedo, G. A. “The Use of Cyclic Voltammetry in the Study of the Chemistry of Metal–Carbonyls,” *J. Chem. Educ.* **1988**, *65*, 1020–1022.
- García-Jareño, J. J.; Benito, D.; Navarro-Laboulais, J.; Vicente, F. “Electrochemical Behavior of Electrodeposited Prussian Blue Films on ITO Electrodes,” *J. Chem. Educ.* **1998**, *75*, 881–884.
- Gilles de Pelichy, L. D.; Smith, E. T. “A Study of the Oxidation Pathway of Adrenaline by Cyclic Voltammetry,” *Chem. Educator* **1997**, *2(2)*, 1–13.
- Gomez, M. E.; Kaifer, A. E. “Voltammetric Behavior of a Ferrocene Derivative,” *J. Chem. Educ.* **1992**, *69*, 502–505.
- Heffner, J. E.; Raber, J. C.; Moe, O. A.; Wigal, C. T. “Using Cyclic Voltammetry and Molecular Modeling to Determine Substituent Effects in the One-Electron Reduction of Benzoquinones,” *J. Chem. Educ.* **1998**, *75*, 365–367.
- Heinze, J. “Cyclic Voltammetry—Electrochemical Spectroscopy,” *Angew. Chem, Int. Ed. Eng.* **1984**, *23*, 831–918.
- Holder, G. N.; Farrar, D. G.; McClure, L. L. “Voltammetric Reductions of Ring-Substituted Acetophenones. 1. Determination of an Electron-Transfer Mechanism Using Cyclic Voltammetry and Computer Modeling: The Formation and Fate of a Radical Anion,” *Chem. Educator* **2001**, *6*, 343–349.
- Ibanez, J. G.; Gonzalez, I.; Cardenas, M. A. “The Effect of Complex Formation Upon the Redox Potentials of Metal Ions: Cyclic Voltammetry Experiments,” *J. Chem. Educ.* **1988**, *65*, 173–175.
- Ito, T.; Perara, D. M. N. T.; Nagasaka, S. “Gold Electrodes Modified with Self-Assembled Monolayers for Measuring l-Ascobric acid,” *J. Chem. Educ.* **2008**, *85*, 1112–1115.
- Kissinger, P. T.; Heineman, W. R. “Cyclic Voltammetry,” *J. Chem. Educ.* **1983**, *60*, 702–706.
- Mabbott, G. A. “An Introduction to Cyclic Voltammetry,” *J. Chem. Educ.* **1983**, *60*, 697–702.
- Petrovic, S. “Cyclic Voltammetry of Hexachloroiridate (IV): An Alternative to the Electrochemical Study of the Ferricyanide Ion,” *Chem. Educator* **2000**, *5*, 231–235.
- Toma, H. E.; Araki, K.; Dovidauskas, S. “A Cyclic Voltammetry Experiment Illustrating Redox Potentials, Equilibrium Constants and Substitution Reaction in Coordination Chemistry,” *J. Chem. Educ.* **2000**, *77*, 1351–1353.
- Walczak, M. W.; Dryer, D. A.; Jacobson, D. D,; Foss, M. G.; Flynn, N. T. “pH-Dependent Redox Couple: Illustrating the Nernst Equation Using Cyclic Voltammetry,” *J. Chem. Educ.* **1997**, *74*, 1195–1197.

This page titled 4.6: Additional Resources is shared under a CC BY-NC-SA 4.0 license and was authored, remixed, and/or curated by David Harvey.

- **11.6: Additional Resources** by David Harvey is licensed CC BY-NC-SA 4.0.

4.7: Chapter Summary and Key Terms

Chapter Summary

In this chapter we introduced three electrochemical methods of analysis: potentiometry, coulometry, and voltammetry. In potentiometry we measure the potential at an indicator electrode without allowing any significant current to pass through the electrochemical cell, and use the Nernst equation to calculate the analyte's activity after accounting for junction potentials.

There are two broad classes of potentiometric electrodes: metallic electrodes and membrane electrodes. The potential of a metallic electrode is the result of a redox reaction at the electrode's surface. An electrode of the first kind responds to the concentration of its cation in solution; thus, the potential of a Ag wire is determined by the activity of Ag^+ in solution. If another species is in equilibrium with the metal ion, the electrode's potential also responds to the concentration of that species. For example, the potential of a Ag wire in a solution of Cl^- responds to the concentration of Cl^- because the relative concentrations of Ag^+ and Cl^- are fixed by the solubility product for AgCl. We call this an electrode of the second kind.

The potential of a membrane electrode is determined by a difference in the composition of the solution on each side of the membrane. Electrodes that use a glass membrane respond to ions that bind to negatively charged sites on the membrane's surface. A pH electrode is one example of a glass membrane electrode. Other kinds of membrane electrodes include those that use insoluble crystalline solids or liquid ion-exchangers incorporated into a hydrophobic membrane. The F^- ion-selective electrode, which uses a single crystal of LaF_3 as the ion-selective membrane, is an example of a solid-state electrode. The Ca^{2+} ion-selective electrode, in which the chelating ligand di-(*n*-decyl)phosphate is immobilized in a PVC membrane, is an example of a liquid-based ion-selective electrode.

Potentiometric electrodes are designed to respond to molecules by using a chemical reaction that produces an ion whose concentration is determined using a traditional ion-selective electrode. A gas-sensing electrode, for example, includes a gas permeable membrane that isolates the ion-selective electrode from the gas. When a gas-phase analyte diffuses across the membrane it alters the composition of the inner solution, which is monitored with an ion-selective electrode. An enzyme electrodes operate in the same way.

Coulometric methods are based on Faraday's law that the total charge or current passed during an electrolysis is proportional to the amount of reactants and products participating in the redox reaction. If the electrolysis is 100% efficient—which means that only the analyte is oxidized or reduced—then we can use the total charge or total current to determine the amount of analyte in a sample. In controlled-potential coulometry we apply a constant potential and measure the resulting current as a function of time. In controlled-current coulometry the current is held constant and we measure the time required to completely oxidize or reduce the analyte.

In voltammetry we measure the current in an electrochemical cell as a function of the applied potential. There are several different voltammetric methods that differ in terms of the choice of working electrode, how we apply the potential, and whether we include convection (stirring) as a means for transporting of material to the working electrode.

Polarography is a voltammetric technique that uses a mercury electrode and an unstirred solution. Normal polarography uses a dropping mercury electrode, or a static mercury drop electrode, and a linear potential scan. Other forms of polarography include normal pulse polarography, differential pulse polarography, staircase polarography, and square-wave polarography, all of which use a series of potential pulses.

In hydrodynamic voltammetry the solution is stirred using either a magnetic stir bar or by rotating the electrode. Because the solution is stirred a dropping mercury electrode is not used; instead we use a solid electrode. Both linear potential scans and potential pulses can be applied.

In stripping voltammetry the analyte is deposited on the electrode, usually as the result of an oxidation or reduction reaction. The potential is then scanned, either linearly or using potential pulses, in a direction that removes the analyte by a reduction or oxidation reaction.

Amperometry is a voltammetric method in which we apply a constant potential to the electrode and measure the resulting current. Amperometry is most often used in the construction of chemical sensors for the quantitative analysis of single analytes. One

important example is the Clark O_2 electrode, which responds to the concentration of dissolved O_2 in solutions such as blood and water.

Key Terms

amalgam	amperometry	anode
anodic current	asymmetry potential	auxiliary electrode
cathode	cathodic current	charging current
controlled-current coulometry	controlled-potential coulometry	convection
coulometric titrations	coulometry	counter electrode
current efficiency	cyclic voltammetry	diffusion
diffusion layer	dropping mercury electrode	electrical double layer
electrochemically irreversible	electrochemically reversible	electrode of the first kind
electrode of the second kind	electrochemistry	electrogravimetry
enzyme electrodes	faradaic current	Faraday's law
galvanostat	gas-sensing electrode	glass electrode
hanging mercury drop electrode	hydrodynamic voltammetry	indicator electrode
ionophore	ion selective electrode	junction potential
limiting current	liquid-based ion-selective electrode	mass transport
mediator	membrane potential	mercury film electrode
migration	nonfaradaic current	Ohm's law
overpotential	peak current	polarography
potentiometer	potentiostat	pulse polarography
redox electrode	reference electrode	residual current
salt bridge	saturated calomel electrode	selectivity coefficient
silver/silver chloride electrode	solid-state ion-selective electrodes	standard hydrogen electrode
static mercury drop electrode	stripping voltammetry	total ionic strength adjustment buffer
voltammetry	voltammogram	working electrode

4.7: Chapter Summary and Key Terms is shared under a not declared license and was authored, remixed, and/or curated by LibreTexts.

- **11.7: Chapter Summary and Key Terms** has no license indicated.

CHAPTER OVERVIEW

5: Surface Techniques

5.1: Applications of Surface Techniques

5: Surface Techniques is shared under a not declared license and was authored, remixed, and/or curated by LibreTexts.

5.1: Applications of Surface Techniques

5.1: Applications of Surface Techniques is shared under a not declared license and was authored, remixed, and/or curated by LibreTexts.

CHAPTER OVERVIEW

6: Elemental Analysis

6.1: Neutron Activation Analysis

6: Elemental Analysis is shared under a not declared license and was authored, remixed, and/or curated by LibreTexts.

6.1: Neutron Activation Analysis

6.1: Neutron Activation Analysis is shared under a not declared license and was authored, remixed, and/or curated by LibreTexts.

Index

B

base peak

3.2: Fragmentation Patterns in Mass Spectra

E

Electrospray Mass Spectrometry

3.9.1: Electrospray Ionization Mass Spectrometry

F

Fragmentation Pattern (Mass Spectroscopy)

3.2: Fragmentation Patterns in Mass Spectra

3.13: The Mass Spectra of Elements

Fragmentation Patterns (mass spec)

3.7.2: Mass Spectrometry - Fragmentation Patterns

G

gas chromatography

2.4: Gas Chromatography

I

Injection Stage (Mass Spec)

3.9.2: Injection Stage

Isotopomers

3.5.4: Isotopes- 13C

M

M+1 peak (mass spec)

3.15: The M+1 Peak

molecular ion

3.2: Fragmentation Patterns in Mass Spectra

3.14: The Molecular Ion (M^+) Peak

P

parent ion

3.2: Fragmentation Patterns in Mass Spectra

R

raman spectroscopy

1.5.1: Raman- Application

1.5.3: Resonant vs. Nonresonant Raman Spectroscopy

Glossary

Sample Word 1 | Sample Definition 1

Detailed Licensing

Overview

Title: CC CHM 411: Advanced Analytical Chemistry

Webpages: 90

Applicable Restrictions: Noncommercial

All licenses found:

- Undeclared: 45.6% (41 pages)
- CC BY-NC-SA 4.0: 33.3% (30 pages)
- CC BY-NC 3.0: 10% (9 pages)
- CC BY-NC 4.0: 6.7% (6 pages)
- CC BY 4.0: 4.4% (4 pages)

By Page

- CC CHM 411: Advanced Analytical Chemistry - *Undeclared*
  - Front Matter - *Undeclared*
    - TitlePage - *Undeclared*
    - InfoPage - *Undeclared*
    - Table of Contents - *Undeclared*
    - Licensing - *Undeclared*
  - 1: Spectroscopic Methods - *CC BY-NC-SA 4.0*
    - 1.1: Overview of Spectroscopy - *CC BY-NC-SA 4.0*
    - 1.2: Spectroscopy Based on Absorption - *CC BY-NC-SA 4.0*
    - 1.3: UV/Vis and IR Spectroscopy - *CC BY-NC-SA 4.0*
    - 1.4: Fourier-Transform Infrared Spectroscopy -- Additional Readings - *Undeclared*
    - 1.5: Raman Spectroscopy - *CC BY 4.0*
      - 1.5.1: Raman- Application - *CC BY 4.0*
      - 1.5.2: Raman- Theory - *CC BY 4.0*
      - 1.5.3: Resonant vs. Nonresonant Raman Spectroscopy - *CC BY 4.0*
    - 1.6: Current Applications of IR and Raman Spectroscopy - *Undeclared*
    - 1.7: Atomic Absorption Spectroscopy - *CC BY-NC-SA 4.0*
    - 1.8: Emission Spectroscopy - *CC BY-NC-SA 4.0*
    - 1.9: Photoluminescent Spectroscopy - *CC BY-NC-SA 4.0*
    - 1.10: Atomic Emission Spectroscopy - *CC BY-NC-SA 4.0*
    - 1.11: Nuclear Magnetic Resonance Spectrometry - *Undeclared*
      - 1.11.1: Additional Readings on NMR - *Undeclared*
      - 1.11.2: Applications of NMR - *Undeclared*
    - 1.12: Spectroscopy Based on Scattering - *CC BY-NC-SA 4.0*
    - 1.13: Neutron Activation Analysis - *Undeclared*
    - 1.14: Problems - *CC BY-NC-SA 4.0*
    - 1.15: Additional Resources - *CC BY-NC-SA 4.0*
    - 1.16: Chapter Summary and Key Terms - *CC BY-NC-SA 4.0*
  - 2: Chromatographic and Electrophoretic Methods - *CC BY-NC-SA 4.0*
    - 2.1: Overview of Analytical Separations - *CC BY-NC-SA 4.0*
    - 2.2: General Theory of Column Chromatography - *CC BY-NC-SA 4.0*
    - 2.3: Optimizing Chromatographic Separations - *CC BY-NC-SA 4.0*
    - 2.4: Gas Chromatography - *CC BY-NC-SA 4.0*
    - 2.5: High-Performance Liquid Chromatography - *CC BY-NC-SA 4.0*
      - 2.5.1: HPLC Simulator - *Undeclared*
      - 2.5.2: HPLC Method Development - *Undeclared*
    - 2.6: Other Forms of Chromatography - *CC BY-NC-SA 4.0*
    - 2.7: Electrophoresis - *CC BY-NC-SA 4.0*
    - 2.8: Problems - *CC BY-NC-SA 4.0*
    - 2.9: Additional Resources - *CC BY-NC-SA 4.0*
    - 2.10: Chapter Summary and Key Terms - *CC BY-NC-SA 4.0*
  - 3: Mass Spectrometry - *Undeclared*
    - 3.1: Accelerator Mass Spectroscopy - *Undeclared*
    - 3.2: Fragmentation Patterns in Mass Spectra - *CC BY-NC 4.0*
    - 3.3: GC/MS Combination- Shockwave - *Undeclared*

- 3.4: How the Mass Spectrometer Works - *CC BY-NC 4.0*
- 3.5: Introductory Mass Spectrometry - *CC BY-NC 3.0*
  - 3.5.1: Fragmentation - *CC BY-NC 3.0*
  - 3.5.2: High Resolution vs Low Resolution - *CC BY-NC 3.0*
  - 3.5.3: Introduction to Mass Spectrometry - *CC BY-NC 3.0*
  - 3.5.4: Isotopes- 13C - *CC BY-NC 3.0*
  - 3.5.5: Isotopes- Br and Cl - *CC BY-NC 3.0*
  - 3.5.6: Molecular Ions - *CC BY-NC 3.0*
  - 3.5.7: Molecular Ion and Nitrogen - *CC BY-NC 3.0*
  - 3.5.8: The Mass Spectrometry Experiment - *CC BY-NC 3.0*
- 3.6: MALDI-TOF - *Undeclared*
- 3.7: Mass Spectra - *Undeclared*
  - 3.7.1: Interpreting a Mass Spectrum - *Undeclared*
  - 3.7.2: Mass Spectrometry - Fragmentation Patterns - *Undeclared*
  - 3.7.3: Mass Spectroscopy- Quizzes - *Undeclared*
- 3.8: Mass Spectra Interpretation- ALDEHYDES - *Undeclared*
- 3.9: Mass Spectrometers (Instrumentation) - *Undeclared*
  - 3.9.1: Electrospray Ionization Mass Spectrometry - *Undeclared*
  - 3.9.2: Injection Stage - *Undeclared*
  - 3.9.3: Mass Analyzers (Mass Spectrometry) - *Undeclared*
- 3.10: Mass Spectrometry- Isotope Effects - *Undeclared*
- 3.11: Organic Compounds Containing Halogen Atoms - *CC BY-NC 4.0*
- 3.12: Selected Ion Monitoring- Shockwave - *Undeclared*
- 3.13: The Mass Spectra of Elements - *CC BY-NC 4.0*
- 3.14: The Molecular Ion (M^+) Peak - *CC BY-NC 4.0*
- 3.15: The M+1 Peak - *CC BY-NC 4.0*
- 3.16: Current Applications of Mass Spectrometry - *Undeclared*

4: Electrochemical Methods - *CC BY-NC-SA 4.0*
- 4.1: Overview of Electrochemistry - *CC BY-NC-SA 4.0*
- 4.2: Potentiometric Methods - *CC BY-NC-SA 4.0*
- 4.3: Coulometric Methods - *CC BY-NC-SA 4.0*
- 4.4: Voltammetric and Amperometric Methods - *CC BY-NC-SA 4.0*
  - 4.4.1: Cyclic Voltammetry - *Undeclared*
  - 4.4.2: Anodic Stripping Voltammetry - *Undeclared*
- 4.5: Problems - *CC BY-NC-SA 4.0*
- 4.6: Additional Resources - *CC BY-NC-SA 4.0*
- 4.7: Chapter Summary and Key Terms - *Undeclared*

5: Surface Techniques - *Undeclared*
- 5.1: Applications of Surface Techniques - *Undeclared*

6: Elemental Analysis - *Undeclared*
- 6.1: Neutron Activation Analysis - *Undeclared*

Back Matter - *Undeclared*
- Index - *Undeclared*
- Glossary - *Undeclared*
- Detailed Licensing - *Undeclared*